Sensitivity to Change:
Black Sea, Baltic Sea and North Sea

NATO ASI Series

Advanced Science Institutes Series

A Series presenting the results of activities sponsored by the NATO Science Committee, which aims at the dissemination of advanced scientific and technological knowledge, with a view to strengthening links between scientific communities.

The Series is published by an international board of publishers in conjunction with the NATO Scientific Affairs Division

A Life Sciences	Plenum Publishing Corporation
B Physics	London and New York
C Mathematical and Physical Sciences	Kluwer Academic Publishers
D Behavioural and Social Sciences	Dordrecht, Boston and London
E Applied Sciences	
F Computer and Systems Sciences	Springer-Verlag
G Ecological Sciences	Berlin, Heidelberg, New York, London,
H Cell Biology	Paris and Tokyo
I Global Environmental Change	

PARTNERSHIP SUB-SERIES

1. Disarmament Technologies	Kluwer Academic Publishers
2. Environment	Springer-Verlag / Kluwer Academic Publishers
3. High Technology	Kluwer Academic Publishers
4. Science and Technology Policy	Kluwer Academic Publishers
5. Computer Networking	Kluwer Academic Publishers

The Partnership Sub-Series incorporates activities undertaken in collaboration with NATO's Cooperation Partners, the countries of the CIS and Central and Eastern Europe, in Priority Areas of concern to those countries.

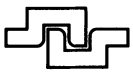
NATO-PCO-DATA BASE

The electronic index to the NATO ASI Series provides full bibliographical references (with keywords and/or abstracts) to more than 50000 contributions from international scientists published in all sections of the NATO ASI Series.
Access to the NATO-PCO-DATA BASE is possible in two ways:

- via online FILE 128 (NATO-PCO-DATA BASE) hosted by ESRIN,
Via Galileo Galilei, I-00044 Frascati, Italy.

- via CD-ROM "NATO-PCO-DATA BASE" with user-friendly retrieval software in English, French and German (© WTV GmbH and DATAWARE Technologies Inc. 1989).

The CD-ROM can be ordered through any member of the Board of Publishers or through NATO-PCO, Overijse, Belgium.



Series 2: Environment – Vol. 27

Sensitivity to Change: Black Sea, Baltic Sea and North Sea

edited by

Emin Özsoy
Institute of Marine Sciences, METU,
Erdemli, İçel, Turkey

and

Alexander Mikaelyan
Shirshov Institute of Oceanology,
Moscow, Russia

Springer-Science+Business Media, B.V.

Proceedings of the NATO Advanced Research Workshop on
Sensitivity of North Sea, Baltic Sea and Black Sea to
Anthropogenic and Climatic Changes
Varna, Bulgaria
14–18 November 1995

A C.I.P. Catalogue record for this book is available from the Library of Congress.

ISBN 978-94-010-6429-3 ISBN 978-94-011-5758-2 (eBook)
DOI 10.1007/978-94-011-5758-2

Printed on acid-free paper

All Rights Reserved
© 1997 Springer Science+Business Media Dordrecht
Originally published by Kluwer Academic Publishers in 1997
Softcover reprint of the hardcover 1st edition 1997

No part of the material protected by this copyright notice may be reproduced or utilized in any form or by any means, electronic or mechanical, including photocopying, recording or by any information storage and retrieval system, without written permission from the copyright owner.

TABLE OF CONTENTS

Preface ix

List of Participants xi

A Synopsis and Recommendations for Future Studies xvii

Changes of Mean Sea Level and Ice Conditions in Gdynia as Indicators of Climate Changes in the Gulf of Gdañsk
M. Sztobryn, M. Kałas and A. Staskiewicz 1

Variability of Northwestern Black Sea Hydrography and River Discharges as Part of the Global Ocean-Atmosphere Fluctuations
A. Polonsky, E. Voskresenskaya and V. Belokopytov 11

Recent Man-Made Changes in the Black Sea Ecosystem
Yu.P. Zaitsev and B.G. Alexandrov 25

Seasonal and Long-Term Variability of the Black Sea Optical Parameters
V.L. Vladimirov, V.I. Mankovsky, M.V. Solov'ev and A.V. Mishonov 33

The Nutrient Stock of the Romanian Shelf of the Black Sea during the Last Three Decades
A. Cociasu, V. Diaconu, L. Popa, I. Nae, L. Dorogan and V. Malciu 49

Distribution and Fluctuation of Dominant Zooplankton Species in the Southern Black Sea in Comparison to the North Sea and Baltic Sea
U. Niermann and W. Greve 65

Some Aspects of Phytoplankton Long-Term Alterations off Bulgarian Black Sea Shelf
S. Moncheva and A. Krastev 79

Sensitivity to Anthropogenic Factors of the Plankton Fauna Adjacent to the Bulgarian Coast of the Black Sea
A. Konsulov and L. Kamburska 95

Long-Term Variability of Phytoplankton Communities in Open Black Sea in Relation to Environmental Changes
A.S. Mikaelyan 105

Mnemiopsis Leidyi Abundance in the Black Sea and its Impact on the Pelagic Community
T.A. Shiganova 117

Seasonal Variation of Surface Pigment Distribution in the Black Sea on CZCS Data
N.P. Nezlin 131

The Effect of Hydrological Conditions on the State of Herring Stocks in the Baltic Sea
T. Raid 139

Role of Fishing in the Black Sea Ecosystem
A.C. Gücü 149

Environmental Impact on Fish Resources in the Black Sea
K. Prodanov, K. Mikhailov, G. Daskalov, K. Maxim, A. Chashchin, A. Arkhipov, V. Shlyakhov and E. Ozdamar 163

Variations in the Vertical Structure of Water Chemistry within the Three Hydrodynamically Different Regions of the Black Sea
Ö. Baştürk, S. Tuğrul, S. Konovalov and İ. Salihoğlu 183

Spatial Isopycnal Analysis of the Main Pycnocline Chemistry of the Black Sea: Seasonal and Interannual Variations
S. Konovalov, S. Tuğrul, Ö. Baştürk and İ. Salihoğlu 197

Suspended Matter as an Index of Productivity in the Western Black Sea (Application for Productivity and Eutrophication Control)
S.V. Vostokov 211

Particulate Organic Matter of Black Sea Euphotic Zone: Seasonal and Long-Term Variation of Spatial Distribution and Composition
Z.P. Burlakova, L.V. Eremeeva and S.K. Konovalov 223

Time-Series Profiles of ^{134}Cs, ^{137}Cs and ^{90}Sr in the Black Sea
K.O. Buesseler and H.D. Livingston 239

The Black Sea Cold Intermediate Layer
L.I. Ivanov, Ş. Beşiktepe and E. Özsoy 253

Physical Oceanography Variability in the Black Sea Pycnocline
L.I. Ivanov, Ş. Beşiktepe and E. Özsoy 265

The Black Sea Bottom Homogeneous Layer: A Simple Model of Formation
V.N. Eremeev, L.I. Ivanov, A.S. Samodurov and M. Duman 275

Physical Processes of Surface-Deep Layers Exchange in the Black Sea
E. Demirov, M.A. Latif and V. Diaconu 285

Convection in the Baltic Sea: A Numerical Process Study
J.O. Backhaus and H. Wehde 295

An Ice/Ocean Model for North and Baltic Sea
C. Schrum 311

Quantification of Transports to Skagerrak: A Modeling Approach
M.D. Skogen, G. Eriksrød and E. Svendsen 327

Eddy Dynamics Controlled by Basin Scale, Coastline and Topography
N.H. Rachev and E.V. Stanev 341

Seasonal Variability of the Black Sea Climatic Circulation
D.I. Trukhchev and R.A. Ibrayev 365

Cold Intermediate Water Formation in the Black Sea. Analysis on Numerical Model Simulations
J.V. Staneva and E.V. Stanev 375

Circulation in Semi-Enclosed Seas Induced by Buoyancy Flux through a Strait
G.K. Korotaev 395

Modelling of Strait Dynamics: The Baltic Experiments
E. Sayin 403

Heat and Salt Intrusions in the Pycnocline from Sinking Plumes. Test Case for the Entrainment in the Black Sea
J.A. Simeonov, E.V. Stanev, J.O. Backhaus, J.H. Jungclaus and V.M. Roussenov 417

Coastal Eutrophication of the Southern Bight of the North Sea: Assessment and Modelling
C. Lancelot, V. Rousseau, G. Billen and D. Van Eeckhout 439

Modelling the Functioning of the North-Western Black Sea Ecosystem from 1960 to Present
D. Van Eeckhout and C. Lancelot 455

Towards Coupling Three Dimensional Eddy Resolving General Circulation and Biochemical Models in the Black Sea
T. Oğuz, P. Malanotte-Rizzoli and H. Ducklow 469

Coupled Hydrodynamic Ecosystem Model of the Black Sea at Basin Scale: Model Description and First Results
M. Grégoire, J.-M. Beckers, J.C.J. Nihoul and E. Stanev 487

Atmospheric Transport of Desert Dust Toward European Seas: Model Parameterisation and a Simulated Case
S. Dobricic 501

Index 509

PREFACE

Recent decades have seen a degradation of the environmental quality in semi-enclosed seas, which are particularly sensitive to population pressures due to their naturally low flushing rates related to their geometry. The North Sea, Baltic Sea and the Black Sea are amongst the most seriously threatened seas in the Euro-Asian region.

Each semi-enclosed sea has a distinct pattern of circulation, transport, mixing, associated with the particular geometry, topography, boundary processes, interior stratification, atmospheric forcing, ice formation, straits / sill controls, and the specific inputs of freshwater, nutrients and pollutants. The workshop investigated the distinctive physical and ecological characteristics of the three seas in a comparative manner, in order to identify the types of driving forces and dynamic controls operating on productivity, nutrient cycling, physical transport and mixing mechanisms. A comparative study of these controlling mechanisms would allow us to better understand ecosystem sensitivity in these different environments.

The workshop presentations highlighted the complexity of the semi-enclosed seas related to the interaction amongst the physical, chemical and biological fields, and differences in time and space scales in each of the systems. Further, a strong climate signal exists in these systems, manifest in the interannual, interdecadal and longer term variability. Part of the variability appears connected with background climatic variability. On the other hand, changes which could not be explained by climate alone are also present, and these are strongly related to human activity - the most significant of these effects is eutrophication. The end results of such changes could be traced in all levels of marine productivity and in the realization of fish catch.

The systems under investigation ranged from almost totally enclosed domains to marginal seas adjoining a large ocean body, and from shallow, dissipative, and tidally dominated shelf regions to deep basins with energetic shelf regions adjoining relatively stagnant waters, and from completely anoxic to oxygen saturated chemical environments. Physical controls include: freshwater balances, strait exchanges, surface fluxes, effects of sea-ice, frontal dynamics and exchange, cross-shelf exchange, pycnocline mixing, shelf and boundary mixing, intrusions of waters cascading from the shelf or entering from straits, convection, upwelling and meso-scale dynamics. Chemical controls include: nutrient and pollutant input levels and temporal changes in their composition, suboxic and redox zone dynamics, and the geochemical residence time and removal rates of compounds in marine systems in general. Biological controls include: the mediation of nutrient cycling, food-web relationships, invasions by opportunistic species, as well as biological influences on optical properties. It was evident that the seasonal cycles of the above variables often modulated the interannual and long-term changes.

The synopsis and recommendations in the following section were developed as a result of common discussions in two working groups organised during the Workshop.

All of the participants contributed to the working group discussions. We thank Ken Buesseler, Leonid Ivanov, Ulrich Niermann and Denis Van Eeckhout for leading the discussions and formulating the results. We also thank Tsonka Konsoulova, Emil Stanev and Sergey Semovski as members of the Workshop Organising Committee.

We thank the NATO Science Committee for giving us the opportunity to carry out this Workshop, and to Dr. L. Veiga da Cunha, Director for the Priority Area on Environment of the Scientific and Environmental Affairs Division of NATO for his support, and to Ümit Ünlüata, Director of the Institute of Marine Sciences of METU, Erdemli, Turkey, for motivating the Workshop. We also thank TÜBİTAK, the Turkish Scientific and Technical Research Council, for providing travel support for some of the participants.

We are grateful to the Bulgarian Academy of Sciences, to Zdravko Belberov, Director of the Institute of Oceanology, Varna, to Mihail Ganchev, of the National Oceanographic Committee of Bulgaria , and to Chavdar Ormanov, Head of the Naval Department of the Bulgarian Army Defence Research Institute, for their enthusiastic support for the Workshop. Simeon Bozhanov, Environmental Adviser to the President of the Republic of Bulgaria kindly provided his support and motivated informal discussions during the meeting.

It was very pleasing for us, the organisers, that the truly multi-disciplinary group of participants of the Workshop enjoyed the great meeting environment in Varna, at the pleasant premises of the International House of Scientists 'F. J. Curie', but also to take part in frequent scientific discussions during the meeting and in splendid times at the evening social hours. We thank Ivan Janev, the director of the IHS, for his hospitality.

The success of the Workshop in large part owes to the efforts of our local hosts, Tsonka Konsoulova, Asen Konsulov and Avram Avramov, who fully employed their talents and diligently took care of fine the details of meeting organisation in all stages. Together with them, a number of other people from the Institute of Oceanology also provided valuable efforts whenever needed.

EMİN ÖZSOY
Institute of Marine Sciences,
Middle East Technical University,
P.K. 28, Erdemli, İçel 33731 Turkey

ALEXANDER MIKAELYAN
Shirshov Institute of Oceanology,
Krasikova 23,
Moscow 117218 Russia

LIST OF PARTICIPANTS

Avram M. Avramov, Institute of Oceanology, Varna 9000, P.O. Box 152, Bulgaria. Tel: +359 52 77 41 83, Fax: +359 52 77 42 56, E-mail: avram@emona.io-bas.bg

Jan O. Backhaus, Universität Hamburg, Zentrum für Meeres- und Klimatforschung, Institut für Meereskunde, Troplowitzstrasse 7, 22529 Hamburg, Germany. Tel: +49 040 41 23 26 04, Fax: +49 40 560 57 24, E-mail: backhaus@dkrz.d400.de

Job Baretta, Ecological Modelling Center, EMC/DHI Joint Department DHI/VKI, Agern Alle, 2970 Horsholm, Denmark. Tel: +45 45 769 555, Fax: +45 45 768 778 144, E-mail: baretta@dhi.dk

Özden Baştürk, Institute of Marine Sciences, Middle East Technical University, P.O. Box 28, Erdemli 33731, İçel, Turkey. Tel: +90 324 521 2406, Fax: +90 324 521 2327, E-mail: basturk@deniz.ims.metu.edu.tr

Jean-Marie Beckers, GHER, Sart Tilman B5, University of Liege, B-4000 Liege, Belgium. Tel: +32 41 66 33 58, Fax: +32 41 66 23 55, E-mail: jmb@ocean.oce.ulg.ac.be

Şengül Beşiktepe, Institute of Marine Sciences, Middle East Technical University, P.O. Box 28, Erdemli 33731, İçel, Turkey. Tel: +90 324 521 2406, Fax: +90 324 521 2327, E-mail: sengul@deniz.ims.metu.edu.tr

Ken Buesseler, Marine Chemistry and Geochemistry, Wood Hole Oceanographic Institution, Clark-447, MS #25, Woods Hole, MA 02543, U.S.A. Fax: +1 508 457 2139, E-mail: kbuesseler@whoi.edu (present address: National Science Foundation, Division of Ocean Sciences, Room 725, 4202 Wilson Blvd., Arlington, VA 22230, U.S.A. Tel: +1 703 306-1589, E-mail: kbuessel@nsf.gov)

Adriana Cociasu, Romanian Marine Research Institute, 300 Mamaia Blvd., Constansa 3-8700, Romania. Tel: +40 41 643 288, Fax: +40 41 831 274, E-mail: acociasu@alpha.rmri.ro

Encho Demirov, Institute of Oceanology, Varna 9000, P.O. Box 152, Bulgaria. Tel: +359 52 77 45 49, Fax: +359 52 77 42 56, E-mail: encho@emona.io-bas.bg

Vasile Diaconu, Romanian Marine Research Institute, 300 Mamaia Blvd., Constansa 3-8700, Romania. Tel: +40 41 643 288, Fax: +40 41 831 274, E-mail: diaconu@alpha.rmri.ro

Srdjan Dobricic, University of Athens, Department of Applied Physics, Ippocratous 33, Athens 10680, Greece. Fax: +30 1 3605080, E-mail: sdobri@etesian.meteolab.ariadne-t.gr (present address: TP-690 Space Applications Institute, 21020 Ispra (Va), Italy. Tel: +39 332 78.52.32, Fax: +39 332 78.96.48, E-mail: srdan.dobricic@jrc.it)

Ali C. Gücü, Institute of Marine Sciences, Middle East Technical University, P.O. Box 28, Erdemli 33731, İçel, Turkey. Tel: +90 324 521 2406, Fax: +90 324 521 2327, E-mail: gucu@deniz.ims.metu.edu.tr

Yusuf Sinan Hüsrevoğlu, Institute of Marine Sciences, Middle East Technical University, P.O. Box 28, Erdemli 33731, İçel, Turkey. Tel: +90 324 521 2406, Fax: +90 324 521 2327, E-mail: ysinan@deniz.ims.metu.edu.tr

Leonid I. Ivanov, Marine Hydrophysical Institute, 2 Kapitanskaya Str., Sevastopol 335000 Crimea, Ukraine. Tel: +38 0692 520452, Fax: +38 0692 444253, E-mail: ocean@mhi2.sebastopol.ua

Maciej Kalas, Institute of Meteorology and Water Management Maritime Branch, Ul. Wazsingtona 42, 81-342 Gdinya, Poland. Tel: +48 48 20 52 21, Fax: +48 58 20 71 01, Fax: +48 58 20 16 41, E-mail: kalas@stratus.imgw.gdynia.pl

Sergey K. Konovalov, Marine Hydrophysical Institute, 2 Kapitanskaya Str., Sevastopol Crimea 335000, Ukraine. Tel: +38 0692 520452, Fax: +38 0692 444253, E-mail: vlvlad@mhi2.sebastopol.ua

Asen Konsulov, Institute of Oceanology, Varna 9000, P.O. Box 152, Bulgaria. Tel: +359 52 77 45 49, Fax: +359 52 77 42 56, E-mail: avram@emona.io-bas.bg

Tsonka Konsoulova, Institute of Oceanology, Varna 9000, P.O.Box 152, Bulgaria. Tel: +359 52 77 45 49, Fax: +359 52 77 42 56, E-mail: avram@emona.io-bas.bg

Gennady K. Korotaev, Marine Hydrophysical Institute, 2 Kapitanskaya Str., Sevastopol 335000 Crimea, Ukraine. Tel: +38 0692 520779, Fax: +38 0692 444253, E-mail: korotaev@mhi2.sebastopol.ua

Cristiane Lancelot, Groupe de Microbiologie des Milieux Aquatiques, Université Libre de Bruxelles, Campus de la Plaine, Blvd. de Triomphe, CP 221, B-1050 Bruxelles, Belgium. Tel: +32 2 650 59 88, Fax: +32 2 650 59 93, E-mail: lancelot@is3.ulb.ac.be

Yüksel Malkoç, Faculty of Marine Science, Karadeniz Technical University, Çamburnu, 61530 Trabzon, Turkey. Tel: +90 462 7522031, Fax: +90 462 7522158

Victor V. Melnikov, Institute for the Biology of the Southern Seas, 2 Nakhimova Ave., Sevastopol 335011 Crimea, Ukraine. Tel: +38 0692 522 484, Fax: +38 0692 592 813, Fax: +38 0692 444 477, Telex: 197301 bios ux (country code 680), E-mail: melnikov@seatrf.sebastopol.ua

Alexander Mikaelyan, Shirshov Institute of Oceanology, Krasikova 23, Moscow 117851, Russia. Tel: +7 095 124 77 49, Fax: +7 095 124 59 83, E-mail: mikael@ecosys.sio.rssi.ru

Snejana Moncheva, Institute of Oceanology, Varna 9000, P.O. Box 152, Bulgaria. Tel: +359 42 77 45 49/168, Fax: +359 42 77 42 56, Fax: +359 42 77 42 56, E-mail: avram@emona.io-bas.bg

Yu. R. Nalbandov, Shirshov Institute of Oceanology, Krasikova 23, Moscow 117851, Russia. Tel: +7 095 124 77 49, Fax: +7 095 124 59 83, E-mail: yuri@nalbandov.msk.ru

Nikolay P. Nezlin, Shirshov Institute of Oceanology, Krasikova 23, Moscow 117851, Russia. Tel: +7 095 124 77 49, Fax: +7 095 124 59 83, Fax: +7 095 124 79 40, E-mail: nezlin@ecosys.sio.rssi.ru

Ulrich Niermann, Institute of Marine Sciences, Middle East Technical University, P.O. Box 28, Erdemli 33731, İçel, Turkey. Tel: +90 324 521 2406, Fax: +90 324 521 2327, E-mail: uli@deniz.ims.metu.edu.tr (present address: E-mail: uniermann@t-online.de)

Temel Oğuz, Institute of Marine Sciences, Middle East Technical University, P.O. Box 28, Erdemli 33731, İçel, Turkey. Tel: +90 324 521 2406, Fax: +90 324 521 2327, E-mail: oguz@deniz.ims.metu.edu.tr

Emin Özsoy, Institute of Marine Sciences, Middle East Technical University, P.O. Box 28, Erdemli 33731, İçel, Turkey. Tel: +90 324 521 2406, Fax: +90 324 521 2327, E-mail: ozsoy@deniz.ims.metu.edu.tr

Kamen Prodanov, Institute of Oceanology, Varna 9000, P.O. Box 152, Bulgaria. Tel: +359 52 77 45 49, Fax: +359 52 77 42 56, E-mail: avram@emona.io-bas.bg

Titka N. Patzireva, Institute of Oceanology, Varna 9000, Bulgaria, P.O. Box 152. Tel: +359 52 77 41 83, Fax: +359 52 77 42 56, E-mail: titka@emona.io-bas.bg

Alexander Polonsky, Marine Hydrophysical Institute, 2 Kapitanskaya Str., Sevastopol, Crimea 335000, Ukraine. tel: +38 0692 520452, Fax: +38 0692 444253, E-mail: ocean@mhi2.sebastopol.ua

Nikolay H. Rachev, Department of Meteorology and Geophysics, University of Sofia, 5 J. Bourchier Str., 1126 Sofia, Bulgaria. Tel: +359 2 625 61 (ext. 289), Fax: +359 2 689 085, E-mail: nick@phys.uni-sofia.bg

Tiit Raid, Estonian Marine Institute, 32 Lai Str., EE0001 Talinn, Estonia. Tel: +372 2 441 198, Fax: +372 6 313 004

Vasille Roussenov, Department of Meteorology and Geophysics, University of Sofia, 5 J. Bourchier Str., 1126 Sofia, Bulgaria. Tel: +359 2 625 6 289, Fax: +359 2 689 085, E-mail: vasil@phys.uni-sofia.bg

Cemal Saydam, Institute of Marine Sciences, Middle East Technical University, P.O. Box 28, Erdemli 33721, İçel, Turkey. Fax: +90 324 521 2327, E-mail: saydam@deniz.ims.metu.edu.tr (present address: Middle East Technical University, Ankara, Turkey. E-mail saydam@rorqual.ims.metu.edu.tr)

Erdem Sayin, Institute of Marine Science and Technology, Dokuz Eylül University, 1884/8 Sokak No. 10, İnciralti - İzmir 35340, Turkey. tel: +90 232 278 55 65, Fax: +90 232 278 50 82, E-mail: sayin@neptune.imst.deu.edu.tr

Corinna Schrum, Universität Hamburg, Institut für Meereskunde, Troplowitzstrasse 7, 22529 Hamburg, Germany. tel: +49 040 41 23 59 89, Fax: +49 040 560 57 24, E-mail: Schrum@ifm.uni-hamburg.de

Sergey V. Semovski, Institute of Oceanology, Polish Academy of Science, P.O. Box 68, Sopot, PL-81-712 Poland. Tel: +48 58 51 72 83, Fax: +48 58 51 21 30, E-mail: siergej@iopan.gda.pl

Tamara A. Shiganova, Shirshov Institute of Oceanology, Krasikova 23, Moscow 117851, Russia. Tel: +7 095 124 77 49, Fax: +7 095 124 59 83, E-mail: shiganov@ecosys.sio.rssi.ru

Kazimeras M. Shimkus, Shirshov Institute of Oceanology, Southern Branch 353470, Gelendzhik - 7, Russia. Tel: +86141 232 61, Fax: +86141 231 89, E-mail: kosyan@sdios.sea.ru

Julian Simeanov, Department of Meteorology and Geophysics, university of Sofia, 5 J. Bourchier Str., 1126 Sofia, Bulgaria. Tel: +359 2 625 61 (ext. 289), Fax: +359 2 689 085, E-mail: stanev@phys.uni-sofia.bg

Morton D. Skogen, Institute of Marine Research, Pb. 1870, N-5024 Bergen, Norway. Tel: +47-55238461, Fax: +47-55238584, E-mail: morten@imr.no

Emil V. Stanev, Department of Meteorology and Geophysics, University of Sofia, 5 J. Bourchier Str., 1126 Sofia, Bulgaria. Tel: +359 2 625 6 289, Fax: +359 2 689 085, E-mail: stanev@phys.uni-sofia.bg

Joanna Staneva, Department of Meteorology and Geophysics, University of Sofia, 5 J. Bouchier Str., 1126 Sofia, Bulgaria. Tel: +359 2 625 289, Fax: +359 2 689 085, E-mail: joanna@phys.uni-sofia.bg

Marzenna Sztobryn, Institute of Meteorology and Water Management Maritime Branch, Ul. Waszyngtona 42, 81-342 Gdynia, Poland. Tel: +48 58 20 52 21, Fax: +48 58 20 71 01, E-mail: sztobryn@stratus.imgw.gdynia.pl

Dimitur I. Trukhchev, Institute of Oceanology, Varna 9000, P.O. Box 152, Bulgaria. Tel: +359 52 77 41 83, Fax: +359 52 77 42 56, E-mail: truhi@emona.io-bas.bg

Denis Van Eeckhout, Groupe de Microbiologie des Milieux Aquatiques, Université Libre de Bruxelles, Campus de la Plaine, Blvd. de Triomphe, CP 221, B-1050 Bruxelles, Belgium. Tel: +32 2 650 59 88, Fax: +32 2 650 59 93, E-mail: denisve@ulb.ac.be

Vladimir L. Vladimirov, Marine Hydrophysical Institute, 2 Kapitanskaya Str., Sevastopol, Crimea 335000, Ukraine. Tel: +38 0692 525276, Fax: +38 0692 444253, E-mail: vlvlad@mhi2.sebastopol.ua

Sergey V. Vostokov, Shirshov Institute of Oceanology, Krasikova 23, Moscow 117851, Russia. Tel: +7 095 124 77 49, Fax: +7 095 124 59 83, E-mail: vostokov@ecosys.sio.rssi.ru

Yu. P. Zaitsev, Odessa Branch, Institute of Biology of Southern Seas, 37 pushkinskaya Street, 270011 Odessa, Ukraine. Tel: +38 048 2 25 09 17, Fax: +38 048 2 25 09 18, E-mail: root@inbum.odessa.ua

Observers:

Jean-Marie Martin, Director, Environmental Institute, Joint Research Centre, European Commission, I-21020 Ispra (Va), Italy. Tel: +39-332-789601, Fax: +39-332-789222, E-mail: jm.martin@ei.jrc.it

Maria Ivanova, Student, Environmental Policy, 1079 Blanchard Center, Mount Holyoke College, South Hadley, MA 01075, U.S.A. E-mail: mivanova@mhc.mtholyoke.edu

M. Ganchev, National Oceanographic Committee, tzarigradsko Shosse 125, h.5, Sofia, Bulgaria. Tel/Fax: +359 2 71 80 77

A SYNOPSIS AND RECOMMENDATIONS FOR FUTURE STUDIES

1. SCIENTIFIC BASIS FOR THE WORKSHOP

Recent research activities in the Black Sea, Baltic Sea and the North Sea have produced a large body of new data and hypotheses about the control mechanisms and current state of the environment in these regions. Among these, the Black Sea stands out in that it has been more intensively investigated in recent years following grave concerns about changes in its ecosystem. Perhaps the Black Sea deserves the special attention it received at the Workshop because of its wider ranges of parameters representing its complex geometry and hydrochemical structure, which differs from the shallower (though not necessarily less complex) environments of the other two Seas. With regard to common processes and studies, and in terms of historical data and syntheses, scientists from all three basins appear to have much to learn from each other.

The need to encourage joint interdisciplinary (physics, chemistry, biology, ecology, geology, climatology and meteorology) studies between groups studying semi-enclosed basins was recognised. The current research efforts could be joined and networked by formal and informal means of cooperation. The purpose of such activities is to establish a multi-disciplinary network of scientists allowing them to perform comparative studies of basic processes in different seas.

Initiatives to generate regular scientific meetings to discuss results were widely recommended at the Workshop, in order to enable comparative studies of basic processes in the Seas of interest. These continuing initiatives should be organised through research agreements, common projects, and international workshops involving regional and external partners, with east-west cooperation. Interest was also expressed for establishing common membership to international programs (e.g. ICES, which includes the Baltic and North Sea but not Black Sea) to enhance formal links.

The interest to establish common data requirements was felt by scientific groups working in each area: The suggestions for development of a common data base included improvements in accessibility, the pooling of data on atmosphere-ocean interactions, global or hemispheric climate, a better evaluation of historical data sets, and the generation of basic data to establish boundary conditions or constraints for further specific studies. Unification and standardisation of basic regional climatological data sets in terms of resolution, parameters, and coverage would make comparisons possible between the different regions, and would facilitate better substantiated results in modelling. The need to develop common methods of data processing and data storage (data banking) is also recognised as a basic utility for comparative studies of semi-enclosed seas.

It was agreed that the selection of three European Seas sharing a common fate but with differing environmental settings was a good choice for comparative studies,

Table 1 Priorities for Contaminants in Specific Marine Areas (IOC / INF - 923, Paris, 1 March 1993)

	Olig. Gyre	Red Sea	North FSU	The Gulf	Carib Sea	West Afr.	Medit Sea	North Sea	Balt. Sea	Asian Seas	Black Sea	Summary
Aquatic Toxins	O	L	O	L	H	O	M	M	M	H	M	16
Art. Radionuclides	O	O	H	O	O	O	L	M	L	O	H	10
Herb./Pesticides	L	O	L	O	H	H	M	M	H	H	H	21
Litter	L	M	M	L	M	H	H	L	M	M	H	22
Pathogens	O	M	L	H	H	H	H	H	M	H	H	26
Nutrients	H	L	L	H	H	H	H	H	H	H	H	29
Oxygen	L	O				M	M		H	M	H	
Synth. Organics	L	L	M	L	L	M	M	M	M	L	H	21
Petroleum	L	H	M	H	H	M	M	M	L	H	H	25
PAHs	L	H	M	H	L	M	M	M	M	M	M	22
Susp. Particulates	O	L	L	H	H	M	L	L	M	H	M	19
Trace Metals	L	L	L	L	L	L	L	M	L	L	M	13
Plankton Pigments	O	L	L	O	M	L	M	H	H	H	H	19
Pharmaceuticals	O	O	O	L	O	L	L	M	L	L	L	8
Totals	10	16	18	20	25	25	27	27	29	30	37	

The entries in this table reflect priorities of different contaminants bearing in mind the severity of their effects in a selection of marine regions. The codes for assignment of priorities: O= Insignificant (0), L = Low priority (1), M = Medium priority (2), H = High priority (3); where the numbers in parantheses are the numerical weighting values. The numerical weighting for contaminants and marine areas have been summed and appear respectively at the right hand side and bottom of the table.

Table 2. Comparative features of some semi-enclosed seas

	Mediterranean Sea	North Sea	Baltic Sea	Black Sea
Volume (10^3km^3)	3,750	54	22	540
Anoxic volume (10^3km^3)	-	-	negligible	480
Average depth (m)	1,540	94	60	1,270
Maximum depth (m)	5,120	725	459	2,210
Surface area (10^3km^2)	2,500	575	365	420
Drainage area (10^3km^2)	6,000	500	1,600	2,370
Drain. area / Surf. Area	2.4	0.9	4.4	5.6
Shelf area / Surface area	5%	95%	100%	25%
Temperature (°C)	14-29	3-18	4-13	2-28
Salinity	36-39.5	28-35.4	8-18	17-22.3
Tidal Range (m)	0.5	1-7	0.2	0.2
Avg. residence time (yr)	100	< 1	23	1450
Lateral flow (km^3/yr)	+29,500 (Gibraltar)	+4,800 (Channel)	+740 (North Sea)	+300 (Bosphorus)
	-26,500 (Gibraltar)	-5,900 (N. Atl.)	-1,220 (North Sea)	-600 (Bosphorus)
River runoff., R (km^3/yr)	450	182	450	340
Precipitation, P (km^3/yr)	1,030		200	240
Evaporation, E (km^3/yr)	2,890		210	350
(R+P)/E	0.51		3	1.7
Phosphorus input(10^3t/yr)	390	7	80	150
Nitrogen input (10^3t/yr)	1,100-2,200	120	230-470	430-880
Population (10^6)	350		75	140

because all three are amongst the most threatened semi-enclosed seas of the world (Table 1) and all three are considered, either totally or in parts, Regions of Freshwater Influence Influence (ROFI). Furthermore, the European region is an area of the world where climatic changes and anthropogenic pressures are strongly felt in terms of alterations in marine and terrestrial ecosystems, sea-level change, pollution, etc. The examination of the ranges of some basic controlling parameters and features of each basin yielded a comparative summary of the environmental settings for the three Seas (Table 2), where the Mediterranean Sea has been included for reference purposes. A concise comparison of the European Seas can be seen in Figure 1, where average pigment distribution based on CZCS ocean colour data shows the excessive primary production in the Seas of interest, in relation to poor productivity of some other regions like the Mediterranean Sea.



Figure 1. Pigment pattern based on ocean colour from the CZCS data. The higher concentrations are in lighter in this grey-scale image modified after the Ocean Colour European Archive Network (OCEAN) Project, of the Joint Research Centre, European Commission

2. PHYSICAL AND CHEMICAL CONTROLS

Recent physical and chemical oceanographic investigations have generated novel results, such as the demonstration of a wide range of interacting spatial and temporal scales. New hypotheses were suggested about short-term, seasonal modulation of long-term climatic signatures with synchronism, resulting from atmospheric teleconnections between the different basins. It was shown that interannual and interdecadal variability could arise in relation to the regional hydrological regimen. This indicated strong climatic variability, which is reflected in the forcing functions, or in relation to internal basin modes and non-linear dynamics of circulation and controls at straits, which get amplified because of continental-marine contrasts, and constraints imposed by semi-enclosed or enclosed basin geometry.

There were strong indications of a need to couple physics and chemistry for an improved understanding of the geochemical settings of the individual basins. The need was recognised for a better theoretical understanding of the relative roles of various forcing mechanisms operating on mixing and circulation (e.g. the roles of buoyancy versus wind stress, topographic interactions, instabilities and energy cascade). Simple laboratory models as well as analytical and numerical approaches were recommended. Further measurement programs and process studies are also encouraged, and could be improved with modern tools, high resolution sampling, and mooring deployments with advanced instrumentation.

Development of advanced forecasting capabilities are needed, and can be accomplished with guidance from joint use and comparisons of models and data. For monitoring purposes, as well as for modelling development, the availability of common, well tested, standardised data bases on hydrological and atmospheric fluxes is highly recommended. Further development of basin-scale and regional sub-models are needed to provide realistic and well-resolved simulations and understanding of complex processes such as water mass formation, isopycnal spreading, shelf-interior interactions, and meso-scale energetics.

There is also a need to couple the present studies with paleo oceanographic studies, since climatic and anthropogenic signals are preserved in the sediments. For example, in the Black Sea, water mass history, past excursions of the chemocline, and periods of low and high productivity are recorded in the sedimentary record. The use of these undisturbed and unique sedimentary records in anoxic basins can thus be used to decouple climatic and anthropogenic changes. Support for an intercalibration program for geochemical analyses is also needed to compare results in different basins. Similarly the use of tracers, and their comparisons between different basins can yield improved understanding of the response to various driving factors and identify common sources of change.

3. EUTROPHICATION AND ECOSYSTEM RESPONSE

Coastal eutrophication results from nutrient enrichment driven either naturally (coastal upwelling) or anthropogenically (riverine nutrient inputs). Changes observed

in the coastal areas thus reveal changes occurring in both terrestrial, freshwater and marine systems. Phytoplankton blooms are the most direct visible consequence of coastal eutrophication and are encountered almost equally in the three semi-enclosed seas - North Sea, Baltic Sea and the Black Sea - as revealed by remote sensing (Figure 1).The response of the ecosystem to eutrophication, as determined by the changes induced in the structure and functioning of the pelagic and benthic foodwebs, differs markedly for the three semi-enclosed seas. This indicates different sensitivities of the three basins to ecosystem destabilisation.

A synthetic view of some Workshop presentations suggests that both the North Sea and Baltic Sea coastal ecosystems act as filters for the open sea regions, since they can absorb some of the extra nutrient supply via complex phytoplankton community changes, before the effects are fully transmitted to the open ocean waters.

Conversely the Black Sea has offered little resistance to destabilisation. Perhaps what makes the Black Sea different from the other two Seas is its geography, in which the interacting coastal (shelf) and deep ecosystems are contained in the same enclosure. In this ecosystem eutrophication has caused important modifications in the ecosystem structure and functioning as evidenced by an increase of phytoplankton blooms, loss of biodiversity, increase in frequency and amplitude of dramatic anoxia events near the shelf bottom, diminution of transparency with disappearance of seagrass beds, etc. Moreover in the late eighties both overfishing and the introduction of the opportunistic exotic gelatinous ctenophore, Mnemiopsis leidyi, have contributed to the destabilisation of the ecosystem.

Despite the large difference in eutrophication-related events, the main cause of coastal eutrophication processes of anthropogenic origin can be identified as being driven by quantitative and qualitative changes which have occurred in the nutrient delivery by rivers and the atmosphere. This underlines the importance of studies on eutrophication events occurring in the coastal zone in close relationship with changes observed in the whole drainage basin of the rivers of interest. Furthermore the workshop revealed an important lack of knowledge on the relationships existing between nutrients changes and subsequent changes in the phytoplankton community structure and associated foodweb.

4. RECOMMENDATIONS FOR FUTURE STUDIES

4.1 SCIENTIFIC RECOMMENDATIONS

Investigations concerning the relative significance of different nutrient sources (atmosphere, rivers, upwelling and lateral fluxes) in each of these semi-enclosed seas and their controlling factors are recommended.

Collection and pooling of basic information is needed on the factors governing changes in the structure and functioning of the pelagic and benthic ecosystem, such as nutrient loading and nutrient ratios (Si/N, N/P); reduced vs. oxidised forms (NO_3^- /NH_4^+); inorganic vs. organic nutrient forms; optical properties; oxic vs. anoxic

conditions. Further, process-oriented studies are greatly needed for basic scientific understanding of the machinery responsible for maintaining an ecosystem.

A good understanding of the underlying physical and chemical processes and their climatic variability is needed to interpret the ecosystem response. In this respect, investigations are needed, related to the trapping and dispersion by meso-scale circulation features and unstable current systems, coastal zone -open sea exchanges, upwelling, winter convection, mixed layer development, to yield an understanding of the controlling physical mechanisms. Basic investigations on the cycling of nutrients in various fractions in the ecosystem are necessary to assess the controlling dynamics.

The above-mentioned changes occurring in the governing factors induce several important structural changes in the ecosystem, including a modification of the dominant species of phytoplankton, and the alteration of the structure of pelagic and benthic food-webs. It appears of utmost importance to gain a better knowledge on the underlying mechanisms affecting the stability of a given ecosystem to changes. Basic research is needed to study stabilising vs. destabilising factors with respect to the structure and functioning of ecosystems, and to determine the relevance of specific factors in determining the sensitivity of a given system. These factors may include fundamental physical - chemical processes of the medium (upwelling, convection, meso-scale dispersion and transport processes), as well as the various biochemical interactions affecting the cycling of nutrients.

More precise definitions of some important and frequently used concepts applied to ecosystems appear to be necessary (e.g. sensitivity, carrying capacity, stability and resistance), and would depend on the identification of stabilising and destabilising mechanisms acting on a food-web. Research and comparative analyses of foodweb structures are essential to yield an assessment of the resistance of a given food-web to destabilisation. This approach would require studies of the expected changes in the ecosystem (changes in the relative importance of major pathways within a foodweb) when submitted to perturbations (increased nutrient loads, changes in physical forcing, etc.).

It is also recommended to identify indicator species or some indicator patterns allowing to characterise the state of an ecosystem with respect to its stability or health. The apparition of opportunistic species seems to be a common feature in eutrophied systems. For example, the genera dinoflagellata could serve as overall indicators. Similarly, the opportunistic species Noctiluca appears to be ubiquitous and could be used as an indicator species in the Black Sea. The benthic foodweb structure by its sensitivity to eutrophication could also be used as an indicator.

Research on the gelatinous species (Phaeocystis, Noctiluca, Aurelia, Mnemiopsis, etc.) with regards to their significance in carbon and nutrient cycling is an important and urgent task. For instance, the impact of Mnemiopsis leidyi on the Black Sea ecosystem, and how its fluctuations can be related to external physical factors remains unclear at present. The introduction of a new species to control the Mnemiopsis leidyi plague is not recommended before a sufficient understanding is reached, and because earlier similar experiments in other regions have shown unpredictable risks, ending in further deterioration of the ecosystems.

4.2 PRACTICAL RECOMMENDATIONS

Cooperative research on a basin-scale, and research activities aimed at comparing different basins under specific controls should be intensified. These studies should be designed to detect the underlying reasons for similar patterns of adverse changes (natural climatic fluctuations versus anthropogenic changes). Interdisciplinary cooperation of biological, chemical, physical oceanographers and atmospheric scientists is needed to investigate these effects and their relative roles on the changing ecosystems.

Data banking, including chemical/biological data, is essential for analyses and modelling. In some cases the information exists at basic level but the need for pooling and updating the information is recognised as urgent. For the specific purpose of reaching a synthesis, establishment of monitoring networks and development of a monitoring strategy are essential. The collection of high resolution time series is the only way to address the problem of the scarcity of data needed for calibration and validation of interdisciplinary models. Field measurements and remote sensing have to complement each other for complete assessments of optical properties, primary production estimation and ecodynamics modelling.

The development in modelling depends on a strategy employing a hierarchy of models, and their testing in various combinations to produce understandable results. Integrated modelling approach, coupling river drainage basins with ocean systems should be used for a better representation of man-induced eutrophication. Often the coastal ecosystems are strongly coupled with hydrodynamics, making sophisticated ecohydrodynamical models necessary, although such developments often have to depend on a procedure of hypothesis testing with simpler models to determine optimal components. Collaboration with standardised equipment and methods is recognised as a basic instrument to achieve these goals.

CHANGES OF MEAN SEA LEVEL AND ICE CONDITIONS IN GDYNIA AS INDICATORS OF CLIMATE CHANGES IN THE GULF OF GDAÑSK

M. SZTOBRYN, M. KAŁAS, and A. STASKIEWICZ
Institute of Meteorology and Water Management, Maritime Branch
ul. Waszyngtona 42, PL 81-342 Gdynia, POLAND

Abstract. The Gulf of Gdañsk is located in the eastern part of the Polish coast. For the purpose of this work, long term hydrological observations performed on the hydro-meteorological station Gdynia are used. The changes of mean sea level and the number of days with sea ice are analysed on the basis of observation series for the period 1946-1994. Increase in the mean sea level is found through analyses of coefficients for linear and parabolic trends. The changes in ice conditions, frequency of storm surges, as well the relationship between annual number of days with sea ice and annual number of storm surges in this part of the Polish coast are investigated. We propose that mean sea level and sea ice conditions are good indicators of climate changes in the last half century in the southern Baltic Sea, where influence of human activities is evident.

1. Introduction

The Gulf of Gdañsk, being a part of the Gdañsk Basin, is the southernmost part of the Gotland Basin of the Baltic Sea. Its maximum depth is equal to 118 m and mean depth is *ca.* 50 m.

Because of the wide connection to the open sea, thermohaline structure depends on the open sea and the Baltic Sea proper. Surface salinity during a year does not vary considerably, remaining close to 7 in open parts of the Gulf. The lower salinity values, as a result of river water inflow, occur near the Vistula river mouth, near the Baltiysk Strait (the entrance to Zalew Wislany - the Vistula Lagoon) and in the shallow, western part of the Gulf - Mala Zatoka Pucka (the Little Puck Bay). Water salinity in lower layers, especially at the bottom, is influenced by irregular inflows of saline water from the North Sea. The mean salinity value in deep layer reaches *ca.* 12. The halocline depth is about 60 m.

Thermal conditions make the Gulf of Gdañsk among the warmest basins in the Baltic Sea. The surface water temperature during the summer period exceeds 18°C, with an extreme value of 26°C recorded in August, 1994. During fall and winter seasons water is well mixed by wind action, while during spring and summer a vertical temperature stratification develops with a thermocline located at depths of 20 - 50 m.

E. Özsoy and A. Mikaelyan (eds.), Sensitivity to Change: Black Sea, Baltic Sea and North Sea, 1–9.
© 1997 *Kluwer Academic Publishers.*

Ice cover seldom occurs in the open waters of the Gulf, whereas, in coastal areas, ice phenomena are observed practically every winter.

Coastal areas of the Gulf of Gdañsk belong to densely populated provinces of Gdañsk and Elblag (Poland) and the Kaliningrad province of the Russian Federation. Waters of the Gulf are exposed to severe human impact mainly in three areas:

-the area extending from the mouth of the Vistula river, one of the largest and most polluted rivers entering the Baltic Sea, to the harbour complex of Gdañsk and Gdynia;

-the semi-enclosed and shallow Vistula Lagoon, collecting wastes of its main river Pregel and the largest cities of Kaliningrad and Elblag. Being connected to the open sea by the narrow Strait of Baltiysk, the Vistula Lagoon should be considered as a separate basin;

-the semi-enclosed and shallow Little Puck Bay in the western part of the Gulf of Gdañsk, cut off from the open sea by an underwater ridge.

This study has been undertaken in order to establish the roles of climatic and anthropogenic changes in hydrological conditions in the area from the Vistula river mouth to Gdañsk and Gdynia harbour complex. This area in the Gulf of Gdañsk is most affected by man: by pollution, by great cities and harbour and industrial activity. Sea level observations from Gdynia and the sea ice observations near the port of Gdynia were analysed, for the period 1946 -1994.

The following indicators of climate and anthropogenic changes were investigated:

- seasonal number of storm surges (NSS),
- the number of the days with sea ice during winter (NDI)
- mean seasonal sea level (MSL) calculated as an average of monthly mean values.

These indicators influence productivity, nutrient cycling, transport and mixing mechanisms. They depend on the meteorological factors: atmospheric circulation, direction and speed of wind and air temperature and pressure. Climatic and anthropogenic changes of the atmospheric circulation, air temperature and mean sea level have received much earlier attention and their time variability and periodicity are rather well known.

The comparison of trends and periodicity of these data with trends and periodicity of the investigated indicators should give the information about marine response to climatic changes.

2. Description of the Indicators

2.1. SEASONAL NUMBER OF STORM SURGES (NSS)

Our definition of a storm surge will only cover the hydrological situations when the sea level exceeds the multi-annual mean sea level (NN = 500 cm) by at least 70 cm. The duration of a typical storm surge ranges from a few hours to several tens of hours. Storm surges along the Polish Baltic coast occur mainly between November and March. From April to August storm surges occur only sporadically or they do not

occur at all. Therefore, for purposes of further study, a number of storm surges have been assumed to occur during a season, i.e. a period starting from August and lasting till July of the next year.

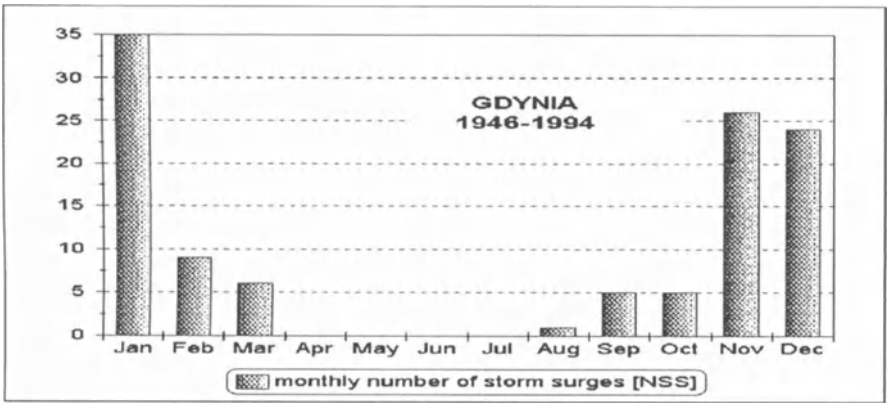


Figure 1. Number of storm surges in particular months

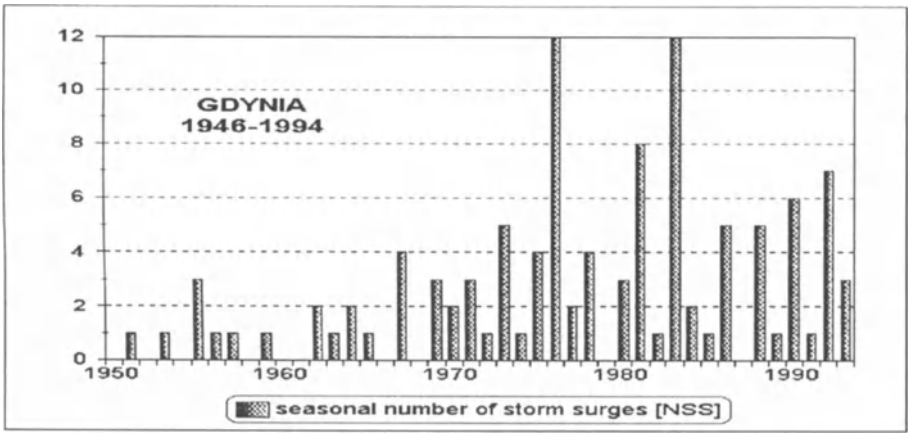


Figure 2. Number of storm surges in particular seasons

The maximum number of storm surges in one season reaches about 12. The number of seasons when no storm surges occurred ranged from 1 to 4 in one decade. The storm surge frequency distribution with respect to months is presented in Fig. 1. The highest number of storm surges recorded during the studied period at the Gdynia sea-level gauge takes place in November, December and January, whereas no storm surges were recorded from April to July during 1946-1994.

The seasonal frequency of storm surge occurrences are examined in Fig. 2. During the late seventies and the early eighties, a rapid growth is noted in the number of storm surges, most likely caused by changes in the Northern Atlantic atmospheric circulation.

After a sharp decrease in frequency in the following period, a systematic growth in seasonal storm surge number occurs in the later part of the eighties. This intensification is statistically significant with respect to 95% confidence level. These results are consistent with those reported earlier by Mietus [8] (intensification of the extreme values of geostrophic wind) and Dziadziuszko and Malicki [3] (more frequent occurrence of high sea level in the water gauge of Wladyslawowo).

2.2. NUMBER OF DAYS WITH SEA ICE DURING A WINTER (NDI)

Number of days with sea ice in the given water area was assumed equal to the number of days when observed sea ice covers more than 10% of the surface, or covers the area with radius of at least 200 m.

The water area of Gdynia, taking into consideration its hydrography and also human activity (necessity of maintenance of navigation on Gdañsk - Gdynia fairway, keeping it open with the assistance of ice - breakers) is a water area characterised by sea ice occurrence with probability of 0.7.

Sea ice appears at the Polish coastal waters in November at the earliest and decays at the very latest in April. The maximum number of days with sea ice at respective decades ranged from 40 to 83 days; since the 1991/92 season, sea ice did not occur at all (not even a sýngle day) in the investigated area. Fig. 3. shows variations of the numbers of days with sea ice for the respective seasons.

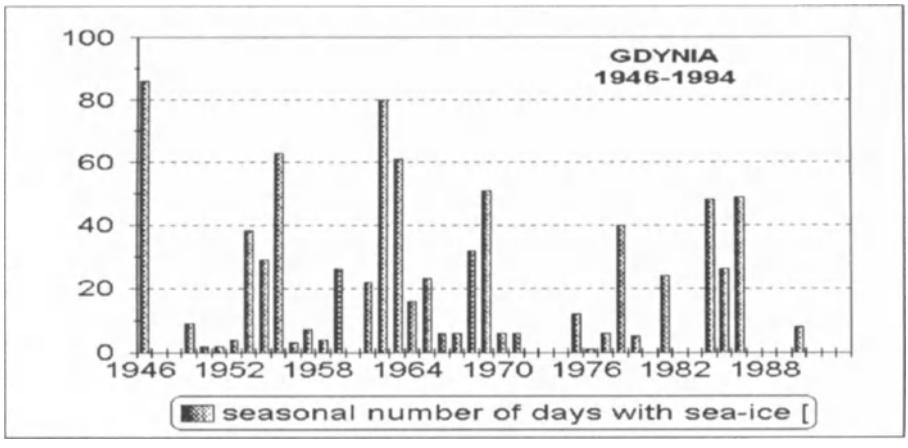


Figure 3. Number of days with sea ice in particular seasons

For the 1946-1994 period - 6 characteristic peaks are noticed: during the 1946 season, in the middle of the fifties, at the beginning of the sixties, with slightly lower numbers at the end of the sixties and seventies, and in the middle at the eighties. After last severe winter 1986/87 a rapid lowering of sea ice phenomenon occurrence frequency is showing off in the water areas close to Gdynia.

2.3. MEAN SEASONAL SEA LEVEL (MSL)

The seasonal variation of sea level observed along the Baltic Sea coasts is strongly connected with annual changes of meteorological factors, such as: the changes in the



Figure 4. Daily mean sea level in the Gulf of Gdañsk

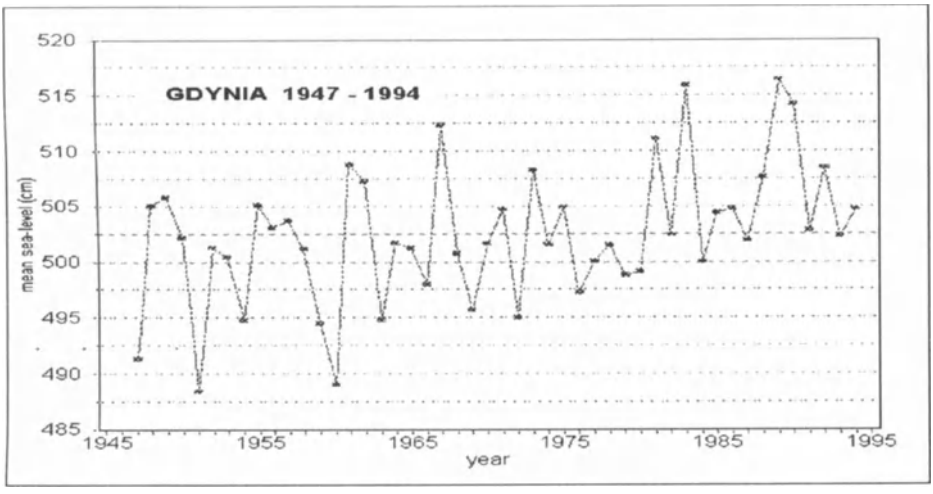


Figure 5. Interannual changes of mean sea level in the Gulf of Gdañsk.

intensity of the zonal circulation and the mean pressure pattern, as well as the variability of local circulation and wind conditions.

Annually averaged daily mean sea level registered at Gdynia tide gauge in the Gulf of Gdañsk is presented in Fig. 4 for the period of 1947-94. The lowest values of the daily mean sea level occur at the beginning of spring (min. value is 489 cm), and the highest occur in early winter (max. value is 520 cm). The annual variability of daily mean sea level, measured by its standard deviation, is largest in the late autumn and

winter (up to 31 cm in January), and lowest in late spring (up to 8 cm in May).

The mean sea level value, computed for the mentioned period for the tide gauge in Gdynia is 504 cm. The difference between the absolute maximum (626 cm) and the absolute minimum (413 cm) of observed levels is 213 cm.

The time series of annual mean sea level in the Gulf of Gdañsk (Fig. 5) shows significant interannual variability, with differences between successive years reaching a magnitude of 20 cm. We can also see a tendency of mean sea level rise (Kalas [4]).

Mean sea level values have been computed for two types of seasons:

- MSLs - mean sea level at Gdynia from August to July (in regard to occurrence of storm surges),
- MSLi - mean sea level at Gdynia in November-April (for cold half of the year).

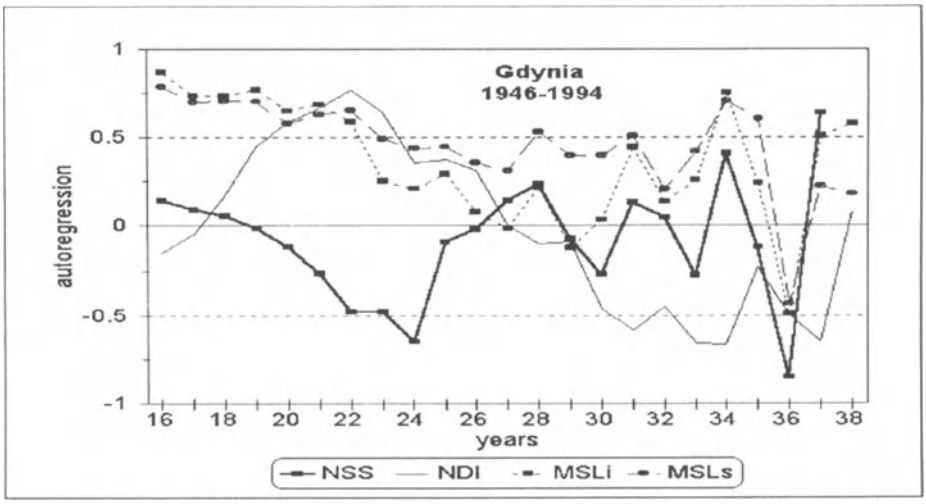


Figure 6. Autoregression function of 8-years moving average of NSS, NDI, MSLi and MSLSs.

3. Periodicity

To analyse periodicity, thereby repeatability, of the hydrological conditions of the Gulf of Gdañsk, NSS, NDI, and MSL have been used.

Statistical analyses of the data series were made, using the MA (moving average), AR (autoregression), ARMA (autoregression of moving average) and ME (maximum entropy) methods. For smoothing (MA, ARMA), 3, 8 and 12 years filters were used. Results of the calculation using ARMA with a 8-years filter are shown in Fig. 6

Our investigations indicate an existence of 3 main periods: 3-4 years, 7-8 (exactly 7.7) years and 11-13 years. These results are in a very good agreement with the previous study of periodicity of sea ice conditions along the Polish coast (Sztobryn [9, 10]) and with results of other climatological research (for example, Cyberski [1]).

Periodicity investigations of the zonal index of the surface atmospheric pressure, by Kozuchowski [6], demonstrated similar periods, e.g. 13.2 years, in time series of the

monthly mean value for 1899 - 1990. His investigations of the seasonal index demonstrated 7-8 years periodicity for December, February, and March, i.e. for months with common sea ice occurrence and the largest number of storm surges.

4. Trends

To determine trends, the time series of investigated indicators were normalised with respect to multiannual mean values and presented in dimensionless form. Multiannual variability of normalised and dimensionless values of indicators (dNSS, dNDI, dMSLs and dMSLi) smoothed by 8-years filter is shown in Fig. 7.

Multiannual variation of sea ice conditions represented by dNDI reflects a significant and very rapid decrease at the beginning of the seventies (Dziadziuszko and Jednoral [2]). On the contrary, multiannual variation of the number of storm surges shows very significant and rapid increase during the same time. The course of mean sea level value represented by dMSLi and dMSLs also reflect accelerated increases, starting with the beginning of seventies.

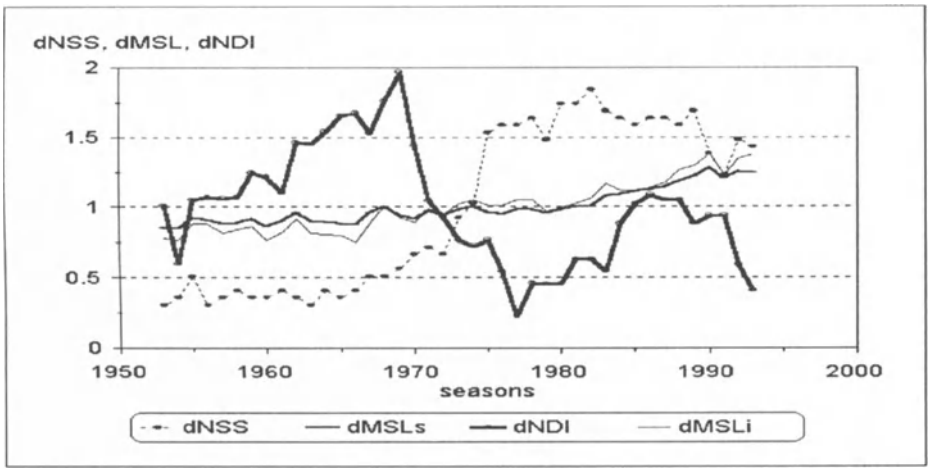


Figure 7. Multiannual variation of indicators smoothed by 8-years filter.

All of these indicators reflect abrupt changes during the 1970s, at a time of major changes, with the intensification of the zonal atmospheric circulation in the Baltic Sea, North Atlantic, as well as Pacific Ocean and North America (Karl [5], Kozuchowski [6], Lorenc and Suwalska-Bogucka [7], Mietus [8], among others). These results are very important in determining the marine response to the climatic change. The repeatability and intensity of the eastern and western circulations are related to each other. Detailed investigations [7] indicate a decrease in intensity of the north-eastern and eastern anticyclonic circulations (the so called Siberian high pressure), especially during the last few years. This change has caused, on the one hand, an increase of the

number of mild winters (without ice or with a small number of days with ice along the Polish Baltic coast), and, on the other hand, an increase in the repeatability and intensity of pressure systems generating rapid sea level changes, as shown in Fig. 7.

Linear and parabolic trends were calculated by the least squares method, with the trend equation of standard regression functions. From the calculation of the annual mean sea level, it follows that:

$$MSL = a + b * year \qquad \text{linear}$$
$$MSL = c + d * year + e * year^2 \qquad \text{parabolic}$$

$$\text{linear} \qquad a = 504.2 \text{ cm} \quad b = 0.2 \text{ cm/y},$$
$$\text{parabolic} \qquad c = 495.7 \text{ cm} \quad d = -0.09 \text{ cm/y} \quad e = 0.03 \text{ cm/y}^2.$$

The values of coefficient demonstrate the increase in mean sea level. The linear trend of other indicators were also analysed, yielding coefficients with values of of 0.22 cm/y for MSLs, and 0.34 cm/y for MSLi.



Figure 8. Comparison of multiannual variation of NDI observed on various areas of the Gulf of Gdañsk smoothed by 8-years filter.

The differences between NDI in Gdynia, Little Puck Bay and Vistula Lagoon were analysed to detect influences of human activity. The Gdynia area is much more affected by this activity than the Little Puck Bay or the Vistula Lagoon regions. The two latter basins are closed to navigation in winter. Multiannual variability in normalised and dimensionless values of dNDI, smoothed by 8-years filter is compared in Fig. 8.

The rapid decrease of NDI observed in Gdynia is also shown in the Little Puck Bay and the Vistula Lagoon but the intensity of this decrease is much smaller in either of the last two basins. The investigated difference can be regarded as probable effect of human impact, connected to navigation during the winter season.

5. Conclusions

Our results indicate that rapid changes of hydrological conditions represented by the indicators NSS, MSL and NDI are in very good agreement with the observed climate changes, as well as with their periods and trends. These results indicate that climate changes strongly affect the hydrological system of the sea. It appears that more rapid decrease of NDI in the seventies for Gdynia compared to the Puck Bay and the Vistula Lagoon is a result of human activities.

6. Acknowledgements

This paper was made possible by research within the EC project ERB CE PDCP 925076 and IMGW project H-7/95. Prof. S. Zerbini and prof. T. Jednoral are acknowledged for coordination of the projects and for their interest in our studies.

7. References

1. Cyberski, J. and Szefler, K. (1993) Climate variations and ice conditions in the Baltic Sea. Workshop of International Geosphere Biosphere Programme, Poland (oral presentation).
2. Dziadziuszko Z. and Jednoral, T. (1993) Sea ice warnings for the Puck Bay, Gdañsk, Poland, Report of the Project No. 6-0001 91 OC, Maritime Institute, Gdañsk, Poland (in Polish).
3. Dziadziuszko Z. and Malicki, J. (1993) Increase of storm surge threat along the Polish Baltic coast. *Gazeta Obserwatora IMGW* **4-5**, 6-12 (in Polish).
4. Kalas, M. (1993) Characteristics of sea level changes on the Polish coast of the Baltic Sea in the last forty five years. Proc. of International Workshop, SEACHANGE '93 - Sea Level Changes and their Consequences for Hydrology and Water Management", Nordwijkerhout, Netherlands, **1**, 51-60.
5. Karl, T.R. (1995) Detecting and communicating information on climate changes: The role of indices. Proc. International Conference on Past, Present and Future Climate, Finland, 197-202.
6. Kozuchowski, K.M. (1993) Variations of hemispheric zonal index since 1899 and its relationships with air temperature. *International J. of Climatology* **13**, 853-864.
7. Lorenc, H. and Suwalska-Bogucka, M. (1995) Thermal tendencies of winters in Poland as an indicator of climate variability. *Wiadomoœci IMGW* **17**, 3-28 (in Polish).
8. Mietus, M. (1994) Vector of geostrophic wind in the Baltic Sea region as an index of local circulation and its relationship to hydro-meteorological characteristics along the Polish coast. Proc. European Workshop on Climate Variation, Finland, 278-292.
9. Sztobryn, M. (1992) Periodicity in ice season persistence at the southern coast of the Baltic Sea. (St. Petersburg, Russia) Proc. XVIII Conference of the Baltic Oceanographers.
10. Sztobryn, M. (1994) Long term changes in ice conditions at the Polish coast of the Baltic Sea. Proc. 12th International Symposium on Ice of the International Association for Hydraulic Research (IAHR), Trondheim **1**, 345-354.

VARIABILITY OF NORTHWESTERN BLACK SEA HYDROGRAPHY AND RIVER DISCHARGES AS PART OF GLOBAL OCEAN-ATMOSPHERE FLUCTUATIONS

A. POLONSKY, E. VOSKRESENSKAYA, V. BELOKOPYTOV
Marine Hydrophysical Institute of Ukrainian Academy of Sciences, Sevastopol, 2 Kapitanskaya St., the Crimea

Abstract. Regional hydrological data sets of the Marine Hydrophysical Institute for 1950 - 1992 were used for the analysis of interannual and inter-decadal variability of temperature, salinity and density of seawater in the Northwest Black Sea. It was shown that high amplitude fluctuations of all fields occurred during the analysed period. These fluctuations are mainly due to the low-frequency changes of the river run-off in the Northwest Black Sea. The variability of the river discharges is the same as the typical amplitude of the seasonal cycle. They are mainly due to natural changes in the coupled ocean-atmosphere system over the globe.

1. Introduction

Variability of the coupled ocean-atmosphere system manifests itself in regional low-frequency variations of hydrometeorological and hydrophysical fields (e.g., Polonsky & Sizov, 1991). In particular, year-to-year and trend-like variations of the Black Sea river discharges are due to low-frequency processes on the globe. Low-frequency change of river discharges leads to interannual and inter-decadal variability of the hydrographic fields in the coastal zone, especially in the North West Black Sea (Simonov and Al'tman, 1991; Polonsky et al., 1995).

The questions to be asked are: How strong are the natural year-to-year and decade-to-decade (trend-like) fluctuations of the Black Sea river discharges and associated sea variability in comparison with the magnitude of a typical seasonal cycle and with the human-induced changes ? What are their main causes.? These questions are addressed, by studying the variability of the Black Sea hydrographic fields and river discharges, with respect to the global and North Atlantic variability of the coupled ocean-atmosphere system.

E. Özsoy and A. Mikaelyan (eds.), Sensitivity to Change: Black Sea, Baltic Sea and North Sea, 11–24.
© 1997 *Kluwer Academic Publishers.*

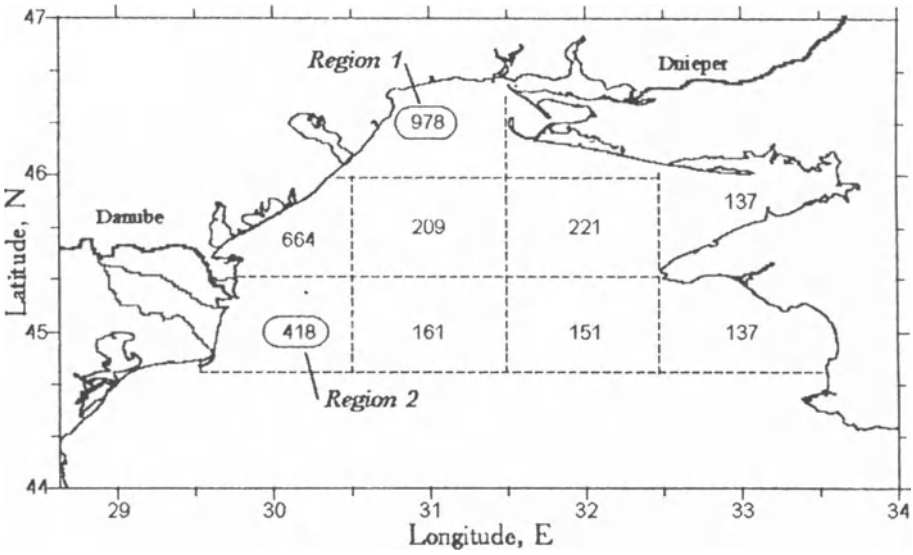


Figure 1. Total number of SST/SSS observations for the month of May in the northwestern Black Sea within 40x40 mile squares in 1924-1994. The wo regions in which the year-to year variability is analysed are marked.

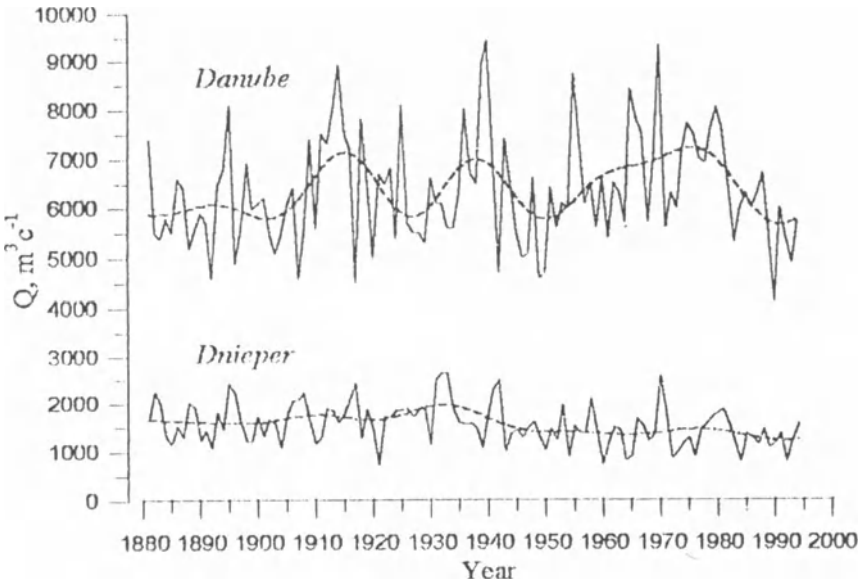


Figure 2. Year to year variability of the average annual discharges of Danube and Dnieper in the 1881-1994 period. Dashed lines are low-pass filtered (20 year cutoff period) discharges.

2. Data and Processing Procedure

We analysed historical data of temperature and salinity at 0 and 20 m depths for the 1924 - 1994 period (Fig. 1), monthly river discharges for 1921 - 1992, the annual discharges of Danube and Dnieper for 1855 - 1994 (Fig. 2), using published data (Ozsoy et al.., 1992; Koval'chuk, 1986), as well as monthly sea surface temperature (SST) in a regular 5°x5° grid in the North Atlantic for 1957 - 1990, and the monthly sea level pressure (SLP) and Rossby index (RI) for 1894 - 1988 (Polonsky and Sizov, 1991).

The river discharges of Danube, Dnieper, Dniester and Uzhny Bug, analysed here contribute about 80% of total Black Sea river discharge. Monthly river discharges were quite accurately determined; especially after the second world war, to allow reliable estimates of their interannual and inter-decadal fluctuations. Typical errors are less than 5 % of the average monthly values, mostly resulting from the inaccuracy of an empirical function Q=f(H), used in the every day practice of the hydrometeorological services (Q is the river discharge, H is the river level). Their anomalies will be correlated with the SST, SLP and RI anomalies (SSTA, SLPA and RIA, respectively).

The RI was calculated as a difference of the SLP in the Asores High and Iceland Low areas. The monthly SLP in the Asores High and Iceland Low was determined as an average of (10 by 10 degree) squares centered on 35°N, 25°W and 65°N, 20°W, respectively using volunteer ship observations. These observations were used also for the calculation of monthly SST. Besides, the monthly position of Asores High an Iceland Low and SLP magnitudes within them after 1891 were received from Monthly Data Sets, 1988... and Monthly Synoptic Bulletins, 1986/1991.

Hydrographic parameters (temperature and salinity) were monthly averaged over regular mesh 40 by 40 miles. If the number of observations was more than four within each box for a given month, the intramonth variance was calculated . This variance is due to day-to-day and relatively small scale variability (typical space scales are less than 40 miles). The variance of monthly averaged magnitudes is due mostly to year-to-year and decade-to-decade changes.

Observation accuracy, the level of relatively high-frequency noise, and aliasing problems for hydrometeorological fields were discussed by Polonsky and Sizov (1991). They concluded that typical random error of calculation of monthly average sea level temperature anomalies (SLTA), SSTA and SLPA in 5°x5° squares in the North Atlantic Ocean varied in the ranges of 0.2-1°C and 1-5 mb, respectively. Therefore, the high-amplitude large-scale SLTA, SSTA and SLPA may be determined with typical relative errors of 15-50%.

First the average annual cycle of each of the analysed parameters and monthly anomalies were calculated. Then the trends and Fourier spectra of all monthly series were estimated. Finally, the correlation of SST anomalies, RI, and river discharge anomalies for various lags were calculated.

3. Results and Discussion

3.1. VARIABILITY OF TEMPERATURE, SALINITY AND DENSITY IN THE N.W. BLACK SEA

Spatial distributions of surface hydrographic fields show strong r.m.s. variability, especially in the coastal zone. The r.m.s. is at a maximum during spring when the discharges of Dnieper and Danube and their rates of change increase. For instance, the total May SSTA r.m.s is about 3.0°C, in comparison to the annual cycle SST r.m.s. of about 7.0°C, and a typical intramonthly r.m.s. (shown in Figures 3 and 5) of about 1.5°C. Similarly the total May SSSA r.m.s. is 4.4 and the annual cycle SSS r.m.s. is 2.2. In essence, the r.m.s. due to the average annual cycle and r.m.s. due to variability at the other space-time scales are the same order. About 50% of total r.m.s. after removing the seasonal signal are due to low-frequency interannual and inter-decadal variability. The remaining part of the r.m.s. is due to relatively smaller scale variability with the typical time/space scales less than 1 month/40 miles (Table 1). Low-frequency variability of the surface density in the N.W. Black Sea is mostly due to SSS change. For instance, the correlation of monthly SSS and surface density anomalies in May 1955/1994 reaches 0.98 in the regions 1 and 2.

The variance of sub-surface salinity decreases rapidly in contrast to the variance of sub-surface temperature, especially within the sharp seasonal thermocline (Table 1). However, the low-frequency change of vertical stability (stratification) of the upper layer of the N.W. Black Sea is mostly due to changes in SSS (Figs. 4,5).

Integrated periodogrammes of the time series basically show two typical scales of low-frequency variability in the hydrographic fields of the N.W. Black Sea. The first is at 10-30 years, while the second one has is at periods of a few years. Each of these are responsible for 30-45% of total variance of monthly salinity and density fields during 1955-1994 (see Table 4). Co-spectra of the river discharges and SSS in the vicinity of the inflow regions show two or three significant peaks (not shown here), with typical periods of these coherent variations being as follows: 2 to 3 years, around 4 years and around 15 years. Significant trends of temperature, salinity, density and stratification are absent in the N.W. Black Sea in the periods studied.

We observe that the N.W. Black Sea hydrography is characterised by strong natural year-to-year and decade-to-decade variability associated with changes in river discharges. We will show below the relationship of these changes to variability of the global coupled ocean-atmosphere system.

TABLE 1. May r.m.s. of temperature, salinity and density due to intramonthly (1) and year-to-year (2) variability in regions 1 and 2 (see Fig.1).

Depth	r.m.s in region 1.						r.m.s. in region 2					
(m)	T_1	T_2	S_1	S_2	σ_{t1}	σ_{t2}	T_1	T_2	S_1	S_2	σ_{t1}	σ_{t2}
0	1.6	2.15	2.74	2.73	2.25	2.17	1.26	1.14	2.88	2.00	2.25	1.42
20	1.3	1.55	0.46	0.36	0.39	0.32	1.63	1.50	0.52	0.31	0.48	0.32

3.2. AVERAGE SEASONAL CYCLE OF THE RIVER DISCHARGES

The seasonal cycle of river discharge depends on precipitation in catchment areas. About 60 % of total annual discharge of Danube occur in March to July. The form of seasonal variability is close to the annual harmonic with maximum in May and a minimum in October. However, the relative amplitude of the annual harmonic of Danube discharge is not so large as Dnieper. There are two principal origins of Danube water, as opposed to the other rivers analysed. Alpine snow-melt is responsible for the May discharge maximum of Danube. Relatively strong summer rainfall in Central Europe (Climate of Europe, 1995) is responsible for strong flood discharges of Danube during that time. The origin of Dnieper is at the Mid-Russian Plateau, whereas the Dniester and Uzhny Bug origins are in the vicinity of the Carpathians. Summer precipitation in Eastern Europe is smaller compared to Central Europe, and therefore the sharp maxima of Dnieper and Dniester/Uzhny Bug discharges respectively occur in the early spring (Simonov and Al'tman, 1991).

Average annual portion of Danube discharge in total Black Sea river discharge exceeds 60%. However, this portion changes from less than 60% in February till May to about 70% in July till September. Dnieper and Dniester are characterized by strong artificial regulation after 1955 when the reservoir hydrosystems and hydroelectrical power stations were built. As a result, the amplitude of seasonal variations of discharges of Dnieper and Dniester reduced significantly after 1955 (Simonov and Al'tman, 1991). However it is not a case for the average annual discharges of both rivers (especially of Dniester, see below). Typical portion of the variance associated with the annual harmonic in total 5 years' running variance of Danube discharge in 1945 to 1984 was about 40%. However it changed from about 25% (around 1972) to about 55% (around 1977). Significance of the annual harmonic/seasonal fluctuations (without annual harmonic) decreases/increases in the variability of discharges of Dnieper, Dniester, and especially Uzhny Bug. For instance, the portions of annual harmonic and seasonal fluctuations (without annual harmonic) in total variance of the Uzhny Bug discharge were about 20% and 70%, respectively with quite strong interannual change. So, the interannual variability of river discharges manifests in year-to-year fluctuations of the average annual values and change of seasonal cycle magnitude (Polonsky et al., 1995).

3.3. YEAR-TO-YEAR AND DECADE-TO-DECADE VARIABILITY OF THE RIVER DISCHARGES

Figures 2 and 6 demonstrate the high-amplitude interannual and inter-decadal fluctuations of all analysed river discharges. Artificial variability due to human activity in the Dnieper and Dniester basins does not manifest itself in the average annual discharges. Moreover, in spite of the building of Dubossar hydroelectrical power station in 1955, the discharge of Dniester was increasing after 1955 at least during two decades. Averaged (over all period of quite precise observation after the First World War) linear trends are a positive practically for all rivers and months except the spring

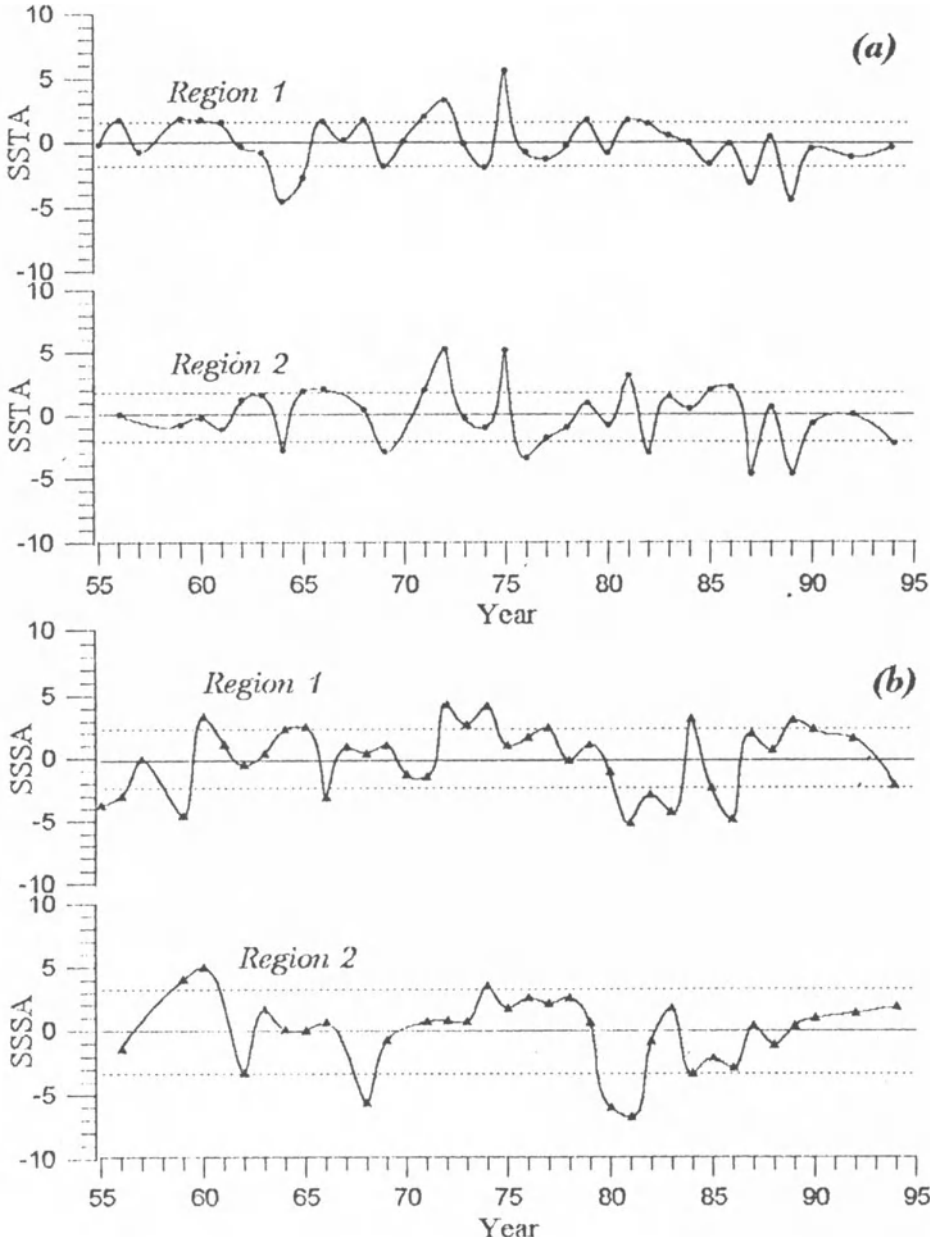


Figure 3. Monthly sea surface anomalies for the month of May in 1955-1994 in two regions of the north-western Black Sea: (a) temperature (°C), and (b) salinity. Dashed lines denote typical intra-month r.m.s.

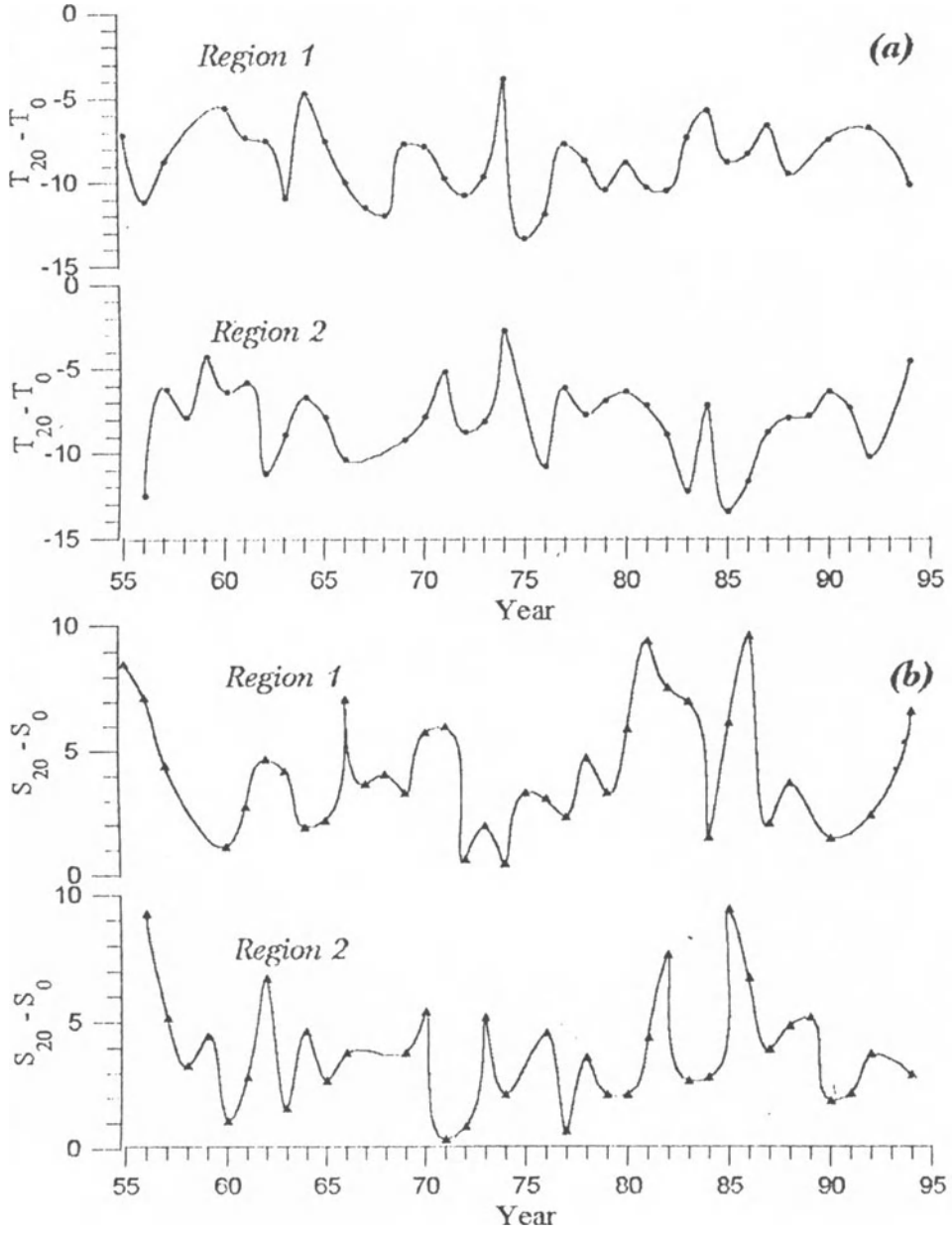


Figure 4. Time series of differences between monthly (a) temperature (°C) and (b) salinity at depths of 0 and 20m for the month of May in 1955-1994 in regions 1 and 2 of the N.W. Black Sea.

/ summer and the except for the annual discharges of Dnieper (Fig.6). The negative trend of the average annual discharge of Dnieper reduced and became insignificant after 1955, in spite of strong artificial regulation of the seasonal cycle. Certainly, the linear trend is not the best approximation of low-frequency variability of the average annual discharges for the most rivers. For example, the linear trend of Danube discharge is insignificant for the period from 1947 to 1992, whereas the second order trend is significant up to 95% confidence level for most of the months (Table 2). Fig.2 makes clear that this trend is in fact due to the high-amplitude quasi-periodical variability of the Danube discharge. The above results confirm that the variability of the river discharges is mainly due to the natural processes.

Time series and periodogrammes of average annual river discharges show that there are three typical scales of natural variability, namely quasi-biennial, 3.5-6.5 year and inter-decadal periods. Typically, the first and second of these scales are respectively responsible for 5-10% and 10-20% of the total variance of annual discharges in the range of periods from 2 to 33 years, whereas the third one is responsible for about 20-30% of the variance (Polonsky et.al., 1995; and Table 4). The relative part in total variance, of the interannual fluctuations of river discharges in periods ranging from 2 months to 5 years, is the same as the part of the annual harmonic. However, these relative contributions are changed significantly during the period of observation. Uzhny Bug has the minimum level of interannual fluctuations in discharge. The discharges of Dnieper and, especially of Danube, vary strongly from year-to-year (Polonsky et al., 1995). Apparently this is a consequence of the larger catchment areas (S) of the last two rivers (S= 63,700; 72,100; 504,000; and 817,000 square km for Uzhny Bug; Dniester; Dnieper; and Danube, respectively).

TABLE 2. Magnitudes of the second order trends in 1947-92. Significant (95 % confidence level) magnitude (cubic km per square year) of monthly Danube discharge are underlined

Month	J	M	M	J	S	N
Coefficient of trends * 10	-0.1	-0.1	-0.15	-0.1	-0.9	-0.05

The following question arises: what is a reason of interannual and inter-decadal fluctuations of the river discharges? Results of Bunker (1980), Hastenrath (1991), Polonsky & Sizov (1991), Sizov, et al.. (1991), Deser and Blackmon (1993), Gray (1993), Dzhiganshin & Polonsky (1994), Kushnir (1994), Voskresenskaya & Polonsky (1993; 1994) and Stocker (1994) show that this may be due to ocean-atmosphere interaction over the globe and especially over the Atlantic Ocean.

3.4. LOW-FREQUENCY VARIABILITY OF SEA-AIR INTERACTION IN THE NORTH ATLANTIC OCEAN

There are two distinct temporal scales of inter-decadal and interannual variability of hydrometeorological fields in the North Atlantic. Both are due to natural fluctuations of the atmosphere-ocean system. Their typical time scales are from one to several decades and from 2 to 7 years, respectively. Similar scales occur in the time series of

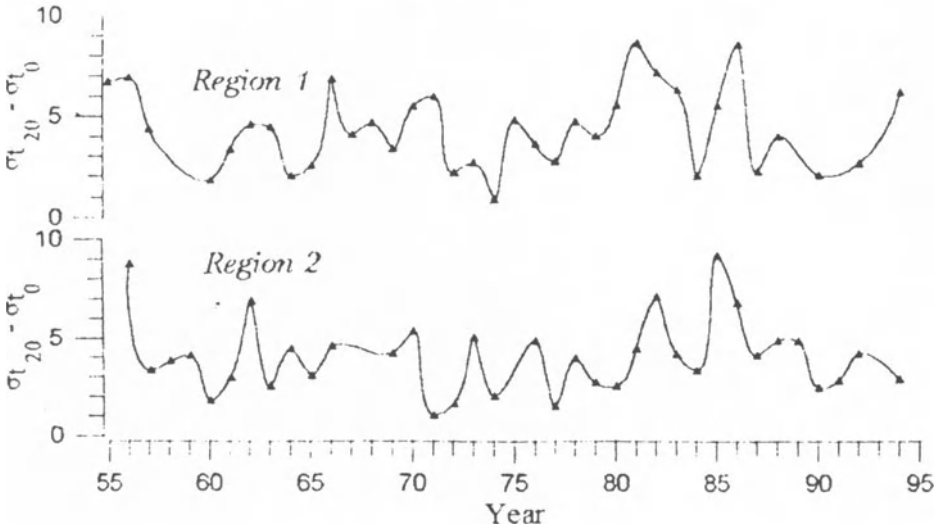


Figure 5. Time series of differences between density at 0 and 20m depths for the month of May in 1955-1994 in Regions 1 and 2 of the north-western Black Sea

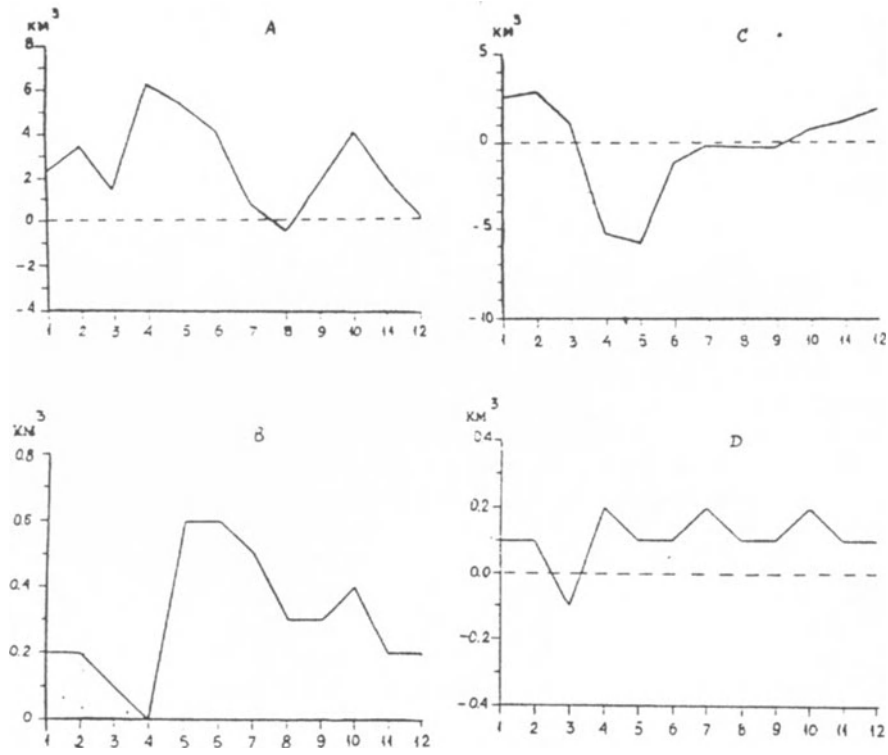


Figure 6. Increase (average linear trend) in the average monthly discharges (in cubic km) in the observation period of 1921-1992. (a) Danube, (b) Dniester, © Dnieper, (d) Uzhny Bug

the hydrographic fields and river run-off in the N.W. Black Sea, as shown above. The first type of variability appears as a trend, if the analysed data sets cover a few decades. Only such data are available for the reliable detection of low-frequency variability of the coupled system. As a result, high-amplitude natural fluctuations of the coupled system in the North Atlantic Ocean could completely mask (damp or intensify) the greenhouse warming of the lower troposphere. Variability of the "conveyor belt" is the possible cause of the natural decadal and inter-decadal changes of the coupled system (Stocker, 1994). The North Atlantic plays a crucial role in their generation. Polonsky and Voskresenskaya (1996) showed that the coherent variability of the northward heat transport resulting from changes in Ekman currents in the tropical North Atlantic, and the high-latitude SST changes in the North Atlantic are the principal manifestations of the decadal mode. Multi-decadal variability is governed by thermohaline circulation in the North Atlantic (Gray, 1993; Stocker,1994). The active role of the North Atlantic Ocean in multi-decadal variability of the global coupled ocean-atmosphere system is confirmed by significant linear trend of RI in 1957-1988, and by an absence of significant trends in the Pacific Southern Oscillation Index in that period. The second-order RI trend was insignificant in the same period. However, it becomes significant if the analysed period increases by about 10 years (Voskresenskaya and Polonsky, 1993).

The SLP (and SST) changes over the North Atlantic Ocean associated with the low-frequency variability of the coupled system are most interesting from the point of view of the present study. Tables 3 and 4 make clear that on decadal scales, the intensification of the Asores High (SLP rise) is accompanied by shifts to North or North-East, while on multi-decadal scale it is linked with shifts to the South-East. The typical magnitude of decadal Asores High displacements are of the several hundreds of km. A similar result for multi-decadal changes was published by Kushnir (1994), who also showed that the sea surface cools in the North Atlantic during multi-decadal intensification of the atmospheric circulation over the same area.

The second type of low-frequency changes appears as a quasi-periodical (random?) signal due to year-to-year fluctuations of the coupled system on the globe. El Nino-Southern Oscillation (ENSO) and North Atlantic Oscillation (NAO) are the main manifestations of this signal in the North Atlantic (Polonsky and Sizov, 1991).

The global ENSO-events are often manifest in the North Atlantic fields. Strong change in amplitude and phase of the annual and semi-annual harmonics occurring in various hydrometeorological parameters, and anomalies in annual average values during ENSO events were found and documented by Hastenrath (1991), and Polonsky & Sizov (1991). Anomalous conditions simultaneously develop in the North/Tropical Atlantic and in the equatorial Pacific. However, the Atlantic anomalies seem to reach their mature phase faster than the Pacific ones, owing to the difference in size and geographical particularities of the two Oceans.

Before typical ENSO-events (in winter), the atmospheric centers of action shift to the North-East and the circulation intensifies in the North Atlantic. Concurrently, negative and positive SSTA are generated over the eastern tropical and subtropical /mid-latitude North Atlantic areas, respectively. After the ENSO-event beginning, the atmospheric circulation becomes weaker in the North Atlantic/Pacific Ocean

simultaneously with a displacement of the Asores High to the South-West (Table 3). Change in seasonal cycle amplitude of the coupled system parameters is the principal manifestation of the ENSO-events in the North Atlantic Ocean. Before the ENSO-event (during anomalous warming of the mid latitudes), the cyclone trajectories shift to the North-East by about 800 km (Monthly synoptic bulletin, 1986/1991; see also Table 4). This is especially important from the point of view of the present study.

Individual features of the ENSO events could partly explain some contradictions concerning lag-lead relationship between Atlantic and Pacific variability. About 20 to 50% of total variance of the hydrometeorological fields due to year-to-year variability in the North Atlantic coupled system do not correlate significantly with the ENSO-type variability. However, its seems, the ENSO-induced variability in the coupled ocean-atmosphere system over the North Atlantic is the principal manifestation of the year-to-year changes (see also, Sizov et al., 1991).

TABLE 3. Correlation matrix of SLP, latitude (positive to the North) and longitude (positive to the West) for the Asores High. Winter data sets 1891-1990 were used. The three values respectively are the correlations after high-pass filter with 5 yr cut-off, band-pass filter with 5 and 20 yr cut-off and low-pass filter with 20 yr cut-off.

	SLP	Latitude	Longitude
SLP	1.0	0.51/0.52/-0.65	-0.46/-0.16/0.79
Latitude		1.0	-0.65/-0.54/-0.44
Longitude			1.0

TABLE 4. The r.m.s of winter pressure in Asores High (SLP), latitude (Lat), longitude (Long) in 1891-1990, annual discharges of Danube (Q1) and Dnieper (Q2) in 1881-1994, May salinity in 1955-1994 in regions 1 (S1) and 2 (S2) of Fig. 1. The first row is based on data without filtering, second row- after band pass filtering with 5 and 20 yr cut-offs, and third row- after low-pass filtering with 20 yr cut off.

SLP (mb)	Lat (degree)	Long (degree)	Q1 (m^3c^{-1})	Q2 (m^3c^{-1})	S1 (psu)	S2 (psu)
2.1	4.7	8.7	1089	432	3.2	1.8
1.2	2.1	4.4	580	270	1.4	0.87
0.85	1.9	3.6	490	140	0.81	0.76

3.5. CORRELATION OF RIVER DISCHARGE ANOMALIES WITH NORTH / TROPICAL ATLANTIC OCEAN ANOMALIES

With the above considerations, we test the correlation of river discharge anomalies with North/Tropical Atlantic SSTA associated with atmospheric circulation anomalies. Figure 7 demonstrates the strong correlation of monthly anomalies of Danube discharge and SSTA in the North Atlantic Ocean. The coefficient of correlation is at a maximum in the N.W. Tropical Atlantic and in the vicinity of the Gulf Stream and North Atlantic Current, reaching respective values of about -0.6 and -0.5 in those regions. The correlation coefficient tends to increase when the lag of Danube discharge anomalies increases from zero to one year in the Gulf Stream and North Atlantic Current vicinity, and from zero to two years in the N.-W. Tropical Atlantic

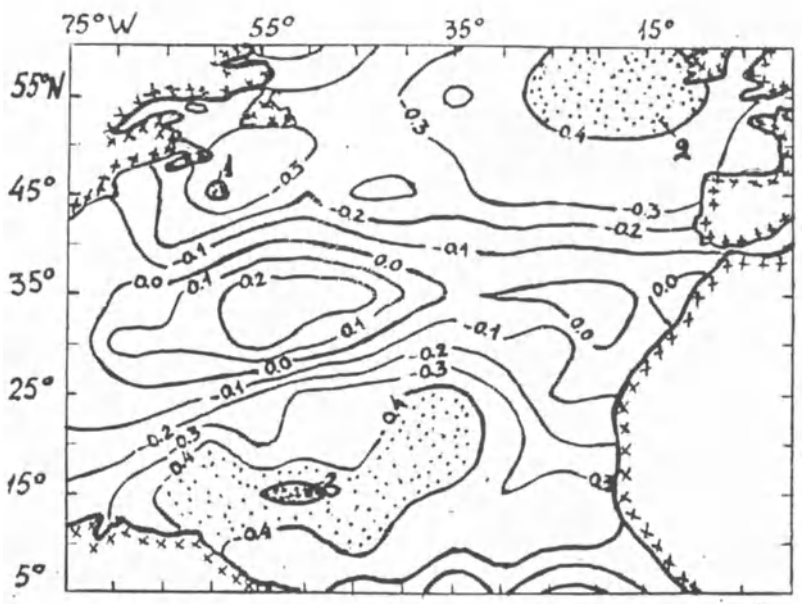


Figure 7. Spatial distribution of correlation coefficient between monthly anomalies of Danube discharege and north Atlantic SSTA averaged over a 5°x5° grid. Time series of 1957-1990 were used. Lag of Danube discharge is 12 months. Numbers 1, 2 and 3 show the areas for which the lag-lead correlation is calculated in Fig. 8.

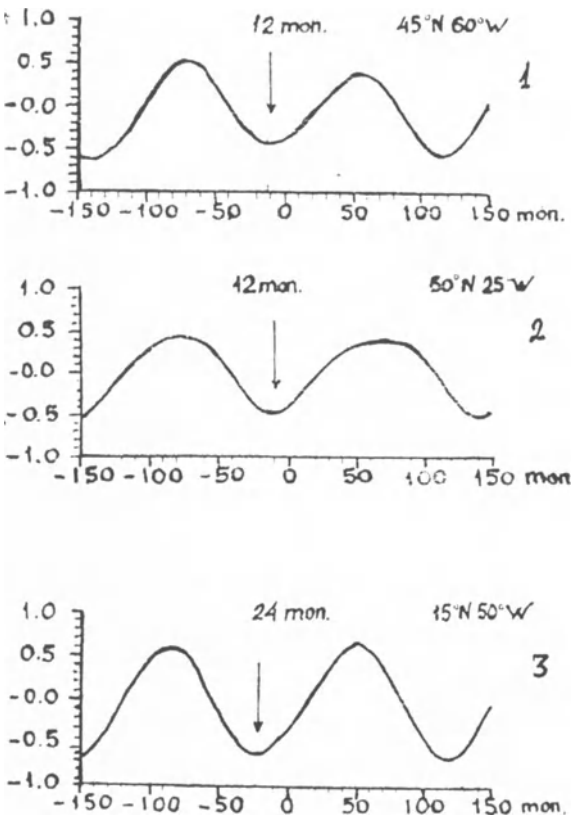


Figure 8. Lag-lead correlation of monthly anomalies of Danube discharge and monthly SSTA in the vicinity of the Gulf Stream (1), North Atlantic Current (2), and North West Tropical Atlantic (3). Running annual harmonic was removed.

(Fig. 8). In other words, following anomalous cooling in the North and especially N.W. Tropical Atlantic, the Black Sea river discharges tend to be larger for one or two years (the correlation coefficients between low-frequency variations of the monthly discharges of Danube, Dnieper, Dniester and Uzhny Bug in 1921 to 1992 vary from 0.55 to 0.95). Increasing the lag results in an increase of the correlation coefficient to about 0.5 on decadal scale, which is statistically significant to 99% confidence level. It should be emphasised that the spatial pattern of the correlation coefficient of SSTA and Danube discharge is similar to the spatial pattern of monthly SST trend in the North Atlantic for 1957-1990 (cf., our Fig.7, and Fig.3 of Voskresenskaya and Polonsky, 1993). This confirms the crucial role of the coupled ocean-atmosphere system variability in inter-decadal changes of river discharge. It should be noted that ENSO-like variability was mostly filtered out during correlation analysis because the current (not averaged) seasonal cycle was removed from SST and Danube discharge).

The predictability of the low-frequency river discharge is associated with the long-term memory of the Ocean. Simultaneously with anomalous decadal warming of the Subtropical Atlantic and cooling of the high latitudes, low-tropospheric zonal circulation is intensified in subtropical latitudes. This leads to an increase in the RI magnitude corresponding to a change in the positions of Asores High/Island Low and cyclone trajectories (shifting North or North-East). As a result, the snow cover and precipitation over the Central and Eastern Europe decrease, following which the negative anomalies of river discharge have to increase with some lag. For instance, the Danube discharge lags behind the SSTA by about one or two years.

Results of Deser and Blackmon (1993) and Table 3 show that the circulation mechanism of decadal variability differs from the multi-decadal one. At the same time, the time series are relatively short and results concerning inter-decadal variability is poor from the statistical point of view. Moreover, the statistical structure of time series is not steady. For instance, Fig.2 shows the strong changes in the amplitude of decadal harmonic of Danube discharge during the period of observations.. Therefore, the statistical forecast of long-term river discharge variability may be successful only for the rather short periods of steady patterns of the large-scale atmospheric and oceanic anomalies. It seems unlikely that these periods occupy more than a few decades.

4. Conclusions

We found strong interannual and inter-decadal variability of the N.W. Black Sea hydrographic fields and river discharges (especially of the large rivers, such as Danube and Dnieper). The typical low-frequency fluctuations of these parameters is of the same order of magnitude as the typical amplitude of their seasonal cycles. It seems these fluctuations are mostly due to natural changes in the global coupled ocean-atmosphere system, and consequently in the North Atlantic. Geophysical mechanisms of year-to-year and decade-to-decade variations differ from each other. The first one is mainly due to ENSO-type variability, and hence related to changes in the coupled system in the tropical Pacific Ocean. The second one is mainly due to variability of the

meridional heat flux and hence to North Atlantic changes. Finally, both types of variability lead to changes of the cyclone trajectories, precipitation river catchments, changes of the river discharges, resulting in changes in the N.W.Black Sea hydrography. Unfortunately, the statistical structure of the time series is not steady; thus the forecast skill of river discharge/hydrographic anomalies could be reasonably good only for the periods of quasi steady patterns of large scale anomalies over the North Atlantic. The problem is to determine when these periods occur, something that could not be determined *a priori,* because of the complexity of dynamics of the coupled ocean-atmosphere system.

5. References

1. Bunker, A.F. (1980) Trends of variables and energy fluxes over the Atlantic Ocean from 1948 to 1972. *Mon.Weather Rev* 108, 720-732.
2. Deser, C., and Blackmon, M.L. (1993) Surface climate variations over the North Atlantic Ocean during 1900-1989. *J.Climate* 6, No.8.
3. Dzhiganshin, G.F.,and Polonsky, A.B. (1994) The Interannual Variability of Sea/Air Temperature in the North Atlantic. *Marine Hydrophysical Journal*, N4, 50-59 (in Russian).
4. Gray, W.M. (1993) Atlantic conveyor belt alterations as a possible cause of multi-decadal global surface temperature change. *4th Symp. Global Change Study,* Anaheim, Calif., prep. Boston (Mass.), 384-388.
5. Hastenrath, S. (1991) *Climate Dynamics of the Tropics.* Kluwer Academic Publishers. Dordrecht/Boston/London. 488p.
6. Koval'chuk, V. (1986) On a regulation of the Black Sea river discharges. *Automatics*, No.4, Kiev (in Russian).
7. Kushnir, Y (1994) The Change in Atmosphere Circulation Associated with North Atlantic Inter-decadal SST Variability. AGS 1994 Spring Meeting (23-27 May, Baltimore,Maryland).Suppl. to EOS, 90.
8. *Monthly data sets on centers of action of the atmosphere.* (1985) Obninsk. 395, (in Russian).
9. *Monthly synoptic bulletin.* (1986/1991) Part 2. Obninsk. (in Russian)
10. Ozsoy, E., Latif, M.A., Tugrul, S., and Unluata, U. (1992) Water and nutrient fluxes through the Bosphorus, and exchanges between the Mediterranean and Black Sea. *Problems of the Black Sea. Plenary Reports. International Conference.* Sevastopol. UKRAINE (November 10-15, 1992) MHI NAS.
11. Polonsky, A., and Sizov, A. (1991) *Low-frequency North Atlantic variability associated with Pacific ENSO events.* Obninsk, 247p. (in Russian).
12. Polonsky, A., and Voskresenskaya, E. (1996). Low-frequency variability of the meridional drift transport over the Northern Atlantic. *Meteorology and Hydrology,* N7, 89-99 (in Russian).
13. Polonsky, A., Voskresenskaya, E., Kadeev, D., Kolinko, A. (1995) Low-frequency change of the Black Sea river discharges associated with the coupled ocean-atmosphere variability in the North Atlantic Ocean. (Proceedings of the second international Conference on the Mediterranean coastal environment (*Medcoast 95*) 3, 1719-1732.
14. Simonov, A.I., and Al'tman, E.N. (1991). *Hydrometeorology and hydrochemestry of the USSR seas, v.4 (Black Sea), is.1 (hydrometeorological conditions).* Hydrometeoizdat. St.Peterburg (in Russian).
15. Sizov, A.A., Voskresenskaya, E.N., and Novoselova, A.A. (1991) On the interrelationship between dynamic processes in the atmosphere and surface temperature anomalies in the Tropical Atlantic. *Marine Hydrophysical Journal,* No.2, 29-34 (in Russian).
16. Stocker, T.F. (1994) The variable ocean, *Nature* 367, No.6460, 221-222.
17. Voskresenskaya, E.N., Zelen'ko, A.B.,and Polonsky, A.B. (1992) The ENSO of 1991-92 and its appearance in the Atlantic Ocean. IBID., N6, 62-70 (in Russian).
18. Voskresenskaya, E.N., and Polonsky, A.B. (1993) The trends and interannual variability of the parameters of the large-scale variability of the ocean and atmosphere in the North Atlantic. *Meteorology and Hydrology,* No.11, 73-80 (in Russian).
19. ·Voskresenskaya, E.N., and Polonsky,A.B. (1994) Low-frequency variability of the heat fluxes in the North Atlantic in 1957 to 1990. IBID., No.9, 59-68 (in Russian).

RECENT MAN-MADE CHANGES IN THE BLACK SEA ECOSYSTEM

YU. P. ZAITSEV, B. G. ALEXANDROV
Odessa Branch, Institute of Biology of Southern Seas (OB IBSS), 37, Pushkinskaya Street, 270011 Odessa, Ukraine

Abstract. The Black Sea is the largest heavily eutrophicated marine area in the Mediterranean basin. The consequences of eutrophication are important for the marine ecosystem, especially in the NW shelf area. The biomass of phytoplankton and blooming areas have increased more than tenfold and corresponding changes in zooplankton populations occurs. Among them there are the replacement of large crustacean species by smaller ones, increasing in populations of gelatinous species, such as Noctiluca, jellyfish and ctenophores. The exotic carnivorous comb jelly, *Mnemiopsis leidyi* , introduced in the 1980s, caused a sharp decline in zooplankton and small pelagic fish populations. Decreasing of water transparency is the main reason for bottom macrophytes populations degradation. One of effective ways of local deeutrophication of marine waters is the installation of special artificial reefs. Positive biological and ecological results of such reefs in the Odessa Gulf area discussed.

Introduction

Since the late 1960s, a wide spectrum of man-made influences on the Black Sea ecosystem was revealed. There are the organic matter (OM) from agricultural and industrial runoff, and domestic sewage, nutrients from the same sources. Toxic substances are originated from industries, pesticides from agriculture. Also for the Black Sea toxic materals from rice culture are characteristic in the north-western (NW) coastal lowlands.

Important sources of solid particles in the Black Sea, except the river runoff, are the dumping, sand extraction on the shelf, and bottom trawling of fish. Microbiological pollution by organisms of public health interest, such as bacteria and virus, are usually from sewage outlets. Macrobiological impact is a result of introduction of exotic marine organisms from ballast waters and ships fouling communities.

Till the present there is little evidence for a direct influence of toxic substances on Black Sea organisms under the natural conditions [1]. Maybe the sharp decline in population of neustonic copepods, Pontellidae and megalops of crabs can be explained by the concentration of heavy metals, PCBs and other toxicants in the surface microlayer of water. Maybe the high number of aberrant specimens in the population

E. Özsoy and A. Mikaelyan (eds.), Sensitivity to Change: Black Sea, Baltic Sea and North Sea, 25–31.
© 1997 *Kluwer Academic Publishers.*

of the moon jelly, *Aurelia aurita* from impacted Black Sea zones is another evidence of a direct toxic influence on marine animals. And maybe the disappearance of the brown alga *Cystoseira barbata* along the NW coast is another proof, because this species is very sensitive to the amount of detergents in the water [2].

Among all kinds of recent man-made impacts in the Black Sea, the most important, in terms of large-scale biological and ecological consequences, there are two: eutrophication and introduction of exotic harmful species [3].

A sharp increasing of the Black Sea eutrophication in 1960s- early 1970s was observed. It is interesting to note, that practically in the same period, similar phenomena in other marine areas were revealed: in the north-western Adriatic Sea, south-eastern North Sea, Louisiana shelf area in the Gulf of Mexico, in Chesapiake Bay, in Saanich Inlet, in Tokyo Bay and in other marine areas. Such a temporal coincidence points out a general reason of this global-scale event.

It is possible to suppose, that one of the major preconditions of excessive nutrient enrichment of estuaries and bays, gulfs, marginal and inland seas in the 1960s and later, was the Indicative World Plan for Agricultural Development (IWP), which has been nicknamed the "Green Revolution".

The Black Sea is the largest heavily eutrophicated marine area in the Mediterranean basin and one of the largest in the World Ocean [4].

The consequences of eutrophication of the Black Sea are diverse and very important for its ecosystem [3].

Eutrophication leads to an increase in the growth of aquatic plants and to algal blooms. Only some examples can be proposed, concerning phytoplankton density and biomass increasing in the NW shelf area.

Average biomass of phytoplankton in this area in the 1950s was 670 $mg.m^{-3}$, in the 1960s- 1,030, in the 1970s- 18,690 and in the 1980s- 30,000 $mg.m^{-3}$ [3]. Average density of *Skeletonema costatum* in Romanian waters of the Black Sea in 1962-1965 was about 2 million $cells.1^{-1}$, and in the 1970s- 97 million $cells.1^{-1}$ [5].

Up to 1960, the summer biomass of peridineans in the NW shelf areas was on average about 18% of the total phytoplankton biomass [6]. In the 1980s, 90% of the total biomass during phytoplankton blooms was made up of dinoflagellates [7]. As a general rule, relatively large unicellular alge, such as *Rhizosolenia calcar avis*, *R .fragillisima*, *Nitzschia seriata* and others were replaced by small-size species, such as *Prorocentrum cordatum*, *Hillea fusiformis*, coccolithophorids and others.

The area of phytoplankton blooms in the NW Black Sea in the 1960s was about 500-700 km^2. In the 1980s it increased about tenfold and more.

The abundant phytoplankton create a good trophic base for herbivores and detritivores, although there is no direct correlation in all cases. Populations of some zooplankton species including herbivores, have become sparse, like copepods, *Pseudocalanus elongatus*, *Centropages kröyeri pontica*, *Pontella mediterranea* and the cladoceran, *Penilia avirostris*. Large species of crustacean plankton have been replaced by smaller species [1]. Of an original seven species of cladocerans, four remained in the 1980s in the plankton, the smallest, *Pleopis polyphemoides*, the most abundant. It is an example of biodiversity decline, very characteristic for the last two decades.

On the contrary, the population numbers of gelatinous plankton greatly increased. It was a bloom of the jellyfish *Rhizostoma pulmo* in late 1960s and early 1970s, a bloom of the moon jelly, *Aurelia aurita* in the 1970s and 1980s, of the protozoan *Noctiluca scintillans* in late 1970s and 1980s, and an outburst of the rainbow comb jelly, *Mnemiopsis leidyi*, an introduced species, in late 1980s. It was a succession of gelatinous species of zooplankton with corresponding impact on Black Sea biota, including fish fauna.

Due to the large amounts of phytoplankton, detritus, *Noctiluca*, jellyfish and other suspended organisms and particles, the transparency of Black Sea water has significantly decreased. In the 1960s, Secchi disk readings in central NW shelf area were recorded at depths of 10-18 m. In the 1980s, recordings were 7-8 m only. As a result, benthic algae growing at depths more than become shaded [3].

The reduction of the unique community "Zernov's *Phyllophora* field" in the center of the NW shelf is a typical example of seaweed population degradation. During the last two decades, the stocks of eelgrasses, *Zostera* have decreased tenfold in the shallow waters. The reason was the mobilizing of sediment particles from the sea bottom when dredging sand in coastal zones.

Actually, macrophytes are confined to the narrow belt near the shore itself, at depths less than 5-6 m.

A very important consequence of man-made eutrophication is the formation of large hypoxic areas, first recorded in 1973 on the NW shelf over an areas of 3,500 km^2. In more recent years, cases of mass mortality of bottom organisms from hypoxia have become ordinary phenomena, their scales depending on the meteorological, hydrological, hydrochemical and biological conditions of each year. In 1978, 1980, 1983, 1990 extremly large hypoxic areas on the NW shelf of 30,000-40,000 km^2 were observed.

The biological losses due to hypoxia on the NW shelf are estimated at 100-200 t of organisms per square kilometre of bottom. The total losses in 1973-1990 are estimated at 60 million t, including 5 million t fishes [8]. The hypoxic zones in the NW shelf area were recorded at depths from 8 to 40 m.

In the recent state of the shelf ecosystem, relatively favourable environmental conditions remained only at the edge of the sea, at depths not more than 5-7 m. Sufficient oxygen content, amounts of nutrients and solar radiation provide normal life conditions for plants and animals.

An increase of population of some algae, which prefer eutrophicated waters (*Enteromorpha*, *Ceramium* and others), invertebrates (mussels, crustaceans) and coastal fish, such as the silverside, *Atherina mochon pontica*, sand lance, *Gymnammodytes cicerellus*, some species of gobies and others has even been observed in the last years. Populations of some interstitial meiobenthic organisms (Harpacticoida, Ostracoda, Halacaridae) are also increasing in eutrophicated waters [9].

Like other eutrophicated seas, the Black Sea proved to be a favourable receiver of exotic organisms, transported in ballast waters from other seas. The list of alien

animals and plants, naturalized into the Black Sea in the twentieth century is quite long one [3].

One of the first accidentally introduced species was the black eyed hydromedusa, *Blackfordia virginica* firstly observed in 1925. It was followed by polychaeta, *Mercierella enigmatica* in 1929, white fingered mud crab, *Rhithropanopeus harrisi tridentata* in 1937, snail, *Rapana thomasiana* in 1946, soft shelled clam, *Mya arenaria* in 1966, blue crab, *Callinectes sapidus* in 1967, nudibranch mollusc, *Doridella obscura* in 1980, bivalve, *Cunearca cornea* in 1982, rainbow comb jelly, *Mnemiopsis leidyi* in 1982. The last settler the brown alga, *Desmarestia viridis* was revealed in 1990 [10].

The eutrophication of marine waters and its various consequences is one of the most heavy man-made impact on the sea. Some results of first experiences for local deeutrophication of waters in the Black Sea, using artificial reefs (AR) in the coastal zone, present certain interest.

On the Azov-Black Sea basin first investigations on AR have been carried out in the region of the Odessa seashore. Here, starting with 1976 many researches on peculiarities of fouling of various substrates and biocenoses formation on AR of several types have been carried out, such as "sprawled reef" of concrete and granite, "littoral reef" of pontic lime stone and "reef of tyre-covers". A significant positive effect has been reached: *Enteromorpha* biomass has increased 20 times, *Cladophora* with *Chaetomorpha* - 15 times, *Ceramium* - more than 40 times, total polychaets, crustaceans and molluscs biomass have increased more than 100 times [11, 12]. Good results were gained by the works on increasing fish productivity in the Sea of Azov. From 1984 to 1985 about 2,5 thousand tyre-covers were installed in Obitochny and Belosarajsky Bays. As a result the composition of ichthyofauna has increased from 8 to 15 species. According to the estimation data the increase of additional volume of gobies catch was 100-120 t at the expense of increasing the number of spawns and survival of fry as the result of AR construction [13].

However the data received on the considerable intensification of autotroph processes in the nearshore sea zone at the expense of AR construction testify to the danger of detritus accumulation with further formation of oxygen deficiency zones [11].

Thus, after-effects of AR installation is analogous to mussel plantations have marked local character and their effect is extremely variable. On the one hand it is discovered that mussel farms can keep up to 30% of carbohydrate, 42% of nitrogen, 60% of chlorophyll "a" [14] and can reduce water pollution by bacteria up to 40-50% even in cases of its high concentration, namely, coliforms 10^{10} cells.l^{-1} [15], to speed the process of biosedimentation more then thrice [16]. In some works, quite a definite conclusion is drawn that mollusc farms not only positively influence the ecosystem but are also the unique possibility for active conteraction to eutrophication [17, 18]. On the other hand by some estimates, 80% of matter assimilated by mussels is used for faecal production [19]. In the region of mass mollusc cultivation dissolved OM concentration may be increased 3-4 times [20], secretion of ammonia by mussels in cases of its complete consumption by phytoplankton leads to a considerable rise of primary

production [21]. In southern eutrophicated seas, like the Black Sea, in areas of water with slow water exchange high mollusc-filtrator concentrations cause pollution and degradation of pelagic and benthic communities [22] in which case it will take from 3 to 8 years to restore the biocenoses [19].

The main reason of structure changes of the Black Sea ecosystem and worsening of the sea waters quality is the break of production and destruction balance of OM, first of all at the expense of the sharp increase of content of mineral compounds of nitrogen and phosphorus, carried out by rivers to the sea, as it has been described before.

The complex analysis of the production and destruction processes taking place in the coastal aquatories made by OB IBSS in the NW shelf during the last 5 years led to the following conclusions:

-the contribution of macrophytes into the primary production is 60-70% of the total production, that is, the functional role of phytoplankton is supressed at the expense of mussel feeding and life secretions of the seaweeds;

-the process of destruction prevailed over the primary production 7-10 times. This testifies to the fact, that about 90% of general flow of energy of the coastal ecosystem goes through the stage of the dead OM (detritus, faecal pelets etc.);

-from spring to autumn the dominating role of the fouling community in OM destruction passes to benthos as a result of sedimentation and the decomposition of some part of biomass.

Mussel, *Mytilus galloprovincialis* and seaweeds, *Ceramium rubrum*, *C.elegans*, *C. diaphanum*, *Chaetomorpha aerea*, *Enteromorpha intestinalis*, *E. linza*, *Cladophora vagabunda* are the main components of fouling community of the coastal ecosystem in eutrophicated areas of the Black Sea. In particular, the average annual mussel biomass in hard substrate fouling has increased 2.1 time for the last ten years and has reached 18.9 $kg.m^{-2}$. Gross output of macrophyte production has increased 2.5 - 3 times to 1.4 $kg.m^{-2}.month^{-1}$ [23,24]. As a rule the fouling community (for example on the AR) determines the transformation of OM. Utilization of macrophytes goes on detritus way. More than 40% of primary production turns into detritus and 37% turns into dissolved organic matter. In mussels' food, the content of detritus, zooplankton, phytoplankton and bacteria corresponds to their composition in seston: 63, 17, 16 and 4% accordingly. The main part of matter ingested by mussels (60.4%) is spent on respiration, 23% - on production and 17% - on excretion, 80% of which is disolve OM.

It has been established that fouling of AR in eutrophic areas is characterised by a high functional activity and a more short period of turnover of matter and energy. In particular, the efficiency of extracting mineral nitrogen and phosphorus by algae per square metre of AR in the Odessa Bay is 420 - 1550 and 60 - 240 $mg.day^{-1}$, correspondingly. Animal foulers such as filtrators as mussels and barnacles, *Balanus improvisus* during the same period extract 3-22 g $C.m^{-2}$ particulate OM.

At the same time the incidental detachment of fouling may cause secondary contamination of the area. The volume of these losses near the Odessa coast for the period of May-November for each metre of coastline (for the belt of coastal shallow water to a width of 100 m) was 1 kg algae and 6 kg mussels.

The threshold indices were determined for functional activity of fouling and intensity of entry of OM into bottom sediments the excess of which leads to an unpermissible lowering of the quality of the marine environment. The production of macrophytes should not exceed 8.5 g $OM.m^{-2}.day^{-1}$ while the rate of biosedimentation - 4.5 g $OM.m^{-2}.day^{-1}$. Regular withdrawal of part of the produsedbiomass of fouling is one of the necessary conditions for using AR in eutrophic waters.

The main restrictions of AR used for local purifying of waters in the eutrophic area are the followings:

1. The periodicity of forming biomass extraction must be obligatory defined considering the intensity of hydrobiont metabolism and their production.
2. The technological methods of processing the fouling biomass from the reefs must correspond to the level of the pollution. Only in this case the local purification of waters that requires considerable expenses on construction can prove profitable at the expence of the selling the products of fouling processment. The products thus received must not be obligatory used for food needs.
3. The location and sizes of AR must take into consideration the speed of current and the content of the main polluting substances in the aquatoria. The presence of the strong current preventing the accumulation of organic sediments in the regions of mass hydrobiont settlements divides in space the zones of positive and negative influence. In this case the reduction of concentration of mineral and organic matters, bacteria and phytoplankton can be observed directly in the AR zone, while at a considerable distance from it, as a result of accumulation of hard metabolites and detritus, the zones of oxygen deficiency will be formed with further death of flora and fauna.

Hydrobiologic improvement (purification) of water environment based on the filtration ability of inchabitans of AR, mariculture farms, and other biopositive installations, with ensure the delay and absorption of matter (including the pollutants) has no prospects without preliminary taking into account the peculiarities of ameliorated area of water, appraisal of matter moving, structure and functional activity of fouling community.

Real improved quality of the environment in case of increasing input of matter can be reached only by organizing their adequate carrying out beyond the borders of ameliorated area of water. It can be realized either, if there are natural currents, ensuring carrying out of accumulated metabolites into the open sea areas or by organizing their extractions and their processing on the land. This process can be profitable only in case the whole complex of measures (amelioration of aquatories, mariculture, utilization of sediments and of fouling organisms) is performed simultaneously and its production will become not only the products of processed biomass, sediments, but also purified aquatoria.

References

1. Zaitsev, Yu.P. (1992a) Recent changes in the trophic structure of the Black Sea, *Fisheries Oceanography* **1**, 2, 180-189.
2. Gerlach, S.A. (1985) *Marine Pollution. Diagnosis and Therapy*, Gidrometeoizdat, Leningrad (in Russian, translated from English)
3. Zaitsev, Yu.P. (1993) Impacts of eutrophication on the Black Sea fauna, Studies and Reviews. *General Fisheries Council for the Mediterranean* **64**, 59-86.
4. Zaitsev, Yu.P. (1991) Cultural eutrophication of the Black Sea and other South European Seas, *La mer* **29**, 1-7.
5. Mihnea, P.E. (1985) Effect of pollution on phytoplankton species, *Rap.Comm. int. Mer Medit.* **29**, 9, 85-88.
6. Ivanov, A.I. (1967) Phytoplankton, in K.A.Vinogradov (ed.), *Biology of the northwestern part of the Black Sea*, Naukova Dumka Publ., Kiev, pp. 59-75 (in Russian).
7. Nesterova, D.A. (1987) Peculiarities of phytoplankton successions in the northwestern part of the Black Sea, *Hydrobiologichesky Zhurnal* **23**, N 1, 16-21 (in Russian).
8. Zaitsev, Yu.P. (1992b) Ecological state of the Black Sea shelf zone near the Ukrainian coast (a Review), *Hydrobiologichesky Zhurnal* **28**, N 4, 3-18 (in Russian).
9. Vorobyova, L.V., Zaitsev, Yu.P., Kulakova, I.I. (1992) *Interstitial meiofauna of sandy beaches of the Black Sea*, Naukova Dumka Publ., Kiev, (in Russian).
10. Minicheva, G.G. Eremenko, T.I. (1993) Algological finds from the northwestern part of the Black Sea, *Algologia* **3**, 4, 83-87 (In Russian).
11. Eremenko, T.I., Minicheva, G.G. (1983) Primary productivity of the macrophytes on the hydrotechnical constructions like artificial reefs, in *Conditions, perspectives of improvement and consumption of the Crimean coastal ecosystem* (Sevastopol,1983), Sinegub, I.A. (1987) The zoocoenosis formation on the different artificial reefs in the north-western part of the Black Sea, in *Artificial reefs for fisheries*, Rep. All-Union Conference (Moscow, December 2-4, 1987), Moscow, pp.57-59 (in Russian).
12. Alexeev, R.P., Zaitsev, Yu.P., Ivanova, E.V., Sinegub, I.A. (1987) The zoocoenosis formation on the different artificial reefs in the north-western part of the Black Sea, in *Artificial reefs for fisheries*, Rep. All-Union Conference (Moscow, December 2-4, 1987), Moscow, pp.57-59 (in Russian).
13. Janovskij,E.G., Grout, G.G. (1990) Artificial reefs in Obitochny Bay of the Sea of Azov, in *Artificial reefs for fisheries*, Moscow, pp. 86-93 (in Russian).
14. Cabanas, J.M., Gonzalez, J.J., Marino, J., Perez, A., Roman, G. (1979) Estudio de mejillon y de su epifauna en los cultivos flotantes de la Ria de Arosa.III. Observaciones previas sobre la retencion de particulos y la biodeposicion de unabatea, *Boletin del Instituto español de oceanografia* **5** (268), 45-50.
15. Govorin, I.A. (1991) Character of the Black Sea mussels in elimination process of allochthonic bacteria from marine environment, *Hydrobiologichesky Zhurnal* **27**, N4, 33-38 (in Russian).
16. Dahlbäck, B., Gunnarsson, L.A.H. (1981) Sedimentation and sulfate reduction under a mussel culture, *Mar. Biol.* **63**, N3, 269-275.
17. Larsson, A.-M. (1985) Blue mussel sea farming-effects on water quality, *Vatten* **41**, 218-224.
18. Rodhouse, P.G., Roden, C.M. (1987) Carbon budget for a coastal inlet in relation to intensive cultivation of suspension-feeding bivalve molluscs, *Mar.Ecol.Progr. Ser.* **36**, N3, 225-236.
19. Rosenberg, R., Loo, L.O. (1983) Energy- flow in *Mytilus edilus* culture in western Sweden, *Aquaculture* **35**, 151-161.
20. Kulakovsky, E.E., Koonin, B.L. (1984) Influence of mussel mariculture on the ecosystem of adjacent regions of Chupa Bay of the White Sea, in *The problems of nature protection in the White Sea basin*, pp.131-136 (in Russian).
21. Solovjova, A.A., Galkina,V.P., Garkavaja, G.P. (1977) Experimental investigation of the influence of mussel metabolites on nature phytoplankton community of the White Sea, *Oceanologija* **17**, v.3, 449-458 (in Russian).
22. Gershanovich, D.E. (1987) Ecological character of the artificial reefs in the sea, in *Artificial reefs for fisheries*, Rep. All-Union Conf. (Moscow, December 2-4, 1987), Moscow, pp. 10-13 (in Russian).
23. Minicheva, G.G. (1993) Structural and functional peculiarities of formation of benthic algae sea communities, *Algologia* **3**, N1, 3-12 (in Russian).
24. Alexandrov, B.G. (1994) Biotic balance of the water ecosystems in hypertrophic urbanized regions of the coastal zone of the Black Sea, in *Urbanization as a Factor of Change of Biogeocoenotic Cover* (Lviv - Jaremcha, September 21-23, 1994), Lviv, Academic Express Ltd., pp.93-94.

SEASONAL AND LONG-TERM VARIABILITY OF THE BLACK SEA OPTICAL PARAMETERS

V.L. VLADIMIROV, V.I. MANKOVSKY, M.V. SOLOV'EV and A.V. MISHONOV
Marine Hydrophysical Institute, National Ukrainian Academy of Sciences, 2, Kapitanskaya St., Sevastopol, Crimea, 335000, Ukraine

Abstract.

Seasonal and long-term variability of the Secchi disk visibility depth and spectral optical parameters of the Black sea water are analyzed using valuable data set from the data base of the Marine Hydrophysical Institute. The drastic decrease of the water transparency was observed during 1986-1992. It coincided with the big changes of the spectral distribution of water optical parameters. The main causes of these changes are eutrophication and influence of biological invader *Mnemiopsis leidyi* on the sea ecosystem structure.

1. Introduction

In situ measurements of the optical parameters have been conducted in the Black Sea since 1970s and Secchi disk depth measurements have been conducted since 1920s. A valuable data set of the Black Sea optical characteristics is available at present. MHI's Black Sea database contains now data of 10300 Secchi disk visibility depth (Z_d) measurements for 1922-1995, 2050 vertical profiles of the light attenuation coefficient ($c(\lambda)$) for 1964-1994, 400 color index (I_c) measurements for 1974-1988, etc. These data permit to estimate the seasonal and long-term variability of some optical parameters of the Black Sea.

In framework of this paper we have considered the Secchi disk data, for which the longest and biggest data set exist, and which correlate well with the mean biooptical properties of the upper water layer [15], spectral light attenuation and radiance index data. These data are also very interesting from the ecological point of view.

2. Seasonal variability of the Secchi disk depth

Seasonal variability of the Secchi disk depth was analyzed using monthly mean values, calculated for 1922-1985 for the central deep part of the Black Sea, limited by the lati-

E. Özsoy and A. Mikaelyan (eds.), Sensitivity to Change: Black Sea, Baltic Sea and North Sea, 33–48.
© 1997 *Kluwer Academic Publishers.*

tudes 42°20' and 44°15'N and longitudes 31° and 38° E and for the western part of the Black Sea (Figure 1). The monthly mean, maximum, minimum values and standard deviations for each month are presented in Table 1.

The amount of data for January are very limited and cannot be used to calculate the mean value. There are two minimum in the interannual variability of Z_d namely in spring and at the end of autumn and two maximums, namely in summer and at the end of winter. The difference between maximum and minimum mean month values is about 6.2 metres or 37% of mean annual value (16.8 m).

The interannual variability of water transparency connects with the annual cycles in phytoplankton, which can be explained by meteorological and hydrological factors. In winter nutrients accumulate in the upper water layer due to the intensive vertical water exchange associated with convection and strong winds. This nutrient supply gives good conditions for the spring plankton bloom, when the radiance is high and surface water

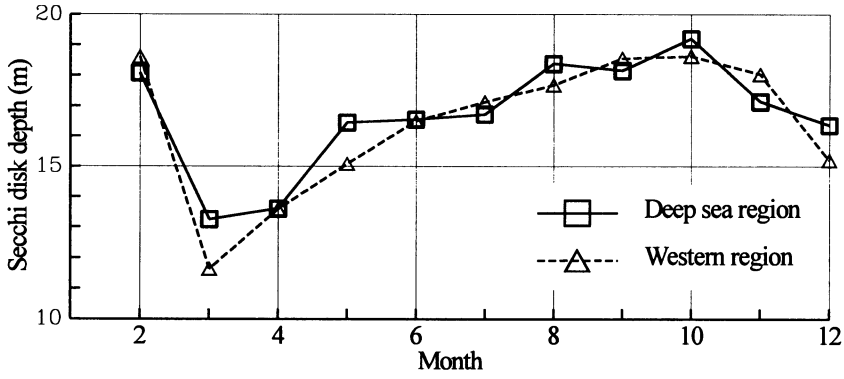


Figure 1. The monthly variation of mean Secchi disk depths in the central deep part and western part of the Black Sea in 1922-1985.

warms. The spring bloom leads to the transparency decrease. After summer thermocline formation, the nutrient migration to the upper layer is strongly limited. Production of phytoplankton considerably decreases and water transparency increases during this thermocline formation in the summer due to the scavenging of the nutrients in the upper layer. In the autumn cooling period, convection leads to the gradual destruction of the thermocline and the elimination of its blocking influence on nutrient fluxes from the deep sea. After full thermocline destruction at the end of autumn, the surface layer is again high in nutrients and a second short plankton bloom occurs, which is interrupted by a quick temperature decrease as a result of winter storms and short insolation during the day.

Correct analysis of the seasonal variability of the hydrooptical parameters can be performed only for the period up to 1985. Further analysis appears to be a fairly tough job, due to the unstable state of the Black Sea ecosystem during the last years. An obvious clear result of that impact is the decreasing of water transparency, which was strongest in the last decade [3].

TABLE 1.The monthly mean, maximum, minimum Z_d values and standard deviations for each month for the central/western parts of the Black Sea

Month	Mean	Max	Min	STD	Number of data points
January	-	-	-	-	-
February	18.1/18.6	28.0/28.0	11.0/11.0	4.64/5.63	11/7
March	13.2/11.6	20.0/28.0	6.0/7.0	4.07/3.23	17/19
April	13.6/13.6	27.0/18.0	9.0/9.0	4.84/3.07	21/12
May	16.5/15.1	31.0/31.0	5.0/5.0	4.63/5.57	39/26
June	16.6/16.5	26.0/26.0	6.0/6.0	4.80/4.59	47/33
July	16.7/17.1	27.0/27.0	7.0/4.0	4.26/3.77	100/56
August	18.4/17.7	28.0/28.0	10.0/2.0	2.78/.0.8	75/79
September	18.2/18.6	29.0/27.0	13.0/13.0	3.25/2.92	51/40
October	19.2/18.6	28.0/28.0	12.0/12.0	2.87/3.22	20/16
November	17.1/18.0	22.0/22.0	12.0/14.0	2.58/2.47	28/19
December	16.4/15.2	22.0/17.0	12.0/11.0	2.77/2.23	11/5

3. Long-term variability of the Black Sea water transparency

Annual mean values of the Secchi disk depth were calculated for all years of measurement to estimate the variability of the water transparency in the Black Sea (Figure 2). These values were calculated for the central deep part of the Black Sea, limited by latitudes 42°20' and 44°15'N and longitudes 31° and 38°E (the same as for the seasonal variability).

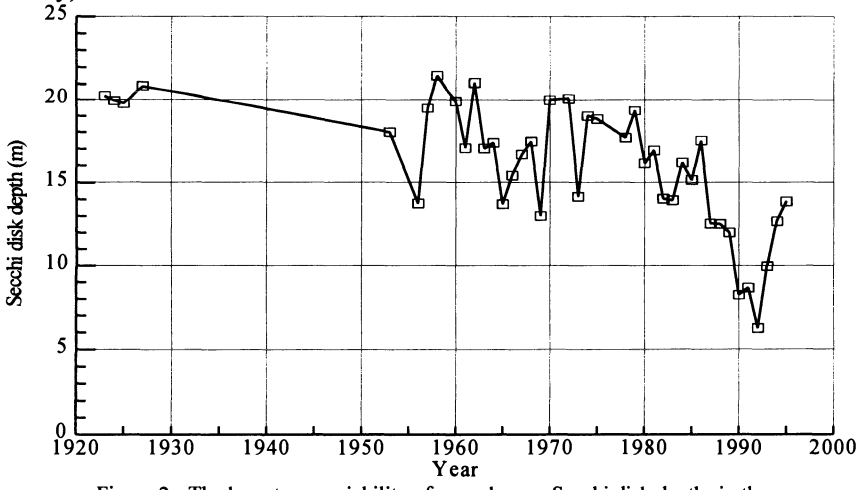


Figure 2. The long-term variability of annual mean Secchi disk depths in the central deep part of the Black Sea in 1922-1995.

The mean values of Z_d were 20-21 m, and a maximum value was 30.5 m in the 1920s. In the early 1980s, the mean annual values decreased to 14-16 m, although

sometimes the values of 25-28 m were found in the central part of the sea. In 1990-1992, the mean values were smallest, reaching 8.2 m in 1990, and 6.2 m in 1992 (Table 2). This is accompanied by the increasing annual variability, which is better marked than seasonal variability. Large variations of the seasonal cyclicity of the optical properties are being observed to take place in the sea as compared with the period prior to 1985.

TABLE 2. The annual mean, maximum, minimum Z_d values and standard deviations for each year for the central part of the Black Sea

Year	Mean	Max	Min	STD	Number of data points
1923	20.2	23.0	19.0	1.44	5
1924	19.9	28.0	13.5	4.18	20
1925	19.8	30.5	11.0	4.32	24
1927	20.9	25.0	16.0	2.70	10
1953	18.0	20.0	17.0	1.22	4
1956	13.8	20.0	8.0	3.99	10
1957	19.5	25.5	13.0	3.53	22
1958	21.5	30.0	10.0	7.31	14
1960	19.9	22.0	19.0	0.99	9
1961	17.1	20.0	13.0	2.08	10
1962	21.1	27.0	16.6	2.92	11
1963	17.0	22.0	11.0	3.74	9
1964	17.4	24.0	3.5	4.21	29
1965	13.7	20.5	9.0	3.78	10
1966	15.4	22.0	9.0	4.58	10
1967	16.7	23.0	10.0	5.31	3
1968	17.4	26.0	9.0	5.69	5
1969	13.0	15.0	10.0	2.12	4
1970	20.0	22.0	18.0	2.00	2
1972	20.1	28.0	13.0	4.10	11
1973	14.1	20.0	6.0	4.22	7
1974	19.0	27.0	15.0	3.12	15
1975	18.8	24.0	9.0	2.86	58
1978	17.7	23.0	14.0	2.35	18
1979	19.3	20.0	18.0	0.94	3
1980	16.1	21.0	7.0	4.31	14
1981	16.9	29.0	12.0	4.33	12
1982	14.0	18.0	9.0	2.92	29
1983	13.9	20.0	10.0	2.82	15
1984	16.2	24.0	5.0	3.29	113
1985	15.1	27.0	6.0	4.87	38
1986	17.5	25.0	6.0	5.10	14
1987	12.5	19.0	7.0	3.11	65
1988	12.5	18.0	8.0	2.45	54
1989	12.0	25.0	2.0	4.73	179
1990	8.2	13.0	3.0	2.16	53
1991	8.7	14.0	5.5	1.92	90
1992	6.2	11.0	2.0	2.51	51
1993	10.0	16.0	7.0	1.76	94
1994	12.7	16.0	9.0	1.52	33
1995	13.9	21.0	6.7	3.89	13

Water transparency measurements using *in situ* sounding instruments, which were performed by MHI during Black Sea surveys, also indicate the same decrease of transparency. Mean, maximum, minimum values and standard deviation of the attenuation coefficients (wavelength 410-420 nm) in the surface layer of the central, deep part of the sea for summer are shown in Table 3. Values for 1977-85 which are considered as the "background" data show large changes compared to 1990, 1991, and 1992 data.

TABLE 3. Attenuation coefficients (wavelength 410-420 nm) in the upper water layer in the central deep part of the Black Sea in summer, $c(\lambda)$ [m^{-1}]

Year	Mean	Max	Min	STD.
1977-1985	0.55	1.38	0.23	0.32
1990	1.17	1.86	0.78	0.23
1991	1.03	2.16	0.69	0.21
1992	1.70	2.76	0.55	0.60

The big shifts in optical water properties have the following ecologically-important consequences:

1. Significant decrease of the thickness of the euphotic layer, in which the primary production takes place.
2. Changes in spectral composition of the light penetrating to the depths.
3. More intense heating of the upper mixed layer can influence water dynamics and climate of the region, besides the change in the plankton life conditions.

It is worth to mention that the water transparency in the Black Sea started to increase since 1993. One of the possible reason for this change is the significant reductions in the agricultural and industrial activities in the former socialist countries of the region.

4. Characteristics of the Secchi disk depth in the Black Sea before 1985

The climatic characteristics of the Black Sea Secchi disk depth in the years preceding the large changes of water transparency were calculated and evaluated for summer and autumn seasons since the most part of the Secchi disk measurements were done during these seasons. Moreover, most of the field surveys in recent years were also done during the same season.

To obtain the map of climatic field of transparency for the Black Sea, the data were gridded using grid size of 10' by longitude and latitude. The averaged values were calculated for a circle with 15' radius. The weights of averaging values were inversely proportional to their square distance to the grid point center. The time period of averaging was rather long (from June to October) to obtain stable data. This choice can be supported by the low variability of mean monthly values during this period. In a hydrological sense, the basin can be characterized as summer type of water structure with a seasonal thermocline during this period. 9200 values were used in this calculation.

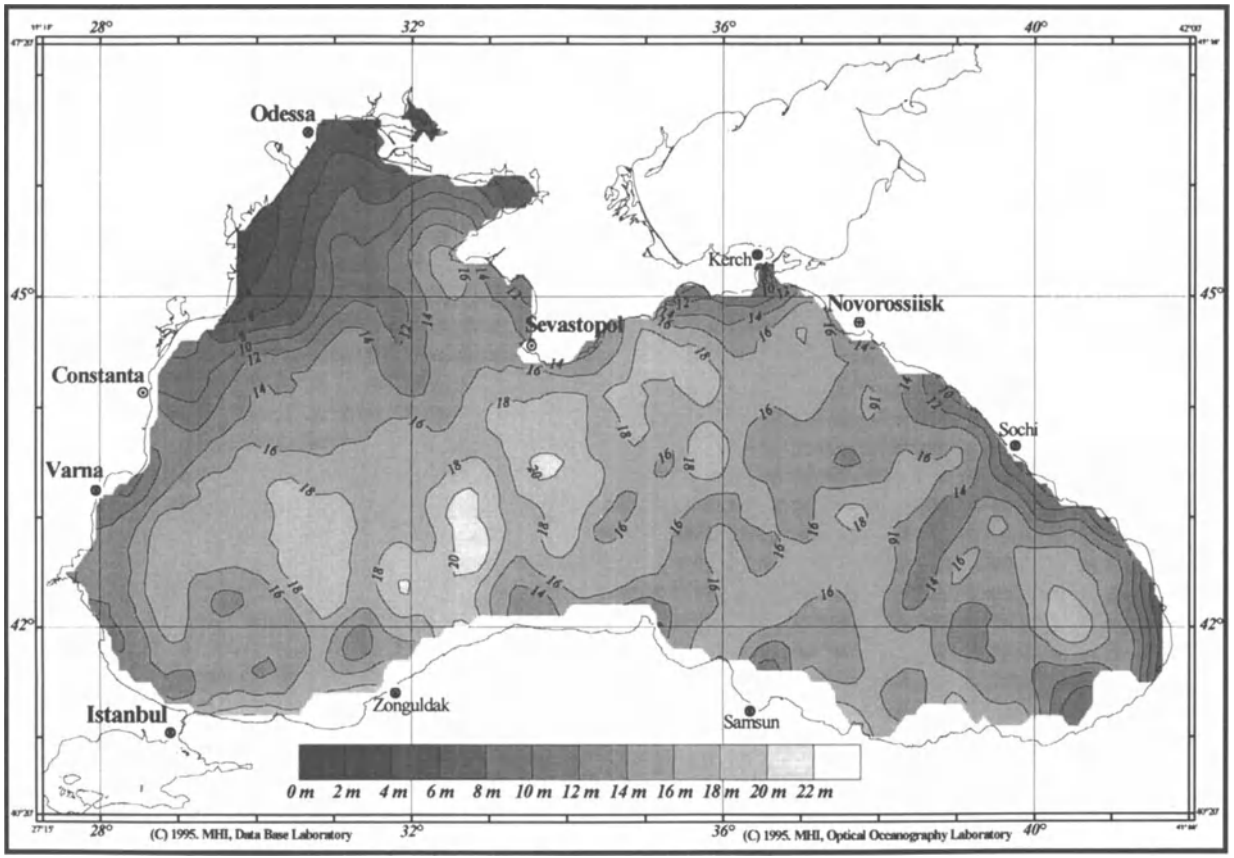


Figure 3. The climatological field of mean Secchi disk depths in the Black Sea for June - October 1922-1985.

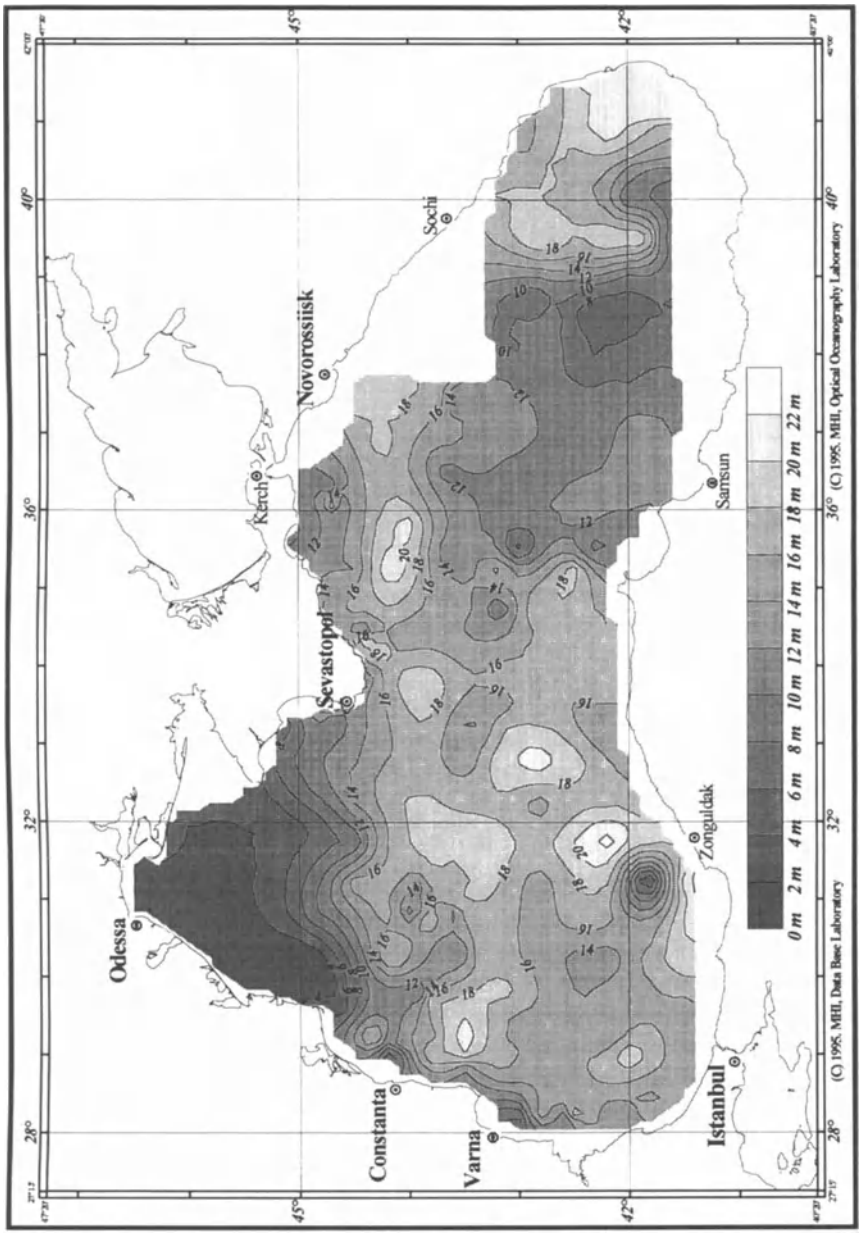


Figure 4. The field of mean Secchi disk depths in the Black Sea for June - October 1984.

The climatic transparency field has the following features (Figure 3). Water with Z_d <6m is found only in a narrow band in the regions of big river mouths: Danube and Dnieper on the northwest shelf, Inguri and Rioni near the Caucasus, and near the Kerch strait. These waters are sharply limited by the 15 psu isoline of salinity on the map of climatic surface salinity field for 1903-1982 in summer [1]. Transparency in nearly 60% of the deep regions of the sea, is more than 16 m. The most transparent waters (Z_d > 22m) occur in the middle parts of the sea where eastern and western cyclonic rings come into contacts with each other and where surface waters with low concentration of nutrients downwells. Relatively higher transparencies (up to 10-20 m) occurs in the shelf zone and often near the coast; for example, near the Bosphorus Z_d exceeds 18 m. There is a difference in the transparency of the eastern and western deep regions of the sea: the eastern part shows considerably lower Z_d values due to higher biological productivity. A map of the planktonic biomass in the Black Sea for the layer 0-100 m in August - September for the 1940-1965 period [7] confirms this conclusion.

In addition to the climatic field it was possible to construct the distribution of the mean Secchi disk field for October 1984 period (Figure 4). This distribution is interesting as it reflects the basin's optical state just before the period of strong decrease in water transparency.

In 1984, the values of Z_d over all the basin were slightly smaller than climatic values, but the general character of transparency distribution was the same. The eastern part of the deep sea region also had smaller transparencies in this period, as it is in the climatic field (Fig.3).

5. Distribution of the Secchi disk depth in the Black Sea in autumn 1991

The Secchi disk depth distribution in the Black Sea was constructed for September/October 1991 using data obtained during the international survey "HydroBlack-91" [2].

The range of Secchi disk values was greatly smaller than climatic values during this survey (1-15 m). The minimum value was measured in northwest shelf near the Danube mouth and the maximum value was in eastern part of the sea, 12 miles off the coast between Tuapse and Gelendzhik (Figure 5).

Waters having Z_d < 6m in 1991 was observed not only in the northwest shelf area of the basin but also down to 41°30' latitude. The area of the region with this low transparency was 5 times greater compared to that in 1922-1985 period. In the earlier period, water having Z_d < 6m was limited in general by the 15 psu isoline, but in 1991 it was approximately 17 psu. Over all the deep part of the Black Sea, values of Z_d ranged between 5--15 m. The most transparent water, with Secchi disk values 10--15 m were, as a rule, in the eastern part of the sea. The distribution of the most transparent water was approximately the same as the distribution of the most saline surface water (S > 18 psu).

Comparison with the climatic optical field for 1922-1985 shows that in central deep part of the sea not only the mean transparency (Z_d =18 m and Z_d =9.4 m, accordingly),

but also the maximum value (Z_d =15 m in 1991) was smaller in September - October 1991 then the climatic mean value. In the climatic field, the transparency of the eastern part of the sea was smaller than in western part, but in September-October 1991 this situation reversed. It's difficult to state exactly the reason for this difference because necessary biological data are lacking.

6. Distribution of the Secchi disk depth in the Black Sea in July 1992

The Secchi disk depth distribution in the Black Sea for July 1992 was constructed by using the data obtained during the international survey "CoMSBlack-92" [12].

It was the unusual period in which the extremely low Secchi disk depth were recorded. Although the water transparency of the northwest shelf area was smaller than climatic values, it was higher than those at 1991. Additionally, the most transparent waters were observed in the northern parts of the region! Very turbid waters with Z_d <4m occupied smaller region than in 1991, whereas the transparencies of the central deep sea region were still smaller; it was only 2-10 metres. Majority of the central parts of the sea was occupied with waters of very low transparency Z_d =2-4m, which were never observed during previous years (Figure 6). It must be noted that the depth of the euphotic zone during this period where the primary production is produced, is limited to upper 6-12 metres [4]. It is interesting that the most turbid waters in the central parts of the basin in July 1992 were in the regions where the most transparent waters were observed in 1991.

7. Evolution of water color and spectral optical properties

Water color also changed considerably, from III-IV (according to the Forel-Ule scale) in deep regions before 1980, to VI-VIII in recent years. Investigators often failed to determine the water color during recent years, because of the water having a marked, dirty-gray or whitish color which has no appropriate indices in the Forel-Ule color scale.

Since the changes in water color are indicative of the changes in the spectral optical properties of the Black Sea water, the investigation of the spectral distribution of the light attenuation coefficient $c(\lambda)$ and of the spectral radiance index $r(\lambda)$ was performed. The data were compared for 1984, prior to the critical deterioration of the Black Sea water transparency, and for 1991 and 1992 periods. A comparison was made for the $c(\lambda)$ and $r(\lambda)$ data, averaged for several stations with Secchi disk depths equal to the mean values in those years.

Spectra of the light attenuation coefficient $c(\lambda)$ for 1984, 1991, 1992, and for the optical's pure sea water [5] are presented in the Figure 7 for the subsurface water of the deep central part of the sea. The Secchi disk depth values corresponding to the each spectrum are showed in a legend.

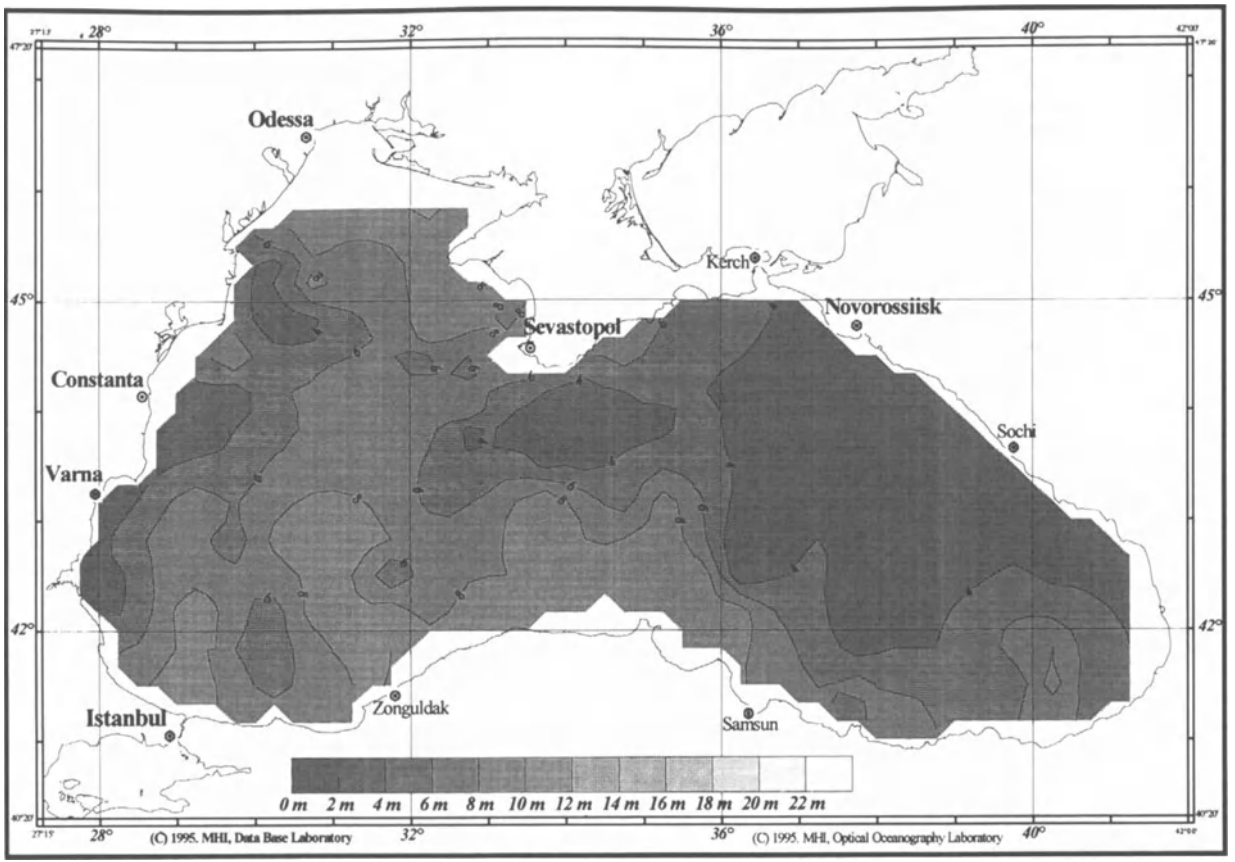


Figure 5. The distribution of Secchi disk depths in the Black Sea obtained during the HydroBlack-91 expedition in September - October 1991.

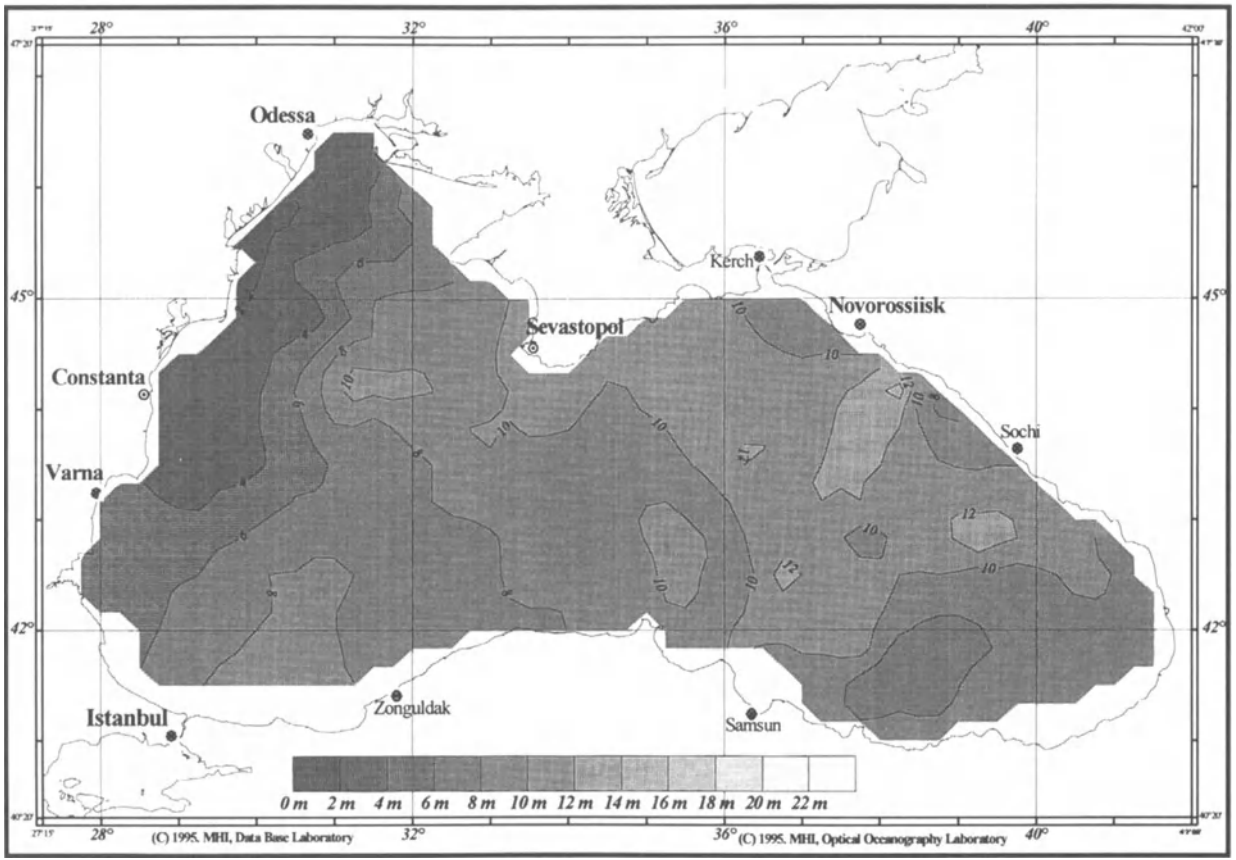


Figure 6. The distribution of Secchi disk depths in the Black Sea obtained during the CoMSBlack-92 expedition in July 1992.

In 1991 and 1992, compared with 1984, not only the values of c(λ) strongly increased, but also the shape of spectral curves changed due to the initial enhanced increase in the short wavelength band. The minimum c(λ), which was in the blue band region of e.m. radiation at 480 nm in 1984, shifted to the green band of spectrum at 550-570 nm in 1992. This shift suggests that the concentration of so-called "yellow substance" (gelbstoff), which is a component of dissolved organic matter produced during the planktonic degradation, increased with time. The absorption spectrum of the yellow substance, $a(\lambda)$, described by the exponential law $a(\lambda) = k \cdot exp(-n\lambda)$ explains why this substance absorbs light strongly in the short wavelength band of the spectrum and doesn't affect the red band. Due to the preferential absorption of the radiation spectrum penetrating through the water having high concentration of the yellow substance is transformed towards the yellow wavelength. The more the concentration of yellow substance, the greater shift in the minimum of light attenuation to the longer wavelength. This effect is clearly observed in Figure 7.

Similar shift in the spectral minimum was also observed in recent years in the spectra of the vertical attenuation coefficients, K(λ), of the sunlight. Measurements of K(λ) were performed by the authors of [11] in the central part of the sea in February-March of 1991 at the Secchi disk depth of 5-6 meters. The spectral minimum of K(λ) at 520-560 nm calculated for these measurements, were observed at 490-530 nm in the central part of the Black Sea [9] before 1979.

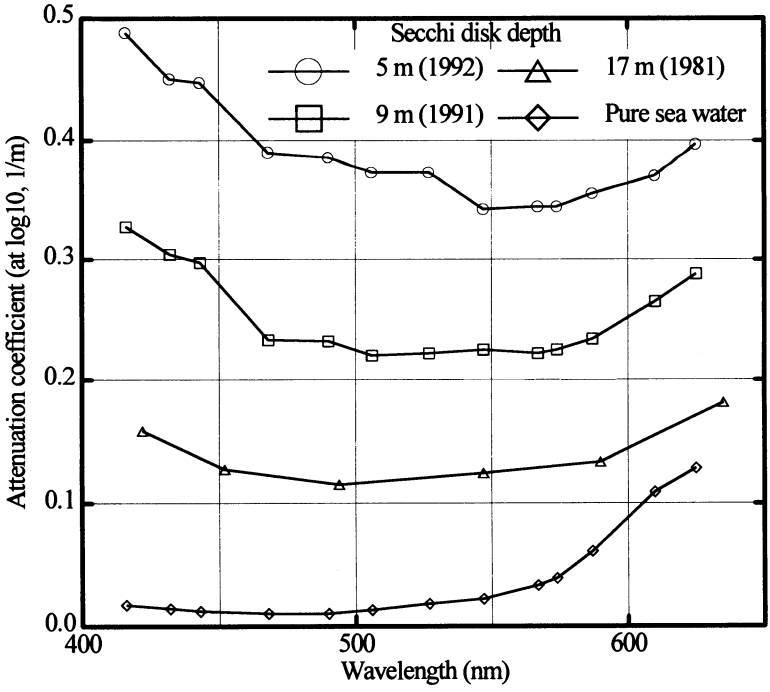


Figure 7. Spectra of the light attenuation coefficient c(λ) for the subsurface water of the deep central part of the sea for the different years and for the pure sea water. The Secchi disk depth values measured at the same station are included in a legend.

Due to this shift of the spectral attenuation minimum, the water color shifted from blue-green (scale number III-IV), which was predominant earlier [10], to the yellow-green (scale number VI-VIII), which was observed during recent years.

Parallel changes have occurred in the radiance spectra of the sea. The radiance index increased four-five times in the band of spectral maximum, and the maximum proper displaced from 480 nm to 540-560 nm in 1992, as compared with 1984 (Figure 8).

Such changes in the spectra of r(λ) show that the concentration of particulate matter, which scatter the light, increased in the upper layer of the sea. This fact caused an increase in the radiance index values and a shift in the maximum of radiance index to the longer wavelengths due to the increase in the dissolved organic matter concentration, especially of yellow substance.

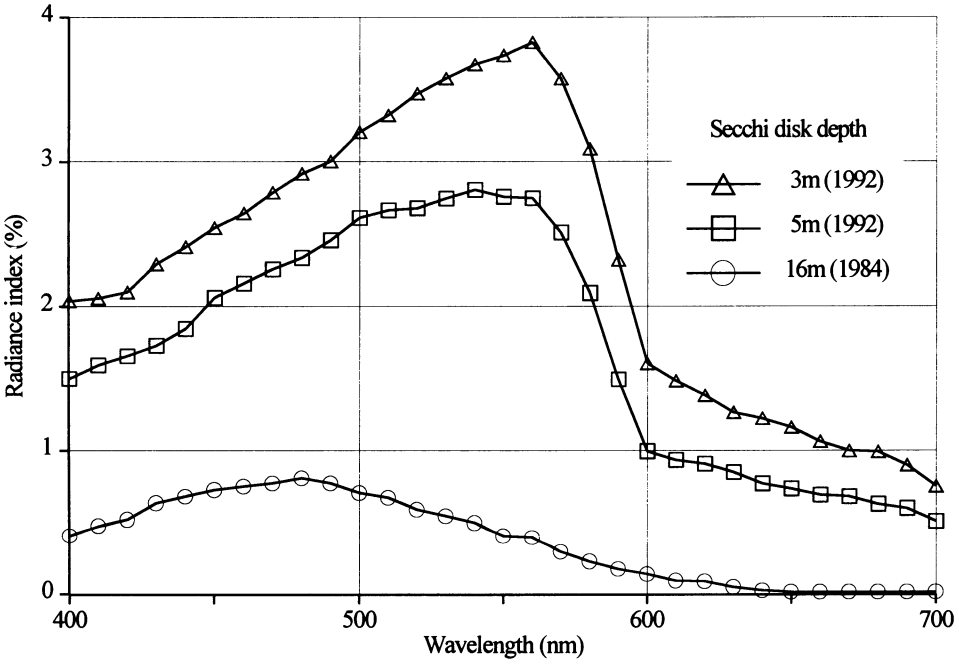


Figure 8. Spectra of the radiance index r(λ) for the deep central part of the sea for different Secchi disk depth and for different years.

A quantitative estimation of the evolution of water color was made for the XYZ colorimetric system, using the spectra of radiance indexes measured in 1984 and 1992. The dominant wavelength, λ_d, and color purity, C_p, were calculated. The color purity indicates in which proportion, the monochrome radiant flux with wavelength λ_d have to be mixed with white color radiant flux to obtain the same color impression.

These parameters are as follows:

in 1984:	Z_d=16 m,	λ_d=486 nm, C_p=41%;
in 1992:	Z_d= 5 m,	λ_d=502 nm, C_p=11%;
and:	Z_d= 3 m,	λ_d=514 nm, C_p=9.5%.

One can see that color purity essentially decreased and λ_d increased in 1992 compared to 1984. This fact accounts for the whitish color of the sea water, frequently observed in recent years, which has no analogue in the color scale. The most part of the radiant flux spreading from the sea in such water is the white light suppressing the dominant wavelength light. This fact is explained by the high concentration of small sized particles in the upper water layer, which nonselectively scatter backward the sun light penetrating into the sea water.

The data published by N.Jerlov for different regions of the World Ocean, shows that the minimum C_p=24% was observed in the Baltic sea at the λ_d=540 nm [6]. For the Black Sea in 1970-th the water purity was found as 51% at the λ_d=492 nm [14].

8. Discussion

Analysis of the total collected information has enabled us to understand the main causes of the drastic transparency decrease in the deep basin of the Black Sea from 1986 to 1992 and to reach the conclusions stated below.

Significant eutrophication occurs both in the near-shore areas of the Black Sea and in the deep ones, being connected with the long-term increasing input of nutrients of anthropogenic origin. For example, an input of biogenic compounds of nitrogen and phosphorus by the Dnieper and Danube waters, which are responsible for 3/4 of the overall river input to the Black Sea, increased 5-7 times from the 1960s to the 1980s. The mean chlorophyll concentration has become one and a half time larger in deep part of the sea throughout the same period.

Water transparency gradually declined due to the increase of the content of optically active matter in the sea. Over 20 years, from the mid-1960s to the mid-1980s, the mean annual decrease of the Secchi disk depth has attained about two metres.

However, the direct cause of the drastic transparency decrease from 1986 to 1992 was the enhanced bloom of *Peridinium* and *Coccolitophores*. Their number in the Black Sea was 1.5 - 2 orders of magnitude larger than in previous years and reached 2-3 billions per cubic meter. A significant increase in the biomass of these planktonic organisms has changed the structure of the plankton community. Now nanoplankton, which contributes immensely to the light scattering, accounts for 90% of the phytoplankton content.

The intense blooms of *Peridinium* might have been also caused by the increased concentration of particulate organic matter, as *Peridinium* can switch to heterotrophyc nutrition.

Coccolitophores also play a significant role in the changes in water transparency, due to their crustal structure containing a number of disks, namely, coccolits, which can be separated. These disks cause an intensive scattering of light. That is why, when the *Coccolitophores* concentration is high, sea water becomes whitish. This effect has been observed in the Black Sea over the last few years.

Phytoplankton structure was also strongly impacted by the biological invaders, such as *Mnemiopsis Leidyi* which appeared in the Black Sea in the early 1980s and is bio-

mass amounted to one billion tons in 1989 [16]. As a result, the amount of herbivorous microzooplankton, which is a part of the *Mnemiopsis* food, has decreased by several times [8], whereas the phytoplankton content conversely, increased. The great amount of dissolved organic matter released by *Mnemiopsis* also facilitated the increase of some types of phytoplankton and bacteria.

Long-term periodical oscillations in the Black Sea water transparency have been found to occur, which seems to be correlated with the 11-year cycle of solar activity. Water transparency increases during the first half of the cycle and decreases during the second one (we assume that the cycle starts when solar activity is at maximum). This fact shows the same cyclicity is inherent to the planktonic community.

Drastic decrease in the transparency in late 1980s coincided with the second half of the 1980-1991 solar activity cycle. However, the magnitude of the transparency decrease was more intense during this cycle than those during the previous cycles.

Analyses of the collected data, it may be concluded that the catastrophic transparency decrease in 1990-1992 took place due to the combined effect of three factors coinciding in time and sign: (1) the natural 11-year cycle, (2) increased eutrophication, and (3) the influence of the biological invader *Mnemiopsis Leidyi* on the ecosystem structure.

It is important to emphasize that the intense decrease in water transparency discontinued in the Black Sea in 1992, and in 1993 water transparency started slightly to improve. As a result, already by the end of 1995, the mean Secchi disk depth in the deep central part of the Black Sea had reached to the levels observed for the early 1980s, i.e. about 17 metres. Regretfully, we have no evidence on the changes that took place in the ecosystem of the sea during these years, which made this transparency to increase, but it coincides with the beginning of a new cycle of solar activity.

9. Acknowledgments

We thank all the scientists and crew of the research vessels participated in data collecting in the Black sea. We wish to thank also Drs. O.Yunev, L.Georgieva and B.Anninsky from IBSS NASU for the very useful discussion on the reasons of catastrophic transparency decrease in the Black Sea. The research described in this publication was made possible in part by Grant No. U1V000 from the International Science Foundation.

10. References

1. Altman, E.N., Gertman, I.F. and Golubeva, Z.A. (1987) *The climatic fields of salinity and temperature of the Black Sea water*, Sevastopol's Department of SOI, Sevastopol (in Russian).
2. Aubrey, D.G., Oguz, T., Demirov *et all* (1991) HydroBlack-91 CTD Intercalibration Workshop; WHOI, Woods Hole, USA, 1-10 December. *IOC Workshop Report* No. **91**. UNESCO.
3. Eremeev, V.N., Vladimirov, V.L., Krasheninnikov, B.N. (1992) Long-term variability of the Black Sea water transparency. *Hydrophysical and hydrochemical investigations of the Black Sea*, MHI NASU, Sevastopol, p. 28-30, (in Russian).

4. Eyvind, A. (1979) Relations between total quanta blue irradiance and Secchi disk observation in the Norwegian and Barents Seas, *Rep. Inst. fer Fysisk Oceanografi Kobenhavns Universitet*, Copenhagen, No. **42**, p. 11-27.
5. Ivanov, A. (1975) *Introduction a l'oceanographie. Proprietes physiques et Chimiques des eaux de mer.* Tome II. Paris, Librairie Vuibert.
6. Jerlov, N.G. (1976) *Marine optics*. Elsevier Scientific Publishing Company, Amsterdam-Oxford-New-York.
7. Kondrateva, T.M. (1979) Quantitative evolution and distribution of phytoplankton. *Principles of the Black Sea biological productivity*, Naukova dumka, Kiev, p. 70-78, (in Russian).
8. Melnikov, V.V., Belokopitov, V.V., Kovalev, A.V., Ostrovskaya, N.A.,. Zagorodnyaya, J.A. and Goubanova A. D. (1996) Long-term variability (1983-1994) of Black Sea Zooplankton in the layer 0-30 m, in E. Ozsoy and A. Mikaelyan (eds.), *Sensitivity of North Sea Baltic Sea and Black Sea to Anthropogenic and Climatic Changes*, Kluwer Academic Publishers, Dordrecht, pp.
9. Neuymin, G.G. (1979) Optical characteristics of the Black Sea waters. *Principles of the Black Sea biological productivity*, Naukova dumka, Kiev, p. 23-33, (in Russian).
10. Neuymin, G.G. (1980) Optical characteristics of the Black Sea waters. *The multidisciplinary oceanographic investigations of the Black Sea*, Naukova dumka, Kiev, p. 198-215, (in Russian).
11. Nikolaev, V.P. (1992) Peculiarities of the Black Sea water optical structure in winter. *Problems of the Black Sea. Abstracts of the conference papers*, MHI NASU, Sevastopol, p. 26-27, (in Russian).
12. Oguz T., S.Besiktepe, O.Basturk *et all* (1993) CoMSBlack'92a Physical and Chemical Intercalibration Workshop. Erdemli, Turkey, 15-29 January. *IOC Workshop Report* No. **98**, UNESCO.
13. Saydam, A. Cemal (1996) Saharan Dust Transport and Its Importance for the Black Sea, in E. Ozsoy and A. Mikaelyan (eds.), *Sensitivity of North Sea Baltic Sea and Black Sea to Anthropogenic and Climatic Changes*, Kluwer Academic Publishers, Dordrecht, pp.
14. Shifrin K.S. (1978) Optics of the ocean. *Physics of the ocean. V.1. Hydrophysics of the ocean*, Nauka, Moscow, p.340-396, (in Russian).
15. Urdenko, V.A., Khalturin, V.I., Afonin E.I. (1985) Empirical interrelations between hydrooptical and biological characteristics and the light field parameters. *Remote sensing of the sea and the influence of atmosphere (Program INTERKOSMOS)*. Ed. by Urdenko V.A., Zimmerman G., USSR Acad. of Sci. - GDR Acad. of Sci. - Ukr. Acad. of Sci., Moscow-Berlin-Sevastopol, p.209-249, (in Russian).
16. Vinogradov, M.E., Sapozhnikov, V.V., Shushkina, E.A. (1992) *The Black Sea ecosystem*, Nauka, Moscow (in Russian).

THE NUTRIENT STOCK OF THE ROMANIAN SHELF OF THE BLACK SEA DURING THE LAST THREE DECADES

A. COCIASU, V. DIACONU, L. POPA, L. BUGA, I. NAE,
L. DOROGAN, V. MALCIU
Romanian Marine Research Institute
300 Mamaia Blvd., 8700, Constantza, ROMANIA

Abstract. Based on systematic hydrographic and nutrient data collected from the Danube between 1980-1995, an onshore station since 1960 and the entire Romanian shelf since 1971, long-term trends in the chemical loads of the Danube to the Black Sea and the nutrient stocks of the shelf have been assessed. The total inorganic nitrogen (IN) and phosphorus (IP) inputs (652,000 and 18,030 tons/y on average, respectively) by the Danube are nearly 3-4 times the total riverine IN and IP influxes to the Mediterranean; but the IN input is comparable with those to the North Sea and Baltic Sea whereas the IP influx is markedly less than the total IP given to the North Sea. Since 1970 the Romanian nearshore water has been enriched in phosphate by industrial discharges (5000 tons-P/y) whose contribution to the chemical stock of the Romanian shelf now is limited relative to the input by the Danube which is known to be one of the severely polluted rivers over the world. In the Romanian shelf region, the silicate and phosphate stocks have decreased slowly since 1974, with an increasing trend in the silicate again in more recent years. The N:P ratio of the shelf water, usually between 20 and 130, is comparable with the large ratios (50-100) observed in the Danube during the last 15 years. Thus algal production on the Romanian shelf should be phosphate-limited.

1. Introduction

The Black Sea, a brackish enclosed basin connected to the Mediterranean via the narrow Bosphorus Strait, receives large volumes of riverine water, which exceed the loss by evaporation [3]. The Danube with an annual water discharge of about 210 km^3, provides nearly 70% of the total runoff to the Black Sea [7]. Therefore, it plays a major role in pumping the `rim current' and the upper layer circulation of the sea.

The investigated Romanian shelf (Figure 1a) with an average depth of about 57m represents about 40% of the northwestern Black Sea shelf area but more than half of the total shelf volume [2]. Because of the large fresh water input, the average salinity of the shelf surface water is nearly 16 and less than that of the open sea. Marked cooling in winter leads to the formation of cold shelf-water, a component of the cold

E. Özsoy and A. Mikaelyan (eds.), Sensitivity to Change: Black Sea, Baltic Sea and North Sea, 49–63.
© 1997 *Kluwer Academic Publishers.*

intermediate layer (CIL) [3,16] which helps transport nutrients from the Danube across the shelf to the open Black Sea.

Large nutrient and organic inputs by the Danube have resulted in intense algal blooms, especially on the Romanian shelf, followed by hypoxia and consequent destruction of - mainly benthic - organisms. A marked decrease in biodiversity - which has also been affected by alien opportunistic species, has been observed [6,10,15].

Drastic changes in the Black Sea ecosystem have prompted the riparian countries to develop comprehensive monitoring and research programs for the better understanding of the damaged marine ecosystem. In this context, the Romanian Marine Research Institute has collected systematic data from the region of the Danube delta since 1980 and on the Romanian shelf since 1970, including daily measurements on the shore since 1960. From these data sets, this report assesses the nutrient stock of the Romanian shelf as well as long-term trends in inorganic nutrient discharged to the Romanian shelf both by the Danube and direct discharges of industrial and domestic waste waters.

2. Data Collection and Processing

Figure 1a shows the locations, in particular the Sulina station on the Danube and the Constantza station on the shore of the Romanian shelf, where water was collected daily during the periods given in Table 1. The water discharged by the Danube was also measured daily. Monthly averages of chemical concentrations were derived from the daily data. Monthly nutrient fluxes to the Romanian shelf by the Danube were calculated from the monthly averages of both chemical concentrations and water flux.

TABLE 1. Period of data sets collected at the Sulina branch of the Danube, Constantza onshore station and Romanian shelf water

Parameter	Constantza	Sulina (Danube)	Romanian shelf
PO_4, SiO_4	1959-1995	1980-1995	1971-1995
NO_3, NO_2	1976-1995	1988-1995	1980-1995
NH_4	1980-1995	1981-1995	1980-1995

Shelf data were collected from the sampling grid of about 20,000 km^2 indicated in Figure 1a. Though, a total of 49 cruises were carried out on the Romanian shelf between 1971 and 1995, data sets from only 29, covering the whole shelf area in Figure 1a, have been utilized in this study.

Chemical constituents in water samples were mostly determined using methods described by Grasshoff et al. [14]. Comparisons of old [1,8,13] and conventional standard methods used in the course of this study were carried out by Cociasu and

colleagues, and insignificant differences were observed, justifying the reliability of long-term data sets.

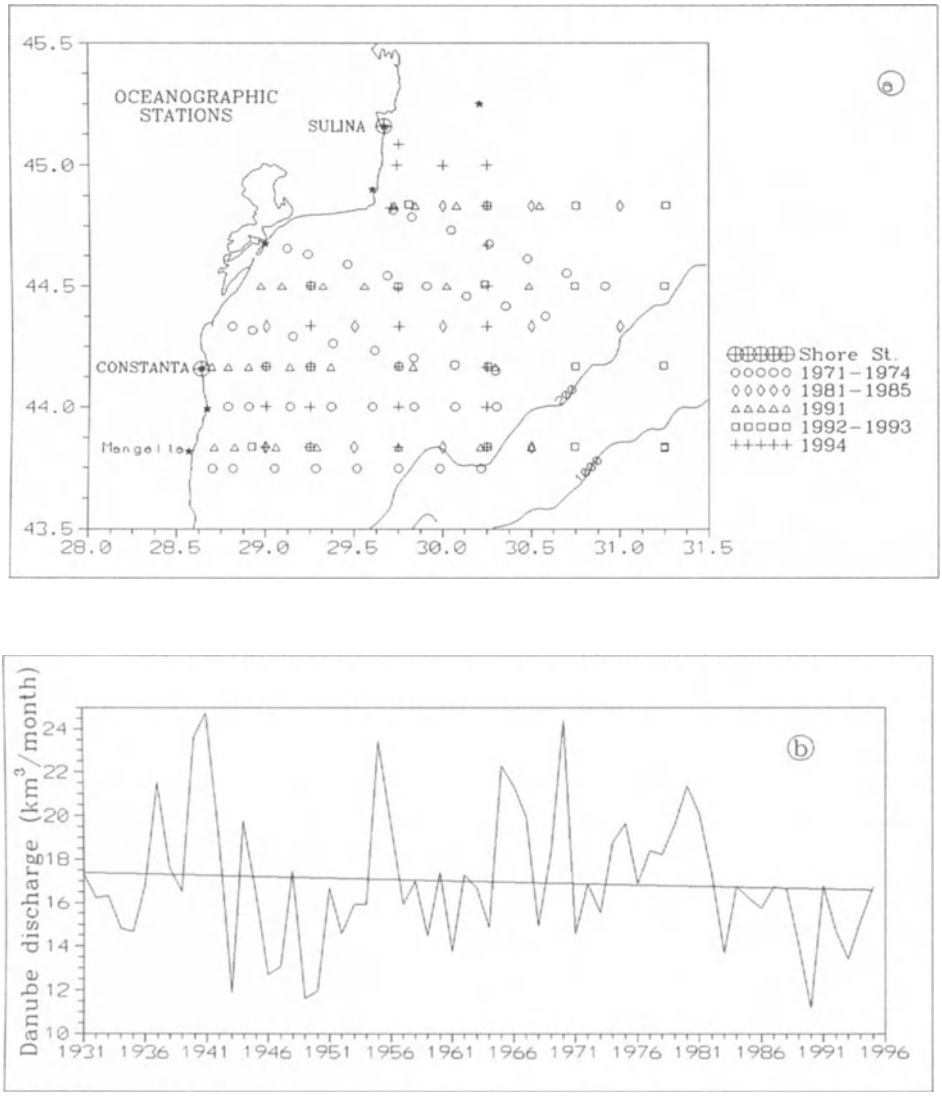


Figure 1. Location map (a) and time evolution of the Danube discharge (b).

The nutrient stock of the shelf water has been computed for each cruise by vertical integration of the concentration, using the trapezoidal rule, at every station. In order to correct for the different station distributions, the results were transferred to the nodes of a rectangular 10 km grid. The total nutrient content was then obtained by horizontal integration using the two-dimensional trapezoidal method.

3. Results and Discussion

3.1. THE DANUBE INPUT TO THE BLACK SEA

Figure 1b, showing the annual water discharged by the Danube into the Black Sea from 1931 to 1995, indicates significant annual fluctuations and some decadal trends, in addition to the expected seasonality (Table 3). These fluctuations, therefore, have a major influence on the nutrient budgets of the western shelf water [12].

The annual means of nutrient concentrations, measured at the Sulina Branch of the Danube since 1980, are depicted in Figures 2 and 3. The phosphate (IP) concentrations measured in the Danube discharge imply a consistent increase during the period of 1980-1990 with some remarkable interannual variations, from levels of 0.8-1.0 μM to 6.5 μM in 1990 (Figure 2a). In this period, three maxima appeared in 1983, 1987 and 1990 during which the Danube flow regime was minimal (Figure 1b). The interannual minima were recorded in 1981, 1984 and 1988, corresponding to a higher flow regime in the Danube. This apparent opposite trend between the water flow and IP concentration of the Danube is most probably the result of dilution of the anthropogenic IP to the Danube by increasing fresh water from its tributaries as observed in the river Elbe during the period 1985-1989 [17]. Since 1990, IP content of the Danube discharge has decreased steadily from its peak value of 6.5 μM to about 2.0 μM in 1993-1995. This is still nearly 3 times the minimum concentration (0.8 μM) observed in 1981. The mean of the annual IP concentrations for 1980-1995 is 3.3 μM.

Contrary to the IP trend, the annual averages of silicate (Si) concentrations ranged merely between 55 and 70 μM during 1980-1989, with a mean value of about 65 μM (Figure 2a). A sharp interannual minimum and maximum observed in 1990 and 1991 respectively coincide with similar trends in the Danube flow regime (Fig 1b). After 1991, Si concentration declined dramatically to its lowest observed value of 30 μM in 1994-when the phosphate and ammonia values were also at their minimum levels as the nitrate+nitrite (NO_X) continued to decrease. In 1995 the Si concentration has increased again to over 50 μM. Ignoring the annual changes, the long-term trend suggests a systematic decrease of 1.0 μM Si per year in the Danube water.

Again, significant interannual changes have been observed in the ammonia concentrations since 1981, levels being much less than the NO_X measured in the Danube discharge since 1988. The highest values were 18.4, 19.7, 15.9 μM in 1981, 1982 and 1987, respectively, followed by a small maximum of nearly 10.8 μM in 1989. If the two maxima in the late 80's are excluded, a nearly ten-fold decrease in the ammonia content of the Danube is obvious during the period of 1981-1994 (Figure 3a). However, in 1995, as for Si, the ammonia concentration increased again over to 8 μM whereas the NO_X and IP have sustained their lowest concentrations in the Danube discharge. The NO_X values obtained between 1988-1995 ranged from 326 μM in 1989 to 176 μM in 1995, indicating a significant and continuous decrease since 1989 (Figure 3a). Comparison of ammonia and NO_X data reveals that NO_X dominates (>95%) the total inorganic nitrogen (TIN) in the Danube discharge. The annual nutrient loads, derived from the monthly averages of concentrations and the water

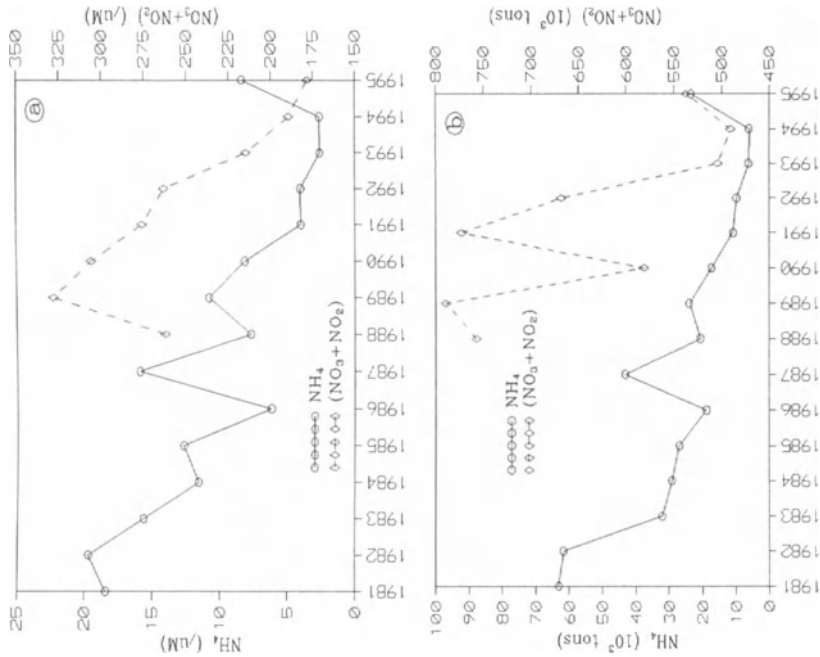


Figure 3. Annual averages of the NO_3+NO_2 and NH_4 concentration (a) and discharge cycles (b) at Sulina station

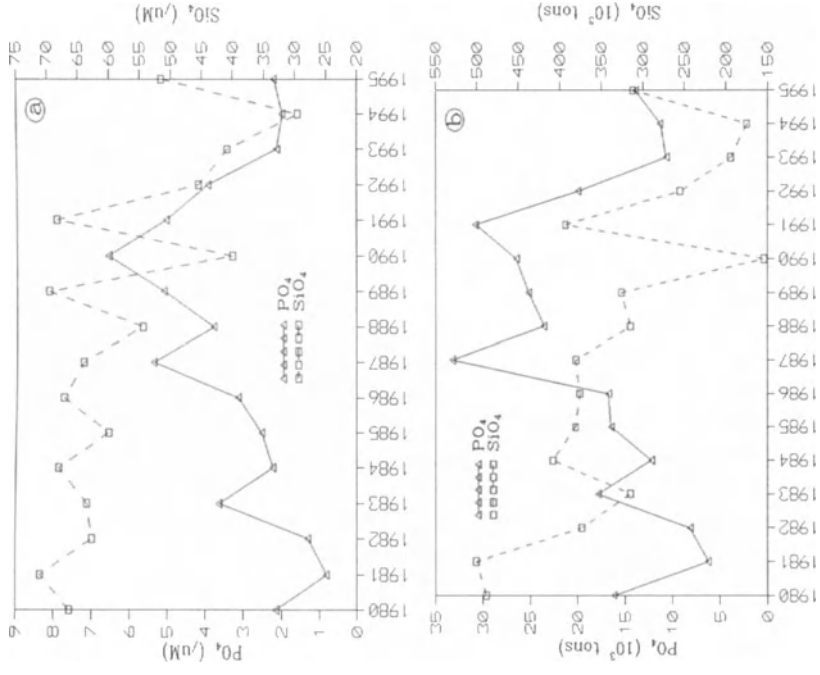


Figure 2. Annual averages of the phosphate and silicate concentration (a) and discharge cycles (b) at Sulina station

fluxes, also display interannual changes (Figures 2b, 3b). In particular, since the minimum discharge of water in 1990 (Figure 1b) coincided with the minimum in Si concentrations (Figure 2a), a dramatic decrease appeared in the Si input (154,000 tons/y) to the Black Sea by the Danube. During the last 15 years, the annual input of Si decreased from 500,000 tons in 1980-1981 to 175,000 tons in 1994. However, the decrease was discontinuous, the changes being very steep in both the early 80's and 90's due to concurrent decreases both in the volume and the concentration. The average annual discharge of Si by the Danube for the 1980-1995 period was 336,000 tons, a half of the estimated Si input before 1970 [1].

On the other hand, the annual IP load, ranging between 6,200 tons in 1981 and 33,200 tons in 1987, displays a similar trend to the concentration because the annual variation in the IP concentration generally exceeded the changes in the water flux. The annual average IP load for the whole 1980-1995 period was nearly 18,000 tons, which is about 50% greater than the flux in 1960 [1], and much larger than those (12,000 tons) in the three most recent years due probably to reduction in the consumption of phosphate-based fertilizers in the drainage area of the Danube.

The changes in annual input of ammonia by the Danube parallel the corresponding concentrations, indicating a net decrease during the last 15 years. The annual loads discharged in recent years (6,100-6,200 tons) are about ten times smaller than the maximum discharges, nearly 60,000 tons, in the early 1980's. In fact the discharge declined nearly 2 fold in 1983, then more slowly till the end of 1994 - save for the one exceptional maximum in 1987.

The NO_X input from the Danube, obtained in 1988-1995, ranged between 490,500 tons/y in 1994 and 789,300 tons/y in 1989, yielding an annual average of 638,000 tons for this period. Since NO_X concentrations are much higher than those of ammonia in the Danube, NO_X has always dominated the TIN input by the Danube. This TIN load (652,000 tons/y, on average) is in good agreement with that given by Cociasu et al. [11] but is 4 times higher than previous estimates [1].

In addition to the remarkable annual changes, there exists a prominent seasonal variation in both the chemical concentrations and the loads of the Danube discharge (see Table 3). For instance, the concentrations decline smoothly from winter-spring to summer-autumn. The lowest IP and Si concentrations were observed in late summer and early autumn, respectively. Such a time lag of about 2 months may have been the result of differences in biological uptake and regeneration rates of nutrients by different planktonic species both in the Iron Gate dam waters and perhaps in downstream of the Danube. NOx displays its maximum concentrations in March as the water flow is still increasing, whereas the Si maximum appears in the winter months.

Similarly the Si and IP input by the Danube decreases steadily during the period of spring to late summer; the maxima in April (Table 3) are the result of the marked seasonal changes both in the water fluxes and in the chemical content of the Danube; monthly water flow is as large as 23.2 km^3 in April, decreasing to 10.9 km^3 in September. Briefly, the maximum NO_X and Si inputs are as large as 3-4 times the summer-autumn influxes whereas the seasonality in the IP load is less pronounced.

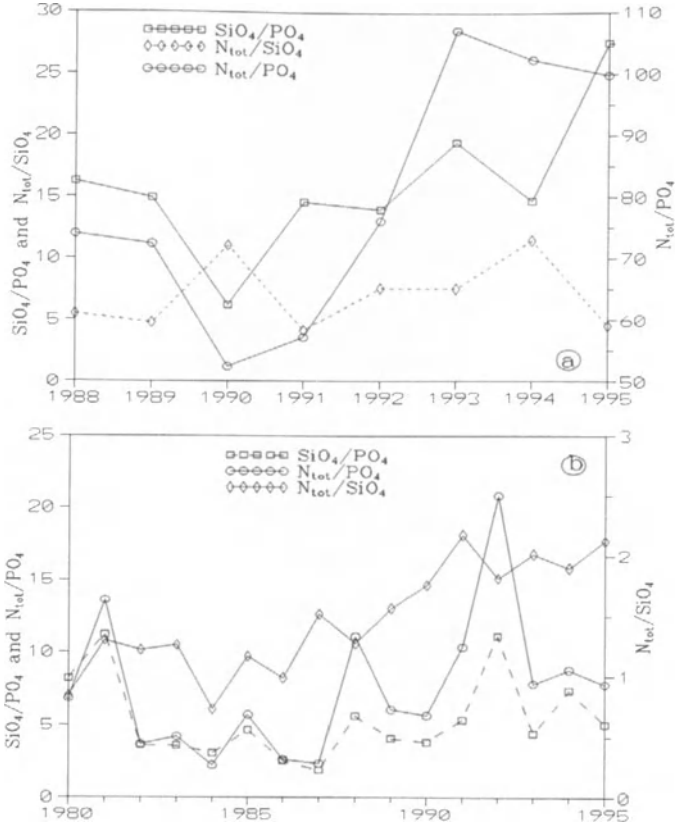


Figure 4. Annual averages of the nutrient ratios at Sulina (a) and Constantza (b) stations

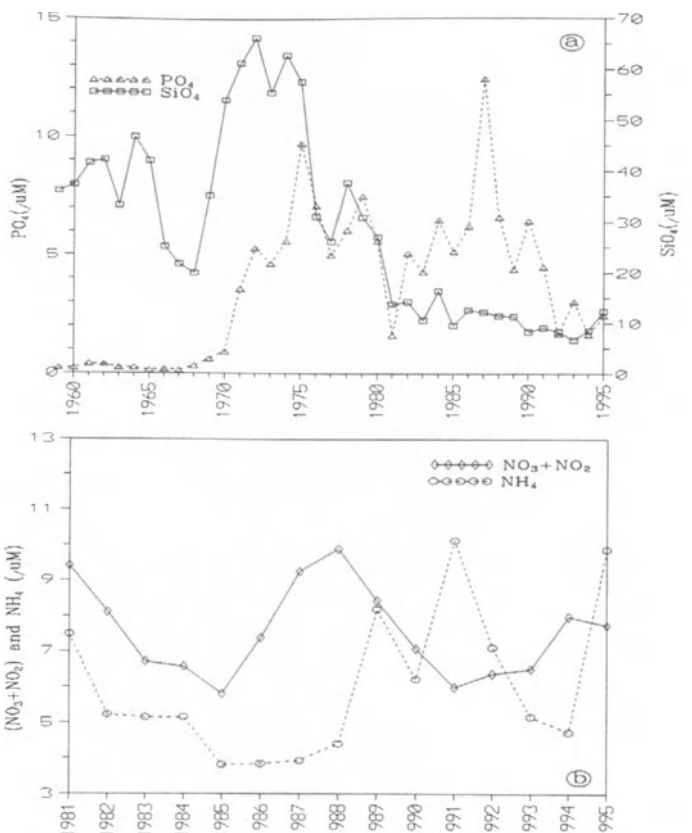


Figure 5 .Annual averages of the phosphate and silicate concentration (a) and NO_3+NO_2 and NH_4 concentrations (b) at Constantza station.

The present nutrient data permit us to estimate their molar ratios and their seasonality in the Danube. As shown in Figure 4a, during the last eight years the N:Si ratio has ranged merely between 5 and 11, with a mean value of 7. The annual averages of the Si:P ratio were mostly in the range of 15-20, with the exception of a marked decrease in 1990 and an increase in 1995. On the other hand, the N:P ratios, always higher than 50, increased remarkably after 1990 due to a net decrease in the IP content of the Danube (Figure 2a) rather than to the increase in inorganic nitrogen. The N:P and Si:P minima in 1990 were the result of the maximum IP concentrations being measured in the Danube which had its lowest water discharge in that year.

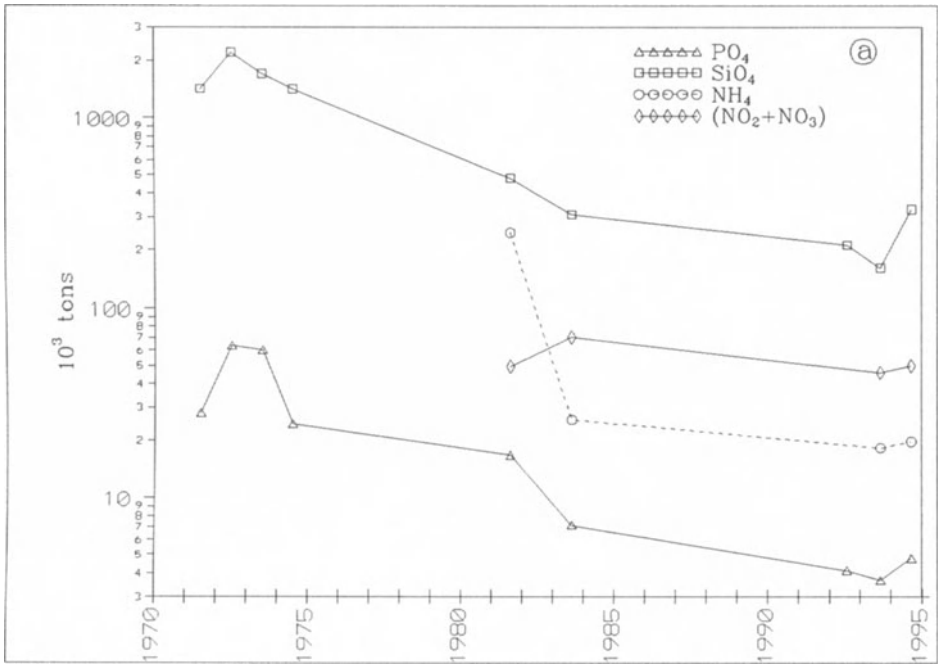
3.2. NUTRIENTS IN THE ONSHORE WATERS

Figures 5a and 5b show the annually-averaged concentrations of nutrients in Romanian onshore waters from 1959 to 1995. The IP concentrations increased sharply after 1970 when a fertilizer plant started discharging its wastewater into the very shallow coastal water 12 km beyond Constantza. This P-rich waste has also markedly modified the N:P ratio in the Constantza onshore water, which is less than in the Danube (Figure 4b). Similar low values relative to those in the Danube have been recorded for both Si:P and N:Si ratios due to excessive utilization of inorganic nitrogen during non-diatom production.

The mean IP concentrations ranged from 0.13 to 0.92 μM between 1959 and 1970 (average 0.33 μM). After 1970 when P-rich waste discharged into the region, the IP content of the nearshore waters increased dramatically [9], reaching 9 μM in 1975 and 12 μM in 1987 (see Figure 5a), with a marked minimum of 1.6 μM in 1981. With the beginning of wastewater treatment in 1975 and subsequent improvement in 1987, a noticeable decreasing trend has been recorded in the IP content of the onshore waters since 1988. Accordingly, in recent years the concentrations have been in the range of 1.6-3.0 μM.

Long-term changes in the mean Si content of the Romanian onshore water differ totally from the changes in IP concentrations and appear to be related to the decreasing trend in the Si content of the Danube (see Figures 2a and 5a). Annual averages, ranging between 33 and 46 μM in 1960-1965, dropped to minimal levels of 19-25 μM in 1966-1968 and then increased again to peak values of 54-66 μM during 1970-1975. After the construction of the Iron Gate dam on the Danube in 1974 a consistent and significant decrease was observed in the Si content of the Constantza coastal waters between 1975-1980 (Table 3). However, during the last 15 years the onshore water concentrations have changed merely between 6.7 and 16.4 μM, yielding an average value of 11.0 μM for this period. The average linear change in the annual mean concentrations of these two nutrients are 0.15 μM/y for IP and -1.1 μM/y for Si, but their statistical significance is low.

The annual means of TIN concentrations in the onshore waters have also shown considerable variation since data were first collected in 1981 (Figure 5b). Between 1981-1990 the NO_X concentrations slightly exceeded the ammonia values; both concentrations decreased from 1980 till 1985. Then the mean NO_X concentration



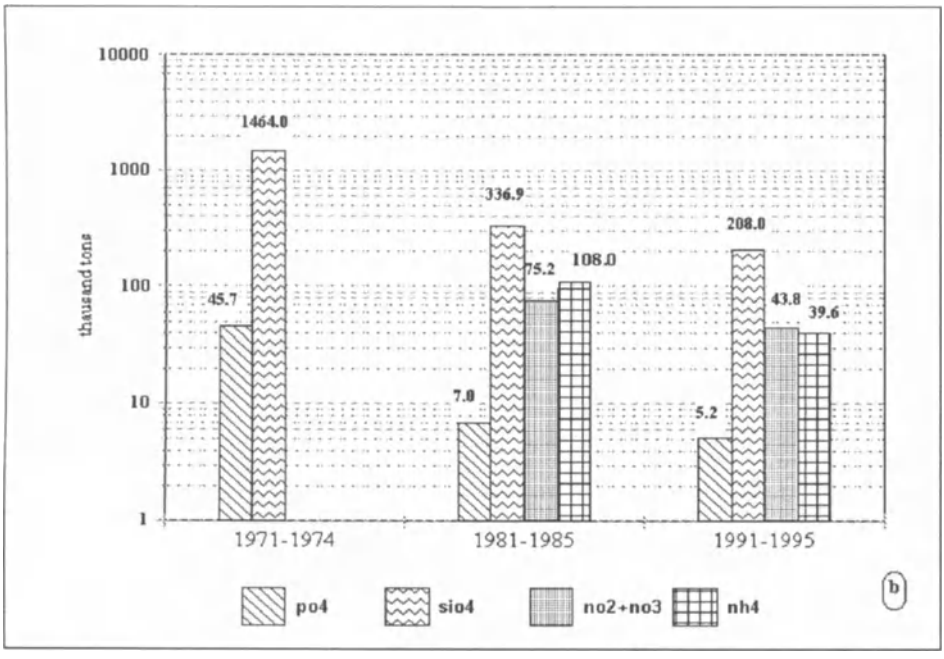


Figure 6. Time evolution of the nutrient stocks on the Romanian shelf.

increased again to peak values of 9-10 μM in 1987-1988 though no marked change was observed in ammonia. However, between 1989 and 1991 the NOx decreased whilst the corresponding ammonia concentrations generally increased. Subsequently the NO_x concentration increased till 1995 during which time the ammonia concentration of the onshore waters occasionally exceeded the corresponding NO_x values.

3.3. NUTRIENT STOCK OF THE ROMANIAN SHELF

Various interacting processes control the spatial and temporal distribution of the inorganic nutrients in the Romanian shelf waters. The major external factors are riverine (mainly the Danube) and the effects of wastewater discharges. The internal parameters are the lateral and vertical mixing of water masses and the circulations, and the intensities of biological activity both in the water column and in the benthic layer. Accordingly, one expects marked spatial and temporal variations in the labile chemical properties of the shelf waters of the western Black Sea.

The long-term changes in the total inorganic nutrient stock of the Romanian shelf, derived from summer data, can be realized from Figure 6. Though there was no measurements from the summer of the late 70's and late 80's, Comparison of the existing data indicates a semi-decadal decrease in the IP and Si stocks of the region from the early 70's (before the Iron Gate dam) to the early 80's (after the dam). During this period, the Danube discharge (see Figure 1b) and the Si content of the river decreased. Though IP data from 70's were very limited, it has been suggested a net increase in the IP input to the shelf water from the Danube during the last two decades [15]. Contrary to the trend in the Danube input, a long-term (semi-decadal) decrease has been observed in the IP stock of the shelf, most probably originating from large increases in the TIN input by the Danube and thus large N:P ratios in the riverine inflow since 1980's.

The largest summer IP stock of the Romanian shelf region was determined in the early 70's. It increased from about 20,000 tons in 1971 to peak values of 63,900-60,500 tons in 1972-1973 when the shelf water contained average concentrations of 1.62-1.53 μM. This maximum was nearly one order of magnitude greater than the minimum stock of 3,700-4,100 tons estimated in the early 1990's when both the Danube flow regime and its IP concentration were at minimal levels (see Figures 1b and 2a). Comparison of the Danube inflow and the IP stock of the shelf reveals that the fluctuations in the nutrient loads of the Danube and thus the ratios of labile nutrients in the riverine inflow dominate the inorganic nutrient stock of the Romanian shelf.

The silicate summer stock of the shelf has also declined significantly in the last two decades from nearly $2x10^6$ tons in 1972 to a level of $2x10^5$ tons in the early 90's (Figure 6a). On the other hand, in 1970's interannual changes in the Si stock of the shelf were not as large as in the IP. The Si stock in 1980's was comparable with that in 1990's (see Figure 6a), indicating an insignificant long-term change since 1980's. However, before the completion of the Iron Gate dam in 1974, the Danube discharge introduced more silicate to the shelf as also suggested recently by Cociasu et al. [11]. Since 1970's the nutrient content of the shelf waters has decreased markedly (by 7 to

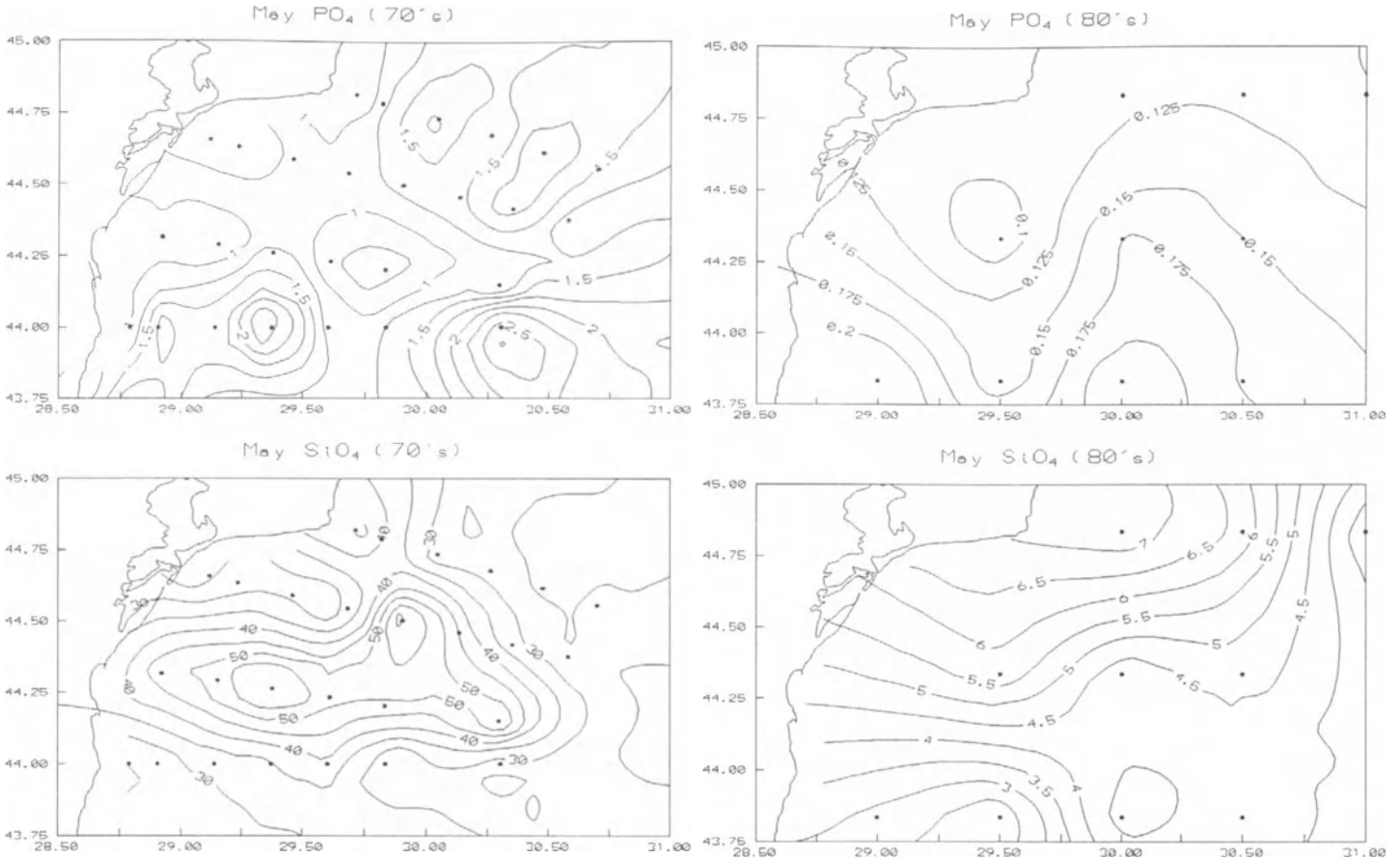


Figure 7. Average surface distribution of PO_4 and SiO_4 in May 70's and 80's.

10-fold). For instance, the post-spring Si concentrations in the surface waters of the shelf were as high as 30-50 μM in the 1970's and decreased to levels of 3-7 μM in the 80's (Figure 7). A similar decadal trend was recorded in the IP concentrations of the surface shelf waters, declining from 1-2.5 μM in the 70's to 0.1-0.2 μM in May of 80's.

Unfortunately no data on NO_X and ammonia concentrations in the Danube are available from the 70's. However, limited winter NO_X data from the Constantza onshore station obtained in the 60's [8] strongly suggest that the TIN content of the Danube and thus of the shelf waters increased markedly in the early 1980's, leading to similar changes in the inorganic nitrogen stock of the shelf. As clearly shown in Figure 6a, ignoring the data from 1981, the summer NO_X stock of the Romanian shelf water are consistently larger than that of ammonia. Limited summer data imply insignificant long-term change in the TIN stock of the shelf during the last 15 years. Nevertheless, in the early 1980's the ammonia stock of the shelf displayed a drastic decrease from 247,000 tons in summer, 1981 to 25,800 tons in 1983 (Figure 6a), probably originating from a decline in Danube discharge, and in the riverine TIN input to the shelf in this period (Figures. 1b and 3b). The NO_X summer stock of the shelf varied merely between 49,600-70,300 tons in 1981-1983 and 45,900-49,900 tons in 1993-1994 (see Figure 6a). Long term data indicate that in the early 80's the TIN stock of the Romanian shelf water was twice larger than the average for the recent period. (Figure 6b).

TABLE 2. Estimates of the molar nutrient ratios in the Romanian shelf waters at surface water and 75m depth.

	1981-1985		1991-1994	
Ratio\Depth	surface	75m	surface	75m
N:P	20-130	18-138	34-61	36-61
Si:P	26-167	22-167	16-66	14-53
N:Si	0.4-5.0	0.4-6.0	1.0-5.0	0.1-4.0
NO_X:NH_4	0.1-12.0	0.2-13.0	0.7-4.0	0.7-4.0

Molar ratios of inorganic nutrients over the Romanian shelf displayed great seasonal variability. Data compiled from measurements in the surface water and at 75m are given in Table 2. In the surface water, the N:P ratio has generally ranged between 20 and 130, with exceptionally high values of 435-715 in May of 1982 and 1983 (the post-bloom period in the region) indicating phosphate-limited algal production. Interestingly, the N:P ratios at 75 m depth, ranging from 18 to 138, were much larger than the conventional Redfield ratio. The seasonality in the N:P ratio was much larger in 1981-1985 than in 1991-1994 during which the Danube flow regime displayed less annual fluctuations (see Figure 1b). The NO_X:NH_4 ratios usually exceeded unity, though unexpectedly low ratios were observed throughout the entire water column in the late summer-autumn of 1981 due to the development of hypoxia (DO<100 μM) in the near bottom waters of the shelf [10]. Similar temporal variations were also recorded in the Si:P and N:Si ratios. interestingly, the variability in the ratios of 75m was as large as those appeared in the surface waters.

Table 3. The mean annual cycle of the nutrient parameters

PAR.	Period	Jan.	Feb.	Mar.	Apr.	May	Jun.	Jul.	Aug.	Sep.	Oct.	Nov.	Dec.
						Danube nutrient discharge (thousand tons)							
$Q(km^3)$	1980-1995	16.6	14.9	17.4	23.0	22.8	20.2	16.2	12.7	10.5	10.9	12.1	14.6
PO_4	1980-1995	1.9	1.6	1.8	2.2	2.1	1.5	1.1	1.0	1.0	1.0	1.2	1.5
SiO_4	1980-1995	35.0	30.5	35.7	38.8	36.3	28.7	23.7	16.3	10.1	16.2	19.6	29.5
NO_x	1988-1995	55.4	46.4	70.1	89.4	78.6	67.1	51.2	30.7	27.2	32.5	33.9	46.3
NH_4	1981-1995	4.8	2.2	2.8	1.8	2.1	2.1	1.3	1.3	0.9	2.0	1.6	2.4
ΣN	1988-1995	57.1	47.1	71.3	90.3	80.0	63.4	52.6	32.0	35.1	33.8	35.0	47.7
						Nutrient concentrations at Sulina station (μM)							
PO_4	1980-1995	4.1	3.9	3.6	3.4	3.0	2.4	2.1	2.6	3.3	3.4	3.4	3.9
SiO_4	1980-1995	75.4	74.3	68.8	59.9	55.2	47.3	47.6	40.4	29.9	48.3	56.6	68.8
NO_x	1988-1995	267.4	282.9	334.6	322.9	276.6	251.8	231.1	202.8	197.3	219.1	199.2	219.6
NH_4	1981-1995	19.0	10.1	11.1	5.2	6.8	7.0	5.4	7.2	5.0	13.0	10.6	14.3
ΣN	1988-1995	276.2	287.7	340.6	326.0	282.3	238.8	236.5	202.4	225.8	227.8	206.1	227.1
						Nutrient concentrations at Constantza station (μM)							
PO_4	1959-1969	0.4	0.3	0.3	0.1	0.1	0.2	0.2	0.2	0.2	0.3	0.4	0.5
	1970-1995	7.0	6.9	5.6	3.9	2.8	3.0	3.3	4.9	6.5	6.7	6.2	4.9
SiO_4	1959-1974	55.6	56.7	56.0	38.0	37.1	31.7	33.1	35.2	37.5	37.3	43.2	50.3
	1975-1995	25.0	25.8	21.1	17.2	15.7	14.3	15.3	13.7	14.6	15.7	17.2	19.9
NO_x	1976-1995	12.6	14.7	14.9	11.3	10.5	6.4	4.8	5.3	5.8	7.3	9.8	10.5
NH_4	1980-1995	7.3	6.7	5.5	5.9	6.0	5.4	7.2	5.8	6.2	7.0	7.0	7.3
ΣN	1980-1995	17.0	17.1	16.7	16.2	15.4	10.2	11.7	10.4	10.9	13.5	15.2	15.3

4. Conclusions

Monthly and long-term changes in the nutrient load of the Danube have originated from the variation in both the flow of water and in the concentrations of nutrients borne by the flow. The water and chemical influxes by the Danube have displayed a decreasing trend in recent years. The nutrient content of the Danube is comparable with the polluted rivers, Rhine, Rhone, Elbe, and Po, whereas its Si concentrations are much less than the average value of 175 μM for the world's rivers [5], indicating a decrease of more than 100 μM since 1974.

The annual discharge of IP by the Danube is about 18,000 tons for 1980-1995, which is about 50 % greater than the flux in 1960 [1]. The TIN input from the Danube for 1988-1995, ranging annually between 500-800 thousand tons, is 4 times higher than previous estimates [1]. During 1988-1995, NO_X comprised nearly 97% of the TIN input from the Danube. The TIN and IP inputs by the Danube are nearly 3-4 times the total riverine IN and IP influxes to the Mediterranean. TIN input is comparable with those to the North Sea (about 650,000 tons/y) and Baltic Sea whereas the IP influx is markedly less than the total IP (50-80,000 tons/y) flux to the North Sea [17].

The Romanian coastal water has been enriched in phosphate not only by the Danube but also by the discharge of (mainly) industrial wastes (400 tons/month). The contribution of waste to the IP stock of the offshore (shelf) waters is now limited in comparison with the Danube input (1000-2200 tons/month, see Table 3). The IP concentrations of the Romanian shelf surface waters in the last 15 years are about 3-7 times less than the those measured before 1974, though an opposite trend has appeared in the onshore waters due to direct waste discharges. The construction of the Iron Gate dam on the Danube and the excessive utilization of silica by diatoms have caused great reductions in the silicate concentrations of the Romanian shelf waters since the 1980's.

During the last two decades the phosphate and reactive silicate stocks of the Romanian shelf region (comprising nearly 40% of the total northwestern shelf) have decreased slowly. In contrast to the low Redfield ratios in the Constantza onshore water, the N:P ratio of the entire shelf surface water ranged between 20 and 130, being consistent with those (50-100) of the Danube. Large N:P ratios in the shelf waters strongly suggest phosphate-limited algal production in the Romanian coastal region. Similar anomalous N:P ratios determined in the near bottom waters of the Romanian shelf where the cold intermediate water layer (CIL) evolves with large nitrate but low phosphate concentrations as also emphasized in Basturk et al. [4].

5. Acknowledgment

The authors express special thanks to Dr. S. Tugrul and Dr. A. Gaines for their suggestions and help in revising the final form of the manuscript.

6. References

1. Almazov N. M. (1961) Stok rasverennykh solej I biogennykh veshchestv kotorye vynoseatsya rekami SSSR v Chernom More, *Naukovi Zapisi Odess. Biol. St.*, **3**, pp. 99-107.
2. Altman E. N. (1990) Osnovhye cherty gidrometeorologicheskaya rezhima I gidrologii bassejna, in V.P. Keondjan, A.M. Kudina and Yu. V. Terekhina (eds.), *Practical ecology of the marine regions: Black Sea*, Naukova Dumka, Kiev, pp. 11-33.
3. Andrianova O. R. and Ovchinnikov I. M. (1991) Osobennosti transformatsii raspresnennykh vod v zapadnoj chasti Chernogo Morja, *Meteorology and Hydrology*, **7**, pp. 74-79
4. Basturk O.,Tugrul S., Salihoglu I.,Konovalov S. (1995) Variations in the vertical chemistry within three hidrodynamically different regions of the Black Sea. *Sensitivity of North Sea, Baltic Sea and Black Sea to anthropogenic and climatic changes.* Varna, 14-18 November.
5. Bennekom A. S. , Salomons W. (1980) *River inputs to Ocean System* . Joint copyright UNEP and UNESCO, pp. 33-51.
6. Bodeanu N. (1992) Algal blooms and development of the main phytoplanktonic species at the Romanian Black Sea littoral in conditions of intensification of the eutrophication process. *Science of the Total Environment, Supplement*, pp. 891-906.
7. Bondar C., State I., Cernea D., and Harabagiu E . (1991) Water flow and sediment transport of the Danube at its outlet into the Black Sea, *Met. and Hydrol.*, **21**, 1, pp.21-25.
8. Chirila V. (1965) Observatii asupra conditiilor fizico-chimice ale Mării Negre la Mamaia în anii 1959-1960. In *Ecologie marină* I , pp. 139-185. Editura Academiei Republicii Socialiste Romania,Bucuresti.
9. Cociasu A. and Popa L. (1980) Observations sur l'evolution des principaux parametres physico-chimiques de l'eau marine de la zone de Constanta, *Rech. Mar.*, **13**, pp.51-61.
10. Cociasu A., Popa L., Dorogan L. (1983) Modification survenues dans la dynamique de l'oxygen des eaux marines littorales Roumaines. *Cercetari marine*, **16**, pp. 39-54.
11. Cociasu A., Dorogan L., Humborg C. and Popa L. (1996) Long term ecological changes in Romanian coastal waters of the Black Sea, *Marine Pollution Bull.*, **23**, 1, pp. 32-38
12. Dorogan L., Popa L., Cociasu A.and Voinescu I. (1985) L' apport de sels nutritifs des eaux du Danube dans la Mer Noire, *Rapp. Comm. int Mer Medit.*, **29**, 7, pp. 57-59.
13. Ghidrometeoizdad (1959) *Rukovodstvo Po Morskim Ghidronimiceskjm Issledovaniam.* Hydrometeorological Publication Series, Kiev.
14. Grasshoff K., Erhardt M., Kremling K. (1976) *Methods of the Sea Water Analysis*, 314 pp. Verlag Chemie, Weinheim.
15. Mee L. D. (1992) The Black Sea in a crisis. A need for concerted international action. *Ambio* , **21**, 4, pp. 278-285.
16. Ovchinnikov I. M. and Popov Yu. I. (1987) Formirovanie kholodnogo promezhutchnogo sloja v Chernom More, *Oceanology*, XXVII, 5, pp. 739-746.
17. Skjoldal H. (1993) *Eutrophication and algal growth in the North Sea.* Symposium "Mediterranean Seas 2000", pp. 445-487.

DISTRIBUTION AND FLUCTUATION OF DOMINANT ZOOPLANKTON SPECIES IN THE SOUTHERN BLACK SEA IN COMPARISON TO THE NORTH SEA AND BALTIC SEA

U. NIERMANN[1] and W. GREVE[2]
[1]*Institute of Marine Sciences, PO. Box 28, 33731 Erdemli / IÇEL, Turkey;*
[2]*Biologische Anstalt Helgoland, Notkestr. 31, 22607 Hamburg, Germany*

Abstract. The fluctuation of dominant pelagic species >300µm (copepoda, chaetognatha, scyphozoa, ctenophora and ichtyoplankton) of the southern Black Sea were compared with that of dominant species of the North Sea and Baltic Sea. In all three seas similar changes in the zooplankton compositon took place in end of the 1980's, beginning of the 1990: - decreasing or increasing abundances of certain species, - occurrence of new species (North Sea: *Muggiaea atlantica* Lusitanean fish species; Black Sea: *Mnemiopsis leidyi*), - changes of the blooming period of certain species, which starts earlier and last longer, - high interannual fluctuations of some species, which were obvious since end of the 1980's. The changes in the zooplankton of all three seas could be related to a rise in temperature during 1988/89 (North Sea, German Bight: sudden rise in the annual average temperature and salinity during 1988/89; Baltic Sea, Kiel Bight: rise in the temperature of the subthermocline water during 1988/89; Black Sea: extraordinary cold winter 1987/88 followed by an extraordinary warm winter during 1988/89. It was concluded, that the changes in the zooplankton community since end of 1980's in the Black Sea, North Sea and Baltic were triggered in all probability by climatic variability.

1. Introduction

The Black Sea, North Sea and Baltic Sea faced similar environmental problems since 1960 [40], [Zaitsev, this volume], as high fishery exploitation, eutrophication, oxygen deficiencies, which led to changes in marine communities [23],[4],[11]. The outburst Ff the accidentally introduced species *Mnemiopsis leidyi* 1988 [37],[39],[18] and the collapse of the anchovy fishery during 1989 [4] draw the attentions of many researchers to the Black Sea. The Institute of Marine Sciences started the investigation and monitoring of zooplankton and ichthyoplankton in the southern Black Sea in June 1991.

E. Özsoy and A. Mikaelyan (eds.), Sensitivity to Change: Black Sea, Baltic Sea and North Sea, 65–77.
© 1997 *Kluwer Academic Publishers.*

This paper attempts to trace some common features of the distribution and fluctuation of dominant zooplankton (>300 μm) in the southern Black Sea in comparison with the fluctuation of same or similar species in the North Sea and Baltic Sea. To compare the abundances of the species in the different seas is difficult, since the numbers and biomasses of the species are strongly dependent on the methods of collecting. In the southern Black Sea the zooplankton was collected by vertical Hensen Net (mesh size 300 μm, opening diameter: 0.7 m) hauls from the anoxic layer to the surface.

2. Zooplankton Species

The considered dominant zooplankton species (>300μm) occurring in the southern part of the Black Sea are shown in Figure 1. The species, which are living most time above the thermocline are placed in the upper part, the species living most time below the thermocline are drawn in the lower part of Figure 1.

These species, *Sagitta setosa*, *Pleurobrachia pileus* and the copepods *Pseudocalanus elongatus*, *Calanus euxinus* and the North Sea *C. finmarchicus*, display diel vertical migrations [36]. During night these species are concentrated in the upper water, mostly just below the thermocline. In the early morning the species migrate down to the deep layers, stay there during day and rise again to the surface in the late afternoon / early evening. During day these species are concentrated in a narrow horizon just above the HS_2-layer in depths between 80 - 150 m with oxygen concentrations between 0.4-0.5 ml O_2 l^{-1}.

Many species, occurring in the Black Sea occur in the North Sea and Baltic Sea as well. Some Black Sea species are represented in the other seas by species of the same genus with similar behaviour. Due to the low salinity many zooplankton species occurring in the Black Sea and in the North Sea are not present or very rare in the Baltic Sea. Many species are present only in the south western more saline area with a salinity S > 7 [1]. Other species, which are dependent on a higher salinity, serve as indicator species for an inflow of higher saline North Sea water and are distributed only in the southern part of the Baltic Sea.

Four species of gelatinous animals are common in the Black Sea: two scyphozoans, *Aurelia aurita* and *Rhyzostoma pulmo* and two ctenophores, *Pleurobrachia pileus* and *Mnemiopsis leidyi*. While *Rhyzostoma pulmo* is most common in coastal areas, the three other species are distributed in all parts of the Black Sea [37]. *Mnemiopsis leidyi*, which originated from eutrophic lagoons in North America, was accidentally introduced into the Black Sea in the mid 1980's and affected radically the entire pelagic fauna of the Black Sea [37],[39],[4],[25]. *Aurelia aurita* is a very common jelly fish in the Black Sea and Baltic Sea, but is rare in the North Sea, where it is controlled by the jelly fish *Chrysaora quinquecirrha*. *Pleurobrachia pileus* exhibits a single dominant population maximum in the German Bight (North Sea) from mid of May till the end of June [13]. In the Baltic Sea the occurrence of *Pleurobrachia pileus* is strongly dependent on the inflow of North Sea water. In the Kiel Bight the variations

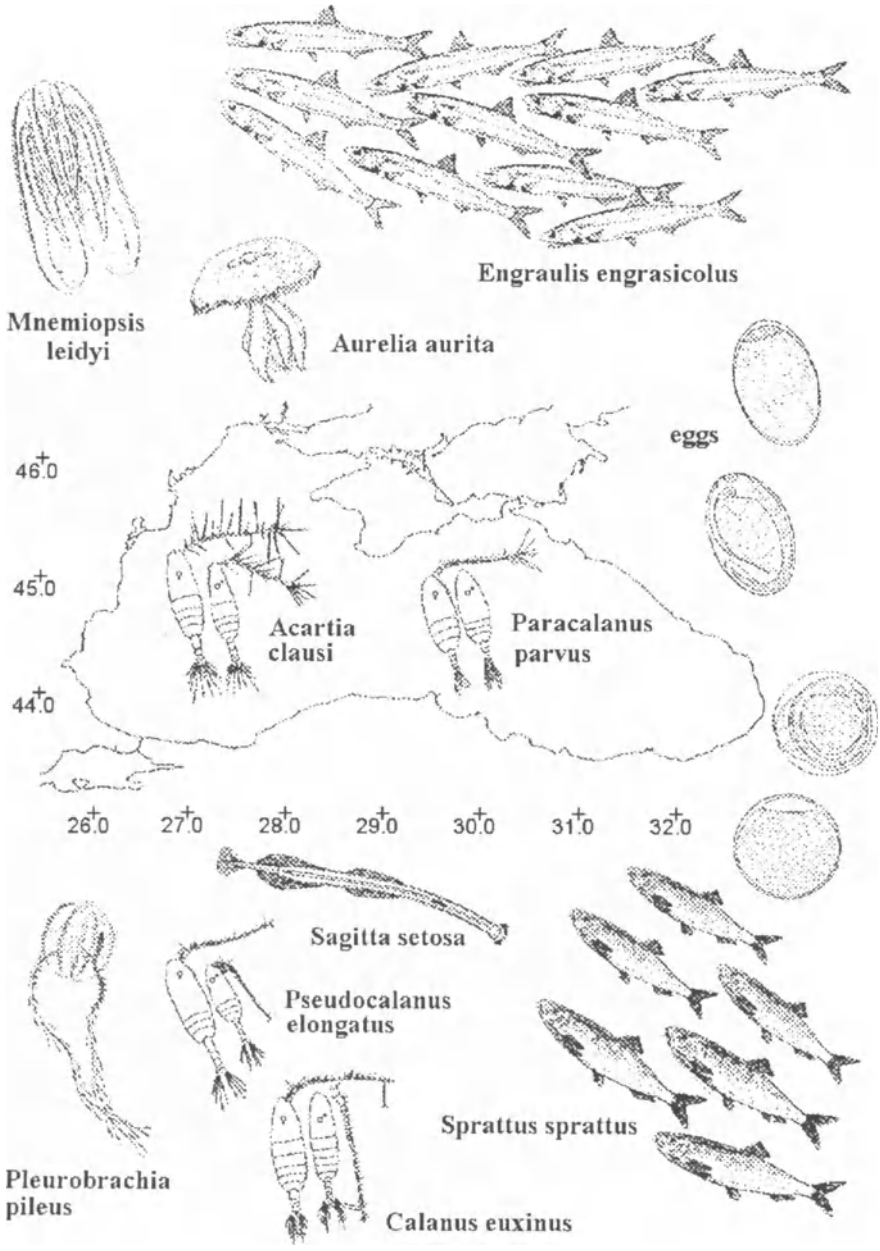


Figure 1: Dominant species (>300μm) of the southern Black Sea

of the ctenophore stock are primarily caused by advection and did not reflect the biological population cycle of this species [34].

Apart from *Oithona nana*, a species which is to small to be caught with a 300 µm gauze, *Acartia clausi* is one of the most abundant copepod species in the upper water layers of the Black Sea. The blooming period is during midsummer all 3 enclosed seas under concideration [37],[3],[19]. *Centropages kröyeri* (*ponticus*) and the cosmopolitan species *Paracalanus parvus* are typical species of the upper layer. They are not very common species in the southern Black Sea, occuring only in low numbers during summer [10]. In the North Sea *Paracalanus parvus* is very abundant in the central North Sea and in the coastal waters of Netherlands and Germany [19]. The distribution of *Paracalanus parvus* in the Baltic Sea is restricted to the south western part dependent on the salinity [1]. Below S = 7.8 this species does not occur. *Centropages kröyeri* does not occur in the North Sea and Baltic Sea. In the North Sea the genus is represented by the species *C. hamatus* and the Atlantic species *C. typicus* [19]. In the Baltic Sea *Centropages hamatus* occurs in low abundance in areas with a salinity S > 7 [1],[35].

Calanus euxinus exhibits the highest biomass of all copepod species in the Black Sea. In the North Sea *Calanus euxinus* is replaced by *C. finmarchicus* and *C. helgolandicus*. *C. finmarchicus* is very common in the deeper northern North Sea, while *Calanus helgolandicus*, a summer/autumn species, occurres mainly in the southern more shallow areas [19].

Pseudocalanus elongatus, a cold water species, with a upper temperature limit of occurrence of about 13°C is very common in the whole Black Sea and in the North Sea. In the low saline Baltic Sea this species acts together with *Calanus finmarchicus* and *Calanus helgolandicus* as indicator of inflows of higher saline North Sea water into the Baltic Sea [1],[34].

The chaetognath *Sagitta setosa* is the dominant chaetognath species in the Black Sea with a peak occurence in July/August. In the North Sea the peak bloom of *Sagitta setosa* is between September and November [27]. In the Baltic Sea *Sagitta setosa* is not common. Its presence in the south western Baltic Sea is always related with an inflow of high saline water of the Kattegat [1]. The distribution of the deep dwelling *Sagitta setosa* reflects the topography and the overall hydrographic situation in the Black Sea (Fig. 2a). Thus the abundance is low at the shelf area. The individuals are accumulated in the rim current and drifting as big clouds along the shelf edges around the basin. The numbers of *Sagitta setosa* coincides with the branches of the current into the open sea, but the numbers are low in the central gyres (Fig. 2b).

A total of 29 taxa of ichthyoplankton were caught during all cruises from 1991 - 1994 in the southern Black Sea. The eggs of the two most economically important species *Engraulis encrasicolus* and *Sprattus sprattus* dominated the ichthyoplankton in summer and winter respectively (Fig. 1). From other fish species eggs and larvae in considerable amounts were only present of *Merlangius merlangus*, *Platichthys flesus*, *Mullus barbartus* and *Mugil sp.* (IMS, unpublished data).

The sprat *Sprattus sprattus* occurs in all three seas. The sprat spans throughout the whole year. In the southern Black Sea and southern North Sea the main spawning time

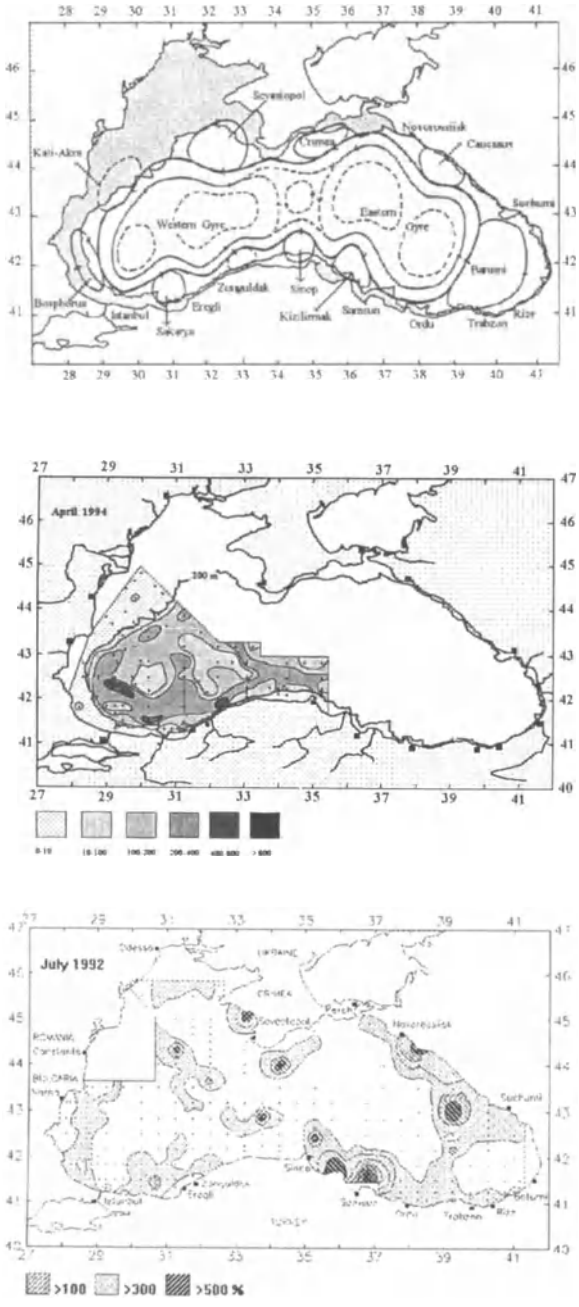


Figure 2 a: General circulation of surface currents in the Black Sea. The bold line shows the rim current. b: *Sagitta setosa*: Distribution in April 1994. c: Distribution of anchovy eggs in comparison to the current system in July 1992 [26]. Indicated are the areas with egg numbers 100 % of the average of the total number.

is in winter, with a peak in January/February. In the northern North Sea the peak spawning season starts with one month delay [17],[32].

The anchovy *Engraulis engrasicolus* is the most dominant fish in the Black Sea [5], but it is not frequent in the North Sea, and it does not occur in the Baltic Sea. In contrast to the sprat, anchovy eggs and larvae are very common during summer from mid of July to mid September. Due to their ellipsoid shape anchovy eggs are very easy to identify [9]. The distribution of anchovy eggs, which are drifting in the upper water layer, reflects as well the hydrographical features of the Black Sea [26]. The bulk of eggs is distributed in the main spawning areas between shelf areas and the rim current (Fig. 2c). After spawning the eggs are transported with the rim in open waters. This is obvious in the area between the eastern gyre and Batumi eddy and in the western area. Regions with no or very small abundances are the cyclonic gyres in the central part and the Batumi eddy in the eastern part of the Black Sea. No anchovy eggs as well were found in the upwelling region west of Sinop with surface temperatures of 12°C. In contrast to the anchovy eggs the cold water species *Pseudocalanus elongatus* was 15 times higher in the upwelling area compared to the average value of 2210±720 individuals m^{-2} of the whole southern Black Sea area (Ergün, 1994).

3. Changes in the pelagic ecosystems

The present state of the Black Sea, North Sea and Baltic Seas are determined by a continuing eutrophication process, which effect especially coastal communities [4]; Lancelot, this volume). Eutrophication effects in the open waters are obvious as well, but still moderate. In the Black Sea changes in the ecosystem started in the sixties with increasing eutrophication, pollution and exploitation of the fish stocks [40]. How these changes are reflected in the life patterns of single species should be highlighted exemplary for the anchovy stock.

The two subspecies of the Black Sea anchovy *Engraulis engrasicolus ponticus and Engraulis engrasicolus euxinus* undergo extensive migrations all over the Black Sea from the overwintering to the spawning areas [17],[6]. According to earlier surveys the anchovy spawns throughout the whole of the Black Sea but mainly in the northern half, especially in the shelf area [17].

Changes in the spawning areas of anchovy were noticeable off the Crimea coast by 1988, when the areas observed to be most abundant with anchovy eggs and larvae were towards the open sea rather than the typical distribution at the shelf areas found during 1950 to 1980. In 1992 and 1993 the bulk of anchovy eggs were obtained from the southern and particularly the south-eastern Black Sea and not from the northern Black Sea as usual. Comparison of the egg numbers found during an earlier survey about 40 years ago in July 1957 showed, that the northern part of the Black Sea displayed nearly the same numbers of anchovy eggs as in 1957, whilst the egg numbers for the southern region were significantly higher in 1992 than in 1957 [26].

The authors concluded, that the low egg and larvae numbers in 1957 and 1959 possibly reflect the mesotrophic state of the Black Sea in the late 1950s. With

increasing eutrophication, the anchovy stock enlarged in the early 1960s, and consequently egg and larval numbers increased. The decrease in spawning of the anchovy in the northern Black Sea during the 1980s is consistent with the northern area of the Black Sea having become excessively eutrophic and more polluted than the southern area over the last two decades as a result of major rivers flowing into this region. It was suggested, that the environmental deterioration of the shelf area due to dystrophication and the improved food conditions in the open sea due to eutrophication, has resulted in a shift of the spawning grounds to the open sea. Increasing eutrophication of the former mesotrophic coastal areas of the southern Black Sea could also be assumed as reason for the expansion of the spawning grounds from the Bosphorous area to the eastern Black Sea coast of Turkey.

A sudden decline of anchovy eggs and larvae, reflecting the collapse of anchovy catches for the whole of the Black Sea, were recorded in 1989, coinciding with the outburst of *Mnemiopsis leidyi*. This species competes for zooplanktonic food with the anchovy and is an important potential predator of anchovy eggs, and, especially, of yolk-sac larvae [8]. *Mnemiopsis* could, therefore, be a threat to fishery year-class recruitment [24].

Why the outburst of *Mnemiopsis leidyi* happened just at the end of the eighties and its relationship to the decline of the zooplankton biomass and the collapse of anchovy stock is still under discussion [37], Zeitsev, 1992; Prodanov, this Volume; Shiganova, thìs volume). Mny authors put the outburst of *Mnemiopsis leidyi* in connection to overfishing and to eutrophication effects, which caused changes in the planktonic species composition. Comparing the fluctuations of the zooplankton in all enclosed seas under consideration it is striking that major changes in the zooplankton community happened in the end of the 1980's as well in the Baltic Sea and in the North Sea.

3.1 BALTIC SEA

The comparison of the August months from 1953 - 1988 (data of the Baltic Sea Fishery Research Institute in Riga) showed a steep increase of zooplankton biomass in the Baltic Proper during the 1970's [35]. The increase of the zooplankton biomass was caused especially by the high increase of *Pseudocalanus elongatus* and *Acartia sp.* After maintaining of a high level during the 1980's the population of *P. elongatus* and *Acartia sp.* declined rapidly in 1988, while small zooplankton species as Bosmina increased (Fig. 3).

In the Kiel Bight a change in the zooplankton community was apparent in 1988 as well: the abundances of many zooplankton species increased, the blooming time of late summer/autumn zooplankton species started earlier and some species show high interannual fluctuations [2]. Increasing abundances after 1988 were observed as well in ichthyoplankton [33] and in zoobenthic species [31] after an abundance and diversity minimum during 1985-1988.

In contrast to the zooplankton stock of the Baltic Proper the stock of *Pseudocalanus elongatus* in the Kiel Bight increased since 1988 after a period of

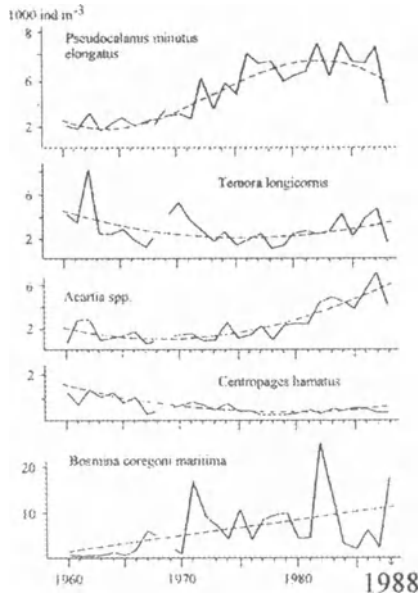


Figure 3: Fluctuation of main zooplankton species in the eastern and south eastern part of the Baltic Proper during August 1960 - 1988 in 0 - 100 m depth [35].

extremely low abundance between 1986 and 1987. The individual numbers of the copepod *Othiona similis* and the appendicularia *Oikopleura diocica* increased very strong since 1988/89 in the summer and displayed since then high seasonal fluctuation (Fig. 4a). Since 1988 the blooming period of *Oikopleura diocica* starts already in July, two month earlier than in previous years and continues as before till November (Fig. 4b).

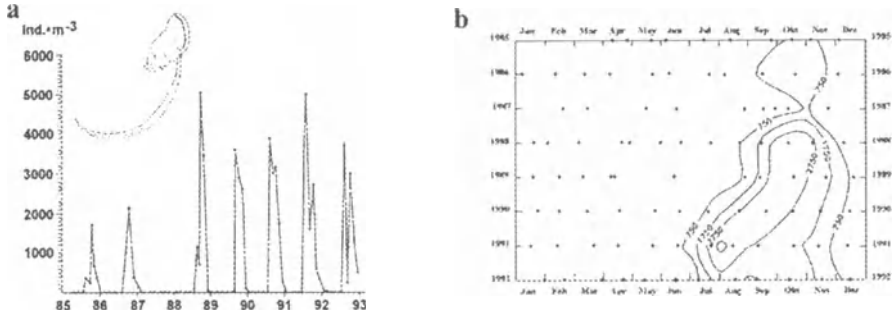


Figure 4: *Oikopleura diocia*: Fluctuation (a) and seasonal distribution (b) in the Kiel Bight, Baltic Sea during 1985 -1993 [2].

In the Kiel Bight the increase of *Oikopleura* and *Oithona* were significantly related with the rise in the temperature at the 20 m depth for the season July to December

1988, while the years with low densities of *Pseudocalanus elongatus* correspond to years with low salinity at 5 m and partly at 20 m depth before and during the reproduction season [2].

3.2 NORTH SEA

Sudden changes in the abundance of some species were detected as well in the German Bight (North Sea), at Heligoland Roads during 1988/89 [14]. For example the abundance of *P. elongatus* and *Paracalanus sp.* decreased after 1987-1992 after a blooming period from 1983-1986 (Fig. 5a). After a blooming period 1983-1989 the stock of and *Acartia sp.* declined rapidly till 1993 (Fig. 5b). After 1988 the actinotrocha, the larval stage of *Phoronis mülleri*, increased after a period of low abundance (Fig. 5c). The abundance of *Sagitta setosa* decreased as well end of the 80's after a blooming period (1983 - 1988). Since 1987 *Sagitta setosa* fluctuated with a high amplitude till 1991 (Fig. 5d).

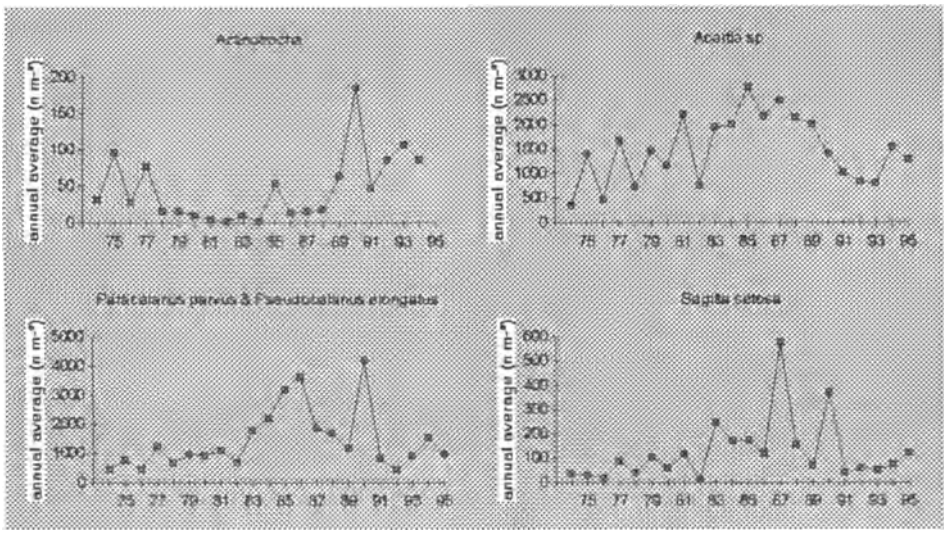


Figure 5: Fluctuation of dominant zooplankton species at Helioland Roads, German Bight, North Sea during 1974 -1995. Data from MABIS (Marine Biological Information System of the Biologische Anstalt Helgoland).

As in the Black Sea a new species *Muggiaea atlantica* (Siphonophora, lusitanian plankton) invaded the North Sea in 1989 and caused changes in the biocoenosis [12]. As evidence for a exceptional inflow of Atlantic water into the North Sea during 1989 an extraordinary population of *Doliolum nationalis* (Tunicata) was observed in the central an south eastern North Sea [21]. Lusitanian fish species *Trachurus vipera, Zeus faber, Mullus surmuletus* and other species where found in the North Sea since 1989 as well [15].

In the German Bight the temperature and salinity of the surface water increased in similarity to the Baltic Sea suddenly in the end of 1980's (Fig. 6). The average surface temperature was in the years 1984-1987 below 10°C. The temperature increased since 1988 and was about 11°C in 1989/90. After 1990 the average temperature varies between 10 and 10.5°C, on a higher level than in the mid 1980's. The salinity S > 33 as well was very high during 1988/89 and remained on a higher level as in the period 1977-1987 with salinities below S = 32.5.

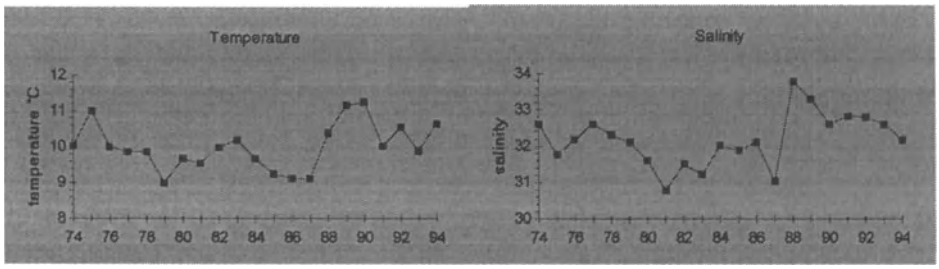


Figure 6: Changes in the mean annual temperature (a) and salinity (b) at Heligoland Roads during 1974 - 1994 according to [14].

3.3 BLACK SEA

In the open Black Sea the average air temperature decreased after 1986, was extremely low in 1987, raised up in 1988 and decreased till 1994 [28] Ovchinnikov, unpublished). Obvious is, that sudden changes in the zooplankton community of the Black Sea occurred as well during 1987-1989 as seen in the North Sea and Baltic Sea. The abundance and biomass of many zooplankton species in the Black Sea, as *Aurelia aurita, Acartia sp., Oithona sp., Sagitta setosa* decreased during 1987/88 [37],[39], [Melnikov, this volume; Shiganova, this volume]. In the same period the combjelly *Mnemiopsis leidyi* stock increased suddenly and the anchovy stock collapsed in 1989 [4],[26].

4. Conclusions

Similar changes in the zooplankton community of the Black Sea were obvious in the North Sea and Baltic Sea:

- changes in the meso zooplankton community structure due to decrease or increase of the abundance of dominant species
- occurrence of new species (North Sea: *Muggiaea atlantica,* lusitanian fish species; Black Sea: *Mnemiopsis leidyi*)
- changes of the blooming periods of some species, which start earlier and last longer
- high interannual fluctuations of some species, which started since end of the 1980's

High fluctuation in communities indicate a period of instability, which often is induced by a change of environmental parameter [29]. The changes in the seas under consideration occurred in the Black Sea after a extraordinary cold winter 1987/88 and a very warm winter during 1988/89, in the German after a sudden increase in temperature and salinity during 1988/89 and in the Kiel Bight after a rise in temperature of the subthermocline water during 1988/89. It could be concluded, that the changes in the zooplankton community since end of 1980's in the Black Sea, North Sea and Baltic Sea are forced by the same overall climatic event.

Of course, the importance of eutrophication as a major forcing function for zooplankton, especially in coastal waters, e.g. in the German Bight [16], most bays of the Baltic Sea [35] and the shelf area of the Black Sea [40] should always be considered. But the effects of eutrophication can be override or masked by hydrographic changes [38], [Reed, this volume]. Besides the possible eutrophication effect the changes of temperature and salinity in the Baltic Proper had an overall influence on the composition of the zooplankton community. The years in cold water periods 1962-1970 and 1979-1988 with severe winters displayed lower level of zooplankton development, than those years of warm water periods with mild winters 1954-1961 and 1971-1978 [35].

Examples for sudden changes of the community structure due to climatic variability as extreme cold winters, changes in the strength of currents or due to or high wave action triggered by strong storms are well known in the North Sea and Atlantic [7], [30]. Mann & Lazier [22] summarized the biological consequences of major perturbation of the North Atlantic during 1960'-1980's which affected the North Sea as well. Influences of forcing conditions have been discussed by Lindeboom *et al.* [20], who stated sudden changes in the biota of the North Sea at the seventies to eighties. Changes in the same period were obvious as well in the composition of phytoplankton (Diatom/Dinoflagellate ratio) and in the duration of the blooming period of Diatoms, Fagellates and small copepods in the German Bight [11].

Up to now the events in the Black Sea after 1988, and especially the collapse of the anchovy fishery, were often related to pollution, overfishing and to the outburst of *Mnemiopsis leidyi* [37],[40],[39]. Keeping in mind, that changes in the zooplankton community in the late 80's were evident in all seas under consideration, a climatic impact could have triggered the changes in the zooplankton community in the Black Sea as well, which caused the conditions for the outburst of *M. leidyi* and the decline of the anchovy stock.

Up to now the approach to evaluate existing zooplankton long term data of the Black Sea in relation to climatic variability has not been carried out. Therefore more effort should be made in near future to evaluate the existing zoo- and phytoplankton data of the Black Sea in relation to physical and meteorologic changes.

5. Acknowledgement

This work was funded by the Turkish Scientific and Technical Research Council (TUBITAK), and by the Scientific Affairs Division of NATO within the framework of the Science for Stability Program. We are indebted to the crews of the RV "BILIM", RV "Prof. VODYANITSKY", RV "AKADEMIK" and the vessels of the Biologische Anstalt Helgoland "Ade", "Utörn" and "Diker" as well the helpers ashore F. Hennemann, Goemann, F. Reiners and J. Nast. Our thanks go to Dr. U. Piatkovski and Dr G. Behrends for their kind support of our data research and to A.M. Kideys for correcting the English of the text.

6. References

1. Arndt, E.A. and Stein, H. (1973) Biologische Untersuchungen während des Internationalen Ostseejahres (International Baltic Year, IBY) 1969/70, *Beiträge zur Meereskunde* 32, 33-55.
2. Behrends, G. (in press) Long-term investigation of seasonal mesoplankton dynamics in Kiel Bright, Germany, *Proceedings of the 13th BMB Symposium, Riga (1-4 September, 1993).*
3. Behrends, G. and Schneider, G. (1995) Impact of *Aurelia aurita* (Cnidaria, Scyphozoa) on the standing stock and community composition of mesozoopankton in the Kiel Bight, *Marine Ecology Progress Series* 127, 39-45.
4. Caddy, J.F. (1993) Toward a cooperative evaluation of human impacts on fishery ecosystems of enclosed and semi-enclosed seas, *Fishery Science* 1 (1), 57-95.
5. Caddy, J. and Griffiths, R. (1990) A perspective on recent fishery relatedevents in the Black Sea, *Studies and Review. General Fisheries Council for the Mediterranean* 63, 43-71.
6. Chashchin, A.K. (1995) Abundance, Distribution and migration of the Black Sea anchovy stocks, *Tr.J. of Zoology* 19, 173-180.
7. Colebrook, J.M. (1986) Environmental influences on long-term variability in marine plankton, *Hydrobiologica* 142, 309-325.
8. Cowan, Jr. V.G. and Houde, E.D. (1993) Relative predation potentials of scyphomedusae, ctenophores and planktivorous fish on ichthyoplankton in Chesapeake Bay, *Marine Ecology Progress Series* 95, 55-65.
9. Demir, N. (1959) Notes of the variations of eggs of anchovy (*Engraulis encrasicolus* Cuv.) from Black Sea, Marmara, Aegean and Mediterranean Seas, *Publications of the Hydrobiological Research Institute, Faculty of Sciences, University Istanbul*, (Ser.B) 4, 180-187.
10. Ergün, G. (1994) Distribution of five calanoid copepod species in the southern Black Sea, *Master Thesis-Middle east technical University, Institute of Marine Sciences, Erdemli, Turkey*, 117 pp.
11. Gerlach, S. (1990) Nitrogen, Phosphorous, Plankton and Oxygen deficiency in the German Bight and Kiel Bight, *Kieler Meeresforschungen, special issue* 7, 357pp.
12. Greve, W. (1994) The 1989 German Bight invasion of *Muggiaea atlantica*, *ICES Journal of Marine Sciences* 51, 355-358.
13. Greve, W. and Reiners, F. (1988) Plankton time -space dynamics in German Bight- a systems approach, *Oecologia* 77, 487-496.
14. Greve, W., Reiners, F., Nast J., in press. Biocoenotic changes of the zooplankton in the German Bight: the possible effects of eutophication and climate, *Symposium on "Changes in the North Sea Ecosystem and their Causes", 11-14 July, 1995, Aarhus University, Aarhus, Denmark.*
15. Heessen, H.J.L., (in press) Long term trends in fish species caught during the internationeal bottom trawl survey, *Symposium on "Changes in the North Sea Ecosystem and their Causes", 11-14 July, 1995, Aarhus University, Aarhus, Denmark.*
16. Hickel, W., Mangelsdorf, P. and Berg J. (1993) The human impact in the German Bight: Eutrophication during three decades (1962-1991), *Helgoländer Meeresuntersuchungen* 47, 243-263.
17. Ivanov, L. and Beverton, R.J.H. (1985) The fisheries resources of the Mediterranean. Part two: The Black Sea. *Studies and Reviews, General Fisheries Council for the Mediterranean* 60, pp 135.

18. Kideys, A.E. (1994) Recent dramatic changes in the Black Sea ecosystem: The reason for the sharp decline in Turkish anchovy fisheries, *Journal of Marine Systems* 5, 171-181.
19. Krause, M., Dippner J.W. and Beil J. (1995) A review of hydrographic controls on the distribution of zooplankton biomass and species in the Sea with particular reference to a survey conducted in January - March 1987, *Prog. Oceanog.* 35, 81-152.
20. Lindeboom, H.J., van Raaphorst W., Beukema, J.J., Cadee, G.C. and Swennen C. (1994) Sudden changes in the biota of the North Sea: Oceanic influences underestimated, *ICES C.M. 1994/L:27*, 1-16.
21. Lindley, J.A. Gamble J.C. and Hunt, H.G. (1995) A change in the zooplankton of the central North Sea 55^{o} to 58^{o}: a possible consequence of changes in the benthos, *Mar.Ecol.Prog.Ser.* 119, 299-303.
22. Mann, H. and Lazier J.R.N. (1991) Dynamics of marine Ecosystems, *Blachwell Scientific Publications, Oxfort, London, Berlin*, pp 466.
23. Mee, L.D. (1992) The Black Sea in crisis: The need for concerted international action. *Ambio 21* 3, 278-286.
24. Monteleone, D.M. and Duguay, L.E. (1988) Laboratory studies of the predation by the ctenophore *Mnemiopsis leidyi* on early stages in the life history of the bay anchovy, *Anchoa mitchilli. Journal of Plankton Research* 10 (3), 359-372.
25. Mutlu E., Bingel, F., Gücü, A.C, Melnikov, V.V., Niermann U., Ostr, N.A., Zaika, V.E. (1994) Distribution of the new invader *Mnemiopsis sp.* and the resident *Aurelia aurita* and *Pleurobrachia pileus* populations in the Black Sea in the years 1991-1993. *ICES Journal of Marine Sciences* 51, 407-421.
26. Niermann U., Bingel, F., Gorban, A., Gordina, A.D., Gücü, A.C., Kideys, A.E., Konsulov, A., Radu, G., Subbotin, A.A. and Zaika, V.E. (1994) Distribution of anchovy eggs and larvae (*Engraulis encrasicolus* Cuv.) in the Black Sea in 1991 and 1992 in comparison to former surveys. *ICES Journal of Marine Sciences* 51, 395-406.
27. Øresland, V. (1986) Temporal size and marturity-stage distribution of the chaetognath *Sagitta setosa* in the western English Channel, *Marine Ecology Progress Series* 29, 55-60.
28. Ovchinnikov, I.M. and Osadchy, A.S. (1991) Secular variability of winter climatic conditions influencing pecularities of hydrological conditions in the Black Sea, in M.E.Vinogradov (ed.), *Variability of the Black Sea ecosystem*, Nauka, Moscow, pp. 85-89. (In Russian)
29. Pearson, T.H. and Rosenberg, R. (1978) Macrobenthic succession in relation to organic enrichment and pollution of the marine environment, *Oceanogr. Mar. Biol. nn.Rev.* 16, 229-311.
30. Rachor, E. and Gerlach, S.A. (1978) Changes of macrobenthos in a sublitoral sand area of the German Bight, 1967 to 1975, *Rapp.P.-v.Reun.Cons.int.Explor.Mer.* 172, 418-431.
31. Rumohr, H. (1993) Erfahrungen und Ergebnisse aus 7 Jahren Benthosmonitoring in der südlichen Ostsee, in J.C. Duinker (ed.), *Das biologische Monitoring der Ostsee im Institut für Meereskunde 1985-1992.* Ber.Inst.Meereskunde 240, 90-110.
32. Russell, F.S. (1976) The eggs and planktonic stages of British marine fishes, *Academic Press London*, pp 524.
33. Schnack, D. (1993) Fischbrutuntersuchungen als Beitrag zum Biologischen Monitoring in der Ostsee, in: J.C. Duinker (ed.), *Das biologische Monitoring der Ostsee im Institut für Meereskunde 1985-1992*, Ber.Inst.Meereskunde 240, 186-199.
34. Schneider, G. (1987) Role of advection in the distribution and abundance of Pleurobrachia pileus in Kiel Bight, *MAR.ECOL.PROG. SER.* 41, no.1, 99-102.
35. Schulz, S., Ertebjerg, G., Behrends, G., Breuel, G., Ciszewski, P., Horstmann, U., Konogonen, K., Kostrichkina, E., Leppanen, J.M., Mohlenberg, F., Sandsröm, O., Viitasalo, M. and Willen, T. (1990) Baltic Marine Environment Protection Commission -Helsinki Commission- *Second periodic assesmement of the state of the marine environment of the Baltic Sea, 1984-1988; Backround document. Ba*

SOME ASPECTS OF PHYTOPLANKTON LONG-TERM ALTERATIONS OFF BULGARIAN BLACK SEA SHELF

S. MONCHEVA and A. KRASTEV
Institute of Oceanology, BAS, Varna, 9000, PO Box 152, Bulgaria

Abstract. The present paper focus on the alterations of spring-summer phytoplankton communities (1961/70-1991/94), the expansion of "bloom" phenomena and the shift of Bacillariophyta:Dinophyta biomass ratio on long-term basis (1955-1994) off the Bulgarian Black Sea shelf. The results reveal a substantial increase in the total biomass (2 times in spring and more than 7 times in summer) and the total abundance (about 9 and 12 times respectively). An apparent expansion in the frequency and intensity of phytoplankton "blooms" is reported with dramatic shift in the taxonomic composition and number of species involved (27 out of total 255 species found off the Bulgarian shelf). The share of Bacillariophyta in the total biomass decreases from 86% (up to 1970) to 42% in 1970-1990 and 53% in 1991-1994, the shift in the nutrients ratios (Si:N and Si:P) deemed to be the possible controlling factor.

1. Introduction

The north-western Black Sea ecosystem has been subjected to the strongest anthropogenic pressure as about 80% of the fresh water runoff is discharged there, the drainage area exceeding the basin area about 5 times [16]. The river plume is the main pathway of freshwater distribution southwards along the western coast of the Black Sea [53] with a strong impact on the chemical and biological processes in the north-western basin [7, 8, 38-40, 50]. This together with the natural peculiarities of Black Sea lie behind its extremely high sensitivity to pollution and eutrophication [16, 57]. Results of recent investigations suggest that the interplay of the Danube anthropogenic load with the natural hydrological fronts and gradients provide opportunities for enhanced biological activity, thus contributing to the global environmental changes in the Black Sea north-west shelf [1].

Eutrophication is considered to play a key role in the substantial alterations in the structure and function of phytoplankton as the first target of the increased nutrient load in this part of the basin [2-4, 18-20, 25, 27, 28]. Changes in the biodiversity of phytoplankton species [29], as well as structural and succession aspects of

E. Özsoy and A. Mikaelyan (eds.), Sensitivity to Change: Black Sea, Baltic Sea and North Sea, 79–93.
© 1997 *Kluwer Academic Publishers.*

phytoplankton development in the close coastal zone off Bulgarian Black Sea area have been well documented [18-20], providing enough evidence of best expressed perturbations in spring and summer. Moncheva et al. [21] published a review on blooms and possible mechanisms of fish and benthic mortalities and claimed the bloom related hypoxia to play the principal devastating role. The established shift in the biomass ratio of Bacillariophyta:Dinophyta in the period 1970-1980 have been related to the changes in solar activity [26], the increased organic load in the basin and the mixotrophy of the dinoflagellates [25]. However, no attention has been paid to the role of nutrients ratios off Bulgarian coast, although there is an evidence in the literature that Si:N and Si:P could be responsible for the changes in the dominance of these main taxonomic groups along the Romanian coast [3, 4].

Prerequisite for assessment of anthropogenic effects is that there is knowledge of the variability of a natural ecosystem [13]. It is perceived that the long-term data can provide valuable clues about structural and functional aspects of phytoplankton communities changes.

Based on an overview of the existing phytoplankton data off Bulgarian Black Sea area, in the present paper are discussed: the basic trends in the variability of spring-summer phytoplankton communities (comparison between the period 1961/1970 — 1991/1994) in terms of taxonomic structure and abundance; the "bloom" phenomena on long-term basis (1955-1994) and the role of nutrients ratios (Si:N and Si:P) as a possible controlling factor in the inversion of Bacillariophyta:Dinophyta biomass ratio.

2. Materials and Methods

The study area is the Bulgarian shelf in the Western Black Sea to 40 miles offshore. The station network covered by RV "Akademik" for the period 1991-1994 is a part of the global sampling grid of the CoMSBlack International Field Program and NATO TU Black Sea Project. As the historical survey (1961-1970) is at transect c. Galata only for a rigorous comparison of the structural features of phytoplankton communities the recent data from this transect have been discussed. A detailed information on station number, station coordinates, sampling depths and cruise inventory is given in Table 1.

The analyses of phytoplankton communities structure is based on spring-summer data sets of both published data for the period 1961-1970 [23-28] and unpublished personal data (1991-1994) — see Table 1, analysed by the same method. Bottle samples from standard sampling depths (including thermocline for the 1991-1994 data set) are processed by the Utermol method [54] on inverted microscope for the two data sets. Phytoplankton species larger than 5 μm are enumerated and the biomass calculated using the standard individual weight of each species. In some cases the comparison is hampered by the insufficiency of published raw data, as for example data on phytoplankton numerical abundance (1964-1970) and on taxonomy and abundance for the period 1980-1990. The inventory of blooming phenomena and the

Bacillariophyta:Dinophyta biomass ratio is based on published data [26, 28] and our unpublished data (1991-1994).

TABLE 1. Cruise data inventory (transect c. Galata).

Station No.	Station coordinates		Distance from the shore	Sampling depths	Cruises
	Lat. (N)	Long. (E)		m	May and August for 1961-1970
1	43°09'	28°03'	3 n.m.	0, 10, 20	May 1991;
2	43°09'	28°10'	10 n.m.	0, 10, 25	September, 1991;
3	43°09'	28°20'	20 n.m.	0, 10, 25, 46	June 1992;
4	43°09'	28°30'	30 n.m.	0, 10, 25, 50, 75, 85	July, 1992;
5	43°09'	28°40'	40 n.m.	0, 10, 25, 50, 75, 100	April, 1994

3. Results

The comparative assessment of phytoplankton biomass in spring-summer between the two periods (1961/70 and 1991/94) reveal a significant increase in 1991/94 — Fig. 1a-c. The interannual variability in the 3 n.m. zone in spring during the first period is in the range 189-29 380 mg.m^{-3}, while during the second — 132-31 710 mg.m^{-3} — Fig. 1a. Large ranges are also observed for the 10 n.m. and 20-40 n.m. area but the difference is smaller — Fig. 1a,b. The average phytoplankton biomass in the 3 n.m. zone in 91/94 exceeds that in 61/70 1.5 times in spring and 12 fold in summer (508 versus 7 896 mg.$^{m-3}$). The overall mean biomass for the entire area in the 1991/1994 period is almost 3 times higher (5 163.8 versus 8 338 mg.m^{-3}) in spring and more than 7 times higher (524.24 versus 3 970 mg.m^{-3}) in summer than that in 1961/1970 period — Fig. 1c.

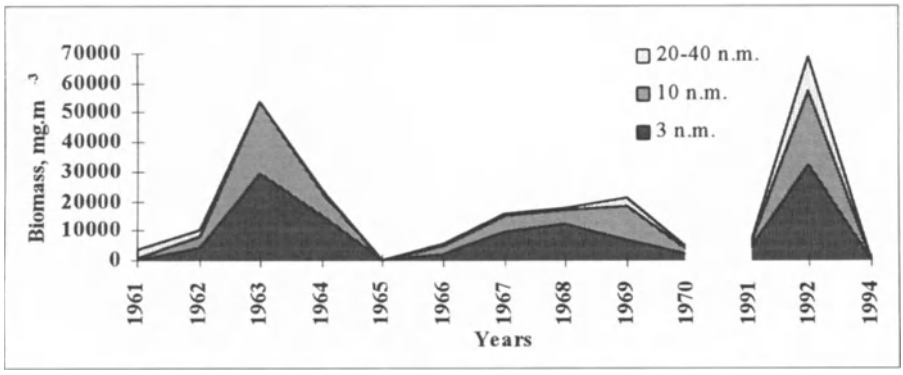


Figure 1a. Interannual variability in spring phytoplankton biomass for the periods 1961-70 and 1991-94 at transect c. Galata.

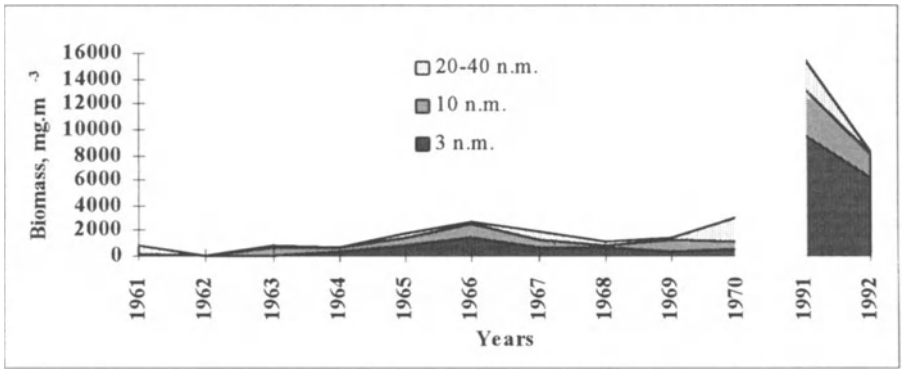


Figure 1b. Interannual variability in summer phytoplankton biomass for the periods 1961-70 and 1991-94 at transect c. Galata.

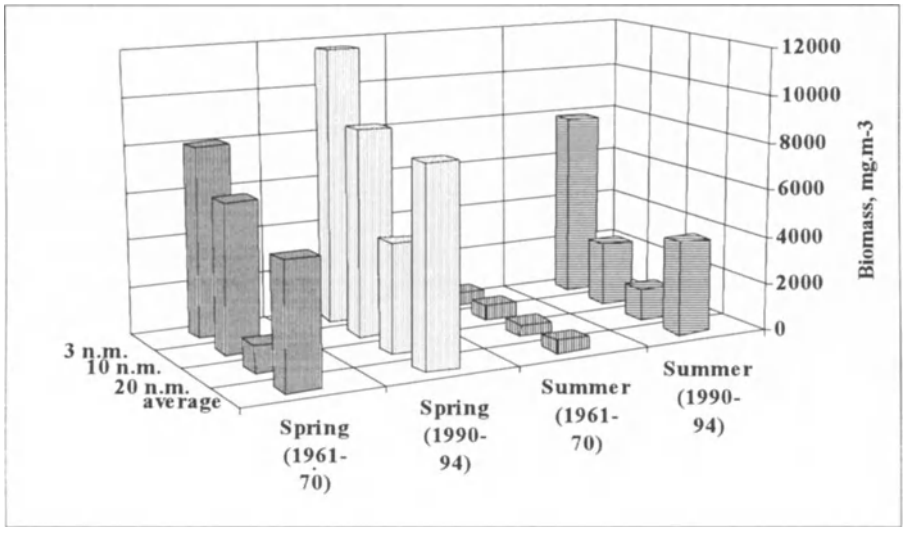


Figure 1c. Average phytoplankton biomass for the periods 1961-70 and 1991-94 at transect c. Galata.

Similar differences are even better expressed in phytoplankton numerical abundance and biomass:abundance (B:N) ratio. The average spring abundance in 91/94 is about 9 times higher than in 61/64 ($302x10^6$ cells.m^{-3} versus 2 $599x10^6$ cells.m^{-3}) and the summer one — more than 12 times ($55x10^6$ — $702x10^6$ cells.m^{-3}) — Fig. 2.

By contrast the B:N ratio as indication of the mean size of the phytoplankton population exhibits the opposite trend especially in spring — a decrease about 5 times (23.9 versus 5.1) — Fig. 2, which obviously could be related to changes in phytoplankton species composition (see the text bellow).

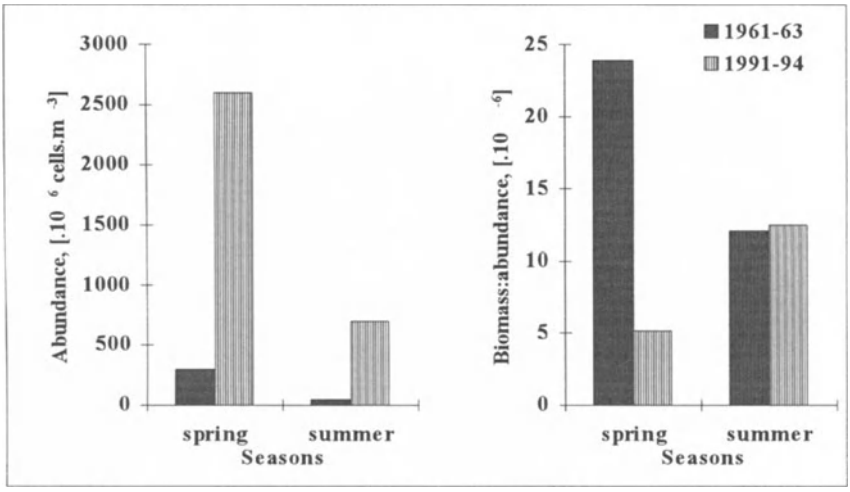


Figure 2. Phytoplankton average numerical abundance and biomass:abundance ratio in spring-summer (1961/63 — 1991/94) at transect c. Galata.

The analysis of biomass ratio of the dominant phytoplankton groups (Bacillariophyta:Dinophyta) reveals a dramatic inversion since 1970. Despite the oscillations in the interannual variability this inversion trend is stable — Fig. 3. The average share of Bacillariophyta in the total biomass up to 1970 is 86% (versus 14% of Dinophyta), decreasing during 1970/90 to 42% (versus 58% of Dinophyta respectively) and slightly increasing in the 1991/94 period to 53% (versus 44% of Dinophyta).

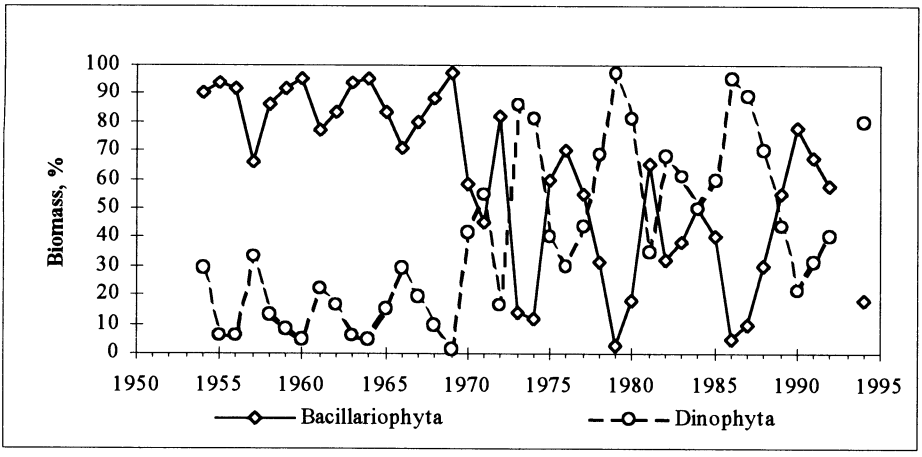


Figure 3. Long-term trend in Bacillariophyta:Dinophyta biomass ratio (for the period 1954-90 redrawn from Petrova-Karadjova, 1992).

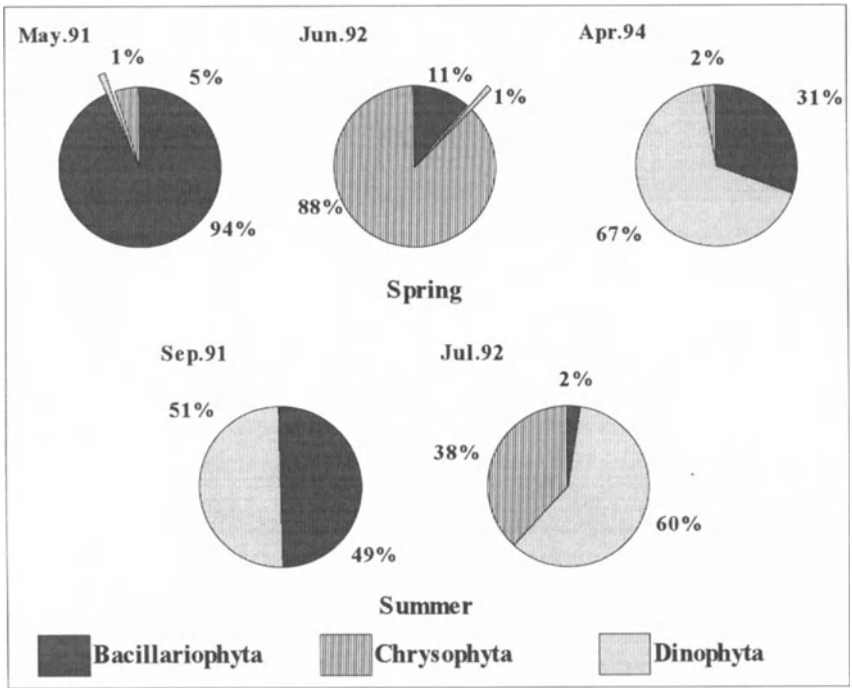


Figure 4. Taxonomic structure of phytoplankton abundance (in percent) in spring-summer (1991-94) at transect c. Galata.

If we consider the taxonomic structure in terms of numerical abundance (only the recent data set, as historical data are not accessible) a sizable portion of Chrysophyta is evident, especially in June and July'92 (87.5-38.4% from the total abundance respectively) — Fig. 4. Consequently one should refer to both numerical abundance and biomass when such a heterogeneous community like phytoplankton is considered.

TABLE 2. Census of the number of phytoplankton species and red-tide species off the Bulgarian coast.

Class	Total no. of species*	No. of red-tide species	No. of red-tide species in the World ocean**
Bacillariophyta	108	14	45-86
Dinophyta	101	7	93-127
Chrysophyta	12	3	8-15
Xanthophyta	1	0	-
Cyanophyta	13	2	3-4
Chlorophyta	11	0	5-6
Euglenophyta	9	1	6-8
Cryptophyta	0	0	5-8
Total	255	27	165-254
% from the total		10.1	6

* Reference No. 29;
** Reference No. 49.

As apparent from Table 2 the number of species registered in blooming densities is 27 out of total 255 species and forms found off the Bulgarian coast [29], representing about 10% of the total. This is about 1.6 times higher than the world statistics [49]. As compared to the number of red-tide species listed for the world ocean (165-254) they account for less than 10% (6-9%). Unlike the world statistics the variability among Bacillariophyta red-tide species is higher than that of Dinophyta species — Table 2.

There has been a dramatic increase both in the number of species involved, the frequency of the blooms and an apparent perturbations in the species succession with a shift towards Dinophyta species (1 before 1970 versus 7 thereafter) and Crysophyta species, among which there are some novel species for the Black Sea and its Bulgarian area like *Phaeocystis pouchettii*, *Gessnerium mochimaensis*, *Scrippsiella trochoidea* and *Oxyphisis oxytoxoides* (Table 3). Another obvious trend is that even the common species such as *Skeletonema costatum, Cerataulina pelagica, Cyclotella caspia*, etc. attain much higher abundance (Table 3). The same stands for the average bloom densities of Bacillariophyta and Dinophyta when considered as taxonomic groups. For example the Bacillariophyta species average bloom density before 1970 is $3.7x10^6$ cells.l^{-1} (the highest — $10.4x10^6$), while during the period 1970-1980 it is more than twice higher — $7.8x10^6$ (so does the maximum density — $20.1x10^6$) and during 1980-1990 — $5.3x10^6$ cells.l^{-1} (max, $27.7x10^6$). This trend in Dinophyta group is even more clear during the same selected time intervals: $1.3x10^6$ cells.l^{-1} before 1970 versus $64.9x10^6$ (max. $280x10^6$) during 1970-80 and 73.6 (max, $220x10^6$) thereafter.

If we go further into some ecophysiological features of the dominant species one can distinguish the following peculiarities. For example the shift in the biodiversity of the blooming species is towards phytoplankters producing high DMSP (per unit cell volume — Table 3 and Table 4), which might affect the climate at least on local bases [6]. Although almost all species presented in Table 3 are noxious species, nine of them have been cited as harmful (Table 4), which should be kept in mind especially in terms of the reported induced toxicity by the shift in nutrient ratios in the environment [55]. However the coexistence of toxic and nontoxic ecotypes of the same species [56] makes direct reference to cases reported for other regions rather speculative which points to the necessity of autochtonous investigations.

Before 1970 the established **dominant** species in spring summer seasons are: *Cyclotella caspia*, *Cerataulina pelagica*, *Thalassionema nitzschioides*, *Leptocylindrus danicus*, *Nitzschia delicatissima*, *Rhizosolenia calcar-avis* from Bacillariophyta (comprising between 53-66% from the total number of species listed) and *Prorocentrum minimum*, *Ceratium fusus*, *Ceratium furca*, *Peridinium crassipes*, *Peridinium divergens* from Dinophyta [23, 24]. During the recent period the spring summer phytoplankton communities are dominated mainly by Dinophyta species: *Heterocapsa triquetra, Scrippsiella trochoidea, Prorocentrum minimum, Prorocentrum micans, Gonyaulax polyedra*. Among Bacilariophyta the most common, registered even in blooming density are the species *Sceletonema costatum, Cerataulina pelagica, Nizschia delicatissima* and among Chrysophyta — *Emiliania huxleyi* and in 1990 *Phaeocystis pouchettii*. *Eutreptia viridis* (Euglenophyta) is typical only for the close coastal area.

TABLE 3. Taxonomic and quantitative characteristic of "blooming" phytoplankton species off the Bulgarian Black Sea coast (1955-1994).

Taxon	Bacillariophyta											
Species / Years	CERATAULINA PELAGICA	CHAETOCEROS CURVISETUS	CHAETOCEROS SOCIALIS	CYCLOTELLA CASPIA	DETONULA CONFERVACEAE	NITZSCHIA CLOSTERIUM	NITZSCHIA DELICATISSIMA	NITZSCHIA SERIATA	NITZSCHIA TENUIROSTRIS	RHIZOSOLENIA CALCAR-AVIS	RHIZOSOLENIA FRAGILISSIMA	SKELETONEMA COSTATUM
1955										8		
1956												
1957												
1958												
1959								2,5				
1960				5								5
1961	8											
1962												3
1963	5			5								4
1964	3,5											2
1965												3
1966							2,6					
1967												3
1968	5						5					2,3
1969	11	5		8	2		9					3
1970				8			6					11
1971				8				3				2,3
1972	11		11		2			5				3
1973			5									5
1974												
1975												
1976												3
1977												
1978												
1979												
1980	8											
1981	5,6											3,4
1982	5											3
1983	8											6,7,8
1984	9	5,6	6	5,6								4,7
1985												3,7,8
1986	8		5				3,5				5	3,4,5
1987					3							5
1988			7					3,5				
1989			1							7	8	5,6
1990	5		1			8					7	2,6
1991	8,9				8		7	7				5
1992	6,7		7,8									
1993	7,9		7									9
1994	6,9			6					6			
Legend	0.5-1.10⁶ cell/l			1-1.5.10⁶		5-10.10⁶		10-50.10⁶		over 50.10⁶		

TABLE 3. *(continue)* Taxonomic and quantitative characteristic of "blooming" phytoplankton species of the Bulgarian Black Sea coast (1955-1994).

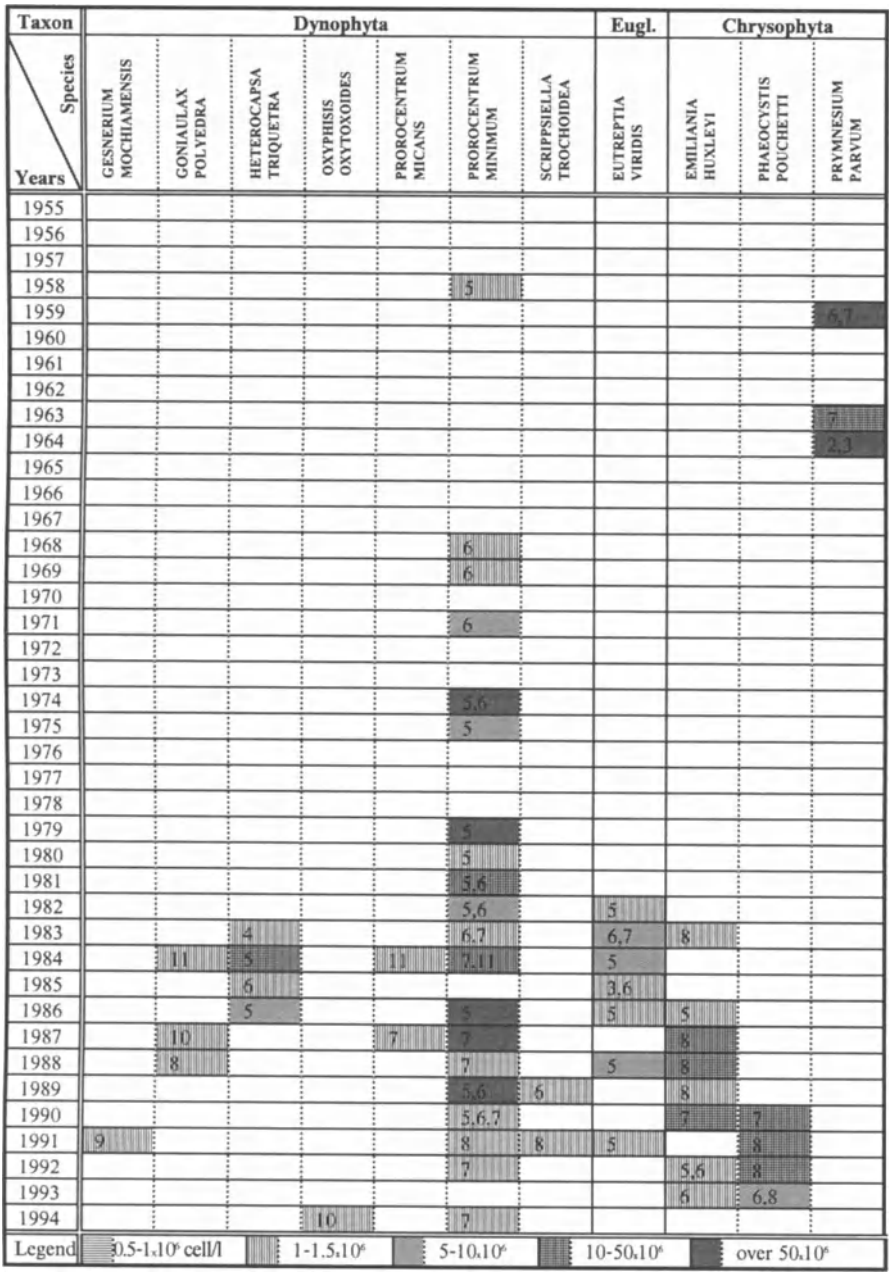


TABLE 4. List of Black Sea species cited* as harmful and Dimethyl sulfide production (DMSP) per unit cell volume**.

Species	$1x10^{-6}$ cells.l^{-1}***	Effect	DMSP per unit cell volume [$\mu M.cm^{-3}$]
Chrysophyta			
Prymnesium parvum	150	toxicity	-
Phaeocystis pouchettii	90	physical effect (foam) fish escape	260
Dictyocha speculum	0.01	gill irritation (asphyxia)	-
Emiliania huxleyi		-	166
Dinophyta			
Prorocentrum minimum	480	human poisoning	886
Scrippsiella trochoidea	1.9	fish mortality	350
Dinophysis acuta	0.02	DSP	-
Dinophysis sacculus	0.15	DSP	-
Bacillariophyta			
Chaetoceros curvisaetus	1	asphyxia	-
Chaetoceros socialis	3.5	asphyxia	-
Skeletonema costatum	280	-	22
Thalassiosira sp	-	-	2

* ICFS Cooperative research report No. 182, 1982; Taylor, 1989.
** Keller et al., 1989, 1990.
*** Maximum numerical abundance of the Bulgarian shelf.

TABLE 5. Specific growth rates (divisions per day) of domminant phytoplankton species.

Species	$div.day^{-1}$		
	Lanskaya [15]	Senicheva [44]	Mihnea [17]
Bacillariophyta			
S. costatum	8.0	5.9	
C. caspia	1.8		
Rh. calcar-avis	1.2		
Ch. curvisaetus	2.2		
Ch. socialis f. vernalis	2.2-2.4		
Ch. socialis f. autumnalis	3.0		
C. pelagica	2.2	2.7	
Th. nitzschioides	1.3-1.5		
N. closterium	3.2		
N. tenuirostis	2.0		
Dinophyta			
P. minimum	2.4	2.8	4.6
P. micans	2.5		
S. trochoidea	1.8		
H. triquetra	2.4		
G. polyedra	1.8-2.0		
C. furca	0.5		
C. fusus	1.0		
P. steinii	1.6		
P. crassipes	0.8		
Chrysophyta			
E. huxleyi	4.8		

The comparison of the species by their specific growth rates dominating the phytoplankton communities before 1970, and thereafter suggests a shift towards species of higher colonization rate as a general trend (Table 5), which is quite in conformity with the general trends established in the mean size of the phytoplankton assemblages and their biomass attained. Nonetheless this suggestion should be treated rather tentatively (see the discussion below).

4. Discussion

As obvious from the results presented, there is a well documented alterations in the phytoplankton structure — a several fold increase in the total biomass and numerical abundance, a decrease in the average size and a consequent dramatic shift in the dominant species composition, an obvious increase in the phytoplankton blooms in frequency and species involved with some novel species for this area and the Black Sea ecosystem.

Recently GESAMP [13] has identified several indices of population structure or species assemblages that measure ecological response to eutrophication among which changes in the type or abundance in the dominant species, alterations in the succession pattern of the communities, reduction in the mean size of the population, increase in the total abundance and biomass as well as the increase in phytoplankton blooms are pointed to be the most sensitive. According to Smetacek [48] a reliable indication of anthropogenically induced eutrophication especially for the temperate latitude basins would be sustained high phytoplankton biomass during the nutrient impoverished late spring-summer seasons.

The chemical data also point to significant changes in both the nutrients concentrations and their ratios — Table 6. All these give evidence to be stated that the perturbations in phytoplankton communities in general could be attributed to the alterations in the chemistry of the environment e.g. the progressive eutrophication.

While nitrogen and phosphorus are the two most important nutrients governing overall algal growth [14], the ratios of nutrients present [52] and the variability of Si concentration [12] can regulate the taxonomic composition of phytoplankton assemblages. According to the Si depletion hypothesis formulated by Schelske and Stoermer [42, 43] the increased nutrient loading causes an increase in phytoplankton production, especially diatoms as they are regarded as species with fast response rates to induced environmental changes [52]. Further increase in nutrient loading enormously increase diatom accumulation rates with a marked increase in the dominance of winter-early spring blooming species which is well documented elsewhere in our investigations [21]. Thus being species with fast respond rates they grow rapidly and by stripping there environment of nutrients change their growth conditions [9] in our case resulting in significant change in the ratios Si:N and Si:P as illustrated in Table 6. As evident from our results before 1970 the diatoms constitute the bulk of the phytoplankton population, the decreasing trend in Si starting since 1964 (Fig. 5).

TABLE 6. Long-term average concentrations of the principal nutrients [μg.l^{-1}] and their ionic ratios at c. Galata (3 n.m.).

Periods	NO_3	PO_4	SiO_4	Si:N	Si:P	N:P
1962-1968*	20.9	24.7	1022.8	32.9	42.7	1.3
1969-1975*	36.3	24.2	529.0	9.8	22.5	2.3
1976-1980*	73.1	66.3	402.9	3.7	6.2	1.7
1986-1990*	22.3	32.4	-	-	-	1.1
1991-1992**	36.9	11.1	352.4	6.4	32.7	5.1

*Data of Rojdestvenskyi [43-45]. **CoMSBlack data.

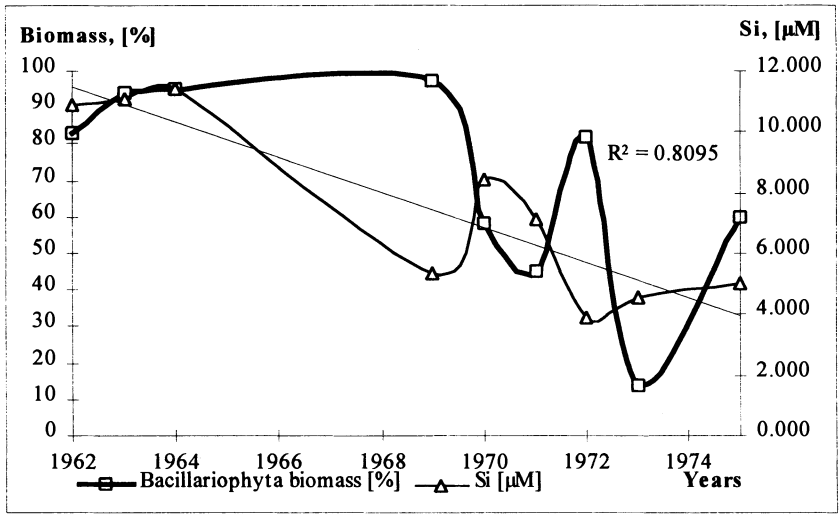


Figure 5. Concentration of Si [μM] in sea water and Bacillariophyta biomass as a % from the total phytoplankton bomass (Si data from Rojdestwenskyi [30-40]).

The reduction in Si content before 1975 could not be attributed to the reduction in Si content in the Danube inflow as the decreasing trend in the Danube waters is marked since 1975 [7] while the inversion in Bacillariophyta:Dinophyta ratio — in 1970. As already mentioned in the results the decrease in Bacillariophyta biomass is relative to Dinophyta biomass only, the diatom blooms increasing in number and biomass attained (Table 3). Factors contributing to the reduction of Si in the North-western Black Sea could be the reduction of the input by the Danube waters [8], may be to a certain extent the massive development of *Aurelia aurita* in the early 80-ties and *Mnemiopsis leidyi* since 1986 [5], but most likely the diatoms play the most signifficant role.

However the annual cycle of Si should not be confused with the long-term historical decrease in the water column. The development of diatoms in winter-early spring (as typical for the Black sea phytoplankton annual cycle) being also enhanced by the increased N and P (e.g. a higher biomass attained) result in more Si incorporated into organic biomass and in an alteration in Si:N and SI:P ratios unfavorable for the further

development of the diatoms, which could be the possible reason in late-spring-summer season other phytoplankton groups to dominate (like for example Dinophyta and Chrysophyta in our case). The degree of recurrence of this scenario most likely is responsible for the degree of the established oscillation in the Bacillariophyta:Dinophyta ratio. Obviously Si could not be considered a limiting nutrient for the development of diatoms on long-term scale although a stable decreasing trend in Si is evident — Table 5. Petrova-Karadjova and Apostolov [26] have related the shift in the Bacilariophyta:Dinophyta ratio to the possible control of solar activity or to the increased organic load in the basin and the mixotrophy of Dinophyta species [25]. As our results suggest it is most likely that Si could be the controlling factor switching the inversion and oscillation in this ratio indirectly by the modified Si:N and Si:P ratios in the environment as a result both of the increased anthropogenic eutrophication and the selectivity of phytoplankton species respond discussed above.

Smayda [46, 47] also has stated that increasing novel and toxic phytoplankton blooms observed globally and locally are a direct consequence of increases in total N and P concentrations and consequent modification of the Si:N and Si:P molar ratios. The fact that only some blooming species are recurrent and the majority variable in their appearance makes attempts at explaining patterns of occurrence based on single features such as phylogeny, size or growth rate of an organism not very successful [45]. Although long-term data can give valuable clues by showing the degree of variability or recurrence in species appearance in relation to environmental features the wide morphological and phycological diversity established makes it impossible to define a single microalgal type adequate as a target organism to the environmental changes. A possible solution could be to pay more attention to the life history strategies of individual plankton species if one is to explain their distribution in time and space [10], which ultimately suggests that smaller time-scales of investigations would be of greater importance, the priority given to process oriented studies.

The alterations of the phytoplankton communities taxonomic structure and abundance may have a significant impact on the structure and functioning of the entire food web. Unlike the other taxonomic groups diatoms are suggested to enhance the transfer in energy to higher trophic levels either through fewer trophic links or higher food quality [11], so phytoplankton species composition may affect both the trophodynamic and the nutrients recycling in the ecosystem.

5. References

1. Aubrey, D., Moncheva, S., Demirov, E., Dimitrov, A. (1995) Environmental mhanges in the western Black Sea related to anthropogenic and natural conditions, *J. Mar. Systems* (in print).
2. Bodeanu, N. (1991) Phytoplankton blooms (eutrophication) hypoxy along the Romanian Black sea coast, *International Workshop on the Blak sea: Focus on the Western Black sea Shelf.*, Varna, Bulgaria, 30 Sept.-4 Oct., 1991.
3. Bodeanu, N. (1993) Microbial blooms in the Romanian area of the Black Sea and contemporary eutrophication conditions, *In: Toxic Phytoplankton Blooms in the Sea,* T.J.Smayda and Y. Shimizu [eds]., Elsev. Amsterdam 203-209.

4. Bodeanu, N. (1995) Algal blooms in Mamaia Bay (Romanian Black Sea coast), *In: Harmful Marine Algal Blooms,* Lassus, P., Arzul, G., Denn, E., Gentien, P., Marcaillou-le Baut, C. [eds], Lavoisier Publ.Inc. 127-132.
5. Borodkin, S. O., Korzhikova, L. I. (1991) The chemical composition of the Ctenophore Mnemiopsis Leidyi and its role in the nutrient transformation in the Black sea, *Oceanologia* **25,** 73-79.
6. Charlson, R. J., Levelock, J. E., Andreae, M. O., Warren, S.G. (1987) Oceanic phytoplankton, atmospheric sulphur, cloud albedo and climate. *reprinted from Nature* **326,** 6114, 655-661.
7. Cociasu, A., Dorogan, L., Humborg, Ch., Popa, L. Long-term ecological changes in Romanian coastal waters of the Black Sea, *Marine Pollution Bulletin* (in press).
8. Cociasu, A., Diaconu, V. The role of the nutrient fluxes on the western shelf in the overall Black Sea eutrophication in the last three decades (this volume).
9. Conley, D. J., Schelsce, C. L., Stoeremer E. F. (1993) Modification of the biogeochemical cycle of silica with eutrophication, *Mar. Ecol. Prog. Ser.* **101,** 179-192.
10. Davis, C. O. (1982) The importance of understanding phytoplankton life strategies in the design of enclosure experiments, *In: G. D. Grice and M.R. Reeve (eds), Marine Mesocosms. Spinger — Verlag, New York* 323-332.
11. Doering, P. H., Oviatt, C. A., Beatty, L. L., Banzon, V. F., Rice, R., Kelly, S. P., Sullivan, B. K., Frithsen, J. B. (1989) Structure and function in a model coastal ecosystem: silicon, the benthos and eutrophication, *Mar. Ecol. Prog. Ser.* **52,** 287-299.
12. Edge, J. K., Aksnes, D. L. (1992) Silicate as regulating nutrient in phytoplankton competition, *Mar. Ecol. Prog. Ser.* **83,** 281-289.
13. GESAMP, reports and studies No. 55 (1995) Biological indicators and their use in the measurement of the condition of the marine environment, 55.
14. Hecky, R. E. and Kilham P. (1988) Nutrient limitation of phytoplankton in freshwater and marine environments: a review of recent evidence on the effects of enrichment, *Limnol.Oceanogr.* **33,** 796-822.
15. Lanskaya, L. A., Finenko, Z. Z. (1971) Growth kinetic of phytoplankton species in limited volume, *In: Ecological physiology of marine plankton organisms, Kiev* 22-50.
16. Mee, L. D. (1992) The Black sea in crisis: A need for concerted international action, *AMBIO — J. of the Human environment, RSAS* 278-286.
17. Mihnea, P. E., (1979) Some Specific Features of Dinoflagellates Exuviaella cordata Ostf. Blooming in the Black Sea, *In: Toxic Dinoflagellates blooms. Ed. Taylor D. L., Seliger,Els. North Holland, NY.* **1,** 77-82.
18. Moncheva, S. (1991) *Ecology of common species from Black Sea under the conditions of anthropogenic eutrophication,* Ph.D. Thesis, IO-BAS, Varna.
19. Moncheva, S., Russev, Ch., Sofronov I. (1991) On influence of the eutrophication on the biological cyclicity of phytoplankton species from the Bulgarian Black Sea coastal zone, *Oceanology, BAS* **21,** 31-38.
20. Moncheva, S. (1992) Cysts of blooming dinoflagellates from Black Sea, *Rapp. Comm .int.Mer.Medit.* **33,** 261.
21. Moncheva, S., Petrova-Karadjova, V., and Palasov, A. (1995) Harmful Algal blooms along the Bulgarian Black Sea coast and possible patterns of fish and zoobenthic mortalities, *In: Harmful Marine Algal Blooms,* Lassus, P., Arzul, G., Denn, E., Gentien, P., Marcaillou-le Baut, C. [eds], Lavoisier Publ.Inc. 193-198.
22. Officer, C. B., Ryther, J. H. (1980) The possible importance of silicon in marine eutrophication, *Mar. Ecol. Prog. Ser.* **3,** 83-91.
23. Petrova, V. (1965) The phytoplankton along the Bulgarian coast of the Black Sea during the 1961-1963 period, *Proc.Research Inst. Fisheries and Oceanography, Varna* **6,** 63-75.
24. Petrova, V. (1973) Dynamics of the biomass of the phytoplankton in the Black sea of the Bulgarian coast during the period of 1964-1970, *Proc. Res. Inst. Ocean. Fish.* **12,** 41-66.
25. Petrova-Karadzova, V. (1984) Changes in planktonic flora in Bulgarian Black Sea waters under the influence of eutrophication, *Proc. Inst. Fish.* **21,** 105-112.
26. Petrova-Karadjova, V., Apostolov, E. M. (1988) Influence of solar activity upon the Diatoms of Black Sea plankton, *Rapp. Comm. Int. Mer. Medit.* **31,** 2.
27. Petrova-Karadjova, V. (1990) Monitoring of the blooms along the bulgarian Black Sea coast, *Rapp. Comm. int. Mer Medit.* **31(1),** 209.
28. Petrova-Karadjova, V. (1992) Solar Control upon the phytoplankton in the Black Sea, *Rapp. Comm. Int. Mer. Medit.* **33.**
29. Petrova-Karadjova, V., Moncheva, S. Biodiversity of phytoplankton off the Bulagarian Black Sea shelf, *In: Biodiversity of Bulg. Black Sea Area. Nat. Rep.* (in press).
30. Rozhdestwenskiy, A. (1962) Hydrochemical, hydrobiological and meteorological characteristic of the year 1961 regarding the Black Sea fishing activities, *Fish farming* **4,** 6-9.
31. Rozhdestwenskiy, A. (1963) Hydrochemical, hydrobiological and meteorological characteristic of the year 1962 regarding the Black Sea fishing activities, *Fish farming* **7,** 23-25.

32. Rozhdestwenskiy, A. (1964) Hydrochemical, hydrobiological and meteorological characteristic of the year 1963 regarding the Black Sea fishing activities, *Fish farming* **5,** 5-8.
33. Rozhdestwenskiy, A. (1969) Hydrochemical, hydrobiological and meteorological characteristic of the year 1968 regarding the Black Sea fishing activities, *Fish farming* **6,** 4-6.
34. Rozhdestwenskiy, A. (1970) Hydrochemical, hydrobiological and meteorological characteristic of the year 1969 regarding the Black Sea fishing activities, *Fish farming* **5,** 11-14.
35. Rozhdestwenskiy, A. (1971) Hydrochemical, hydrobiological and meteorological characteristic of the year 1970 regarding the Black Sea fishing activities, *Fish farming* **4,** 7-9.
36. Rozhdestwenskiy, A. (1972) Hydrochemical, hydrobiological and meteorological characteristic of the year 1971 regarding the Black Sea fishing activities, *Fish farming* **5,** 24-26.
37. Rozhdestwenskiy, A. (1973) Hydrochemical, hydrobiological and meteorological characteristic of the year 1972 regarding the Black Sea fishing activities, *Fish farming* **8,** 1-5.
38. Rozhdestwenskiy, A. (1986) *Hydrochemistry of the Bulgarian sector of the Black sea,* BAS Publishing house, Sofia.
39. Rozhdestwenskiy, A. (1990) On Long-year dynamics of the most important hydrochemical indices in the Bulgarian part of the Black sea, *Oceanology, BAS, Sofia* **19,** 15-26.
40. Rozhdestwenskiy, A. (1992) Hydrochemical characteristic of the Bulgarian Black Sea water area for the period of 1986-1990, *Proc. of Inst of Oceanology, BAS, Sofia* **1,** 9-18.
41. Sanders, H. L. (1968) Marine benthic diversity: A comparative study, *Amer. Nat.* **102,** 243-282.
42. Schelske, C. L., Stoermer, E. F. (1971) Eutrophication, silica depletion, and predicted chenges in algal quality in Lake Michigan, *Science* **173,** 423-424.
43. Schelske, C. L., Stoermer, E. F. (1972) Phosphorus, silica and eutrophication in Lake Michigan, In: Likens, G. E. (ed) *Nutrients and eutrophication,* Am. Soc. Limnol. Oceanogr., Lawrence, KS, pp. 157-171.
44. Senicheva, M. I. (1980) Dynamic of Sceletonema costatum Grev. in Sevastopol Bay, *Ekologia moria* **1,** 11-15.
45. Smayda, T. J. (1980) Phytoplankton species succesion, In I. Morris (ed.), *The Physiological Ecology of Phytoplankton.* Blackwell, Oxford, pp. 493-570.
46. Smayda, T. J. (1989) Primary production and the global epidemic of phytoplankton blooms in the sea: a linkage, In: Cosper, E. M., Bricelj, V. M., Carpenter, E. J. (eds) *Coastal and estuarine studies, Novel phytoplankton blooms Springer-Verlag, New York* **35,** 449-483.
47. Smayda, T. J. (1990) Novel and nuisance phytoplankton blooms in the sea: evidence for a global epidemic, In: Graneli, E., Sunstrom, B., Edler, L., Anderson, D.M. (eds) *Toxic marine phytoplankton. Elsevier, Inc., Amsterdam* 29-40.
48. Smetacek, V. Bathmann et al (1991) Coastal eutrophication: causes and consequences, In: *Ocean Margin Processes in Global Change,* Ed. by R.F.C.Mantoura, J.M. Martin and R. Wollast. pp. 251-279
49. Sournia, A. (1995) Red-tide and toxic marine phytoplankton of the world ocean: an inquiry into biodiversity, *In: Harmful Marine Algal Blooms,* P.Lassus, G.Arzul, E.Denn, P.Gentien, C.Marcaillou-le Baut [eds], Lavoisier Publ.Inc. 103-112.
50. Stoyanov, A. (1992) Changes in the biogeochemical cycle of N and P along the Bulgarian Black Sea under influence of eutrophication, *Compt. rend de Acad. Bulg. Scienc* **45,** 12, 99-101.
51. Taylor, J. K. (1989) Red tides, brawn tides and other harmfull Algal blooms: the view into the 1990, (Conference overview) *In: Toxic Marine phytoplankton,* ed by Graneli, E, Sundstrom, B., Edler, L., Anderson, D. M., Elsev. Publish. New York, pp. 527-533.
52. Tilman, D., Kilham, S. S., Kilham, P. (1982) Phytoplankton community ecology: the role of limiting nutrients, *A. Rev. Ecol. Syst.* **13,** 349-372.
53. Tolmazin, D. (1985) Changing coastal oceanography of the Black Sea, *In: North-Westrn shelf. Prog. Oceanog.* **15,** 217-276.
54. Utermol, M. (1958) Zur Vervollkommung der Quantitativen Phytoplankton Methodic, *Mitt. Int Verein. Theor. angew. Limnol.* **9,** 1-38.
55. Wyatt, T. (1989) Do Algal blooms play homeostatic roles, *Toxic Marine Phytoplankton* ed by Graneli, E., Sundustrom, B., Edler, L., Anderson, D. M., Elsev. Publish. New York, pp. 249-252.
56. Yasumoto, I., Fnoe, A., Bangis, R. (1979) New toxic Dinofagellate found in association with Ciguatera, *In: Toxic Dinoflagellate Blooms, Els. North, Holland* **I,** 221-224.
57. Zaitzev, Yu. P. (1991) Eutrophication in the Black sea waters, *International Workshop on the Black sea: Focus on the Western Black Sea Shelf,* Varna, Bulgaria, 30 Sept.-4 Oct., 1991. R.F.C. Mantoura, Martin, J. M. and Wollast, R., 251-279.

SENSITIVITY TO ANTHROPOGENIC FACTORS OF THE PLANKTON FAUNA ADJACENT TO THE BULGARIAN COAST OF THE BLACK SEA

A. KONSULOV and L. KAMBURSKA
Institute of Oceanology, BAS, Varna, 9000, PO Box 152, Bulgaria

Abstract. The present paper focuses on the qualitative and quantitative changes in zooplankton composition on the western Black Sea area on the basis of long term data (1970-1995 period). The results reveal a decreasing tendency in diversity of mesozooplankton as well as a slight increase in total zooplankton biomass. The investigations of the ecological status of some zooplankton species (*Noctiluca scintilans*, *Mnemiopsis leidyi*), including their adaptation, give some grounds to consider them as potential bioindicators in the high eutrophication zones.

1. Introduction

The Black Sea is a unique part of the World Ocean for a number of reasons, the most outstanding of which is its geographically determined doom.

The worst form of pollution in the Black Sea at present is the high rate of eutrophication, which results in a series of changes in the physical properties of the water mass, causes phobic loss in the lower layers and affects the mechanism of the zooplankton diurnal migrations. The high degree of eutrophication is also a reason for significant changes in the composition and structure of the pelagic ecological category of organisms [10].

Detailed analysis of the data concerning qualitative composition and quantitative development of zooplankton under conditions of high eutrophication allows us to accept that the plankton fauna almost totally lack the species *Anomalocera patersoni* and *Pontella mediterranea*. A rapid decrease in the quantity of these species to the degree of extinction has occurred in the nearshore zone, where they were abundant in summer 20-25 years ago [2,3,4,8].

The purpose of the present report is to highlight the effects of eutrophication affecting the Black Sea plankton fauna adjacent to the Bulgarian coast, and to explain the role of zooplankton in its occurrence in the shallow shelf and open sea zones.

E. Özsoy and A. Mikaelyan (eds.), Sensitivity to Change: Black Sea, Baltic Sea and North Sea, 95–104.
© 1997 *Kluwer Academic Publishers.*

2. Materials and Methods

The main zooplankton sampling stations were located at 3, 10, 20, 30 and sometimes 40 and 50 miles offshore along the profiles 115° from cape Galata, 100° from cape Emine, 90° from cape Maslen nos and 90°-100° from cape Kaliakra, Achtopol and Rezovo. The data were obtained in 1994, 1995 and the 1970-1988 period. The data in 1991, 1992 and 1995 were collected from the stations of the HydroBlack and CoMSBlack networks. Sampling has also been carried out at many additional stations defined during the cruises (Fig. 1).

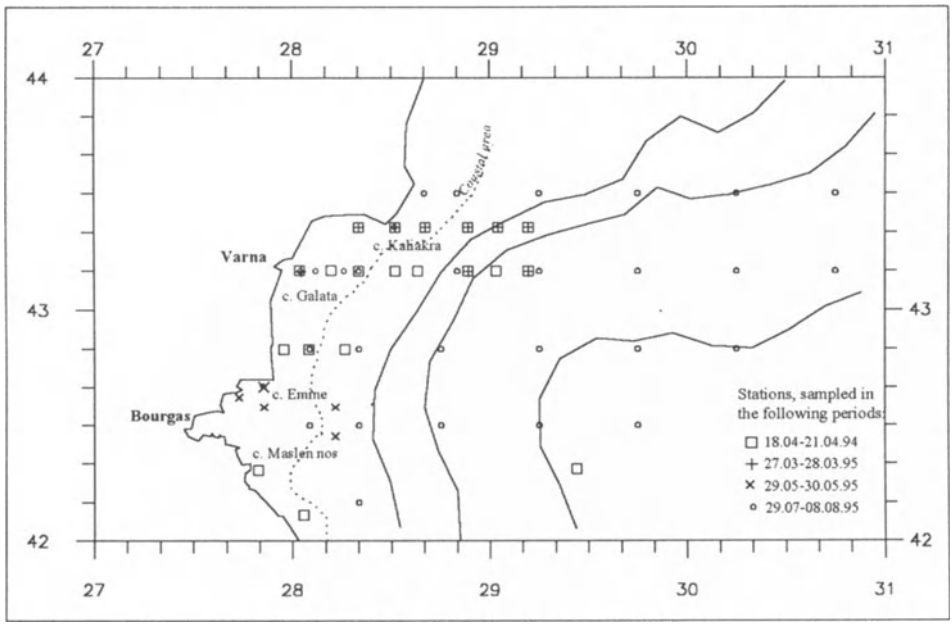


Figure 1. Sampling stations adjacent to the Bulgarian Black Sea coast during spring and summer (1994-1995)

Table 1. Time and place of observation.

Year	Date	Number of stations		Research Vessel
		coastal region	open sea area	
1994	18-21 April	10	9	Navy Hydrographic Ship "Adm. Ormanov"
1995	27-28 March	4	5	
1995	29-30 May	3	2	
1995	29July-08 August	10	19	R/V "Akademik"

Zooplankton samples were collected by a vertical net of the Jedi type with 36 cm opening diameter and a mesh size of 150 μm. The plankton samples were taken at standard depth intervals of 10-0, 25-10, 50-25, 75-50, 150-75, 150-100, 100-0 m. After counting and

identifying the size of *Mnemiopsis leidyi* and *Aurelia aurita*, the samples were fixed with 4 % formalin solution aboard the ship. The quantitative data processing was done according to Dimov [1]. Biomass was calculated on the basis of standard species weight obtained from Marine Hydrophysical Institute-Sevastopol. Field work for this paper was carried out between 18 April 1994 and 8 August 1995 with R/V "Akademik" and Navy R/V "Adm. Ormanov" (Table 1). The discussion was based on the data from the coastal region (up to 10-12 miles offshore) and the open sea area.

3. Results and discussion

On the basis of analysis of the results obtained from many years of study, the trends in the change of the qualitative composition and quantitative development of the zooplankton species in the waters adjacent to the Bulgarian coast are pointed out.

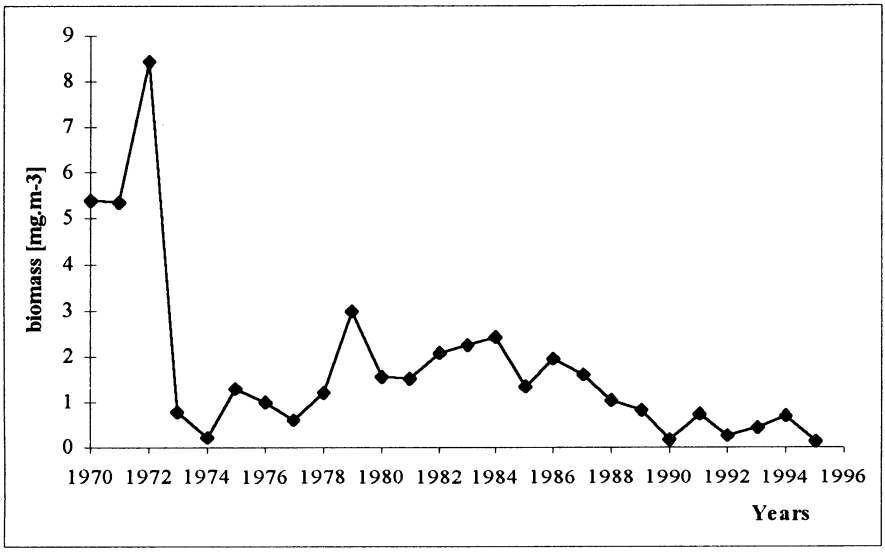


Figure 2. Multiannual trend in the variability of the mean biomass [mg.m^{-3}] of *Oithona minuta* in the Bulgarian Black Sea area for the period 1970-1995 (spring-summer).

In the 1970-1972 period, the average biomass of *Oithona minuta* in the Black Sea adjacent to the Bulgarian coast was 6.39 mg.m^{-3} (STDEV=1.77) (Fig. 2). In the 1973-1989 period it decreased to an average of 1.46 mg.m^{-3} (STDEV=0.72), and in 1990-1995 the average biomass of the same species was 0.41 mg.m^{-3} (STDEV=0.25). The average biomass values of *Centropages kroyeri* observed during the corresponding periods respectively were 14.29 mg.m^{-3} (STDEV=5.79), 2.37 mg.m^{-3} (STDEV=1.69) and 0.95 mg.m^{-3} (STDEV=0.73) (Fig. 3).

The most recent data in 1994 on the state of the zooplankton adjacent to the Bulgarian Black Sea coast, show that, under the spring (April) conditions with quasi-

homogeneous structure of the surface waters, the qualitative composition of the coastal zone (10 miles offshore) is dominated by the species of *N. scintilans*, *Acartia clausi* together with her copepodit and nauplii stages, *Paracalanus parvus*, *Pleopis polyphemoides*, larvae of *Polychaeta*, *Lamellibranchia* and *Cirripedia* as well as the *Rotatoria* species — *Synchaeta vorax*. Among them *N. scintilans* and the representatives of *Rotatoria*, *Cladocera* and *Copepoda* account for the highest percentage of biomass (Fig. 4a).

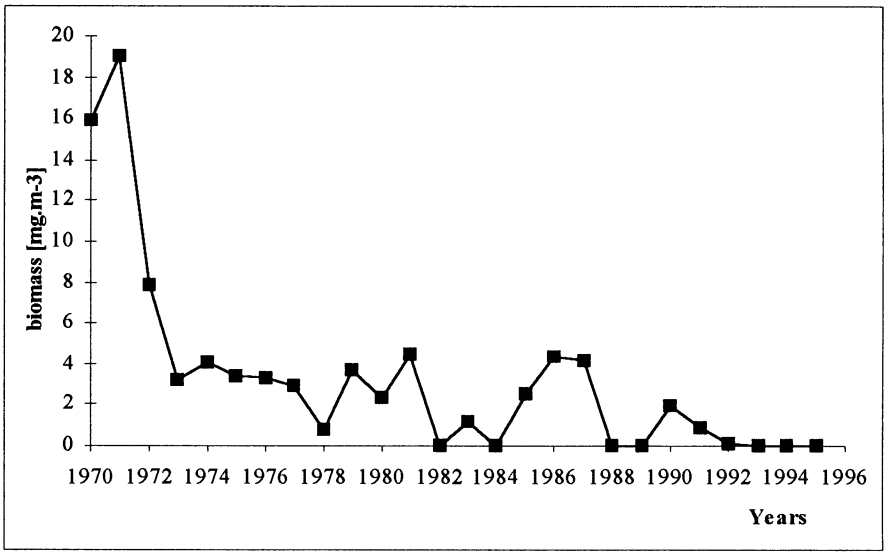


Figure 3. Multiannual trend in the variability of the mean biomass [mg.m^{-3}] of *Centropages kroyeri* in the Bulgarian Black Sea area for the period 1970-1995 (spring-summer).

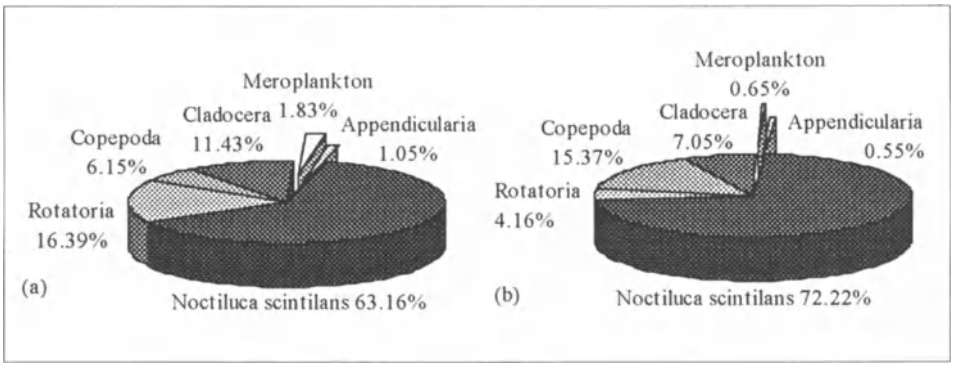


Figure 4. Zooplankton mean biomass structure in the coastal zone (a) and the open sea (b) in April, 1994.

At the same time, the open sea plankton fauna is dominated by *A. clausi*, *Ps. elongatus*, *C. helgolandicus*, *O. similis*, *S. setosa*, *Pl. rhodopi* and *N. scintilans*,

the latter of which occupies the greatest part of the average biomass (Fig. 4b).

In the coastal region, the eurytherms and the thermophile species are still not well developed, and determine a small part of the biomass. *N. scintilans* mean biomass amounts to 83.65 mg.m^{-3} in the coastal zone and 216.38 mg.m^{-3} in open sea (Fig. 5a).

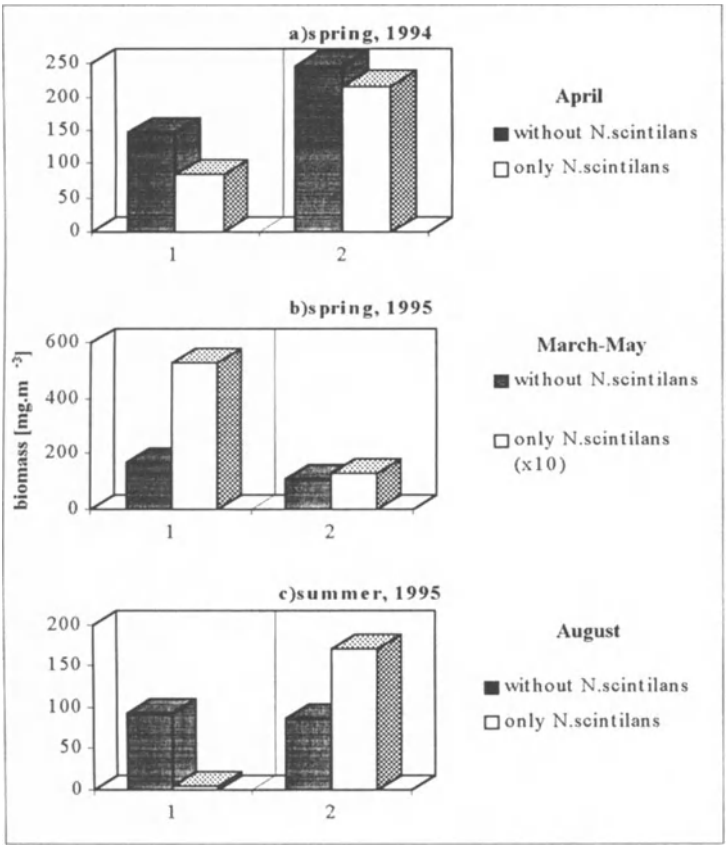


Figure 5. Mean valuesof the Black Sea zooplankton biomass in mg.m^{-3} adjacent to the Bulgarian coast excluding *Noctiluca scintilans* and *N.scintilans* separately in a coastal (1) and an open-sea (2) region.

The mean spring value of the zooplankton biomass excluding *N. scintilans*, amounts to 146.72 mg.m^{-3} in the coastal zone and reaches 246.15 mg.m^{-3} in the open sea, about 10-12 miles offshore. The higher biomass values in open sea are due to the significant part of stenothermal and cryofile species *Ps. elongatus*, *C. helgolandicus* and *O. similis* High numbers of the ctenophore *M. leidyi* were established in this survey, 20 ind.m^{-3} and 12 ind.m^{-3}, respectively in the coastal and open sea areas.

The spring zooplankton biomass in 1995 contained the same species as the previous year, equally valid for coastal and open-sea regions. Percentage composition of the average biomass without *N. scintilans* is shown in Figure 6. Differences are

observed in terms of quantitative comparison: The mean coastal biomass of 169.28 mg.m^{-3} excluding *N. scintilans,* is considerably higher in comparison to 1994, while the open sea biomass (110.29 mg.m^{-3}) is two times smaller. Obviously, *N. scintilans* has a pronounced presence. During this period its biomass has reached 5283.54 mg.m^{-3} in the coastal region and 1301.15 mg.m^{-3} in the offshore zone (Fig. 5b). In same period *M. leidyi* amounted to 18 ind.m^{-3} in the coastal region, and 17 ind.m^{-3} in the open sea.

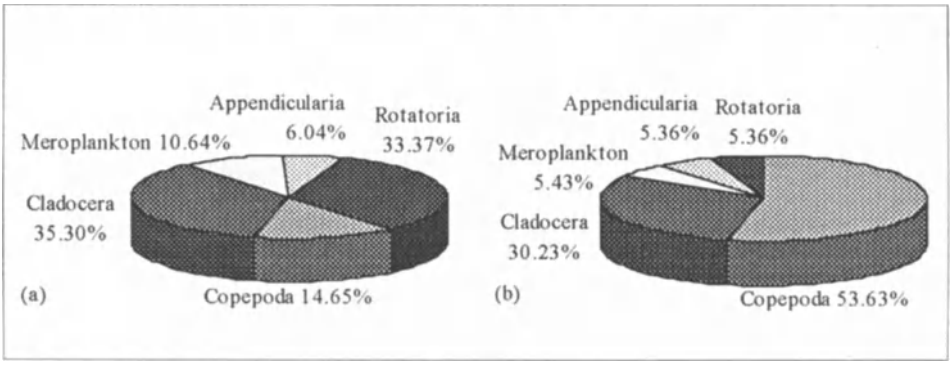


Figure 6. Zooplankton mean biomass structure in the coastal zone (a) and the open sea (b) in spring (March-May), 1995.

During the summer of 1995, in the isothermal waters of the coastal region, zooplankton were mainly represented by eurythermal and thermophile species of *Cladocera* and *Copepoda*, and the larvae of *Cirripedia*, *Polychaeta*, *Lamellibranchia* and *Gastropoda*. Among them *Cladocera* and *Copepoda* species constituted the highest percentage of biomass (Fig. 7a). Significant quantities of *M. leidyi*, Pisces ova and Pisces larvae have also been registered. *N. scintilans* abundance in this zone is much lower in comparison to that recorded in spring of the same year.

In the quasi-homogeneous structure of the open sea, the summer zooplankton is comprised of three components: a thermophile complex above the thermocline; a eurythermal one at depths of 25-50 m and a stenothermal cryofile complex below 50m. In this zone *N. scintilans* has high percentage in biomass. The percentage shares of *S. setosa*, *Copepoda* and *Cladocera* are similar (Fig. 7b).

The mean values of the summer biomass in the coastal and the open sea areas excluding *N. scintilans* are respectively 93.33 mg.m^{-3} and 87.49 mg.m^{-3}. The biomass of *N. scintilans* in the same regions are respectively 4.38 mg.m^{-3} and 171.34 mg.m^{-3} (Fig. 5c).

In summer of 1995 the highest quantities of ctenophore *M. leidyi* have been registered in the coastal region. The abundance of *M. leidyi* exceeded 100 ind.m^{-3} in the coastal zone south of cape Kaliakra (120 ind.m^{-3}), in Varna Bay, adjacent to the Kamchia river mouth (115 ind.m^{-3}) and in Bourgas Bay (135 ind.m^{-3}). Towards the open sea, the quantity of this species gradually decreased and only single individuals were found there (Fig. 8). It was noticeable that young stages with size up to 1 cm prevailed in

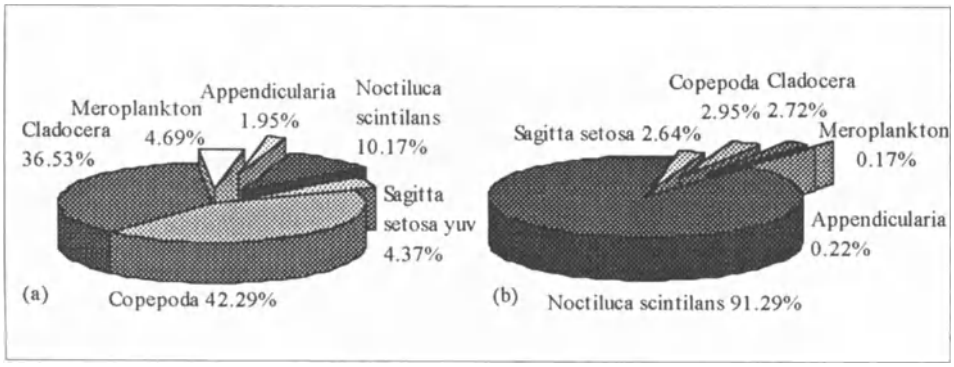


Figure 7. Zooplankton mean biomass structure in the coastal zone (a) and the open sea (b) in August, 1995.

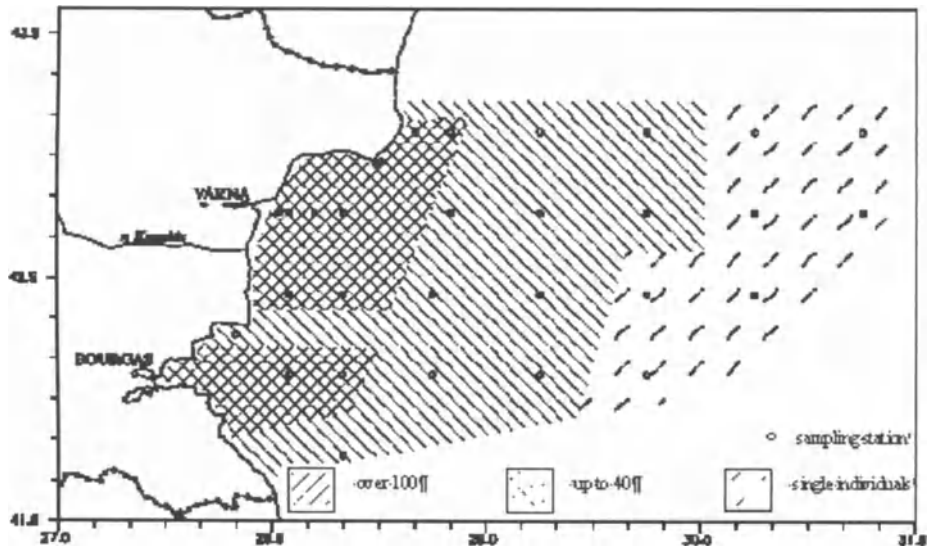


Figure 8. Distribution of Mnemiopsis leidyi [ind.m^{-3}] adjacent to the Bulgarian Black Sea area in August, 1995

the coastal zone, while in the open sea, individuals over 13 cm in size were registered.

After 1991, long standing records of zooplankton quantitative development exhibit an increase in the coastal area (Fig. 9), which could be explained by the lower number of *Mnemipsis leidyi* at that time (Fig. 10). The increase in ctenophore number after 1994 seems to be the most probable cause for zooplankton sustainable characteristics.

The progressive increase of the unicellular euryphage *Noctiluca scintilans,* which appears to have a role as a eutrophicant in the coastal zone, and as a de-eutrophicant with trophic potential in the open sea, is probably due to the high degree of primary and secondary eutrophication of the Black Sea adjacent to the Bulgarian coast [5]. The number of *N. scintilans* has always been higher in the coastal region (Fig. 11) where

higher values of zooplankton biomass were also registered. This type of correlation has been exhibited during the entire period (1971-1995).

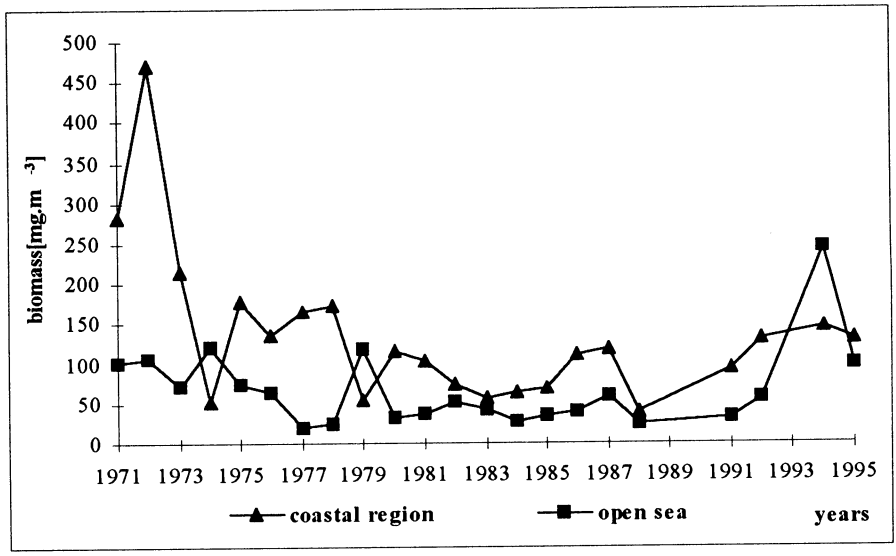


Figure 9. Long-term dynamics of zooplankton biomass in the Bulgarian Black Sea area for the period 1971-1995 (spring-summer, without *Noctiluca scintilans*).

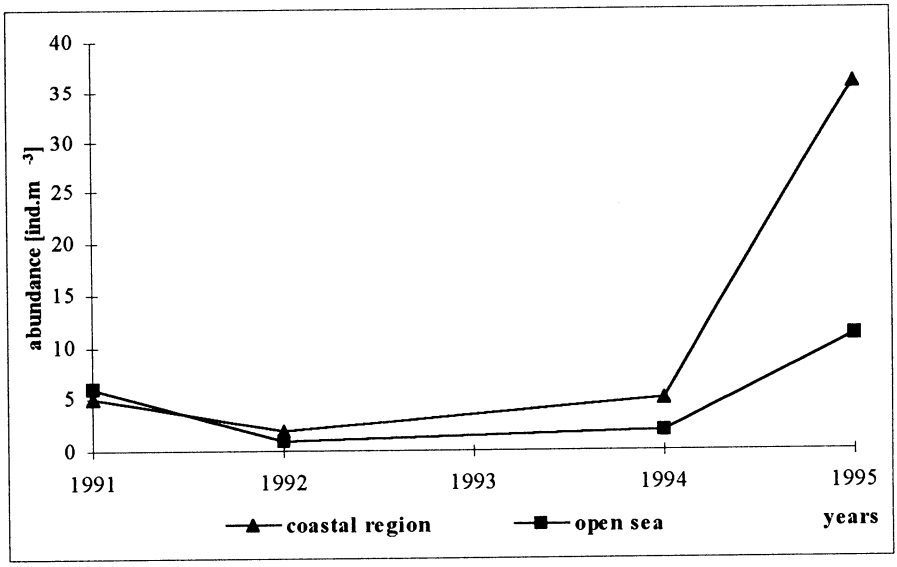


Figure 10. Average abundance of *Mnemiopsis leidyi* in the Bulgarian Black Sea area for the period 1991-1995 (spring-summer).

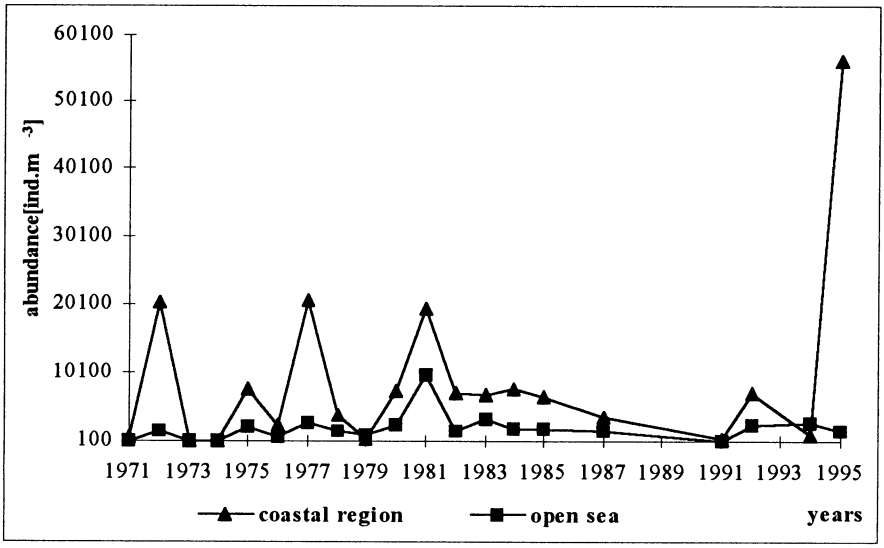


Figure 11. Average abundance of *Noctiluca scintilans* in the Bulgarian Black Sea area for the period 1971-1995 (spring-summer).

Today the coastal zone is highly eutrophic, which is probably the cause of serious disturbances in the structure of its pelagic ecosystem [9]. These structural changes are pronounced not only in the biodiversity decrease of the coastal plankton but also in the progressive increase in the number and biomass of those of its components that are adapted to the high degree of eutrophication. Thus, the exclusively great quantities of the unicellular euryphage *N. scintilans* in the coastal region and open sea during recent years and the mass development and reproduction of ctenophore *M. leidyi* in the nearshore zone, indicate active eutrophic processes in the western part of the Black Sea. This allows us to suggest that these two representatives of the pelagic fauna are exclusively sensitive to changes in the environment caused by anthropogenic factors, and hence can be used as bio-indicators.

4. Conclusion

In conclusion, it can be stated that, during recent years, the state of the zooplankton, in terms of its number and qualitative composition, has been affected by the following factors:

Centropages kroyeri and *Oithona minuta* are strongly reduced in quantity, and *Anomalocera patersoni* and *Pontella mediterranea* are almost extinct from the coastal water species.

The mean zooplankton biomass increase after 1991, excluding *N. scintilans* increase after 1991 is retained within limits of 131 $mg.m^{-3}$ in the coastal region and

99 mg.m^{-3} in the open sea, suggesting a process of pelagic ecosystem recovery due to *Mnemiopsis leidyi* pressure.

Mnemiopsis leidyi development influences to a great extent the zooplankton number and biomass.

Noctiluca scintilans, being a constant component of the pelagic ecosystem adjacent to the Bulgarian Black Sea coast, appeared highly adaptive to eutrophicaton.

The high values in number and reproductiveness of these two species in highly eutrophied regions (in the nearshore zone south of cape Kaliakra, in Varna and Bourgas Bays, and in the Kamchiya river mouth), confirm their adaptiveness.

This circumstances allow one to suggest that these two components of the zooplankton could be used as bio-indicators of the degree eutrotrophication in relation to anthropogenic activities. Their nutrition, development and reproduction patterns in highly eutrophied zones give us reason to assume that they could play a positive role in the processes of de-eutrophication.

5. References

1. Dimov, I. (1959) Improved Quantitative Zooplankton Sampling Method. *Rep. BAS,* 12, 5, 427-429.
2. Dimov, I. (1962) The Zooplankton adjacent to the Black Sea Western Coast during the Period 1957-1959. *Processing of the Institute of Fisheries,* 2, 5-8, Varna.
3. Dimov, I. (1963) Formation of the Zooplankton Composition and its Quantity in the Black Sea Western Part. *Processing of the Institute of Fisheries,* 3, 5-29, Varna.
4. Konsulov, A. (1975) The Black Sea Zooplankton adjacent to the Bulgarian Coast. *Ph.D. Thesis* (in Bulgarian).
5. Konsulov, A. (1984) The Part of Noctiluca Scintilans in the Shallow Water Eutrofication. *Ribno stopanstvo (Fish Industry),* 3, 17-18.
6. Konsulov, A. (1989) One more New-comer. A New Species in the Black Sea-Dangerous or Harmless for Ecology, *Morski Svjat* 2, 8.
7. Konsulov, A. (1990) New Species for the Black Sea. *BAS, Oceanology* 19, 98-99.
8. Konsulov, A. (1991) Investigation on Biology, Ecology and the Meaning of the Zooplankton in the Black Sea adjacent to the Bulgarian Coast. *D.Sc. Thesis* (in Bulgarian).
9. Vinogradov, M.E, Ý.A.Shushkina, E.I.Musaeva, P.Yu.Sorokin. (1989) Ctenophore Mnemiopsis leidyi (A.Agassiz) (Ctenophora:Lobata)-New Settlers in the Black Sea. *Oceanology,* Institute of Oceanology, 29, 293-299, Moskva.
10. Vinogradov, M. E. Ý. A.Shushkina, V.V. Sapozhnikov. (1992) The Black Sea Ecosystem. Institute of Oceanology, 5-109, Moskva.

LONG-TERM VARIABILITY OF PHYTOPLANKTON COMMUNITIES IN OPEN BLACK SEA IN RELATION TO ENVIRONMENTAL CHANGES

ALEXANDER S. MIKAELYAN
Shirshov's Institute of Oceanology RAS,
Krasikova 23, 117851 Moscow

Abstract. Data on total biomass and taxonomic structure of phytoplankton communities, collected in the Black Sea during the period 1978-1992 were analysed. Comparisons were restricted to the biological summer-autumn season, when the ecosystem is in most stable state. Changes in phytoplankton communities were investigated in the entire basin as well as in five regions of the Black Sea: central cyclonic gyres, central convergence zone, western and eastern parts of Rim Current. The range of interannual oscillations was comparable with seasonal changes. The mean biomass of the total phytoplankton in the water column varied by about 5 times, from 4 to 21 g m^{-2}, in the period. The general trend of biomass increase from 1978 to 1992 was observed in the 5 studied regions as well as in the entire basin. The highest phytoplankton biomass was observed in the western part of Rim Current. An increase in large phytoplankton groups was evident in the 1992-1995 period, during which an increase of diatoms and a decrease of dinoflagellates was also observed. The analysis of changes in zooplankton communities occurring after the *Mnemiopsis* intrusion have shown that grazing control was not the main factor determining total phytoplankton abundance in deep waters of the Black Sea. Changes in grazing control could have defined the changes in size and taxonomic structure of the phytoplankton community. On the other hand, interannual oscillations of average air temperature in winter appears inversely correlated to mean phytoplankton biomass in summer, suggesting that bulk of the phytoplankton in the summer-autumn season is linked to intensification of general hydrodynamic activity in the Black Sea driven by climatic variations. A review of earlier data on phytoplankton, collected during the 1948-1976 period is also consistent with this hypothesis.

1. Introduction

During the recent years, extensive attention was paid to the problem of drastic changes in the Black Sea ecosystem. The changes in the chemical and biological environment have been reported in the north-western part of the Black Sea [9, 28]. These changes were mainly related to eutrophication caused by a net increase in river discharges to

E. Özsoy and A. Mikaelyan (eds.), Sensitivity to Change: Black Sea, Baltic Sea and North Sea, 105–116.
© 1997 *Kluwer Academic Publishers.*

the sea [4]. As concerns the open waters of the Black Sea, eutrophication is not so clearly evident. The anthropogenic impact on the ecosystem of open waters is often modulated by natural climate fluctuations reflected by environmental parameters such as river outflows, intensity of circulation, mixing and winter cooling conditions [26].

Well defined interannual changes in chemical and biological parameters have been observed in the open waters of the Black Sea during the last 3-4 decades. The concentration of nutrients in the upper mixed layer decreased more than 10 times from 1950 to 1987 [2,16]. In contrast, the content of the chlorophyll *a* and the level of primary production increased by a factor of *ca* 2 from 1960 to 1991 [25]. Decreases in water transparency occurred during last decade, with minimum transparency (disk Secchi readings) observed in 1992 [27].

Various data obtained in the central part of the Sea from 1948 to 1956 by the Institute of Biology of the Southern Seas, Sevastopol shows the obvious trend of increasing of phytoplankton biomass at the beginning of 50's [6]. In the eastern part of the Sea, within the coastal and Rim Current area, phytoplankton biomass increased *ca* 3-4 times from 1961 to 1976 [11]. In this data series, the maximum phytoplankton biomass was observed at the beginning of 80's. The analysis of more recent data from 1978 to 1995 in the present study revealed an increase of biomass in 1991-1992.

Unfortunately, long-term data on phytoplankton are virtually impossible to compare, due to principal differences in methods of collection and treatment of the samples. Before the 60's, phytoplankton were collected with nets [15], and, hence, only large algae cells were counted. In the 60-70's, the settling technique was used, which shifted the size of collected phytoplankton to more small cells (over 8 μm). Since 1978, phytoplankton are collected using filtration over Nuclepore filters with pore size of 1 μm [22]. Simultaneously, small flagellates were counted in natural samples without pre-filtration, in order to be able to count the fragile cells destroyed during the filtration process. It was expected that all phytoplankton cells were enumerated. Starting from 1984 the fluorescent count was applied to enumerate the small algae [24]. It was shown that the count of flagellates under light microscope in natural waters substantially underestimates the number of small algae and totally misses the picophytoplankton [10, 14]. Therefore, quantitative comparisons of algae biomass and size composition of phytoplankton communities are not possible in the long term.

In this paper, the quantitative comparisons of data obtained in the cruises of Institute of Oceanology, Moscow from 1978 to 1995 are presented. During this period the phytoplankton were collected and enumerated usind rather similar techniques. Changes in phytoplankton communities, related to physical, chemical and biological environment are studied in five Black Sea regions as well as in the entire basin.

2. Material and Methods

Samples were collected at 87 stations during the period from 1978 to 1995. According to Morozova-Vodyanitsckaya [15], summer-autumn is the biologically stable season in the Black Sea. During this period the vertical stratification in the photic zone occurs.

Species composition and the level of phytoplankton biomass are more or less the similar. In order to avoid the influence of seasonal changes, which exceeds 1 fold [29], only data collected from June to mid November were taken into account. List of data sources used is presented in the table 1.

TABLE 1. Data sources

Year	Period	Stn.	Cruise	Source
1978	25.09-31.10	12	64 "Vityaz"	Suchanova, Belayeva [23]
1978	01.08-31.10	5	"Priboy"	Zernova, Nezlin [29]
1979	20.09-29.10	5	"Priboy"	Mikaelyan [12]
1980	25.09-02.11	2	"Priboy"	Mikaelyan [12]
1985	21.09-01.11	6	7 "Rift"	Rat'kova [18]
1986	11.06-29.06	5	8 "Rift"	Rat'kova [18]
1989	23.07-10.09	23	44"Mendeleev"	Senichkina et al. [20]
1991	18.08-13.11	10	23"Vityaz"	Mikaelyan, Georgieva, Kokurkina, Vavilova (unpublished data)
1992	28.09-14.10	12	26"Vityaz"	Mikaelyan, Kokurkina, Vavilova (unpublished data)
1995	20.09-25.09	7	"Akvanavt"	Mikaelyan, Zav'yalova (unpublished data)

Samples were collected by means of a 150-liter plastic sampler (Institute's construction). The vertical sampling series consisted of 7-10 samples down to depths of 75-130 m. Cells of microphytoplankton (over 15 μm in length) from 1 to 5 l were concentrated over 1.0 μm Nuclepore filter. Cells were examined and enumerated under light microscopes in non-fixed concentrates (from 30 to 40 ml) on the day of collection. In 1978-1980 the small flagellates (under 15 μm) were counted under light microscope in natural water samples without concentration. In 1985 and later, small cells were enumerated using epifluorescence microscopy. Aliquots (25 to 50 ml) of the collected samples were fixed with glutaraldehyde (up to 1% of final concentration). After 20 minutes, the aliquots were filtered through 0.2 μm Nuclepore filters previously stained with Sudan Black to prevent filter autofluorescence. After filtering, algae cells were stained with primulin [3]. Slides with the filters were examined microscopically (LUMAM-I3, LOMO, Russia) using blue excitation. Eukaryotes fluoresced red and cyanobacterial cells yellow-orange. Cells were counted by transects or fields of vision and a part of the total filter area was investigated. In the case of nanophytoplankton (from 2 to 15 μm), this part corresponded to 0.1-1 ml of the filtered water. In the case of picophytoplankton (under 2 μm) it varied from 0.001 to 1.0 ml. Cell volumes were calculated based on measurements of cell's approximate dimensions using geometrical formulae. Wet biomass was assumed to be equal to cell volume.

The method of counting small cells under light microscope in natural waters has strong bias against numbers of small algae [10, 14], not being able to enumerate cells under 4-6 μm.. In order to compare the data obtained before and after 1984, the former were corrected using a conversion factor. This factor was found from the relationship between the total phytoplankton biomass and the share of cells over 6 μm in total phytoplankton biomass (fig. 1). The correction was substantial when the biomass was

low (less than 10 g m^{-2}). With high biomass values (more than 15 g m^{-2}) no correction was applied.

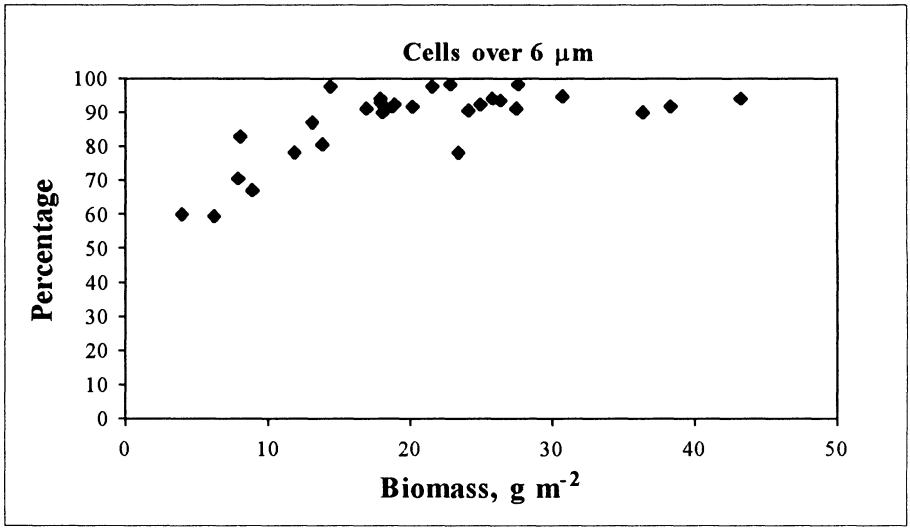


Figure 1. Percent of algae with the cell size over 6 μm in the total phytoplankton biomass on average under water column.

3. Results and Discussion

During the period from 1978 to 1995 the total phytoplankton biomass in the water column varied *ca* 10 times, from 4 to 40 g m^{-2} . Changes were observed in the entire basin, as well as in the 5 regions studied: western and eastern parts of Rim Current, western and eastern cyclonic gyres and Central Convergence zone between the two gyres (fig. 2). The highest values (40-43 g m^{-2}) were recorded in the two cyclonic gyres (fig. 2, C, D). The lowest level of phytoplankton biomass (under 20 g m^{-2}) was observed in the Central Convergence (fig. 2, B). The range of interannual oscillations was comparable with seasonal fluctuations. In the eastern part of the Rim Current, the phytoplankton biomass varied from 2 g C m^{-2} to 20 g C m^{-2} during the 1980's [29]. In the eastern cyclonic gyre, the total phytoplankton abundance reached a maximum of 120 g m^{-2} in winter 1991 [13], and decreased to 30 g m^{-2} in summer 1991 (this study). The mean total phytoplankton biomass in the water column varied *ca* 5 times from 4 to 21 g m^{-2} from 1978 to 1995.

The general trend of biomass increase from 1978 to 1992 could be seen in the 5 regions as well as in the entire basin. The only station surveyed in the center of the eastern cyclonic gyre evidently showed a decrease in phytoplankton abundance in 1995 (fig. 2, D). A decrease in algae biomass was also observed in the eastern part of the Rim Current in 1995 (fig. 2, F).

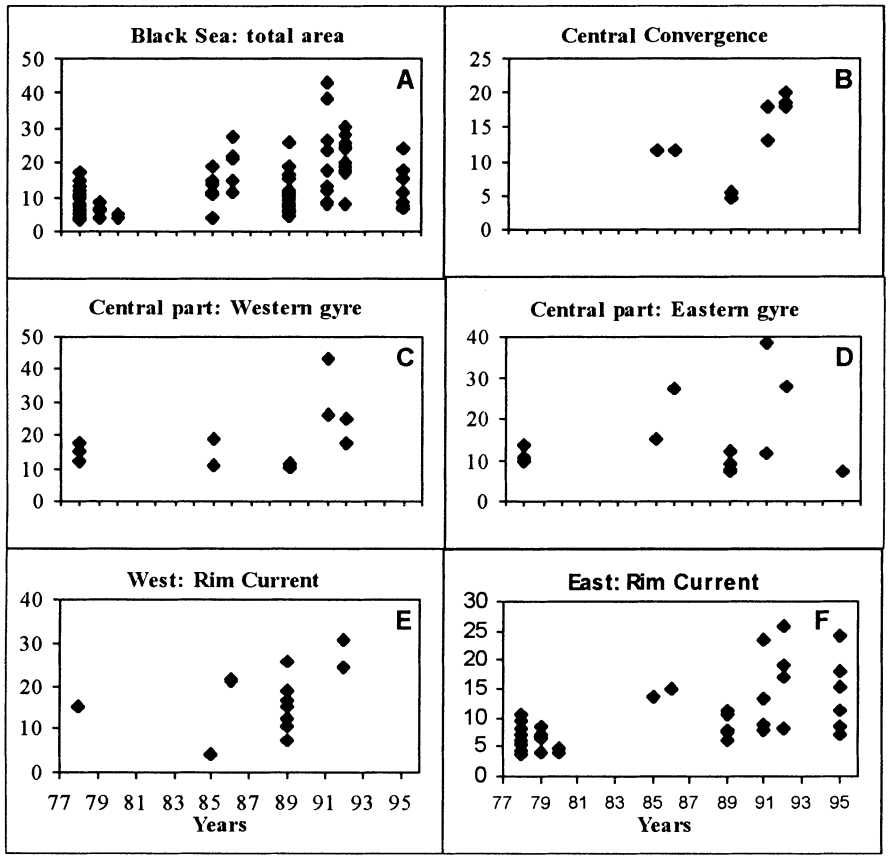


Figure 2. Changes in phytoplankton biomass (g m^{-2}) in the open waters of the Black Sea. Entire basin (A) and 5 regions: eastern (D) and western (C) cyclonic gyres; eastern (F) and western (E) periferal areas and Rim Current; convergence between two central gyres (B).

The highest phytoplankton abundance was observed in the western part of the sea in the region of Rim Current and peripheral areas (fig. 3, A). Significant difference (Student's test, $p<0.02$) in phytoplankton biomass was found between this region and the eastern part of Rim Current. Comparison of other regions revealed no significant differences in phytoplankton biomass in those regions (fig. 3, A)

The most simple explanation of this observation is the influence of anthropogenic input reaching the open waters of the western part of the basin. This suggestion is confirmed with the nutrients content in the upper mixed layer. Phosphate concentration in the western part of Rim Current was significantly higher than that in other regions (fig. 3, B). The nitrogen concentration displayed a maximum in the center of the western cyclonic gyre (fig. 3, C). Combining two nutrients it could be suggested that the western part of the sea was more saturated with nutrients than the eastern one. This suggestion is consistent with many observations, including satellite photos, from which the meanders and rings along the western coastal current could be

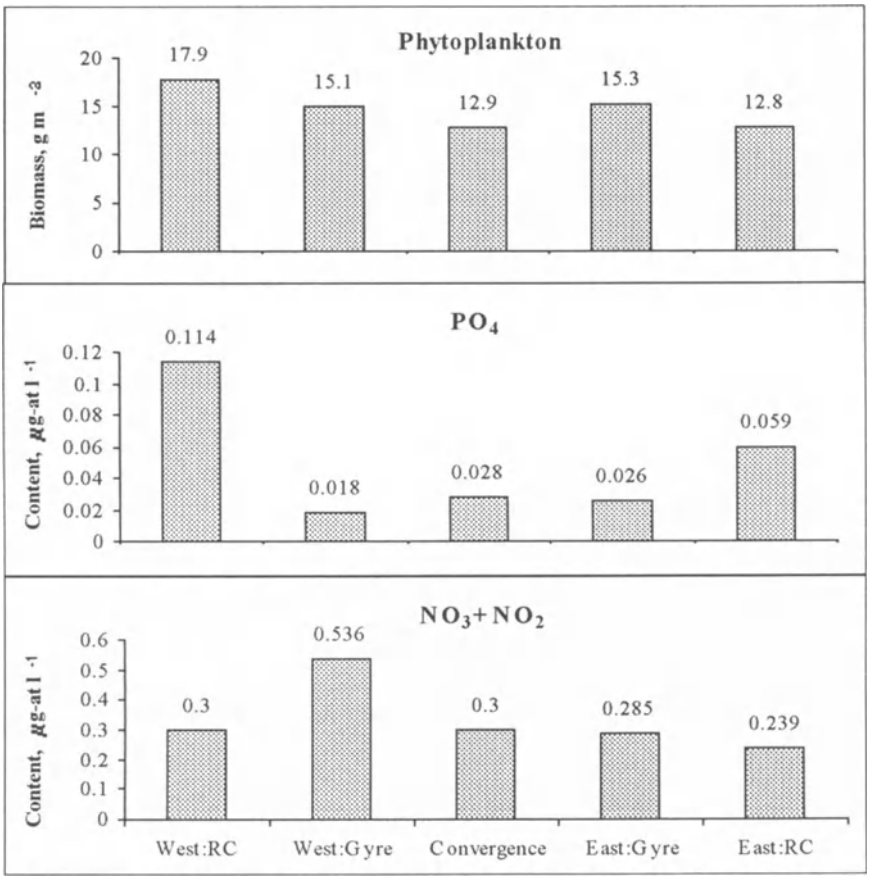


Figure 3. Phytoplankton biomass under water column, content of phosphates and nitrates+nitrites in the upper mixed layer in five regions of the Black Sea. West:RC and East:RC- western and eastern parts of Rim Current; West:Gyre and East:Gyre - western and eastern central cyclonic gyres; Convergence - region between two central gyres.

seen. Some intrusions of nutrient replenished coastal water reach the center of the western part, but these events seem to be occasional [1]. As a result, the highest phytoplankton biomasses were observed in the western part of Rim Current, excluding the center of the western cyclonic gyre. The eutrophication of the eastern part of the sea is not evident from these data.

Interannual changes in the sizes and taxonomic structures of phytoplankton communities were also observed. An increase in the share of microphytoplankton in the total phytoplankton biomass was recorded in 1992 and 1995 (fig. 4, A). An increase of diatoms and a decrease of dinoflagellates in the summary biomass of both groups occurred after 1991 (fig. 4, B).

After intrusion of ctenophora *Mnemiopsis* into the Black Sea ecosystem in 1988, the number of mesozooplankton decreased [26]. Decline in small copepods abundance

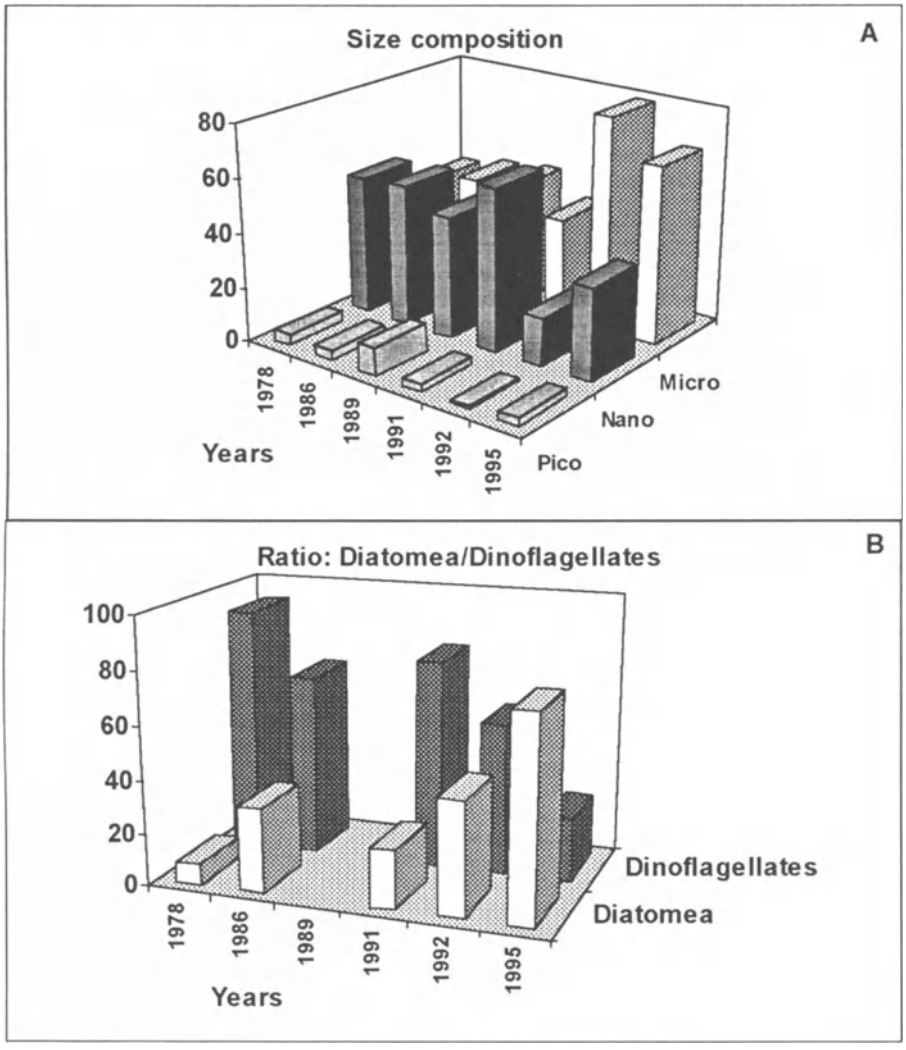


Figure 4. Changes in share (%) of 3 size groups (pico-, nano- and microphytoplankton) in the total phytoplankton biomass (A). Changes of ratio (%) between biomass of diatoms and dinoflagellates (B).

(under 3 mm) was recorded since 1988, while the biomass of *Calanus euxinus* decreased later in 1991 (fig. 5).

It could be expected that the anthropogenic eutrophication of the open waters in the Black Sea would not be equal to the entire basin, because of the main source in the north-western part of the sea. The evident increase in phytoplankton biomass from 1980 to 1992 in the whole basin might have had other reasons, which could be grouped as two main factors: changes in the general hydrodynamic activity, or a decrease of grazing on phytoplankton. The increase in hydrodynamic activity leads to enrichment

by nutrients in the upper mixed layer, promoting the development of phytoplankton and shifting the size spectrum of phytoplankton to large cells, especially to diatoms [7]. On the other hand, a decrease in number of copepods, as main consumers of large cells, could also have increased the share of large cells in the phytoplankton biomass. Thus, both factors could influence the size and taxonomic structure of phytoplankton community in the same direction, and therefore their contributions to this event could not be easily separated. It is only noted that the increase in total phytoplankton biomass was observed in 1985-1986, before the zooplankton decline in 1988 (fig. 5). In 1995, the decrease in phytoplankton biomass was observed on a background of low, constant level of zooplankton biomass. This suggests that grazing is probably not the main factor which determines total phytoplankton levels. Nevertheless, changes in grazing control might have defined the changes in size and taxonomic structure of phytoplankton community. For instance, an increase in the share of microphytoplankton, as well as of diatoms in the total phytoplankton biomass were recorded in 1991, and clearly observed in 1992 and 1995, coinciding with the lowest level of copepod abundance swo far observed (fig. 5).

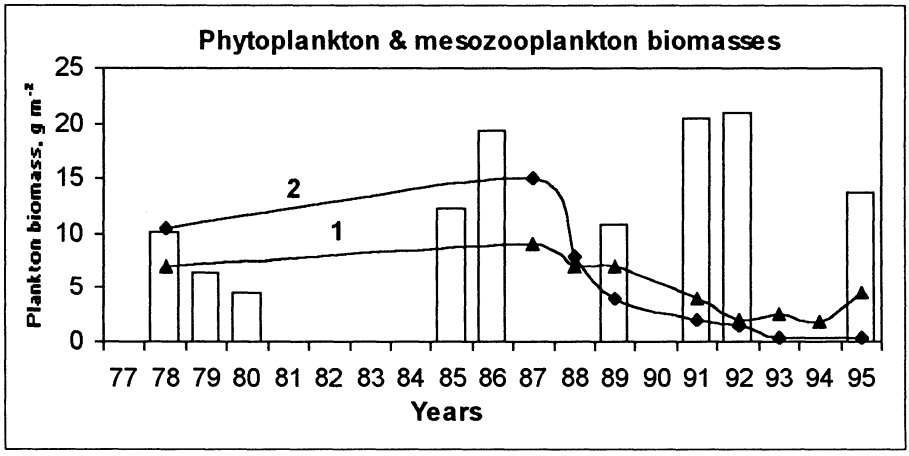


Figure 5. Biomass of *Calanus euxinus* (1) and other copepods (2): data from 1978 to 1992 by Vinogradov [25]; data from 1993 to 1995 by Shiganova [21]. Summer phytoplankton biomass (columns).

The general hydrological activity in the Black Sea strongly depends upon winter convection and hence on climatic variations [5]. According to Ovchinnikov and Osadchiy [17], the average winter air temperature has quasi-periodic 20-years oscillations. During the coldest years of the period, the low winter temperatures could cause intense water uplift in the centers of both gyres and would intensify the circulation of the Rim Current, which would be effective in winter as well as in summer. During the period from 1980 to 1993, a gradual decrease in winter mean air temperatures were observed, along with an increase in phytoplankton biomass in the summer (fig. 6). The high value of mean biomass obtained in 1986 (fig. 6. point 5), to some extent had methodological origin. A thin layer (3-5 m) with a very high diatom

abundance, occurred at the thermocline in June 1986 [19]. This layer was discovered and sampled with high resolution from the submersible "Argus", with results that seriously differed from other surveys, due to the methods of data collection. When recalculated using standard profile resolution (10 depths), the mean total phytoplankton biomass diminished from 19 to 16 g m^{-2}. The latter value (fig. 6, curve 4) therefore seems to be more suitable for interannual comparison.

The lowest and the highest phytoplankton biomasses corresponded to high and low temperatures in 1980 and 1992 respectively. The decrease in biomass from 1978 to 1980 and from 1992 to 1995 corresponded to inverse changes in air temperature (fig. 6). This permits us to put forward the following hypothesis: Cold and warm weather periods with corresponding low and high hydrodynamic activity respectively are the main factors determining the level of productivity in the Black Sea. Although the earlier available data could not be compared with modern ones as mentioned above,. nevertheless the position of peaks within a group of data which are methodologically similar could show the principal relationship between phytoplankton biomass and air temperature. Data on phytoplankton biomass obtained in the eastern part of the sea from 1961 to 1976 [11] confirm the correspondence of low winter air temperatures and maximum of algae abundance in summer (fig. 6, curve 3). The similar pattern could also be seen from a review of the earlier data collected from 1948 to 1956 [6]. The cold winter period from 1948 to 1952 corresponded to the highest summer-autumn phytoplankton biomasses (fig. 6, curve 2).

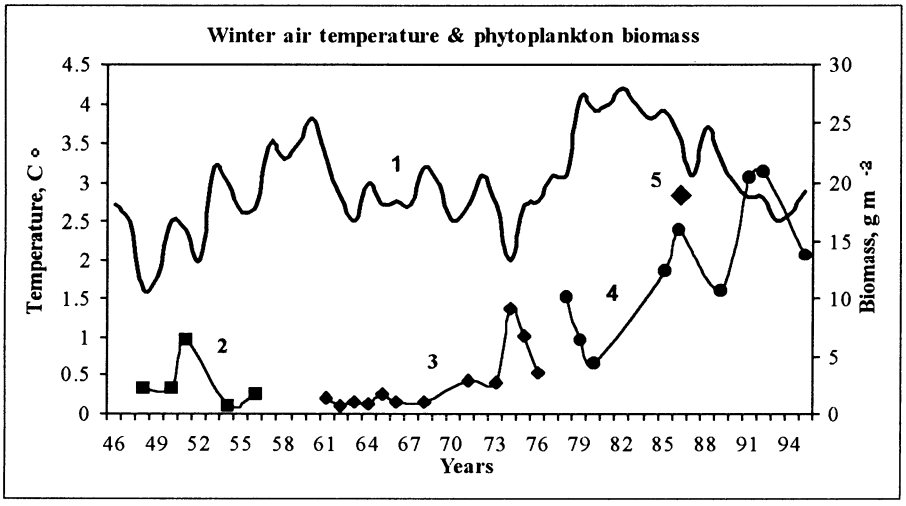


Figure 6. Average winter air temperature (curve 1, from Ovchinnikov and Osadchy [17], modified with data by Ovchinnikov, unpublished) and total phytoplankton biomass in summer: 2-from Georgieva [6]; 3- from Mashtakova and Roukhiyainen [11]; 4 - from this paper; 5 - measured value (see explanation in the text).

The presented curve of winter air temperature is the result of 5 year sliding average applied to the data. The year-to-year comparison of temperature and phytoplankton biomass provides more worse correlation. The Black Sea current system is inert. As

example, the inertia of the system could be seen from interannual changes of mean temperature in Cold Intermediate Layer. In spite of the fact that the winter of 1994 was warmer than of 1993, the cooling in the lower part of the pycnocline continued during this year and the temperature started to increase only in 1995 [8]. It seems that the sequence of cold years is necessary to result in an intense circulation and to increase the productivity of the basin.

Projecting into the future, the next warm and cold extremes are expected in the years 1998-2000 and 2010-2012 respectively. Therefore, the level of productivity of the sea should be compared between the years 1980 and 2000, and between 1990 and 2010. This implies that the eutrophication of the basin could be determined only on the basis of an analysis using at least 20-years of data.

4. Conclusions

1. The range of interannual oscillations is comparable with seasonal changes.
2. The anthropogenic influence on the open waters of the Black Sea is evident only in the western part of the sea.
3. Mesozooplankton grazing on phytoplankton does not define the total level of biological productivity, but, possibly, influences on size and taxonomic structure of phytoplankton community.
4. The bulk of the phytoplankton biomass is linked to general hydrodynamic activity in the Black Sea caused by climatic variations.
5. Taking into account the 20 years oscillations in weather conditions, anthropogenic changes in the ecosystem can only be assessed by a comparison of at least 20 years of data.

5. Acknowledgements

The author is grateful to Dr. T.Rat'kova for data on microscopic observations during the expedition of 1986, and to Dr. I.M. Ovchinnikov for the data on winter air temperature. The data in 1995 were collected and studied with financial support of Russian Scientific Foundation (grant N 95-05-15626).

6. References

1. Besiktepe, S., Solakov, D., Diaconu, V. and Oguz, T. (1996) Cross-frontal mixing of the coastal and the interior waters of the Black Sea, in E.Ozsoy and A.Mikaelyan (eds.), *Sensivity of North Sea, Baltic Sea and Black Sea to Anthropogenic and Climatic Changes*, Kluwer Academic Publishers, Dordrecht.
2. Bryantsev, V.A., Fashchuk, D.Y. and Finkelshtein, M.S. (1991) Symtoms of hydrological fluctuations in the Black Sea, in M.E.Vinogradov (ed.), *Variability of the Black Sea ecosystem*, Nauka, Moscow, pp. 89-93. (In Russian)
3. Caron, D. (1983) Technique for enumeration of heterotrophic and phototrophic nanoplankton using epifluorescence microscopy and comparison with other procedures, *Appl. Env. Micr.* **46**, 2, 491-498.

4. Cociasu, A. and Diaconu, V. (1996) The role of the nutrient fluxes on the western shelf in the overal Black Sea eutrophication in the last three decades, in E.Ozsoy and A.Mikaelyan (eds.), *Sensivity of North Sea, Baltic Sea and Black Sea to Anthropogenic and Climatic Changes*, Kluwer Academic Publishers, Dordrecht.
5. Fillipov, D.M. (1968) *Circulation and structure of the Black Sea waters*, Nauka, Moscow. (In Russian)
6. Georgieva, L.V. (1993) Species composition of phytoplankton communities, in A.V.Kovalev and Z.Z.Finenko (eds.), *Plankton of the Black Sea*, Naukova Dumka, Kiev, pp. 33-55. (In Russian)
7. Goldman, J.C. (1993) Nutrient and energy flow through marine plankton food chains: impact an new and regenerated primary production, in *Problems of the Black Sea.* International Conference, Sevastopol, Ukraine, Nov.10-15,1992, Plenary reports. MHI UAS, pp. 111-127.
8. Ivanov, L.I., Besiktepe, S., Ozsoy, E., Duman, M., Diaconu, V. and Demirov, E. (1996) Recent changes in the Black Sea pycnocline, *Submitted.*
9. Konsulov, A. and Kamburska, L. (1996) Sensivity to antropogenic factors of the Black Sea plankton fauna in front of the Bulgarian coast, in E.Ozsoy and A.Mikaelyan (eds.), *Sensivity of North Sea, Baltic Sea and Black Sea to Anthropogenic and Climatic Changes*, Kluwer Academic Publishers, Dordrecht.
10. Kopylov, A.V. and Sazhin, A.F. (1989) Heterotrophic nanoplankton in the oxygen zone of the Black Sea, in M.E.Vinogradov and M.V.Flint (eds.), *Structure and productive characters of planktonic communities of the Black Sea,* Nauka, Moscow, pp. 139-155. (In Russian)
11. Mashtakova, G.P. and Roukhiyainen, M.P. (1979) Seasonal dynamics of phytoplankton, in V.N.Greese (ed.), *Productivity of the Black Sea*, Naukova Dumka, Kiev, pp. 79-85. (In Russian)
12. Mikaelyan, A.S. (1984) Diurnal changes in the phytoplankton communities in the eastern part of the Black Sea, *Ph.D. Thesis*, Institute of Oceanology RAN, Moscow. (In Russian)
13. Mikaelyan, A.S. (1996) Winter bloom of diatom Nitzschia delicatissima in the open waters of the Black Sea, *Mar. Ecol. Progr. Ser.*, **129**, 241-251.
14. Mikaelyan, A.S. and Vedernikov, V.I. (1983) Estimation of number of small phytoplagellates, in M.E.Vinogradov (ed.), *Modern methods of quantitative estimates in studies of planktonic distributions*, Nauka, Moscow, pp. 106-144. (In Russian)
15. Morozova-Vodyanitskaya, N.V. (1954) The phytoplankton of the Black Sea. Part II, *Trudu of Sevastopol Biological Station AN USSR* **8**, 11-99. (In Russian)
16. Nalbandov, Yu. (1996) The climatic changes of the hydrochemical regime of the open part of the Black Sea, in E.Ozsoy and A.Mikaelyan (eds.), *Sensivity of North Sea, Baltic Sea and Black Sea to Anthropogenic and Climatic Changes*, Kluwer Academic Publishers, Dordrecht.
17. Ovchinnikov, I.M. and Osadchy, A.S. (1991) Secular variability of winter climatic conditions influencing pecularities of hydrological conditions in the Black Sea, in M.E.Vinogradov (ed.), *Variability of the Black Sea ecosystem*, Nauka , Moscow, pp. 85-89. (In Russian)
18. Rat'kova, T.N. (1989) The phytoplankton of the open areas of the Black Sea, in M.E.Vinogradov and M.V.Flint (eds.), *Structure and productive characters of planktonic communities of the Black Sea*, Nauka, Moscow, pp. 38-52. (In Russian)
19. Rat'kova, T.N., Kopulov, A.I., Sazhin, A.F. and Flint, M.V. (1989) Accumulation of diatoms Nitzschia spp. in the cold intermediate layer of the Black Sea, in M.E.Vinogradov and M.V.Flint (eds.), *Structure and productive characters of planktonic communities of the Black Sea*, Nauka , Moscow, pp. 105-116. (In Russian)
20. Senichkina, L.G., Georgieva, L.V., Nesterova, D.A., Fashchuk, D.Y. and Lifshiz, A.V. (1991) Phytoplankton of the Black Sea in summer period, 1989: biomass and connection with hydrological conditions, in M.E.Vinogradov (ed.), *Variability of the Black Sea ecosystem*, Nauka , Moscow, pp. 104-116. (In Russian)
21. Shiganova, T. (1996) Investigations of the state of main plankton components of the Blak Sea ecosystem after invasion of Mnemiopsis leidyi, in E.Ozsoy and A.Mikaelyan (eds.), *Sensivity of North Sea, Baltic Sea and Black Sea to Anthropogenic and Climatic Changes*, Kluwer Academic Publishers, Dordrecht. (In Russian)
22. Shushkina, E.A. and Vinogradov, M.E. (1991) Fluctuations of the pelagic communities in the open regions of the Black Sea and changes influenced by ctenophora Mnemiopsis, in M.E.Vinogradov (ed.), *Variability of the Black Sea ecosystem*, Nauka , Moscow, pp. 248-261. (In Russian)
23. Sukhanova, I.N. and Belyaeva, T.V. (1980) Species composition, distribution and diurnal variations of phytoplankton in the Black Sea in October 1978, in M.E.Vinogradov (ed.), *Ecosystems of the Black Sea*, Nauka, Moscow, pp. 65-91. (In Russian)

24. Sukhanova, I.N., Georgieva, L.V., Mikaelyan, A.C. and Sergeeva, O.M. (1987) Phytoplankton of the open waters of the Black Sea in late spring in M.E.Vinogradov (ed.), *The modern state of the Black Sea ecosystem*, Nauka, Moscow, pp. 86-96. (In Russian)
25. Vedernikov, V.I. and Demidov, A. (1993) Primary production and chlorophyll in the deep regions of the Black Sea, *Oceanology* **33**, 2, 229-235. (In Russian)
26. Vinogradov, M.E. (1993) Long-term variability of the pelagic community structure in the open Black Sea, in *Problems of the Black Sea,* International Conference, Sevastopol, Ukraine, Nov.10-15,1992, Plenary reports. MHI UAS, pp. 19-33.
27. Vladimirov, L., Mankovsky, I., Solovev, M. and Mishonov, V. (1996) Seasonal and long-term variability of the Black Sea optical parameters, in E.Ozsoy and A.Mikaelyan (eds.), *Sensivity of North Sea, Baltic Sea and Black Sea to Anthropogenic and Climatic Changes*, Kluwer Academic Publishers, Dordrecht.
28. Zaitsev, Yu.P. and Alexandrov, B.G. (1996) Recent man-made changes in the Black Sea ecosystem, in E.Ozsoy and A.Mikaelyan (eds.), *Sensivity of North Sea, Baltic Sea and Black Sea to Anthropogenic and Climatic Changes*, Kluwer Academic Publishers, Dordrecht.
29. Zernova, V.V. and Nezlin, N.P. (1983) Seasonal changes of phytoplankton in the western part of the Black Sea in 1978, in Yu.I.Sorokin and M.E.Vinogradov (eds.), *Seasonal changes of plankton in the Black Sea*, Nauka, Moscow, pp. 12-33. (In Russian)

MNEMIOPSIS LEIDYI ABUNDANCE IN THE BLACK SEA AND ITS IMPACT ON THE PELAGIC COMMUNITY

T. A. SHIGANOVA
P.P.Shirshov Institute of Oceanology RAS
23, Krasikova, 117851 Moscow, Russia

Abstract. This study is an attempt to give a short synthesis of the present knowledge of the development of the ctenophore *Mnemiopsis leidyi* invader in the Black Sea and a brief review in other seas of the Mediterranean basin, based on the published data, and new field studies (1992-1995). This assessment confirms interannual fluctuations in the abundance of *M. leidyi*, characterised by sharp increases and decreases, depending mainly on food availability. *M. leidyi* seasonal dynamics populations in the Black Sea and in the other seas of the Mediterranean basins are similar. Maximal biomass occurs in August-October, maximal numbers coincide with reproduction peak. The reproduction starts in some areas of the inshore waters during the late July-August (1991, 1992, 1994) or sometimes in August-September (1993, 1995), and lasts till October-November. Reproduction peaks up about one month after its beginning, first in the inshore waters; then part of spawning population and the new generations penetrate into the open sea, where reproduction is expected to continue. The main factors controlling the spatial distribution of *M.leidyi* are combined effects of temperature and salinity, and the main factor controlling its abundance is food availability. Assessment of the state of main parameters of the pelagic ecosystem before the *M. leidyi* outbreak shows that the reduction of resources of planktivorous fishes -its main competitors- can be one of the possible reasons for the great burst of *M. leidyi*.

1. Introduction

Mnemiopsis leidyi, a gelatinous predator, was introduced into the Black Sea at the beginning of the 1980's from the north-western Atlantic coast, possibly with the ballast waters of ships. It has spread over the Black Sea, the Seas of Azov and Marmara. At present, its impact is a serious problem for the pelagic ecosystems of these basins [44-47, 16, 22, 35].

The introduction of a new species into a biotope can often be harmful for the ecosystem, especially in the case of semi-enclosed seas, which are more sensitive to impacts compared to the open sea [5]. It is important to know the degree of tolerance of the invader to a new environment, peculiarities of its biology in a new habitat,

E. Özsoy and A. Mikaelyan (eds.), Sensitivity to Change: Black Sea, Baltic Sea and North Sea, 117–129.
© 1997 *Kluwer Academic Publishers.*

interrelation with all the trophic layers of the biota, relationship between introduced and indigenous species, its preys and competitors. All these factors determine the abundance, distribution of the invader and its impact on the ecosystem.

2. Material and methods

One of the goals of this study was to determine the dependence of ctenophore abundance and pattern of its distribution on environmental variables such as temperature, salinity, prey biomass (meso-zooplankton, fish eggs and larvae) and competitors' abundance (*Aurelia aurita*, planktivorous fishes).

This approach ignores aspects of patchiness and the peculiarities of local distribution, certainly important factors in for Black Sea populations. Only long-term fluctuations in *M. leidyi* development and distribution were examined, using averaged values for the Black Sea. Proximity of the interior (depth > 200 m) and shallow waters (<200 m) was considered to be the most important division for *M.leidyi* distribution.

The determination of the *M. leidyi* age structure and main parameters of its life cycle (somatic growth, reproduction and elimination/mortality) were made on the basis of numbers, biomass, average individual weight fluctuations and the ratios between the three main size groups of individuals in the samples.

In order to gain some insights into the *M. leidyi* population dynamics in the Black Sea and other seas of Mediterranean basin, all published and new data are summarised in the following. The spatial and (interannual, seasonal) temporal patterns of ctenophore distribution were analysed, based on these data.

Published data used in the present assessment

year	reference.	Authors
1988	36	Vinogradov et al. (1989)
1989	9, 25, 26	Shushkina and Musaeva (1990 a,b); Khoroshilov (1993)
1990	27, 28, 37	Shushkina and Vinogradov (1991), Shushkina et al. (1992), Vinogradov (1990)
1991	9, 38	Vinogradov (1992); Khoroshilov (1993)
1992	37, 39, 40, 44	Vinogradov et al. (1992); Vinogradov (1992, 1993)

Material was collected according to the standard methods used at the P.P.Shirshov Institute of Oceanology, as presented elsewhere [36]. Only during July, 1992, samples were taken from the surface layer with a Pleyston Net, that is why only the ratio between size groups was used from that cruise data. Data prior to 1992 were extracted from the published literature of P.P.Shirshov Institute of Oceanology [Table], recalculating the ratio between size groups and in some cruises, average individual weight. All the other published data, obtained by different nets were used without comparison of the numbers and biomass.

The data from 1992 to 1995 were collected during 10 cruises: 1992, (July north-western, north-eastern area of the Black Sea; October - the Sea of Marmara); 1993

(August- north-eastern, southern part of the Black Sea, November- central, north-eastern part of the Black Sea, area off Syria in the Mediterranean Sea); 1994 (August, September- north-eastern, central parts of the Black Sea), 1995 (March, August, September- the north-eastern Black Sea). During all these cruises special attention was given to the stations in the open part of the Black Sea where monitoring observations were regularly conducted by P.P..Shirshov Institute of Oceanology [36-44].

Calculation numbers, biomass and averages were made with using compute program of Dr.Gorbunov A.E., which was always the same for P.P.Shirshov Institute of oceanology data of estimations. Correction factors for insufficient catchability were used for the Bogorov Rass Net [42]. The individuals of *M. leidyi* were segregately counted within three sized groups: l< 10 mm, l = 10-45 mm, l > 45 mm.

3. Results and Discussion

3.1 LONG TERM CHANGES

Long-term fluctuations of ctenophore biomass, numbers, average individual weight and ratio between three sized group of *M. leidyi* are given in Figures 1,2,3,4,5.

The ctenophore *Mnemiopsis leidyi* was, for the first time, found in Sudak Bay of the Black Sea in November 1982 [19]. Later it was found in the north-eastern coastal water in 1986 [47]. In 1987 it occurred in the north-eastern, north -western inshore waters and in the Bosporus area. And only in the autumn (September) of 1988 did it penetrate everywhere in the Black Sea and its average biomass reached to about 1 kg.m^{-2}, and average numbers increased to about 310 ind.m^{-2} [42,11]. (Figure 1,2,3).

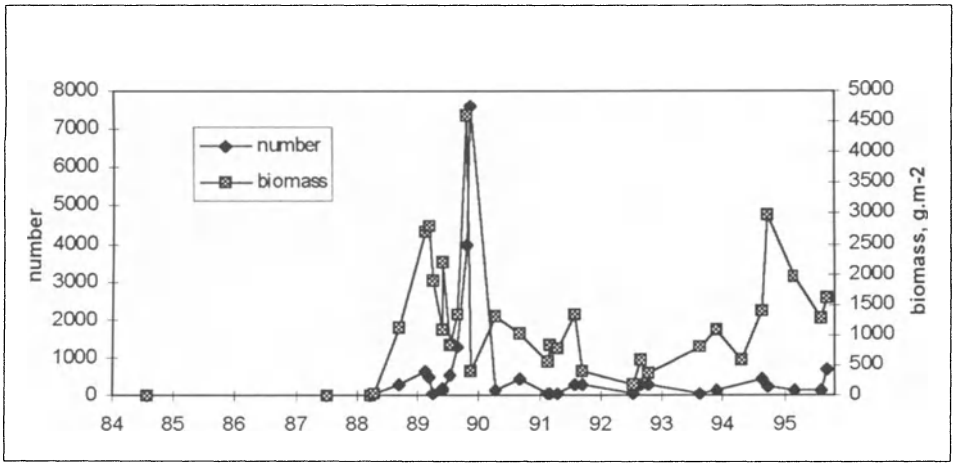


Figure 1 Long-term fluctuation of *M. leidyi* biomass and number in the open sea

In October 1989, *M. leidyi* reached its peak biomass (4,6 $kg.m^{-2}$) and in November its peak number of individuals (7600 $ind.m^{-2}$) in the open part of the sea [9,36], representing the all-time maximum values measured since the present time [38].

In 1990 and 1991, the abundance of *M. leidyi* started to decrease, particularly in the open part of the sea. In April 1990, the open sea biomass (1,3 $kg.m^{-2}$) was about twotimes lower than the same season of 1989. In September 1990, the biomass was lower (1 $kg.m^{-2}$ - in the open sea, 1,6 $kg.m^{-2}$ -in the inshore waters). (Figure 4) [26,28,37]. In February 1991, the biomass decreased to about half of that in 1990 (0,57 $kg.m^{-2}$), but increased back temporarily (1,32 $kg.m^{-2}$ - in the open sea, 1 $kg.m^{-2}$ -in the inshore waters) in August: [9,29,38]. (Figures 1,2,3,5)

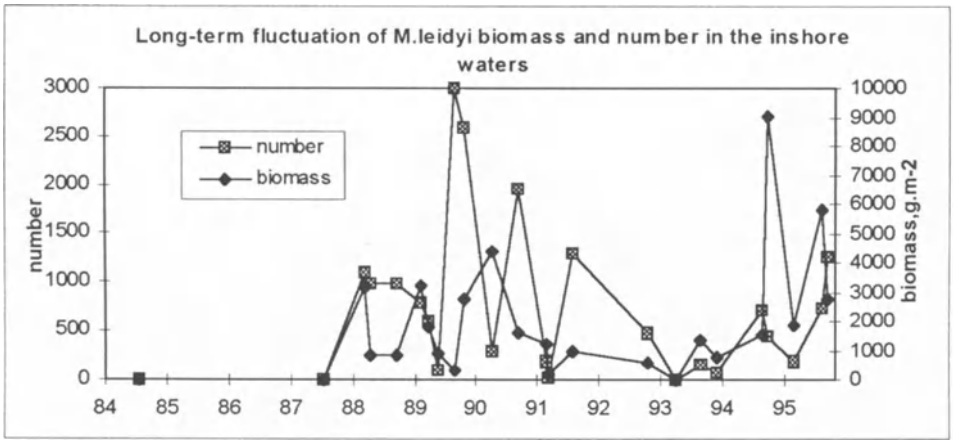


Figure 2 Long-term fluctuation of *M. leidyi* biomass and number in the inshore waters

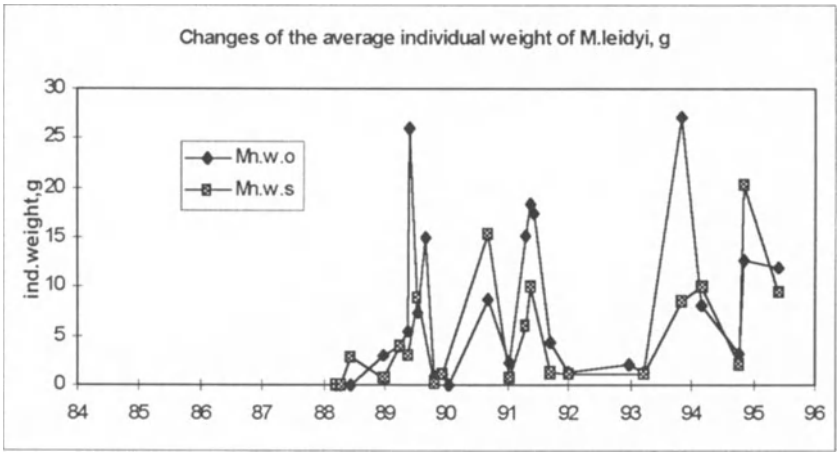


Figure 3 Changes of average individual weight of *Mnemiopsis leidyi:*
1-in the open sea, 2-in the inshore waters

In 1992, the *M. leidyi* abundance remained low, but in the open area in September it increased slightly in biomass (0,6 kg.m^{-2}), increasing in numbers in October [50]). (Figures 1,2,3,6)

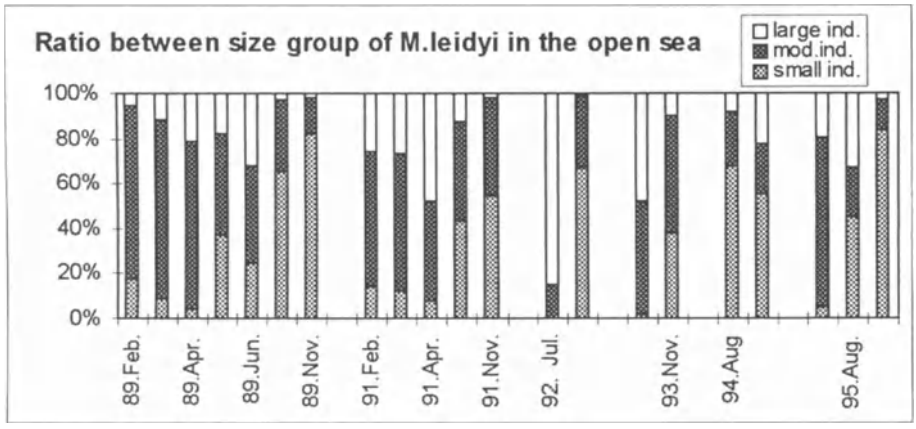


Figure4 Ratios between size groups of *Mnemiopsis leidyi* in the open sea.

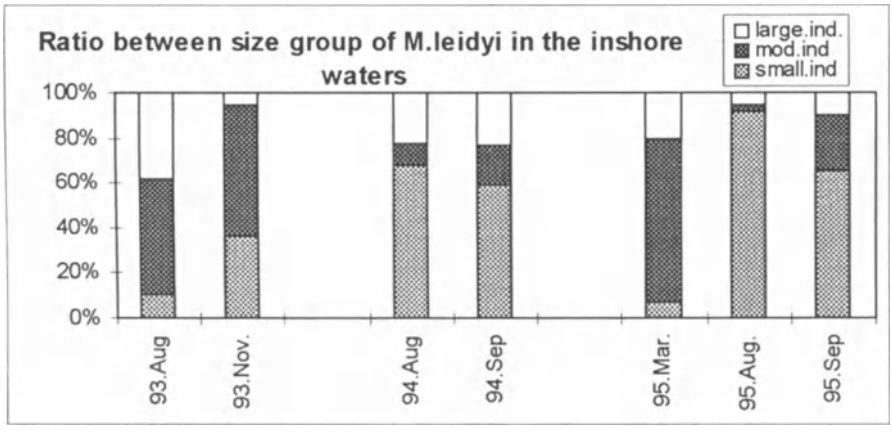


Figure5 Ratio between size groups of *Mnemiopsis leidyi* in the inshore area in 1993-1995

In spring 1993 the abundance of *M. leidyi* reached its minimum in the open sea since the beginning of the its outbreak [24]. In August 1993 its biomass begun to increase particularly in the open sea (0.82 kg.m^{-2} in the open sea; 0,32 kg.m^{-2} -in the inshore waters) and the trend continued in November (the biomass was 1,1 kg.m-^{2},in the open sea, 0,8 kg.m^{-2} -in the inshore waters). The number was maximal in November [24,42].

M. leidyi abundance continued to increase later, reaching in September 1994 a peak biomass (2,7 $kg.m^{-2}$) in the open sea, about three times larger than that in 1993, and much larger values (9 $kg.m^{-2}$) in inshore waters. This peak abundance corresponded to a second explosion since 1989, only second in magnitude compared to the first one.

In March 1995 the biomass was very high, considering the season, both in inshore and offshore waters (about 1,9 $kg.m^{-2}$ in both areas). In August and September of 1995 the biomass decreased, particularly in the open sea. In August 1995, the open sea biomass remained at the level of 1994 (about 1,3 $kg.m^{-2}$), but in September it was lower (1,6 $kg.m^{-2}$) than the previous year. In the inshore waters, the biomass was very high in August (5,8 $kg.m^{-2}$), which was also lower than the previous year. Number was maximal in September in both area.

For a number of years after the first appearance of *M. leidyi* in the Black Sea in 1982 (or possibly in 1986, if we don't take Pereladov's information into consideration), it was only found in some parts of the inshore waters. Then, for the first time in autumn 1988, it appears to have started spreading over the rest of the Black Sea. Afterwards, *M. leidyi* seems to have begun being assimilated actively in a new biotope, following a rather long adaptation period; reaching a peak abundance in autumn 1989, thereafter decreasing steadily until the summer of 1993; when a second increase of abundance occurred, with a peak in autumn 1994, partially extending into 1995. From this review, it is evident that *M.leidyi* abundance is characterised by sharp interannual fluctuations, probably depending strongly on its environmental interactions.

Some evidence suggests that *M. leidyi* from the Black Sea may have penetrated through the straits to adjacent basins. In August 1988 it was observed in the Sea of Azov for the first time. Since we expect the organisms can only survive there during the warm part of the year (when temperature is in excess of 18° C, and salinity is more than 3), it would possibly have to be re-introduced in spring or summer months through the Kerch Strait. First it occurs only in the southern area adjacent to the Kerch Strait, and later in August - September *M. leidyi* is found to spread throughout the Sea of Azov where the minimum temperature is 18°C and minimum salinity is about 3. Its biomass reaches its peak during this period. The variation in time and the dynamics of *M. leidyi* penetration in the Sea of Azov largely depends on wind-driven currents. [30, 45].

In 1989-1990 it probably appeared in the Sea of Marmara., According to our investigations, high densities of *M. leidyi* were observed in the Sea of Marmara in October 1992, probably being the first outburst there, with an average biomass of 4,2 kg m^{-2}.suggesting local mass reproduction. All of the population was located in the upper layer of the Sea originating from the Black Sea. [22,23] In July 1993, there was a low abundance of only adult individuals in the Sea of Marmara [11].

In the late spring of 1992, rather high numbers of *M. leidyi* consisting of both small and large individuals were observed in Kusadasi Bay on the Turkish coast of the Aegean Sea, and in Mersin Bay along the eastern coast on the Mediterranean. During the following investigations in July 1993, no individuals were found in Mersin Bay, and only two adult individuals were caught in Kusadasi Bay [11,35]. My own samples

in the eastern part of the Aegean Sea did not contain any individuals of *M. leidyi* in October 1993, but indicated other occurrences of *M. leidyi* close to the Syrian Mediterranean coast in late October.

The pattern of occurrence and temporal variations in the Marmara and eastern Mediterranean seem to suggest that *M. leidyi* was most probably introduced from the Black Sea through the Turkish Straits with the surface currents flowing out from the Black Sea. However, separate introduction into these regions with ballast waters of the ships is equally likely, and the exact reasons clearly can not be identified with certainty. Optimal conditions for maintaining *M. leidyi* may exist continuously in the upper layer waters of the Sea of Marmara, whose origin is the Black Sea. On the other hand, *M. leidyi* can survive in the Aegean and Mediterranean in spring and autumn when the temperature is not higher than 24-26°C, but it is difficult to judge how it can survive under high summer temperatures and constant high salinity of about 39.

3.2. SEASONAL DYNAMICS OF *M. Leidyi*.

Preliminary seasonal dynamics of *M. leidyi* can be described as follows: in February, moderate sized individuals predominate the population. In general the smaller and larger sized individuals occur in a small numbers (Figs. 4-5). The presence of small individuals most probably depends on reproduction in late autumn of the previous year and survival through the winter without much growth, or possible shrinking in size, at low temperatures.

From February to June in the open sea, mainly somatic growth of the overwintering individuals occurs. There is an increase of biomass due to prevalent growth of individuals; individual weight increases but numbers remain approximately the same (Figure 3). Simultaneously in the inshore waters, there is a general decrease in biomass and numbers caused by the transport of individuals with currents to the open sea, as well as an absence of recruitment of the new generations.

In June and July virtually everywhere the biomass and particularly numbers remain relatively low. The population is made up of mainly adult individuals and new generations are absent (Figs. 4-5) [46].. At this time, the average individual weight is rather high; it reaches a peak in August or September, when the biomass and later September-November, the numbers tend to increase. The reproduction starts in some areas of the inshore waters in the second part of July or in August (as observed in 1991, 1992, 1994) or later in August-September (1993, 1995) and continues till October-November. Reproduction peaks in August-September or September-October, first in the inshore waters. Later a part of spawning population and new generations penetrate out to the open sea, where reproduction most probably continues. At that time the individual weight decreases due to the appearance of high number of small sized individuals. In around October or November the biomass drops because of elimination of adult individuals after reproduction (Figures 1,2). During the winter there is a small population consisting of small and moderate sized individuals.

In 1989 the seasonal dynamics of *M. leidyi* differed from the dynamics of the following years which is probably connected with processes of adaptation to a new

environment and assimilation to a new biotope . From February to April the decrease of biomass occurred, perhaps, due to prevalent processes of elimination. In that period of the year, adult and even juvenile mortality could take place [12]. That is probably why large individuals were in small numbers since summer. In June and particularly in July the numbers of small individuals increased in the samples and in July an active reproduction started and continued till November. Thus in 1989 *M. leidyi* reproduced during a period from June to November. Perhaps it was connected with its assimilation to the new biotope after appearance of favourable conditions after period of adaptation, as found in ctenophore behaviour [20].

Analysis of seasonal dynamics of *M. leidyi* population in the Black Sea and other seas of the Mediterranean basin indicates similarities despite some differences in the timing of maxima in biomass and numbers.

Data on *M. leidyi* population dynamics in its native region (Atlantic coastal area of North America) suggest differences in seasonal abundance patterns in different areas. There is a peak of abundance and reproduction in summer and late autumn in the north [12, 13,15], while in the middle latitude coastal systems in the United States, biomass was greatest in spring and autumn and very low in summer [3,13,20], and in the south, it highest abundance occurred in September [20]. In some areas of native region, the patterns of seasonal dynamics are similar to those of the Black Sea. However, most of these seasonal dynamics studies deal mainly with the biomass. For a full examination of seasonal population dynamics, it is very important to study biomass and abundance as well as reproductive rate. The seasonal dynamics of these parameters appear to be different in the Black Sea. That is why separate evaluations do not necessarily demonstrate the real pattern of seasonal dynamics of *M. leidyi* population.

4. Discussion: Possible Reasons for the M. leidyi Outbreak and its Impact on the Planktonic Community

Why did the period of adaptation of *Mnemiopsis leidyi* last such a long time, taking several years (from 1982 or 1986 till 1988), despite the well known tendency of *M. leidyi* for a dramatic increase in biomass within short periods under optimal conditions [15, 20]. The determination of the probable factors suppressing *M.leidyi* development during such a long period will help to assess the factors which control its abundance.

The Black Sea began to change from an oligotrophic to an eutrophic body of water in the 1970's and early 1980's as a result of antropogenic factors. Firstly the pelagic community reacted to environmental changes. At the end of 1970s, eutrophication and blooms of *Noctiluca miliaris* became common in the Black Sea [10,48]. At the beginning of the 1980's, explosive development of *Aurelia aurita* started (reaching an average biomass of 0,6-1 $kg.m^{-2}$, Figure 6), possibly connected with eutrophication [40].

The growth in the population of *Aurelia aurita* led to a decrease in the abundance of zooplankton [16]. At the same time, changes in abundance and species composition of fishes were observed. After 1979, a major decline was recorded in the resources of

mackerel, bonito and bluefish [10]. Therefore it seems that the decreases in the stocks of most traditional fish species were caused by the increase in the amount of fishing of planktivorous fishes, and first of all, the most abundant species -anchovy. The share of anchovy in the catches of all countries increased gradually during the 1980's. In the 1960's, anchovy catches amounted to 14,6% of total catches, in the 1970's to 47%, then since the 1980's to more than 50%, and in 1988 to 64% [6] (Figure9). The catch of anchovy should make up 50-53% of the resources but it comprised 60-80% since

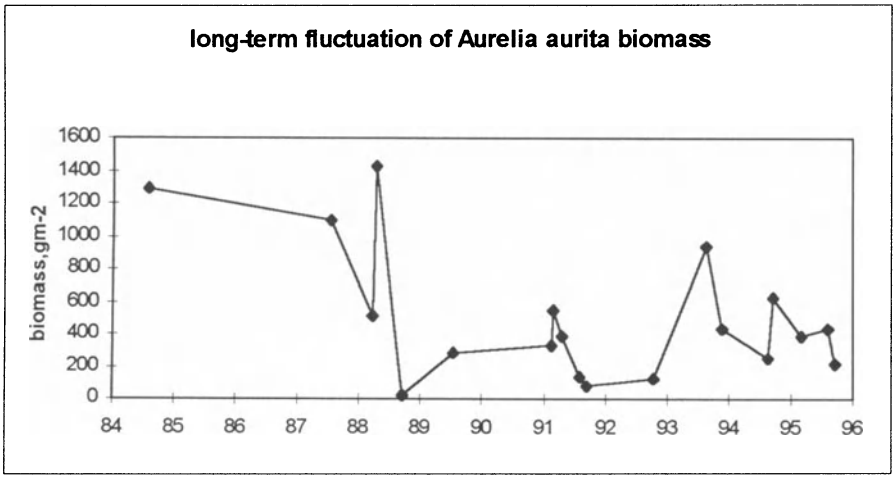


Figure 6. Long-term fluctuation of *Aurelia aurita* biomass

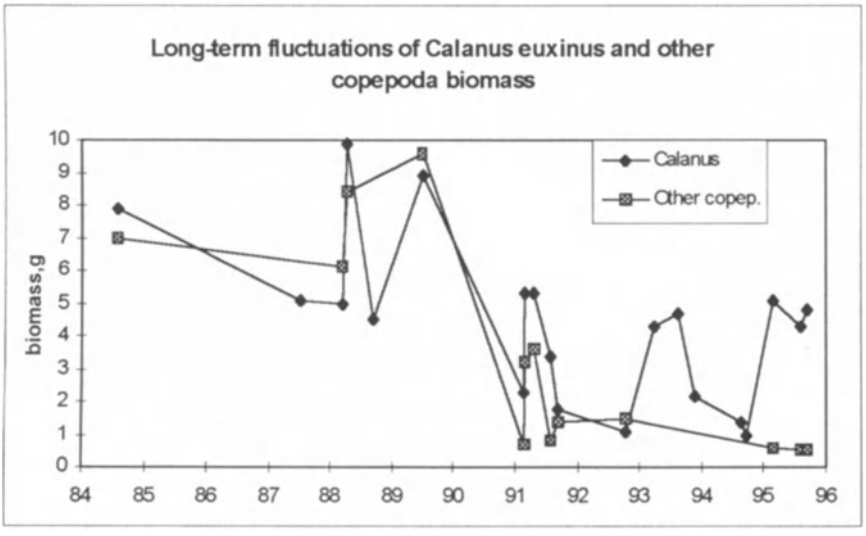


Figure 7.. Long-term fluctuation of *Calanus euxinus* and other copepoda biomass:
1- *Calanus euxinus* biomass, 2- other *Copepoda*

1984 [5,6]. Anchovy is a fish with short life-cycle: its life duration is 3-4 years, but in general, the catch of anchovy consists of two generations: 2+ and 1+. During the 1980's there were more and more generations of 1+ and 0+ [8,18]. In spite of all the adverse factors, the quantity of anchovy was still rather high before 1989. The total catch of anchovy was a maximum in 1988, following a most productive year in new generation anchovy [1] in 1987, carried out with the highest resources (spring resources was 245 thousand .tons in 1988, data of YugNIRO) and the highest percent of anchovy in the total catch occurred (Figures. 8,9), amounting to about 80 % of resources [5]. In 1988, new generation of anchovy was only one-fourth of that in 1987 [1], due to a decrease of the spawning stock after overfishing in 1987. That is why after such a high catch in 1988, fishing resources in 1989 were about one-seventh of those in 1988. Thus overfishing was the main reason for the decline in the number of anchovy *Engraulis engrasicholus* in 1989 [6]. Even a worse situation occurred with the Black Sea scad, *Trachurus mediterraneus ponticus*. The sprat *Sprattus sprattus sprattus* suffered least of all. In 1988 a maximum catch of anchovy was obtained, and of the Black Sea scad in the 1980's; the smallest spawning anchovy stock also occurred in 1988. In addition, in 1988 there occurred the last phase of the population cycle of *Aurelia aurita,* which accompanied a sharp decline in its abundance (Figure 6) [3].

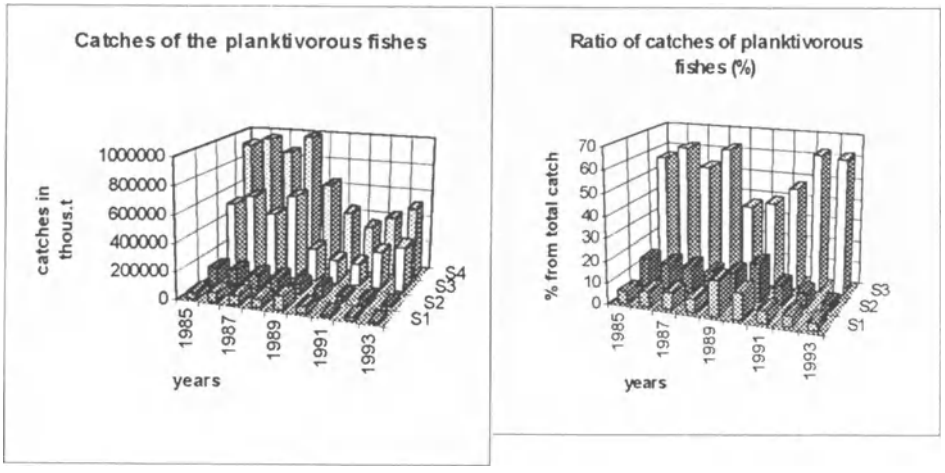


Figure8 (a) Changes of the catches of the planktivorous fishes: S1 - sprat, S2- Black Sea scad, S3- anchovy, S4- total catch, and (b) ratio between catches of planktivorous fishes and total catch in the Black Sea: S1- sprat; S2 - Black sea scad; S3- anchovy

These events with important ecological consequences occurred before the mass development of the *M. leidyi* in 1988-1989. Probably, the existence of serious food competitors *Aurelia aurita* and planktivorous fishes, abundant before 1988, and the lower abundance of valuable zooplankton as food suppressed the bloom of *M. leidyi* before the autumn of 1988. Possibly due to these reasons, the abundance of mesozooplankton significantly increased during the spring and summer of 1988

(Figure 7). In autumn 1988, a mass development of *M. leidyi* was observed, and a decrease in zooplankton abundance followed. Zooplankton biomass increased again in 1989 in conditions of small abundance of the main consumers and reached its peak during July -September 1989 (Figure7). Exactly around that time the mass explosion of *Mnemiopsis* occurred, during the period of high food availability and low number of competitors. This explosion reached its maximal biomass in autumn 1989 (Figures 1,2).

During the next years 1990-1992, the mass development of *M. leidyi* decreased the total abundance of mesozooplankton. *Pontellidae, Oithona minuta* and *Sagitta setosa* species virtually disappeared. These species were usually present in the food chain of *M. leidyi* during the first years of its mass development, but during the last years, its main food are *Acartia clausi* and *Calanus euxinus* in the open sea, and *Cladocera, Pleopis polyphaemoides* in the inshore waters [31-34]. The catches of planktivorous fishes continued to drop due to the *M.leidyi* burst (Figure 8).

Biomasses of *M. leidyi* and *Aurelia aurita* have been inversely correlated during all years as a result of competition between them (Figure 6) [16, 40].

After *M. leidyi* abundance considerably declined in 1992-1993, zooplankton abundance began to increase (Figure7), consisting mainly of *Calanus euxinus, Pseudocalanus elongatus,* and *Sagitta setosa.* The number of anchovy fish eggs and larvae also increased. The abundance of the other fish eggs and larvae remained at low level [17,24]. The catches of anchovy began to increase since 1992, while the catches of other species remained at low level. The recent increase in anchovy abundance may be connected with its short duration of life and points to the possibility of rehabilitating its stocks. Under optimal conditions (mainly high food availability), the anchovy population could be reconstructed within a few years [18]. On the other hand the Black Sea scad has a longer life-cycle and would need several years with favourable conditions for its reconstruction [18].

Increased zooplankton productivity followed by the increase of *M. leidyi* abundance occurred in summer 1993. In the autumn of 1994 when the *M. leidyi* biomass was highest, the zooplankton biomass dropped again, and in spring and summer 1995, the biomass of zooplankton, particularly *Calanus euxinus* increased in spite of high abundance of *M. leidyi* (Figure 7). Perhaps the ecosystem is gradually adapting to the new invader. If this is the case, the measures for improving the environment of the Black Sea, could be the following: strict control of fishing on planktivorous fishes; restoration of the predator fishes. These measures may reduce the abundance of *M. leidyi* and its impact on the Black sea ecosystem.

In conclusion we would propose to restore the Black Sea ecosystem to the situation that prevailed before *M. leidyi* introduction by consistent improvements in its health. The results of such restoration might make the introduction of any other kind of predator for diminishing *M. leidyi* abundance [7] unnecessary. If any another species is introduced now, the damaged ecosystem of the Black Sea can suffer further deterioration.

5. Acknowledgement

This study was conducted with funds from the Russian Foundation for Fundamental Investigation (RFFI 96-04-51051). I am grateful to V. S. Khoroshilov for an examination of mesozooplankton samples.

6. References

1. Arkhipov A.G. 1993 Assessment of abundance and pattern of distribution of commercial fishes of the Black Sea in early stages of ontogenes. Voprosy of ichthyology. 33(4), p. 511-522. (in Russian).
2. Burrel V.G., Van Engel W.A.1976 Predation by and distribution of a ctenophore, *Mnemiopsis leidyi* (A.Agassiz) in the York River Estuary,. Estuar. Coast. Mar.Sci. V.4., p.235-242.
3. Caddy J.F. and Griffiths 1990. A perspective on recent fishery-related events in the Black Sea. Studies and Reviews. GFCM, No 63, p.43-71
4. Caddy J.F. 1993. Toward a Comparative Evaluation of Human Impacts on Fishery Ecosystems of Enclosed and SemiEnclosed Seas. Reviews in Fisheries Science 1(1), p.57-95
5. Chazchin A.K. 1995. Abundance, distribution and migrations of anchovy stocks in the Black Sea. Turkish Jornal of Zoology. N 4
6. GFCM. (1995) Statistical Bulletin, nominal; catches 1985-1993. FAO Bull. of Fishery Statistics 34 (11). 257 pp.
7. Harbison G.R. Volovik S.P. Methods for the control of population of the Ctenophore *Mnemiopsis leidyi* in the Black Sea and Azov Sea. FAO report.p. 1-22.
8. Ivanov L., Beverton R.J.H. (1985) The fisheries resources of the Mediterranean. Part two.Black Sea. GFCM. FAO.Rome. 70 pp.
9. Khoroshilov V.S. (1993) Seasonal Dynamics of the Black Sea Population of Ctenophore *Mnemiopsis leidyi* . Oceanology. 33(4), p. 558-562 (in Russian).
10. Kovalev A.V., Melnikov V.V., Ostrovskaya N.A., Prusova I.Yu. 1993.Macroplankton. in: Plankton of the Black Sea. Kiev. Naukova dumka, p.183-204 (in Russian).
11. Kideys A.E.,Niermann U. 1994. Occurrence of *Mnemiopsis* along the Turkish coast ICES J. mar. Sci.51: 423-427.
12. Kremer P.(1976) Population dynamics and ecological energetics of a pulsed zooplankton predator, the Ctenophore *Mnemiopsis leidyi*. Estuarine processes.Voll. Uses, Stresses and Adaptation to Estuary. p.197-215.
13. Kremer P. (1993) Ctenophore population dynamics: patterns of abundance for *Mnemiopsis leidyi* in U.S. coastal waters. ICES Statutory meeting L.36. p.1-9.
14. Lebedeva L.P.,Shushkina E.A. (1991). The estimation of population characteristics of *Aurelia aurita* in the Black Sea. Oceanology. 31(3) p.434-441..
15. Miller R.J.(1974) Distribution and Biomass of an Estuarine Ctenophore Population, *Mnemiopsis leidyi* (A. Agassiz) Chesapeake Science Vol. 15. No 1. p. 1-8
16. Mutlu E., F.Bingel, Gucu A.S., Melnikov V.V., Niermann U., Ostr N.A., Zaika V.E. 1994. Distribution of the new invader *Mnemiopsis sp.* and the resident *Aurelia aurita* and *Pleulrobrachia pileus* populations in the Black Sea in the years 1991-1993. ICES. J.mar.Sci.p.407-421.
17. 19.Niermann U., Bingel F., Gorban A., Gordina A.D.,Gugu A.C., Kideys A.E., Konsulov A., Radu G., Subbotin A.A., Zaika V.E. 1994. Distribution of anchovy eggs and larvae (*Engraulis engrasicolus* Cuv.) in the Black Sea in 1991-1992. ICES J. mar. Sci.,51: 395-406.
18. Pavlovskaya R.M. 1979. General feathures of form of the number of generations of the main commercial fishes. In "Resources of the Black Sea" Moscow "Pizthevaya promyshlennost", p.5-24.(in Russian).
19. Pereladov M.V. (1983) Some observations for biota of Sudak Bay of the Black Sea. III All-Russian conference of marine biology. Kiev. Naukova dumka.t.1,p. 237-238. (in Russian).
20. Raymont D. Plankton and ocean productivity. M. Agroprom. T.2. 278 pp.(in Russian).
21. Rass T.S.(1992). Changes in the fish resources of the Black Sea. Oceanology 32(2).p.197-203 (in Russian).
22. Shiganova T.A.(1993) Ctenophore *Mnemiopsis leidyi* and ichthyoplankton in the Sea of Marmara in October of 1992.Oceanology. 33(6), p. 900-903.(in Russian).
23. Shiganova T.A. B.Ozturk, A.Dede (1994) Distribution of the ichthyo-, jelly- and zooplankton in the Sea of Marmara. FAO Fisheries report No 495. p.141-145

24. Shiganova T.A., Niermann U., Gugu A.C., Multu E., Khoroshilov .1996.Investigations of the structure of planktonic community in the Black Sea in 1993. Deep Sea Research Special Volume on the Black Sea: Oceanographic Variability (in press).
25. Shushkina E.A., Musaeva E.I. 1990. Structure of epilegic community and changes related to the invasion of Mnemiopsis leidyi in the Black Sea. Oceanology 30(2), p.306-310. (in Russian).
26. Shushkina E.A., Musaeva E.I. 1990. Increasing abundance of the immigrant ctenophore *Mnemiopsis* in the Black Sea (report of an expedition by the R/Vs "Akvanavt" and "Gydrobiolog" in April 1990). Oceanology. 30(4), p.521-522.
27. Shushkina E.A. and Vinogradov M.E. 1991. Long-term changes in the biomass of plankton in open areas of the Black Sea. Oceanology.31(6). p.716-721.
28. Shushkina E.A. Vinogradov M.E. 1991. Changes of the plankton community of the open part of the Black Sea and impact of *Mnemiopsis leidyi* on it. In: Ecosystem variabilities in the Black Sea: natural and antropogenic factors. Moscow. Nauka.p.248-261. (in Russian).
29. Shushkina E.A.,Vinogradov M.E., Nikolaeva G.G., Musaeva E.I.(1992). Mesoplankton distribution and analysis of structural and functional properties of the pelagic communities in the open part of the Black Sea in winter 1991. In: Zimnee stoyanie ecosystemy otkrytoi chasti Chernogo morya.M. Inst.ocean. RAN p.119-130. (in Russian)
30. Studenikina E.I., Volovik S.P., Miryozan I.A., Luts G.I. (1991) The Ctenophore *Mnemiopsis leidyi* in the Sea of Azov. Oceanology. 31(6), p. 722-725
31. Tzikhon-Lukanina E.A.,Reznichenko O.G., Lukasheva T.A.(1991a) Quantitative aspects of feeding in the Black Sea ctenophore *Mnemiopsis leidyi*. Oceanology. 31(2). p.272-276).
32. Tzikhon-Lukanina E.A.,Reznichenko O.G. (1991b). Feeding peculiarities of different size speciments of ctenophore *Mnemiopsis* in the Black Sea. Oceanology. 31(3).p.442-446.
33. 38.Tzikhon-Lukanina E.A.,Reznichenko O.G.,Lukasheva T.A. (1992). What ctenophore *Mnemiopsis* eats in the Black Sea inshore waters ? Oceanology. 32(4). p.724-729.
34. 39.Tzikhon-Lukanina E.A., Reznichenko O.G.,Lukasheva T.A.(1993) Predation Rates on Fish Larvae by the Ctenophore *Mnemiopsis leidyi* in the Black Sea inshore waters. 1993. Oceanology 33(6) p.895-899.
35. Uysal Y., Mutlu E.1993. Preliminary note on the occurence and biometry of *Ctenophora Mnemiopsis leidyi* finallz invaded Mersin Bay. Doga (1993). Tr.J.of Zoology. 17,229-236
36. Vinogradov M.E., Shushkina E.A., Musaeva E.I., Sorokin P.Yu.1989. Ctenophore *Mnemiopsis leidyi* (A.Agassiz) (Ctenophora: Lobata) - new settlers in the Black Sea. Oceanology 29 (2), p.293-298.
37. Vinogradov M.E. 1990 Study of ecosystem of the Black Sea pelagial (44-th cruise of R/V "Dmitry Mendeleev". Oceanogogy. 30(2). p.344-346.
38. Vinogradov M.E.1992 Long-term variability of the pelagic community structure in the open Black Sea. In:Problems of the Black Sea. MHI UAS. pp.19-33.
39. Vinogradov M.E. 1993. Monitoring of the open areas of the Black Sea (the 26-th cruise of the R/V "Vityaz" (September 26-October 19,1992). Oceanology. 33(2). p.312-316.
40. Vinogradov M.E., Sapozhnikov V.V., Shushkina E.A. 1992 The Black Sea ecosystem. Moscow. Russia. Nauka, 112 pp. (in Russian).
41. Vinogradov M.E., Shushkina E.A. 1992. Temporal changes of the zoocene structure of the open area of the Black Sea. Oceanology. 32(4), p. 709-717.
42. Vinogradov M.E., Shiganova T.A., Khoroshilov V.S. 1995 The state of main organisms of plankton community in the Black Sea in 1993. Oceanology 35(3), p.418-422.
43. Vinogradov M.E., Shushkina E.A., Bulgakova Yu.V., Serobaba I.I. 1995. The consumption of Zooplankton by Comb-jelly *Mnemiopsis leidyi* and pelagic fishes in the Black Sea. Oceanology. 35(4), p. 569-573.
44. Vinogradov M.E., Shushkina E.A., Nikolaeva G.G. 1992. The state of zoocene in the open areas of the Black Sea during late summer . Oceanology. 33(3).p.382-387.(in Russian).
45. Volovik S.P., Mirzoyan I.A., Volovik G.S.1993 *Mnemiopsis leidyi*: biology, population dynamics, impact to the ecosystem and fisheries. ICES. Statuary meeting, p1-12.
46. Zaika V.Ye.,Sergeeva N.G. 1990. Morphology and development of *Mnemiopsis mccradyi (Ctenophora, Lobata)* in the Black Sea.(in Russian). Zoologicheskyi zhurnal.69(2). p.5-11. (in Russian).
47. Zaitsev Yu.P., Vorob'eva L.V., Aleksandrov B.G.1988. New species Ctenophora in the Black Sea. VINITI.pp 1-6. (in Russian).
48. Zaitsev. Yu.P.1993 Impact of eutrophication on the Black Sea fauna: Fao Rome 64(2).

SEASONAL VARIATION OF SURFACE PIGMENT DISTRIBUTION IN THE BLACK SEA ON CZCS DATA

N. P. NEZLIN
P. P. .Shirshov Institute of Oceanology, RAS,
Krasikova 23, 117851 Moscow, Russia

Abstract. The remote sensing data obtained by Coastal Zone Color Scanner (CZCS) on the satellite "Nimbus-7" collected during the period from 1978 to 1986 were used to analyse the seasonal variation of surface plant pigments distribution in the Black Sea, presented here on maps for each climatological month. The pattern of seasonal variations is typical for subtropical regions rather than for the temperate ones. The range of the absolute value of plant pigment surface concentration measured by remote sensing does not differ greatly from the values measured by direct methods.

1. Introduction

The data obtained by Coastal Zone Colour Scanner (CZCS) on the satellite "Nimbus-7" [6] during the period of November 1978 to June 1986 were used for both the evaluation of seasonal patterns of phytoplankton variability over the wide ocean areas [1, and many others] and the estimation of the global values of of primary production and plankton stock of the World Ocean [7, 12, 17]. In the Black Sea region they were successfully used for analysis of the influence of the boundary currents on the productivity of the coastal and slope waters [13, 14]. The present paper is an attempt to analyse the seasonal variation of surface pigment distribution in the Black Sea, using its climatically averaged images.

2. Material and Methods

The satellite Nimbus-7 was launched in 1978 and obtained information until 1986. The methods of recalculating the optical properties of the water surface to yield pigment concentration were described in [4, 5]. The information was summarised in Goddard Space Flight Centre and presented as a set of CD-ROMs [3]. The data were obtained from the NASA Physical Oceanography Distributed Active Archive Center at the Jet Propulsion Laboratory / California Institute of Technology. The monthly maps of chlorophyll *a* distribution all over the World Ocean were presented. The data obtained

E. Özsoy and A. Mikaelyan (eds.), Sensitivity to Change: Black Sea, Baltic Sea and North Sea, 131–138.
© 1997 *Kluwer Academic Publishers.*

during 7.5 years of observations were averaged as a set of climatological maps. For analysis of these data received from NASA special software was developed together with V. Yu. Dyakonov. This software gave us the opportunity to obtain data for any month for the ocean surface, and either to prepare them for statistical analysis, or to display them in maps. While preparing the grid for mapping we use smoothing (so-called two-dimensional cosine-filtering) to overcome small-scale variability.

The maps of spatial distribution of chlorophyll *a* were constructed for all 12 climatological months. The colours used for mapping were chosen according to the colour scale developed in the Laboratory of Functioning of Ocean Pelagial of P. P. Shirshov Institute of Oceanology [12, 17]. The maps were slightly smoothed, radius of cosine filtration for each month being equal to 20 nautical miles (about 1/3 of degree of latitude). The levels of surface pigment concentration are given in Table 1. Average values of the most important productive characteristics of plankton community for temperate regions calculated on the base of large amount of data are given in the same Table. It is worth noting that the characteristics of oligotrophic waters (surface chlorophyll *a* concentration below 0.1 $mg \cdot m^{-3}$) are not presented in the table because they were not observed in the Black Sea.

Table 1. The levels of surface pigment concentration typical for various productivity levels and average values of productivity characteristics for temperate regions of various productivity levels [17].

Productivity level	1	2	3	4	5
Productivity level	hypertrophic	eutrophic		mesotrophic	
Surface chlorophyll range, $mg.m^{-3}$	>1.0	0.7-1.0	0.3-0.7	0.15-0.3	0.1-0.15
Transparency, m	5±1.0	10±0.6	12±0.7	16±0.6	22±0.8
Photosynthetic layer depth, m	22±1.5	52±3.0	56±2.6	75±5.7	106±5.6
Light attenuation, m^{-1}	0.091±0.007	0.080±0.002	0.062±0.009	0.050±0.004	0.040±0.002
Surface chlorophyll, $mg.m^{-3}$	1.95±0.22	0.80±0.03	0.48±0.04	0.23±0.01	0.11±0.01
Chlorophyll in 0-200 m layer, $mg.m^{-2}$	124.4±38.9	48.2±7.3	31.5±4.6	19.6±1.7	14.5±1.1
Primary production, mg $C.m\text{-}2.day^{-1}$	1400±300	900±500	800±100	500±100	300±100

3. Results

The seasonal fluctuations of plant pigments distribution over the surface of the Black Sea are illustrated by monthly averages displayed Figure 1.

In January the major part of the Black Sea surface was evenly covered by hypertrophic waters with chlorophyll concentration above 1.0 $mg \cdot m^{-3}$. Only the southern part of the central region of the Sea was occupied by eutrophic waters. The data in the eastern part of the Black Sea were insufficient for mapping.

In February the average level of surface pigments concentration decreased, the patchiness increasing greatly. The eastern, south-western and north-western parts of the Black Sea were occupied by hypertrophic waters, the central part being occupied by eutrophic waters. Both the eastern part of the Black Sea and the major part of north-western shelf had no data.

The pattern of surface plant pigments distribution changed greatly in March. Almost all the area of the sea was covered by eutrophic waters with surface chlorophyll

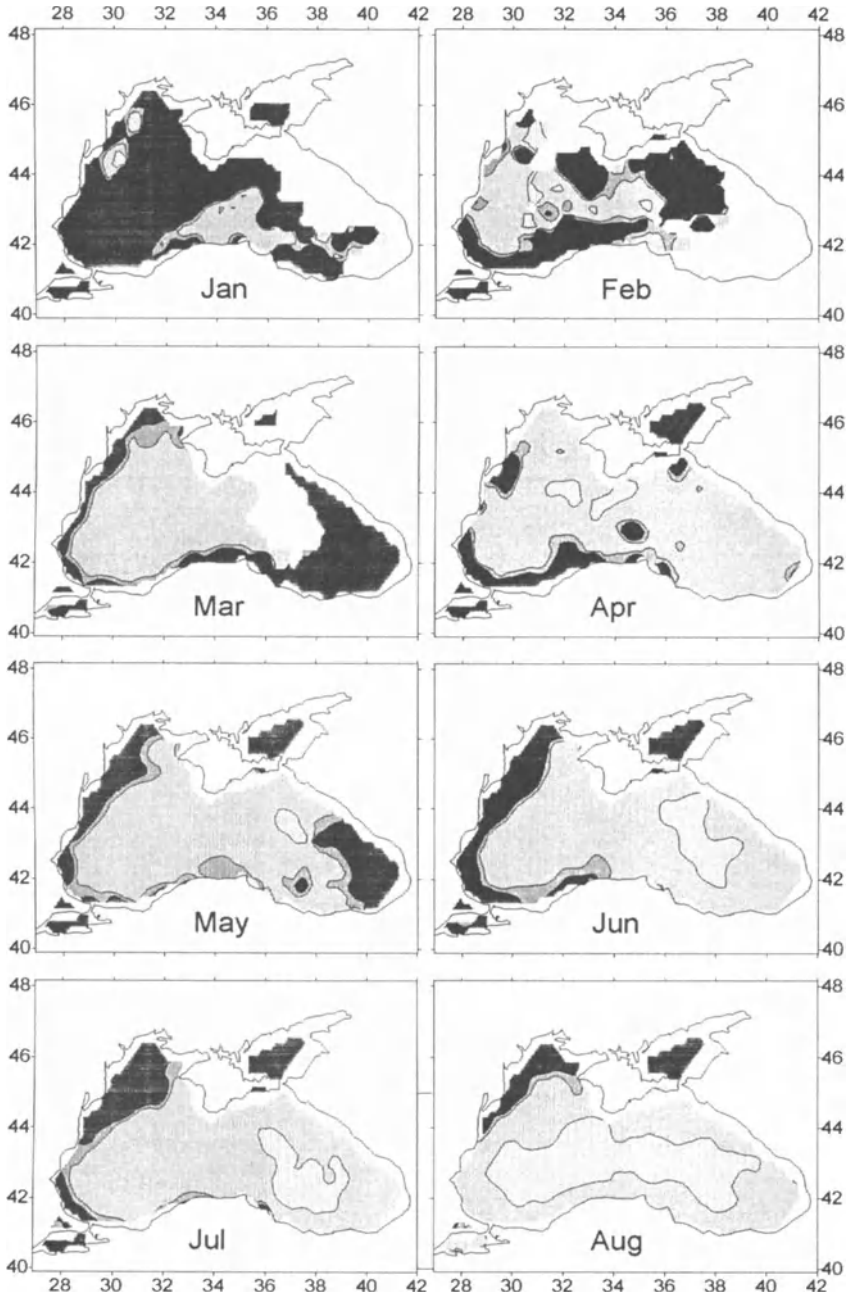


Figure 1. Surface average pigment concentration, January - December 1978-1986.

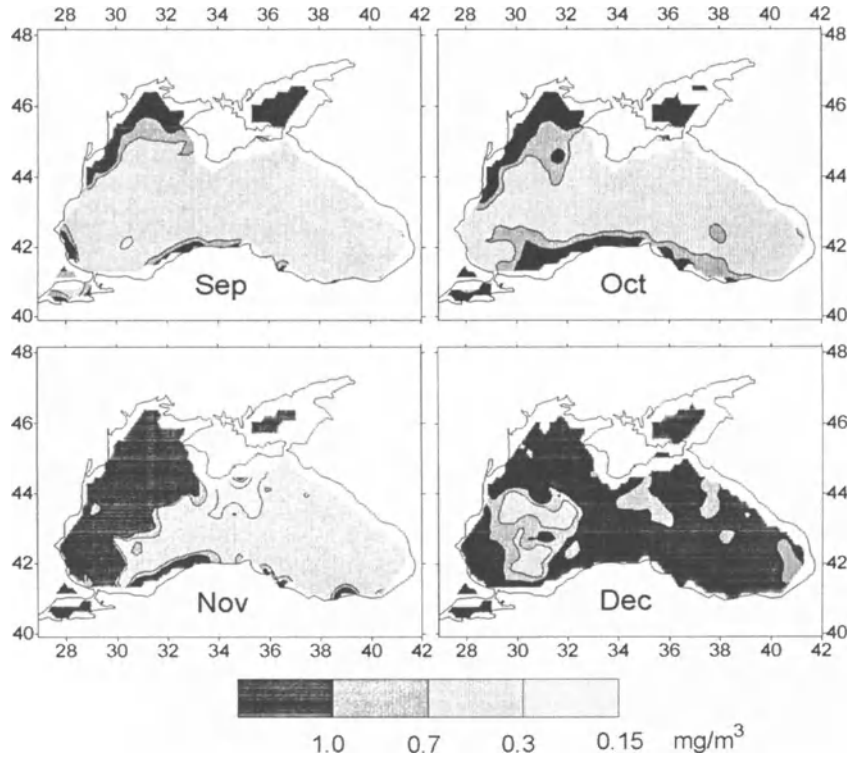


Figure 1. (continued).

a concentration about 0.3-0.7 mg·m^{-3}. Hypertrophic waters remained only along the coast and in the eastern part of the sea.

In April almost all the surface of the Black Sea was covered by eutrophic waters (0.3-0.7 mg·m^{-3}). Only along the south-western coast there were some areas of hypertrophic waters, and in the central part of the sea few patches of mesotrophic waters appeared.

In May the coastal areas occupied by hypertrophic waters spread along all the western coast; hypertrophic waters being observed in the eastern part of the sea.

In June all the open regions of the Black Sea were occupied by eutrophic waters, the region of eastern gyre being occupied by mesotrophic waters with surface concentration of plant pigments less than 0.3 mg·m^{-3}. The hypertrophic waters remained along the western coast.

The same pattern of plan pigments distribution was observed in July, the band of hypertrophic waters along the western coast being slightly weaker.

In August the area of mesotrophic waters with surface plant pigments concentration 0.15-0.3 mg·m^{-3} spread over all the open regions of the Black Sea. All the coastal regions were occupied by eutrophic waters, the hypertrophic waters being observed only in north-western shelf region.

In September the eutrophic waters covered the central part of the sea, the pattern of pigments' distribution with hypertrophic region at the north-western shelf remaining as before. A thin band of hypertrophic waters appeared along the southern coast.

In October the band of hypertrophic waters along the southern coast became more distinct. The level of surface plant pigments in the north-western shelf region increased, exceeding in some localities 3 $mg \cdot m^{-3}$.

In November all the western part of the sea was covered by hypertrophic waters.

In December all the area of the Black Sea was occupied by hypertrophic waters, the pattern being just the same as in January.

4. Discussion

The pattern of surface pigment concentration in winter appears to differ from typical winter phytoplankton distribution. As usual, winter blooming of phytoplankton occurs in the central part of the Black Sea, coastal zones being less rich by phytoplankton biomass [9] and associated plant pigments concentration. Meanwhile measured by CZCS values do not display this pattern. The reason for this discrepancy is not yet obvious, though it could have several reasons.. One of the reasons could be that in coastal regions the pigment concentration measured by satellite radiometer is overestimated.

One of the factors disturbing the instantaneous pattern of plant pigment distribution according to CZCS image seems to be the variety of the atmospheric correction values first of all depending on aerosol type and optical depth [8]. The response from coastal regions could differ from the offshore regions of the Black Sea according to this feature during the winter time. The second reason could be the alternative species composition of phytoplankton during winter in the near-shore and offshore areas. The third reason could be the higher concentration of terrigenous suspension along the coast.

It is not easy to distinguish the comparative importance of these factors affecting the obtained pattern of plant pigment distribution. We should only mind, that the systematic errors of CZCS pigment values as compared with the field observations were already observed in various regions of the ocean [2, 10].

In order to describe the general pattern of seasonal variation of plant pigments in the Black Sea, the concentrations of plant pigments over the total area of the Black Sea were averaged for each month. The median values, rather than the average, were used to describe seasonal changes of surface pigment concentration, because the statistical distribution of pigment concentrations is far from symmetrical. The range of variation is characterised by 25% and 75% percentiles (Figure 2). From autumn till the spring (October-February) the bulk of the observed values falls within the range of hypertrophic productivity levels (up to 2.3 $mg \cdot m^{-3}$). From March to September, the productivity level is eutrophic, except in August, when part of the values can be assigned to mesotrophic productivity level.

First of all, the pattern of seasonal variations of surface plant pigments concentration in the Black Sea needs to be compared with the ones typical for temperate and subtropical regions ([11], Figure 8.8). Evidently the pattern of seasonal variations characterised by one winter maximum is typical for subtropical regions rather than for the temperate ones.

The median values of surface plant pigment concentration were compared with the pattern of seasonal variation of surface chlorophyll *a* content described in the review of Vedernikov and Demidov ([16], data on mean content in the photosynthetic layer were taken from Table 2 and recalculated into the surface concentrations by the equation from Table 1 of these authors). These values are presented by dotted lines in Figure 2.

It is obvious that the range of variations is the same, concerning both CZCS data and field measurements. Only in summer the measured values seem to be rather lower. It can be explained by the fact that Vedernikov and Demidov's data refer to open sea regions only, while CZCS data refer to the whole area of the Black Sea, including coastal regions with permanently high pigment concentration values.

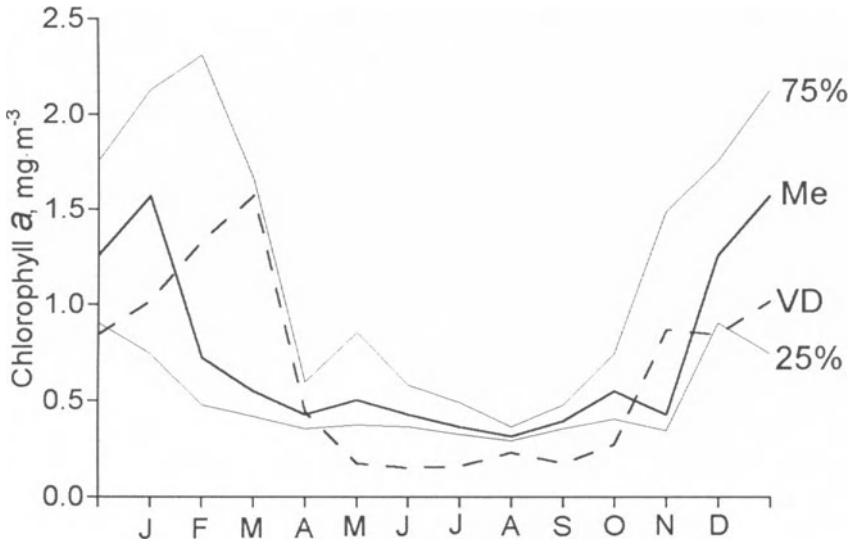


Figure 2. Seasonal variation of surface pigment concentration. CZCS data: Me - median, 25% and 75% - 25% and 75% percentiles respectively, VD - data from [16].

The month when maximum surface pigment concentration occurs in the Black Sea, according to CZCS data, is January-February, while according to Vedernikov and Demidov's review, [16] the maximum occurs in March. The reason for this inconsistency seems to be lack of data obtained during the winter season by both CZCS and field measurements. Meanwhile in an earlier review of the same authors [15], in the figures showing seasonal changes of chlorophyll *a* vertical distribution, it is evident that the surface chlorophyll *a* concentration decreases from February to March. In any

case, the question on the correlation between remote sensing data and field measurements seems to be crucial in investigation of the problem.

The seasonal variation of surface pigment concentration in the open sea area along the cross-section from western to eastern part of the Black Sea is displayed in Figure 3. Evidently, the seasonal variation differs greatly in the western and eastern parts of the Black Sea. In the western part, the winter bloom starts earlier (in October) and decreases earlier (in February), whereas in the eastern part of the sea the winter bloom starts later (in December) and continues much later (up to April-May). The reason for these differences seems to be the same: lack of valid data during winter-spring time.

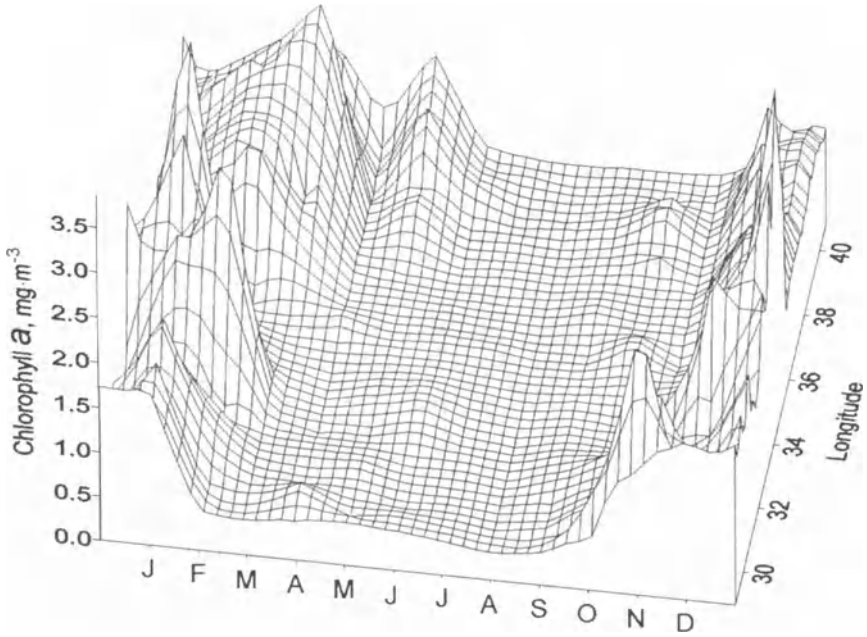


Figure 3. Seasonal variation of surface average pigment concentration at cross-section via central part of the Black Sea. X-axis - month (January - December); Y-axis - longitude, Z-axis - surface chlorophyll concentration.

5. Conclusions

The CZCS data are used for evaluation of chlorophyll concentration and primary production over wide areas of the World Ocean, though the level of reliability of the data is questionable for coastal regions. There are opinions, suggesting that in the coastal region, the CZCS data are overestimated about 2-4 times (e.g. [7]). The

comparison of CZCS data and field observations seems to prove the validity of the satellite information for evaluation of productive properties of the Black Sea, according to absolute values and the pattern of seasonal variation. Such evaluation should be the next step of our study.

6. References

1. Banse K. and English D. C. (1994) Seasonality of coastal zone color scanner phytoplankton pigment in the offshore oceans,
2. *Journal of Geophysical Research*, **99**, C4, 7323-7345.
3. Chavez F. P. (1995) A comparison of ship and satellite chlorophyll from California and Peru, *Journal of Geophysical Research*, **100**, C12, 24855-24862.
4. Feldman, G. C., Curing, N., Ng, C., Esaia, W., McClain, C. R., Elrod, J., Maynard, N., Edres, D., Evans, R., Brown, J., Walsh, S., Carle, M. and Podesta, G. (1989) Ocean colour: availability of the global data set, *Eos Trans. Amer. Geophys. Union.* **70**, 634-641.
5. Gordon, H. R. and Clark, D. K. (1980) Remote sensing of optical properties of a stratified ocean: an improved interpretation, *Applied Optics*, **19**, 3428-3430.
6. Gordon, H. R., Clark, D. K., Brown, J. W., Brown, O. B., Evans, R. H. and Broenkow, W. W. (1983) Phytoplankton pigment concentrations in the Middle Atlantic Bight: comparison between ship determination and Coastal Zone Scanner estimates, *Applied Optics*, **22**, 20-36, .
7. Hovis, W. A., Clark, D. K., Anderson, F., Austin, R. W., Wilson, W. H., Baker, E. T., Ball, D., Gordon, H. R., Mueller, J. L., El Sayed, S. Y., Sturm, B., Wrigley, R. C. and Yentsch, C. S. (1980) Nimbus-7 coastal zone colour scanner: system description and initial imagery, *Science*, **210**, 60-63.
8. Longhurst, A., Sathyendranath, S., Platt, T., Caverhill,.C. (1995) An estimate of global primary production in the ocean from satellite rediometer data, *Journal of Plankton Research*, **17**, 6, 1245-1271.
9. Martin D. L. and Perry M. J. (1994) Minimizing systematic errors from atmospheric multiple scattering and satellite viewing geometry in coastal zone color scanner level IIA imagery, *Journal of Geophysical Research*, **99**, C4, 7309-7322.
10. Mikaelyan A. S., Nesterova D. A. and Georgieva L. V. Winter blooming of the algae Nitzschia delicatula in the open regions of tha Black Sea, in M. E. Vinogradov (ed.), *Ecosystems of Open Black Sea in Winter*, Moscow, 58-72. (in Russian).
11. Mitchell B. G. (1992) Predictive bio-optical relationship for polar oceans and marginal ice zones, *Journal of Marine Systems*, **3**, 91-105.
12. Raymont, J. E. G. (1980) *Plankton and productivity in the oceans.* Vol. 1 *Phytoplankton.* 2nd ed., Pergamon Press, New York.
13. Shushkina, E. A., Vinogradov M. E., Sheberstov, S. V., Nezlin, N. P. and Gagarin, V. I. (1995) Characteristics of the epipelagic ecosystems of the Pacific Ocean based on satellite and measured data. Stocks of plankton in the epipelagial, *Oceanology*, .**35**, 5, 705-712. (in Russian, English summary).
14. Sur H. I., Ozsoy E., Ilyin Y. P. and Unluata U. (1996) Coastal/deep ocean interactions in the Black Sea and their ecological/environmental impacts, *Journal of Marine Systems*, 7, 2/4, 293-320.
15. Sur H. I., Ozsoy E., and Unluata U. (1994) Boundary current instabilities, upwelling, shelf mixing and eutrophication processes in the Black Sea, *Progress in Oceanography*, **33**, 4, 249-302.
16. Vedernikov, V. I. and Demidov, A. B. (1992) Seasonal variability of the primary production and chlorophyll in the open regions of the Black Sea, in M. E. Vinogradov (ed.), *Ecosystems of Open Black Sea in Winter*, Moscow, 77-89. (in Russian).
17. Vedernikov, V. I. and Demidov, A. B. (1993) Primary production and chlorophyll in deep regions of the Black Sea, *Oceanology. English Translation*, **33**, 2, 193-199.
18. Vinogradov M. E., Shushkina, E. A., Vedernikov, V. I., Gagarin, V. I., Nezlin, N. P. and Sheberstov, S. V. (1995) Characteristics of the Pacific epipelagic ecosystems based on the satellite and expedition data: Abiotic parameters, and production indices of phytoplankton, *Oceanology, English Translation*, .**35**, 2, 208-217.

THE EFFECT OF HYDROLOGICAL CONDITIONS ON THE STATE OF HERRING STOCKS IN THE BALTIC SEA.

TIIT RAID
Estonian Marine Institute
32 Lai Str. Tallinn EE0001 Estonia

Abstract. The Baltic herring (*Clupea harengus membras. L*) is one of the most essential commercial fish species in the Baltic Sea. The annual landings of herring have varied from 300,000 to about 480,000 tonnes in recent 20 years. Herring in the Baltic Sea can be treated as a complex of several stoks, each linked to separate spawning grounds. The hydrological, particularly salinity conditions vary from 1-2 on the herring spawning grounds in the Eastern Gulf of Finland to above 10 in the Southwestern Baltic. This shows good adaptation of herring to the low and variable salinity conditions in the Baltic Sea. Despite of that, changes in salinity conditions, depending on occurrence or absence of inflows from the North Sea, seem to have an essential effect on both herring growth and behaviour. The prolonged period of absence of big inflows of saline water into the Baltic Sea can probably even affect of the stock structure of herring. That points at the importance of regular inflows of saline water as the stabilizing factor in the ecosystem of the Baltic Sea.

1. Introduction

A unique transitional ecosystem, connecting the oceanic and freshwater conditions occurs in the Baltic Sea. Salinity conditions in that sea depend on the balance between the runoff of freshwater from the drainage area of 1.6 million km^2, precipitation and water exchange over shallow Darss and Drogden sills, with depths just 18 m and 7 m and cross-sections 0.8 and 0.1 km^2, respectively. The existence of shallow sill areas constitute the main reason, why the Baltic Sea has become a brackish water basin with typically two-layered vertical salinity distribution.

Salinity, decreasing from nearly oceanic level in the Danish Straits to 1-2 in the Gulf of Bothnia and the Gulf of Finland, play the key role in the formation of the structure and dynamics of the Baltic Sea ecosystem. As a result, the ecosystem can be characterized by the gradual decrease of the share of marine species and increase of the fresh-water species from the transition area to the north and north-east.

Despite of the shortness of the evolution of the contemporary Baltic Sea (approximately 10 000 years), a number of species, inhabiting the sea are well adapted to the low and variable salinity conditions. The Baltic spring spawning herring (*Clupea harengus membras L.*) is one of the most important commercial fishes in the Baltic Sea. The total biomass of herring in the main basin of the sea has been estimated at the level of 3 000 000 - 4 300 000 t in recent two decades [1].

Herring, being widely distributed all over the sea, form several different geographical groups (stocks), linked to the different spawning grounds and differing from each other by the morphometrical characteristics, growth rate, behaviour etc. According to E. Ojaveer [8], at least 9 such groups can be distinguished (Figure 1).

E. Özsoy and A. Mikaelyan (eds.), Sensitivity to Change: Black Sea, Baltic Sea and North Sea, 139–147.
© 1997 *Kluwer Academic Publishers.*

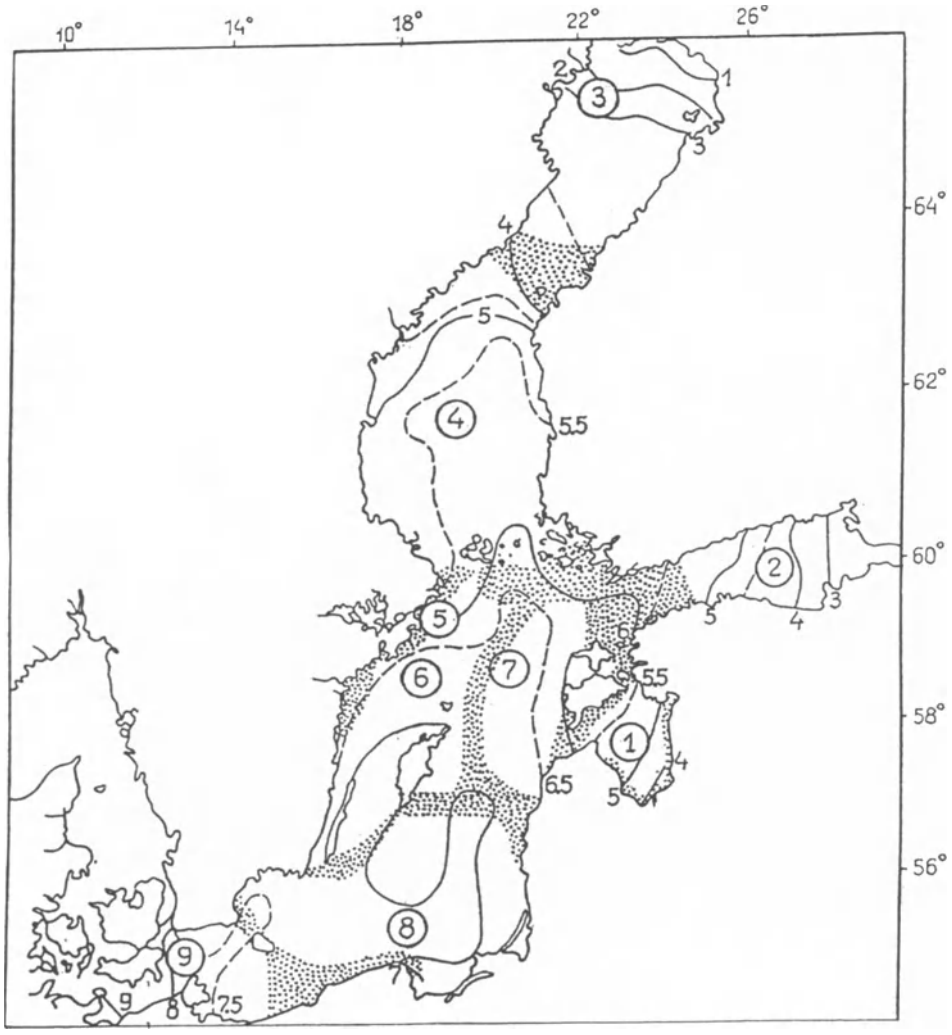


Figure 1. Mean surface salinity (isolines) in June and location of main herring stocks. (dotted areas). 1- Gulf of Riga, 2- Gulf of Finland, 3- Gulf of Bothnia, 4- Bothnian Sea, 5- Swedish fjord herring, 6- Western Central Baltic, 7- Eastern Central Baltic, 8- Southern Baltic, 9- Western Baltic [8, 14].

2. Effect of Salinity on Herring Stocks

The salinity conditions undergo continuous alterations, induced by the periodical occurrence of inflows of saline oceanic water into the Baltic Sea over the sills. During the present century, 12 strong or very strong and 19 moderate inflows have been registered (Figure 2). Strong inflows have recurred after almost every 10-16 years. The intensity of influxes of oceanic water is influenced by the climatic variability, driving the river runoff [4].

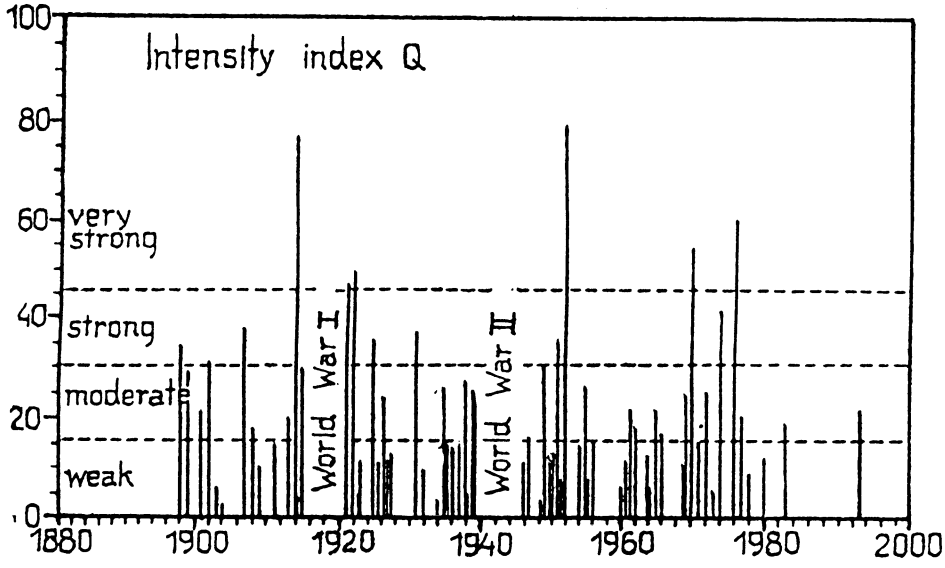


Figure 2. The major Baltic Inflow events during the present century [6].

Against the historical background of regular occurrence of big inflows, the period since 1977 can be characterized as an exceptional one, during which just two moderate inflows (in 1983 and 1993, were observed. As a result, the mean salinity of the sea has decreased during the period mentioned by 20-25%, both in deeps and gulfs. The decrease was accompanied by the weakening of stratification of water column and intensifying of vertical transport [2,3]. Simultaneously to those alterations in hydrological regime, changes in some basic ecological parameters of the Baltic herring, like mean weight at age, abundance, biomass etc., can be observed in 1980s-1990s.

2.1. MEAN WEIGHT AT AGE

The mean weight at age of herring, being relatively stable in 1960s, started to increase gradually in 1970s in all regions of the sea. So in the Gulf of Finland the the mean weight reached its highest values in younger age groups in the late 1970s and, in the older age groups, in the early 1980s. Later, in 1986 - 1990, the mean weight decreased in most abundant age groups (1-6) to the level of 1976 - 1980 (Figure 3). The declining trend has continued in 1990s.

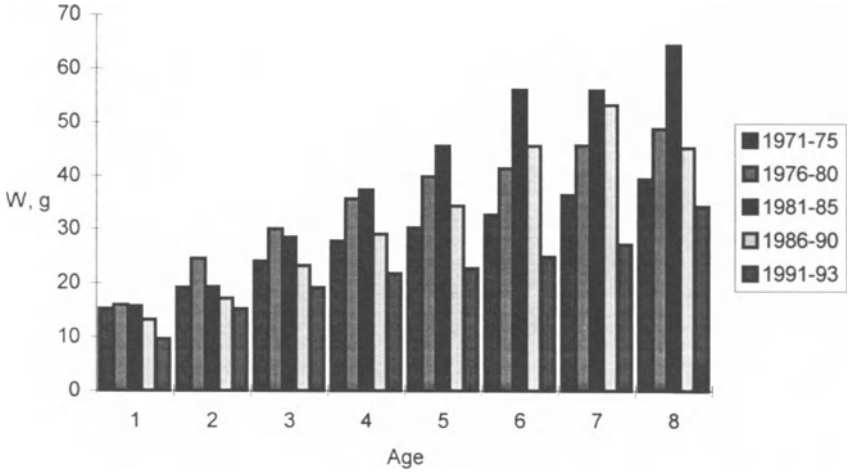


Figure 3. Mean weight of herring in the Gulf of Finland in 1971-1993.

The decrease in mean weight was accompanied by deterioration of body condition of fish and an increase of the share of dystrophic fish, often invaded by various parasites [10,13]. The recent investigations have revealed the following two major changes in herring feeding and feeding conditions of herring in the Northeastern Baltic since mid-1980s:

1. Share of herring with no food in the guts has increased since the second half of 1980s remarkably in all age groups, reaching 80 - 90% in 1991 - 1992 (Figure 4). The increase was particularly obvious in older (bigger) herring, known as grazing mostly on big, energy-rich nektobenthic prey (Mysids).
2. Prey composition of herring has changed in late 1980s, compared with "traditional" food spectrum. So, the importance of smaller zooplankton, particularly of *Acartia* and *Temora* has increased in the diet of all age groups, while the share of "traditional" prey like Mysids has remarkably decreased (Figure 5). *Limnocalanus* has also lost its position as important prey object for herring. The latter, is in good accordance with changes in the composition of planktonic communities, where, the abundance of *Limnocalanus* has declined dramatically in late 1980s [12].

The increasing share of starving fish and changes in prey composition indicate the deterioration of feeding conditions of herring since the mid-1980s. A. Lumberg and E. Ojaveer [5], analyzing the dynamics of zooplankton abundance and biomass in the Gulf of Finland during the recent 30 years, revealed the occurrence of zooplankton-rich period in 1974 - 1982, followed by a sudden decrease in zooplankton abundance in 1982 - 1984. The difference in zooplankton abundance between the two periods was estimated to be two- to three-fold.

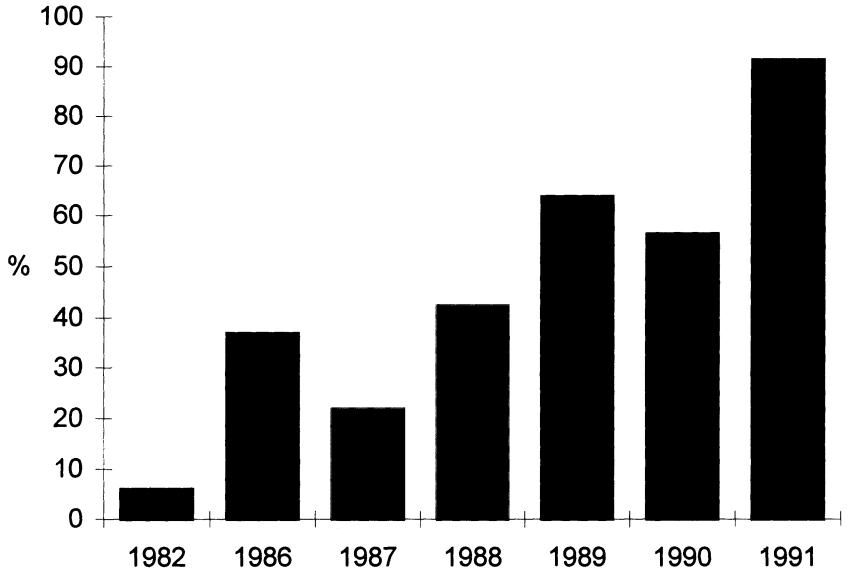


Figure 4. Mean share of unfed herring in the Northeastern Baltic and the Gulf of Finland in April 1982-1991.

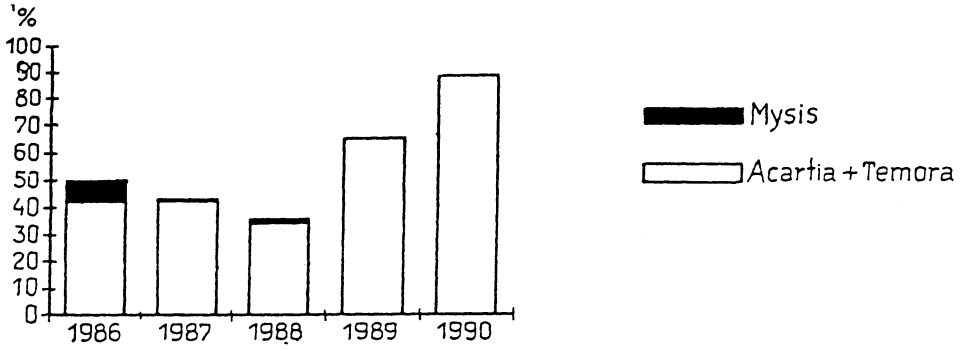


Figure 5. Share of *Acartia* + *Temora* and *Mysis* in the Gulf of Finland in April 1986 - 1990.

The high abundance of zooplankton and high mean weight at age of herring in late 1970s and early 1980s coincided with the period of increased salinity in the Baltic [4]. The virtual absence of big inflows from the North Sea after 1983 has created present period of low salinity and active vertical mixing. The decreased salinity has caused both, changes in species composition of zooplankton and the decrease in zooplankton abundance [12]. As a consequence of increased vertical mixing, the stratification of water column has weakened, providing the planktonic and nektobenthic animals with much wider zone of optimum living conditions (particularly better oxygen conditions), compared to the period of strong stratification, observed in early and mid-1980s after a series of strong or moderate inflows of 1970s [11]. That has caused the scattering of high plankton concentrations, observed at the well developed halocline during the period of strong stratification. The scattered food could have been at least partly responsible for the dramatic decrease in the mean weight at age of herring in late 1980s-early 1990s.

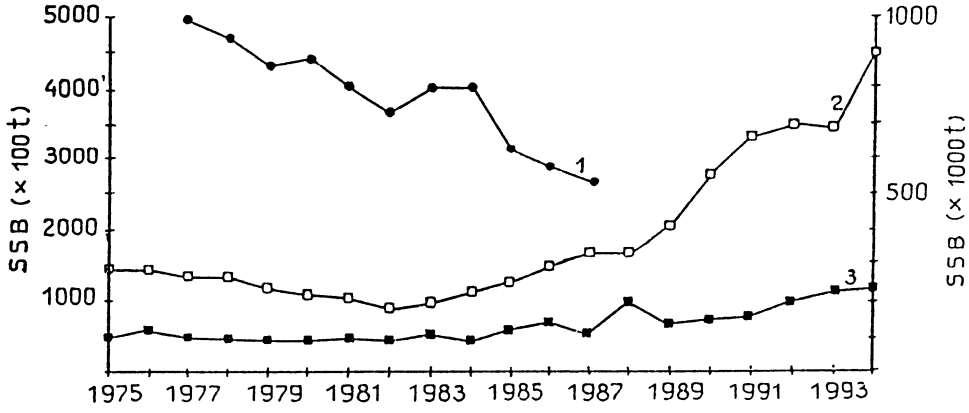


Figure 6. Dynamics of spawning stock biomass in some herring stocks in the Baltic: 1- Southern + Western and Central Baltic (x 1000 t [8]), 2- Bothnian Sea, 3- Gulf of Riga (x 100 t [1]).

2.2. STOCK STRUCTURE

Salinity conditions on the spawning grounds of the main Baltic herring stocks vary considerably, decreasing from 10-15 in transition area at the Danish straits to 1-2 in the eastern Gulf of Finland and in the Gulf of Bothnia (Figure 1).

The investigations of embryonal development of herring have shown, that success of the embryol performance of each herring group is the highest at salinity and temperature conditions, prevailing on the main spawning grounds of the given group [7]. Non-optimum conditions in the spawning grounds cause an increase of embryonal and larval

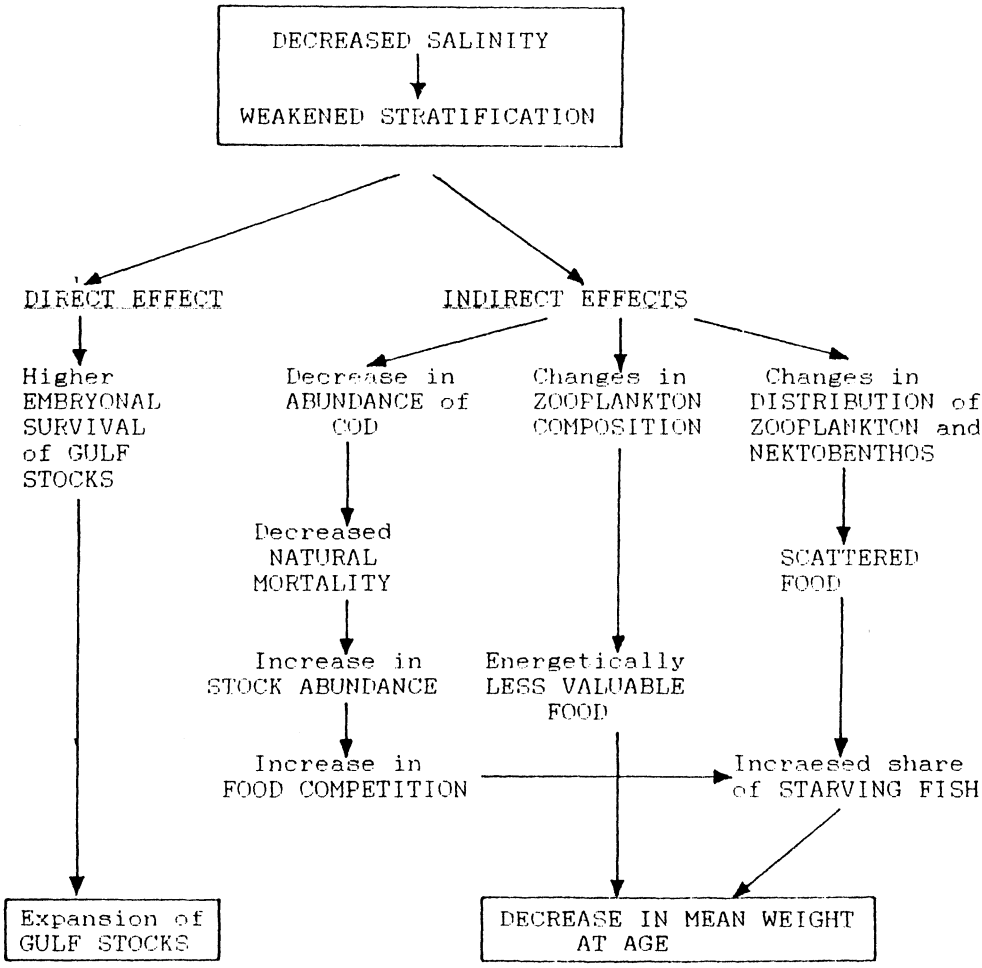


Figure 7. The possible pathways of the effects of prolonged period without big inflows on the Baltic herring.

mortality. Therefore, the adaptation of herring to the different mean salinity and temperature conditions, occurring at different spawning sites along the Baltic coasts serve probably as an evolutionary basis for the formation of those herring groups within such a limited space [9].

The decrease of salinity, observed in the Baltic Sea since mid-1980s has probably also affected the reproduction success of different herring stocks resulting eventually in different pattern of stock dynamics. So, the decreasing trend in open-sea stocks of the Southern and Western Baltic, adapted to the higher salinities, can be followed since the end of 1970s, up to the late 1980s (Figure 6). At the same time, the biomass of the stocks, adapted to the lower salinities, e.g. the Gulf of Finland stock, the Gulf of Riga stock and the stock of the Bothnian Sea have clearly gained in biomass during the period of absence of oceanic inflows to the Baltic Sea.

Of course, the possible effect of fishery on dynamics of open-sea stocks cannot be ruled out, particularly in 1970s, but the continuing decrease of open-sea herring even in the conditions of low exploitation level of 1990s still indicate on the effect of natural factors [1].

Low salinity, observed in spawning areas of cod, located in the Bornholm Deep and the Gotland Deep has caused a series of cod recruitment failures since 1982 [1]. As a result, the stock abundance of cod has declined dramatically since second half of the 1980s. The absence of main natural predator of herring in most of the northern part of the Baltic Sea during the recent decade has also supported to the increasing trend in several herring stocks.

3. Conclusions

The absence of oceanic inflows to the Baltic Sea in the 1980s - 1990s has induced a number of changes in sea ecosystem, affecting on biology and stock structure of Baltic herring (Figure 7). The following two major effects can be pointed out:

- decrease in mean weight at age of herring as a result of unfavourable feeding conditions (scattering of food concentrations, forced transition to the use of energetically less valuable prey etc.);
- the expansion of herring stocks, adapted to the lower salinity.

The regular occurrence of inflows from the North Sea can be regarded as an obligatory stabilising factor for herring stocks, maintaining the historically established infraspecific pattern of herring and interactions within the ecosystem.

4. References

1. Anon.(1995). *Report of the Working Group on the Assessment of Demersal and Pelagic Stocks in the Baltic*, ICES C.M. 1995/Assess: 18, 1-258.
2. Astok, V., Tamsalu, R., Nomm, A., Suursaar, Y. (1990). Gulf of Finland. Baltic Marine Environment Protection Commission-Helsinki Commission-1990. Second Periodic Assessment of the State of the Marine Environment of the Baltic Sea, 1984-1988; Background Document, *Baltic Sea Environment Proceedings* **35B**, 54-58.
3. Dahlin, H., Fonselius, S., Sjoberg, B. (1993). The changes of the hydrographic conditions in the Baltic proper due to 1993 major inflow to the Baltic Sea, ICES C.M.1993/ C:58 Session V: 1-15.
4. Kalejs, M. and Ojaveer, E. (1989) Long-term fluctuations in environmental conditions and fish stocks in the Baltic, *Rapp. P.-v. Reun. Cons. int. Explor. Mer* **190**, 153-158.
5. Lumberg, A. and Ojaveer, E. (1991) On the environment and zooplankton dynamics in the Gulf of Finland in 1961-1990, *Proc. Estonian Acad. Sci. Ecol.* **1**, No. 3, 131-140.
6. Matthaus, W., Nehring, D., Nausch, G. (1994) Effects of the inflows of salt-rich water during 1993 and early 1994 in the Central Baltic Sea, ICES C.M. 1994/Q:3, 1-17.
7. Ojaveer, E. (1981) Influence of temperature, salinity and reproductive mixing of Baltic herring groups on its embryonal development.- *Rapp. P.-v. Reun. Cons. int. Explor. Mer.* **178**, 409-415.

8. Ojaveer, E. (1991) On the condition and management of herring stocks in the Baltic, Proc. Int. Herring Symp. Anchorage, Alaska, 521-531.
9. Ojaveer, E. and Raid, T. (1988) Role of reproduction in Baltic population differentiation, ICES EHL Symp. Paper No. 37, Bergen, 1- 14.
10. Parmanne, R. (1992) Changes in growth of herring in the northern Baltic Sea, ICES C.M. 1992/J:42, 1-14.
11. Raid, T. and Lankov, A. (1995). Recent cahanges in in growth and feeding of herring and sprat in the northeastern Baltic Sea, *Proc. Estonian Acad. Sci. Ecol.* **5**, 1/2, 38-55.
12. Sidrevics, L., Line, R., Berzinsh, V., Kornilovs, G. (1993) Long-term changes of zooplankton abundance in the Gulf of Riga, ICES C.M. 1993/L:15, 1-14.
13. Turovsky, A., Aps, R., Raid, T. (1992) The parasitic infestation and growth of clupeids in the North-eastern Baltic, ICES C.M. 1992/J:27, 1-9.
14. Voipio, A. (editor). (1981). *The Baltic Sea*. Elsevier, Amsterdam, Oxford, New York.

ROLE OF FISHING IN THE BLACK SEA ECOSYSTEM

A. C. GÜCÜ
Middle East Technical University, Institute of Marine Sciences
P.O.Box 28, Erdemli, 33731, İçel, Turkey

Abstract. The Black Sea anchovy has experienced the most severe decline of the past 50 years and the responsible factors are not yet clearly understood. This is mainly due to the possible existence of several factors which may be equally probable. Some of these factors are: the increased eutrophication which changed the oligotrophic character of the Black Sea into a dystrophic one; the introduction of ctenophore medusa, *Mnemiopsis* sp; the outstanding exploitation pressure of the over-capitalised fishing fleet, and alterations in river discharges and hydrologic conditions at the straits. In this study, the contribution of fishery to anchovy collapse has been evaluated. For this purpose, **i)** the increase of fishing power by the recent introduction of purse seiners and sonars and their effects on over-wintering stocks along the Turkish coasts, **ii)** the condition index as an indicator of starvation of anchovy for pre and post *Mnemiopsis* period, **iii)** the spawning behaviour of anchovy, and **iv)** the coexistence of anchovy and *Mnemiopsis* during the anchovy spawning season, have been reviewed. It was concluded that effects of over-capitalisation of the fishing sector, especially of Turkey, on anchovy collapse and to an extent on the catastrophic changes in the Black Sea ecosystem, should not be overlooked as secondary.

2. Introduction

The state of the Black Sea, with its unique features, such as being the largest enclosed catchment basin, sets an excellent example demonstrating the adverse human impact on a marine ecosystem in regard to what could happen in the very near future to the other parts of the world oceans. Since the early fifties noticeable alterations have been observed at various levels of the Black Sea ecosystem. These changes, such as manipulation of hydrologic regimes of the out-flowing rivers (Bondar, 1977), changes in nutrient composition (Bologa et al., 1984; Gomoiu, 1990), introduction of exotic species (Vinogradov et al., 1989; Mutlu et al., 1994), selective and excessive fishing (Ivanov and Beverton, 1985; Stepnowski et al., 1993; Bingel et al., 1993), are well studied and reviewed by various authors (Sorokin, 1983; Tolmazin, 1985; Caddy and Griffiths, 1990; Mee, 1992; Zaika, 1992; Niermann et al., 1994). The rivers, such as the Danube, Dnepr, Denstr, Don and Kuban, constitute llinks between land and sea,

E. Özsoy and A. Mikaelyan (eds.), Sensitivity to Change: Black Sea, Baltic Sea and North Sea, 149–162.
© 1997 *Kluwer Academic Publishers.*

and play a crucial role in the modification and in the later deterioration of the ecosystem. These rivers are loaded by anthropogenic wastes from various sources in Central and Eastern Europe and drain them into northern part of the Black Sea. Their influence is, therefore, more pronounced in the Northwestern Shelf area and the Azov Sea, compared with other areas such as the Turkish Coast. Figure 1 is an arbitrary representation of different zones subjected to different types of changes.

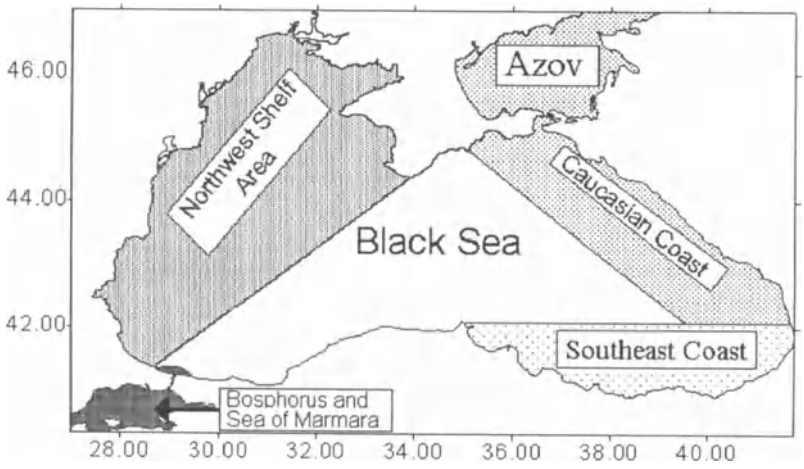


Figure 1 Arbitrary zones of the Black Sea used in the text.

In 1989, the *Mnemiopsis sp.*, which is an introduced species, suddenly appeared in the Black Sea in huge quantities. Its appearance has been synchronously followed by a sudden decline in various fish stocks. The purpose of this study is to evaluate the changes in the Black Sea ecosystem from the fisheries point of view and review -the catalysing effects of excess fishing on *Mnemiopsis* outbreak and on the deterioration in the ecosystem.

3. Zones of the Black Sea

3.1. NORTHWESTERN SHELF AREA, NWS

Until recently, the Northwestern Shelf Area was the most important zone in the Black Sea for the majority of the fish fauna. This area was reported as the main spawning and nursery ground for commercial species, like anchovy (*Engraulis encrasicolus ponticus*), turbot (*Psetta maxima)*, Atlantic bonito (*Sarda sarda*) and blue fish (*Pomatomus saltator*) (Slastenenko, 1956; Ivanov and Beverton, 1985). The primary reasons for the high preference of this region were the river induced productivity; and the underlying shallow and broad shelf area inhabited by macrophytes, which were

abundant enough to oxygenate the water column down to 60 meters (Ivanov and Beverton, 1985; Zaitsev, 1993).

As the level of nutrient enrichment increased gradually, primary production and in turn, the carrying capacity of the ecosystem for planktivorous species has increased (Caddy, 1990). In the 1980's a significant drop in the stocks of large pelagic fish, like *Scomber scombrus*, *Sarda sarda*, *Pomatomus saltator* was observed. As a result of improved food availability and removal of predation control by large pelagics, the ecological situation in the NWS area turned in favor of the small pelagic fishes like *Engraulis encrasicolus ponticus* and *Sprattus sprattus balericus*. On the other hand, stocks of some other commercial demersal species, such as *Psetta maxima* declined considerably (GFCM, 1993).

By further increase in the nutrient enrichment, the frequency and extent of phytoplankton blooms and consequently turbidity in the waters have also increased. Light attenuation by the particles increased and this resulted in regression of macrophyta meadows. Today, human induced excess autotroph production, which is not transferred to higher trophic level sediments at the bottom; are decomposed by bacterial activity and cause high level of oxygen utilization. Due to lack of oxygen, hypoxia and even local anoxia became common phenomena in the shallow coastal waters of NWS. Along with macrophytes, mussels, other demersal invertebrates and fish either died or were reduced drastically. In summary, this precious habitat for almost all living resources was dystrophied (Zaitsev, 1993).

3.2. THE AZOV SEA

Although it a has different hydrological and biological structure than Black Sea, from the fishery point of view, the Azov Sea is in close connection with the Black Sea. Like the NWS area, the Azov Sea, with its shallow, less saline waters supplied with suitable nutrients, formerly served as important nursery and spawning grounds for commercial fishes such as anchovy (*Engraulis encrasicolus ponticus*) and kilka (*Clupea cultrivensis*). Starting from the early fifties, due to the construction of reservoirs, dams, diversion of river water for irrigation, dumping of industrial, agricultural and domestic wastes into water bodies, the water quality and hydrological regime of the Azov Sea has been changed. Eutrophication and desalination of the water has eventually adversely affected fish stocks (Volovik et al, 1992; 1993a; 1993b).

3.3. THE BOSPHORUS AND THE SEA OF MARMARA

Apart from being a strait between the Sea of Marmara and the Black Sea, the Bosphorus is also a passage for the warm water components of the fish fauna, which spawn and feed in the Black Sea and over-winter in the Marmara and the Aegean Seas. During their seasonal migrations, these fish become extremely vulnerable to the fishery activities in the Turkish Straits, and hence they are over-fished. Moreover, domestic and industrial pollution, heavy sea traffic and coastal erosion in the Bosphorus are other important factors preventing annual fish migration between the two seas. Several

authors (Caddy and Griffiths, 1990; Zaitsev, 1993) have attributed total disappearance of large pelagics from NWS area to a combination of these factors.

3.4. THE SOUTHERN COAST

The man-made disturbances listed above for the NWS and Azov Sea and their influences on ecology, are not yet at a recognisable level along the Turkish coast. Turkish rivers discharging into the Black Sea are not utilised for energy generation, and human-induced changes in their hydrological regimes are not significant. The nutrient load and industrial or domestic wastes are not as concentrated as in the other two basins (Balkas et al., 1990). Until the fishery crisis in 1989 when anchovy catch collapsed from some 300 thousand tons to 96 thousand tons (Anon, 1993), Turkey had not been faced with a serious problem concerning drastic changes of the ecosystem as reported in NWS area and Azov Sea.

4. Aurelia Aurita and *Mnemiopsis sp.* in the Context of the Changing Ecosystem of the Black Sea

Due to the induced eutrophication, the overall biomass at nearly all levels of the pelagic food web increased in the Black Sea (Zaitsev, 1993; Caddy, 1990; 1993; Kideys, 1994, Ivanov and Beverton, 1985). Many species which were formerly abundant disappeared and were replaced by their counterparts having higher ecological tolerance, such as *Noctiluca scintillans* and *Aurelia aurita.* In addition, some newly introduced opportunistic species, like *Mnemiopsis sp.* appeared, invaded the whole basin and reached to dramatic quantities in biomass.

Aurelia aurita is a common component of the Black Sea fauna. In 1959-1962 jelly-fish total biomass in the 0-80m water layer of the Black Sea was 90-1600 thousands tons (wet weight; average $\approx$ 670 thousand tons). In 1978, in the 0-10m layer there were 47 million tons of *Aurelia aurita* with a total biomass of 300-450 million tons (wet weight) for the whole Black Sea (Gomoiu, 1981). Since there was no external control mechanism, such as predation or exploitation over *Aurelia aurita*, a considerable part of the biomass flow in the food-web was diverted in favour of *Aurelia aurita.* Consequently this species attained a biomass of 400 million tons just before the *Mnemiopsis* outburst in 1988 (Shushkina and Musayeva, 1983; Flint et al., 1989; Shushkina and Vinogradov, 1990; Vinogradov et al., 1985; Mutlu et al., 1994).

As opposed to *Aurelia aurita, Mnemiopsis* sp. is an introduced species first reported in 1982 (Shushkina and Musayeva, 1990; Zaika and Sergeeva, 1990) in the Black Sea. In 1989, this new species replaced *Aurelia aurita* by a sudden increase reaching to 800 million tons of total biomass and spread out all over the Black Sea. Later, between 1991-1993, the biomass leveled out and remained more or less stable around 100 million tons (Mutlu et al., 1994). A schematic representation of the fluctuation in the coexistence of these two species are depicted in Figure 2.

After the surprising outbreak of *Mnemiopsis sp.* in the Black Sea, coinciding with a drop in anchovy catch, the earlier studies disregarded the steadily increasing *Aurelia aurita,* and focused on possible predation of *Mnemiopsis sp.* on anchovy egg and larvae

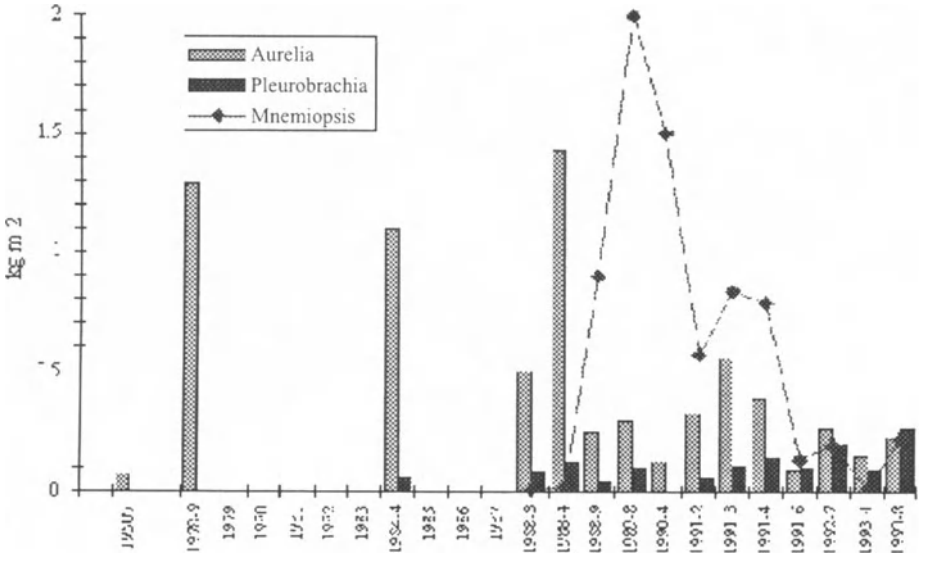


Figure 2. Fluctuation of the biomass (wet weight kg^{-2}) of *Mnemiopsis sp.*, *Aurelia aurita*, and *Pleurobrachia pileus* in offshore areas of the Black Sea from 1958-1993. Taken from Mutlu et al., 1994

and sought correspondence with collapse of anchovy fishery (Vinogradov, 1992; Zaika, 1992; Harbison and Volovik, in press). Recent studies, however, showed that anchovy egg and larvae constitute only a minor part of the *Mnemiopsis* diet (Tsikhon-Lukanina et al., 1990; Tsikhon-Lukanina and Reznichenko, 1991; Mutlu, in prep.). Both anchovy and *Mnemiopsis* feed mainly on copepods, hence compete for the same food source.

5. Review of Total Landings of Black Sea Countries

Figure 3 represents total fish landings from the Black Sea reported by the riparian countries. The collapse of fisheries was not only experienced in Turkey. Other countries faced the same problem even earlier. The Bulgarian fishery was ahead of the party confronted with a fishery crisis. In the seventies, moderate degree of nutrient enrichment increased the over-all production, reflected in the fishery by increased landings. The highest catch was obtained in 1981 and in the following period, landings decreased with nearly the same trend of the former increase. An almost similar picture

was observed in Romania and former USSR, whose highest catches were obtained in 1986 and 1982, respectively. Along the Turkish coast, the increase in total fish landings kept its pace until 1988, thereafter underwent a very sharp decline in 1989.

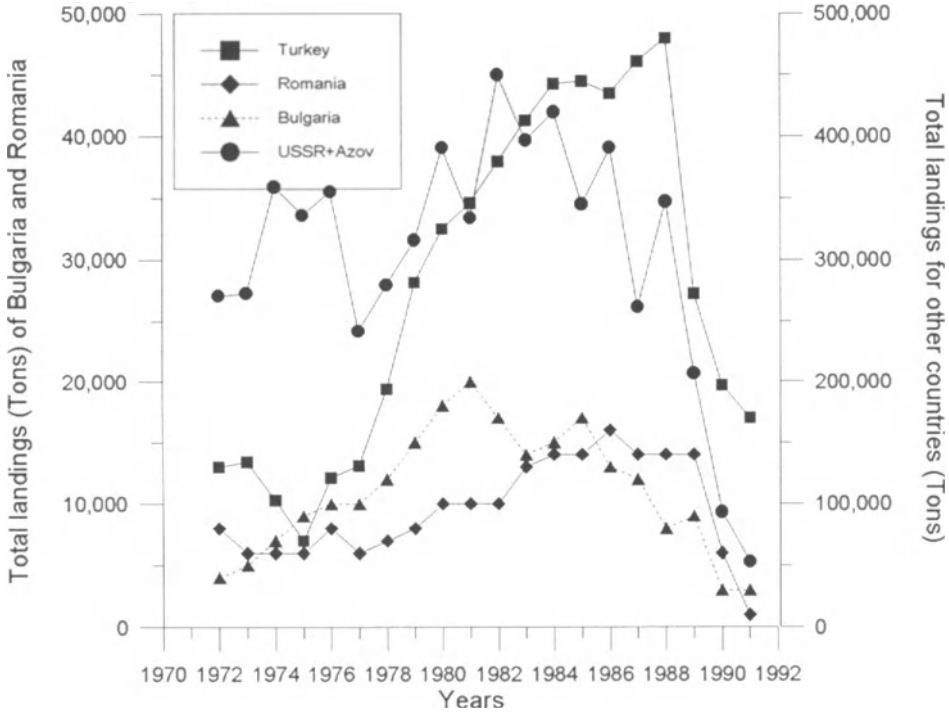


Figure 3. Total landings of Black Sea riparian countries (GFCM, 1993).

5.1. TURKISH FISHERY AND CHANGES IN THE CATCH COMPOSITION

Today, the Turkish fishing fleet operating in the Black Sea is characterised by three distinct categories: purse seining, trawling and artisanal fishery. The latter one is carried out with small wooden boats 4-10 m in length, using beach seine, trammel and gill nets. Their contribution to the total landing is quite insignificant.

Trawl nets are designed and rigged to work on the bottom. Considering the complex topography, i.e. narrow and steep continental shelf, canyons, and troughs, the Turkish coast of the Black Sea, in general is not suitable for trawling activity. Moreover, trawling is completely banned at the eastern-most section of the coast.

Purse seine nets used by the Turkish fishing fleet are about a kilometer long and approximately 150 meters high (Anon, 1992). These nets catch the fish by surrounding them from the sides. The sea bottom or the underlying permanent H_2S layer prevents the fish from escaping in deep waters by diving downwards. Boats operating purse seine nets are usually equipped with powerful sonars having one kilometer scanning range on each side of the boat, which enables them to point precisely the position of

fish schools. Once the school of fish is encircled, an auxiliary skiff equipped with a fish pump comes alongside and empties the catch in a short time. This fishery setup, is extremely suitable to exploit dense school forming pelagic species, such as anchovy. As reported by the fishermen, a single set of purse seiner may catch up to 300 tons of anchovy in a single operation.

Although the total landing of fishery collapsed in 1989 and remained low since then, not all the species exploited by Turkish fishing fleet showed the same trend. Table 1 represents the main commercial fishes exploited by the Turkish fishing fleet along with their catch records of the past 12 years. It is evident that main pelagic species like *Engraulis encrasicolus*, *Pomatomus saltator* and *Sarda sarda* decreased during that period, some others, such as *Merlangius euxinus*, *Scomber japonicus* and *Sprattus sprattus* increased. Like anchovy, the other species lay pelagic eggs and they are strictly dependent on copepods for feeding during their early life stages. Here, one of the most important argument requires the settlement of the question as to why only the pelagic fish have declined, while others have increased or did not change.

The species which shows a negative trend is mostly school forming pelagic species and they are the target species of purse seines. On the contrary, most of the species, which increased or remained unchanged during the past 12 years, are either demersal or do not form dense schools, hence are not vulnerable to purse seines. As an example, whiting is a demersal species caught mainly by trawlers. Similarly sprat is a pelagic species, but because it does not form dense school during the fishing season (November to April), it is not effectively caught by purse seine nets.

5.2. FISHING POWER OF THE TURKISH FISHING FLEET

As a consequence of man-induced eutrophication, the carrying capacity of the Black Sea, and in turn, the surplus production of small pelagics have increased. The purse seines, introduced in late 50's, rapidly developed in the later years. The number of boats, usage of sonars and fish finders, fish pumps and number of auxiliary skiffs increased very sharply (Figure 4). All these factors have increased the fishing power of the Turkish purse seine fleet by the factor of ten (Gücü, in prep.).

Due to poor coordination in the sector and lack of reliable stock estimates, the same reasons misled the policy makers to encourage investments on fish processing factories, such as fish oil and meal plants. Today, the fishing and processing capacities are not properly matched, i.e., the total capacity of fish processing factories have reached 6700 tons/day which is 4 times higher than the total annual production of the whole country, including catches from Mediterranean, Aegean, Marmara Sea and inland waters (Bingel et al., 1995).

6. Anchovy as an Indicator of the Ecological Changes in the Black Sea

The anchovy is the dominant species of the Black Sea. It comprises more than 50% of the total landings from the Black Sea. The anchovy has two subspecies in the Black

Sea. The Black Sea anchovy, *E. encrasicolus ponticus* and the Azov anchovy, *E. encrasicolus maeoticus*. Until recently, the Black Sea anchovy was mainly spawning in the Northwestern Shelf area in summer. During winter, the whole population was

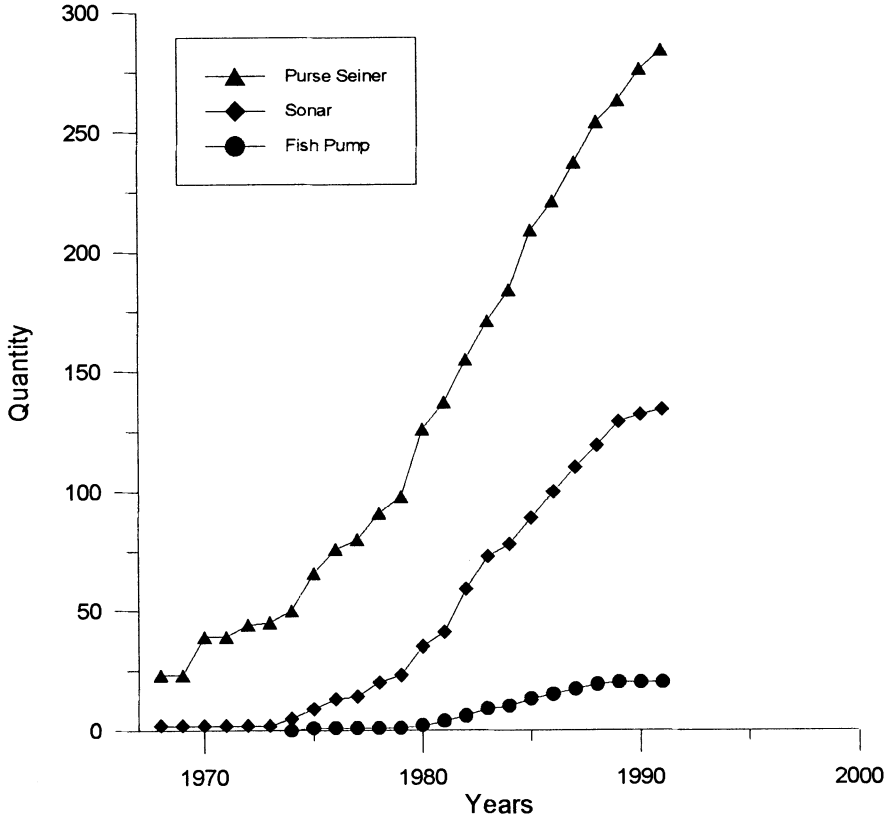


Figure 4. Number of Turkish purse seiners, boats with sonar and fish pump operated in the Black Sea (Anon., 1992).

migrating to the south and hibernating along the eastern part of Turkish Black Sea coast and Georgia (Ivanov and Beverton, 1985). Azov anchovy was spawning in the Azov Sea during summer and migrating to south for over-wintering. More recent studies carried out by joint efforts of various Black Sea countries, have revealed that there is an evident shift in the spawning grounds of the Black Sea anchovy, which are nowadays located in the southern part of the Black Sea, contrary to their past preferences (Niermann et al., 1994). Hydroacoustic studies in offshore waters support the hypothesis that major spawning and nursery grounds of anchovy have shifted to the south (Caddy, 1992).

The southward shift in the spawning ground of Black Sea anchovy is in good agreement with deterioration of the ecological features of the northwestern shelf area (Zaitsev, 1993). The period of summer algal blooms developing in the NWS area and

finally associating with hypoxia and even anoxia, coincides with the period when anchovy spawning reaches it maximum.

Similarly, a southward shift in the spawning ground of Azov anchovy has been reported by Chashchin (1995). The author explained this situation by desalination in the Azov Sea as a result of hydrological manipulation on the in-flowing rivers, like Kuban. Consequently moving south, the spawning grounds of the Azov and Black Sea anchovy have been overlapped, and the share of hybrids (Black Sea X Azov anchovy) in the Black Sea has increased considerably (Chashchin, 1995).

6.1. FACTORS RESPONSIBLE FOR THE ANCHOVY DECLINE

Several hypotheses for explaining the decline of anchovy stocks have been advanced, but only two appear scientifically sound: the impact of *Mnemiopsis sp.* and the effects of over-fishing. The effects of the latter is evident from the variations in length composition of anchovy landed by the Turkish fishing fleet, depicted in Figure 5 along with the total amount of fish caught. In the 1987/88 fishing season, relatively larger and older fishes were dominating the catch. This is an appreciable figure for fisheries management purpose, unless total catch exceeds the limit of "recruitment over-fishing" in which the size of the spawning stock is reduced so that they can not produce enough offspring to sustain former population size. However, as it is evident from a comparison of the 1987/88 and 1988/89 fishing seasons, the anchovy stock was over-fished and only small sized premature individuals dominated the catch during 1988/89 period. Neither fishermen nor governments recognised this obvious sign of "recruitment over-fishing", and due to mismanagement, potential spawners of the next year were removed from the system before they could spawn. Finally in the 1989/90 period, nearly no anchovy was left and Turkish fishing fleet could only catch 1/3 of the amount in the previous seasons (Anon, 1993).

As a consequence of drastic decline in the stocks, the catch per effort, and in turn, total income of the fishermen reduced. Faced with declining anchovy catches, Turkish fishing fleet of the Black Sea, which had attained enormous quantities, shrunk in size. Some of the people involved switched to alternative businesses, others moved to the Aegean and Mediterranean Sea regions to cope with crisis. According to the latest catch statistics of Turkey a slight recovery was experienced in 1994.

Another evidence on the role of over-fishing in anchovy fishery collapse is the condition index of the hibernating anchovies. In Figure 6, condition of different size groups of anchovy are depicted. This figure is contradictory with the concerns about the starvation of anchovy as a consequence of heavy predation of *Mnemiopsis* on calanoid copepods, which is the common food source of both species. The figure, on the other hand, is in good agreement with the feeding biology of the anchovy, such that they stop feeding during winter and consume fat deposited during summer, such that their condition index is decreased. As it is clear from the figure, the condition index of the over-wintering anchovy has decreased considerably in all examined fishing periods.

As the condition indices of the smallest size group of over-wintering anchovy are compared for pre- and post *Mnemiopsis* periods, they were less conditioned before *Mnemiopsis* outbreak during 1988/89 fishing season. In 1989/90, the condition index of the youngest individuals of hibernating anchovies increased considerably. It is crucial to note that this period coincides with the anchovy collapse. This is in contrast

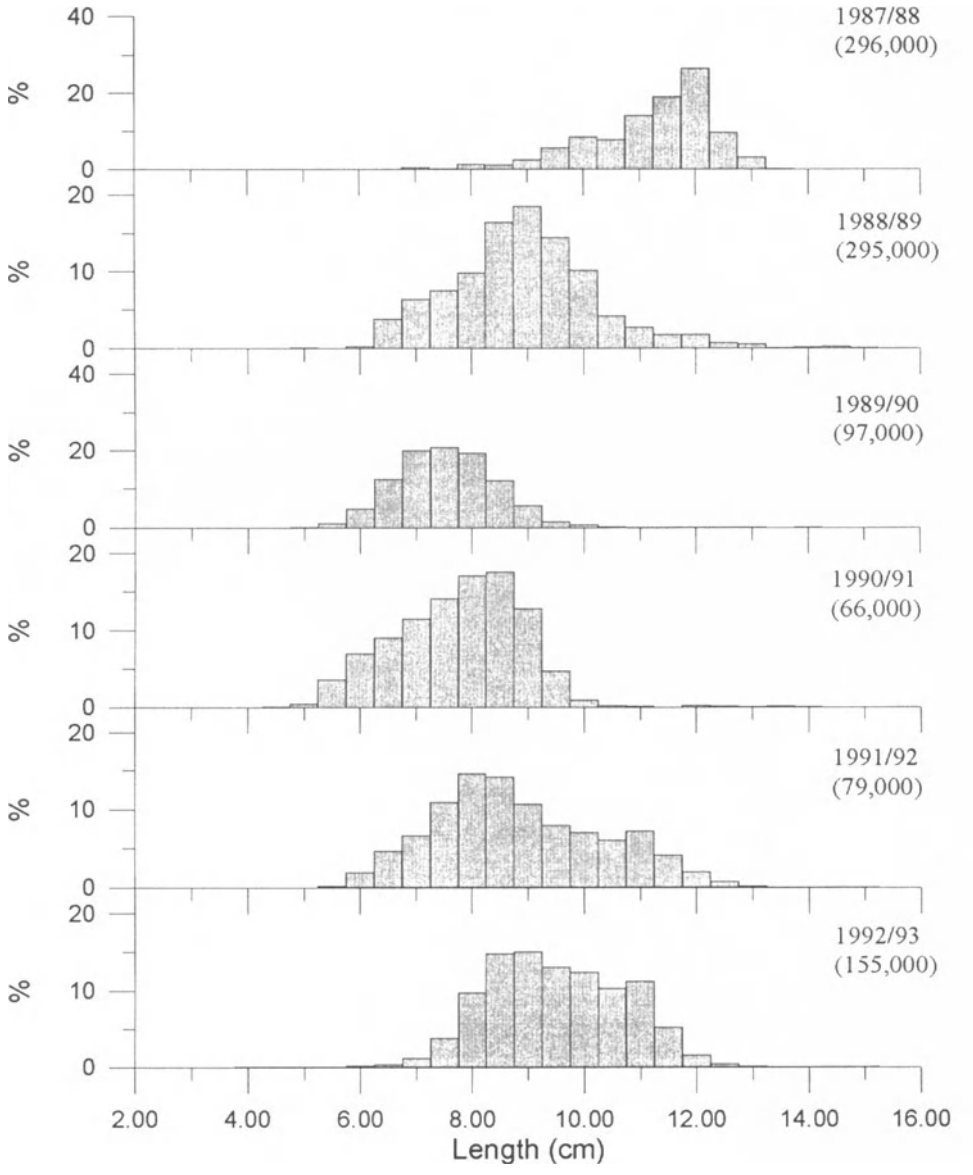


Figure 5. Length composition of the anchovy landed by the Turkish fleet during 1987-1993

with the expectations, because within this period *Mnemiopsis* attained the maximum biomass level ever recorded, during which predation of anchovy spawns by *Mnemiopsis*, if any, and competition between *Mnemiopsis* and anchovy for calanoid copepods should expected to be very high.

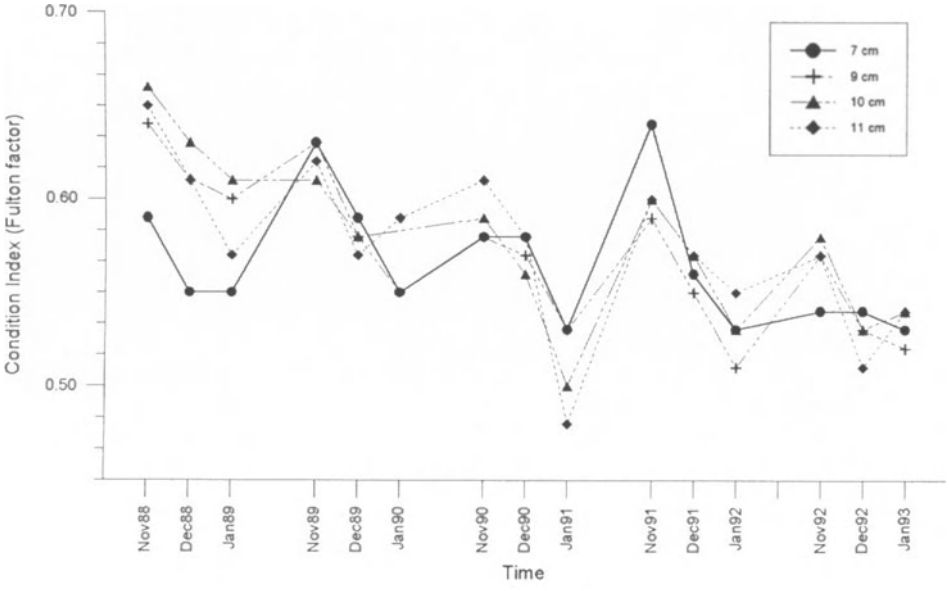


Figure 6. Condition index of anchovies caught during 1988-1993

7. Conclusion

Nutrient enrichment, in general, has raised the carrying capacity of the Black Sea for small pelagic fishes, hence the catch per unit effort increased and provoked governmental and private investments in the fishing sector. Towards the end of 1980's, the fishing sector reached a state that can catch and process more than the Black Sea could sustain.

As a result, over-wintering anchovy, which forms very dense schools and are concentrated in a narrow coastal band, became extremely vulnerable to the Turkish purse seiners. Finally size of the spawning stock was reduced to the extent that not enough young fish were produced to ensure the future of the stock. Following the abrupt decline in the stock, the niche formerly occupied by anchovy was re-occupied by *Mnemiopsis* sp.

The collapse of the fishery in the Black Sea, besides causing significant loss to economy, in terms of the value of catch, the value of vessels and plants, and employment, also had a significant side effect due to its contribution to enhance the eutrophication. Using the respective ratios of 1/417 and 1/35 for phosphorus and nitrogen in fish tissue, given by Anderson and Ursin (1977), Caddy (1992) has roughly

calculated that the total removal of phosphorus and nitrogen simply by fishery activities to be on the order of 2158 tons and 26000 tons, respectively, in the pre-collapse period. At present, these values have decreased to 480 tons of phosphorus and 5760 tons of nitrogen. In other words, 1,700 tons of phosphorous and 20,000 tons of nitrogen have remained in the system.

As it was repeatedly emphasised by nearly all authors working on Black Sea ecological problems, to mitigate the situation in the Black Sea the following remedies are advisable:

–substantial reduction of flow of nutrient into the system,

–implementation of control measures over jelly predators,

–recovery of fish stocks through a sound international fishery management policy.

It is worth noting that the above listed remedies are often very costly and therefore nearly improbable to implement. On the other hand, by simply regulating the fishery and achieving a level exceeding the former catch records;

i) economic loss (human food, employment, re-utilization of waste, investment capital) can be retrieved,

ii) energy flow to jelly organisms can be diverted to fishes, and hence population of the former can also be controlled,

iii) considerable part of the excess nutrient pumped by the rivers into the Black Sea can be removed from the system in a very profitable way.

8. Acknowledgements

This work was supported by the Turkish Scientific and Technical Research Council (TUBİTAK), and by the Scientific Affairs Division of NATO within the framework of the Science for Stability Program. I am indebted to the personnel of Yomra Fisheries Research Institute for their helps in various ways. I should also extend my sincere thanks to Dr. Ulrich Niermann, Mr. Can Bizsel and Mr. Mumtaz Tirasin.

9. References

1. Anon. (1992) *Determination and quantification of fishing gears and technology in Black Sea.* Ministry of Agriculture and Rural Affairs of Turkish Republic, Research Institute of Aquatic Products. Trabzon. 106 p (in Turkish).
2. Anon. (1993) *Fishery Statistics 1989-90.* State Institute of Statistics, Prime Ministry of Turkish Republic. Publ., No., 1583.
3. Andersen, K.P. and Ursin, E.A. (1977) A multispecies extension to the Beverton and Holt theory of fishing, with accounts of phosphorus circulation and primary production. *Meddr. Danm. Fisk.-og Havunders.* N.S.7:319-435
4. Balkas, T., Dechev, G., Mihnea, R., Serbanescu, O. and Ünlüata, Ü. (1990) State of marine environment in the Black Sea Region. *UNEP Regional Seas Reports and Studies*, 124.
5. Bingel F., Kideys A.E., Ozsoy E., Tugrul S., Basturk O. and Oguz T. (1993) *Stock assessment studies for the Turkish Black Sea coast.* NATO-TU Fisheries Final Report. Institute Of Marine Sciences. METU Içel Turkey 108p.

6. Bingel F., Gücü A.C., Stepnowski A., Niermann U., Dogan M., Kayikci Y., Mutlu E., Avsar D., Kideys A.E., Uysal Z., Ismen A., Bekiroglu Y., Genc Y., Okur H., and Zengin M. (1995) Stock assessment studies for the Turkish Black Sea coast. Final Report. Institute of Marine Sciences. METU Içel Turkey 159p.
7. Bologa A.S., H.V. Skolka and Frangopol P.T. (1984) Annual cycle of planktonic primary productivity off the Romanian Black Sea coast. *Marine Ecology-Progress Series* 19:25-32.
8. Bondar, C. (1977) Changes in hydrological pattern induced by engineering works on the lower Danube. *Hidrotecnica*, 22(7):87-9 (in Romanian).
9. Caddy, J.F. (1990) A contrast between recent fishery trends and evidence for nutrient enrichment in two large marine ecosystems: the Mediterranean and the Black Sea. The Large Marine Ecosystems (LME) concept and its application to regional marine resource management.
10. Caddy, J.F. (1992) Update of the fishery situation in the Blacks Sea, and revision of the conclusions of the 1990 GFCM Studies and Reviews No.63, by Caddy and Griffiths: "A respective on recent fishery-related events in the Black Sea". World Fisheries Congress. May 3-8, 1992 Athens, Greece.
11. Caddy, J.F. (1993) Toward a comparative evaluation of human impacts on fishery ecosystems of enclosed and semi-enclosed seas. *Reviews in Fisheries Science,* 1(1):57-95
12. Caddy, J., and Griffiths, R. (1990) A perspective on recent fishery related events in the Black Sea. *Studies and Review. General Fisheries Council for the Mediterranean*, 63:43-71.
13. Chashchin A.K. (1995) Abundance, distribution and migration of the Black Sea anchovy stocks. *Tr. J. of Zoology* 19:173-180.
14. Flint M.V., Arnautov G.N. and Shushkina E.A. (1989) Quantitative distribution of jellyfish Aurelia. Structure and productional characteristics of plankton communities in the Black Sea. *Nuaka, Moscow*: 315-322.
15. GFCM (1993) Statistical Bulletin, nominal catches 1979- 1991. *FAO Bulletin. of Fishery Statistics*, 32(9): 237 pp.
16. Gomoiu, M.T. (1981) Some problems concerning actual ecological changes in the Black Sea. *Cercetari Marine.*, 14: 109-127.
17. Gomoiu M.T. (1990) Marine eutrophication syndrome in the north-western part of the Blacks Sea. In: Vollenweider R.A., Marchetti R. and Viviani R [Eds.] Marine Coastal Eutrophication. Elsevier Publ. 683-703.
18. Harbison G.R. and S.P. Volovik (in press). The ctenophore, Mnemiopsis leidyi, in the Black Sea: A holoplanktonic organism transported in the ballast water of ships. In: Cottingham D., ed. In press. Non-indigenous and Introduced Marine Species. *NOAA Technical Report.*
19. Ivanov L. and Beverton R.J.H. (1985) The fisheries resources of the Mediterranean. Part Two: Black Sea. *G.F.C.M. Studies and Reviews* No.60, Rome: FAO, 135p.
20. Kideys, A.E. (1994) Review of "recent dramatic changes in the Black Sea ecosystem: the reason for the sharp decline in Turkish anchovy fisheries. *Journal of Marine Systems*
21. Mee, L.D. (1992) The Black Sea in crisis: The need for concerted international action. *Ambio*, 21(3):278-286.
22. Mutlu E, Bingel F., Gücü A.C., Melnikov V.V. Niermann U., Ostr, N.A., and Zaika V.E. (1994) Distribution of the new invader *Mnemiopsis* sp. and the resident *Aurelia aurita* and *Pleurobrachia pileus* populations in the Black Sea in the years 1991-1993. *ICES J. Mar. Sci.* (51): 407-421
23. Niermann U., F. Bingel, A. Gorban, A.D. Gordina, A.C. Gücü, A.E. Kideys, A. Konsulov, G. Radu, A.A. Subbotin & V.E. Zaika. (1994) Distribution of anchovy eggs and larvae (*Engraulis encrasicolus* Cuv.) in the Black Sea in 1991 and 1992 in comparison to former surveys. *ICES J. Mar. Sci.* (51): 395-406
24. Shushkina, E.A., and Musayeva, E.I. (1983) The role of jellyfish in the energy system of Black Sea plankton communities. *Oceanology,* 23 (1): 92-96.
25. Shushkina, E.A., and Vinogradov, M.YE. (1991) Long-term changes in the biomass of plankton in open areas of the Black Sea. *Oceanology*, 31(6): 716-721.
26. Shushkina, E.A., and Musayeva, E.I. (1990) Structure of planktonic community of the Black Sea epipelagic zone and its variation caused by invasion of a new ctenophore species, *Oceanology*, 30(2): 225-228.
27. Slastenenko E. (1956) Karadeniz havzasi baliklari., *E.B.K. yay.*, 1-770, Istanbul, 711 sayfa
28. Sorokin, Y.I. (1983) The Black Sea. Ecosystems of the world. In Estuaries and enclosed seas. 26: pp.253-291. Ed. by P. H. KETCHUM. Elsevier, Amsterdam.
29. Stepnowski A., Gücü A.C., and F. Bingel. (1993) Assessment of the pelagic fish resources in the southern Black Sea using echo integration and Dual-Beam processing. *Archives of Acoustic, Polish Academy of Science Journal*, 18 (1), pp. 83-104.
30. Tolmazin D. (1985) Economic impact of the riverine-estuarine environment of the USSR: The Black Sea basin. *Geo.* Jl, 11:137-152

31. Tsikhon-Lukanina E.A., Reznichenko O.G. and Lukasheva T.A. (1990) Diet of the Ctenophore Mnemiopsis in the inshore waters of the Black Sea. *Oceanology* (31) 4, 496-500.
32. Tsikhon-Lukanina E.A. and Reznichenko O.G. (1991) Diet of the Ctenophore Mnemiopsis in the Black Sea as a function of size. *Oceanology* (31) 3, 320-323
33. Vinogradov, M.E. (1992) Long - term variability of the pelagic community structure in the open Black Sea. In: Problems of the Black Sea. International Conference on Problems of the Black Sea. International Conference. Sevastopol, Ukraine. November 10 - 15: 19 - 33.
34. Vinogradov, M.YE., Flint, M.V., and Shushkina, E.A. (1985) Vertical distribution of mesoplankton in the open area of the Black Sea. *Marine Biology* 89: 95-107.
35. Vinogradov, M.Ye. (1990) Investigation of the pelagic ecosystem of the Black Sea (44th Cruise of the R/V Dimitriy Mendeleyev, 4 July - 17 September 1989. Oceanology 30(2): 254-256.
36. Vinogradov M.YE., E.A. Shushkina, E.I. Musayeva and P.YU. Sorokin (1989) A newly acclimated species in the Black Sea: The ctenophore Mnemiopsis leidyi (Ctenophora: Lobata). *Oceanology* 29(2): 220-224.
37. Volovik, S.P., Makarov, E.V. and Semyonov, A.D. (1992) The state of the ecosystem and fish stock of the Azov Sea, measures aimed at their protection. World Fisheries Congress, 3 - 8 May 1992, Athens, Greece.
38. Volovik, S.P., Dubinina, V.G. and Semenov, A.D. (1993a) Fisheries and environment studies in the Black Sea system. Part 1: Hydrobiology and dynamics of fishing in the Sea of Azov. *Studies and Reviews. General Fisheries Council for the Mediterranean.* No.64. Rome, FAO : 1 - 58.
39. Volovik, S.P., Myrzoyan, Z.A., and Volovik, G.S. (1993b) *Mnemiopsis leidyi* in the Azov Sea: Biology, population dynamics, impact to the ecosystem and fisheries. *ICES* C:M.1993/L:69: 11 pp.
40. Zaika, V.E. (1992) The ecosystem degradation is increasing. In: Problems of the Black Sea. International Conference on Problems of the Black Sea. International Conference. Sevastopol, Ukraine. November 10 - 15: 97 - 100.
41. Zaika, V.YE., and Sergeeva, N.G. (1990) Morphology and development of *Mnemiopsis mccradyi* (Ctenophora: Lobata) in the Black Sea, *Zoologichesky Zhurnal*, 69(2): 5-11 (Abstract in English).
42. Zaitsev, Yu.P. (1992) Recent changes in the trophic structure of the Black Sea. *Fish. Ocean.*, 1(2): 180 - 189.
43. Zaitsev, Yu.P. (1993) Fisheries and environment studies in the Black Sea system. Part 2: Impact of eutrophication on the Black Sea fauna. *Studies and Reviews. General Fisheries Council for the Mediterranean.* No.64. Rome, FAO : 59 - 86.

ENVIRONMENTAL IMPACT ON FISH RESOURCES IN THE BLACK SEA

K. PRODANOV[1], K. MIKHAILOV[2], G. DASKALOV[2], K. MAXIM[3], A. CHASHCHIN[4], A. ARKHIPOV[4], V. SHLYAKHOV[4], E. OZDAMAR[5]
[1]*Institute of Oceanology-Varna, Bulgarian Academy of Sciences*
[2]*Institute of Fisheries-Varna, Bulgaria*
[3]*Institul Roman de Cercetari Marine-Konstanta, Romania*
[4]*YugNIRO-Kertch, Ukraine*
[5]*Ondokuz Mayis University Faculty of Fisheries-Sinop, Turkey*

Abstract.. Stock assessments for anchovy, sprat, whiting and horse mackerel during 1950-1994 is performed. The VPA analysis showed that the decline of these populations, mainly as a result of the intensification in fishing activity, is probably one of the major reasons for the mass development of the ctenophore *Mnemiopsis leidyi*. It is considered that the reduction of the fishing effort, especially on immature fish, may have rapid effects on the recovery of their stocks.

1. Introduction

During the last 30 - 35 years, the Black Sea ecosystem has been subjected to dramatic changes due to the increased pollution of the basin and the over-exploitation of some commercial fish species. According to Rass [19], the pollution of the northwestern part of the Black Sea is the reason why bonito and blue fish avoid this region, although their stocks in the Sea of Marmara have not decreased.

The period of "eutrophied sea" date back to the early 70's and is characterised by structural and functional alterations in the ecosystem as a result of the intensification and spreading of both local and regional phytoplankton blooms. In the last decade, these blooms are known to attain their maximum intensity in the late spring - summer period, in a way that is abnormal for the Black Sea, where peak production normally occurs in early spring and autumn. Changes have also been registered in the taxonomic composition of blooms - producing phytoplankton species with succession shifted towards the predominance of Dynophyta and since 1989 - towards an increasing importance of Crysophita species - *Emiliania huxleyi* and *Phaeocystis pouchettii* [9, 10]. Recently some phyto- and zooplankton species new for the Black Sea ecosystem have invaded the basin resulting in dramatic alterations in the food web [11]. During the period of consideration, the abundance of most commercial carnivores like bonito (*Sarda sarda* Bloch), blue fish (*Pomatomus saltator* Linnaeus) and mackerel (*Scomber*

E. Özsoy and A. Mikaelyan (eds.), Sensitivity to Change: Black Sea, Baltic Sea and North Sea, 163–181.
© 1997 *Kluwer Academic Publishers.*

scombrus Linnaeus) has sharply decreased. The mackerel has almost become extinct in the Black Sea since 1968. This has been the period of rapid intensification of fishing, particularly of sprat (*Sprattus sprattus phalericus* Risso), horse mackerel (*Trachurus mediterraneus ponticus* Aleev) and anchovy (*Engraulis encrasicolus ponticus* Aleksandrov), for which catches have been extended from 3.1, 4.9 and 128.3 thousand tons (1970) up to 105.2 (1989), 147.7 (1985) and 485.5 (1984) thousand tons, respectively. Shlyakhov et al. [23] claim that the rapid decline of the anchovy stock could be related both to the deteriorated environmental conditions and the over-catch during some years (1985-1986). In the early 80's (1982), the ctenophore *Mnemiopsis leidyi* = *Mnemia mccradyi* has invaded the Black Sea [24, 26] with a biomass increase resulting in several fold reduction of the nutritive zooplankton biomass; Copepoda species in particular [6, 27]. The above anthropogenic factors should be discriminated from the natural factors, in particular from global climatic changes and their impact on the hydrology, hydrochemistry and primary production of the basin. A typical example in this sense is the established periodicity in the qualitative and quantitative composition of phytoplankton in Black Sea in relation to the solar activity variability [14,15]. Another important natural and anthropogenic factor is the decline registered in the water budget of the Black Sea, related to the decreases in river inflow [1]. The global climatic changes influence river runoff through the overall amount of rainfall. The importance of the subject calls for annual stock assessments and catch projections of commercial fish species in relation to the environmental conditions.

2. Material and Method

On the basis of combined (Bulgarian, Ukrainian, Romanian and Turkish) data for the age compositions of the catches of anchovy, sprat, horse mackerel and whiting, an assessment of the dynamics of their stocks was accomplished. For this purpose the results from the ichthyoplankon survey annually carried out by YugNIRO-Kerch were also used. In order to establish the values of the fishing mortality coefficient for the oldest age group (Fst), the available data for fishing effort by gears and ships were used. The coefficient was then calculated, alternatively by Teylor's method [26]. The natural mortality coefficient was determined by the methods of Kutty and Quasim [8]; Pauly [12] or using data from literature. For defining the same coefficient for the youngest age group of sprat (0+) the relationship derived by Petersen and Wroblewski [13] was applied.

In the present work the stock assessments are made by different modifications of VPA: traditional and with ad hoc tuning [25]. For sprat three methods were applied: the Separable VPA (SVPA) [16], the VPA with ad hoc tuning [16] and the Extended Survivors Analysis (XSA) [21, 22]. The first one assumes separable fishing mortality pattern and the last two use additional information (CPUE, surveys indices) for tuning the model parameters (fishing mortality, abundance).

Determination of the recruitment abundance was investigated by many different methods:

(1) $R = a*B*\exp(-b*B)$ [20]
(2) $R = a*B - b*B^2$ [3]
(3) $R = f(X1;X2;X3....Xn)$ multicorrelation analysis

For establishing the influence of fishing mortality on the stock recruitment relationship of whiting we used the following equations:

(4) $R = a*B - b*B^2 - c*B*F$
(5) $R = a*B - b*B^2 - c*B*F - d*B^2*F$

where: R - recruitment; B - spawning biomass; X1, X2, X3 .... Xn - independent variables reflecting the influence of the biotic and abiotic factors of the environment. The influence of fishing mortality rate on the dynamic of the anchovy exploited stocks were investigated by following equations:

(6) $Bex = a*F_{(1+ - 4+)}*\exp[-b*F_{(1+ - 4+)} - c*F_{0+}]$
(7) $Bex = a*F_{(1+ - 4+)}*\exp[-b*F_{(1+ - 4+)} - c*F_{0+} + d*B + e*R]$

3. Results and Discussion

3.1. BLACK SEA ANCHOVY

On Figures 1 and 2 are presented the results for anchovy stock assessments during the period 1967-1994. According to VPA conducted by seasons, the spawning and exploited anchovy biomasses have ranged from 137.5 (1990) to 768.1 (1979) thousand tons and from 271.0 (1990) to 1427.4 (1979) thousand tons, respectively. The assessments were performed with M=0.82.

The steady decline of the exploited biomass is associated with the poor environmental condition in the Black Sea, one of the result being the outburst of ctenophore *Mnemiopsis leidyi*, and the over exploitation of the anchovy stock during 1987-1989. During the considered period the coefficient of exploitation ($U=Y/B_{0+}$) ranged between 0.422 and 0.567 with the corresponding F values 0.81 and 1.44, respectively.

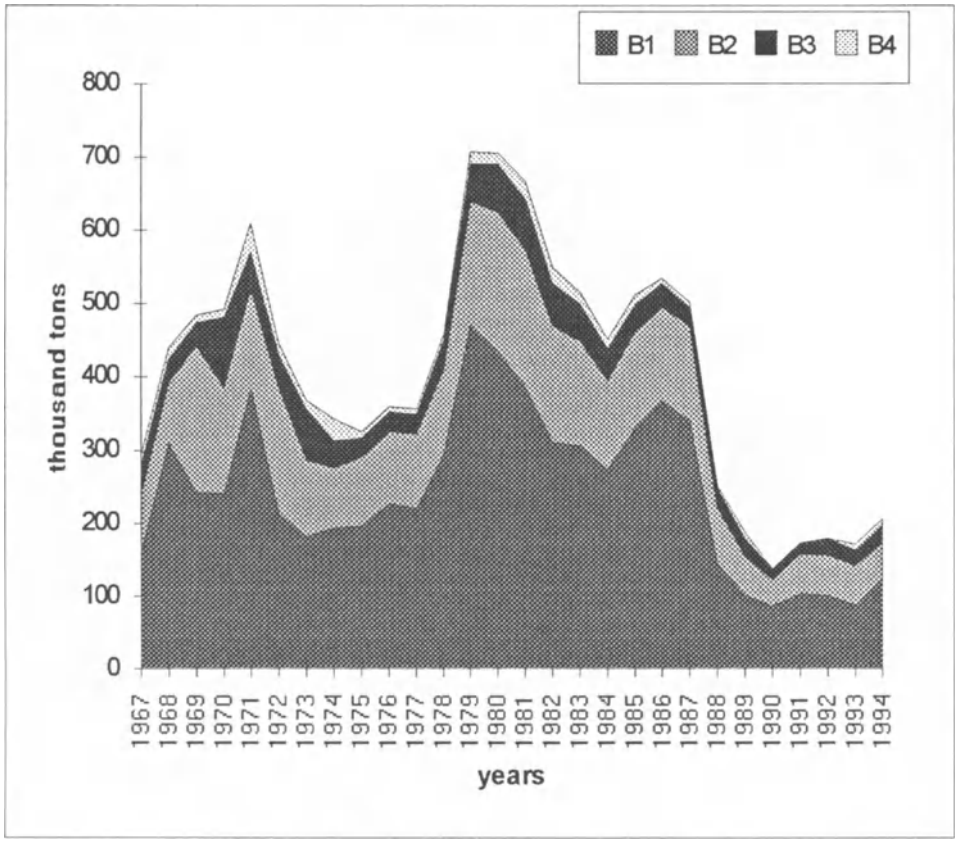


Figure 1. Anchovy spawning biomass in the beginning of May (shortly before the spawning season) during the period 1967-1994

The anchovy stock size assessments are agree with that performed by Johannesson and Loose [6]; Ivanov and Beverton [4]; Ivanov and Mikhailov [5]. The first estimate was obtained from trawl - hydroacoustic survey that took place in March 26 - 31, 1976 off the Turkish coast. According to this survey, the anchovy biomass during this year has been 990.0 thousand tons. On the basis of these data and the fact that assessment was only related to the wintering stock off the Anatolian coast, Ivanov and Beverton [4] adopted that its stock in the whole Black Sea has been around 1500.0 thousand tons. The conclusion of Ivanov and Mikhailov [5] gave an average estimate of the exploited anchovy biomass of 1000.0 thousand tons assuming that in some years it has peaked at 1300.0 thousand tons.

The influence of the fishing mortality rate on the anchovy exploited biomass was investigated by the equations (4) and(5). The values of the parameters in equation (4) are as folow:

$$Bex=5540.9*F_{(1+-4+)}*\exp[-0.940266*F_{(1+-4+)}-2.337497*F_{0+}] \quad r=0.532$$

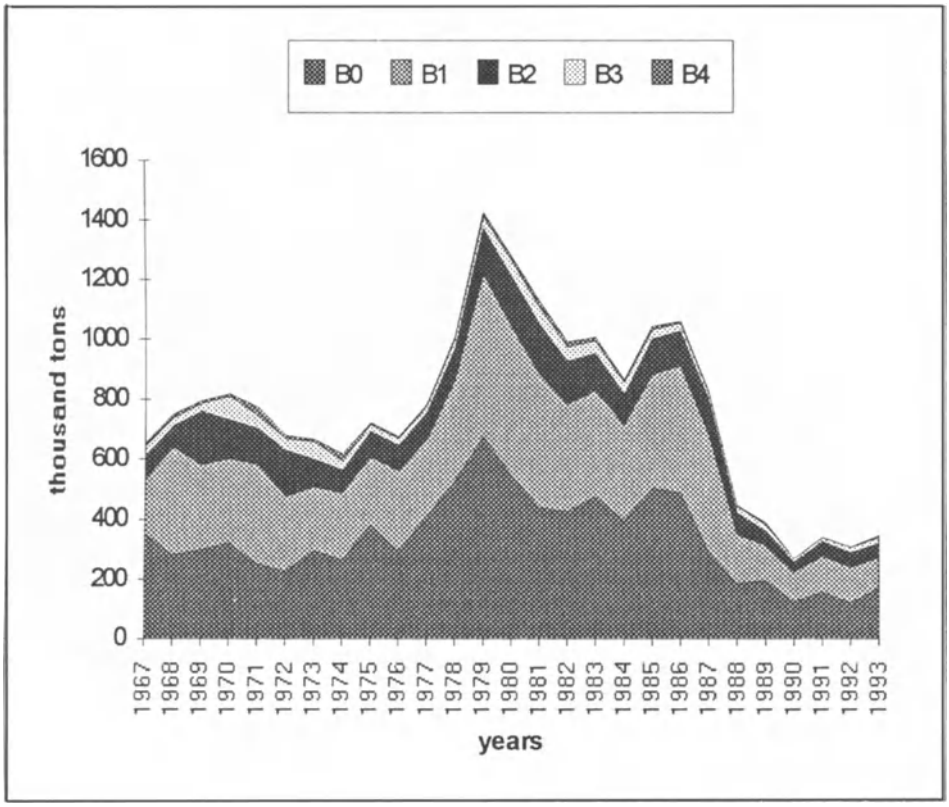


Figure 2. Anchovy exploited biomass (by age groups) in the beginning of November during the period 1967-1994

The relationship between the exploited biomass and fishery mortality rate is derived on the basis of the VPA results. According to the estimated values of the parameters under consideration, at F0+ = 0.1 the optimum value of F(1+ - 4+) is 1.0635. The last value does not change with increasing of the values for F0+ but the curve's forms, reflecting the relationship between the exploited biomass and fishing mortality rate (F1+ - 4+), change strongly (figure 3). On the pointed figure it is seen that at F0+ = 0.1, Bmax = 1716.0 thousand tons. The estimates show that the anchovy exploited biomass can stabilize on its maximum level on condition that the abundance of recruitment is always 162.0×10^9 number of specimens [F(1+ - 4+) = 1.0635]. Under these conditions the annual catch will be 583.9 thousand tons (34.0% from the initial exploited biomass). At F0+ = 0.3, Bmax=1076 thousand tons. In order to stabilize on this level 113.0×10^9 0+ old fishes has to recruit annually. In this case the annual catch will be 434.8 thousand tons (40.4% from the initial exploited biomass). At F0+=0.5, Bmax=675 thousand tons. In this case the anchovy exploited biomass will stabilize on its maximum level if the recruitment is 78×10^9 0+ old fishes annually. The annual

catch at F(1+ - 4+) = 1.0635 will be 315.4 thousand tons (46.7% from the initial exploited biomass).

From the above stated facts it is clear that according to equation (6) the increase of fishing mortality rate on the juvenile 0+ old fishes will lead to reduction of the anchovy exploited biomass although the exploitation level increases - from 34 to 46.7%.

The anchovy stock-recruitment relationship was established by means of equations (1) and (2). The parameters in these equations are as follows:

(1) $R = 0.3008648*B*\exp(-0.000352155*B)$ $r = 0.714$

(2) $R = 0.3044772*B - 0.0000898145*B^2$ $r = 0.719$

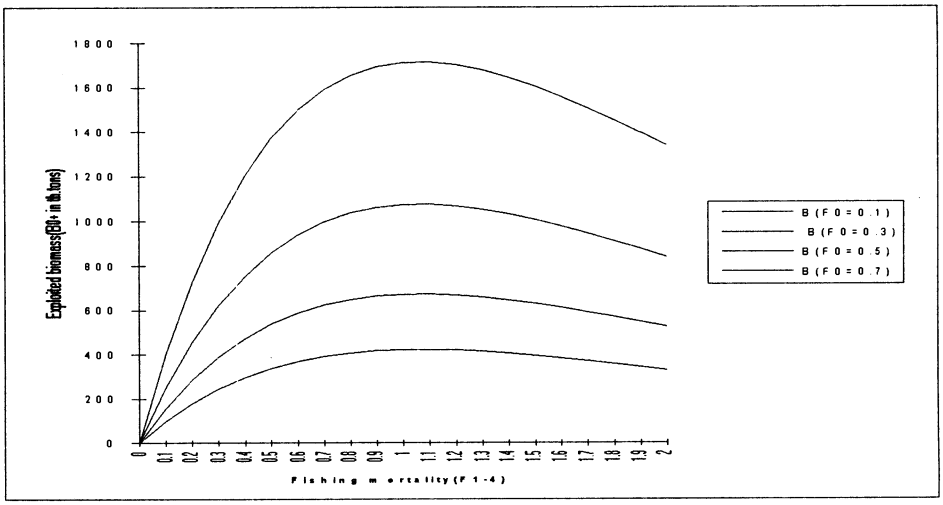


Figure 3. Anchovy exploited biomass (Âex) in dependence on the fishing mortality rate on the stock (F1+ - 4+) and recruitment (F0+)

According to equation (1), Bopt and Rmax are 2839.7 thousand tons and 314.3 x 10^9 specimens of 0+ old fishes, respectively. At F=0 for all age groups, the spawning biomass (Br) stabilizes when its biomass reaches 3402.0 thousand tons. This stock produces annually 308.0x10^9 0+ old fishes.

According to equation (2), Bopt and Rmax are 1694.6x10^3 tons and 258.05x10^9 specimens of 0+ old fishes. At F=0, the spawning biomass will stabilize when its biomass reaches 2380.0 thousand tons, that will annually produce 215.9x10^9 specimens of 0+ old fishes.

From these results, it can be concluded that up to the present, the anchovy spawning biomass has never reached its theoretically estimated level, since the real abundance of recruits was considerably lower, except those of 1979 year-class - 217.0x10^9 specimens. Besides, the estimates were accomplished at F=0 while in the reality the anchovy stock was subject of intensive commercial fishery. That is why the established equations, reflecting the relationship between anchovy exploited biomass

(Bex) and the fishing mortality rate (on the stock and recruitment, separately) and the spawning biomass (B) and recruitment was combined in a single generalised equation (6). Its parameters are as follows:

$$Bex = 2137.18*F_{(1+-4+)}*\exp [-1.21343*F_{(1+-4+)} - 1.23539*F_{0+} + 0.0008139*B + 0.003271*R], \quad r=0.975$$

This equation describes significantly the empirical data for anchovy biomass during the period 1967-1992. According to it Fopt is 0.82411. The annual catch that has to be realized by the given year depends on the concrete state of the anchovy exploited biomass. The last one depends on the spawning biomass and recruitment. The pointed biomasses as well as the catches depend on the level of fishing mortality on the stock and recruitment. The deduced equation shows that when the fishing mortality rate on the 0+ old fish increases the anchovy exploited biomass will begin to decrease. This will lead to reduction of the spawning biomass, because of which the recruitment will also decrease.

The mean number of recruits during the period 1978-1980 is 187.3×10^9 specimens of 0+ old fishes. During the same period the spawning biomass is at the average 624.2 thousand tons. According to equation (1) the pointed spawning biomass has to produce recruitments with abundance of 155.1×10^9 number of specimens. During the period under consideration the mean values for F(1+ - 4+) and F0+ are 0.4590 and 0.2667, respectively. For these values of the pointed fishing mortality coefficients the mean exploited biomass has to be 1116.0 thousand tons. In fact it had been 1238.0 thousand tons. The difference is due to the fact that the theoretically estimated abundance of recruitment is lower than that estimated by VPA. If the VPA value for R (187.3×10^9 numbers of specimens) is used, the exploited biomass would be 1239.9×10^3 tons.

During the period 1986-1988, i.e. slightly earlier than the mass development of the new species *M. leidyi*, the value of the above mentioned parameters had been as follows: R=103.5×10^9 numbers of specimens; B=429.6 thousand tons; F(1+ - 4+)=0.8331; F0+ = 0.5200. For these values Bex has to be at the average 678.3 thousand tons. In fact it had been 777.8 thousand tons. According to equation (1), at B=429.6 thousand tons the abundance of recruitment has to be 114.2×10^9 number of specimens. From the above facts, it becomes clear that the observed decrease in the exploited biomass of anchovy is nothing unusual. It is basically a result of the irrational manner in which the commercial fishery is operated, i.e. a sharp increase of fishing mortality coefficient towards the recruitment (from 0.2667 to 0.5200). The latest value has reached 0.6669 in 1989. During the same year, the other population parameters were as follows: F(1+ - 4+)=0.7534; B=188.1 thousand tons; R=63.1 x 10^9 numbers of specimens (R_t=54.1 x 10^9 numbers of specimens). For these values of the pointed parameters, Bex has to be 405.7 thousand tons. In fact the exploited biomass decreased to 389.6 thousand tons. The following decrease of the above mentioned biomass is mainly due to the reduced spawning biomass, found to materialise over the years as follows (in thousands of tons): 1990: 137.5; 1991: 173.2; 1992: 197.6; 1993: 172.1. According to equation (1), in correspondence with these

spawning biomass values, the produced recruitments would be as follows (number of specimens $x10^9$): 40.2 (40.2); 50.0 (50.7); 56.7 (39.5); 49.7 (54.6). In the brackets are shown the actual abundance of the corresponding year-classes. It is clear that, with the exception of 1992 year-class, the coincidence between theoretically expected abundance of recruitments and their actual values (in relation to VPA data) is very high. Hence, the series of low- abundance anchovy year-classes during the period 1988-1993 is due to the reduced spawning biomass. The decreasing of both exploited and spawning biomasses was conditioned by the irrational way of accomplishing the commercial fishery - too high catches of juvenile specimens. In our opinion, the sharp decline of the anchovy biomass, together with those of the other more abundant zooplanktivores (mainly the sprat and horse mackerel), can be one of the reasons for mass development of *M. leidyi* after 1988, since fish search much more actively their food compared to the medusae and ctenophores. In the created situation, the most troubling fact is the following: although it occurs in small quantities, ctenophores feed with eggs and larvae of spawning fishes. That is why the survival rate of new generations of fish would have to decrease when the ctenophore biomass is on rise. In this situation, the most rapid and effective way for recovering the anchovy stocks, despite the increased ctenophore biomass, is decreasing of the fishing effort on 0+ year old fishes.

3.2. BLACK SEA SPRAT

In Figure 4, we present the stock assessment for sprat, according to the different modifications of VPA, following the methods of Prodanov et al. (1994) (Fig. 5).

The observed cyclic recurrence in biomass dynamics argues for the stock sensitivity to natural environmental parameters. During certain times, the fishing effort can reinforce natural trends or can have dominant impact on the lowering of stocks. Since 1988, the sharp decline of sprat biomass was accompanied by fishing mortality increase in 1989 owing to the high fishing effort and catch in the sprat fishery of the former USSR. During 1989-1991, the *Mnemiopsis* biomass reached a maximum. To date, there is no direct evidence for ctenophore feeding on sprat larvae, so that it is difficult to assert this as a cause for the weak 1989-1991 year classes. Nevertheless, data available offshore, on vertical distribution during the cold season, coinciding with the spawning peak, and the seasonal maximum of *Mnemiopsis* biomass (27) are reasons to consider ctenophore feeding as a factor for negative changes in sprat stock.

Till now, the relations between plankton feeding invertebrates and fishes were regarded only one-way i.e. the former were pointed out as the reason for the stock decline of the latter. In our opinion the reverse is also possible: the lowering of fish stocks owing to the heavy and uncontrolled fishery could have resulted in a surplus of zooplankton that would favour the "outburst" of megaplankters.

In Table 1 we present the parameters in equation 3, reflecting the relationship between sprat offspring abundance and environmental factors. It is notable that the value of "r" does not exceed 0.712, which suggests a weak dependence of the offspring

abundance on investigated factors since the influence of random factors does not decrease below 49.3%.

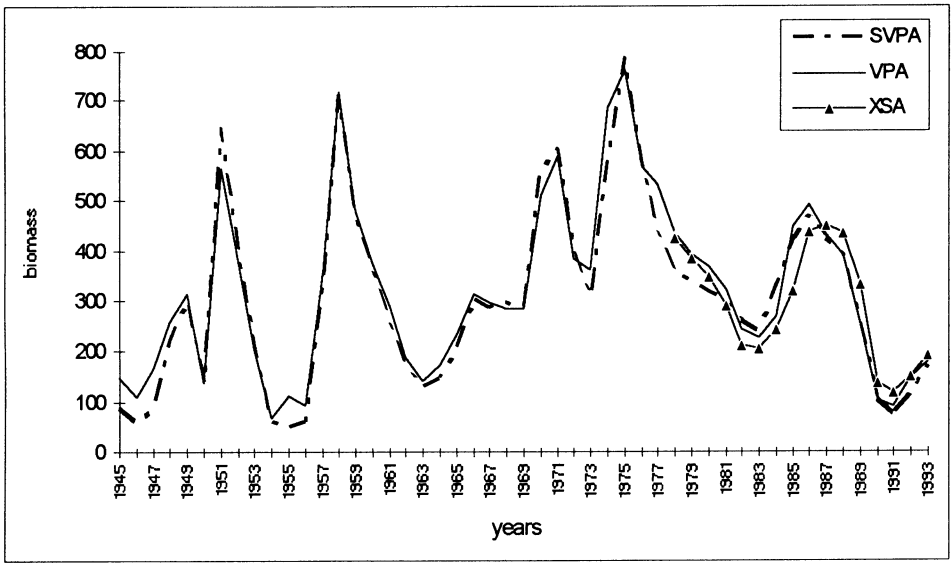


Figure 4. Sprat biomass (in tons) over the years obtained by three methods: Separable VPA (SVPA), VPA with *ad hoc* tuning (VPA) and Extended Survivor Analysis (XSA)

TABLE 1. Parameter values of equations reflecting the relationships between the abundance of sprat fingerlings and some environmental factors

Para-meters	R=f(B)	R=f(B, X1)	R=f(B, X2)	R=f(B, Z)	R=f(B,.. X3)	R=f(b,.. X4)	R=f(B,.. X5)	R=f(B,.. X6)
a								
b	0.0684	0.0721	0.0507	0.0670	-0.06473	-0.08325	-0.03402	-0.11140
c		-0.0073	-0.0045	-0.0043	0.04437	0.04914	0.05284	0.03108
d			-0.2217	-0.3274	-0.30074	-0.44648	-0.45368	-0.27971
e				-32.659	-24.0001	-28.5162	-27.0093	-25.3243
f					-1.30726	-1.22958	-1.67992	-1.36845
g						-3.67857	-5.60691	-5.67867
h							-0.12479	-0.14030
i								-190.610
r	0.137	0.144	0.207	0.323	0.667	0.683	0.687	0.712
D%	1.88	2.07	4.29	10.44	44.49	46.65	47.20	50.70
S%	98.02	97.93	95.71	89.56	55.51	53.35	52.80	49.30

R is abundance of sprat fingerlings ($N \times 10^3$); B - sprat spawning biomass (B1+); X1 - phytoplankton biomass; X2 - zooplankton biomass; Z - total mortality rate; X3 - sea water temperature; X4 - solar activity; X5 - cosmic rays intensity; X6 - Earth's geomagnetism

In Table 2 we present the values of the parameters reflecting the relationships between sprat offspring abundance along the Bulgarian coast and its spawning biomass (B1+), the fishing mortality rate (F), the duration (X1 and X3) and the average speed of winds

with an westerly component (X2 and X4) during November-December and January-March, the intensity of cosmic rays (X5) and solar activity (X6).

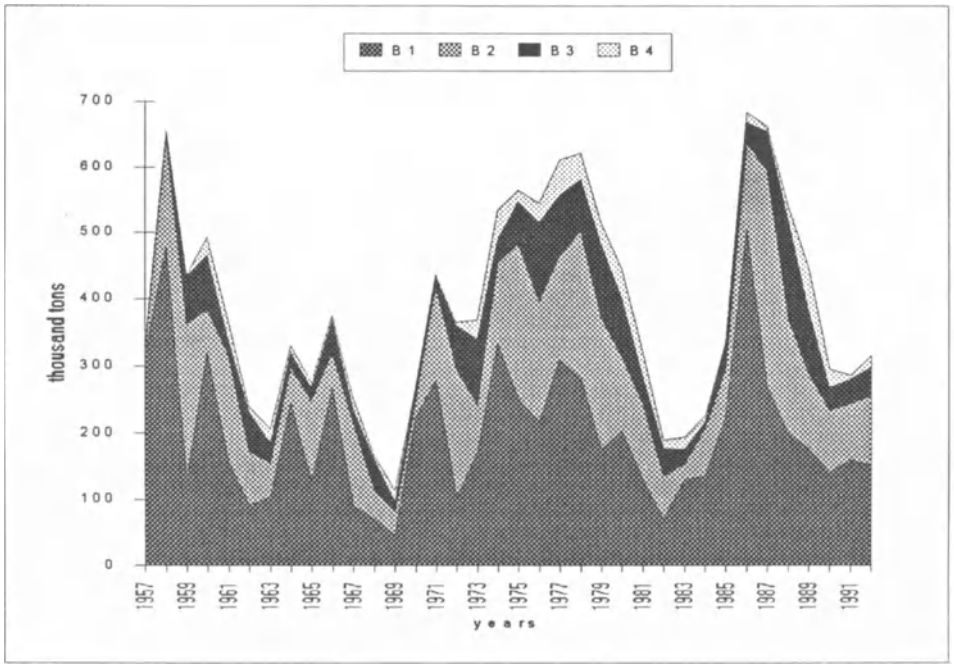


Figure 5. Sprat spawning biomass (by age groups) in the western part of the Black Sea during 1957-1992 (after Prodanov et al., (1994) [18])

It is evident from the Table 2 that the coefficient "r" reaches a value of 0.869, meaning that the influence of random factors is 24.53%. Among the examined variables, the westerly winds during November-December and January-March prove to be of greatest significance, i.e. when the sprat is intensively spawning at depths of 25-100m. This could be due to upwelling of deep waters and shoreward transport resulting from westerly winds, bringing waters rich in nutrients near the coast, which could contribute to summer phytoplankton blooms. Because of low temperature and 0_2 content, and possible H_2S content of the produced waters, they could be responsible for regional zoobenthic mortality including fish species. In winter, similar upwelling of deep waters take place, but unlike summer, they would be warmer than the surface waters.
In Table 2, the wind velocity is favourable, while its duration seems unfavourable. The integral impact of these variables on the sprat fingerling's abundance is considerable - the value of "r" is 0.843 (D% = 73.02; S% = 26.98). Further complexity introduced by the including the rest of the variables in the equation does not result in a significant increase in the value of "r", suggesting that the sprat fingerlings depend on some other factors. According to Stoyanov (1966), the sprat generations and spawning biomass depend both on the predator abundance and on the number of days with temperature of

TABLE 2. Parameter values in the equations reflecting the relationships between sprat fingerlings along Bulgarian Black Sea coast and the investigated environmental factors

Para-meters	R=f(X1)	R=f(X1,. X2)	R=f(X1,.. X3	R=f(X1,.X4	R=f(X1,. B)	R=f(X1,. F)	R=f(X1,.. X5)	R=f(X1,..X6)
a	41.979	-73.01	-55.89	-192.6	-187.076	-152.426	-153.762	75.698
b	-0.0005	-0.068	-0.065	-0.021	-0.0185	-0.0210	-0.0209	-0.0171
c		16.296	15.527	8.7793	8.0138	7.9136	7.9090	4.1665
d			-0.023	-0.065	-0.0551	-0.0526	-0.0522	-0.0624
e				21.313	20.1659	17.9572	17.9165	21.688
f					0.0485	-0.0079	-0.0083	0.0935
g						-39.2660	-39.1342	-14.487
h							0.0004	-0.0520
i								-0.2607
r	0.107	0.543	0.558	0.843	0.845	0.855	0.855	0.869
D%	1.14	29.46	31.12	71.02	71.41	73.02	73.02	75.47
S%	98.86	70.54	68.88	28.98	28.59	26.98	26.98	24.53

B is the spawning biomass; F is the fishing mortality rate; X_1 and X_3; X_2 and X_4 are the duration and the average speed of winds with an western component during November-December and January-March, respectively; X_5 is the intensity of cosmic rays; X_6 is solar activity.

TABLE 3. Multiple regression analysis of sprat recruitment (indep. variable) and environmental data (dep. variables)

A			B		
Multiple R	0.8792		Multiple R	0.9839	
R square	0.7729		R square	0.9680	
Obser-vations	27		Obser-vations	17	
	Coefficients	P value		Coeffcients	P value
Intercept	202.75	0.3872	Intercept	-57.278	0.0639
X_1	-5.8377	0.6795	X_1	-0.0200	0.1689
X_2	-0.0846	0.5758	X_2	-0.1322	0.1609
X_3	-2.3786	0.4748	X_3	-0.1159	0.0158
X_4	-0.4639	0.0051	X_4	1.6002	0.0075
X_5	-0.0381	0.0833	X_5	0.8100	0.0001
X_6	0.3934	0.0002	X_6	-0.1485	0.2001
			X_7	-3.3435	0.0005
			X_8	0.8561	0.0001

A: X1 - sea surface temperature mesured in Batumi bay , X2 - river outflow in the North Western part of the Black Sea , X3 - total phosphorus amount in the Danube river delta (Vilkovo), X4 - zooplankton biomass in Western part of the Black Sea , X5 - phytoplankton biomass in Western part of the Black Sea , X6 - sprat parental stock biomass;

B:X1 - phytoplankton biomass in Western part of the Black Sea, X2 - zooplankton biomass in Western part of the Black Sea, X3 - horse mackerel parental stock biomass; X4 - whiting recruitment, X5 - whiting parental stock biomass, X6 - dog-fish parental stock biomass, X7 - turbot parental stock biomass, X8 - sprat parental stock biomass.

the water below 6°C during November - March. The same author pointed out that the influence of water temperature is indirect, via the food web. Bryantzev (1990) showed the great importance of annual atmospheric circulation characteristics on the productivity of the Black Sea, and noted that this relation is better expressed in anchovy and less in sprat.

Table 3 shows the results of multiple regression analysis including the important factors for sprat offspring abundance, which is seen to be only directly proportional to

spawning stock size and inversely proportional to the thermal background, the river inflow, phosphates, and phyto- and zooplankton biomass in the western Black Sea.

3.3. BLACK SEA WHITING

Figure 6 presents the results for whiting biomass in the western part of the Black Sea according to VPA with tuning of the Fst values for the oldest age group. It is found that the whiting biomass has ranged between 44.5 to 181.2 thousand tons. After 1984 its biomass began to decrease and nowadays it is about 50-60 thousand tons.

In Figure 7, presenting the results for the whiting biomass in the eastern part of the Black Sea, it is seen that the whiting biomass has ranged from 73.0 (1990)- 73.9 (1989) to 489.3 (1978) thousand tons. The fluctuations in the biomass of the eastern population coincide with those of the western population, but the former had higher absolute values (about two fold). The differences between the whiting biomasses in the eastern and western parts of the Black Sea are primarily due to the heavier weights, and lengths, of the fish from the eastern part of the basin. The whiting weights by age groups in the two areas are given in Table 4.

In Figure 8 are shown the VPA data for 0+ year-old fish abundance and that from trawl surveys carried out by YugNIRO, usually in May. The assessment of the total 0+ year fish abundance, performed by the two methods had similar trends, and did not differ substantially in their absolute values. Relatively higher differences were detected for the areas, primarily in 1982, since the results from ichthyoplankton survey showed that the recruitment abundance in the western and the eastern parts of the basin were 5.3 and 14.1 x 10^9 specimens respectively; overall value being 19.4 x 10^9 specimens, and from VPA: 13.0 and 3.6, total 16.6 x 10^9 specimens. Despite these differences, there is good coincidence, especially on the the total recruitment abundance in the entire Black Sea.

The impact of fishing mortality rate on the whiting fingerling abundance is established by equations (6) and (7) - Table 5. It is evident from the data that the fishing mortality rate exerts a significant impact on stock-recruitment relationships. The influence of random factors decreased from 68.09% (according to Ivanov's equation) to 36.6%.

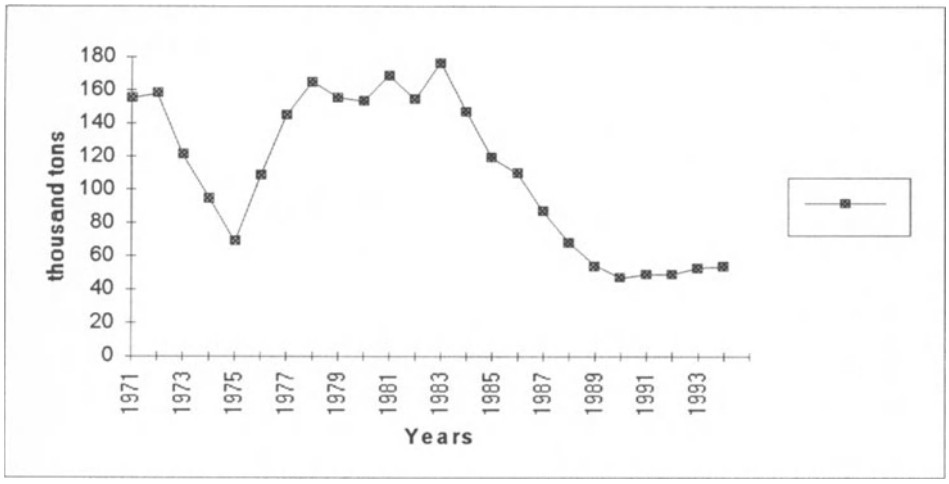


Figure 6. Whiting biomass (B_{1+} in th. tons) in the western part of the Black Sea

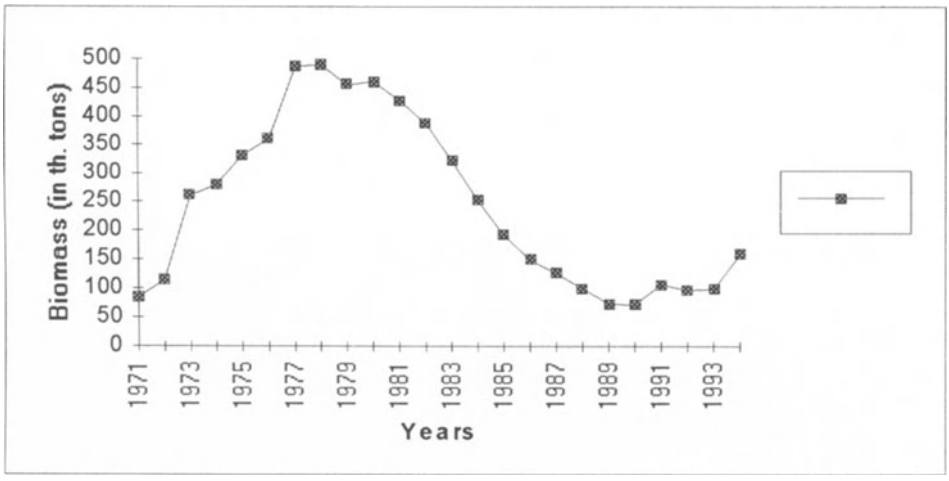


Figure 7. Whiting biomass (B1+ in th. tons) in the eastern part of the Black Sea

The results of the multiple regression analysis in Table 6 reflect the relationship between the whiting offspring abundance and the environmental factors in the Black Sea. The abundance is in direct proportion to river inflow and inversely proportional to phosphate concentration, zooplankton biomass and the spawning biomass. The last probably is due to the fact that cannibalism occurs in whiting.

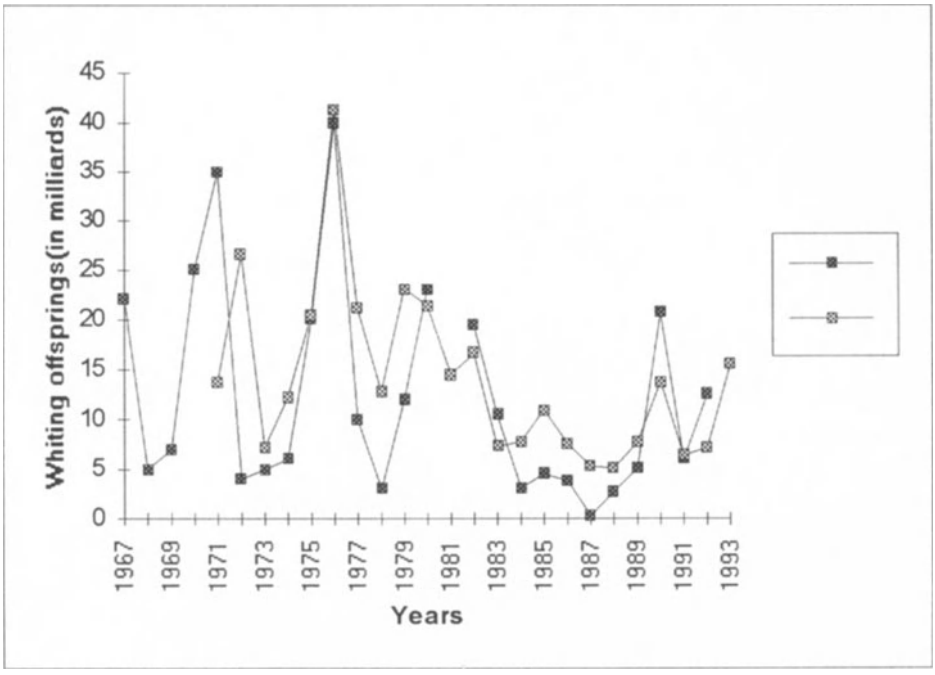


Figure 8. Number of whiting offsprings (in milliards) in the Black Sea during the period 1967-1993 (red-ichthyoplankton surveys; green- VPA)

TABLE 4. Weigths by age groups of whiting

Age	Eastern Black Sea W (g)	Western Black Sea W (g)
0+	4.0	4.2
1	12.8	11.6
2	23.4	21.4
3	44.4	33.7
4	71.7	48.2
5	104.2	63.3
6	140.9	79.2
7	180.2	
8	222.0	

TABLE 5. The parameter values in equations (6) and (7) reflecting the influence of fishing mortality rate on the stock-recruitment of whiting in the western part of the Black Sea

Equa-tions	a	b	c	d	r	D%	S%	Bopt	Rmax
6	1.1356	0.0041	1.4732		0.771	59.47	40.53	139.8	79.4
7	1.1082	0.0035	0.9109	0.009	0 796	63.40	36.60	158.0	87.5

TABLE 6. Multiple regression analysis of whiting recruitment (indep. variable) and environmental data (dep. variables)

A			B		
Multiple R	0.8511		Multiple R	0.9839	
R square	0.7243		R square	0.9680	
Obser-vations	16		Obser-vations	17	
	Coefficients	P value		Coeffcients	P value
Intercept	-7.6003	0.1514	Intercept	8.0037	0.3035
X_1	0.1054	0.0001	X_1	0.0544	0.3631
X_2	-0.3965	0.4120	X_2	0.0149	0.5123
X_3	-0.0553	0.0229	X_3	-0.0518	0.3456
X_4	-0.0652	0.0444	X_4	-0.1949	0.0036
			X_5	-0.0398	0.0234
			X_6	-0.0242	0.1504
			X_7	-0.0305	0.0725
			X_8	0.1255	0.0014
			X_9	1.2116	0.0031

A: X1 - sea surface temperature mesured in Batumi bay , X2 - river outflow in the North Western part of the Black Sea , X3 - total phosphorus amount in the Danube river delta (Vilkovo), X4 - zooplankton biomass in Western part of the Black Sea , X5- phytoplankton biomass in Western part of the Black Sea , X6 - sprat parental stock biomass; B: X1 - phytoplankton biomass in Western part of the Black Sea, X2 - zooplankton biomass in Western part of the Black Sea, X3 - horse mackerel parental stock biomass; X4 - whiting recruitment, X5 - whiting parental stock biomass, X6 - dog-fish parental stock biomass, X7 - turbot parental stock biomass, X8 - sprat parental stock biomass.

3.4. BLACK SEA HORSE MACKEREL

The results of VPA for the dynamic of horse mackerel biomass in Figure 9 show that both the total and spawning biomasses during the period of consideration, varied widely, owing to the different strengths of the new year classes. The latter have ranged during the period 1950 - 1959 from 1420.27 x 10^6 (1959) to 5891.19 x 10^6 (1957) specimens. During the same period the total (B0+) and spawning (B2+) biomasses have respectively ranged from 54.7 (1950) to 129.3 (1953) thousand tons and from 12.3 (1950) to 54.1 (1953) thousand tons. In the next decade (1960 - 1969) these biomasses have respectively varied from 76.6 (1964) to 267.9 (1969) and from 29.9 (1965) to 96.3 (1967) thousand tons. It is clear that there is no coincidence between the total and the spawning biomasses which is due to the increased fluctuation in the strength of the year classes. For instance the size of the total biomass in 1969 was determined by the strong 1969 year class - 27443.83 x 10^6 specimens. During the next three years, the new year classes were weak, especially that of 1971 amounting to 833.12 x 10^6 specimens, as a result of which the total stocks have declined from 303.2 (1970) to 181.0 (1973) thousand tons. Subsequently, they increased up to 332.3 (1978) thousand tons. In the late 1970's and the beginning of the 1980's (1982 included) the total biomass have ranged from 235.7 (1980) to 337.3 (1982) thousand tons. In 1983 and 1984, the biomass grew up to 650.4 and 689.7 thousand tons, the reason being the very strong successive 1983 and 1984 year classes, especially the first one, with the

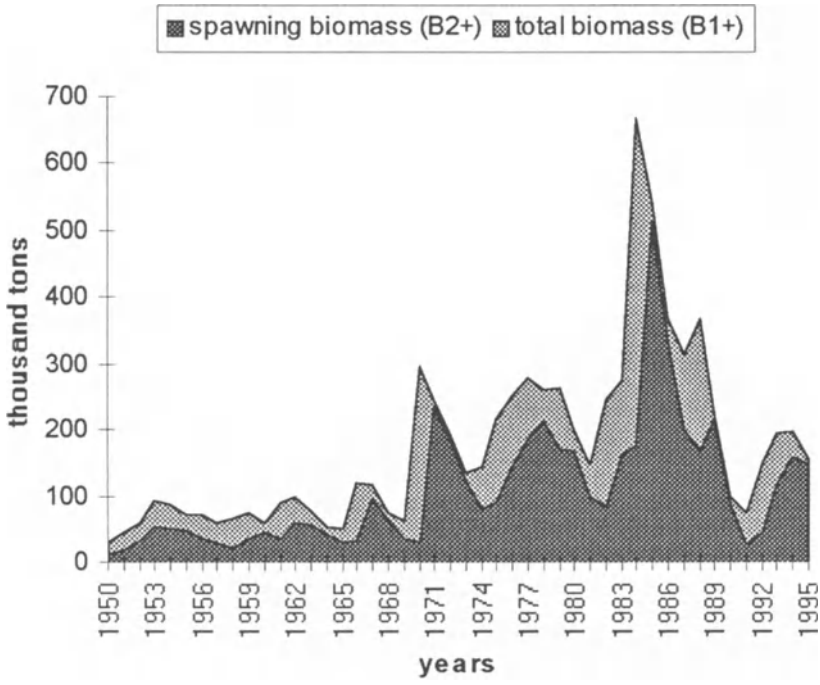


Figure 9. Horse mackerel spawning and exploited biomasses in the Black Sea during the period 1950-1994

extreme value of 50195.58 x 10^6 specimens. However, the next two year classes (1985 and 1986) were weak, resulting in the decline of the total biomass as a result of the rise of the spawning biomass that reached its maximum value in 1985 of 514.7 thousand tons. The successive 1986 - 1987 year classes were relatively strong (on the average) and the total and spawning biomasses remained comparatively high - 456.9 - 471.1 and 313.3 - 200.1 thousand tons, respectively. Weak successive 1988-1989 year classes - 1609.90 x 10^6 and 1333.96 x 10^6 specimens caused the sharp decline to the total and spawning biomasses - 136.1-154.5 and 87.0-26.9 thousand tons in 1990 and 1991, respectively. The 1991-1993 year classes varied among 4153.80 x 10^6 (1993) and 10641.33 x 10^6 (1991), as a result of which, the total and the spawning biomasses increased to 224.6 and 115.2 (1991) thousand tons, respectively. The last 1994 year class was very weak - 1106.3 x 10^6 numbers of specimens. As it was noted the estimation of the year - class strength during the last 1-2 years, is quite difficult and the errors are perhaps the largest. Nevertheless the spawning biomass would remain at the level of 1994 and even it would be lower from 157.4 to 145.9 thousand tons. If the estimated abundance of 1994 year class does not differ seriously from the real one it can be expected that the exploited stock (B1+) would continue to reduce from 197.9 to 156.5 thousand tons. As it was pointed out the accuracy of the assessments depends exclusively on the fishery statistics data. Therefore, the lack of information for the horse mackerel catches or its understatement by Russia, Ukraine, Georgia, Roumania

and Bulgaria enhances the risk of incorrect assessment of its biomass. For example according to the Turkish data, the catches in 1994 were threefold higher than in 1993.

The Turkish catches of horse mackerel, as it was the case with the anchovy catches, are taken primarily in winter, when the species has almost sedentary pattern of life and forms dense concentrations in the wintering grounds. This makes the fishery more effective and raises the possibilities to harvest larger amounts of fish, despite the fixed stock size.

The improvement in fishing gears and the application of modern echo acoustics have further contributed to a more effective fishery, and has an immediate effect on the fishing mortality. When the level of the horse mackerel stock was low, even small catches caused higher fish mortality and vice versa. For example, during 1956-1958, the catches varied between 17.370 and 29.735, on average 24.675 thousand tons and the mean value of F_{2-6} - from 0.7022 to 0.8929, with an average of 0.7271. In the 1985-1988 period when the species biomass was high, the catches of the order of 93.741 - 141.078 thousand tons caused fishing mortality in the range of 0.2867-0.4367, with an average of 0.3373. All of this stresses the necessity for stock size assessments and of TAC to be made every year, as well as for clarifying the causes (natural and anthropogenic) determining the fluctuations in the year - class strength. This is of vital importance, as in most cases, the spawning biomass of fish species concerned have less effect on the recruitment than the environment, especially after the eutrophication of the basin and the invasion of a number of new species, the greatest impact among them being made by the ctenophore Mnemiopsis. It is not unlikely that at present, the new species experience a time of adaptation to the current environmental conditions, and after some years they may not cause population outburst that could further disrupt the balance the Black Sea ecosystem is striving for.

4. Conclusions

The abundance of the different year-classes of the fish species in consideration depends on many abiotic and biotic factors. The determinants for the fish part of the ecosystem are the fishing mortality rate and the changes in the food web, due to the mass development of *Mnemiopsis leidyi* and the more frequent phytoplankton blooms provoked by the eutrophication of the basin.

In the cases of anchovy, and partially in horse mackerel and sprat, the first factor has decisive importance in lowering of the biomass. The first two fish species reproduce in the summer months in almost the whole Black Sea aquatory. During these months the *Mnemiopsis* biomass is highest, because of this its negative impact being the highest. This ctenophore mainly inhabits waters above the thermocline, i.e. where the eggs and larvae of anchovy and horse mackerel are developing. As previously pointed out, the latter can serve as food for *Mnemiopsis leidyi*, although in small quantities, which would thus exert direct influence on their abundance. The observed decline in the small zooplankton (Copepod) in summer months also lowers the survival of the larvae and alevins of the two species. All of this ultimately caused the dramatic

decline in the anchovy stock in 1990 and 1991. The reduced fishing mortality during the next years is the major reason for the positive trends toward increase of its biomass.

The reasons for the depletion of sprat biomass in the western part of the basin after 1987-1988 have complex character. On the one hand, the environmental conditions deteriorate, and on the other hand, the fishing mortality increases. This imbalance inevitably leads to the depletion of the heavily fished stocks. In such cases the best approach is to reduce the fishing mortality, which would enable the relevant species to overcome the unfavourable conditions, leading to their improvement [17]. The sprat spawns in almost the entire Black Sea aquatory, which allows it to adequately utilise the trophic potential of the basin. After reducing of the fishing effort its stocks have shown a rising trend. Similar trend is observed concerning the stocks of whiting and especially that of the shad. In the case of turbot, spiny dogfish, and Russian sturgeon, the situation is much more complicated, since their catches are highly underestimated. Furthermore the regulation measures prohibiting the catch of immature fish are not observed, primarily in the case of turbot and Russian sturgeon. The depletion of the mullet stocks is determined by decrease in surface area of the nearshore lakes and their industrial pollution, practically concerning all Black Sea countries.

5. References

1. Berenheim, D.Ya. (1960) Changes in the Azov and Black Sea water levels and river inflow. Proc. of Aztcher NIRO **18**, 3-20 (in Russian).
2. Eremeev, V.N., Chudinovski, T.V. (1990) Hydrobiology of the Black Sea. Applied Ecology of Sea Regions. The Black Sea, Kiev, 57-106. (in Russian).
3. Ivanov, L.S. (1977) A symmetrical reproduction curve in fish population studies. Proceedings of the Institute of Fisheries-Varna, XV, 1-15 (in Bulgarian)
4. Ivanov, L.S., Beverton, R.J.H. (1985) The fisheries resources of the Mediterranean. Part two: Black Sea. FAO Studies and reviews **60**: 135 pp.
5. Ivanov, L.S., Mikhailov, K. (1991) On the relation between catch, stock and production of the Black Sea anchovy (*Engraulis encrasicolus* Aleksandrov). Oceanology, Sofia **20**, 16-25. (in Bulgarian).
6. Johannesson, K.A., Loose, G.F. (1977) Methodology of acoustic estimations of fish abundance in some UNDP/FAO resources survey projects. Rapp. Proc.-Verbau des Reun. CIEM **170**: 296-318.
7. Konsulov, A., Konsulova, Tz. (1993) Biodiversity on the Black Sea plankton and benthos. National Biological Diversity Conservation Strategy, Sofia, 473-514. (in Bulgarian and Inglish).
8. Kutty, M.K., Quasim, G.Z. (1965) The estimation of optimum age of exploitation and potential yield in fish populations. J. Cons., Int. Explor. Mer.**32**, No 22: 191-202.
9. Moncheva, S. (1991) Eutrophication /phytoplankton blooms/ hypxia. International workshop on the Black Sea, Varna, 30.09-04.10.1991.
10. Moncheva, S. (1991) Ecology of common Black Sea phytoplankton species under the influence of anthropogenic eutrophication. Ph.D thesis. (in Bulgarian).
11. Moncheva, S., Petrova-Karadjova, V., Palasov, A. (1993) Harmful algal blooms along the Bulgarian Black Sea coast and associates fish and zoobenthothic mortalities. Proc. of 6th Int. conf. toxic marine phytoplankton, 18-22 Oct. 1993, Nant, France.
12. Pauly, D. (1980) On the interrelation between natural mortality growth parameters and mean environmental temperature in 175 fish stocks. J. Cons. CIEM, **39** (2), 175-192.
13. Peterson, I., Wroblevski, J.J. (1984) Mortality rate of fishes in the pelagic ecosystem. Can. J. Fish. Aquat. Sci., **41**: 1117-1120.
14. Petrova-Karadjova, V.J., Apostolov, E.M. (1988) Influence of solar activity upon the diatoms of Black Sea plankton. Rapp. et Proces-Verbaux des Reunions, CIESM 31, 2.
15. Petrova-Karadjova, V.J. (1992) Solar control upon the phytoplankton in the Black Sea. Rapp. et Proces-Verbaux des Reunions, CIESM 33, 265.

16. Pope, J.G., Shephered, J.G. (1982) A simple method for consistent interpretation of catch-at-age data. J. Cons. Int. Explor. Mer. **40**: 176-184.
17. Prodanov, K. (1989) On the problem of determining the optimum value of fishing mortality coefficient (Fopt) and total allowable catch (TAC). Hydrobiology, Sofia **34**, 79-90.
18. Prodanov, K., Mikhailov, K., Daskalov, G., Maxim, K., Chashchin, A., Arkhipov, A., Shlyakhov, V., Ozdamar, E. (1994) Stock assessment of sprat (*Sprattus sprattus* L.) and whiting (*Merlangius merlangus euxinus* Nordmann) in the western part of Black Sea and Bulgarian Black Sea coast during 1957-1992 in relation to some natural and anthropogenic factors. First International CEOS meeting. Monterey, 05-09. 1994, USA (in press).
19. Rass, T.S. (1987) Present notions about taxonomic composition and changes in ichthiophauna of the Black Sea. Vopr. Ichthyol. **27**, No 2 ,179-187. (in Russian).
20. Ricker, W.E. (1979) Computation and Interpratation of Biological Statistics of Fish Populations, pp 408 (in Russian).
21. Shepherd, J.G. (1994) Extended survivors analysis: an improved method for the analysis of catch-at-age data and CPUE data. ICES W.P. 22 pp. (mimeo).
22. Shepherd, J.G., Darby, C.D. Combination of recruit indices by weighted averages using RTC3: A user's guide MAFF Direct. Fish. Res., Lowestoft. (in press - personal communication).
23. Shlyakhov, V.A., Chashchin, A., Korkosh, N.I. (1990) Fishing intensity and dynamics of the Black Sea anchovy stock. Coll. reprint of VNIRO, 80-92. (in Russian).
24. Sorokin, Yu.I. (1982) The Black Sea : Nature, Resources, Nauka, Moscow, 216 pp. In Russian.
25. Sparre, P. (1987) Computer programs for fish stock assessment. FAO Fisheries Technical Paper 101, Suppl. 2.
26. Teylor, C.C. (1959) Temperature and growth. J. Conseil Explor. Mer. **25(1)**, 93-101.
27. Vinogradov, M.E., Shushkina, E.A., Musaeva, E.I., Sorokolit, P.Yu. (1989) Ctenophore Mnemiopsis leidyi (A.Agassis) (Ctenophora: Lobata) - new setlers in the Black Sea. Oceanology, Acad.Sci. USSR **29 (2)**, 293-299. (in Russian).
28. Vinogradov, M.E., Sapozhnikov, V.V., Shushkina, E.A. (1992) The Black Sea Ecosystem, 110 pp. (in Russian).
29. Zaika, V.E and Sergeeva, N.G. (1991) Diural variations in populations structure and vertical distribution of jellyfishes Mnemiopsis mcCradyi Mayer (Ctenophora) in the Black Sea. Gidrobiol. Journal **27**, No 2, 15-19. (in Russian).
30. Zaitzev, Yu.P. (1993) Impacts of eutrophication on the Black Sea fauna. In Fisheries and environmental studies in the Black Sea system, pp.63-85 FAO Studies and reviews,

VARIATIONS IN THE VERTICAL STRUCTURE OF WATER CHEMISTRY WITHIN THE THREE HYDRODYNAMICALLY DIFFERENT REGIONS OF THE BLACK SEA

ÖZDEN BAŞTÜRK[1], SÜLEYMAN TUĞRUL[1],
SERGEI KONOVALOV[2] AND İLKAY SALİHOĞLU[1]
[1]*Institute of Marine Sciences (IMS), P.K. 28,*
33731 Erdemli, İçel, Turkey
[2] *Marine Hydrophysical Institute (MHI), Ukraine*

Abstract. High-resolution, basin-wide chemical data reveal that the Black Sea upper layer possesses distinct chemical features at specific density surfaces, but with some noticeable regional differences in their positions and magnitudes. The nitracline, is consistently established at smaller density surface relative to the phosphocline over the basin; thus, N:P molar ratios appear to be unexpectedly high (40-80) within the upper nutricline, especially in the anticyclonic regions (ACR). The ratio drops to levels of 4-8 at the nitrate maxima formed within the base of the main oxycline. Phosphate profiles display a prominent minimum within the suboxic zone of the cyclonic regions (CR), which weakens markedly within the coastal regions and rim current. Vertical distributions of chemical ratios have led to valuable information on the relative fluxes in the oxic/anoxic transition zone as well as the quality of data sets from different years.

1. Introduction

The Black Sea ecosystem has been dramatically modified by various factors since the 70's [1]. Though the changes in the biological components of the ecosystem are well documented [2,3,4], those of the chemical properties are still poorly understood, due to a lack of high-quality and high-resolution data in the historical data base. Nevertheless, comparison of combined data relative to water density, rather than depth, has permitted us to minimize regional variations due to appearance of similar hydrographic features at different depths. Density dependent chemical profiles have been shown to be more informative in collating basin-wide data sets [5,6,7,8,9] and thus in defining possible long-term changes in the vertical chemistry of the Black Sea. However, the chemocline boundaries and magnitude of the characteristic chemical features in the Black Sea are most probably subject to noticeable regional and seasonal variations, which partly limit the reliability of long-term changes to be inferred from

E. Özsoy and A. Mikaelyan (eds.), Sensitivity to Change: Black Sea, Baltic Sea and North Sea, 183–196.
© 1997 *Kluwer Academic Publishers.*

basin-wide composite profiles. With this goal, the present report discusses the density-dependent chemical profiles from hydrodynamically different regions in detail, based on the data collected in September 1991, and those collected by the June-July 1988 cruise of R/V Knorr, and the April 1969 cruise of R/V Atlantis.

2. Materials and Methods

Water samples were collected from the locations listed in Table 1, either by a rosette or by Nansen bottle casts at selected depths and/or density surfaces. In September 1991, chemical measurements were carried out on board the R/V Bilim (IMS-Turkey) and R/V Prof. Kolesnikov (MHI-Ukraine); nutrients by a two channel Technicon Autoanalyzer or manual colorimetric methods whereas dissolved oxygen (DO) and hydrogen sulphide (H_2S) with the modified iodometric titrations in sample bottles (flushed with argon). Physical data were collected *in situ* by a Sea-Bird Model-9 CTD probe. The Knorr-88 and Atlantis-69 data were obtained from the technical reports [9,10].

Table 1. The station names and coordinates used in the text for three different regions of the Black Sea and different cruises.

CYCLONIC GYRE	ANTICYCLONIC EDDY	RIM CURRENT
Station. Latitude Longitude	Station. Latitude Longitude	Station. Latitude Longitude
R/V BILIM - 1991		
N30N45 43°30'N 31°45'E	L50Y15 41°50'E 40°15'E	L30W45 41°30'N 38°45'E
M50T45 42°50'N 36°45'E	L15Y15 41°15'E 40°15'E	L30W15 41°30'N 38°15'E
M10V15 42°10'N 37°15'E	L30X45 41°30'E 39°45'E	L15W15 41°15'N 38°15'E
M50P45 42°50'N 32°45'E	L30Y50 41°30'E 40°50'E	L32M13 41°32'N 30°13'E
M50N45 42°50'N 31°45'E	L30Y15 41°30'E 40°15'E	L30V45 41°30'N 37°45'E
M30N45 42°30'N 31°45'E	M10X45 42°10'E 39°45'E	L31V22 41°31'N 37°22'E
M30P15 42°30'N 32°15'E	L30X15 41°30'E 39°15'E	M19R45 42°19'N 37°45'E
N10R45 43°10'N 34°45'E	L50X15 41°50'E 39°15'E	L45T45 41°45'N 36°45'E
R/V PROF. KOLESNIKOV - 1991		
N30N45 43° 30'N 31° 45'E	L50Z15 41°50'E 41°15'E	N30X15 43°30'N 39°15'E
N30P15 43° 30'N 32° 15'E	M10Y15 42°10'E 40°15'E	P10T45 44°10'N 36°45'E
N30V45 43° 30'N 37° 45'E	M10X45 42°10'E 39°45'E	
N50N15 43° 50'N 31° 15'E	M50Y45 42°50'E 40°45'E	
N30N15 43° 30'N 31° 15'E	M30Z15 42°30'E 41°15'E	
R/V KNORR - 1988		
CR4-0903 41°52'N 31°18'E	CR4-1907 41°31'N 40°45'E	CR3-0308 41°35'N 32°00'E
R/V ATLANTIS - 1969		
1444 43°49'N 31° 41'N	1468 42°00'N 40°00'E	1431 42°10'N 33°00'E
1442 44°45'N 31° 58'E	1469 41°24'N 40°41'E	1438 41°58'N 35°40'E
1446 42°13'N 31° 29'E	1470 42°02'N 41°18'E	1440 42°12'N 34°21'E
1445 43°08'N 31° 27'E	1477 41°34'N 39°03'E	1447 41°22'N 30°59'E

3. Regional Variations in the Physical Properties

The physical oceanography of the Black Sea upper layer extending down to the anoxic waters is principally determined by cyclonic, anticyclonic type of circulations and boundary rim currents over the deep basin. Boundaries of the areas dominated by these

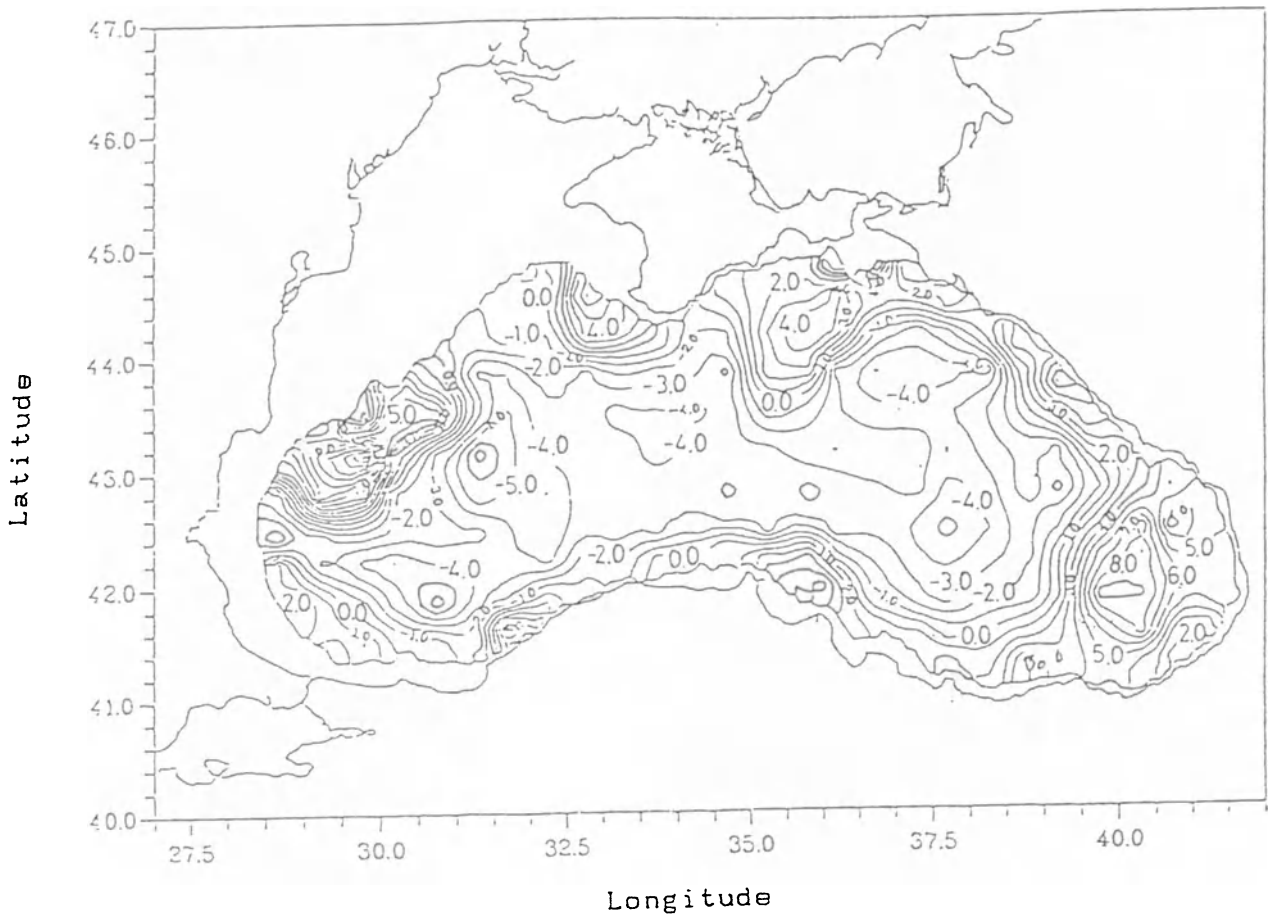


Figure 1. Dynamic height anomalies in cm at 100 Dbar level relative to 900 Dbar level in September 1991

circulations can be defined by dynamic height (DH, in cm) anomalies derived from basin-wide hydrographic data [11]. In the cyclonically dominated regions (CR), DH was <-3 whereas the areas with DH>+5 were called the anticyclonic regions (ACR). In the rim current frontal zone (RCFZ), DH ranged from -2 to +2 [11] for September 1991. During this period, two cyclonic gyres, separated from the anticyclonic eddies in the coastal zone by the cyclonically undulating rim current [8], were established quasi-permanently in the interiors of the eastern and western basins of the Black Sea (Fig. 1).

Figure 2 shows composite depth profiles of θ, S and σ_θ in upper layers of CR, ACR and RCFZ. It appears that the surface water density (σ_θ) is determined mainly by temperature during the stratification period. Below the seasonal thermocline, its change with depth is principally controlled by salinity due to the establishment of a permanent halocline in the upper layer. In this zone, there existed a nearly isohaline and relatively cool isothermal water mass of some 10 meters thick within ACR which became much thinner in CR (Fig. 2). The boundaries of this layer also determine the thickness of the Cold Intermediate Layer (CIL) defined by the upper and lower 8 ^{o}C isothermals [12,13]. Composite profiles of θ, S and σ_θ in CR display similarities below 35-40m, whereas those from ACR possess remarkable spatial differences down to at least 200 meters and those from RCFZ resemble the profiles of CR below 70-80 meters. The Brunt-Väisälä frequency was reported to be minimum at the depth of the σ_θ=14.7 and reached to maximum below σ_θ=14.8 surface which defines not only the approximate base of CIL but also the upper boundary of the permanent pycnocline [14,15]. Thus, the Black Sea surface layer may be homogenized down to the σ_θ=14.7-14.8 surfaces by convective mixing processes in winter as also supported by late winter data.

4. Regional Variations in the Chemical Properties

Density dependent composite profiles of DO and H_2S, and nutrients ($P0_4$, $N0_3$+$N0_2$=TNOx and Si) for the CR, ACR and RCFZ of the Black Sea, displayed in Figures 3-4, indicate similar vertical features in the upper layer as emphasized in recent studies [7,9,16]. However, detailed examination of these profiles has led to the recognition of noticeable and distinct regional differences both in the position and magnitude of the characteristic features inherent to the Black Sea.

Dissolved Oxygen (DO): Composite profiles of DO from the pre-defined three regions (Fig. 3) for September 1991 indicate that the upper mixed layer have possessed nearly saturated levels of DO (250-350 μM), below which the concentrations decreased steeply to 20-30 μM levels at the 15.4-15.5 density surfaces. However, regional profiles revealed that the oxycline onset appeared at greater density surfaces (σ_θ=14.4-14.5) in CR compared to those in ACR and RCFZ (σ_θ=14.2-14.3). The depletion rate of DO in the oxycline appeared to be much higher in CR (7.94 μM/m) than in ACR (3.57 μM/m) and in RCFZ (4.60 μM/m), due to the regional variations in the thicknesses of CIL coinciding with the oxycline. Below the main oxycline, the DO values decline slowly from 20-30 μM at σ_θ=15.4-15.5 surfaces to <5 μM at σ_θ=15.9-16.0, yielding

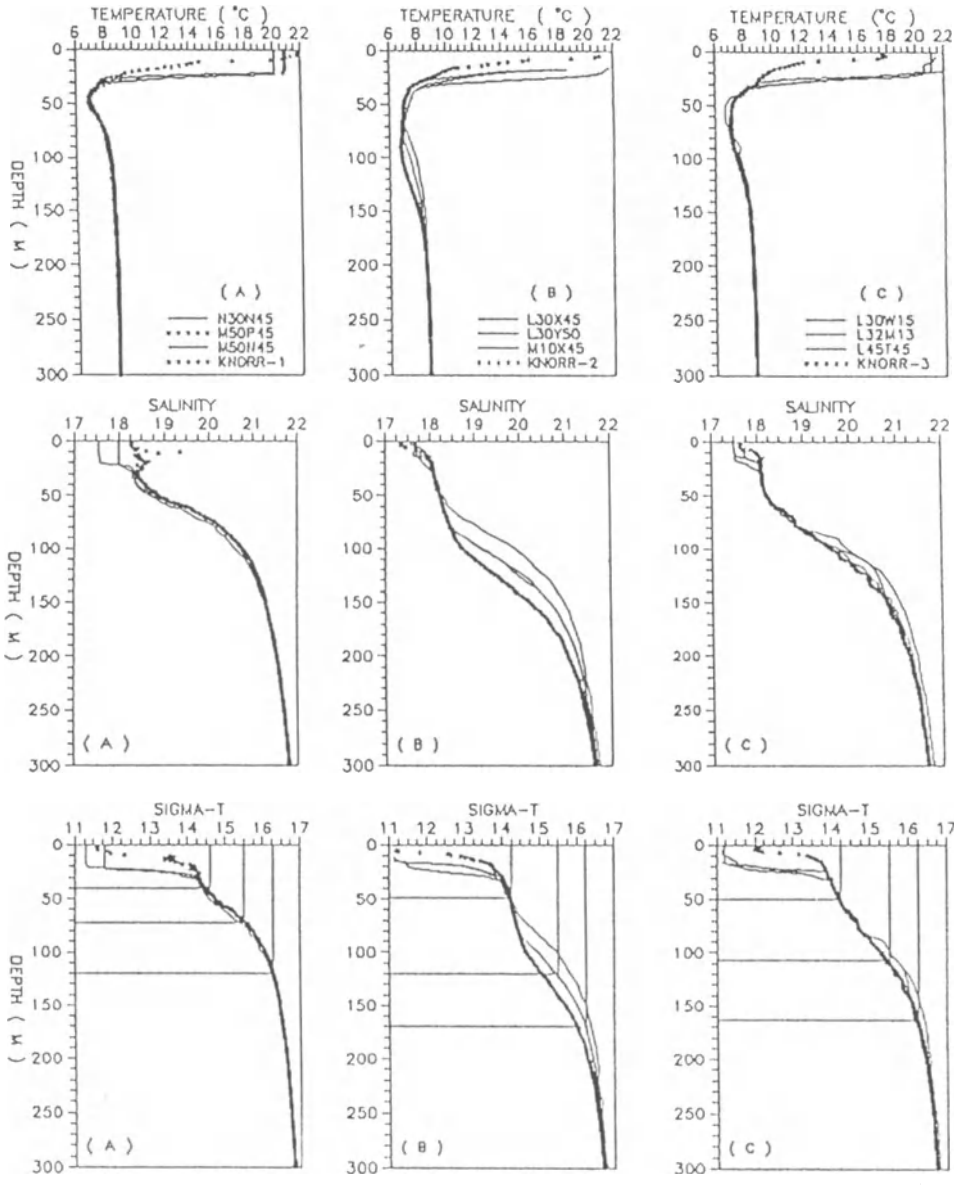


Figure 2. Depth dependent variations of temperature, salinity and sigma-T within dynamically different regions of the Black Sea. (A):cyclonic, (B):anti-cyclonic and (C):meandering rim current for September-1991 period.

gradient values of 0.61, 0.84 and 0.93 μM/m for CR, ACR and RCFZ, respectively. The DO becomes undetectable at about σ_θ=16.15-16.20 surfaces where the sulphidic waters first appear at 1-3 μM levels. In the present study, the DO deficient zone with DO<20 μM and H_2S<1 μM is called the suboxic zone (SOZ). The upper boundary of SOZ, which is suggested to have been enlarged toward the surface during recent decades by at least 0.3-0.4 σ_θ units [17], was also located at smaller densities in CR by at most 0.1-0.2 σ_θ units in late summer.

Hydrogen Sulphide (H_2S): Regional composite profiles of H_2S in Figure 3 were obtained from the titrimetric data of Bilim-91 and high-resolution Knorr-88 data measured by the automated colorimetric method. The Bilim-91 data were consistently overestimated by at least 5 μM within the low-lying anoxic waters due to difficulty in determining adequate system blank of the titrimetric method. Accordingly, the sulphidic waters first appeared at the 16.10-16.20 isopycnal surfaces throughout the deep basin in September 1991, whereas the Knorr-88 data indicate insignificant regional differences both on the sulphidic water onset (H_2S=1 μM at σ_θ=16.15).

Phosphate and TNOx: Composite profiles in Figure 4 demonstrate that the o-$P0_4$ and TNOx poor surface layer extends down to the σ_θ=14.5-14.6 surfaces (30-40 m depths) in CR, but only down to the σ_θ=14.2-14.3 (but 40-60 m depths) in ACR and RCFZ. It appears that the nutricline, coinciding both with the permanent pycnocline and oxycline, was established at greater density surfaces but at shallower depths in CR. Apart from the distinct regional differences, the phosphocline always commences at greater density surfaces by about 0.1-0.2 units relative to the TNO_x and Si onsets at the same locations (Fig. 4). Such a consistent shift between the onsets of the chemical gradients always occurs within the upper CIL where the average salinity values were about 18.19, 18.21 and 18.49 for ACR, RCFZ and CR, respectively. Apparent spatial variations both in the nutricline onsets and the physical properties of the CIL are most probably the result of the regional formation of CIL with different chemical properties and thicknesses. Accordingly, a given concentration value within the upper nutricline is reached at different density surfaces in the physically different regions; for instance, it consistently appears at smaller σ_θ surfaces in ACR.

Composite PO_4 profiles (Fig. 4) exhibit a basin-wide increasing trend within the oxycline down to σ_θ=15.6-15.7 surface. In the lower suboxic zone of the CR, the concentration decreases steeply and drops to minimal levels of 0.05-0.10 μM (mean=0.2 μM) at the σ_θ=15.85-15.90 surfaces where the DO<5 μM. This prominent phosphate minimum zone inherent to the CR was observed to weaken significantly in the ACR (0.97 μM, on average) and almost disappear in the RCFZ (1.0-1.2 μM) (see Table 2). In fact, occasional contact of reducing sediments with the oxic water in the coastal margins [18] introduce the reduced Fe and Mn species directly into oxic waters, as well as dissolved phosphate [19]. Strong rim current (>10 cm/s) undulating along the coast [20] enhances the vertical and horizontal mixing [9] and thus inhibits the development of a prominent phosphate minimum within the ACR and RCFZ. These chemically modified waters are then advected by the meandering rim current towards the open waters [21]. However, it is as yet unclear what major biomediated chemical

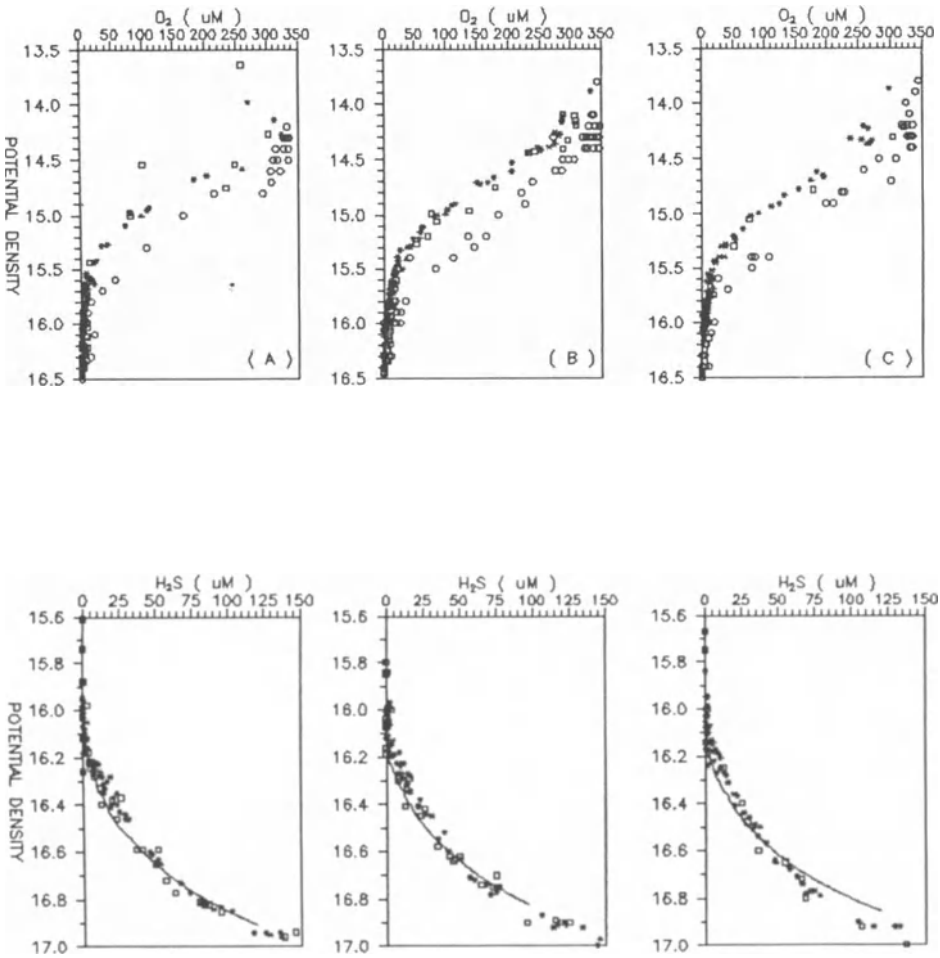


Figure 3. Potential density dependent variations of dissolved oxygen and hydrogen sulfide within dynamically different regions of the Black Sea. (A): cyclonic, (B): anticyclonic and (C): rim current for Bilim–91 (*) Knorr–88 (––), Prof. Kolesnikov–91 (□) and Atlantis–69 (o) data.

processes contribute to the formation of the distinct phosphate minimum zone in the suboxic waters of CR.

Table 2. Averages of saturated dissolved oxygen (SDO), dissolved oxygen (DO), o-PO_4 and TNOx concentrations andcorresponding averaged depths of the density surfaces (DDS) within dynamically different regions of the Black Sea.

	POTENTIAL DENSITY SURFACE INTERVALS								
	σ_θ = 14.20 - 14.30			σ_θ = 15.35 - 15.45			σ_θ = 15.95 - 16.00		
	A	B	C	A	B	C	A	B	C
SDO	331.7	340.6	336.8	327.0	327.1	327.2	321.8	321.8	321.9
DO	323.4	279.8	261.6	21.7	30.2	21.7	3.7	3.3	4.9
o-PO_4	0.02	0.02	0.01	1.07	1.06	1.14	0.21	0.97	1.20
TNOx	0.14	1.23	1.16	8.00	7.84	7.80	1.29	0.93	0.97
DDS	28-32	46-62	40-47	67-69	121-124	90-96	95-99	154-157	119-124

(A): Cyclonic gyre, (B): Anticyclonic gyre, (C): Rim current

The phosphate profiles display a steep increase within the sulphidic water interface of the entire deep basin (Fig. 4). The concentrations, as low as 0.10-1.2 μM at the σ_θ=15.85-15.90 surfaces, reach to peak values of 5-7 μM at the σ_θ=16.20-16.25 surfaces and then decrease slightly in the upper anoxic water. The occurrence of the deep maximum at the sulphidic boundary throughout the deep basin most probably results from the dissolution of phosphate-associated metal (Fe, Mn) oxides in the anoxic waters [6,19]. Comparison of the regional data indicates that the concentrations at the maxima were always lower in RCFZ (4.6-5.30 μM) than in CR and ACR (5.6-6.0 μM).

Composite TNOx profiles, in Figure 4, permit us to define the boundaries of the nitracline in 1988 and 1991; it first appears at about σ_θ=14.2-14.3 surface in the ACR but at greater density values (σ_θ=14.4-14.5) in the CR where the nutricline shoals nearly up to the base of the euphotic zone. The nitrate values increase steadily in the oxycline and eventually reach to distinct maxima (7.8-8.0 μM) between the σ_θ=15.35-15.45 surfaces throughout the basin, corresponding to the oxycline lower boundary where the DO being 20-30 μM, near the suboxic levels (<20 μM) as shown in Figure 4 and Table 2. In the SOZ, the TNOx concentration decreases down to 0.1-0.2 μM levels due to denitrification and eventually vanishes in the upper anoxic water. The TNOx gradient within the oxycline appeared to range from 0.207 μM/m for the CR to 0.123 μM/m for the ACR and 0.133 μM/m for the RCFZ, due to a two fold decrease of the nitracline thickness in CR. In the suboxic layer, below σ_θ=15.5 surface, the nitrate depletion rates were nearly similar over the basin, ranging from 0.216-0.227 μM/m in ACR and CR to 0.240 μM/m in RCFZ. This strongly suggests that the nitrate fluxes in the suboxic zone are almost in balance and subject to small regional variations over the basin.

Depth-integrated nutrient and DO contents of upper oxygenated waters between σ_θ=14.3-15.4 surfaces and the suboxic waters between σ_θ=15.4-15.95 displayed remarkable regional variations (Table 3). The integrated values for the oxygenated waters including the oxycline were much greater in the ACR than in the CR, due to the apparent enlargement of the oxygenated layer in the ACR coinciding with the

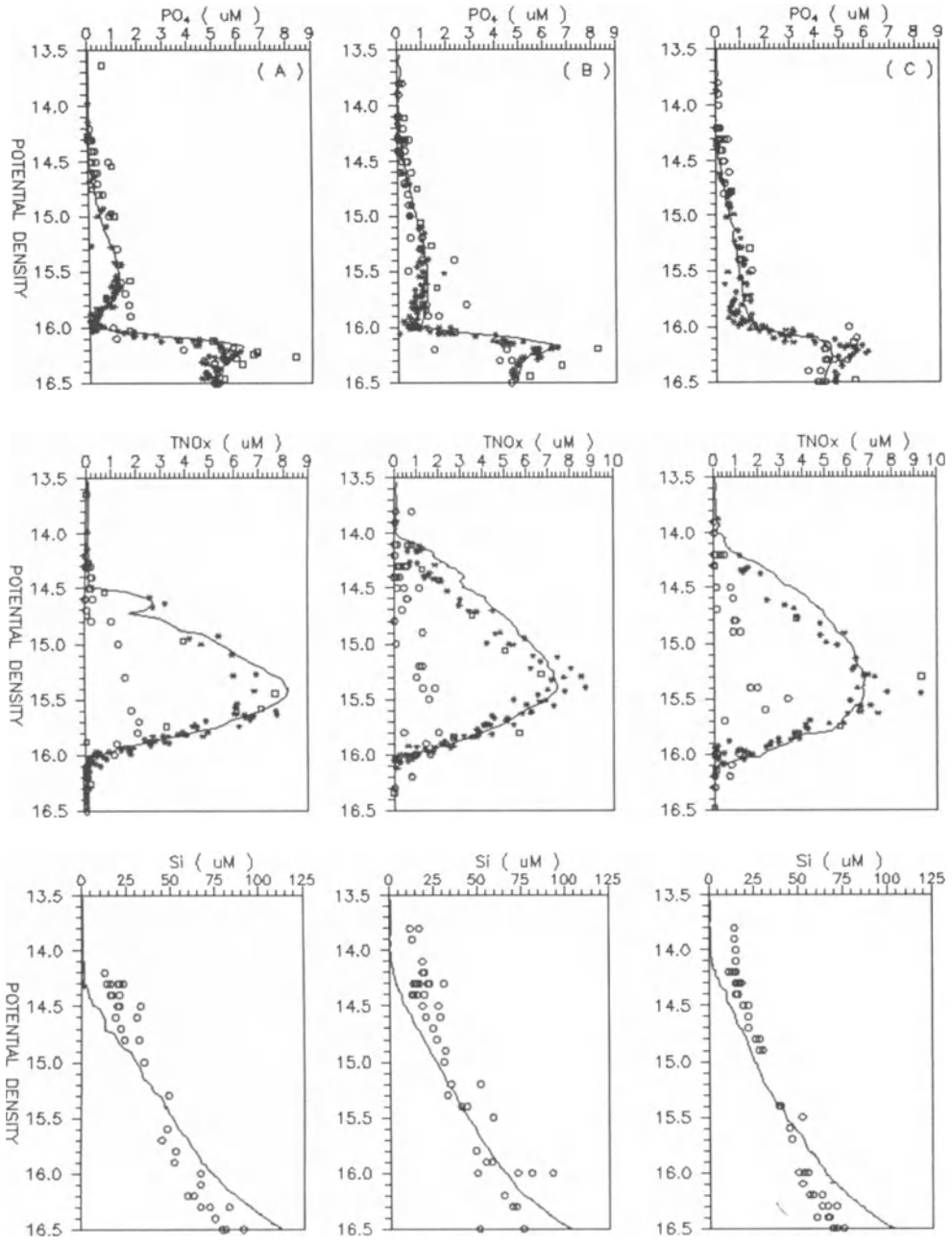


Figure 4. Potential density dependent variations of PO_4, TNOx and Si within dynamically different regions of the Black Sea. (A): cyclonic, (B): anti-cyclonic and (C):rim current for Bilim-91 (*), Knorr-88 (--) Prof. Kolesnikov-91 (□) and Atlantis-69 (o) data.

thickness of CIL which ranges from 30-40 m in the CR to about 70-80 m in the ACR (Figs. 2-3). However, in the SOZ of the ACR, the integrated DO and $P0_4$ values were still relatively large due to disappearance of the phosphate minimum zone, whereas the regional TNOx estimates being comparable (Table 3).

Table 3. Depth integrated totals of dissolved oxygen (DO), o-PO_4 and TNOx concentrations within σ_θ =14.30-15.40 and σ_θ =15.41-15.95 isopycnal surfaces for different dynamic regions of the Black Sea (All are in units of x 10^{-3} moles.m^{-2})

	σ_θ = 14.30 - 15.40			σ_θ = 15.41 - 15.95		
	A	B	C	A	B	C
DO	3371.7	7494.1	4837.0	298.8	602.3	391.2
PO_4	12.4	23.9	21.3	19.9	27.3	28.3
TNOx	86.9	196.1	151.3	130.8	143.7	128.3
N/P	7.0	8.2	7.1	6.6	5.3	4.5

(A): Cyclonic gyre, (B): Anticyclonic gyre, (C): Rim current

Chemical Ratios in the Water Column: Molar ratios of AOU:N:P derived from the depth-integrated values of the BILIM-91 data (Table 2) in the oxycline, markedly differ from the mean oceanic ratios of 175:16:1 [24]. The ratios were estimated as 283:7.5:1, 227:6.4:1, 195:5.9:1 for the CR, ACR and RCFZ of the Black Sea. High molar AOU ratios within the eddies imply, in addition to the utilization of available DO in aerobic decomposition of organic matter, a net export of DO from the oxycline into the relatively thin SOZ of the CR by diffusive processes. Moreover, upward flux of nutrients may partly contribute to the distinct low ratios. The closeness of the AOU:Nutrient ratios in the oxycline of RCFZ to the oceanic averages [22] indicates that diffusive DO losses from the oxycline are nearly compensated by the influx from the upper layer. Anomalous N:P ratios over the entire basin also reveals that the nitrate losses by denitrification in the suboxic zone of the system exceed the phosphate export to the anoxic waters by sedimentation. However, such low N:P ratios may have partially been originated from the distinct chemical composition (low N:P ratios) of biogenic particles as observed in the Sea of Marmara fed by the surface inflow from the western Black Sea [23]. The N:P ratio in the SOZ of the CR displays abnormal regional changes due to formation of the prominent phosphate minimum zone. Moreover, in this zone the oxidation of Fe(II), Mn(II), H_2S and even NH_4 compound most probably takes place through nitrate reduction as suggested by Murray et al. [16]. The molar N:P ratios in the oxycline, ranging merely between 7.0 and 8.2 (Table 3), are at least two times higher than the old ratios computed both from the Atlantis-69 data [10]. However, they are all markedly less than the conventional ratio of about 16 estimated for the oxygenated deep oceans [24].

Density dependent composite profiles of the nutrient ratios in Figures 5-6 would lead to improved understanding of the principal processes responsible for the regional differences in the hydrodynamic properties of the Black Sea. Interestingly, the TNOx:$P0_4$ profiles (Fig. 5) always displayed characteristic maxima of 60-80 at 14.1-14.3 density surfaces within ACR and RCFZ; similar maxima were also observed in CR but at greater density surfaces (σ_θ=14.4-14.5) but with lower N:P (30-40) values, due to the basinwide shift between the nitracline and phosphocline onsets. It should be noted that a similar feature is consistently established in the upper nutricline of the

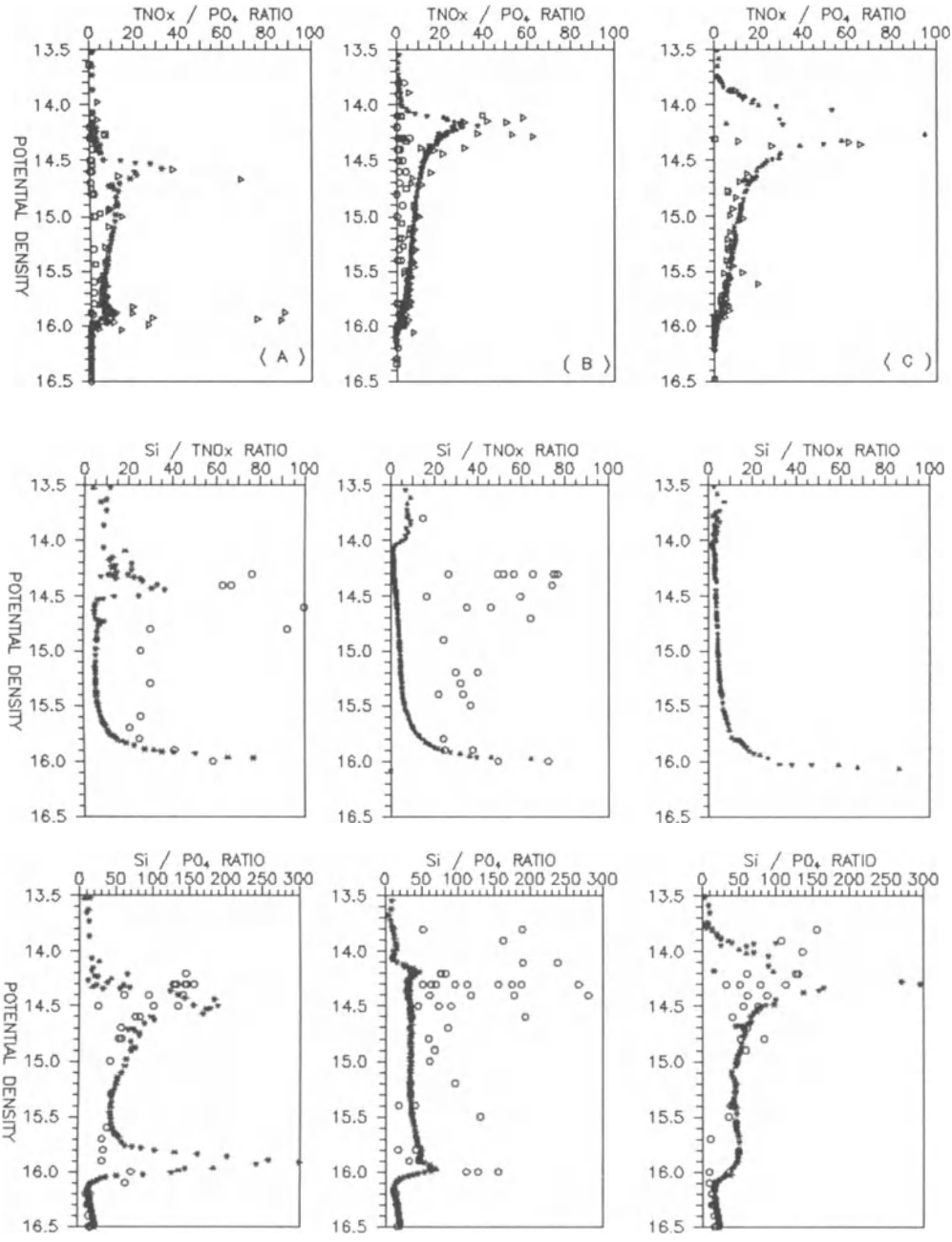


Figure 5. Potential density dependent variations in $TNOx/PO_4$, $Si/TNOx$ and Si/PO_4 ratios within the (A):cyclonic, (B):anticyclonic and (C):rim current regions of the Black Sea for R/V Knorr (*), R/V Atlantis (o), R/V Bilim (▷) and R/V Prof. Kolesnikov (□).

eastern Mediterranean [25]. We suggest that, in the period of late winter-early spring bloom, the cool surface waters sink down below the euphotic zone with relatively high concentrations of dissolved organic nitrogen (DON) and/or ammonia, whereas the majority of fast recycled organic phosphorus leaves the surface layer as particulate phosphorus associated to sinking biogenic particles. Interestingly, no peak values appeared in the composite profiles of the old ratios, indicating remarkable changes in the nutrient cycling in the upper layer as well as the land-based input rates and their transport into the open Black Sea. The ratio decreases slowly within the oxycline from values of 12-14 at the σ_θ=14.7-14.8 surfaces to levels of 6-8 at the depth of nitrate maximum (σ_θ=15.35-15.45) further to levels of 4.5-6.6 in the upper suboxic waters, yielding maxima in the phosphate minimum zone and eventually being less than one in the anoxic interface due to intense denitrification (Fig. 5).

In the productive zone of the Black Sea, The old Si/TNO_X ratios (Fig. 5) within the upper slope of the nitracline are much larger than the recent values due to high silicate content of the surface waters in the late 60's. The ratios within the SOZ's of the CR and ACR do not indicate any shift from late 70's up to 1991. Although there are some remarkable scattering in old Si/$P0_4$ data from the frontal zones (Fig. 5), the ratios remained almost constant in the main oxycline and suboxic waters down to the $P0_4$ minimum zone where the recent ratios display a maximum as large as 200-250 in the CR. Moreover, the ratios of the upper oxycline in CR were much larger than in ACR due to the remarkable downward shift in the phosphocline onset. The appearance of comparable Si/TNOx ratios within the main oxycline together with almost vertically uniform Si/P ratios from the same region (Fig. 5), indicate that both the fluxes and regeneration of reactive silicate in the upper layer of the Black Sea are very similar to those of phosphorus and nitrogen.

5. Conclusions

Comparison of high-resolution, basin-wide data reveals that the phosphocline always commences at greater density surfaces relative to the nitracline onset. Accordingly, the profiles of TNO_X:$P0_4$ and Si:$P0_4$ ratios display the distinct maxima at specific density surfaces of the upper nutricline. The TNOx and DO gradients within the oxycline are markedly larger in CR than in ACR where the thicker CIL has been formed. The sub-surface $P0_4$ minimum is a distinct feature of the suboxic zone in CR; it weakens in ACR and nearly disappears within the RCFZ. This feature was most probably much less pronounced in the 60's due to limited thickness of the old suboxic zone. The depth-integrated values of nutrients and DO between the 14.30-15.95 density surfaces are markedly larger in ACR than in the CR, permitting more nutrient influx from the lower layers of ACR to its surface waters. Comparison of chemical ratios indicate a net DO input from the oxycline into the suboxic zone; the nitrate loss from the suboxic zone by denitrification exceeds the phosphate export to the anoxic waters.

6. Acknowledgments

This work was supported by the Turkish Scientific and Technical Council (TÜBITAK), the NATO-Science for Stability Program and the Ukrainian Academy of Sciences. The authors wish to thank the crews of R/V Bilim (IMS) and R/V Prof. Kolesnikov (MHI), and the technicians in the IMS and MHI for their valuable contributions.

7. References

1. Mee, L.D. (1992) The Black Sea in crisis: The need for concerted international action, *Ambio* **21**, 278-286.
2. Shuskina, Eh.A., and Musaeva, Eh.I. (1990) Structure of planktonic community from the Black Sea epipelagical and its changes as the result of the introduction of a ctenophore species, *Oceanology* **30(2)**, 306-310.
3. Smayda, T.J. (1990) Novel and nuisance phytoplankton blooms in the sea: Evidence for a global epidemic, in E. Granelli, B. Sundstroem, L. Elder and D.M. Anderson (eds.), Lund, Sweden, 26-30 June,1989, pp:29-40.
4. Vinogradov, M.Ye., Shushkina, E.A., Musaeva, Eh.I., and Sorokin, Yu.I. (1989) The comb-jelly *Mnemiopsis leidyi* (A. Agassiz)(Ctenophora:Lobata); a newly introduced species in the Black Sea, *Oceanology* **29(2)**, 293-299.
5. Bastürk, Ö., Saydam, C., Salihoglu, I., Eremeev, L.V., Konovalov, S.K., Stoyanov, A., Dimitrov, A., Cociasu, A., Dorogan, L. and Altabet, M. (1994) Vertical variations in the principle chemical properties of the Black Sea in the autumn of 1991, *Marine Chemistry* **45**, 149-165.
6. Codispoti, L.A., Friederich, G.E., Murray, J.W. and Sakamato, C.M. (1991) Chemical variability in the Black Sea: Implications of continuous vertical profiles that penetrated the oxic/anoxic interface, *Deep-Sea Res.* **38(2A)**, 691-710.
7. Saydam, C., Tugrul, S., Bastürk, Ö., and Oguz, T. (1993) Identification of the oxic/anoxic interface by isopycnal surfaces in the Black Sea, *Deep-Sea Res.* **40(7)**, 1405-1412.
8. Tugrul, S., Bastürk, Ö., Saydam, C., and Yilmaz, A. (1992) Changes in the hydrochemistry of the Black Sea inferred from water density profiles, *Nature* **359**, 137-139.
9. Friederich, G.E., Codispoti, L.A. and Sakamato, C.M. (1990) *Bottle and pumpcast data from the Black Sea expedition*, Monterey Aquarium Res. Inst. Tech. Rep.90-3, 224p.
10. Brewer, P.G. (1971) Hydrographic and chemical data from the Black Sea, Woods Hole Oceanogr. Inst. Technical Report, Reference No:71-65.
11. Oguz, T., Aubrey, D.G., Latun, V.S., Demirov, E., Kovesnikov, L., Limeburner, R. and Eremeev, V. (1994) Meso-scale circulation and thermohaline structure of the Black Sea observed during HydroBlack'91, *Deep-Sea Res.* **41(4)**, 603-628.
12. Filipov, D.M. (1965) The cold intermediate layer in the Black Sea, *Oceanology* **5**, 47-52.
13. Ovchinnikov, I.M. and Popov, YU.I. (1987) Cold intermediate layer formation in the Black Sea, *Oceanology* **27(5)**, 739-746.
14. Buesseler, K.O., Livingston, H.D., Ivanov, L. and Romanov, A. (1994) Stability of the oxic-anoxic interface in the Black Sea, *Deep Sea Res.* **41(2)**, 283-296.
15. Murray, J.M., Top, Z., and Ozsoy, E. (1991) Hydrographic properties and ventilation of the Black Sea, Deep-Sea Res. **38(2)**, S663-S690.
16. Murray, J.M., Codispoti, L.A. and Friederich, G.E.(1995) Oxidation-Reduction Environments: The suboxic zone in the Black Sea, in C.P. Huang, C.R. O'Melia and J.J. Morgan (eds.) *Aquatic Chemistry*, ACS Advances in Chemistry Series No.244, p:157-176.
17. Murray, J.M., Jannasch, H.W., Honjo, S., Anderson, R.F., Reeburgh, W.S., Top, Z., Friederich, G.E., Codispotu, L.A., and Izdar, E. (1989) Unexpected changes in the oxic/anoxic interface in the Black Sea, *Nature* **338**, 411-413.
18. Kempe, S., Diercks, A.R., Liebezeit, G. and Prange, A. (1991) Geochemical and structural aspects of the pycnocline in the Black Sea (R/V Knorr 134-8 Leg 1, 1988), in E. Izdar and J.W. Murray (eds.), *Black Sea Oceanography,* NATO-ASI Series C, **v.351**, Kluwer Acad. Publ., Netherlands, pp:89-110.
19. Shaffer, G. (1986) Phosphate pumps and shuttles in the Black Sea, *Nature* **321**, 515-517.

20. Sur, H.I., Özsoy, E., and Ünlüata, Ü. (1994) Boundary current instabilities, upwelling, shelf mixing and eutrophication processes in the Black Sea, *Prog. in Oceaography* **33(4)**, 249-302.
21. Lewis, B.L. and Landing, W.M. (1991) The biogeochemistry of manganese and iron in the Black Sea, *Deep-Sea Res.* **38(20)**, S773-S803.
22. Takahashi, T., Broecker, W.S., and Langer, S. (1985) Redfield ratio based on chemical data from isopycnal surfaces, *Jr. of Geophysical Res.* **90**, 6907-6924.
23. Polat, C.S. (1995) Nutrient and organic carbon budgets in the Sea of Marmara: A progressive effort on the biogeochemical cycles of carbon, nitrogen and phosphorus, Ph.D. Thesis, Institute of Marine Sciences, Erdemli, Icel, Turkey, June 1995.
24. Takahashi,T., Broecker,W.S., and Langer,S. (1985) Redfield ratio based on chemical data from isopycnal surfaces, *Jr. of Geophysical Res.* **90**, 6907-6924.
25. Krom, M.D., Brenner, S., Kress, N., Neori, A. and Gordon, L.I. (1992) Nutrient dynamics and new production in a warm eddy from the eastern Mediterranean, *Deep-Sea Res.* **39(3/4)**, 467-480.

SPATIAL ISOPYCNAL ANALYSIS OF THE MAIN PYCNOCLINE CHEMISTRY OF THE BLACK SEA:
seasonal and interannual variations

SERGEY KONOVALOV*, SÜLEYMAN TUĞRUL♣
ÖZDEN BAŞTÜRK♣ and İLKAY SALİHOĞLU♣
(*) Marine Hydrophysical Institute (MHI-NASU), Sevastopol, Ukraine.
(♣) Institute of Marine Sciences (IMS-METU), Erdemli-İçel, Turkey.

Abstract. The results of 1991-1994 basin-wide investigations have been analysed using the method of spatial isopycnal analysis. Seasonal and interannual variations of phosphates, nitrates, dissolved oxygen and the suboxic zoneare revised. The range and possible reasons of spatial and temporal variations in the density-dependent vertical profiles of nutrients and oxygen in the layer of the main pycnocline, in the thickness and the position of suboxic zone of the Black Sea are discussed.

1. Introduction

In the Black Sea, only the thin upper layer (50-250 m) is oxygenated due to the existence of a permanent pycnocline at intermediate depth, below which an anoxic water mass occupies the entire basin [1]. Restricted by the presence of this pycnocline, vertical ventilation has resulted in the formation of an oxygen-poor transition layer between oxygenated and anoxic waters [1,2]. The oxic/anoxic transition layer, the so-called "suboxic" (SO) zone [2-4], has been well documented for the nutrient profiles which display explicitly different characteristic features from those observed in the oxygenated oceans. For example, a subsurface maximum of nitrate and phosphate profiles are observed throughout the basin but at different depth depending on spatial and seasonal variations in the hydrographic conditions and the intensity of hydrodynamic processes. However, it has recently been demonstrated that such well distinguished features are principally established on specific density surfaces with small variations over the basin [4-9]. These findings have lead most scientists to examine basin-wide, long-term data extensively, so as to define spatial and temporal variability in the density-dependent profiles of the principal hydrochemical properties in the upper layer, down to the anoxic boundary [7,10-12]. They have demonstra-ted that hydrochemical properties of the main pycnocline in anticyclonically-dominated coastal waters and rim current frontal zone appear to differ noticeably from those in the cyclonic interior of the Black Sea. Regional differences observed in the vertical

E. Özsoy and A. Mikaelyan (eds.), Sensitivity to Change: Black Sea, Baltic Sea and North Sea, 197–210.
© 1997 *Kluwer Academic Publishers.*

distributions of the main hydrochemical properties have been attributed to complicated lateral and vertical mixing processes which are intensified in some regions in winter when the surface layer is thoroughly mixed [13,14], as well as to the rate of organic matter input from the euphotic layer [2].

In the present paper we attempt to define the ranges and to discuss the possible reasons of the spatial and temporal variability in the density dependent vertical distribution of nutrients and oxygen in the layer of the main pycnocline of the Black Sea, based on the chemical data obtained through the 1991-1994 basin-wide surveys.

2. Materials and Methods

Data sets of IMS-METU, Erdemli-Içel, Turkey and MHI-NASU, Sevastopol, Ukraine have been used in this work. These data sets have been obtained as the national contribution of international programmes: CoMSBlack and TU-Black Sea. Net of oceanographic stations covers the main part of the Black Sea (look, for example, Fig. 3). Information on accuracy of data is available in reports prepared for every international multi-ship experiment. Part of this information is in Table 1.

TABLE 1. Information on the accuracy of hydrochemical data.

Parameter	Mean value	Standard deviation	Mean value	Standard deviation
Dissolved oxygen	324	1.4	4.1	1.1
Hydrogen sulfide	39	0.8	1.9	1.3
Phosphates	6.26	0.06	0.03	0.05
Silicic acid	107	1.1	6.9	0.04
Nitrates	5.21	0.13	0.19	0.02
pH	8.41	0.005	7.86	0.008

3. Results and Discussions

3.1. DISSOLVED OXYGEN

Basin-wide density dependent profiles of dissolved oxygen (DO) (Fig. 1) imply that the water mass above the isopycnal surface 14.5-14.6 is well oxygenated, and below that, an oxygen gradient zone (the so-called "oxycline"), coinciding with the upper part of the main pycnocline, is located [5-7]. The oxycline is apparently established between density surfaces of 14.5-14.6 and 15.6-15.9. The thickness of this layer shows marked regional variations. The DO values rapidly diminish to 10-30 μM at 15.6-15.9 density surfaces and gradually decrease to less than 5 μM within the sub-oxic zone [2,5-7,15]. The vertical gradient of oxygen concentration in the oxycline, depends on the

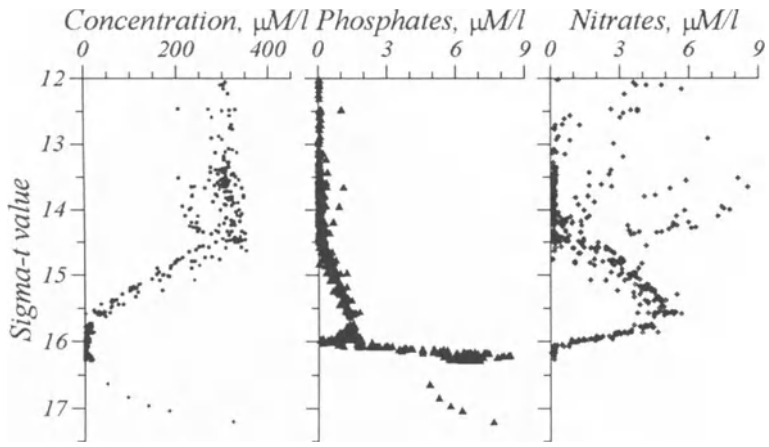


Figure 1. Distribution of dissolved oxygen, hydrogen sulfide, phosphates, and nitrates versus sigma-t in May 1994

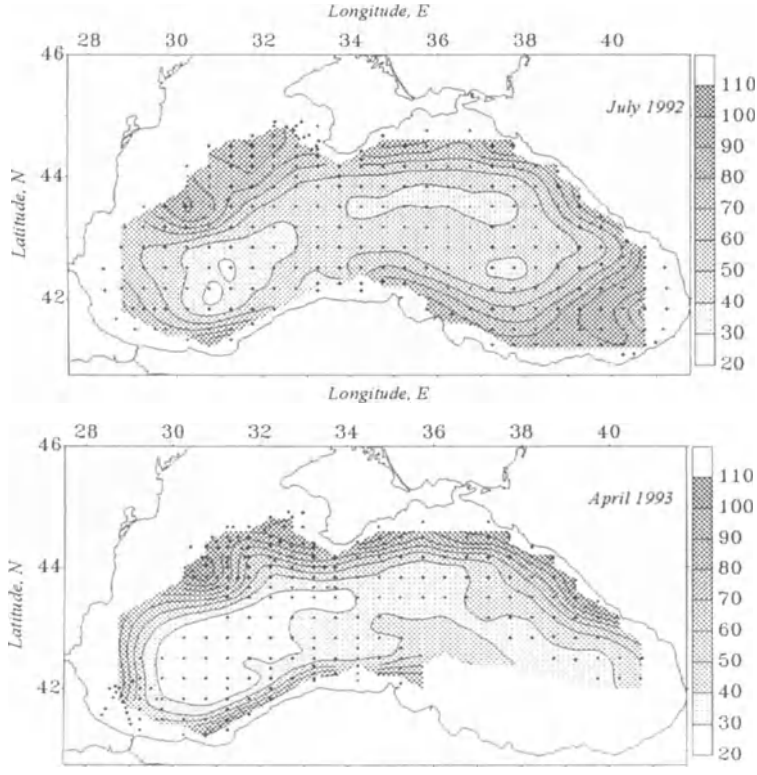


Figure 2. The depth (m) of the 14.6 isopycnal surface in July 1992 and April 1993.

hydrographic structure (Fig. 2). The DO depletion rate at a constant depth increases from coastal margins towards the cores of the cyclonic gyres [16].

The surface oxygen shows remarkable seasonal and year-to-year variations in the subsurface maximum, depending on the water temperature and the level of the primary productivity. The different realizations of the spatial distribution of DO are displayed in Fig. 3 on the 14.6 isopycnal surface, which approximately defines the oxycline onset (Fig. 1) and corresponds to the core of the Cold Intermediate Layer (CIL).

Briefly, the DO concentrations vary from 160 μM to 260 μM over the basin for July 1992 and from 280 μM to 340 μM for April 1993, and up to 310 μM for May 1994 (Fig. 3). The DO concentration in the core of the CIL is consistently higher in the cyclonic regions than in the anticyclonically dominated area near the shelf break. The core of the CIL appears to be more oxygenated, by about 20-40 μM, in April 1993 compared to May 1994 and by 40-80 μM compared to July 1992. The core waters of the CIL are up to 90-115% saturated with oxygen throughout the year.

The processes of winter convective mixing and phytoplankton activity could be responsible for increasing oxygen concentration in the CIL waters. Basinwide variations in the depth of the 14.6 density (σ_t) surface (Fig. 2) indicate that it may be as shallow as 25-30 m (April 1993), or up to a depth of 40-50 m within the cyclonic regions in late spring-summer months. Direct convective mixing in winter can reach depths of the 14.5-14.7 surface[14], but the influence of convective mixing can be detected down to the depths of 15.6-15.7 isopycnal surfaces, in distributions of temperature [11], and chemical properties [17]. Because the 25-30 m depth levels could be the base of euphotic zone in the central region of the Black Sea where the phytoplankton activity could lead to increases of oxygen, it is not yet clear whether the physical or the biological processes are more important in determining the oxygen variations in the CIL waters.

Examination of the DO content of waters at 15.6 the density surface, which roughly defines the lower boundary of the oxycline (Fig. 4), shows oxygen concentration variations in the range of 10-30 μM. Interestingly, in July 1992, hypoxia (DO<10 μM) was recorded at some sections of the central part of the basin where the primary production was also unexpectedly very high, which was limiting the euphotic zone to the upper 10 meters in depth. DO concentrations as high as 80-140 μM (Fig. 4) were recorded in the north and north-eastern parts of the basin, surrounded by the water masses possessing very low DO levels. In April 1993, the lowest concentrations of dissolved oxygen occurred near the same place, but the position of the highest values was different (Fig. 4).

It is rather difficult to explain the elevated DO concentrations in a particular region due to the complexity of mixing processes within the main pycnocline. In general, only physical processes can provide cross-isopycnal fluxes leading to an increase of oxygen in this layer, while the chemical and biochemical Redox processes would be expected to lead to a decrease. The low DO content of waters on the 15.6 density surface indicates limited ventilation of the permanent pycnocline even within central regions during the winter mixing processes, and/or intensive utilisation of DO

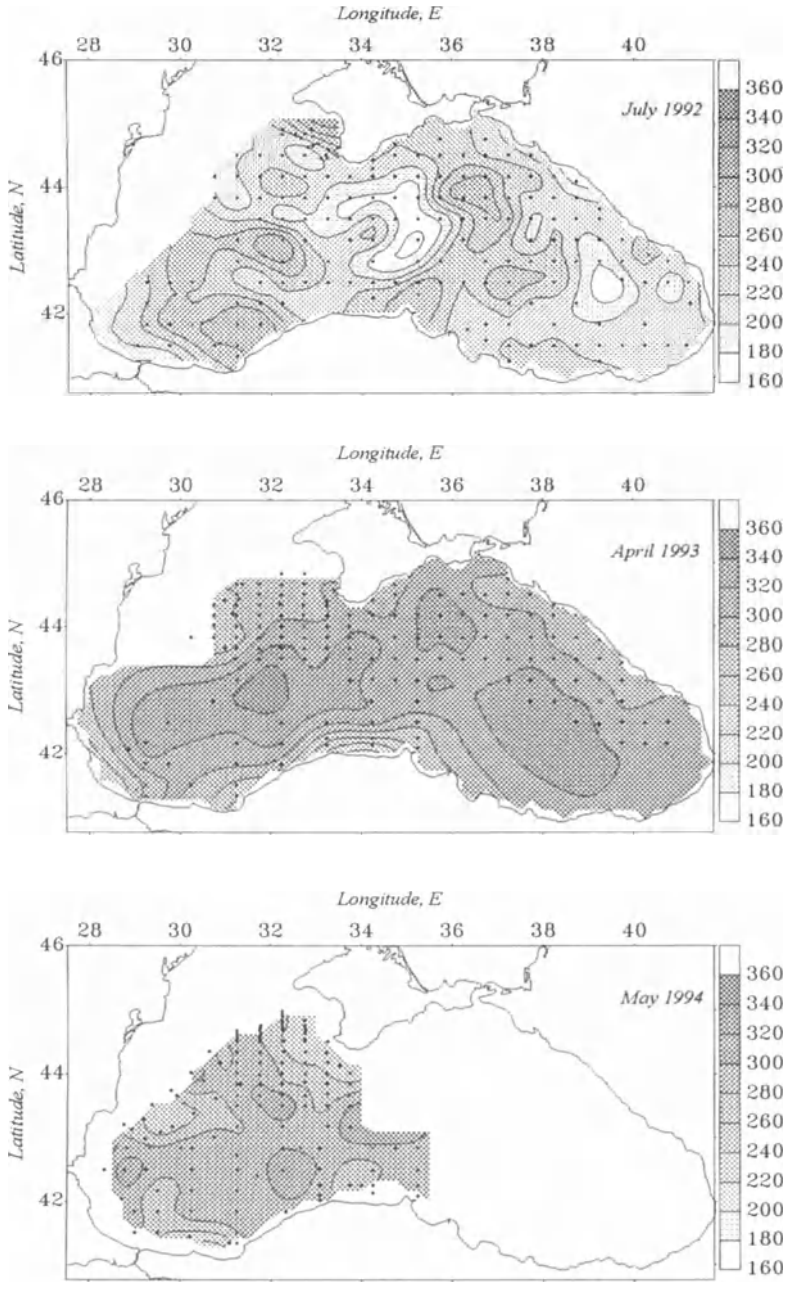


Figure 3. Dissolved oxygen (μM) at the 14.6 sigma-t surface.

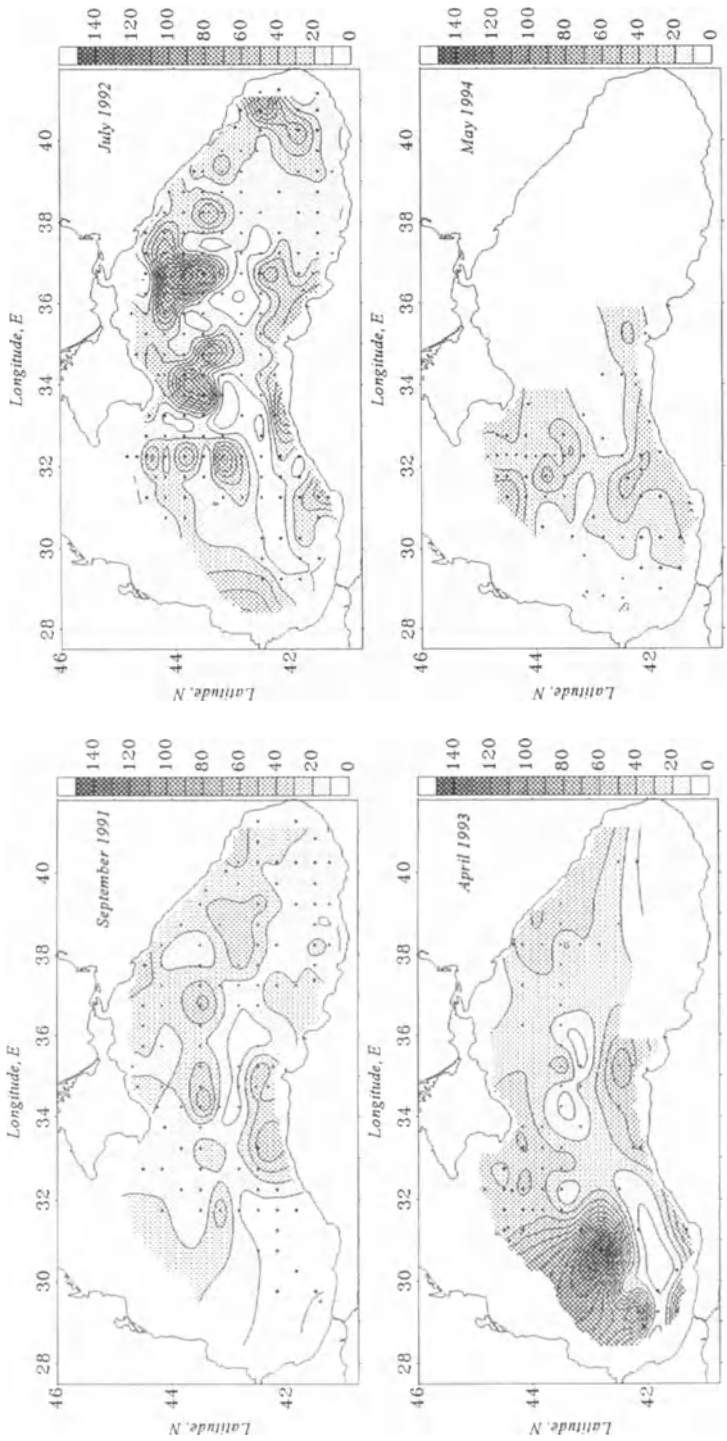


Figure 4. Dissolved oxygen (μM) at 15.6 sigma-t surface.

3.2. THE SUBOXIC ZONE

The "suboxic zone", first introduced by Murray et al. [3], was defined as a zone located "between the layer of oxygen decrease to suboxic levels (less then 5 μM) and that of the first appearance of hydrogen sulfide". Later, Tugrul et al. [5] and Saydam et al. [6] suggested to use the position of subsurface nitrate maximum and the 16.2 density surface as the boundaries of the SO zone. In this study, the DO values of the 20 μM and 16.2 density surfaces define the upper and lower boundaries of the SO zone (Fig. 5). The oxycline extends to the depths of 10-30 μM of oxygen [18]. In this way, we avoid any uncertainties related to the determination of low concentrations of oxygen and hydrogen sulfide, and overcome the questions on variations in the position of the nitrate maximum. Based on these definitions, the basin-wide variations in the thickness of the SO layer in terms of depth (m) and sigma-t (σ_t) units are plotted respectively in Figs. 6 and 7. The thickness of the suboxic layer varies in space and time from 20 to 70 meters and from 0.3 to 0.8 density (σ_t) units (Figs. 6 and 7). These estimates are in good agreement with the values announced by Murray et al [3] and later by Tugrul et al. [5] for the summer period of 1988.

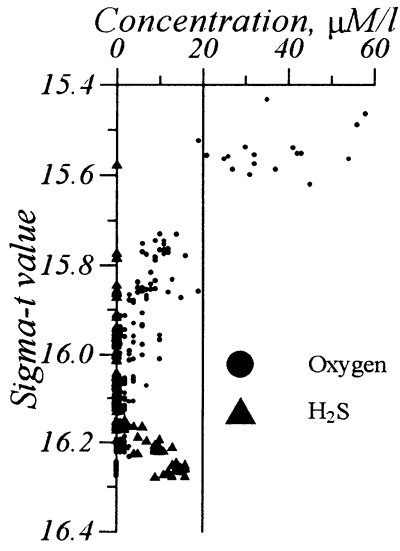


Figure 5. Oxygen and hydrogen sulfide in oxic/anoxic transition zone.

Noticeable spatial and temporal variations of the thickness of SO zone are recognised in the Black Sea waters (Figs. 6 and 7). It is yet unclear what processes are more important for spatial and temporal variations of the thickness of the SO zone, although various physical, chemical, and biochemical processes are expected to be important for different periods of the year. Good correlation between the phosphate concentration in the layer of local minimum (σ_t~15.95) and the thickness of SO zone in spring (Fig. 8) implies considerable role of Redox processes. On the other hand, seasonal weather conditions for similar periods were different from 1991 to 1994, resulting in variable intensity and spatial features of the ventilation of the main pycnocline [19]. This would in turn imply variations in the cross-isopycnal flux of all the other properties, resulting in variable intensity of the Redox processes. Biochemical processes should be more important during the blooms of phytoplankton, when great amounts of particulate organic matter sink from the euphotic zone. For example, the upper boundary of the SO zone rises upward by the 15.1-15.2 density surface in a limited area of the central Black Sea in July 1992, probably due to the excess organic matter input into the permanent pycno-

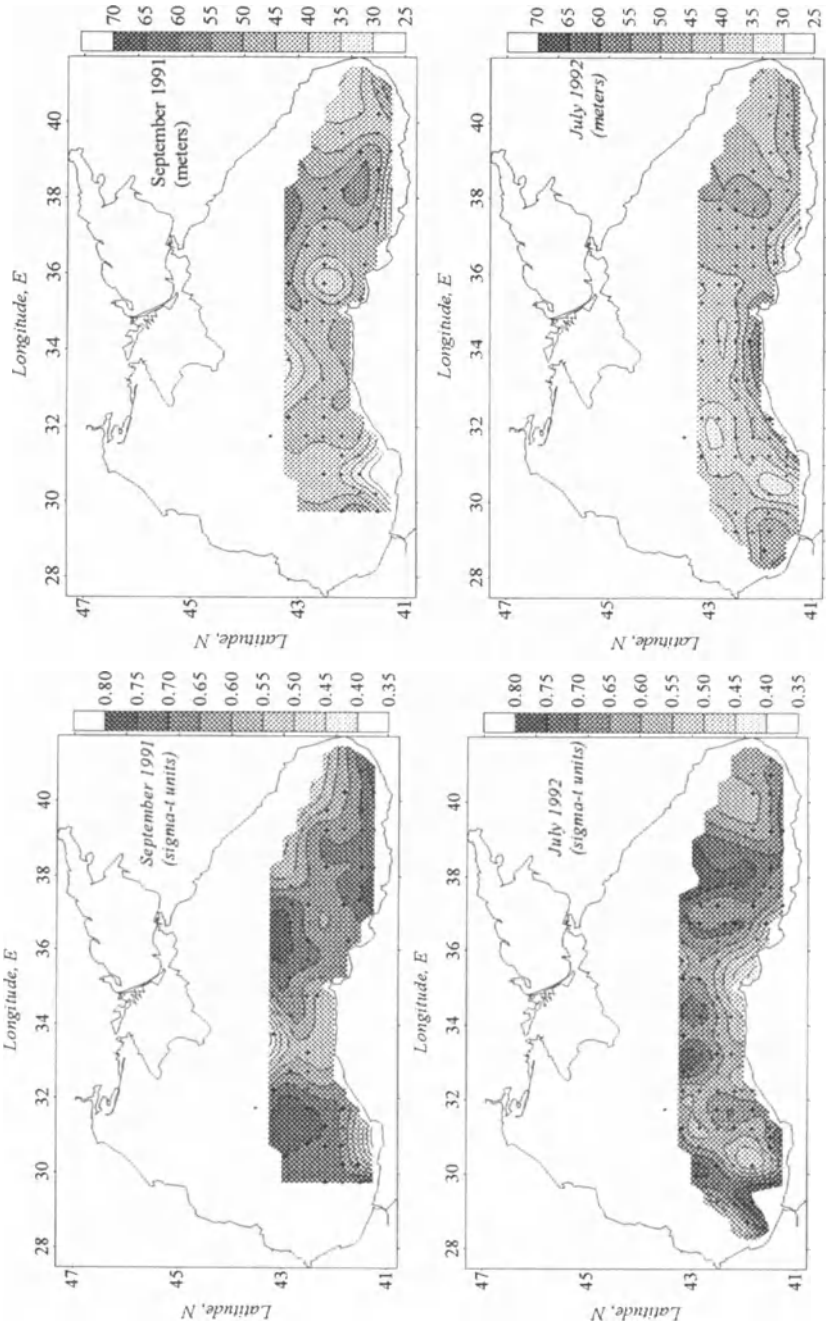


Figure 6. The thickness of SO zone in 1991 and 1992.

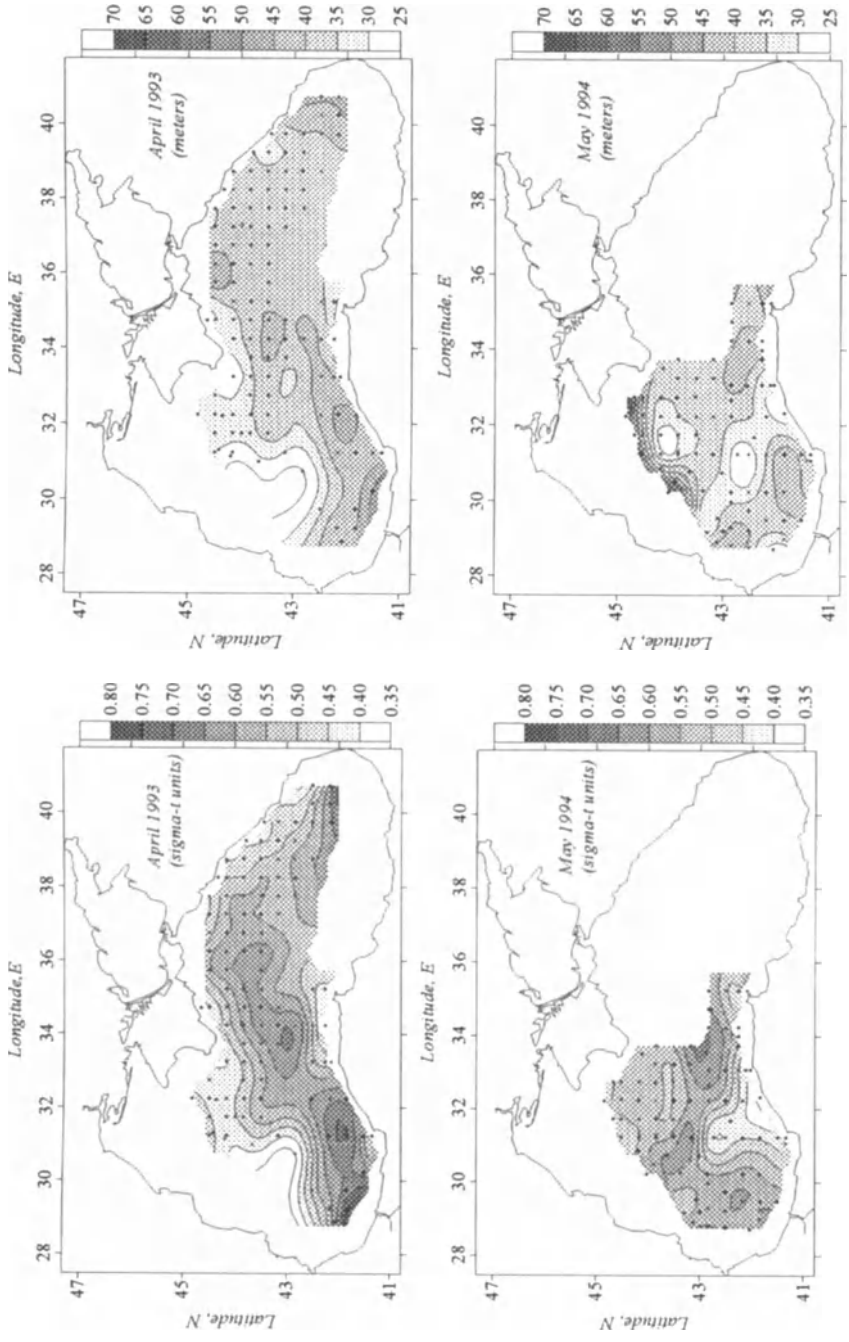


Figure 7. The thickness of SO zone in 1993 and 1994.

cline waters and the weak cross-isopycnal fluxes in the same region.

3.3. PHOSPHATES

The vertical distribution of reactive *ortho*-phosphate indicates the existence of two distinguished features (minimum at σ_t~15.95 and maximum at σ_t~16.20) within the oxic/anoxic transition layer, as it was recently emphasized [4,5,20-22]. Although the depths of these characteristic features are variable over the basin, they are located in a narrow range of density (Fig. 1). On the other hand, the onset of the phosphate gradient consistently appears at different σ_t values across the region. This depth corresponds to about 14.2-14.3 density in the anticyclonic regions and 14.5-14.6

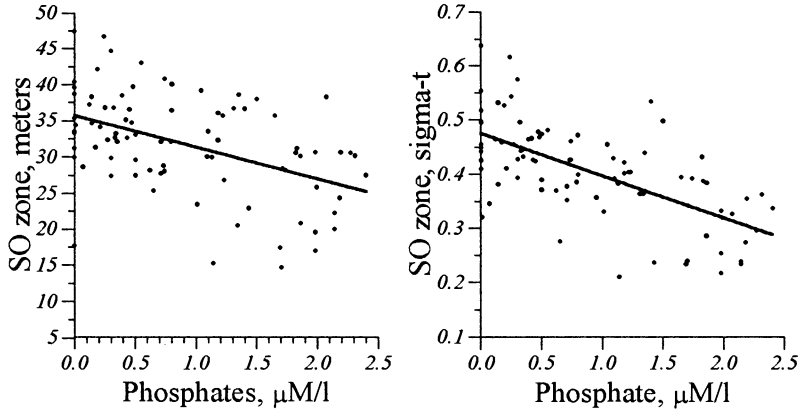


Figure 8. Concentration of phosphates in the local minimum (σ_t~15.95) and the thickness of SO zone.

density in the cyclonic regions in September 1991 [16].

The local phosphate minimum is formed between the primary and deep phosphate maxima within the SO zone. The position of phosphate minimum varies, in general, from 15.85 to 16.05. It was observed to be a permanent feature of the cyclonic regions and tends to weaken or disappear completely towards the periphery of the deeper part of the Black Sea [12,16]. Accordingly, the upper phosphate maximum becomes apparent when a local minimum is formed, otherwise phosphate concentration increases monotonously with sigma-t density from ~14.0 to ~16.2 [12].

The upper broad phosphate maximum is formed by the aerobic oxidation of biogenic organic matter within the oxygenated, upper pycnocline. It is yet unclear if biologically mediated chemical processes could be responsible for creating the local phosphate minimum at sima-t of ~15.95, as suggested by Sapognokov et al. [22]. Phosphate concentrations measured at the depth of P-minimum, between 15.85-16.05 sigma-t and at the depth of P-maximum corresponding to 16.15-16.30 sigma-t for April 1993, depicted in Fig. 9, indicate significant spatial changes, with concentration increasing from the coastal margins towards the interior of the basin. The highest

phosphate concentration corresponding to the deep maximum always occurred within the cyclonic regions, where the subsurface minimum is also a prominent feature of the system. The suggestion of Shaffer [20] linking the local minimum (at around 15.95 sigma-t) and the maximum (at around 16.2) to the transport of the phosphate-associated metal oxides, from suboxic to the anoxic zone seems to be the most reliable hypothesis so far.

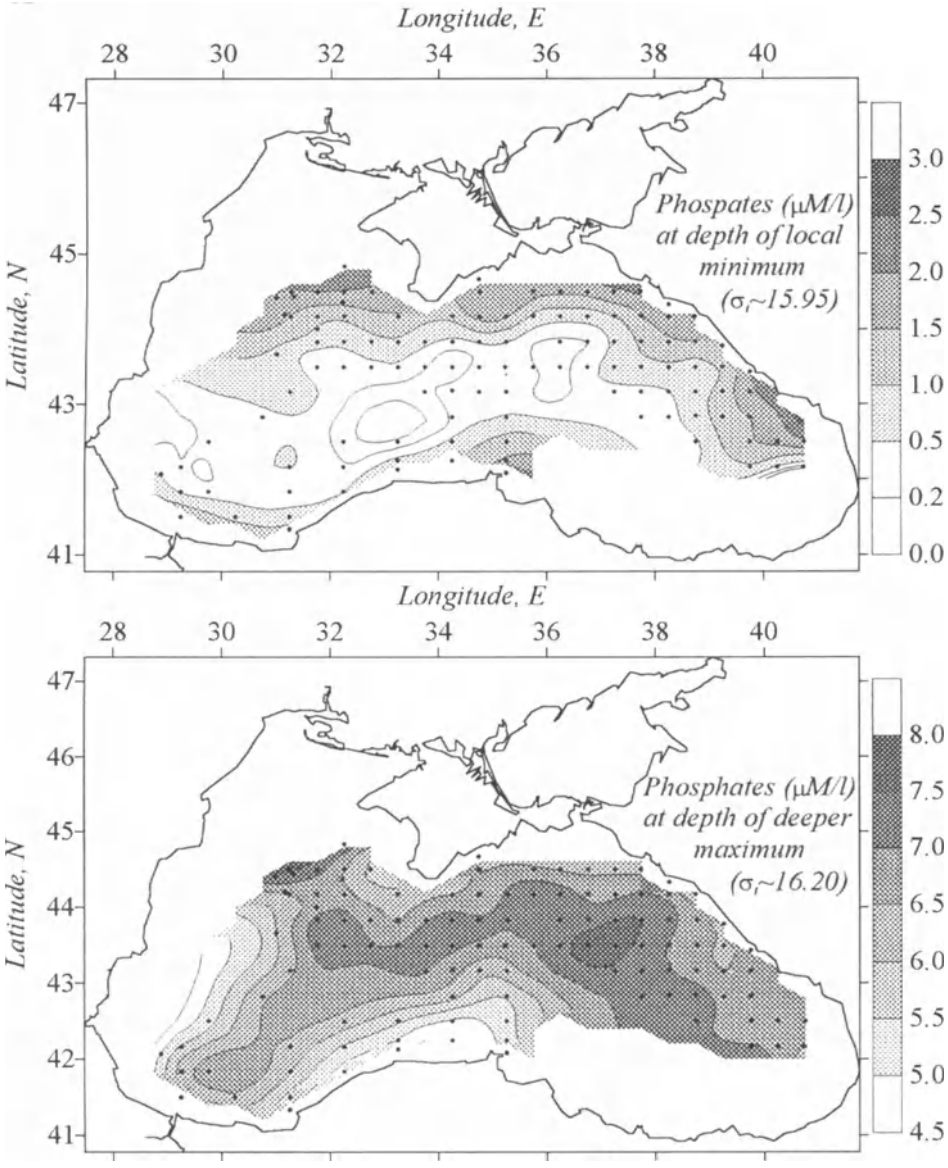


Figure 9. Concentration of phosphates in the layer of local minimum (σ_t~15.95) and deeper maximum (σ_t~16.20) in April 1993.

3.4. NITRATES

As shown in Fig. 1, the nitrate concentrations start to increase below 14.2-14.5 sigma-t and attain peak values of 4-6 μM at intermediate depths of the main pycnocline, where the DO concentrations decrease to 10-40 μM. Markedly higher surface values were also recorded at the north-western shelf where polluted Danube and Dnieper Rivers discharge fresh waters to the surface. In the suboxic zone waters of the system, nitrate values decrease sharply with depth and decrease to undetectable levels within the

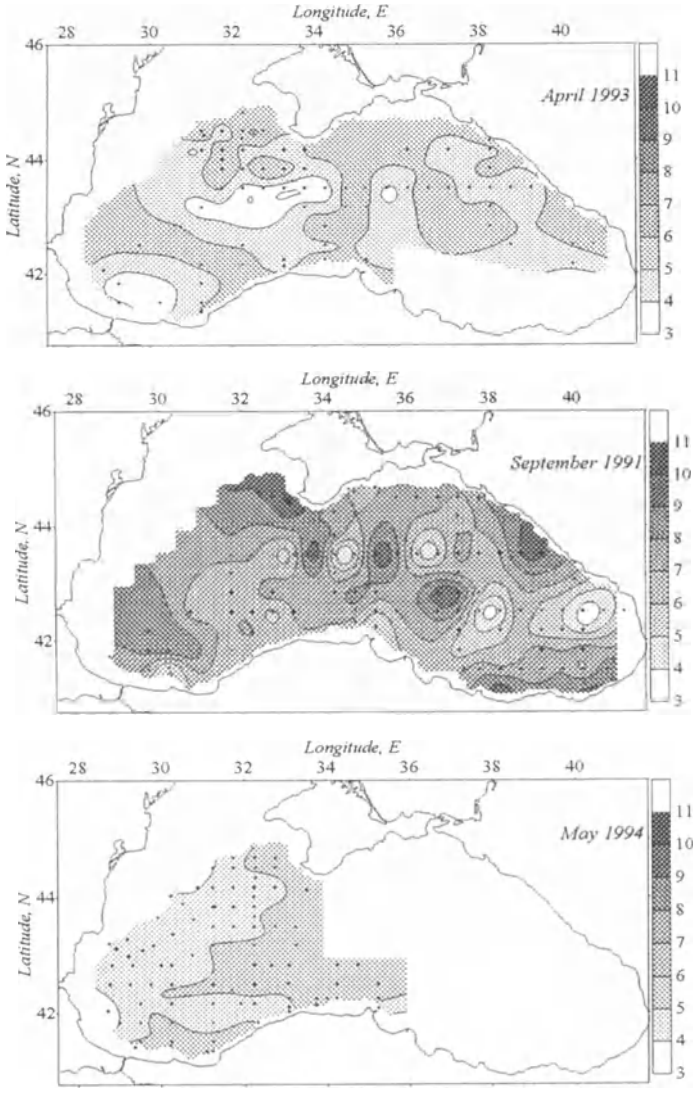


Figure 10. The highest values of nitrate concentration in the layer of the main pycnocline.

anoxic interface. As first noticed by Codispoti et al. [4], individual nitrate-density profiles from different locations are very similar, in particular the nitracline commences at similar density surfaces (Fig. 1). However, it always commences at greater density, but at shallower depths in the cyclonic regions, probably due to the shoaling of the permanent pycnocline near the base of the euphotic zone [16] or as a result of winter convective mixing [11].

The composite profile possesses a maximum established between the density surfaces of 15.4 and 15.6 over the basin (Fig. 1), but in some regions it is located deeper, till the 15.8 isopycnal surface [11]. The nitrate maximum and its depth exhibit spatial and temporal variability (Fig. 10). Interestingly, the peak values of nitrate changed from 4-9 μM in September 1991 to 3-6 μM in April 1993 and May 1994 throughout the entire basin, except in the north-western shelf areas where the Danube and Dnieper discharges are effective. The comparison of long-term data on nitrate reveals that the maximum nitrate concentration varies from 3 to 9 μM [5].

The maximum nitrate increases as a result of oxidation of particulate organic matter sinking from the euphotic zone. Processes that could decrease the nitrate concentration in the layer of the main pycnocline are: denitrification, utilisation by phytoplankton (in cases where the onset of the nitrate gradient is shallower then the base of euphotic zone), and winter convective mixing (if the intensity and depth of this mixing is sufficient to reach the upper part of the main pycnocline). It is unclear yet which of these processes are more important, but they all are relevant for the nitrogen cycle in the Black Sea waters. The seasonal variation in the total mass of nitrate in the layer of the main pycnocline is estimated to be up to $2 \cdot 10^5$ tons [11]. This amount is comparable in magnitude with the total annual input of nitrate by river discharges into the Black Sea. That is why the investigation of nitrate balance at the main pycnocline is extremely important for better understanding of the processes driving the Black Sea ecosystem.

4. Acknowledgements

The main part of this work was carried out under the sponsorship of NATO Science for Stability Program and Turkish Scientific, Technical Research Council (TUBITAK), and National Academy of Sciences of Ukraine (NASU). We also wish to thank the technicians and crew of R/V Bilim and R/V Professor Kolesnikov for their valuable contributions. Part of this work was supported by Grant No8000 from the International Science Foundation.

5. References

1. Skopintsev, B.A. (1975) *Formation of the present state hydrochemical structure of the Black Sea,* Leningrad, Gidrometeoizdat. (in Russian)
2. Murray, J.W., Codispoti, L.A., and Friederich, G.E. (1995) Redox Environments: The suboxic zone in the Black Sea, American Chemical Society Advances in Chemistry Series, No244, 157-176.

3. Murray, J.W. (1989) Unexpected changes in the oxic/anoxic interface in the Black Sea, *Nature*, **337**, 411-413.
4. Codispoti, L.A., Friederich, G.E., Murray, J.W., and Sakamoto, C.M. (1991) Chemical variability in the Black Sea: implications of continuous vertical profiles that penetrated the oxic/anoxic interface, *Deep-Sea Research*, **38**, No2a, 691-710.
5. Tugrul, S., Basturk, O., Saydam, C., and Yilmaz, A. (1992) Changes in the hydrochemistry of the Black Sea inferred from density profiles, *Nature*, **359**, 137-139.
6. Saydam, C., Tugrul, S., Basturk, O., and Oguz, T. (1993) Identification of the oxic/anoxic interface surfaces in the Black Sea, *Deep-Sea Research I*, **40**, No7, 1405-1412.
7. Basturk, O., Saydam, C., Salihoglu, I., Eremeeva, L.V., Konovalov, S.K., Stoyanov, A., Dimitrov, A., Cociasu, A., Dorogan, L., and Altabet, M. (1994) Vertical variations in the principle chemical properties of the Black Sea in the autumn of 1991, *Marine Chemistry*, **45**, No1-2, 149-166.
8. Bezborodov, A.A. (1990) Relationship of the hydrogen sulfide boundary and density structure of the Black Sea waters, *Reports of Academy of Sciences of Ukraine*, B, No12, 3-7.
9. Vinogradov, M.E. and Nalbandov, Yu.R. (1990) The influence of sea water density changing on the physical, chemical and biological properties of the Black Sea ecosystem, *Oceanology (Russian)*, **30**, No5, 769-777.
10. Konovalov, S., Romanov, A., Salihoglu, I., Basturk, O., Tugrul, S., Gokmen, S. (1994) Intercalibration of CoMSBlack-93a chemical data; unification of methods for dissolved oxygen and hydrogen sulfide analyses and sampling strategies of CoMSBlack-94a cruise, *Report of Institute of Marine Sciences, Erdemli - Turkey*, March, 1994.
11. Konovalov, S. (1994) The influence of the winter ventilation processes on the hydrochemical structure of waters in the Black Sea, *"Biochemical Processes in the Arabian Sea", US-CIS Arabian Sea Workshop*, 149-155.
12. Eremeeva, L.V., Konovalov, S.K., Romanov, A.S., and Ovsyaniy, E.I. (1994) Isopycnal analysis in investigation of spatial variability of hydrochemical vertical structure, *Materials of "International conference, Sevastopol, Crimea, September 6-11 1993", MHI, National Academy of Sciences*, 136-144.
13. Ovchinnikov, I.M. and Popov, Yu.I. (1986) Formation of the cold intermediate layer in the Black Sea, *Oceanology (Russian)*, **27**, No5, 739-746.
14. Latun, V.S. (1987) The process of formation of Cold Intermediate layer of the Black Sea in the central parts of cyclonic gyres, *Materials of the conference "Development of management of coastal marine environment", Sevastopol*, VINITI, No5804 - B87, part2, 343-359.(in Russian)
15. Bezborodov, A.A., and Novoselov, A.A. (1989) The new data on oxygen distribution near the oxic/anoxic interface in the Black Sea. Revision of previous point of view, *VINITI*, No6773-B89, 18pp. (in Russian)
16. Basturk, O., Tugrul, S., Konovalov, S.K, and Salihoglu, I. (1996) Variations in the vertical chemistry within three hydrodynamically different regions of the Black Sea, *this volume.*
17. Ivanov, L.I., Besiktepe, S., and Ozsoy. E. (1996) Black Sea Cold Intermediate Layer, *this volume.*
18. Eremeev V.N. and Bezborodov A.A. (1993) *The oxic/anoxic transition zone,* Academy of Sciences of the Ukraine, Marine Hydrophysical Institute, Sevastopol. (in Russian)
19. Ivanov, L.I., Besiktepe, S., Ozsoy, E., Duman, M., Demirov, E., and Diakonu, V. (1995) Recent changes in Black Sea pycnocline. *Proceedings of the Malta 1995 CIESM meeting.*
20. Shaffer, G. (1986) Phosphate pumps and shuttles in the Black Sea, *Letters to Nature. Nature,* **321**, 37-44.
21. Gusarova, A.N. and Sapognikov, V.V. (1989) Peculiarities of the vertical distribution of phosphates in the Black Sea, *Oceanology (Russian),* **29,** No4, 589-594.
22. Sapognikov, V.V., Bibikov, V.A., Faschuk, D.Ya, and Finkelshtein, M.S. (1985) The phosphate minimum in the layer of co-presence of oxygen and hydrogen sulfide in the Black Sea, *Oceanology (Russian)*, **25,** No6, 966-969.

SUSPENDED MATTER AS AN INDEX OF PRODUCTIVITY IN THE WESTERN BLACK SEA (APPLICATION FOR PRODUCTIVITY AND EUTROPHICATION CONTROL)

S. V. VOSTOKOV
P. P. Shirshov Institute of Oceanology, Krasikova 23, Moscow 117851 Russia

Abstract. Suspended matter distribution and composition in relationship with different productivity parameters were investigated in the western part of the Black Sea (BS) for better understanding the scales of river influence and eutrophication in the area. Good correspondence between the total amount of suspended matter (SM), particulate organic matter (POM), total plankton biomass (Bo), algae biomass (Bp) and primary production (Pp) spatial variability is pointed out. The SM concentrations in the western BS change in the range of 0.3-7.0 mg/l, dependent on the level of productivity and river influence. The organic matter contribution to total SM shows general tendency of its insignificant growth from the open sea to the coastal regions. In surface waters the POM/SM ratio rises from 40% in the open sea, to 70% in shallow, more productive regions and from 33% to 55% in the euphotic zone respectively. Below the layer of photosynthesis, the OM portion in suspended material varies in the range of 18-28 without essential difference between shelf and open waters. The role of living biomass in the SM is found to elevate from 11% in the open and outer shelf regions, to 22-26% in shelf zone, on the average. The suspended matter composition analysis shows biogenic indigenous origin of the SM in the most part of the western Black Sea shelf. Results suggest the conclusion that the total suspended and particulate organic matter spatial variability reflects the production processes development in the western BS, induced by the river nutrient inflow and local eutrophication. The possibility of monitoring Black Sea productivity, by in-situ and satellite measurements of suspended matter and its components is discussed.

1. Introduction

The suspended matter (SM) studies in the Black Sea touches upon the interests of different marine disciplines: biology, geology, geochemistry, optics and etc. It is also important for monitoring aquatic environments and remote sensing programs focused on the river influence and eutrophication control.

E. Özsoy and A. Mikaelyan (eds.), Sensitivity to Change: Black Sea, Baltic Sea and North Sea, 211–221.
© 1997 *Kluwer Academic Publishers.*

The western and north-western parts of the Black Sea are characterised by considerable river inputs and eutrophication. Satellite images show the complicated time development of gradient structures existing in close correspondence with river inflows and water mass circulation. With respect to salinity [16], the Danube's influence is noticeable in Romanian and Bulgarian waters. According to satellite information, the suspended matter enriched zone is well defined along the western coast of the Sea extending from the source region to the Bosporus. Differentiation and redistribution of the SM, carried by Danube and other rivers, are the important factors responsible for the SM content and composition in the coastal area. The riverine material, being mixed with marine suspended matter, creates a complicated heterogeneous system. The rate of substitution of terrain suspensions by biogenic matter of marine origin and the resulting suspended matter content and composition depends on biological, chemical and mechanical settling intensity, transport by currents, production-destruction processes, and many other factors.

The river input has dual influence on the fields of SM in coastal zone. The inflow of Danube waters, containing about 100 times higher levels of suspended matter than the adjacent coastal water masses [10], considerably increase concentrations of SM in the regions of discharge. Organic compounds of the river inflow being involved in production cycles of heterotrophs and myxotrophs serve as an additional source of SM represented by living biomass. Large amounts of nutrients in the river waters, with the addition of the regenerated nutrients, directly stimulate primary production. Progressive eutrophication of the western BS, which has resulted in excessive growth of primary productivity [20,4,5], greatly influences the SM content and composition. Explosive development of productivity found in the vicinity of estuarine areas [3,4] leads to fast substitution of terrigenous material by biogenic suspended matter of indigenous origin.

The goals of the present first step of investigation are to study SM distribution, composition, and spatial variability together with other parameters of productivity, and in relation to the river influence and increased production in the western BS; to compare the relative contributions of the main sources of SM in the western BS, to determine their role in suspended matter formation, to validate the SM determinations, and to demonstrate the use for the assessments and control of western BS productivity and eutrophication based on ship and satellite observations.

2. Materials and Methods

The data were mostly collected during an ecosystem expedition - the 6th cruise of R/V "Vitiaz " in April - May 1984 (Figure 1). Water samples were taken by 150-l organic glass bottles from 5-12 predetermined depths based on examination of hydrological, hydrochemical, optical and biological vertical gradients by special instruments [7] and the previous data on the SM and POM vertical gradients [10,11,19,23,26]. The sampling strategy was aimed to determine the essential gradients of the ecosystem vertical structure. At each depth, .the ecosystem parameters including biomass of

plankton groups, primary production (Pp), chlorophyll a concentration (Chl), bacterial activity, total suspended matter (SM), particulate organic matter (POM), important nutrients etc., were measured in water samples by methods described in [7].

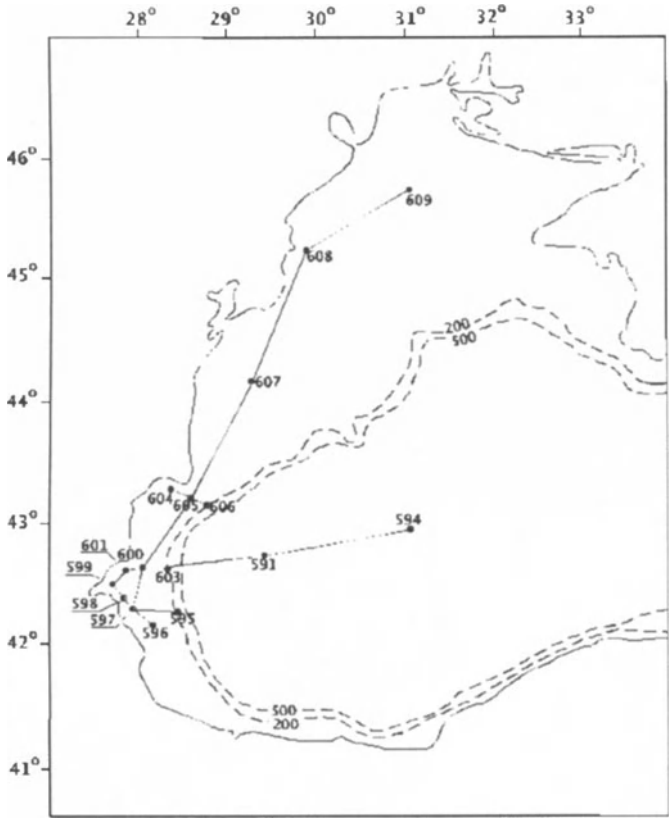


Figure 1. Stations map of the 6th cruise of R/V "Vitiaz" in the western part of the Black Sea (April-May 1984)

The amount of suspended matter, collected on specially prepared [8,15] membrane filters CINPOR (pore size 0.7-0.8 μ) was measured as the difference in weight between washed and dried filters before and after filtration with 5% accuracy. POM was collected at each depth by mild filtration of 2-10 litter sub-sample through pre-combusted Whatman GF/C glass fiber filters (effective pore size 0.8 μ) Particulate organic carbon content was determined in frozen specimens with CHN-autoanalyser and also, by modified wet combustion method [14,27] in parallel. The results were transferred to POM dry weight by taking into account the fact that organic carbon constitutes 50% of organic matter by weight.

3. Results and Discussion

3.1 SUSPENDED MATTER DISTRIBUTION

The analysis of the data (Figures 2,3) shows the absence of sharp gradients in SM distribution in the deep sea regions, adjacent to the western shelf. The SM concentrations in the open sea regions (0.3-1.0 mg/l) is in agreement with previously observed values [10,23]. Vertical distribution of SM in the deep sea oxic layer (Fig. 2) has some important features to be mentioned. Maxima of the SM concentrations (0.8-1.0 mg/l) usually occur in the upper 30-40 meter layer, above the seasonal pycnocline,

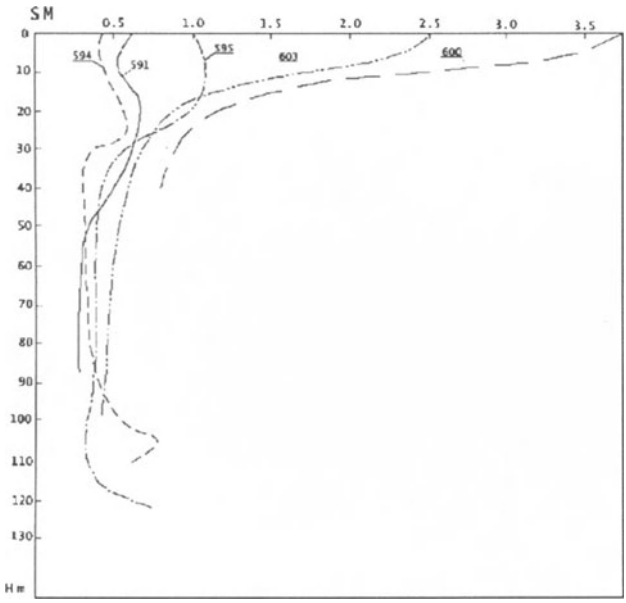


Figure 2. Vertical distribution of suspended matter - SM (mg/l) in the open sea and coastal zone.

and coincide with POM maxima everywhere (Figures 2,3). Between depths of 40-100m, the SM concentrations are nearly uniform, with values of 0.3-0.4 mg/l. The distinct increase of SM (up to 0.7-0.8 mg/l) at depth, known as the "deep layer of high turbidity" [18,19] is usually found in suboxic zone at depths of 100-140 m. The suspended matter from this layers differs by brown and black colour on the filters and suggests manganese suspension. Transition to the shelf area (Figures 2,3) is characterised by considerable increase of the SM and POM concentrations, in close correspondence with each other and also with plankton biomass, algae biomass and primary production [7], which is noticeable even from the continental slope waters (stations 595,603,606). The SM concentration growth is mainly expressed in the surface and the layer of photosynthesis. (Figures 2,3, Table 1). The surface concentration of suspended matter in the near-shore regions (3.0-6.0 mg/l) exceeds that

in the open BS by an order of magnitude. The contrast in SM concentration below 40-50m is not so sharp. Similar tendencies and variability scales are mentioned for POM spatial dynamics [12,13,14], suggesting similar controlling factors. The suspended matter distribution along the western coast (Figure 4) reflects the result of several interacting processes: general current and eddy transport of SM, mechanical, chemical, biological sedimentation; primary production and etc. Satellite information shows that the real distribution of suspended matter along the western shelf is much more complicated and variable than it can be reflected by the present material. However,

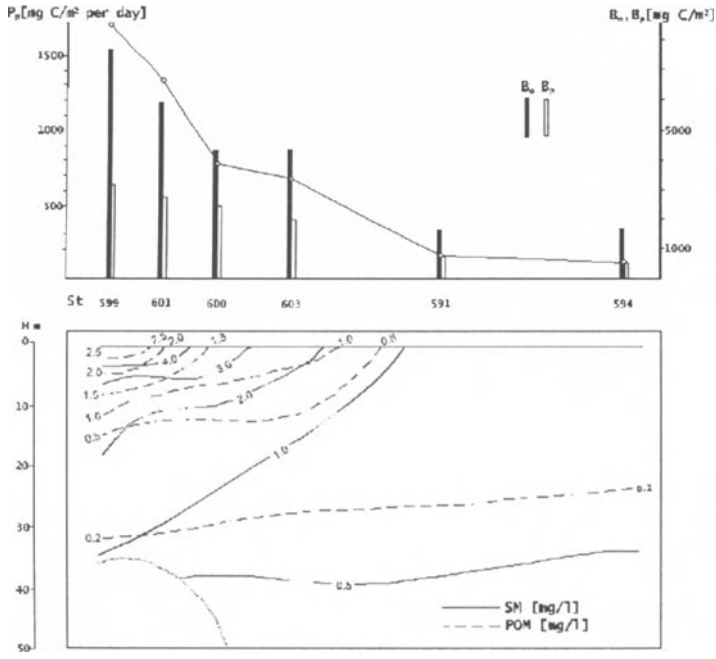


Figure 3. Spatial variability of suspended matter (SM), particulate organic matter (POM), plankton biomass (Bo)*, algae biomass (Bp)** and primary production (Pp)*** across the western Black Sea shelf. *Shuskina *et al*, **Sukhanova *et al.*, ***Vedernikov *et al.* [7].

they provide an an opportunity to study general tendencies of the SM spatial variability in relation to the processes mentioned. The surface SM content 9 miles offshore from the northern branch of Danube's mouth (St. 608) reaches 5.0 - 7.0 mg/l, decreasing sharply down to 0.8 - 1.0 mg/l near the bottom. The average turbidity of Danube's waters is 330 mg/l [17]. Suspended matter concentrations are 1.5 -2.0 mg/l at the surface and 0.3 mg /l in the bottom layer, in the middle part of the Romanian shelf. The shelf region opposite Cape Kaliacra is found to be a specific transition zone, dividing SM enriched waters, situated on the general direction of transport by the main BS current. The SM and POM concentrations in the region are in agreement with the open sea values. In contrast, the waters of Bulgarian shelf contain more suspended matter than the offshore regions situated on the main stream. Similar spatial dynamics

of SM and POM to be found, in good correspondence with Chl and Pp variability in the area [3,5] suggests that SM distribution in the main part of the western BS is controlled by production processes.

3.2 SUSPENDED MATTER COMPOSITION

The studies of suspended matter composition is intended to clarify the result of terrain material dilution by the substance of biogenic origin in different western BS regions

Table 1. Suspended matter and it's components in the western part of the Black Sea.

REGION	STATION	LAYER m	SM dry weight mg/l	POM mg/l (%)	PLANKTON dry weight mg/l (%)
OPEN SEA	591	0-1	0.60	0.30 (50)	
		Hp(50)*	0.60	0.20 (33)	
		0-100	0.45	0.14 (31)	0.050 (11)
	594	0-1	0.50	0.20 (40)	
		Hp(75)*	0.38	0.15 (39)	
		0-100	0.35	0.12 (35)	0.046 (13)
CONTINENTAL SLOPE AND OUTER SHELF WATERS	595	0-1	0.80	0.43 (54)	
		Hp(70)*	0.51	0.21 (42)	
		0-100	0.45	0.18 (40)	0.057 (13)
	596	0-1	0.90	0.56 (62)	
		Hp(40)*	0.45	0.25 (55)	
		0-100	0.48	0.15 (31)	0.053 (11)
	606	0-1	0.60	0.29 (48)	
		Hp(50)*	0.40	0.21 (52)	
		0-100	0.32	0.13 (41)	0.040 (13)
BULGARIAN SHELF WATERS	597	0-1	2.20	1.20 (55)	
		Hp(25)*	1.42	0.70 (50)	
		0-35	1.30	0.60 (46)	0.310 (24)
	599	0-1	3.80	2.65 (70)	
		Hp(20)*	2.50	1.25 (50)	
		0-30	2.10	1.00 (47)	0.540 (26)
	601	0-1	3.60	1.70 (48)	
		Hp(20)*	2.40	1.00 (41)	
		0-25	2.25	0.90 (40)	0.580 (25)
	600	0-1	3.30	1.50 (52)	
		Hp(15)*	2.70	1.00 (37)	
		0-35	1.80	0.60 (33)	0.340 (19)
	604	0-1	6.00	1.40 (23)	
		Hp(13)*	3.50	0.95 (27)	
		0-13	3.50	0.95 (27)	0.850 (24)
ROMANIAN SHELF WATERS	607	0-1	2.00	0.90 (45)	
		Hp(22)*	1.50	0.70 (46)	
		0-45	1.00	0.36 (36)	0.170 (17)
9 MILES FROM DANUBE'S MOUTH	608	0-1	5.80	2.30 (40)	
		Hp(12)*	3.50	1.20 (34)	
		0-20	2.60	0.75 (28)	0.240 (9)

* Hp- photosynthesis layer depth, determined by "in situ" primary production measurements [7].

and to realise river suspensions input and indigenous production influence on the SM spatial dynamics. For that purpose all the plankton groups biomass [7] and POM data are transferred to dry weight according to [6,21,28,29], taking into account that 1 mg of algae wet weight equals to 0.15-0.30 mg of dry weight, as a function of phytoplankton community structure; for microzooplankton the coefficient is taken as 0.16, and for bacteria and protozoans 0.20, respectively. The SM composition in different layers of the western BS is presented in Table 1. The results show that in the open waters surface layers, the SM consists by 40-50% of organic matter. In the layer of photosynthesis which depth was found by direct primary production determinations [7], the OM contribution to the SM constitutes 33-39%, which differs very slightly from the total oxic layer value (31-35%).

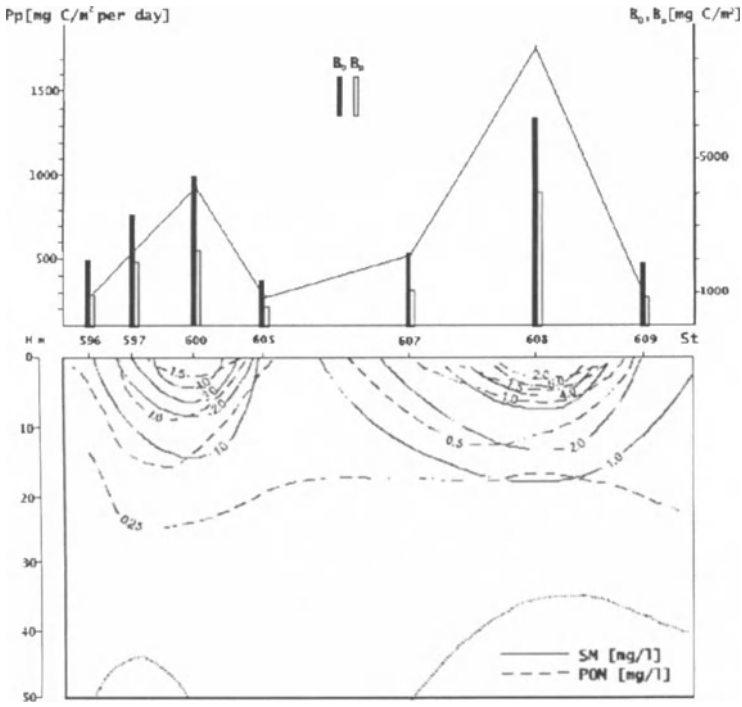


Figure 4. Spatial variability of suspended matter (SM), particulate organic matter (POM), plankton biomass (Bo)*, algae biomass (Bp)** and primary production (Pp)*** along the western Black Sea shelf. *Shuskina *et al*, **Sukhanova *et al.*, ***Vedernikov *et al.* [7].

In the continental slope and shelf regions the relative OM content in suspended matter varies between 20 and 70%. The POM contribution changes from 40% up to 70% in the surface waters, from 31% to 55% in the layer of photosynthesis and from 30 to 46% totally in the oxic zone respectively. The insignificant growth of the OM contribution from the outer shelf and open waters to the coastal regions is noted to be a general tendency in the region investigated. Below the photosynthetic zone, the role of

OM decreases down to an average 23 %, having a range of 18-28% in the area investigated. Generally the SM composition below the euphotic zone is not found to have distinct tendencies of variability across the region. The role of living biomass in the total amount of suspended matter in oxic layer is found to elevate from 11% in the open shelf waters to 22-24% in shallow and more productive regions.

The SM composition variability along the western BS coast is of particular interest. The role of organic fraction in SM in the vicinity of Danube mouth (St. 608) decreases from 40% at the surface down to 15% near the bottom (at 18-20m). With respect to POM/SM ratio, the SM from the surface layers differs greatly from Danube SM, which contains about 15% of organic matter [9]. In contrast, the suspended matter collected near the bottom is characterised by POM/SM ratio similar to riverine material. The SM from the middle part of Romanian shelf region consists of organic matter up to 30-50%, similar to the pelagic matter originated from biogenic sources [9]. Bulgarian near-shore waters are characterised by predominance (up to 70% in the surface) of the organic fraction in total amount of suspended matter and the maximal role of living matter (up to 26%). The rare phenomenon is in good correspondence with the maximum level of biosynthesis, mainly connected with microplankton without mineral skeletons (bacteria, protozoans, flagellates). The SM composition in the eutrophied waters of the Bulgarian and Romanian shelves are similar. The variability of SM composition is usually connected with different levels of productivity. On the average, the organic matter constitutes 50-60% of the SM in the surface coastal waters and about 40% of it in the water column. The living biomass contribution is 17-26%. The role of organic matter and living biomass increase with the primary productivity. Dilution influence of terrigenous matter is noticeable in the region of discharge and also in shallow waters, where turbidity of bottom sediments is possible.

Table 2. Parameters of linear regressions (Y = a + bX) between particulate organic matter (POM), plankton biomass (Bo), algae biomass (Bp), primary production (Pp) and SM in surface* and photosynthetic** layers of the western BS.

LAYER	P A R A M E T E R						NUMBER OF OBSERVATIONS
	Y	X	a	b	R	σ	
SURFACE	POM	SM	-6.5	0.26	0.98	0.02	15
PHOTOSYNT.	POM	SM	-1850	0.27	0.92	0.04	15
SURFACE	Bo	SM	-7.0	0.18	0.97	0.03	15
PHOTOSYNT.	Bo	SM	-3879	0.31	0.94	0.04	15
SURFACE	Bp	SM	-176	0.21	0.89	0.06	15
PHOTOSYNT.	Bp	SM	-1736	0.11	0.85	0.04	15
SURFACE	Pp	SM	-31	0.06	0.98	0.004	15
PHOTOSYNT.	Pp	SM	-1507	0.06	0.95	0.06	15

[SM] - * mg/m3 ; ** mg/m2 dry weight, [POM, Bo, Bp,] - *mgC/m3 ; ** mgC/m2, [Pp] - * mgC/m3 per day, ** mgC/m2 per day.

Analysis of the SM distribution and composition variability in relation to river influence and eutrophication suggest good correlation between SM content and the main productivity parameters: primary production, chlorophyll concentration, algae biomass, total plankton biomass, particulate organic matter and others. The results of regression analyses on the data are presented in Table 2. They reveal close

correspondence between the SM content and the main productivity parameters of the coastal ecosystem. The correlation coefficients increase from the total euphotic layer to the surface, where the maxima of photosynthesis usually occur [3,5]. This result also supports the close relationship between the SM and production processes in the major part of the BS western shelf.

3.3 THE MAIN SOURCES OF SUSPENDED MATTER AND SM FORMATION IN THE WESTERN BS.

The majority of suspended particles found in seas and oceans represent complicated systems, including mineral organic and living matter, tied inseparably. Subsistence forms of SM vary greatly in relation to the origin of particles and environmental conditions. However, a simple division of SM to organic and mineral fractions was used by some authors [11] for distinguishing the genetic types of particulate matter. With respect to organic/mineral proportion two types of suspended matter were distinguished in the BS [10]: (1) autochthonous particulate matter of biogenic origin, characterised by organic matter predominance, (2) terrigenous mineral material, typical for the regions of discharge. The Danube's estuarine area was considered to be a good example of the second type of suspended matter formation.

The SM composition analysis, at the vicinity of Danube mouth, reveals intensive substitution of terrigenous material by biogenic matter displayed even in the area of considerable river solid inflow. The primary production in that specific region exceeds 1.7 g $C/m^2/d$ and equals to 3.5 $g/m^2/d$ of OM or 5.0$g/m^2/d$ of dry algae biomass. At such rates of Pp, the total amount of SM in the water column will be reproduced by algae production in about every ten days.

It is often taken into consideration that river inflow, shore abrasion, bottom sediments, phytoplankton, zooplankton, and anthropogenic inputs are the main sources of suspended matter in the western BS waters [1, 17]. The comparison of relative contributions of terrigenous and indigenous matter can help determine the origin of SM in the Black Sea, and in its sub-domains. Estimates based on published data [9,20,17,22,24,25] show that primary production in the BS constitutes 300 million tons of dry matter annually, and river inputs - 25-87 million tons, abrasion of shores - 17 million tons, atmospheric deposition - 4 million tons respectively. In the shelf waters, the SM flux resulting from photosynthetic production of 120 million tons exceeds the terrigenous contribution. Estimations based on the zonality of western BS shelf primary production [3,4], and the average Pp values published in [20] reveal the predominance of phytoplankton production (90 million tons) in the annual SM flux to the coastal ecosystem, compared to the SM discharge of Danube, Dnestr, Bug and Dnepr rivers (7.5 million tons). A separate estimate of the riverine input of SM into the western BS (50 million tons), is based on the hypothesis that the major part of the solid discharge from western rivers is mainly suspended matter, in contrast with the grain size distribution of riverine solid material examined in [9,11]. The proximity of such estimates results from complexity in determinations of the seasonal and annual biosynthesis, and also from the assessment of the solid inflows remaining in suspended

form after the river-sea geochemical transitions. The results of relevant investigations [9,10,11] show that about 18% of the solid inflow from total western rivers remains in suspended form after penetration of the river waters into the Sea. The portion of riverine solid matter settled in the river-sea transition zone vary from 30 up to 80%, based on granulometric and chemical differentiation [17]. This process is mainly accomplished by biological mechanism of sedimentation. On the other hand, the annual photosynthesis production is a maximum value of the real phytoplankton contribution to SM. The algae biomass produced is consumed by zooplankton, and reduced by mortality, passive settling, and microbial and chemical degradation. Suspended matter formation in nature depends on a great number of processes to be taken to account. Nevertheless the relationships between the main sources are reflected in the SM composition investigated. The direct microscopic analysis in the region [26] supports the present conclusion of biogenic matter predominance in the SM. The indigenous origin of SM in the main part of the western BS and close correspondence of SM, POM, algae biomass, total plankton biomass and other productivity parameters, and their spatial variability makes it possible to interpret the turbidity structures observed by satellites [1], as a zones of high biological productivity induced by the Danube inflow and local pollution. In this sense, the POM and suspended matter contents in sea water, characterise the integrated result of production-elimination processes in marine ecosystems, and thus makes it possible to use the results of SM, POM, Chl and Pp determinations as parameters responsible for temporal and spatial variability scales of productivity. When used together, they can serve for assessment of river influence and biological seasonality, and changes in their balance. The practical application of these ideas are foreseen in the scope of ecosystem data analysis .

4. References

1. Aibulatov N.A., Novikova T.Z. (1984) Quantity distribution of suspended matter in shelf waters of the Black Sea. (rus.), Oceanology. Vol.2. N6. pp.960-968.
2. Vedernikov V.I., Demidov A. B.(1993) Primary production and chlorophyll in the deep of the Black Sea. ,Oceanology. Vol.33 N2. pp.229- 235.
3. Vedernikov V. I. (1987) Primary production in the Black Sea in spring 1984.,Modern state of the Black Sea ecosystem 1984. (rus.), Moscow. Nauka. pp. 105-117.
4. Vedernikov V. I., Bersenieva G.P., Burlakova Z.P.(1981) Primary production, chlorophyll and particulate organic matter in the Burgass Bay in summer (rus.), The western Black Sea ecosystem structure and functioning (Sozopol). Moscow. pp.67-86.
5. Vedernikov V.I., Vostokov S.V.(1984) Production of phytoplankton and particulate organic matter contents in some of the Black Sea regions. (rus.), Rep. All-Union Symp." Biogeochemistry of the continental margins of the ocean." (Nalchick 24-29 sept.1984) Moscow.pp.67-86.
6. Vinberg G. G. (1960) The primary production of water basins. (rus.), Minsk. BAS Publ. 329p.
7. Vinogradov M.E., Flint M.V. eds. (1987) Modern state of the Black Sea ecosystem 1984. (rus.) Moscow. Nauka.240p.
8. Vitiuk D.M.(1970) Determination of organic and mineral compounds of suspended matter on ultra filters (rus.), Hydrobiological journal. Vol.5. pp.111-116.
9. Vitiuk D.M., Dobrjanskaia M.A., Chistenko V.M.(1972) Some data on the organic suspended matter river inflow to the Black Sea. (rus.), Biology of the Sea. Vol. 27. pp.143-152.

10. Vitiuk D.M. (1970) The suspended matter and its components in the Black Sea. (rus.), Hydrobiological journal. Vol.11. N.1. pp.12-18.
11. Vitiuk D.M. (1983) The Suspended matter and its biogenic components.(rus.),Kiev. Naukova Dumka. 210p.
12. Vostokov S.V. (1987) Particulate organic matter in the open Black sea waters (rus), Modern state of the Black Sea ecosystem Moscow. Nauka. pp.59-63.
13. Vostokov S.V. (1987) Living and non living material in the particulate organic matter of coastal Bulgarian waters and adjacent open Black sea regions. (rus.), Modern state of the Black Sea ecosystem 1984. Moscow. Nauka. pp.68-77.
14. Vostokov S.V., Korjicova L.I. (1989) Peculiarities of the particulate organic matter distribution in the epipelagic Black sea. (rus.), Structure and production characteristics of the Black sea plankton communities. Moscow. Nauka. pp.246-255.
15. Vostokov S.V. (1988) The suspended matter and its components in the western part of the Black Sea. (rus.), "Geol. of Seas and Oceans." Rep. 8th AllUnion school mar. geol. vol.3 Moscow. 73-75.
16. Markov H.T. (1981) About river waters transfer and distribution from the north-west along the Bulgarian coast.(rus.), Rep. GOIN. Vol.158. pp. 28-34.
17. Mitropolskiy A.Yu., Bezborodov A.A., Ovsianiy E.Yu. (1982) Geochemistry of the Black Sea.(rus.), Kiev. Naukova Dumka. 142p.
18. Neuimin G.G. (1970) Stable deep-water turbidity layer in the Black Sea. (rus.), Mar. Hydr. Res. Vol.1. N.47. Sebastopol. Publ. MGI. UScA. pp.178-191.
19. Neuimin G.G. (1973) Optical researches of the Black Sea.(rus.), Rep. All Union Symp. Res. of the BS and MS. Sebastopol. Vol.1. Kiev. Naukova Dumka. pp.81-88.
20. Sorokin Yu.I. (1982) The Black Sea.(rus.), Moscow. Nauka. 216p.
21. Sushienia L.M. (1975) Quantitative characteristics of crustacean's feeding. (rus.), Minsk. Nauka and Technika. Publ. 207p.
22. Trimonis E.S. (1975) The main features of the recent sedimentation in deep Black Sea region.(rus), Hydrol. and Geol. Res. of the Bs and .SAS.Publ. pp.182-195.
23. Trimonis E.S. and Shimkus K.M. (1976) Suspended matter quantitative distribution in the Black Sea.(rus.), Oceanology. Vol.16. N.4. pp. 648-654.
24. Shuisky Yu. D. (1981) Sedimentary balance research experience in the coastal zone of the Black Sea.(rus.), Geol. Journ. Vol.41 N.5. pp. 82-89.
25. Hmaladze G.P. (1978) Solid inflow of the Black Sea Caucuses rivers.(rus.), Leningrad. Hydrometeo.Publ. 166p.
26. Dmitrov P.S., Stoanov A.S., Sthereva G.P. (1981) On the distribution of suspended material in the western part of the Black Sea area, Rep. BAN. Vol.34. N.10. pp.1429-1431.
27. Parsons T.R., Maita Y., Lall C.M. (1984) A manual of chemical and biological methods for seawater analysis, Oxford, 180p.
28. Platt T.., Brian I. (1973) Caloric content of phytoplankton, Limnol. Oceanogr. Vol. 18. N.2. pp. 306-310.
29. Stratman R.R. (1967) Estimating of the organic carbon content of phytoplankton from all volume of plasma volume, Limnol. Oceanogr. Vol. 22. N.3. pp. 411-418.

PARTICULATE ORGANIC MATTER OF BLACK SEA EUPHOTIC ZONE: seasonal and long-term variation of spatial distribution and composition

Z. P. BURLAKOVA[#], L. V. EREMEEVA[+], S. K. KONOVALOV[+]*
[#]*Institute of Biology of the South Seas, National Academy of Sciences of Ukraine (IBSS) 33500 Ukraine, Crimea, Sevastopol, Nakhimova 2*
[+]*Marine Hydrophysical Institute, National Academy of Sciences of Ukraine (MHI) 33500 Ukraine, Crimea, Sevastopol, Kapitanskaya 2*

Abstract. Results from 10 years of observation on particulate organic matter (POM) distribution and composition in the euphotic zone of the Black Sea, and information on chlorophyll-a and phaeophytin have been prepared as joint data set to analyse the long-term and seasonal variations of POM distribution. Seasonal variations of POM distribution and composition (C/N and C/Chl) are revealed for the 1985-1994 period, while long-term changes, if any, remain within the bounds of uncertainty of the methods (20%). Peculiarities of POM distribution and composition have been discussed for different seasons and for the month of March, which is a unique period in the Black Sea environment. Explanations are suggested for the observed peculiarities.

1. Introduction

Suspended or particulate organic matter is one of the basic properties of any marine ecosystem, which acts as a bridge between living and non-living matter in the sea. POM is a result of primary biological processes in the sea, except in the near shore regions which are under the influence of river inflows and man-made discharge of pollutants. The quantity of POM in the euphotic zone is the measure of primary biological productivity and a basis for the total productivity of any marine ecosystem. However, the distribution and composition of POM result not only from production, but also from degradation, sinking, and lateral dynamics of water even for regions far from the coast. That is why preliminary data published by Finenko [1], Filipov [2], Vityuk [3], Vostokov [4,5], and some other investigators were extremely important for understanding of the general peculiarities of POM distribution, but an extended, regular data set is needed to investigate the spatial, seasonal, and long-term variations of POM distribution and composition in the Black Sea waters.

E. Özsoy and A. Mikaelyan (eds.), Sensitivity to Change: Black Sea, Baltic Sea and North Sea, 223–238.
© 1997 *Kluwer Academic Publishers.*

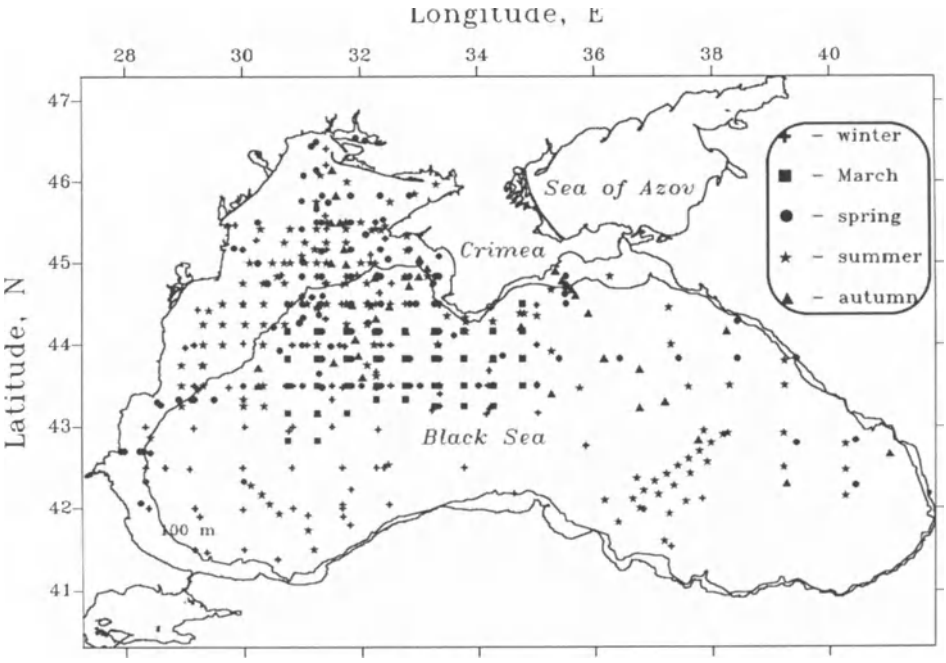


Figure 1. Position of stations where POM data have been obtained from 1985 to 1994.

Periodic investigations of particulate organic matter (POM) in the Black Sea have been carried out by MHI and IBSS since 1984. Observations at 460 oceanographic stations for all seasons (118 for spring, 140 for summer, 46 for autumn, 117 for winter, and 41 for March, as a unique month for the Black Sea ecosystem) have been carried out for nearly all parts of the Black Sea (Fig. 1) and results have been incorporated into the general data set. Part of these data were analysed and results published by Burlakova [6,7], and Agatova [8]. In here we summarise them, analysing the total data set in order to discuss the following questions:

-peculiarities of spatial distribution of POM in the Black Sea;
-seasonal and interannual variations of the POM distribution;
-C/N and C/Chl composition of POM in the Black Sea;
-spatial and temporal variations of C/N and C/Chl composition of POM;
-influence of natural and anthropogenic processes on the POM production, composition and distribution in the Black Sea.

2. Methods

Samples of water were filtered through GF/F or GF/C (for winter) fiberglass filters. Filters were pre heated at 350-400°C for 18-20 hours. Volume of water depended on total amount of suspended material and was 0.5-5 liters. Filters planned for POC and

PON analyses were rinsed with 0.01N solution of hydrochloric acid and dried at 60°C. They were then kept in refrigerator in a dry box protected against pollution. Filters were analysed in the laboratory after cruise. CHN-analyser was used for determination of carbon and nitrogen. Chlorophyll-a was determined by fluorometric method [9].

3. Results and Discussion

Initial data set contains information on C:N:P composition of POM, and data on chlorophyll-a and phaeophytin concentration. A set of plots has been prepared for the analysis of different questions on POM behaviour in Black Sea waters in separate seasons. There are plots of vertical and spatial distribution (for the surface, and the euphotic zone) of carbon, nitrogen, and phosphorus of POM, as well as their relation to chlorophyll-a concentration. Only a small part of them is presented here to enable us discussing the above mentioned questions. We shall discuss the mean values for euphotic zone, as a more representative measure.

A complex vertical distribution of POM exists in the Black Sea euphotic zone, as well as in the underlying region [4,5,7], depending greatly on temperature, light penetration and transparency of water, vertical and spatial dynamics of water, properties of nutrients source, vertical density structure of the water column, and, of course, on the properties of phytoplankton, zooplankton, and bacterial communities. On the other hand, the euphotic zone mean values let us compare different regions of the sea.

The spatial distribution of POM should vary from one year to another as a function of climatic changes. Some "catastrophic" events in the Black Sea environment have been observed and announced for last decade: extremely intensive blooms ("red" tides) of phytoplankton [10], invasion of *Mnemiopsis leidyi* [11], great increases in nutrient discharge by rivers [12], decreases in fish stocks [13], a possible upward shift of the oxic/anoxic interface [14], and even a total crisis of the Black Sea [15]. Nevertheless we have revealed that long term variations of POM properties in the Black Sea waters for individual seasons from 1985 to 1994 are less then the usual errors of POM analysis (~20%). On the other hand, the seasonal variations in the spatial distribution and composition of POM are clear and well defined for individual regions of the sea. Therefore, we used the 10-year data set to prepare synthetic plots for separate seasons (Figs.2-11). The conclusion on seasonal and long-term variations of POM properties is more important for investigation and modelling of general peculiarities of the Black Sea environment. It means that all observed events are local or temporary, they do not influence primary biological properties of the Black Sea environment.

There is clear distinction between the seasonal, spatial variations of POM distribution / composition in comparison to long-term changes (Figs.2-11). Spatial distribution is not uniform for all seasons, but it is more pronounced for spring and summer (Figs.6-9).

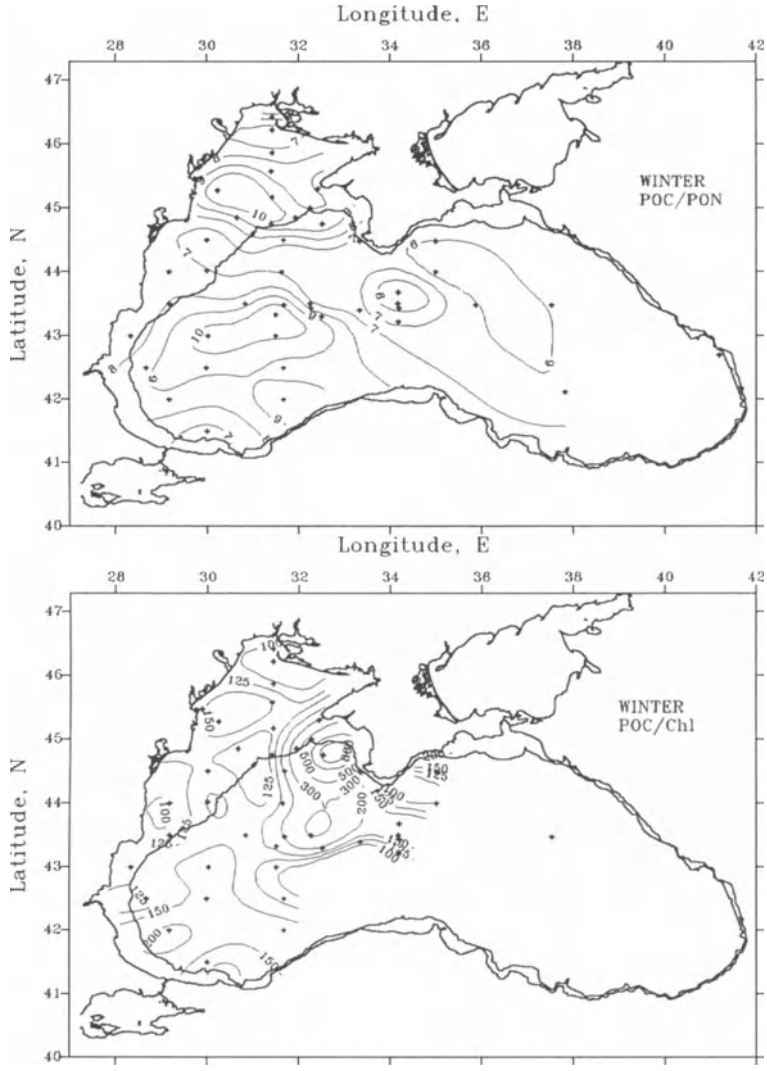


Figure 2. Distribution of POC/PON and POC/Chl values in winter.

The Black Sea could be divided into two parts with radically different oceanographic conditions - the deep sea part and the shelf regions. The shelf (here we use 100m depth as the boundary between deep part and shelf) constitutes ~25% of the total area of the sea. These two parts are comparable in size, and greatly influence each other. The POM composition and distribution in the shelf waters is a function of nutrient discharge by rivers, temperature of water, light penetration, transparency of water, local wind induced dynamics, and exchange with the deep part of the sea. In the deep part of the sea the general circulation, the intensity of vertical mixing, as well as the

light penetration and temperature are the main determinants of POM properties. Therefore, separate analyses of POM are required in the shelf and deep waters.

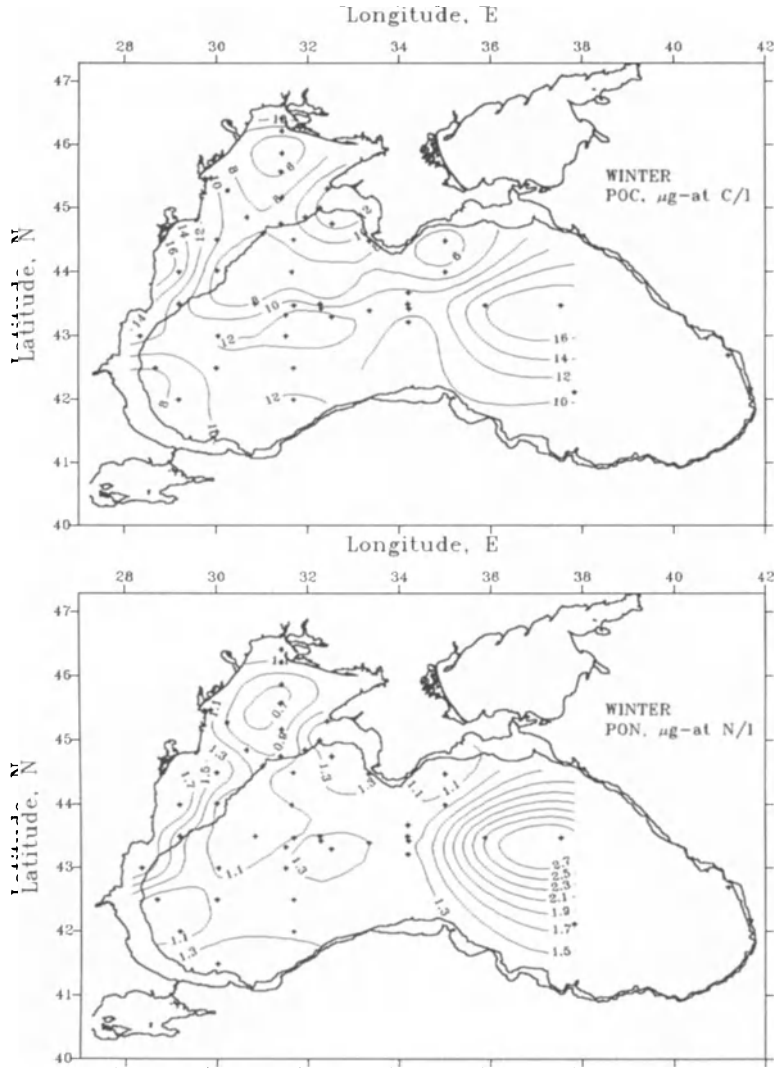


Figure 3. Distribution of POM in winter.

3.1. WINTER

Winter is the season of the smallest concentration of POM in the euphotic zone of both shelf, and deep parts of the sea (Fig.2). The lowest values occur in the central part of the shelf. Concentrations are generally low, even in the region of river influence, where

nutrient concentration is elevated. This low productivity results from poor light penetration and low temperatures.

POM concentrations are increased only in the cores of the main cyclonic gyres (especially in the eastern cyclonic gyre) at the central part of the sea (Fig. 2). Upward flux of nutrients, resulting from winter convective mixing, and higher temperature of deep waters compared to the shelf are the reasons for this spatial distribution of POM.

C/Chl values (as the indicator of biological productivity) vary from 80 to 150, all over the sea, except the region south-west of Crimea (Fig. 2). These values (less then 150) demonstrate that the fraction of living material in POM is typical for the active natural phytoplankton community. Some disagreement exists between C/Chl and C/N spatial distribution. Noting that the total POM concentration is low, we can suppose that spatial distribution and composition of POM in winter is a result of the following processes:

- intensive hydrodynamic processes, and especially, extremely active vertical convective mixing prevent accumulation of POM (living or dead) in euphotic zone;
- above mentioned intensive hydrodynamic process together with low temperature and weak light penetration restrict activity of phytoplankton community;
- low temperature is the reason for slow POM degradation, and chlorophyll-a decomposition, so that C/N and C/Chl do not demonstrate the state of phytoplankton community in winter.

3.2. MARCH

The month of March is a unique time for the Black Sea environment, although this typical period may shift slightly from one year to another, depending the climatic conditions. This is the period when the intensive winter storms cease, and the seasonal pycnocline starts to develop (vertical stability of water column increases), after the winter convective mixing has led to an upward flux of nutrients. These ideal conditions are even better defined at the cores of the central cyclonic gyres [16], because of their specific vertical hydrological and hydrochemical structure. The temperature of the water in the central part of the sea (~7°C) is usually higher then the shelf regions (3-5°C) during this period. As a result of all these conditions, extremely intensive phytoplankton blooms can occur in the core region of the main cyclonic gyres [17].

Concentrations of particulate organic carbon (POC) and particulate organic nitrogen (PON) are twice as greater than the mean values in winter (Figs.2 and 4). Low values of the C/Chl ratio (50-60) and values of C/N close to the Redfild ratio demonstrate that all POM is living organic material of active phytoplankton community.

3.3. SPRING

The distribution and properties of POM at Black Sea shelf regions in spring (Fig.6-7) provide an excellent example of phytoplankton bloom in shallow marine basins. Concentrations of POC (100-120 μg-at C/l) and PON (15-17 μg-at N/l) achieve

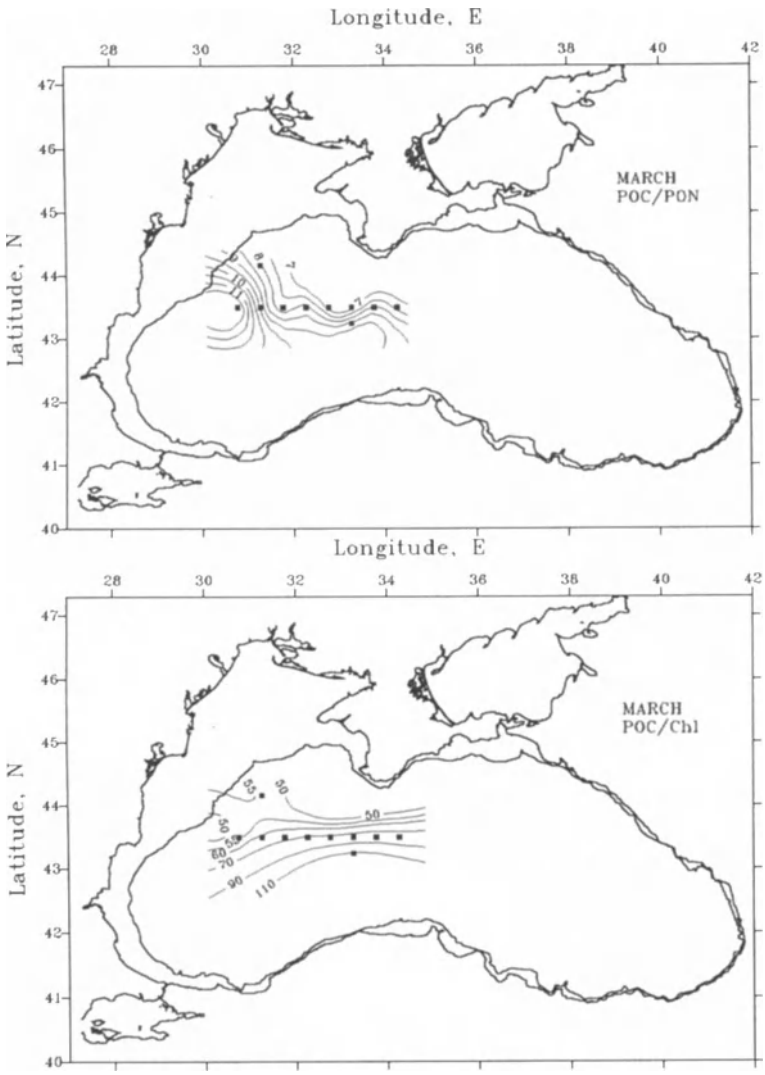


Figure 4. Distribution of POC/PON and POC/Chl values in March.

extremely high values near the Danube and Dnieper mouths, where concentrations of nutrients are elevated. These conditions lead to oxygen deficiency later when POM is oxidised, but initially the oxygen concentration could get as high as 160-180% of saturation values. Area of intensive blooming of phytoplankton, and area of high POM concentrations depends on the combined effects of nutrient discharge by rivers, wind, temperature, and solar irradiance; on the average this region is equal to 1/3 of the north-western shelf. The southern, central, and north-eastern parts of the shelf (except

the most near-shore, shallow part near Crimea) are less productive. But, even in these areas, the concentrations of POC and PON are 1.5-2 times as high as those in winter.

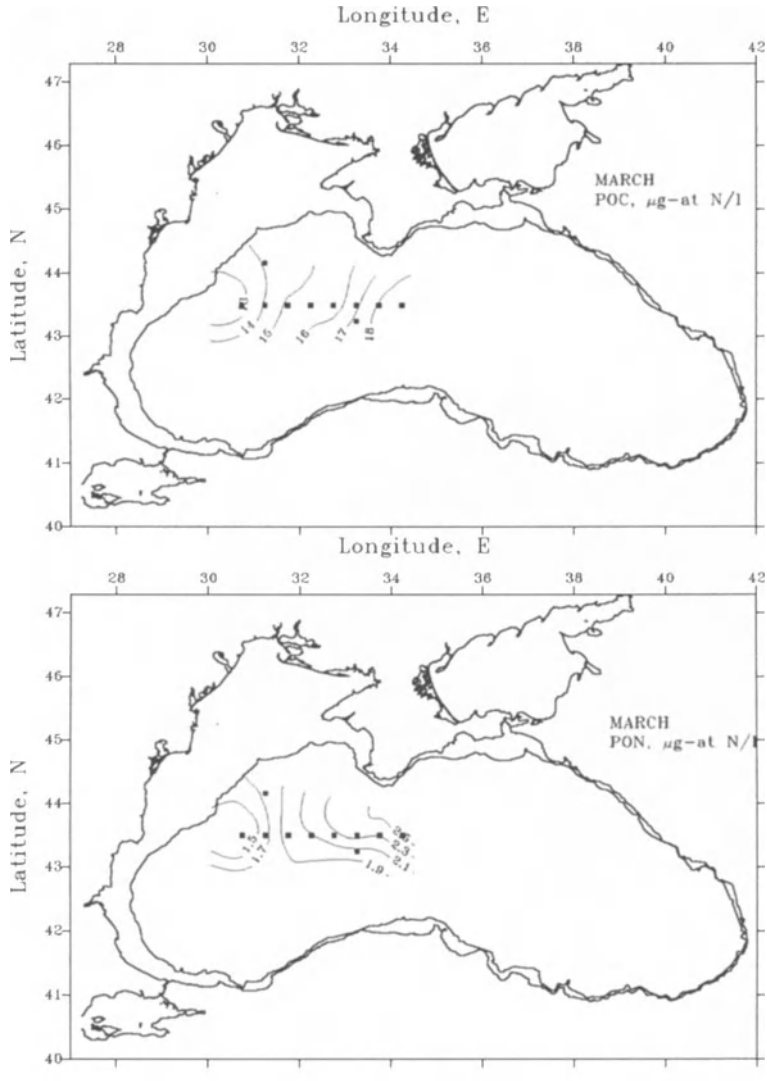


Figure 5. Distribution of POM in March.

The C/N ratio is the same as the Redfield value. The C/Chl ratio is not higher than 300. There is no doubt that spring is the most productive season for the shelf. After winter-time ventilation, there is a lack of detritus, the destruction of POM is weak and it has not influenced C/N and C/Chl ratios yet.

The concentration of POM in the deep part of the sea is nearly the same as it was in March during the post-winter phytoplankton bloom (Fig.6). But the C/N ratio, and especially C/Chl ratio are actually higher (Fig.7). It means that living POM of the deep part of the sea starts to transform into detritus and the structure of phytoplankton community starts developing into the summer situation, with great importance of re-utilisation of nutrients.

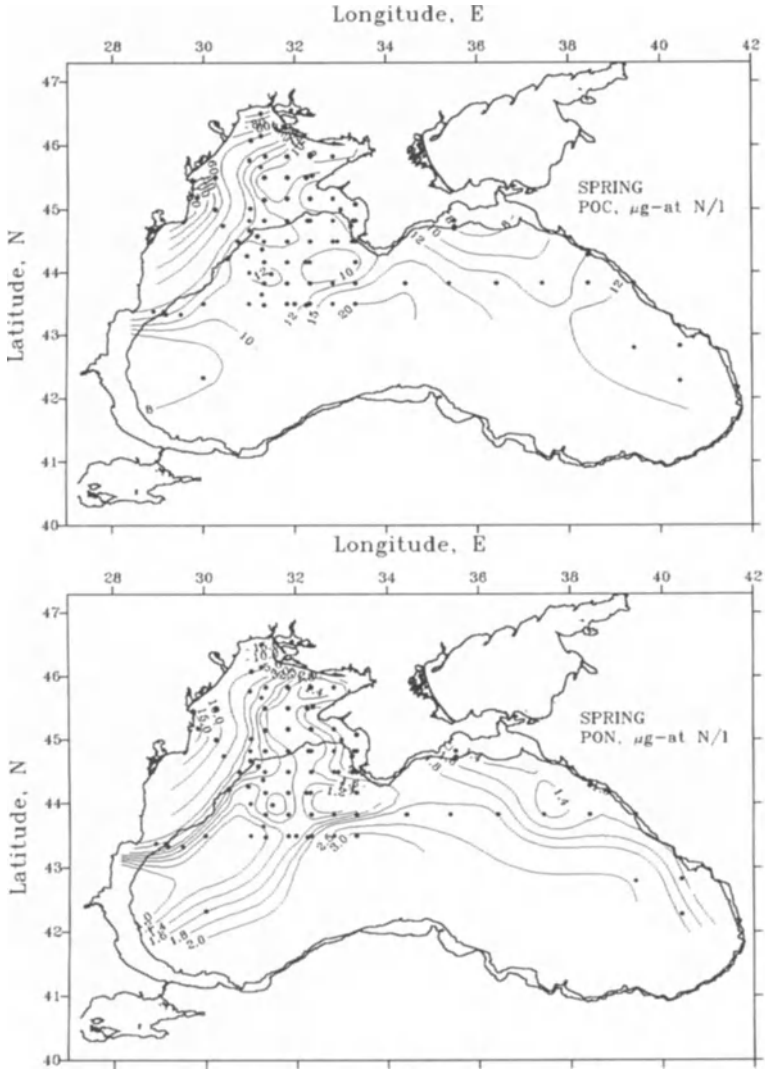


Figure 6. Distribution of POM in spring.

3.4. SUMMER

There are no difficulties to describe and to explain transformation of POM distribution and composition in the Black Sea waters from spring to summer (Fig.8-9).

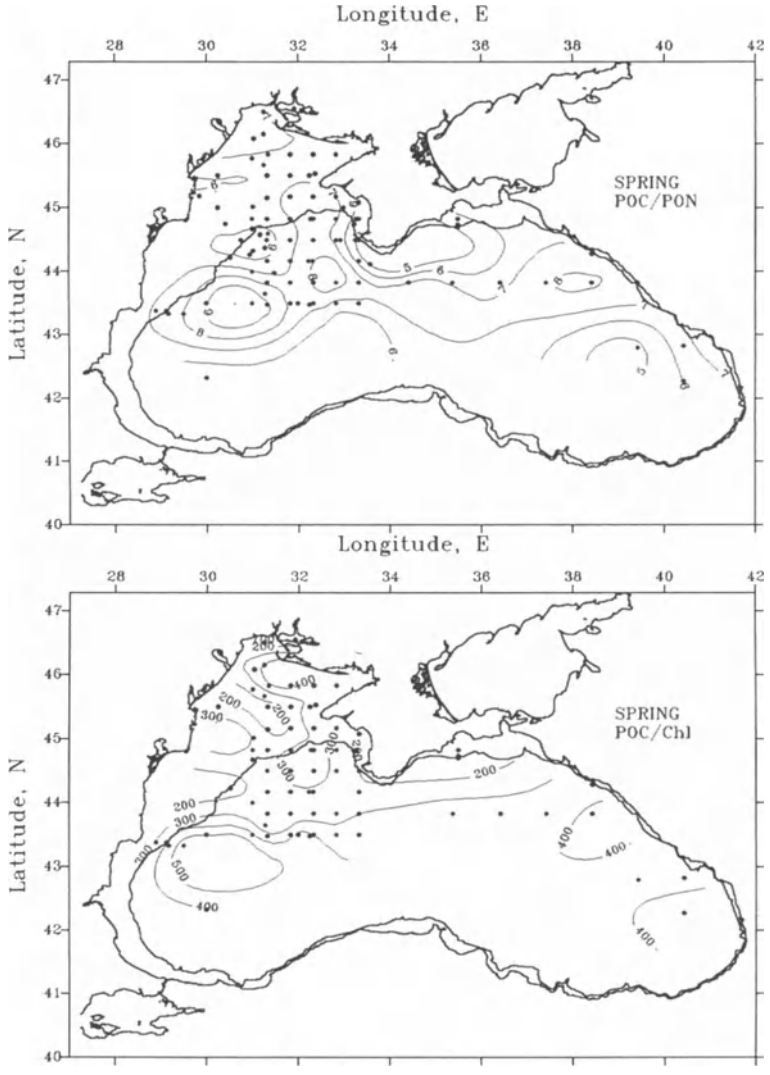


Figure 7. Distribution of POC/PON and POC/Chl values in spring.

The concentration of POM in deep part of the sea multiplies two times. But C/N (up to 12) and C/Chl (up to 1300) values confirm that the main part of POM is non-living and hardly destroyed material. The sharp seasonal pycnocline serving as the bottom for

the surface waters provides accumulation of POM in the euphotic zone, but restricts the upward flux of "new" nutrients from water below it. As a result, the phytoplankton community exists mainly due to the re-utilisation of nutrients, POM and dissolved organic matter.

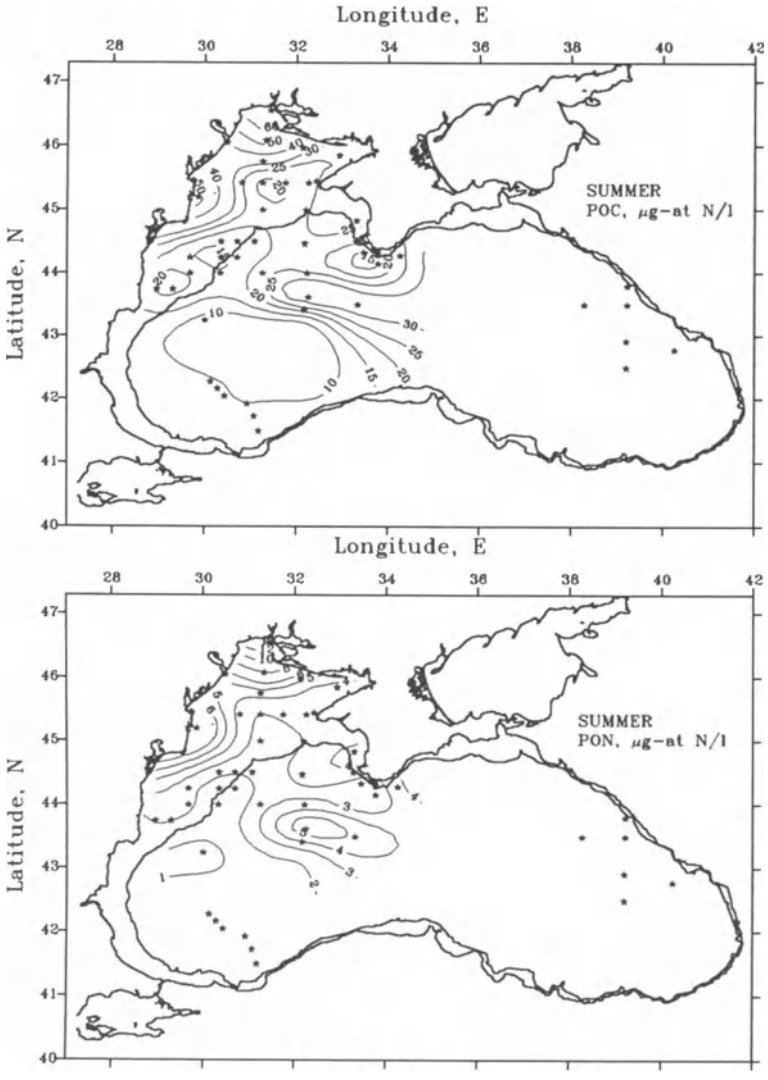


Figure 8.Distribution of POM in summer.

The highest concentrations of POM are located at shelf in the part, where Dnipper-Danube influence is active (Fig.8), but values and area of this region are 2-3 times less then those in spring. The C/Chl ratio is less then 200 in the region (Fig.9). Together

with low values (6-7) of the C/N ratio, it means that the area of Dnipper-Danube influence is the only region of "new" production in the Black Sea. The amount of "new" POM seems to be significant, because the C/N ratio is about 7 nearly all over the shelf, even for the central and north-eastern region of increased C/Chl values (Fig.9).

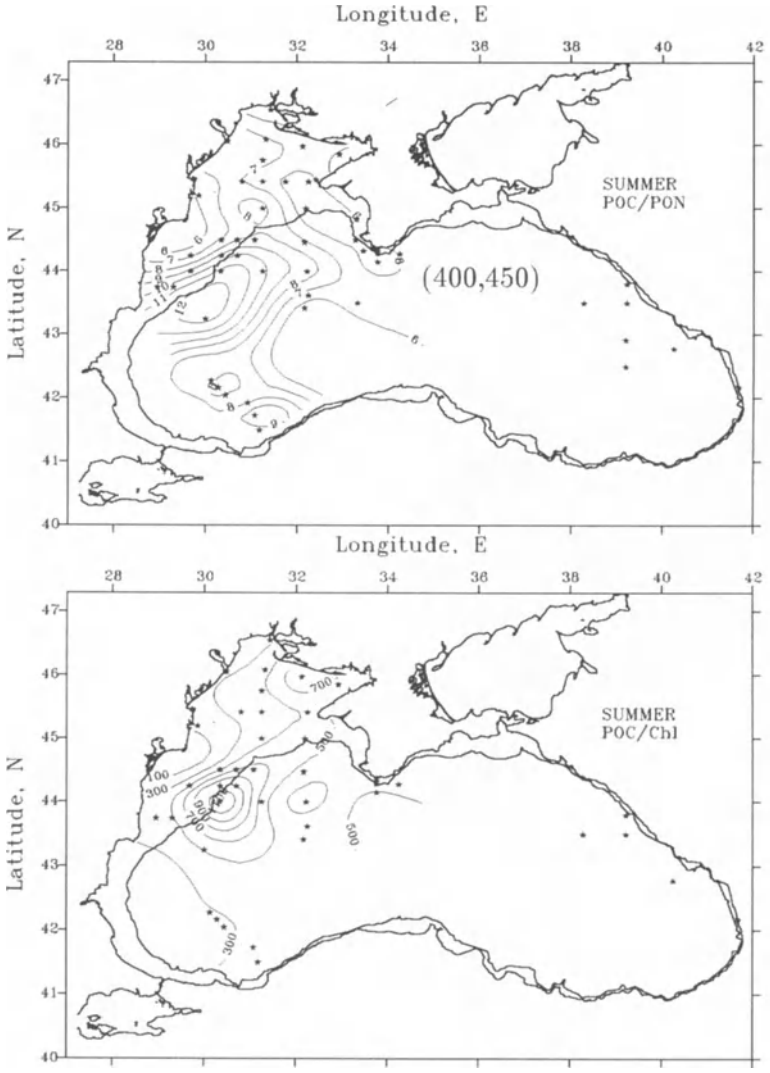


Figure 9. Distribution of POC/PON and POC/Chl values in summer.

3.5. AUTUMN

Concentrations of POM decrease and values of C/N and C/Chl ratio increase from

summer to autumn (Fig.10-11). This change seems to be reasonable. Part of the POM has precipitated below the euphotic zone or it has been consumed by zooplankton. These processes do not change the C/N ratio of POM that has been increased from summer to autumn (Figs.9 and 11). But the phytoplankton community of the deep part of the Black Sea has been using "recirculated" nutrients since the early summer.

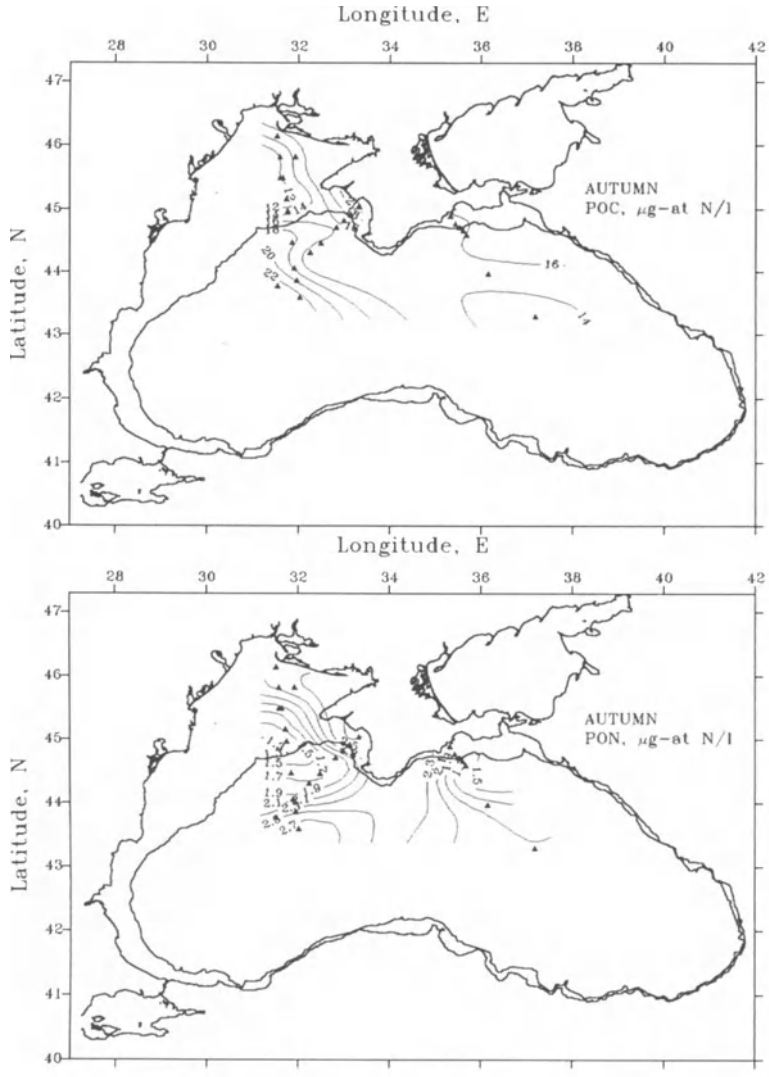


Figure 10. Distribution of POM in autumn.

Part of "new" POM is very small. Labile part of POM has been reutilised. POC concentration has decreased 1.5 times while PON has decreased 2-2.5 times from

summer to autumn. As a result, the C/N ratio is higher than 8 for the deep part of the sea, but could be as mach as 12. The C/Chl ratio varies from 350 to 900 (Fig.11).

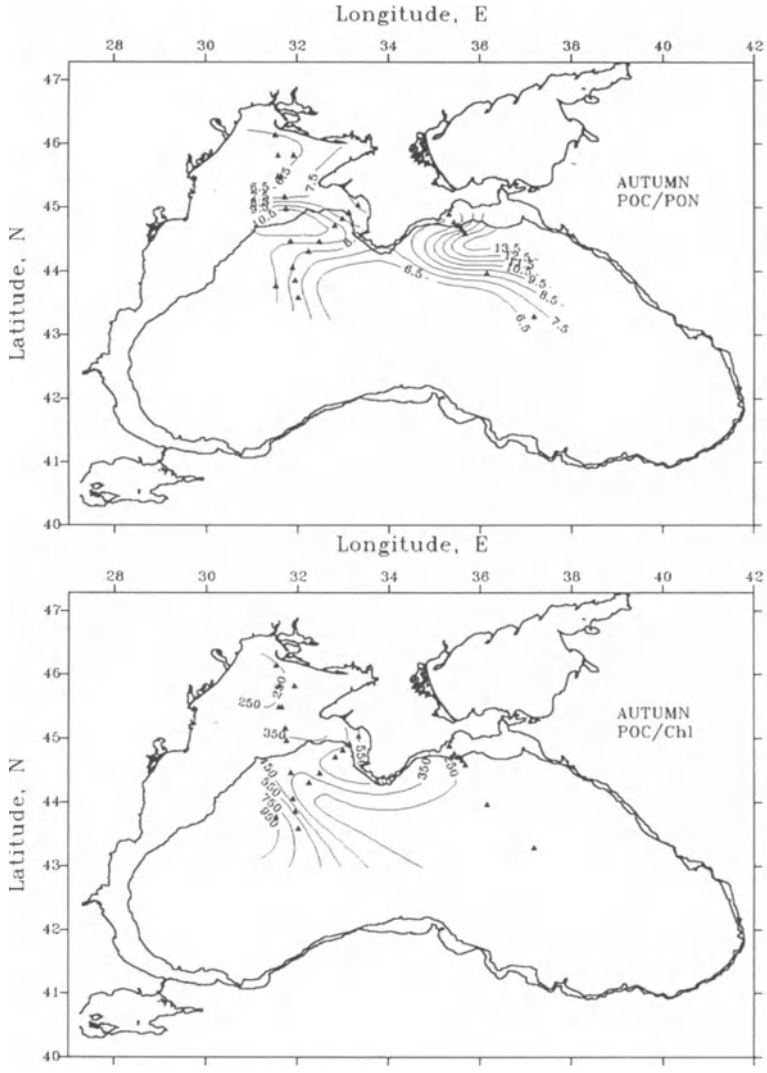


Figure 11. Distribution of POC/PON and POC/Chl values in autumn.

Concentrations of POM have decreased 1.5 times from summer to autumn at the shelf (Figs.8 and 10). But the C/N and C/Chl ratio has not changed for the same period (Figs.9 and 11). It seems to us that the shelf, and especially its western part near the Dnieper-Danube inflow, is the region where nutrients have not restricted productivity of phytoplankton community in autumn, as well as in summer. Decreasing duration of

day-time, irradiance, and nutrient discharge by rivers are the reasons of decreasing of POM concentrations at the shelf in autumn. But abrupt decreases of POM concentration will start with the beginning of winter storms, when the vertical structure of water column, and therefore the euphotic zone, will be destroyed, while temperature and light penetration will reach their lowest values (Figs.10 and 2) of the year.

4. Conclusions

The results of this discussion of the long-term and seasonal variations of POM distribution and composition in the euphotic zone of the Black Sea can be summarised under the following headings:

Seasonal variations of POM distribution and composition (C/N and C/Chl) are real, while the magnitude of the long-term changes are usually smaller than the uncertainty limits of the methods (20%) for the period from 1985 to 1994.

Five different periods of the year, rather then the four traditional seasons, are realised during the annual cycle of POM distribution in the euphotic zone of the Black Sea. This situation results from the presence of two vastly different ecosystems (deep part of the sea and shelf) in the Black Sea, leading to the conditions where the early spring (called here as "March") is the normal time of a spring phytoplankton bloom in the deep part of the sea, but this event occurs in late spring at the shelf region.

The deep part of the sea is the region where dynamics, intensity of vertical mixing, light penetration and temperature are the main determinants of POM properties. Spring is the only time for "new" production, in which the nutrients supplied into the euphotic zone by winter convective mixing are utilised by phytoplankton community. The ecosystem of the deep part of the sea persists mainly by re-utilisation of nutrients from early summer to autumn.

POM composition and distribution at the shelf depends on nutrients discharge by rivers, temperature of water, irradiance, transparency of water, and local wind induced dynamics. In contrast to the deep part of the sea, the shelf is the region where discharge of nutrients via Dnieper-Danube inflow provides intensive production of POM from spring to autumn. Recirculation of nutrients in the euphotic zone of the shelf is not important for the existing phytoplankton community.

5. Acknowledgements

Original data on the particulate organic matter and chlorophyll, have been obtained by participants of several cruises in the framework of National and International programmes carried out by Marine Hydrophysical Institute (National Academy of Sciences of Ukraine) and Institute of Biology of the South Seas (National Academy of Sciences of Ukraine). Part of this work was supported by Grant No8000 from the International Science Foundation.

6. References

1. Finenko, Z.Z. (1965) Organic matter of seston in the Black and Azov Seas, in *Investigation of plankton in the Black and Azov Seas*, Naukova dumka, Kiev, pp.12-17.
2. Filipov, V.S. (1980) Suspended organic carbon in the Black Sea aerobic waters, in *Ecosystems of the pelagic zone of the Black Sea*, Nauka, Moscow, pp.62-64.
3. Vityuk, D.M. (1975) Suspended matter and components of it in the Black Sea, *Hydrobiological journal (Russian)*, **11**, No1, 12-18.
4. Vostokov, S.V. (1987) Particulate organic matter in the central part of the Black Sea in spring of 1984, in M.E.Vinogradov and M.V.Flint (eds.), *Present state of the Black Sea ecosystem*, Nauka, Moscow, pp.59-67.
5. Vostokov, S.V. and Korzhikova, L.I. (1989) Distribution of particulate organic matter in epipelagic zone of the Black Sea (May-June 1986), in M.E.Vinogradov and M.V.Flint (eds.), *The structure and productivity of planktonic communities of the Black Sea*, Nauka, Moscow, pp.246-254.
6. Burlakova, Z.P., Eremeeva, L.V., and Krupatkina, D.L. (1988) C:N:P composition of suspended matter of western and north-western parts of the Black Sea, in V.N. Eremeev (eds.), Formation and seasonal transformation of hydrophysical and hydrochemical structure of the Black Sea, MHI AS Ukraine, Sevastopol, pp.162-172.
7. Burlakova, Z.P., Eremeeva, L.V., and Bezborodov, A.A. (1992) Vertical distribution of suspended organic matter in the Black Sea, *Reports of Ukrainian Academy of Sciences*, No4, 81-84.
8. Agatova, A.J., Burlakova, Z.P., Eremeeva, L.V., and Torgunova, N.J. (1992) Dissolved and suspended organic matter in the Black Sea during the winter-spring period, in *Investigation of the Tropical Atlantic Ocean*, VSP, pp.121-130.
9. Yunev, O.A. and Berseneva, G.P. (1986) Flurometric method for determination of chlorophyll-a and phaeophytin-a in phytoplankton, *Hydrobilogical journal (Russian)*, **2**, No2, 89-95.
10. Bodeanu, N. and Roban, A. (1975) Donnees concentrant la floraison des eaux du littoral roumain de Mer Noire avec la peridinium Exuviaella cordata, *Cero. Mar. Constanta*, No8, 31-42.
11. Vinogradov, M.E., Shushkina, E.A., Musaeva, E.I., and Sorokin, P.Yu. (1989) New settler in the Black Sea - Mnemiopsis leidyi (A.Agassiz) (Ctenophora: Lobata), *Oceanology (Russian)*, **29**, No2, 293-299.
12. Vinogradov, M.E., Sapozhnikov, V.V., and Shushkina, E.A. (1992) *The Black Sea ecosystem*, Nauka, Moscow, pp.88-96.
13. Zaitsev, Yu.P., Garkavaya, G.P., Nesterova, D.A., Polishuk, L.N., and Cokur, A.G. (1987) Present state of the north-western Black Sea ecosystem, in M.E.Vinogradov and M.V.Flint (eds.), *Present state of the Black Sea ecosystem*, Nauka, Moscow, pp.216-230.
14. Murray, J.W. (1989) Unexpected changes in the oxic/anoxic interface in the Black Sea, *Nature*, **337**, 411-413.
15. Mee, L.D. (1994) The Black Sea in Crisis: A Need for Concentrated International Action, *AMBIO*, **21**, No4, 278-286.
16. Konovalov, S.K. (1994) The influence of the winter ventilation processes on the hydrochemical structure of waters in the Black Sea, in materials of the US-CIS Arabian Sea Workshop *Biochemical Processes in the Arabian Sea*, MHI NAN Ukraine, Sevastopol, pp.149-155.
17. Finenko, Z.Z. and Krupatkina, D.K. (1993) Primary production in the Black Sea in winter-spring, *Oceanology (Russian)*, **33**, No1, 97-104.

TIME-SERIES PROFILES OF ^{134}CS, ^{137}CS AND ^{90}SR IN THE BLACK SEA

KEN O. BUESSELER AND HUGH D. LIVINGSTON
Marine Chemistry and Geochemistry,
Woods Hole Oceanographic Institution
Clark-447, MS #25, Woods Hole, MA 02543 USA

Abstract. The water column distributions of the artificial radionuclides, ^{134}Cs, ^{137}Cs and ^{90}Sr are used to examine mixing and ventilation processes in the Black Sea. Samples were collected on 6 cruises between 1986 and 1992. From the isotope ratios, we can separate the pre-existing weapons testing signal which arrived in the mid-60's from the more recent Chernobyl inputs in 1986, both of which arrived predominantly as atmospheric fallout to this basin. The vertical radionuclide profiles are normalized to salinity to allow for a comparison of radionuclide penetration along isopycnal surfaces. These time-series vertical radionuclide data allow one to follow magnitude and depth of penetration of surface oxic waters into intermediate depths below the oxic/anoxic interface (<500m). Some evidence for interannual variations in the strength of ventilation can be seen, which likely reflects the intensity of winter cooling and mixing, and the overall water and salt balances. A subsurface Chernobyl Cs maximum near the Bosporus found in both 1987 and 1988 suggests that at least part of this vertical mixing process occurs as entrainment driven mixing near the Bosphorus. Samples were also collected near the Danube and Dneper rivers, where interleaving low salinity, and for the Dneper, high ^{90}Sr water masses can be detected. Overall however, the riverine sources of these tracers are much smaller than atmospheric deposition and can be ignored for most sites.

1. Introduction

One of the unusual features of the Black Sea is the large volume of permanently anoxic deep waters which are separated from the oxic surface waters by a sharp pycnocline. This oxic/anoxic interface occurs along a constant density surface which is generally dome shaped, being deeper near the margins (approx. 150-200m) than in the central basin (80-100m). The position, or density of this interface appears to be relatively constant on decadal time-scales [2,8]. In studying the sensitivity of this basin to anthropogenic or climatic changes, it is important to account for vertical exchange across this sharp density surface. Recent studies have shown that diffusion alone cannot account for the rapid penetration of Chernobyl derived cesium across the

E. Özsoy and A. Mikaelyan (eds.), Sensitivity to Change: Black Sea, Baltic Sea and North Sea, 239–251.
© 1997 *Kluwer Academic Publishers.*

pycnocline. Some form of entrainment of surface waters and horizontal transport into the intermediate waters is needed to account for the vertical tracer distributions [7]. Such a rapid injection of surface waters below the pycnocline may account for the observed separation between the depths of oxygen depletion and the onset of H_2S across the pycnocline [13,14].

In this paper, we present time-series data on the vertical distributions of ^{134}Cs, ^{137}Cs and ^{90}Sr obtained between 1986 and 1992 in the Black Sea, and use these water mass tracers to follow the rates of mixing across the oxic/anoxic boundary. This work follows on from our previous report of Chernobyl derived cesium isotope depth profiles measured through 1988 [7]. The approach taken here is to combine data from all of our cruises along isohaline surfaces, to enhance out ability to monitor changes in surface water penetration below the densities characteristic of the pycnocline. Both $^{134}Cs/^{137}Cs$ and $^{137}Cs/^{90}Sr$ ratios will be used to distinguish between the earlier weapons testing fallout primarily delivered in the early 1960's, from the more recent Chernobyl sources in 1986.

2. Sampling and Analyses

In September 1986 and May 1987 samples were collected primarily in the SW Black Sea region in collaboration with Turkish colleagues aboard the RV *K. Piri Reis*. In June/July of 1988 samples were collected along the southern margin and in the central basin during the US sponsored RV *Knorr* cruises. Cruises in April 1989, June 1990, and August 1992 were focused in the NW shelf and the western gyre regions, in collaboration with Russian and Ukrainian colleagues aboard the RV *Professor Vodjanitsky*. Sample locations for each cruise are shown in Figure 1.

Two types of water samples were collected for the Cs and Sr isotopes. Large volume samples (>200 liters) for cesium isotopes only, were collected either with a deck mounted or *in-situ* pumping system. Samples were passed through a prefilter followed by a series of Cs adsorber cartridges, the details of which are described in [6,7]. Previous studies have shown that the percent of particulate bound ^{134}Cs and ^{137}Cs is low (<1%) as expected from its soluble behavior in seawater [3,12]. By gamma counting these large volume samples one can separate between the ^{134}Cs and ^{137}Cs activities. Because of the short half-life of ^{134}Cs (^{134}Cs $t_{½}$ = 2.07 years vs. ^{137}Cs $t_{½}$ = 30.2 years) and low absolute efficiency of gamma counting, large volume samples were needed for these analyses. The precise determination of ^{134}Cs activities in subsurface samples became impractical for our purposes beyond 1990 using this technique.

Discrete unfiltered small volume samples (10 to 200 liters) were also collected and analyzed for ^{90}Sr ($t_{½}$ = 29.0 years) and the Cs isotopes. Samples were collected using wire mounted bottles or from bottles mounted on a CTD/Rosette. These samples were processed via radiochemical purification procedures and beta counted as described in [6]. If significant, the ^{137}Cs beta activities were corrected for any contribution from ^{134}Cs betas using $^{134}Cs/^{137}Cs$ data. In this manuscript, all radionuclide data are decay

corrected to May 1, 1986, to separate out any changes due to radioactive decay vs. those related to physical processes. On each cruise, separate salinity samples were also collected and analyzed upon return to the Woods Hole Oceanographic Institution. Temperature data, if available, were obtained from CTD mounted sensors. Activity results for all 240 samples analyzed from this time period can be obtained from the IAEA Black Sea radiochemical database (contact: M. Scott at IAEA Monaco), alongwith sampling dates, station information, propagated counting errors, and ancillary temperature and salinity results.

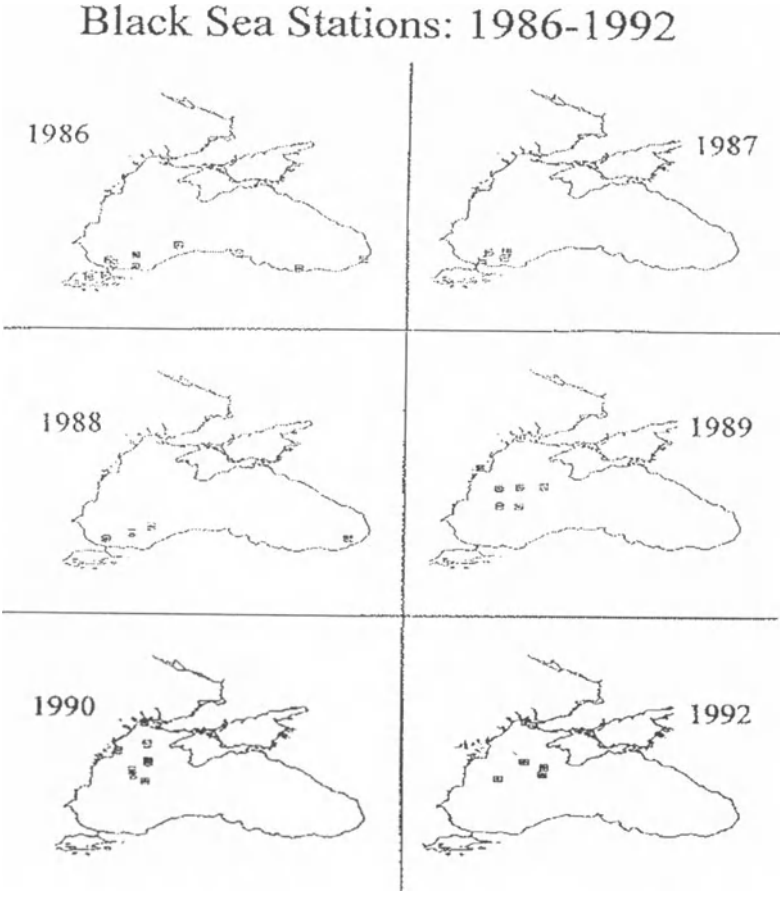


Figure1. Map of Black Sea stations sampled for Woods Hole radiochemical analyses of waters.

3. Results and Discussion

3.1. SEPARATION OF WEAPONS TESTING AND CHERNOBYL SIGNALS

It has been widely recognized that the Chernobyl nuclear reactor accident released significant quantities of a wide range of radionuclides into the environment, and to the Black Sea in particular. Many of these reactor derived radionuclides are the same as those released during nuclear weapons testing, and depending upon the location and specific isotope, activities from either source may be dominant. The vast majority of Chernobyl radionuclides delivered to the Black Sea arrived as a pulse in early May 1986 as atmospheric fallout. Atmospheric fallout is also expected to be the dominant source of the earlier weapons testing radionuclides as well.

Given their longer half-lives, ^{137}Cs and ^{90}Sr from both Chernobyl and weapons testing sources can be found in the Black Sea. In contrast, due to the rapid decay of ^{134}Cs, essentially all of the ^{134}Cs measured in the Black Sea post 1986 can be attributed to the more recent Chernobyl accident. In 1986, the $^{134}Cs/^{137}Cs$ ratio in surface waters was a function of the relative activity of Cs from each source. Using a two end-member model, we showed that the end-member Chernobyl fallout $^{134}Cs/^{137}Cs$ activity ratio in Black Sea surface waters must have been 0.53, identical to that determined from direct atmospheric sampling at the time of the accident [10,1]. Knowing this decay corrected input ratio and the $^{134}Cs/^{137}Cs$ ratio of any sample therefore allows for the separation of the Chernobyl ^{137}Cs fallout from weapons testing signals [7].

Given the two year half-life of ^{134}Cs and the large volume requirements for gamma counting, we desired a second procedure to separate ^{137}Cs derived from Chernobyl and weapons testing sources. For this, we use our 1986 total ^{137}Cs data below the mixed layer to determine the subsurface, Chernobyl-free, ^{137}Cs profile that has been established in the 20+ years since the arrival of weapons testing fallout. Simply subtracting the pre-existing ^{137}Cs activities from any total ^{137}Cs profile in the later years, allows for the determination of a Chernobyl ^{137}Cs profile. The only assumption that we make is that the changes in the vertical distribution of the Chernobyl signal will be large and rapid, relative to any subsequent changes in the pre-existing weapons testing signal. We will show that the results are the same using either this approach or the $^{134}Cs/^{137}Cs$ data (through 1990) as a correction to the total ^{137}Cs activities.

In Figure 2, we show a typical depth profile of ^{137}Cs, $^{134}Cs/^{137}Cs$ ratios and salinity for a station in the western gyre sampled in September 1986. It was clear from this data that the Chernobyl fallout was confined to the upper mixed layer based upon the elevated $^{134}Cs/^{137}Cs$ ratio and high activities of the surface most sample. In the lower panel of this Figure, we show the same ^{137}Cs data plotted for all of the stations sampled in September 1986 vs. salinity. By using salinity as a proxy for density, we can combine data from both shelf and deep water stations, as it is well known that geochemical features follow isopycnal surfaces in this basin [5,11,20,18,8]. This normalization to salinity approximates a density normalized curve, as the greater than four salinity gradient between surface (specifically salinities > 18.2) and deep waters

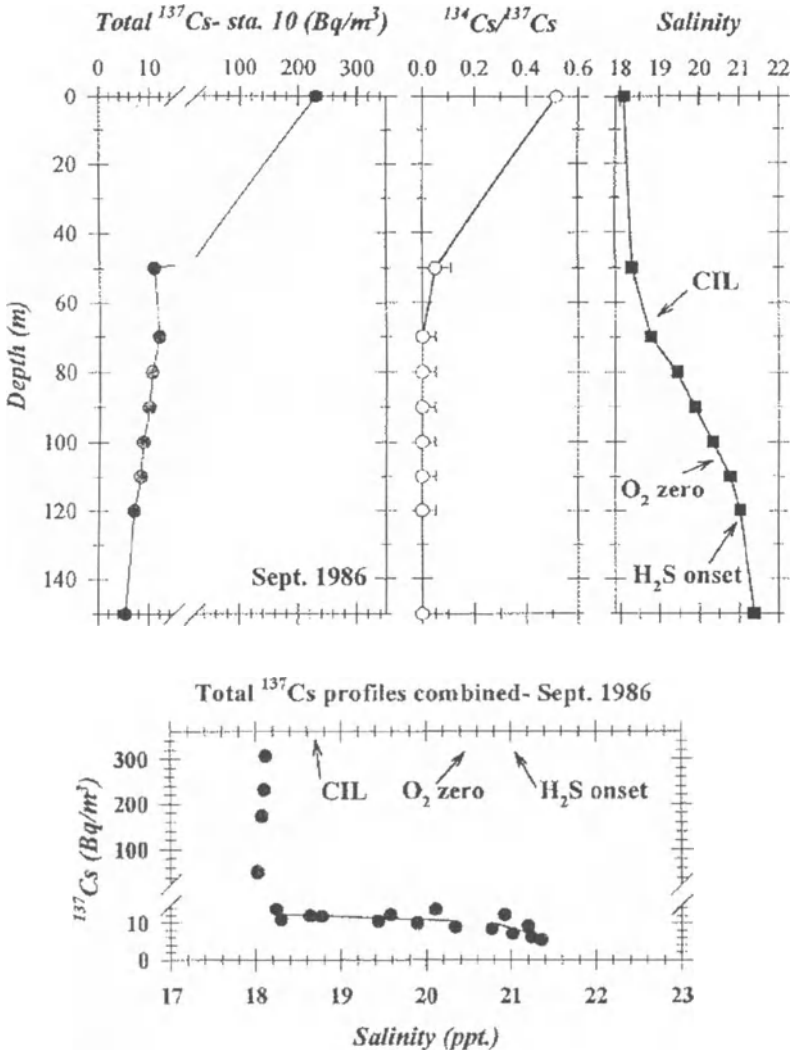


Figure 2. Plot of total ^{137}Cs, ^{134}Cs/^{137}Cs ratios, and salinity vs. depth for a single station from the central western gyre sampled in 1986 (upper panel). In the lower panel, all ^{137}Cs data are combined from the same cruise in September 1986 along isopycnal surfaces. The approximate depths/salinities of the core of the CIL, O_2 zero (O_2<5 μM) and H_2S onset (H_2S >5μM) are also indicated.

determines the bulk of the density changes. We are forced to rely on salinity given a lack of complete temperature data for all samples collected between 1986-1992.

Using this salinity normalization, the core of the Cold Intermediate Layer (CIL waters <7.5 °C) would be found at a salinity of 18.7, the depth of oxygen zero (O_2 < 5 μM) is found at a salinity of 20.5 (density = 15.9σ_τ) and the onset of H_2S (H_2S > 5 μM)

at a salinity of 21.0 (density = $16.3\sigma_t$). Total Cs137 activities in the surface mixed layer in September 1986 were quite high, >100 Bqm^{-3}, relative to pre-Chernobyl activities around 10 Bqm^{-3} [21]. $^{134}Cs/^{137}Cs$ ratios around 0.5 were found for these surface most samples and no detectable ^{134}Cs was found in the deeper samples [7]. In essence, the total ^{137}Cs data in Figure 2 define quite clearly a post-Chernobyl ^{137}Cs signal in the uppermost waters, and the pre-existing weapons testing signal in samples from below the mixed layer.

In any samples where we have both decay corrected ^{134}Cs and ^{137}Cs activities, by knowing the $^{134}Cs/^{137}Cs$ ratio in Chernobyl fallout (=0.53), as stated above, we can correct our subsurface samples for weapons testing derived ^{137}Cs. It is clear that both weapons testing ^{137}Cs profiles are identical, whether obtained from $^{134}Cs/^{137}Cs$ ratios or the 1986 deep water total ^{137}Cs data (Figure 3). There is more scatter around the individual $^{134}Cs/^{137}Cs$ derived points, due primarily to the higher analytical uncertainty in the $^{134}Cs/^{137}Cs$ ratio, particularly in the later years. Given this higher scatter using the $^{134}Cs/^{137}Cs$ approach, we have used the best fit line to the 1986 total ^{137}Cs data between salinities of 18.2 - 21.5 to correct all subsequent total ^{137}Cs profiles for pre-existing weapons testing fallout. It is also important to point out that any model which attempts to examine vertical mixing of weapons testing derived tracers (bomb-^{14}C, tritium, etc.), should result in a relatively similar pattern of tracer penetration. The maximum depth of weapons testing ^{137}Cs that we could clearly see in our studies is around 500m, or a salinity of roughly 22.0. At these lower intermediate water activities (^{137}Cs<0.1 Bqm^{-3}), there are additional concerns about ^{137}Cs blanks and resuspended sediments that make it quite difficult to further define the maximum penetration depth of this tracer. The penetration of weapons testing ^{134}Cs to depths of 500m is consistent with the penetration of anthropogenic tritium and freons into this basin [19,9].

3.2. TIME-SERIES EVOLUTION OF CHERNOBYL ^{137}Cs PROFILES: 1986 THROUGH 1992

The extent of mixing between surface and intermediate waters in the Black Sea can be studied by following the evolution of the derived Chernobyl ^{137}Cs tracer profile with time (Figures 4a-4e). In essence, we are following the introduction of a soluble tracer which arrived to the Black Sea surface waters as a pulse in early May 1986. For this analysis, we corrected all of our total ^{137}Cs results for pre-existing weapons testing ^{137}Cs as discussed in the previous section. The data are combined along constant salinity surfaces (to approximate isopycnal surfaces) and presented here for waters >18 only (to exclude surface most samples influenced by direct river discharges). As shown previously in Figure 2, by September 1986, Chernobyl ^{137}Cs was confined to the surface mixed layer only. By May of 1987, the Chernobyl signal is clearly seen below the depth of the CIL, with low activities (<5 Bqm^{-3}) below the depths of O_2 zero and H_2S onset. This trend of downward mixing continues through 1988, with a clear decrease in the slope of the ^{137}Cs activity vs. salinity profile above the depths of O_2 zero, and with slightly higher ^{137}Cs activities at the depths of the oxic/anoxic interface

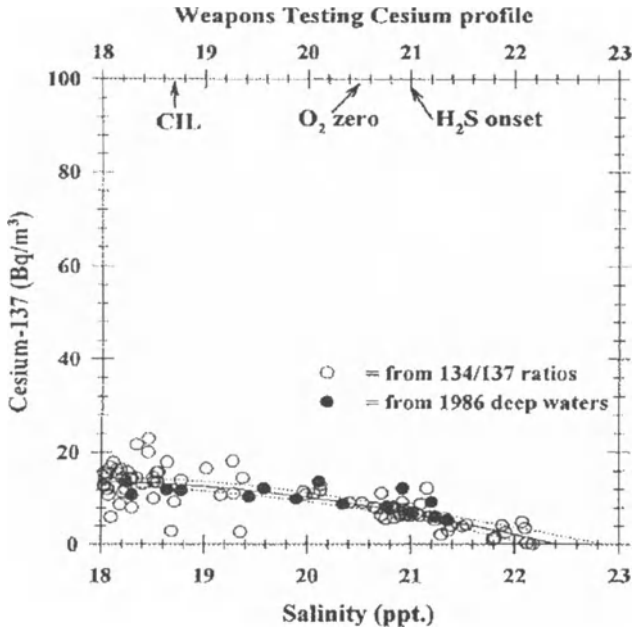


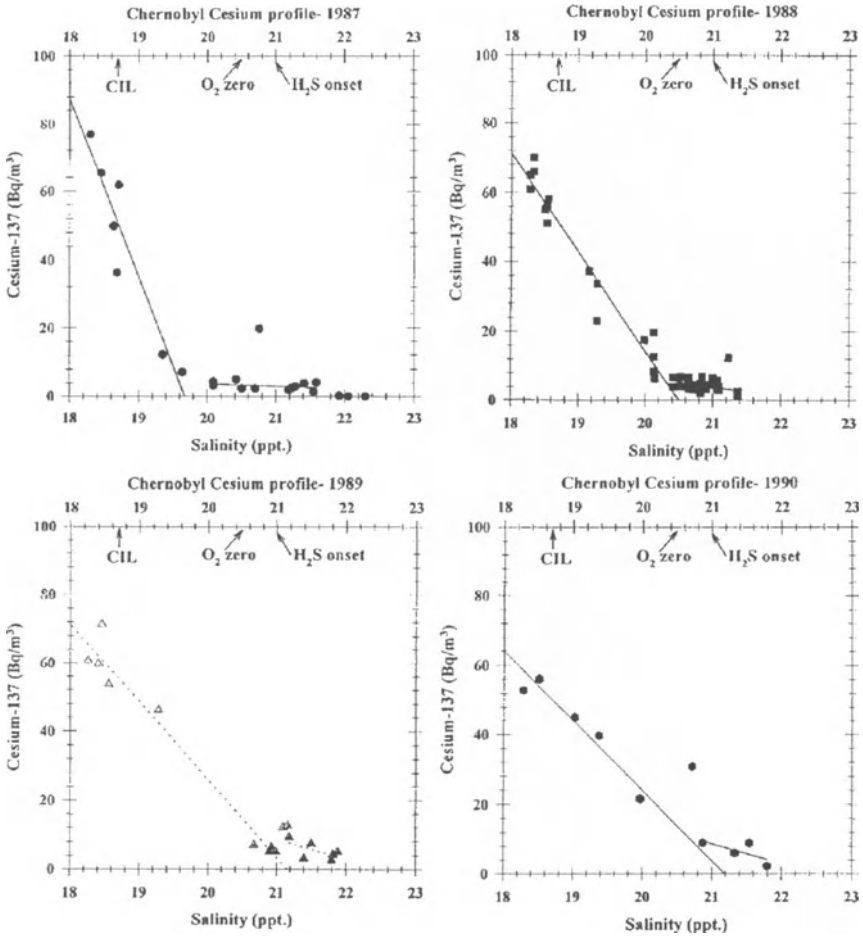
Figure 3. A comparison of the 1986 ^{137}Cs activities below the mixed layer with a weapons testing ^{137}Cs profile derived from measured ^{134}Cs/^{137}Cs ratios and total ^{137}Cs activities for all samples collected between 1987-1990 (see text for details). Both sets of data can be used to define the pre-Chernobyl ^{137}Cs distribution.

(mean Chernobyl ^{137}Cs = 3.1 Bqm^{-3} for 1987 and 4.3 Bqm^{-3} for 1988 between salinity values of 20.2-21.5).

Many of the main conclusions from our previous analysis of a subset of the 1986-1988 ^{137}Cs data vs. depth [7] can be more easily seen in these salinity normalized plots of Chernobyl ^{137}Cs activity. For example, between Sept. 1986 and May 1987 the deepening of the surface mixed layer over the winter months down through the depths of the CIL is evident by the penetration of Chernobyl ^{137}Cs. In addition, these data clearly demonstrate that over a period of only 6 months there is mixing between surface waters and depths below oxygen zero as well, (Chernobyl ^{137}Cs activities in 1987 between 20.2-21.5 are 5% of those at the surface). Since the diffusive rates are too slow to account for such rapid "vertical" mixing, other processes must be sought to explain the rapid downward penetration of tracer. Here again, the salinity normalized Chernobyl ^{137}Cs data can help. In 1987 and 1988, at stations sampled near the mouth of the Bosphorus, we found anomalously high ^{137}Cs activities at densities near the oxic/anoxic interface. Such single point subsurface maxima are found in 1987 (Figure 4b at S=20.8, ^{137}Cs = 20 Bqm^{-3}) and in 1988 (Figure 4c S=21.2, ^{137}Cs = 15 Bqm^{-3}). In both cases, these points are associated with entrainment features near the Bosphorus, where outward flowing Black Sea surface waters and inward flowing Mediterranean waters have formed a tongue of sub-surface water which is injected laterally into the basin (note sampling locations in Figure 1 for these years). Such features are seen on

occasion in this region based upon anomalous T/S properties and sub-surface oxygen anomalies [16,15]. These entrainment processes are presumably responsible for ventilation of the intermediate depths, and can account for the formation of the sub-oxic zone [8].

In 1989, 1990 and 1992, the trend of continued tracer penetration can be seen by the decrease in slope in the Chernobyl ^{137}Cs vs. salinity plot above oxygen zero, and the slow build-up of ^{137}Cs activity below salinity of 21. The data are thus consistent with rapid mixing down to depths near the upper boundary of the pycnocline, and slower mixing between salinity of 21-21.5 (i.e. depths between 150-500m in the central gyres).



Figures 4a-4e. Time-series plots of Chernobyl ^{137}Cs vs. salinity for all stations sampled between 1987-1992. Chernobyl ^{137}Cs is derived from the total ^{137}Cs activity and a correction for pre-existing weapons testing ^{137}Cs activities.

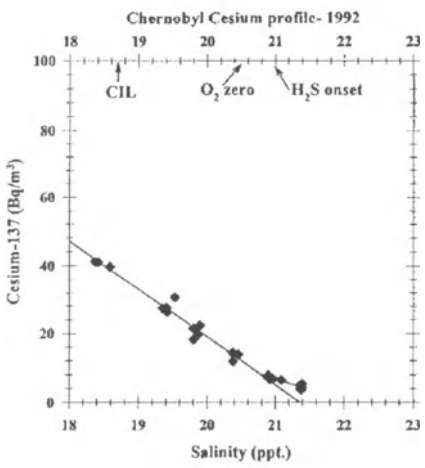


Figure 4 (continued)

There is a single anomalous point at S=21.7, ^{137}Cs = 35 Bqm^{-3}, collected in 1990 at 200m near the center of a quasi-permanent anti-cyclonic gyre off of Sevastopol. This subsurface feature may reflect enhanced surface water entrainment in regions other than the Bosphorus. The elevated ^{137}Cs in this case, is consistent with an elevated $^{134}Cs/^{137}Cs$ ratio of 0.37 for the same sample.

Recent high quality T/S data in the Black Sea are consistent with the observed patterns of ^{137}Cs penetration. Seasonal variations in T/S properties are evident down to salinities of 20.0, and interannual variations down to at least 20.5 (or densities of $<16.0\sigma_\tau$; [8]). It is over these same depths that the surface-derived Chernobyl ^{137}Cs signal is found to penetrate most rapidly. Between salinity values 20.5 to 22.0 (densities of σ_τ=16-16.5), there are only very slight variations in T/S properties on an interannual basis, consistent with the slower penetration of ^{137}Cs to these same depths. In our own ^{137}Cs data set, between 20.5 and 21.5, it is hard to detect any appreciable change in ^{137}Cs between 1989 to 1992. Ventilation at these depths may be restricted to anomalously cold or unusual winter conditions. Below 22.0 (densities of σ_τ=16.5) anomalies in T/S properties in the Black Sea deep waters are not readily detected, and both the Chernobyl derived and earlier weapons testing tracers are absent.

3.3. $^{137}Cs/^{90}Sr$ RATIOS IN THE WATER COLUMN

The post 1986 $^{137}Cs/^{90}Sr$ ratios in Black Sea waters also reflect some combination of Chernobyl and earlier weapons testing sources. Worldwide, the $^{137}Cs/^{90}Sr$ ratio of global fallout from weapons testing sources averages 1.45 in activity units, in surface open ocean waters of 35 salinity [4]. Deviations around this ratio are found near point sources of non-fallout radionucides, such as near Sellafield (Pentreath, 1988), and in estuaries where the higher mobility of Sr relative to Cs in fresh waters decreases the measured $^{137}Cs/^{90}Sr$ ratio [4]. Black Sea surface waters are somewhat brackish,

salinity ranging from around 18 in the central gyres, to much lower values near the mouths of the major rivers and hence lower $^{137}Cs/^{90}Sr$ ratios are expected.

Due to the rapid penetration of the Chernobyl ^{137}Cs to depth, we have relatively few samples where we can examine directly the pre-Chernobyl $^{137}Cs/^{90}Sr$ ratio. In 1986, at depths of 50 and 70m, where Chernobyl ^{137}Cs had yet to penetrate (i.e. $^{134}Cs/^{137}Cs = 0$), the observed $^{137}Cs/^{90}Sr$ ratio was 0.78 ± 0.04. By 90m, we found a somewhat elevated $^{137}Cs/^{90}Sr$ ratio of 1.30 ± 0.23. The slight elevation in $^{137}Cs/^{90}Sr$ may be related to the increase in salinity (and hence ^{137}Cs relative to ^{90}Sr) with depth, however it must also be remembered that the error on this ratio increases rapidly as the activities decrease with depth. Other than these three samples, we did not make any attempt to further refine this pre-Chernobyl ratio, and conclude that a $^{137}Cs/^{90}Sr$ ratio slightly <1 is characteristic of surface waters and one slightly >1 for the deep waters, pre 1986.

In post-Chernobyl samples, we found surface water $^{137}Cs/^{90}Sr$ ratios as high as 5 to 6, consistent with the relative enrichment of ^{137}Cs relative to ^{90}Sr in the atmospheric fallout immediately following the Chernobyl accident [1]. By 1987, those samples with elevated Cs134 clearly show higher $^{137}Cs/^{90}Sr$ ratios, with surface waters being characterized by a $^{137}Cs/^{90}Sr$ ratio of 3.7 ± 0.6 (n=4, salinity<19), and deeper waters having a ratio of 1.5 ± 0.2 (n=3; salinity 19.4 - 21.3). The trend continues throughout 1988-1992, with a slight decrease in this ratio in surface waters and an increase to ratios between 1.5 and 2.0 or higher at depths of the oxic/anoxic interface. In essence, the $^{137}Cs/^{90}Sr$ story is similar to that derived from Chernobyl ^{137}Cs alone, and discussed above. Given the increased difficulty and additional uncertainty when making both ^{137}Cs and ^{90}Sr activity measurements, we did not complete ^{90}Sr analyses on all samples.

While $^{137}Cs/^{90}Sr$ ratios do not add significant new information to the study of penetration of surface waters to depth, the $^{137}Cs/^{90}Sr$ ratio can be used as an indicator of river water intrusions into the Black Sea In figure 5, the 1990 $^{137}Cs/^{90}Sr$ ratios are plotted vs. salinity. In 1990, we sampled near the mouths of the Danube and Dneper rivers (Figure 1) in an attempt to study the riverine influences on the NW shelf water balance. At salinities >18.2, the $^{137}Cs/^{90}Sr$ ratio decreases from around 4 to 1.5, consistent with the mixing of surface waters impacted by Chernobyl with a high ratio, into the low ratio deep waters. Also, it is clear that the general trend at salinities <17, is a decrease in the $^{137}Cs/^{90}Sr$ ratio, consistent with the enrichment of ^{90}Sr in the fresh water end member. More interesting perhaps is the evidence in this data set for anomalously low $^{90}Sr/^{137}Cs$ samples between 17 to 18 salinity. These low ratios correspond to low salinity anomalies in the T/S profile at any given station, and reflect intrusion of river waters onto the shelf. In fact, using $^{137}Cs/^{90}Sr$ information from the Danube (characterized by low salinity / low ^{90}Sr / low ^{137}Cs) and Dneper (low salinity / high ^{90}Sr / low ^{137}Cs) and the measured salinity from any given sample, it is possible to deconvolute the relative percent of Danube, Dneper, and Black Sea surface water (high salinity / low ^{90}Sr / high ^{137}Cs) in the NW shelf region, at least in the late 80's and early 1990's (Stokosov *et al.*, 1994, unpublished results).

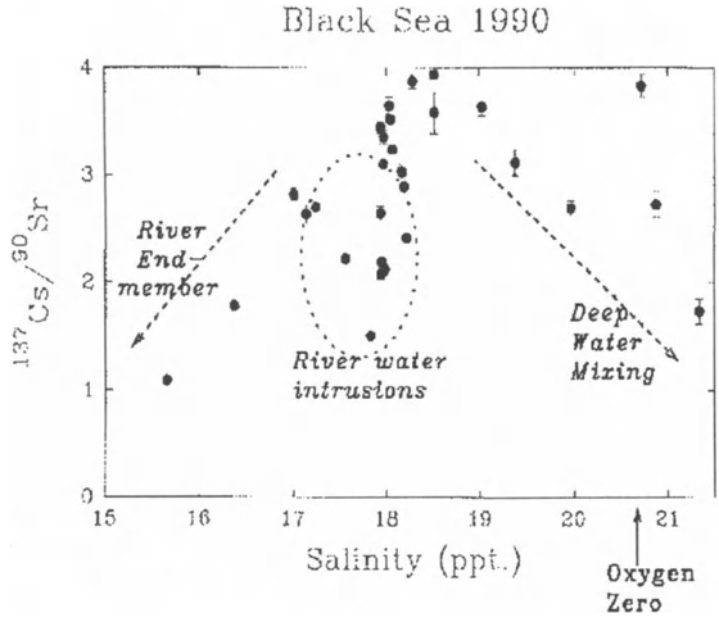


Figure 5. Plot of total $^{137}Cs/^{90}Sr$ ratios vs. salinity for stations sampled in 1990. The general trend of low $^{137}Cs/^{90}Sr$ at low salinities is due to the higher mobility of ^{90}Sr in fresh waters. Note at salinities between 17-18, anomalously low ratios appear due to river water injections along shallow isopycnal surfaces into the Black Sea. The decrease in $^{137}Cs/^{90}Sr$ with depth reflects mixing of post-Chernobyl fallout in surface waters (end member $^{137}Cs/^{90}Sr$ >4) with weapons testing ^{137}Cs and ^{90}Sr activities in deeper waters (weapons testing $^{137}Cs/^{90}Sr$ approx. 0.8 to 1 in Black Sea).

4. Summary

In this paper, we present an overview of ^{134}Cs, ^{137}Cs and ^{90}Sr analyses conducted as part of our studies of Chernobyl fallout in the Black Sea. Since these tracers have a surface source (i.e. fallout from Chernobyl or weapons testing) and a soluble/conservative geochemical behaviour, they can be used to trace vertical mixing processes between surface waters and intermediate and deep layers. By combining data along isohaline surfaces, we have been able to enhance the vertical resolution of this data set, and examine the inter annual variations in the extent of mixing. Using either the $^{134}Cs/^{137}Cs$ ratio, the pre-Chernobyl 1986 total ^{137}Cs profile, or $^{137}Cs/Sr$ ratios, one can separate out the weapons testing fallout ^{137}Cs signal from the more recent Chernobyl ^{137}Cs source.

Our results suggest that during each winter waters regularly mix down to at least the depth of oxygen zero. Mixing of surface waters down to depths of the sub-oxic and sulfidic zone is less rapid, but is clearly evident only one year after the Chernobyl accident. Significant vertical mixing on decadal time-scales appears to be limited to salinities <21.5 (depths <500m). These fallout tracers suggest that mixing occurs, at

least in part, due to the entrainment of surface waters and injection along isopycnal surface in the region near the Bosphorus.

All of these data are now available to the international community via the IAEA database. Combination of these data and similar results collected by other researchers should allow for a quite complete description of vertical penetration of Chernobyl fallout in the Black Sea. Furthermore, the pre-Chernobyl ^{137}Cs data define quite clearly the extent of fallout penetration from sources which were delivered to surface waters in the early 1960s. We feel that these data will provide an important constraint on physical models of mixing in the Black Sea on both annual and decadal time-scales. Ultimately, it is the coupling of such models with biogeochemical parameters, that will allow for a more complete assessment of the impact of anthropogenic activities on this enclosed basin.

5. Acknowledgments

We would not have been able to conduct our Black Sea radionuclide program without the kind assistance of a wide range of Turkish, Ukrainian and Russian colleagues. These colleagues provided us with the opportunity to collect samples on a total of 6 sampling cruises to the Black Sea, and more importantly became out scientific colleagues and friends. Rather than possibly neglect any one individual, we would like to specify our appreciation to the following labs and their personnel - the Institute of Biology of Southern Seas, Sevastopol; the Marine Hydrophysical Institute, Sevastopol; and the Dokuz Eylul University, Izmir. In addition, our first sampling opportunities in 1986 were made possible only through ongoing efforts of researchers from the Univ. of Hamburg (E. Degens, V. Ittekkot, S. Kempe), and S. Honjo at WHOI. Sampling and radiochemical analyses by S. Casso, M. Hartman, W. Clarke, and J. Andrews at WHOI is also highly appreciated. We have had many different funding sources for these efforts, which for these authors specifically includes the US National Science Foundation, the US Environmental Protection Agency, the US Office of Naval Research, and the WHOI Coastal Research Center. This is contribution No. from the Woods Hole Oceanographic Institution.

6. References

1. Aarkrog, A. (1988). The Radiological Impact of the Chernobyl Debris Compared with that from Nuclear Weapons Fallout. *Journal of Environmental Radioactivity* **6**, 151-162.
2. Bezborodov, A.A. (1990). Variability in Position of the Onset of Anaerobic Waters in the Black Sea as Based on Data of the Past Years. In: *Complex Oceanographic Investigations of the Black Sea (Hydrology, Hydrophysics, Hydrochemistry)* V.E. Zaika, ed. [In Russian], Academy of Science of Ukraine, Marine Hydrophysical Institute, Sevastopol, 76-114.
3. Bowen, V.T., Noshkin, V.E.,. Livingston, H.D. and Volchok, H.L. (1980). Fallout Radionuclides in the Pacific Ocean: Vertical and Horizontal Distributions, Largely from GEOSECS Stations. *Earth and Planetary Science Letters* **49**, 411-434.

4. Bowen, V.T., Noshkin, V.E., Volchok, H.L., Livingston, H.D. and Wong, K.M. (1974). Cesium 137 to Strontium 90 Ratios in the Atlantic Ocean 1966 through 1972. *Limnology and Oceanography* **19(4)**, 670-681.
5. Brewer, P.G. and Spencer, D.W. (1974). Distribution of Some Trace Elements in Black Sea and their Flux Between Dissolved and Particular Phases. In: *The Black Sea - Geology, Chemistry and Biology.* E.T. Degens and D. A. Ross (eds.), American Association of Petroleum Geologists, Memoir 20, Tulsa, 137-143.
6. Buesseler, K.O., Casso, S.A., Hartman, M.C. and Livingston, H.D. (1990). Determination of Fission Products and Actinides in the Black Sea Following the Chernobyl Accident. *Journal of Radioanalytical and Nuclear Chemistry Articles* **138**, 33-47.
7. Buesseler, K.O., Livingston, H.D. and Casso, S.A. (1991). Mixing Between Oxic and Anoxic Waters of the Black Sea as Traced by Chernobyl Cesium Isotopes. *Deep-Sea Research* **38(2)**, S725-S745.
8. Buesseler, K.O., Livingston, H.D., Ivanov, L. and Romanov, A. (1994). Stability of the Oxic-Anoxic Interface in the Black Sea. *Deep-Sea Research I* **41(2)**, 283-296.
9. Bullister, J.L. and Lee, B.S. (in press). Chlorofluorocarbon-11 Removal in Anoxic Marine Waters. *Geophysical Research Letters.*
10. Devell, L., Tovedal, H., Bergstrom, U., Appelgren, A., Chyssler, J. and Andersson, L. (1986). Initial Observations of Fallout from the Reactor Accident at Chernobyl. *Nature* **321**, 192-193.
11. Lewis, B.L. and Landing, W.M. (1991). The Biogeochemistry of Manganese and Iron in the Black Sea. *Deep-Sea Research* **38(S2A)**, S773-S804.
12. Livingston, H. D., Buesseler, K.O., Izdar, E. and Konuk, T. (1988). Characteristics of Chernobyl Fallout in the Southern Black Sea. In: *Radionuclides: A Tool for Oceanography.* Guary, J.C., Guegueniat, P. and Pentreath, R.J. (eds), Elsevier, Essex, U.K., 204-216.
13. Murray, J.W., Jannasch, H.W., Honjo, S., Anderson, R.F., Reeburgh, W.S., Top, Z., Friederich, G.E., Codispoti, L.A. and Izdar, E. (1989). Unexpected Changes in the Oxic/Anoxic Interface in the Black Sea. *Nature* **338**, 411-413.
14. Murray, J. W., Codispoti, L.A. and Friederich, G.E. (1993). Redox Environments: The Suboxic Zone in the Black Sea. In: *Aquatic Chemistry.* Huang, C.P., O'Melia, C.R. and Morgan, J.J. (eds)., American Chemical Society, in press.
15. Oguz, T., Latif, M.A., Özsoy, E., Sur, H.I.and Ünlüata, Ü. (1989). *On the Dynamics of the Southern Black Sea.* NATO Advanced Research Workshop on Black Sea Oceanography, Çesme, Turkey, 23-27 October.
16. Özsoy, E., Ünlüata, Ü. and Top, Z. (1993). The Mediterranean Water Evolution, Material Transport by Double Diffusive Instrusions, and Interior Mixing in the Black Sea, *Progress in Oceanography* **31**, 275-320.
17. Pentreath, R.J. (1987). "Sources of Artificial Radionuclides in the Marine Environment." In: *Radionuclides: A Tool for Oceanography.* Guary, J.C., Guegueniat, P. and Pentreath, R.J. (eds). Proceedings of an International Symposium jointly organized by the Société Française pour l'Energie Nucléaire (SFEN) and l'Institut National des Techniques de la Mer (INTECHMER-CNAM), Cherbourg, France, 1-5 June, Elsevier, pg. 12-34.
18. Saydam, C., Tugrul, S., Bastürk, O. and Oguz, T. (1993). Identification of the Oxic/Anoxic Interface by Isopycnal Surfaces in the Black Sea. *Deep-Sea Research I* **40**, 1405-1412.
19. Top, Z., Östlund, G., Pope, L. and Grall, C. (1991). Helium Isotopes, Neon and Tritium in the Black Sea: A Comparison with the 1975 Observations. *Deep-Sea Research* **38(S2A)**, S747-S760.
20. Tugrul, S., Bastürk, O., Saydam, C. and Yilmaz, A. (1992). Changes in the Hydrochemistry of the Black Sea Inferred from Water Density Profiles. *Nature* **359**, 137-139.
21. Vakulovskiy, S.M., Krasnopevtsev, Y.V., Nikitin, A.I. and Chumichev, V.B. (1982). Distribution of ^{137}Cs and ^{90}Sr Between Water and Bottom Sediments in the Black Sea, 1977. *Oceanology* **22**, 712-715.

THE BLACK SEA COLD INTERMEDIATE LAYER

L. I. IVANOV,* Ş. BEŞİKTEPE+ and E. ÖZSOY+
* *Marine Hydrophysical Institute (MHI-NASU)*
2, Kapitanskaia, Sevastopol, Crimea, Ukraine.
+ *Institute of Marine Sciences (IMS-METU)*
Erdemli, İçel, Turkey.

Abstract. We focus on the volumetric temperature/salinity analysis of the Cold Intermediate Water (CIW) masses, based on data sets obtained in years with normal, severe and mild winter conditions. A comparative analysis of the 1991 and 1992 data is used to study a convection event during the winter of 1991-1992, and April 1993 and March-April 1995 surveys are used to characterise Cold Intermediate Layer (CIL) peculiarities after severe (1993) and mild (1995) winter conditions. A new analysis of the CIW formation is presented, based on the new data sets having high resolution, full basin coverage. Comparative volumetric T,S analyses do not confirm replenishment of CIW in the peripheral 'convergence zone' by water from the cyclonic central region, after being formed there by winter convection, as it had been previously claimed by Ovchinnikov [24]. Subtle evidence supports Kolesnikov's hypothesis [16] of CIW production over the shelf. Yet, the contribution of this mechanism is found to be small. We find that the formation process is a result of advective and convective contributions most actively taking place along the 'convergence zone'.

1. Introduction

An accurate understanding of the sources, formation and spreading mechanisms of the Cold Intermediate Water (CIW) is much needed in the Black Sea. Surface mixing results in formation of CIW, and contributes to the direct ventilation of the upper ocean. The impact of surface mixing on the transport of pollutants and organic matter, and on the new production resulting from the entrainment of nutrients into the surface waters need to be studied for a better understanding.

The CIL is characterised by a minimum in temperature, with $T < 8°C$, occurring within a typical depth range of about 50 - 180 m overlying the main pycnocline, where vertical stratification is maintained by the salinity gradient.

The low salinity of the surface waters is maintained by fresh water inputs into the Black Sea, and the shallow (~10 -30 m) mixed layer often reflects the effects of seasonal heating and cooling. Although observations are limited, it is often assumed

E. Özsoy and A. Mikaelyan (eds.), Sensitivity to Change: Black Sea, Baltic Sea and North Sea, 253–264.
© 1997 *Kluwer Academic Publishers.*

that convection driven by wintertime atmospheric cooling should erode the pre-existing thermal structure and establish an isothermal layer reaching from the surface to the core of the CIL. The strong salinity stratification at the pycnocline opposes penetration of turbulent convection into the deeper layers.

We focus on the volumetric temperature/salinity analysis of the CIW, based on recent data sets, covering normal, severe and mild winter conditions. We provide evidence to the claim that the Rim Current prevents direct penetration of the convectively generated waters from the central cyclonic gyres to the periphery of the basin, showing that the CIW in the convergence zone (more than 50 percent of the entire CIL volume) mainly originates from the shelf and the continental slope area.

2. Hypotheses on Winter Convection and CIW Formation

The first attempts to explain the origin of CIL were made by Knipovich [15] and Zoobov [32]. They described the CIL as a remnant of the upper mixed layer formed by winter cooling and convection processes. Continued field studies revealed that, in various parts of the sea, the core of the CIL was often deeper than the lower boundary of the mixed layer observed in winter. In addition, the CIW core properties appeared relatively uniform across the basin, and did not appear to be related to south-north and west-east gradients of air temperature or other meteorological parameters.

These facts served as the ground to formulate hypotheses emphasising the advective nature of CIW formation [7, 8, 16]. In accordance with this theory, the cold waters replenishing the CIL in winter are mostly formed in the northwestern shelf, along the adjoining slope region, as well as in the proximity of the Kerch strait; then advected along the periphery towards south. A number of scientists [4, 30] supported this idea.

The hypothesis on the production of the CIW in the northwest part of the sea dominated until 1984, when Ovchinnikov [24, 25] and MHI scientists [11] strongly argued for the generation of CIW in cyclonic gyres in the central part of the sea. The basic idea of Ovchinnikov was that "there is a slow flow of newly formed cold waters from the centers of cyclonic gyres toward the coasts in the Black Sea but not their advection from the northwest part of the sea as it had been thought previously" [25]. Some other studies added details and provided support to this hypothesis [14].

3. The Surface Circulation in the Basin

The most prominent feature characterising the Black Sea general circulation is a basin-scale cyclonic boundary current referred to as the 'Rim Current' [20].

The existence of forcing by a positive curl of the wind stress [18, 19], thermohaline forcing of nonuniform surface buoyancy fluxes [17, 23, 28] and lateral buoyancy sources from rivers and the Bosphorus inflow [6, 23] have been recognised as driving mechanisms for the cyclonic circulation.

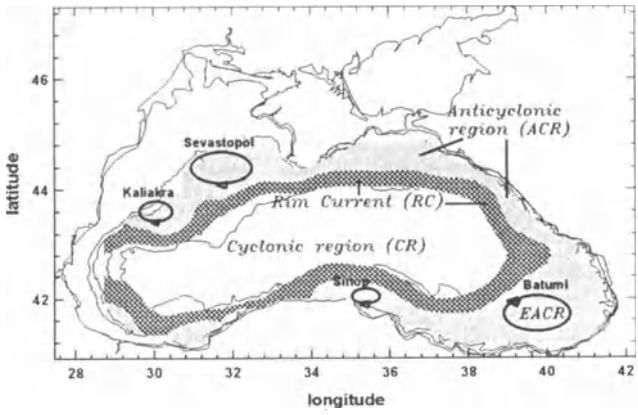


Figure 1. Circulation scheme of the Black Sea based on the 1992 data.

The topography of the pycnocline was used to depict the basic circulation in the basin. The circulation scheme is presented in Fig.1, partially based on the 1992 data: The core of the Rim Current in the scheme corresponds to the zone of maximum pycnocline slope for this survey. The region between the Rim Current and the shelf is typically characterised by a trough formed by the isopycnal surfaces. The anticyclonic cells are often confined to areas of irregular of bottom relief (Sevastopol, Kaliakra, Sinop, Batumi anticyclonic quasi-permanent features) [3, 4, 20, 22]. In analogy with the open ocean cases, this region has been referred to as the 'Convergence Zone' [26], herein referred to as the anticyclonic region (Fig. 1).

4. Data and Analysis Methodology

For the analysis, the data acquired during September 1991 (HydroBlack-91) [1], July 1992 (CoMSBlack-92) [21], April 1993 and March-April 1995 cruises were used. The measurements covered the entire Black Sea in September 1991 and July 1992, and part of it (~50-70 % of total area) in April 1993 and March-April 1995, on a grid allowing to resolve mesoscale features (1/3 degree latitude and 1/2 degree longitude, with increased resolution over slope areas).

The basin-wide data collected during the summer periods of 1991 and 1992 are used to study a convection event that took place in during winter 1991-1992, and the April 1993 and March-April 1995 partial surveys are used to characterise CIL peculiarities after severe (1993) and mild (1995) winter conditions. Although winter 1991-92 data are not available, the comparison of the two summer data sets provide valuable information, because traces of the winter mixing event appear well preserved in the temperature-salinity structure in the following period, particularly due to the peculiarities of the Black Sea pycnocline. It is well known that the density, rather than depth, serves better as a vertical coordinate for studying the vertical structure of various constituents [2, 5] in the pycnocline region. Temperature often acts as a passive tracer,

with a smaller contribution to density as compared to the salinity, and therefore the temperature signature of cooling events are demonstrated well by studying temperature structure on density coordinates of the halocline region.

The core of the CIW occurs at σ_θ = 14.2 - 14.8. The coincidence of the lower boundary of the CIL (defined as the crossing point of temperature at T = 8° C) with the main pycnocline at σ_θ = 15.3 - 15.9 indicates that the convection events have limited, short-term effects in modifying the structure of the main pycnocline on a seasonal time scale.

5. Results

5.1 METEOROLOGICAL CONDITIONS

There are numerous indications that the winter of 1991-1992 was one of the coolest winter seasons in the region, relative to climatological averages [10, 29, 31]. For the considered time period, the winter of 1993 was actually the most severe. Temperatures in the core of the CIL as well as meteorological data reveal a decrease in average winter temperatures for the region in 1991-1993 (averaged temperatures for Odessa, Sevastopol, Yalta and Kerch meteorological stations for winters of 1990-91, 1991-92 and 1992-93 were 2.7°C, 2.3°C and 2.0°C, respectively). In contrast, the CIL temperature in 1995 imply a warm anomaly for this winter period, giving us a possibility to compare results of CIW formation during cold and warm winters.

5.2 CIL IN 1991 & 1992: A COMPARATIVE STUDY

The averaged CIL temperatures for the whole range of σ_θ values in July of 1992 appeared to be cooler than in September of 1991 [13]. The most noticeable differences in the CIL and pycnocline T,S structure were confined to the σ_θ = 14.4-15.0 range and the maximum level of downward 'penetration' due to cross-isopycnal mixing for the central part of the sea was estimated to coincide with the σ_θ=15.5 surface, which is close to the lower boundary of CIL.

For the lower part of the CIL, the largest temperature differences between 1991 and 1992 data were in the cyclonic interior region of the basin. In the July 1992 survey, waters underlying the core of the CIL in the central part of the basin were approximately 0.5°C cooler than the waters within the convergence zone (Fig. 2). On the other hand, above the CIL core, the waters in the convergence zone appeared to be much cooler than those in the cyclonic interior [13], which implied appreciable cooling of the intermediate waters during winter, and their warming during summer, to occur over the dome of the cyclonic gyre where the pycnocline is shallower. This fact strongly supports the claim that cooling/ventilation of the upper pycnocline during cold winters basically takes place in the cyclonic interior.

As it can be seen from Table 1, the total volume of the CIL in July 1992 was larger, by about 1527 km^3, compared to that in September 1991. The volume of the

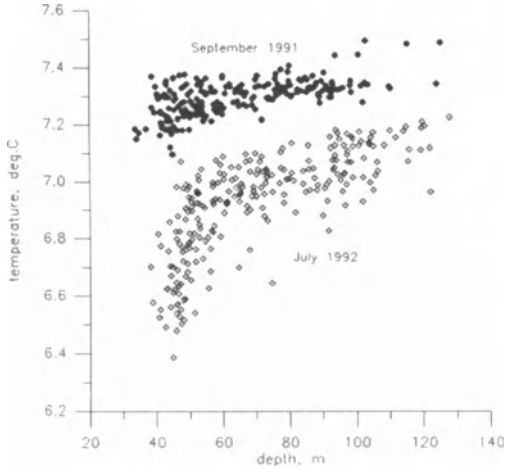


Figure 2. Temperature versus depth on the 14.8 sigma-t.

lower part of the pycnocline was unchanged, to within the accuracy of the estimate. For summer months, Glazkov [9], estimates the average CIL volume to be 16035 km^3. A comparison of this estimate with our calculations implies appreciable interannual variability in CIL thickness. In order to quantify the seasonal cooling effects, we define the CIL negative heat storage per unit area, Q, as follows:

$$Q = \int_{z_2}^{z_1} (T_* - T)\, dz \qquad (1)$$

which excludes the factor ρc_p for simplicity (with $\rho \cong 1 g\ cm^{-3}$ and $c_p \cong 1$ cal g^{-1} $°C^{-1}$ accounting for the density and specific heat of sea water). T_* =8 °C is the upper limit temperature used to identify CIW with $T \leq T_*$ between intermediate depths z_1 and z_2, corresponding to the crossing points at temperature T_*.

The total negative heat storage, QA (A being the survey area), for the September 1991 survey, was smaller by 7070 °C km^3 compared to July 1992, corresponding to a heat loss of 10.4 10^7 J/m^2 from the CIL from September 1991 to July 1992. The differences in negative heat storage of CIL between the 1991 and 1992 surveys can be attributed to the seasonal course of the thermohaline characteristics (possible changes from July 1991 to September 1991) and the interannual variability in the CIW generation in winters of 1990-91 and 1991-92.

To estimate the contribution seasonal variations to the difference, it is reasonable to expect that T,S changes in summer-fall 1991 would be similar to those in 1992. Based on other measurements, we know that the CIL temperature in the northwestern part of the sea has not changed significantly during summer 1992: only a 0.2°C increase in the temperature of the CIW core has been observed in the summer months [12]. Therefore, one would estimate that seasonal changes would only account for about 30-40% of the calculated 1991-92 difference in total negative heat storage, which

would in fact be an underestimate, because it does not include seasonal variations in the total volume of CIW which we do not specifically know. In addition, warming in the upper part of the CIL proceeds faster than in its core, introducing an asymmetry which is difficult to assess here.

TABLE 1. Volumes of water (km^3) for the layers: sea surface - CIL upper boundary, CIL - lower pycnocline (σ_θ =15.6-16.2 surfaces) and the total amount of the CIL negative heat storage Q (°C km^3).

Cruise	Vol.: 0-CIL UB	Vol.: CIL	Vol.: σ_θ=15.6-16.2	Q
September 1991	8398	18361	11787	10430
July 1992	8669	19888	11693	17500

Our rough estimate shows that the interannual variations in CIL total negative heat storage, which are on the same order of magnitude as the seasonal changes, were on the order of 5 10^7 J/m^2 during 1991-1992, with an associated average winter cooling rate of about 7 watt/m^2, if we assume that the cooling period was approximately three months. The heat flux into the cold intermediate layer associated with summer-fall heating (two month period between July and September) can be estimated to be on the order of 10 watt/m^2.

Although the surface area of the cyclonic region (see Fig.1 for definition) is twice as large as the anticyclonic one, the total negative heat storage was calculated to be comparable: 6580 °C km^3 for the convergence zone and 5575 °C km^3 for the cyclonic region. Variations of negative heat storage per unit area in the anticyclonic area (convergence zone), exceed that for the cyclonic domain approximately by a factor of 5. It is evident that the anticyclonic eddies in the Black Sea act as reservoirs where cold waters generated by winter cooling are stored. Whatever changes occur in the Black Sea CIL volume or negative heat storage, these are mostly confined to the areas of the quasi-permanent anticyclonic eddies.

The volumetric T,S diagrams (volumes in km^3 per 0.1°C and 0.1 T,S class) of CIW for the whole Black Sea (excluding the shallow shelf areas) are shown in Figs. 3,a,b respectively for the September 1991 and July 1992 surveys. In general, both figures show that the CIW possesses a prominent core (approximately, between the 14.2 and 14.6 σ_θ interfaces) in the region of the stratified waters of the upper pycnocline, subject to summer warming. On the average, the CIW core in September 1991 is approximately 0.5°C warmer than in July of 1992, as well as being more uniform. In July 1992, the cold core (T<6.2°C) in the cyclonic area was saltier by a difference of about 0.1 as compared to September 1991, linked to deeper convection in 1992.

5.3 CIL VOLUMETRIC STRUCTURE IN 1992

Since features in the temperature - salinity fields are better recognised in 1992, we analyse the July 1992 CIL T,S structure in further detail. For better understanding of the peculiar T,S structure of the whole CIL volume, analogous volumetric T,S diagrams were calculated for the above specified regions (see Fig.1).

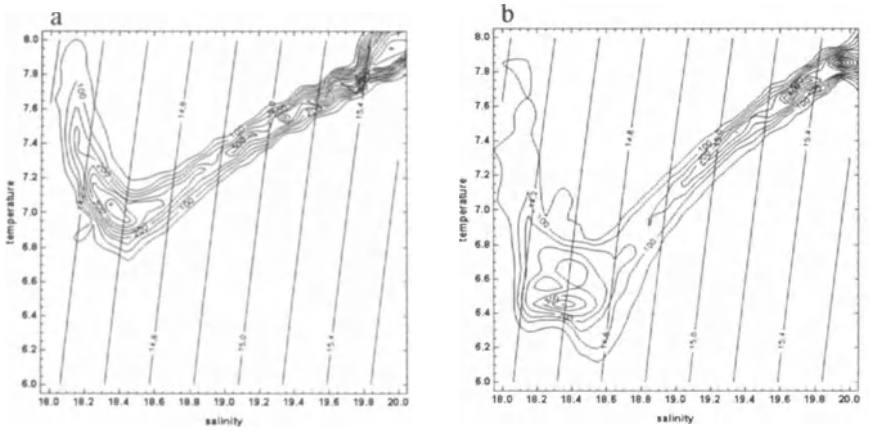


Figure 3 a,b. Volumetric T,S diagrams (km^3 per 0.1°C, 0.1 T,S class) for August-91 (a) & July-92 (b).

These T,S diagrams for different parts of the sea are shown in Figure 4,a-d. For the region of cyclonic circulation (Fig.4,a), maximum volumes were registered in the 6.25° - 6.55°C temperature and 18.55 salinity classes. Comparing Figures 4,a and 3,b, it is possible to verify that, for these T,S classes, waters of the cyclonic interior constitute 50 - 100 % of the volume of the average T,S diagram.

The characteristic feature of the volumetric T,S diagram for this area (see Fig.4,a) is the pattern of isolines within the core of the layer. Waters comprising the core of the layer differ in temperature, but so much in salinity (equal volume contours per T-S class are elongated from low to high temperatures with only a slight slant in salinity), implying that the waters in the cyclonic central domain of the sea were generated locally. The term locally is used here not to identify the *in situ* origin of water but its generation within a specific area of uniform salinity, i.e. of cyclonic circulation. The slant of the elongated contours implies that the salinity CIL core is controlled by winter surface temperature. Cooling implies entrainment and leads to an increase in salinity of the surface waters, as well as the CIL core.

For the anticyclonic region, extremes are observed for the following pairs of (T,S) classes: (6.45° C, 18.15); (6.45° C, 18.35); (6.65° C, 18.35), revealing less saline waters, compared to the central part of the sea (Fig.4,b). The isoline contours within the core of the CIL significantly differ from those for the area of cyclonic circulation. Isoline contours are elongated not 'vertically' but 'horizontally' (broad salinity range), and three water masses can thus be distinguished. For the core of the layer, salinity stratification dominates. In fact, only the upper part of the layer is seen to undergo transformation caused by warming, with most other regions remaining unchanged.

In terms of salinity, both extremes occur for the two salinity classes of 18.1-18.2 and 18.3-18.4 Note that these are waters observed within the deep part of the basin excluding the shallow shelf area. Waters with such low salinities, basically, were not observed in the area of cyclonic circulation. In general, it is reasonable to suppose that

less saline waters are of shelf origin. Waters with medium salinities could be generated in the convergence zone.

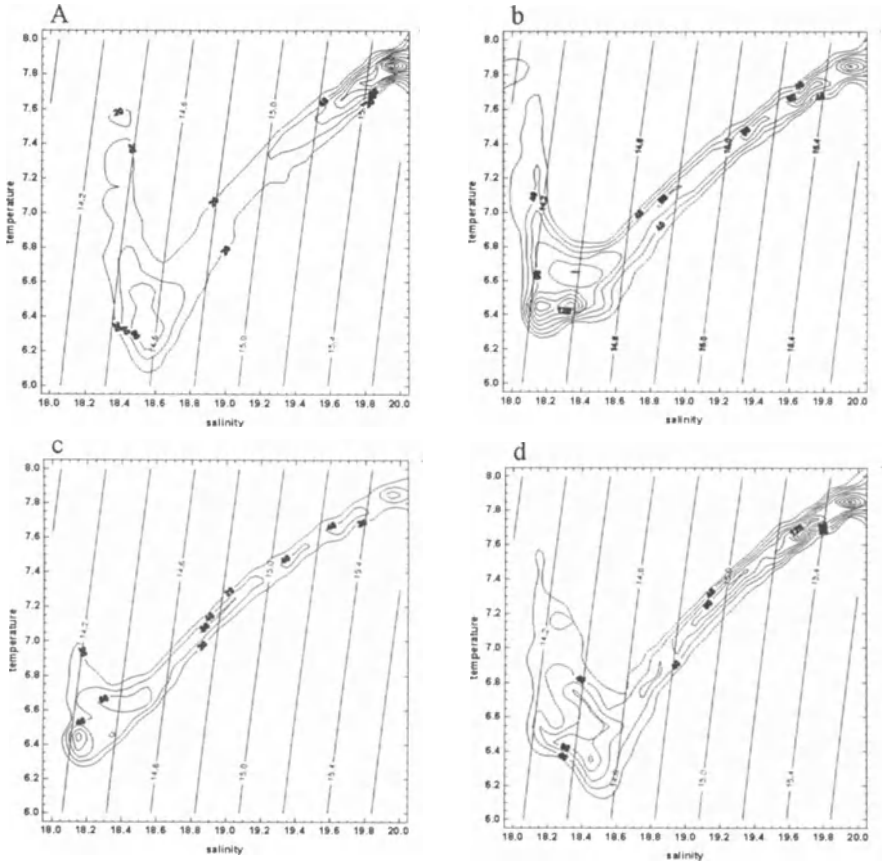


Figure 4 a-d. Volumetric T,S diagrams (as in fig.3) for the CR (a), ACR (b), EACR (c), RC (d).

From a comparison of Figures 4,a and 4,b, it can be easily verified that the CR and ACR T,S diagrams cross each other at only one point. Intersection occurs because of elongation of the upper part of CR T,S diagram induced by summer warming. If we were to focus on the relative position of volume extremes for CR and ACR T,S diagrams, it becomes apparent that they could not be connected in an isopycnal manner. We consider the above facts as strong arguments to show that there is an effective separation of the central and peripheral zones, i.e., from the previous winter formation period until July 1992, CIW from the basin's interior did not replenish the CIL in the convergence zone and *vice a versa.* The Rim Current, being the zone of maximum potential vorticity gradient for the circulation (implicitly, the thickness of the layer characterises the stretching component of potential vorticity), effectively

inhibits the cross stream exchange. Since potential vorticity is a conservative property and major CIW characteristics are preserved during the warm period, significant changes in the entire CR and ACR CIL volumes are unlikely to occur on a seasonal time scale.

The low salinity cold waters, are supposed to be of shelf origin. Their temperatures are close to 6.4-6.5°C and they are concentrated in the region of the eastern anticyclonic eddy (EACR, Fig. 4,c). This fact may have two alternative explanations. These are waters generated in the nearby shelf area or they are from the north shelf of the sea but trapped in the eddy. Such phenomenon can occur if the spring intensification of the eddy coincides in time with the period when low salinity waters reach the region via advection by the Rim Current. In April 1993, low salinity and cold waters have been observed along the Caucasian coast within the convergence zone implying their 'local' origin. More saline waters (18.3-18.4) of the convergence zone were observed in the northern anticyclonic eddies but not in the Batumi eddy.

Climatic data [27] depict southeastern part of the sea as the region with the warmest climate within the Black Sea, and it was never reported as a CIW generation area. Most probably, this low salinity water is formed in the northeastern shelf area.

The CIW present the Rim Current zone (Fig. 4,d) most probably has been formed by waters of the cyclonic gyre and less saline waters of the convergence zone. Thus, the Rim current may be considered as a zone of interaction between waters of the cyclonic region and of the outlying anticyclonic area.

For each volumetric T,S diagram, it is possible to subjectively distinguish a core of newly formed and only slightly transformed cold waters and an 'old' CIW. The 'newly formed, slightly transformed cold waters' are defined, herein, as waters within the layer of relatively weak density stratification (compared to the main pycnocline), with T,S characteristics close to the core values. In the volumetric T,S diagrams, this water volume appears as a 'broad' area with enclosed isoline contours around the CIL core. Since the estimates are subjective, they are used in a qualitative rather than quantitative manner, i.e. for a comparative analysis.

For the anticyclonic area, the volume of the newly formed waters made up about 4000 km^3. This constituted, approximately, 57 per cent of the CIL total volume for this area. For the cyclonic region, the same value was 2700 km^3 (approximately, 50 per cent of the total CIL volume) revealing considerably smaller amount compared to the ACR. The largest portion of newly formed waters characterised the T,S diagram for the Batumi anticyclonic region. For this area, the volume of the CIL 'core' was 1800 km^3 (up to 60 per cent of the total CIL volume). At the same time, the volume of the low salinity waters within this dynamical feature was only 600 km^3, implying relatively insignificant role of the 'shelf source' in contributing to CIW.

5.4 CIL STRUCTURE FOR YEARS WITH ANOMALOUS WINTER CONDITIONS

5.4.1. The case of severe winter meteorological conditions

The April 1993 survey occupied only 70 per cent of the basin, and it was not possible to calculate the exact volume of the CIW. On the other hand, the volumetric T,S diagram of the CIW for the April 1993 survey area revealed major portions of water with different T,S characteristics within the CIL qualitatively similar to the 1992 survey. The largest portion of the newly formed water was rather uniform with temperatures of about 6.0 -6.2° C and with salinities about 18.2-18.3, i.e. with lower salinities than in 1992 for this area. Waters of the northwestern shelf were of anomalously low temperatures (2-5°C) but their total amount was negligible when compared with the CIW volume of anticyclonic and cyclonic areas.

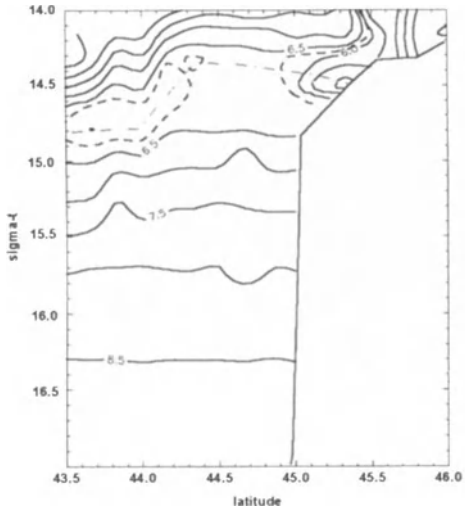


Figure 5. Temperature distribution on a transect along 32° 15' E and across the Rim Current in April 1993.

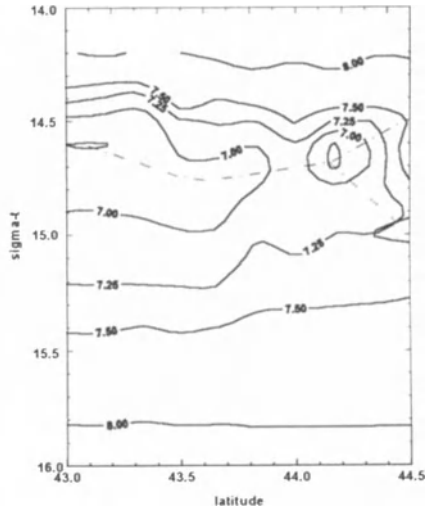


Figure 6. Temperature distribution on a transect along 34° 15' E and across the Rim Current in March 1995.

The above description shows appreciable similarity in CIW T,S structure for the 1992 and 1993 surveys. Note, that some peculiarities were better pronounced in 1993 as a result of severe winter meteorological conditions. For example, CIW salinities (densities) substantially differed across the frontal feature of the 'Rim Current' (Fig.5). The transition zone between denser and less dense waters was less than 20 miles at most of the transects. Salinity differences across the frontal feature were about 0.4 in 1992 and increased up to 0.6 in 1993. Salinities within the anticyclonic eddies were the same, revealing efficient entrainment (erosion of the pycnocline) only in regions with cyclonic circulation.

5.4.2. The case of mild winter meteorological conditions

The temperature distribution in isopycnal coordinates across the 'Rim Current' frontal zone for the 1995 survey is shown in Figure 6, and reveal not only quantitative, but qualitative distinctions between structures for anomalously warm and cold winters. In particular, in contrast with the situation in 1992 and 1993, CIW core densities, in 1995, increased shoreward (up to 14.9). Also, in 1995, the core of the CIL was stratified and its position in the vertical coincided with the largest vertical density gradients, revealing the relict character of the layer.

6. Summary

Since a large portion of new hydrographic data has been analysed, a new perspective on the problem of CIL formation in the Black Sea can be specified in the following section as part of our basic conclusions resulting from the analysis. A schematic illustration of these results is shown in Figure 7. Herein, let us address two basic specific questions: (1) Does the Black Sea CIW have a local or an advective nature? (2) What are the specific CIW source regions?

(1) A basic conclusion derived from the comparative analysis of the Black Sea volumetric T,S diagrams for a number of years and covering different regions is that the water formed by winter convection within the vast central area of cyclonic circulation, does not replenish the CIL in the convergence zone (schematised in the Figure by dashed lines), as it was claimed by Ovchinnikov [24, 25]. The cross frontal exchange within the CIL is strongly inhibited, due to strong cross frontal gradients in potential vorticity. In general, CIW is of 'local' origin if the term 'local' is used to discriminate areas of cyclonic and anticyclonic circulation but not in terms of their *in situ* formation. Within the cyclonic area and the convergence zone, the CIW is advected by currents. Waters of the convergence zone possess strong salinity stratification, which means that the newly formed part of the CIW in this region is of advective nature. Th high occurrence of CIL fine structure anomalies in the periphery of the basin supports this claim [13]. One specific example is the Batumi anticyclonic eddy (shown in Fig.7 by a black spot as a 'sink' region). The CIW found within its area cannot be formed in the southeast but should be advected from the north and the west along the Caucasian and Anatolian coasts within the convergence zone. There are indications of the penetration of a part of shelf generated waters into the ACR but the role of this mechanism is relatively small.

(2) For a cold winter, generation of the CIW within anticyclonic eddies accounts for more than half of the entire Black Sea CIL volume. At the same time, cooling is more 'effective' over the shelf and in the central part of the sea where heat losses per unit volume, apparently exceed the values for the anticyclonic areas. Thus, in terms of efficiency of entrainment, the central part of the sea may be considered as a CIW source region partially in support of Ovchinnikov's hypothesis. For a warm winter,

cross frontal differences in T,S characteristics are small and no quantitative estimates can be provided to support the above claims in this case.

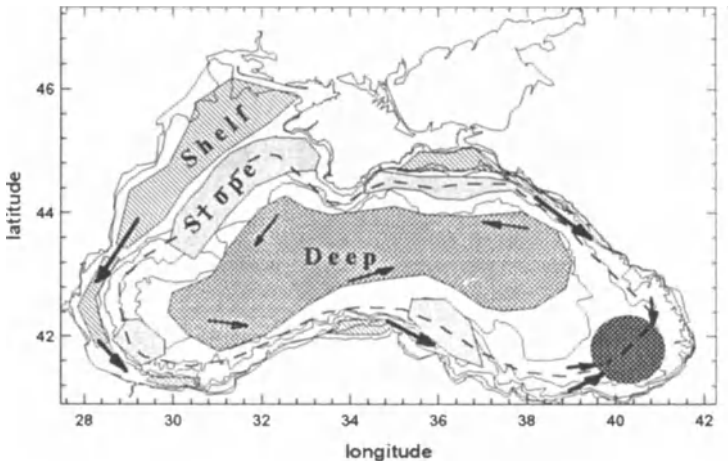


Figure 7. A scheme of CIW formation (source regions) and subsequent spreading. Black spot in the south eastern corner identifies CIW 'storage area' within the Batumi anticyclonic eddy.

7. Acknowledgements

This study has been made possible by support from the Turkish Scientific and Technical Research Council, Ukrainian Agency of Marine Research and Technologies, CoMSBlack and NATO TU-Black Sea Programs.

References

1. Aubrey, D.G., Oguz, T., Demirov, E., Ivanov, V., McSherry, T., Diaconu, V. and Nikolaenko, E. (1993) HydroBlack 91 - Report of the CTD Intercalibration Workshop. *IOC Workshop report* .**91**, 56 p.
2. Basturk, O., Saydam, C., Salihoglu, I., .Eremeeva, L.V., Konovalov, S.K., Stoyanov, A., Dimitrov, A., Cociasu, A., Dorogan, L. and Altabet, M. (1994) Vertical variations in the principle chemical properties of the Black Sea in the autumn of 1991, *Marine Chemistry* **45**, 149-166.
3. Blatov, A.S. (1981) Hydrological structure and energy storage of the Main Black Sea Current eddies, *Meteorologia i Gydrologia* **7**, 86-93.
4. Blatov, A.S., Bulgakov, N.P., Ivanov, V.A., Kosarev, A.N., Tuzhilkin, V.S. (1984) *Variability of hydrophysical fields of the Black Sea*, L.: Hydrometeoizdat (in Russian).
5. Buesseler, K.O., Livingston, H.D., Ivanov, L.I. and Romanov, A.S. (1994) Stability of the oxic/anoxic interface in the Black sea, *Deep-Sea Res.***41**, 283-296.
6. Bulgakov, S.N., Korotaev, G.K., Jwhitehead, J.A. (1996) Salt flux as a mechanism of large scale circulation in the Black Sea, *J. of Marine Res.* (in press).
7. Filippov, D.M. (1965) To the question about the cold intermediate layer in the Black sea, *Okeanologia* **5**, 635-641. (in Russian).
8. Filippov, D.M. (1968) *Circulation and structure of the Black Sea waters*, M.: Nauka. (in Russian)

PHYSICAL OCEANOGRAPHY VARIABILITY IN THE BLACK SEA PYCNOCLINE

L. I. IVANOV* Ş. BEŞİKTEPE+ and E. ÖZSOY+
* *Marine Hydrophysical Institute (MHI-NASU)*
2, Kapitanskaia, Sevastopol, Crimea, Ukraine.
+ *Institute of Marine Sciences (IMS-METU)*
Erdemli, Içel, Turkey.

Abstract. Local variability of the Black Sea permanent pycnocline position is caused, basically, by dynamical processes: Ekman pumping, meandering of the Rim current, mesoscale eddies, etc. Recent CTD measurements allow to filter local effects and to study variations of the pycnocline structure in detail with the focus on understanding of the role of different mechanisms which cause these variations. Gradual deepening of the isopycnal interfaces since 1991 as well as cooling (freshening) tendency has been registered. The total range of migration of the sigma-t interfaces within the pycnocline was 9 - 11 meters, with the shallowest position in 1990-91 and the deepest position in 1994. In the particular case, both cooling and freshening during 1991 - 1994 period, to some extent, occurred in response to changing vertical velocity. Cooling in this sense may not coincide with respective variation of annual mean air temperatures. In speculative manner, there should be a balance between combined variations of the basin's water balance, winter meteorological conditions and the thermohaline structure of the pycnocline layer. Weather conditions for the warm part of the year complicate the response in the pycnocline.

1. Introduction

The Black Sea is globally the largest body of anoxic waters facing rapid environmental deterioration under the impact of increasing contaminant inputs [17]. The evolution of the basin density and chemical stratification in the last few millennia results from the invasion of the Black Sea by the Mediterranean waters [6]; yet very little is known of the short term, interannual variability of the halocline or chemocline. Because the chemical changes including the transition from oxic to anoxic waters (i.e. the chemocline and the oxycline) coincide with the permanent halocline, its shoaling would imply adverse changes.

Claims of oxycline shoaling [7,11,18], supposedly in response to decreased freshwater inputs [18], have been contested and proved to be premature by more recent

E. Özsoy and A. Mikaelyan (eds.), Sensitivity to Change: Black Sea, Baltic Sea and North Sea, 265–274.
© 1997 *Kluwer Academic Publishers.*

results [3,4,9]. The former hypothesis of a rising oxycline could not be supported with positive proof, because comparisons based on depth profiles of oxygen, hydrogen sulfide or other chemical properties in a given region and time period could not isolate vertical displacements associated with local dynamical variability of currents (the meandering Rim Current, eddies, etc.) from processes of irreversible diapycnal mixing or chemical transformation. Typically, when comparisons are made with respect to density, so as to exclude variability resulting from dynamical effects, no justification remains to argue for a recent trend in the depth of the oxycline [2,9,10,24]. However, purely chemical changes can not be excluded; for example in nutrients [2,25] and possibly in the suboxic zone [4, 18, 20], in relation to eutrophication.

The observed stationarity of the present chemocline position with respect to density coordinates [2,9,10,25], raises the question of whether the density stratification itself is stationary on interannual time scales. Any foresight to this end has been limited in the past by the availability of data covering the entire basin.

The upper part of the pycnocline is ventilated effectively by wintertime convective cooling resulting in the formation of the Cold Intermediate Layer (CIL), residing below a warm layer in summer, and above the deep waters where temperature increases with depth [14].The deep waters of the Black Sea have striking stability in physical and chemical properties, as a result of limited turbulent energy penetration into the deep waters [19,23].

Direct ventilation appears to be confined to the layer above the pycnocline (above the 14.5 - 14.7 sigma-t interface) where convection and subsequent isopycnal injection supposedly are the major mechanisms of water mass formation [14,19]. Similarly, ventilation of the lower pycnocline occurs due to entrainment of the Cold Intermediate water (CIW) into the Mediterranean Water near the Bosporus and its subsequent injection in the lower pycnocline region (sigma-t = 15.8 - 16.2) by intrusions of the shelf modified waters [8, 23].

The interannual variations in the thermohaline structure of the pycnocline, acquired from the comparative analysis of the Atlantis II 1969 and Knorr 1988 data were reported in [19] with a suggestion, in a speculative manner, that possible causes for changes in the structure could be increased heat flux to the atmosphere and decreased freshwater input. On the other hand, permanent shifts in the position or structure of the pycnocline are not evident in recent data [9]. This brings into question the existence of possible short term (on a time scale of several years) variations in the pycnocline structure. Our analyses below reveal significant interannual variability in the vertical position and structure of the halocline (pycnocline) [15].

2. Data and Analysis Methodology

Recent CTD measurements (basin-wide and partial surveys within the context of the CoMsBlack program and TU-Black Sea project) in the Black Sea provide a unique opportunity to study variations of the pycnocline structure in detail, and to understand the role of different mechanisms which cause these variations. The data set includes

intercalibrated CTD data from basin wide surveys in September 1991, July 1992 [1,21] and surveys with 40-70 percent coverage of the sea (western part of the sea, mostly, with 10 to 20 miles between the hydrographic stations) conducted in the framework of the CoMSBlack and TU-Black Sea programs in April 1993, May 1994 and March-April 1995. To characterize an overall range of pycnocline temperature variations, the une 1984 data (approximately 60 percent of the whole basin coverage, western and central part, on 20 x 20 miles grid [12]) as well as the data from the joint MHI ASU - IMS METU October 1990 basin wide survey [22] were also included.

Data averaging over the survey area was used to filter effects of local dynamics. Since typical spatial scales of a mesoscale features in the Black Sea are on the order of 50 nm [5], such averaging procedure implies efficient filtering of a mesoscale fluctuations and therefore the averaged data depict the general features of the water body.

3. Results

Temperatures in the core of the CIL, as well as meteorological data reveal a decrease in winter averaged temperatures for the region in 1991 - 1993 [14,26]. The winter of 1994 was warmer (CIL core temperatures in May of 1994 were, approximately, 0.2°C warmer than in April of 1993) and the 1995 winter could be characterized as anomalously warm [14].

Averaged positions of the selected sigma-t surfaces and the temperatures at those surfaces for the 1991 - 1994 period are presented in [15]. The updated results are shown in figures 1a,b, revealing that the deepest position of the pycnocline occurred in 1994. Note that the deepening of the pycnocline did not coincide with the time of maximum surface cooling. Only the 1995 data showed a tendency of reversal in the vertical migration of the interfaces, and the cooling appreciably lagged behind, with increasing lag with depth. The slanted dashed line in fig. 1,b reveals the vertical phase shift in the temperature fluctuations. For the upper pycnocline (14.8 sigma-t), the lowest temperature occurred in 1993, but the cooling in the lower part of the pycnocline continued at least until March 1995 in the form of a delayed response to the earlier surface cooling. Since the only source for water with lower temperatures is at the surface, cooling at the sigma-t interfaces of the pycnocline implies ventilation of the layer continuing in the second and the third years after the extreme surface cooling.

Referring to the analysis of climatological data [16] and individual data sets for one specific year [13], it can be easily shown that the seasonal warming (same for winter cooling) is confined mostly to the layer above the core of the CIL and intraanual changes of temperature and salinity at 75 m and below are small (respectively less than 0.04°C and 0.05 [16]) when compared with interannual variability (see fig.1). Therefore, the recent data obviously show appreciable interannual changes within the pycnocline. Such a comparison also provides confirmation to the claim that various properties are well preserved within the pycnocline region on a seasonal time scale, i.e. the results of the present study are not much affected by seasonal variability.

The total range of excursion of the sigma-t interfaces within the pycnocline was 9 - 11 meters, with the shallowest position in 1990-91 and the deepest position in 1994. The combined effect of the downward pycnocline migration and of the cooling resulted in a considerable changes in the position of the lower CIL boundary [Ivanov et al., this volume], revealing appreciable interannual changes from 77 meters in June 1984 (the warmest year) to 107 meters in 1994 (especially large when compared with the negligible seasonal changes [16]). This fact strongly contests the claim on intraannual stationarity of the total volume of water above the lower boundary of the CIL [16].

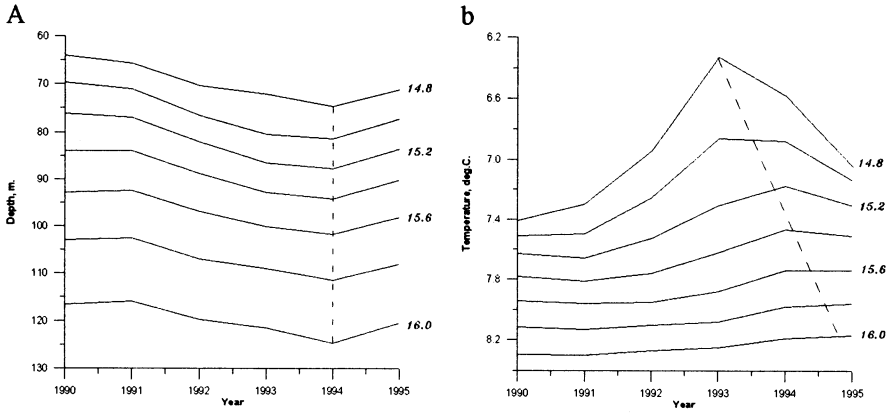


Figure 1. Positions of the 14.8 - 16.0 sigma-t interfaces and temperatures at those surfaces.

The average T,S curves for 1984 and 1990 - 1994 (downward migration phase of the pycnocline) in figure 2 illustrate the overall temperature and salinity variations in the pycnocline region. The arrowhead lines in fig.2 show successive changes in T,S at 70 and 90 m depths. On the T,S plane, 'points' for the 1984 - 1991 period 'shifted' towards denser position since cooling and salinity increase occurred at a fixed depths.

Figures 1 & 2 depict T,S variability of the averaged data. Figure 3 shows the overall range of variations in the position and temperature of the 15.6 sigma-t interface throughout the survey areas for June 1984, September 1991 and May 1994 periods, revealing a consistent decrease in temperature in all regions of the sea.

In June 1984 and May 1994, the temperature distribution has asymmetry, with some data revealing the existence of anomalously (compared to the averaged values) cold water. Water with low temperatures (low salinities) originates from near the Bosphorus region, where mixing of the Mediterranean waters with CIW and the subsequent lateral injection into the basins interior takes place [8,23]. Similar cold water patterns can be seen on other interfaces in the range of 15.2 - 16.2 sigma-t.

Vertical profiles of temperature and salinity vertical gradients for the 1991 - 1994 surveys are shown in figures 4 a,b. It can easily be verified that the temperature gradient varies in much broader range than the salinity gradient, and the same is also valid for the second derivatives. Because the computation of second derivatives proved to be noisy, order of magnitude estimates were made by dividing the profiles to three

density intervals of sigma-t = 14.8 - 15.4, 15.4 - 15.8 and 15.8 - 16.2 respectively, representing the upper, middle and lower pycnocline, so that the second derivatives are calculated at the middle part.

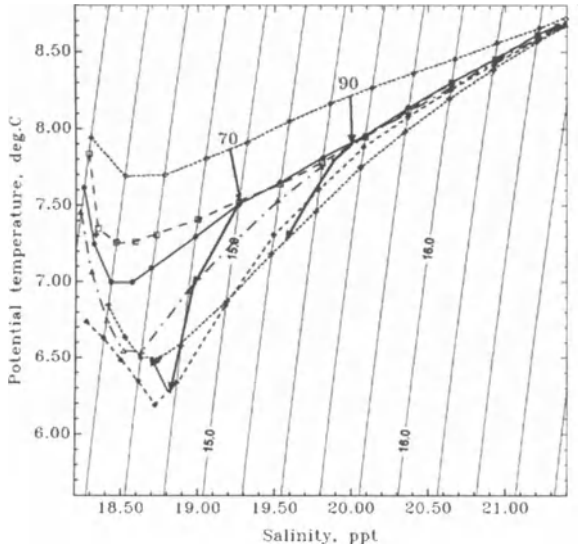


Figure 2. Averaged T,S diagrams for the 1984, 1990-94 surveys. Arrowhead lines show them in succession.

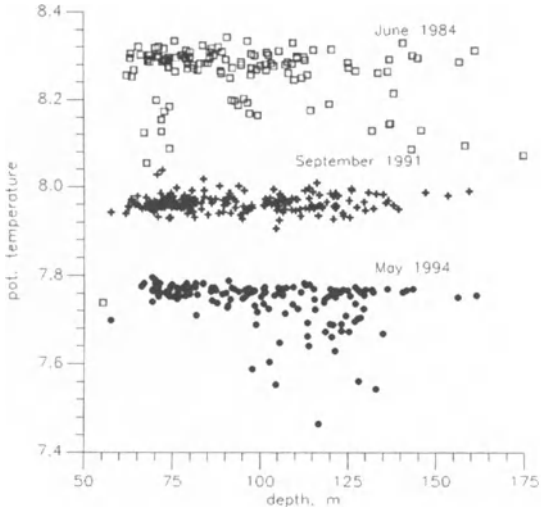


Figure 3. Scatter distribution of potential temperature at 15.6 sigma-t interface for different years.

For the 1991 - 1994 period, cooling and decrease in salinity were observed, resulting in a net deepening of the density surfaces (salinity changes overcompensated the decrease in temperature), proportional to the difference between salinity ($\beta\Delta S$) and temperature ($\alpha\Delta T$) contributions to density variations. The decrease in salinity was more uniform with depth than the decrease in temperature (fig.4,a,b). In the vertical, values of $\Delta T/\Delta t$ decrease faster than $\Delta S/\Delta t$ (t is time) so that the vectors characterizing T,S variations on the T,S plane veer towards isopycnal orientation in the upper layers (see fig.2). The divergence of these vectors in the pycnocline region characterizes changes in density stratification, i.e. a downward 'migration' (in terms of density) of pycnocline (i.e. the layer of maximum vertical density gradient). In 1991, the maximum density gradient was confined to the 14.9 sigma-t level and it shifted to the 15.3 level in May 1994. Variations in density structure can be very important for the Black Sea from a dynamical point of view, since they would also characterize changes in potential vorticity; this last issue is beyond the scope of the present paper.

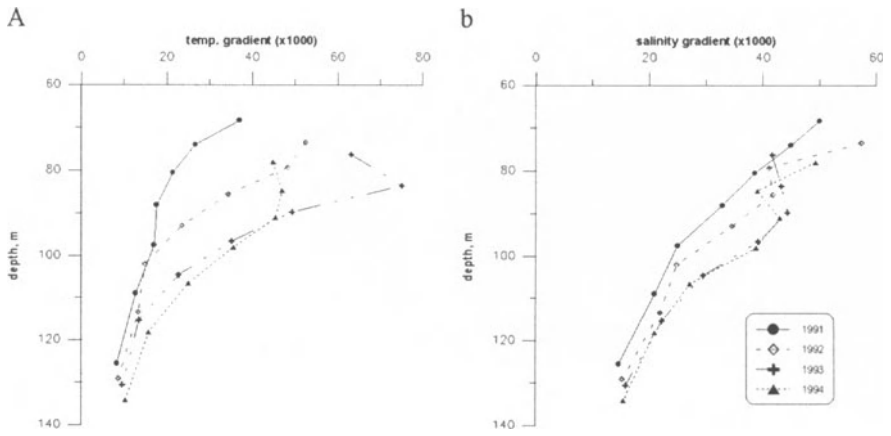


Figure 4. Vertical temperature (a) and salinity (b) gradients versus depth for the 1991 - 1994 period.

4. Discussion

In the following section, we shall scrutinize recent temporal changes in temperature and salinity. Both for temperature and salinity, we may write the following equations which characterize the balance between vertical diffusion, vertical advection and temporal variations:

$$\partial T/\partial t + W\,\partial T/\partial z = k_T\,(\partial^2 T/\partial z^2); \qquad (4.1)$$
$$\partial S/\partial t + W\,\partial S/\partial z = k_S\,(\partial^2 S/\partial z^2),$$

where W is the vertical velocity, k_T and k_S are the vertical diffusion coefficients.

It is assumed, for simplicity, that, vertical variations of the diffusive coefficients within the pycnocline depth range are much less important than variations of vertical

temperature and salinity gradients. Since we consider mean values for the whole Black Sea, horizontal advection is neglected.

4.1. AN ESTIMATE OF VERTICAL VELOCITY

With the existing data, it is difficult to estimate the amount of laterally injected waters, which actually affect the W value, but, for a first order approximation, it is possible to assume that that the ratio of entrainment to Bosphorus inflow varies from about 6-11 [8,24] in the upper pycnocline to 3.3 [19] in the deep layer. The volume of Bosphorus effluent is 312 km^3 per year [27] and, with an averaged (in the vertical) entrainment ratio of about 7, the total volume of intrusions can be estimated as 2.3 x 10^3 km^3 per year and the resulting upward velocity is then 2.1 x 10^{-7}m/s. Most probably this is a lower limit estimate for W, because in [23,24] it was explicitly shown that intrusions resulting from the near bottom mixing of the inflowing Mediterranean waters are confined mostly to the upper layer, which would result in higher values for W in the pycnocline layer.

4.2. AN ESTIMATE OF DIFFUSIVE COEFFICIENTS

There are two equations (4.1) with three unknowns (W, k_T, k_S) and to solve them a certain hypothesis should be applied. We can use the estimate of W made above. Substituting this value (W = -2.1 x 10^{-7}m/s) into (4.1), we obtain k_T and k_S close to (1.2-1.5) $10^{-5}m^2/s$ and (1.0-1.2) $10^{-5}m^2/s$, respectively. Another approach is also possible: We could assume $k_T = k_S$, as it is often considered for the pycnocline region where diffusive coefficients are typically two orders of magnitude larger than those for molecular diffusion. This yields estimatesin the ranges of W = (-3 - -5) 10^{-7}m/s and $k_T = k_S$ = (2-3) $10^{-5}m^2/s$.

4.3. POSSIBLE TIME VARIATIONS OF TERMS

Temporal variations in the pycnocline can occur as a result of changes in vertical velocity, vertical gradients, second derivatives or the diffusion rate. It should be emphasized that basin averaged vertical velocity (excluding the side boundary layers) for the Black Sea is always negative (z axis pointing downward) and its value depends upon total water balance of the basin. An increase in the absolute value of W results in warming and subsequent increase in salinity at a certain depth level.

In the above section it has been revealed that downward migration of density interfaces was also associated with 'deepening' of the profiles of temperature and salinity with respect to density and not only depth. Since the vertical gradient term is accompanied by the vertical velocity W in equations (4.1), its increase (decrease) is equivalent to the effect of an increase (decrease) in vertical velocity. In our further speculations we shall therefore take into consideration the combined effects of W and $\partial S/\partial z$, $\partial T/\partial z$ changes, referring to it as the effect caused by the W variation. Note, that the changes in salinity vertical gradients were for the most time insignificant; hence,

we basically observed a decrease in vertical velocity during 1991 - 1994, rather than the effect of $\partial S/\partial z$, $\partial T/\partial z$ variations. If changes in W were constant in time, the effect would be greater in 1993-94, when the gradients were higher, rather than in 1991-92.

Figure 4 implies appreciable temporal changes in second derivative of temperature and small changes in salinity. For simplicity we consider the diffusive coefficients to be constant.

4.3.1. Changing vertical velocity

Based on a basic balance between diffusive and advective effects, it can be argued that diffusion effects will depress the pycnocline when advective effects recede, or *vice versa*. Note, further, that the variations in the vertical first and second derivatives of temperature are usually larger than that of salinity, as may be verified by figures 4a,b, and the temporal change of salinity gradient at the pycnocline is relatively constant with depth. The latter situation could correspond to vertical shifts of the salinity profile due to changes in vertical velocity.

The decrease in vertical velocity in the 1991-94 period amounts to 15-30 % of the average value. Changes of W affect the temperature, but, for the upper and middle pycnocline, in much less extent than salinity and density. Therefore, the variations of pycnocline position are mostly governed by changes in W. Such variations in vertical velocity affect the profiles of all the other properties (vertical distribution of nutrients, dissolved oxygen, hydrogen sulfide, etc.) in much the same way as salinity, density and temperature profiles, giving an explanation for the observed stationarity of the present chemocline position with respect to density coordinates.

4.3.2. The role of heat flux

Variation in vertical advection has resulted in deepening of the halocline (pycnocline) approximately by 9 - 11 m in 1991-1994 (see fig.1). Using this estimate, and the mean temperature gradients in figure 4a, the mid-pycnocline (90-100 m depth) temperature change accounted by advection during the same period is estimated to be on the order of 0.3^{0}C, or 45 % of the total variance. The remaining part is explained by diffusion of heat.

4.3.3 Comparison with other data

To check consistency of the present observations with the hypothesis claiming long term stability of the Black Sea pycnocline [9], data from the 1969 Atlantis II and the 1988 Knorr surveys [19] can be used for comparison with present results. The 1969 T,S relationship lies somewhere in between the 1984 and 1991 extremes in Figure 1, and the 1988 T,S relationship approximately coincides with the 1992 curve, showing that both cases are within the range of the discussed thermohaline variability from 1984 to 1994. Most probably, there was a cooling phase from 1984 to 1988, followed by subsequent warming before 1990, and the last cooling episode of 1991-94 described in this paper. The observations suggest interannual and interdecadal variations in the pycnocline.

Note, that the cooling may not necessarily coincide with the respective variations of annual mean air temperature. In a speculative manner, more general influences should be expected, involving combined effects of the basin's water balance, the time history of winter meteorological conditions including other variables such as the wind stress, basin averaged surface fluxes, and the averaged curl of wind stress, driving the system through either direct or proxy relationships.

5. Summary

Substantial interannual variability is shown to exist in the pycnocline structure. In the period from 1991 to 1994, appreciable deepening of the pycnocline region occurred mostly due to a decrease in the upward vertical velocity. This result in itself sheds light on the question of remarkable stationarity displayed by the present chemocline [2,4,9,10,24]. Variations in vertical velocity affect all other profiles (vertical distribution of nutrients, dissolved oxygen, hydrogen sulfide, etc.) in the same way as salinity, and temperature profiles, giving an explanation for the observed stationarity of the present chemocline position with respect to density coordinates.

6. Acknowledgments

The study has been made possible through support from the Turkish Scientific and Technical Research Council, Ukrainian Agency of Marine Research and Technologies, CoMSBlack and NATO TU-Black Sea Programs. The research was partly made possible through individual support of L.I. Ivanov by Grant K3M100 from the Joint Funds of the Government of Ukraine and International Science Foundation.

References

1. Aubrey, D.G., Oguz, T., Demirov, E., Ivanov, V., McSherry, T., Diaconu, V. and Nikolaenko, E. (1993) HydroBlack 91 - Report of the CTD Intercalibration Workshop. *IOC Workshop report* .**91**, 56 p.
2. Basturk, O., Saydam, C., Salihoglu, I., Eremeeva, L.V., Konovalov, S.K., Stoyanov, A., Dimitrov, Cociasu, A., Dorogan, L. and Altabet, M. (1994) Vertical variations in the principle chemical properties of the Black Sea in the autumn of 1991, *Marine Chemistry* **45**, 149-166.
3. Bezborodov, A.A., Eremeev, V.N. (1991) Variability of the structure of oxygen - hydrogen sulfide zone in the Black Sea. "Dramatic" or synoptic? *Marine hydrophysical journal* **1**, 59-68.
4. Bezborodov, A.A., Eremeev, V.N. (1993) *Black Sea. Oxic/anoxic zone.* Marine hydrophysical institute, Sevastopol. (In russian)
5. Blatov, A.S. (1981) Hydrological structure and energy storage of the Main Black Sea Current eddies, *Meteorologia i Gydrologia* 7, 86-93.
6. Boguslavskiy, S.G. and Kotovshchikov, B.B. (1984) Formation of Recent Salinity Field in the Black Sea. *Oceanologia* **24**, 313-316.
7. Bryantsev, V. A., Faschuk, D. Ya., Ayzatullin, T. A., Bagotskiy, S. V. and Leonov, A. V. (1988) Variation in the Upper Boundary of the Hydrogen Sulphide Zone in the Black Sea: Analysis of Field Observations and Modeling Results. *Oceanologia* **28**, 80-185.
8. Buesseler, K.O., Livingston, H.D., Casso, S.A. (1991) Mixing between oxic and anoxic waters of the Black Sea as traced by Chernobyl cesium isotopes. *Deep-Sea Res.* **38**, suppl.**2A**, 725 - 746.

9. Buesseler, K.O., Livingston, H.D.,.Ivanov, L.I., Romanov A.S. (1994) Stability of the oxic/anoxic interface in the Black sea. *Deep-Sea Res.* **41**, 283-296.
10. Codispoti, L.A., Friederich, G.E., Murray, J.W., Sakamoto, C.M. (1991) Chemical variability in the Black Sea: implications of continuous vertical profiles that penetrated the oxic/anoxic interface. *Deep Sea Res.* **38**, suppl. **2A**, 691-710.
11. Fashchuk, D.Ya. and Ayzatullin, T.A. (1986) A Possible Transformation of the Anaerobic Zone of the Black Sea. *Oceanologia* **26**, 171-178.
12. Golubev, Yu.N., Tuzhilkin, V.S. (1992) Dynamics and energetics of antyciclonic eddy in the central part of the Black Sea in the summer of 1984. *Okeanologia* **32**, 428-435.
13. Ivanov, L.I. (1993) Cold intermediate water formation in the western Black sea as derived from 1992 data, in. V.N.,Eremeev (ed.), *Problems of the Black sea*, MHI, Sevastopol, p.p. 78-89.
14. Ivanov, L.I., Besiktepe, S., Ozsoy, E. (1996) Black Sea Cold Intermediate Layer, in A.Mikaelyan and E., Ozsoy (eds), *Sensetivity of the North Sea, Baltic Sea and Black Sea to Anthropogenic and Climatic Changes,* Kluwer Academic Publishes, Dordrecht, NAT ASI Series, this issue.
15. Ivanov, L.I., Besiktepe, S., Ozsoy, E., Duman, M., Demirov, E., Diakonu, V. (1995) Recent changes in Black Sea pycnocline. *Proceedings of CIESM Malta 1995 Meeting.*
16. Mamaev, O.I., Arkhipkin, V.S., Tuzhilkin, V.S. (1994) T,S analysis of the Black Sea waters. *Okeanologia* **34**, 178-192.
17. Mee, L.D. (1992) The Black Sea in Crisis: the Need for Concerted International Action. *Ambio* **24**, 278-286.
18. Murray, J.,W., Jannasch, H.W., Honjo, S., Anderson, R.F., Reeburgh, W.S., Top, Z., Friederich, G.E., Codispoti, L.A., Izdar, E. (1989) Unexpected changes in the oxic/anoxic interface in the Black Sea. *Nature* **338**, 411-413.
19. Murray, J.M., Top, Z., Ozsoy, E. (1991) Hydrographic properties and ventilation of the Black Sea. *Deep-Sea Res.* **38**, suppl.**2A**, 663 - 689.
20. Murray, J.W., Codispoti, L.A., and Friederich, G.E. (1993) Redox Environments: The Suboxic Zone in the Black Sea, in Huang, C.P., O'Melia, C.R. and Morgan, J.J. (eds), *Aquatic Chemistry*, American Chemical Society.
21. Oguz, T., Besiktepe, S., Basturk, O., Salihoglu, I., Aubrey, D.G., Balci, A., Demirov, E., Diakonu, V., Dorogan, L., Duman, M., Ivanov, L.I., Konovalov, S., Stoyanov, A., Tugrul, S., Vladimirov, V. and Yilmaz, A. (1993) Report on the CoMSBlack '92a Physical and Chemical Intercalibration Workshop, *IOC Workshop Report* **98**, 1-86.
22. Oguz, T., Latun, V.S., Latif, M.A., Vladimirov, V.V., Sur, H.I., Markov, A.A., Ozsoy, E., Kotovshchikov, B.B., Eremeev, V.V., Unluata, U. (1993, b) Circulation in the surface and intermediate layers of the Black Sea, *Deep-Sea Res.* **40**, 1597-1612.
23. Ozsoy, E., Unluata, U. and Z. Top (1993). The evolution of Mediterranean water in the Black Sea: interior mixing and material transport by double diffusive intrusions, *Prog. Oceanogr.*, **31**, 275-320.
24. Ozsoy, E., Top, Z., White, G., Murray, J.W. (1991) Double diffusive intrusions, mixing and deep convective processes in the Black Sea, in Izdar, E. and Murray, J.W. (eds), *Black Sea Oceanography.* NATO/ASI Series, Kluwer Academic Publishers, Dordrecht, pp.17-42.
25. Tugrul, S., Bacsturk, O., Saydam, C., Yilmaz, A. (1992) Changes in the Hydrochemistry of the Black Sea Inferred from Water Density Profiles. *Nature* **359**, 137-139.
26. Turkes, M., Sumer, U., Kilic, G. (1995) Variations and Trends in Annual Mean Air Temperatures in Turkey With Respect To Climatic Variability. *Int. Journal of Climatology* **15**, 557-569.
27. Unluata, U., Oguz, T., Latif, M.A., Ozsoy, E. (1989) On physical oceanography of the Turkish straits, in L.J.Pratt (ed.), *The physical oceanography of sea straits*, NATO/ASI Series, Kluwer Academic Publishes, Dordrecht.

THE BLACK SEA BOTTOM HOMOGENEOUS LAYER: A SIMPLE MODEL OF FORMATION.

V. N. EREMEEV[♣], L. I. IVANOV[♣], A. S. SAMODUROV[♣] and M.DUMAN[♠].
[♣] *Marine Hydrophysical Institute (MHI-NASU), Sevastopol, Ukraine.*
[♠] *Institute of Marine Sciences & Technologies (IMST-DEU), Inciralti, Izmir, Turkey.*

Abstract. The analysis of field data and the results of a one-dimensional model are applied for the description of the deep water structure in the Black Sea. The results of the model support the claim that the observed bottom homogeneous layer exists as a result of the geothermal heat flux and the dependence of mixing properties on stratification. The bottom mixed layer in the Black Sea can only exist if part of the incoming salt penetrates into the bottom layer.

1. Introduction

The Black Sea is an 'estuary type' basin. Precipitation and riverine discharges exert a freshening influence upon the upper part of the sea, and increase in salinity occurs due to Marmara Sea water entering the basin from the Bosphorus. Complex processes of mixing of the incoming water and upward flux of salt results in the penetration of salt into the upper layers exiting the basin through the Bosphorus, in accordance with the salt balance conditions. As a result, the salinity increases monotonously with depth. In general, the temperature also increases with depth, starting from the core of the Cold Intermediate Layer. Winter-time cooling, the incoming relatively warm waters from the Bosphorus and the geothermal heat flux are the principal factors affecting the formation of temperature stratification. The most prominent feature that occurs due to the geothermal heat flux is the near bottom convective layer, herein defined as the Bottom Homogeneous Layer (BHL).

2. Observational data

To make estimates of the parameters of the BHL, all hydrographic data collected by precise CTD probes during recent years have been utilised (fig.1). The final data set consisted of the CTD data from the R/V Knorr 1988,, the R/V Piri Reis March 1992

E. Özsoy and A. Mikaelyan (eds.), Sensitivity to Change: Black Sea, Baltic Sea and North Sea, 275–283.
© 1997 *Kluwer Academic Publishers.*

cruises and the MHI data collected by R/V 'Professor Kolesnikov' in the framework of the CoMSBlack-92'a, 93' and 95' expeditions. In the Knorr 88, Piri Reis 92 and, partly, in 'Professor Kolesnikov' 1995 cruises SBE probes were used; the other data were collected with an Istok-7 probe. The fact that the hydrographic data were collected by different types of CTDs does not allow one to analyse the variability of deep water features using the pooled data set. However, estimates of the mean properties are reliable and it has been possible to derive spatial variability of the parameters from the data sets of the individual cruises.

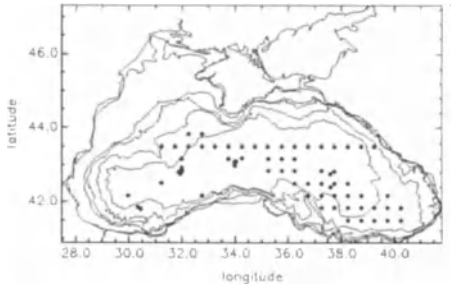


Figure1. Locations of stations comprising the pooled data set.

The results of the observations reveal that, just above the top BHL interface, a transition layer of, approximately 50 m thickness occurs [4]. This layer is characterised by a noticeable increase in the temperature and, to a lesser degree, salinity gradients. The structure of the BHL has been characterised by the position of the BHL top interface, its stability ratio, and vertical gradients of salinity and potential temperature within this zone.

In all of the data, the BHL thickness varied from 60 m to 460 m, which decreased towards the continental slope. A review of all the data yields an estimate for a typical BHL thickness for the open part of the sea to be about 350 m.

The calculated mean value of the stability ratio ($R_\rho = \beta \cdot \Delta S / \alpha \cdot \Delta T$) for the transition layer above the BHL top interface is 2.6 ± 0.18, where T is the potential temperature, S is the salinity, α and β are respectively the thermal and haline expansion coefficients.

3. Modeling

The stable vertical density gradient in the Black Sea is mostly due to salinity stratification and the destabilizing role of temperature is relatively small. That is why a laboratory modeling approach describing the evolution of a stably stratified layer heated from below [3,8] can be postulated as an appropriate model of the Black Sea BHL. In general, the development of convection process is the following. After the initial oscillatory phase of instability, as heating exceeds a critical value, a convective mixed layer is formed over the bottom and its upper boundary moves upwards. The process of double diffusion in the diffusive regime play an important role in evolution of this mixed layer[4,5,6,7]. Due to this mechanism, the growth of the layer at specific moment of time abruptly stops and a new layer is formed at the top of the initial convective layer. As a result, a multilayer structure is usually formed and it controls the vertical exchange of salt and heat. The fact that a single layer of convection is observed

in the Black Sea was explained [4,5,7] by the interface being in the long time limit of the 'low stability regime' [2], which is a result of vanishingly small entrainment by the convective eddies, effectively limited by the interfacial stratification.

The basic objective of modeling within this studies is to assess conditions that determine BHL existence in the Black Sea and to determine the sensitivity of this feature to possible climatic changes.

In modeling, we adopt the idea that, for the Black Sea, the bottom convective layer exists as a result of the geothermal heat flux [4,5,7]. Values for this heat flux are relatively uniform with a slight increase towards the continental slope [1] and may be estimated as $H_Q \approx 3 \cdot 10^{-2} watt / m^2$. It is also assumed that, in stationary conditions, heat and salt fluxes out of the BHL are controlled by double diffusion in diffusive regime.

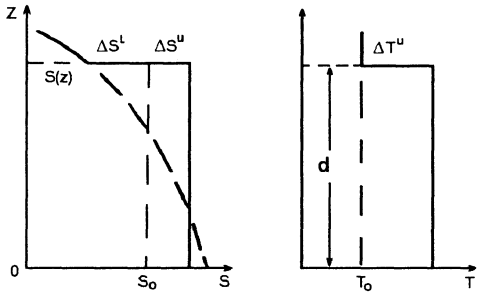


Figure 2. The scheme of the BHL formation

Small variations in the position of the BHL upper interface as well as in the stability ratio values at the BHL upper boundary give evidence to argue on the stationary character of the layer. Estimates of heat flux across the upper BHL interface can be also used as a weighty argument for the hypothesis of stationary character of the layer. For the Black Sea conditions, we acquire estimates of heat fluxes about $4.3 \cdot 10^{-2}$ watt/m^2 and $3.3 \cdot 10^{-2}$ watt/m^2, respectively (the same estimates made using two different flux formulae in [4] were $7.4 \cdot 10^{-2}$ watt/m^2 and $5.2 \cdot 10^{-2}$ watt/m^2). Both estimates are close to the typical value of the geothermal heat flux.

Let us depict the process of the BHL evolution in the framework of the Turner's one dimensional model [8]. Taking into consideration the salt flux originating from the Bosphorus, one can write basic equations in terms of buoyancy in a general form:

$$\int_0^t B_T dt = g\alpha \cdot \Delta T^U d\,, \qquad \int_0^t B_S dt = g\beta \cdot \Delta S^U d\,, \tag{1}$$

where B_T and B_S are buoyancy fluxes into the BHL which are controlled by heat and salt fluxes respectively. The other definitions can be found in Figure 2.

It is possible to formulate the third equation using the condition that potential energy has to be constant during the period of BHL evolution:

$$\frac{1}{2} g\rho_0 d^2 (-\alpha \cdot \Delta T^U + \beta \cdot \Delta S^U) - g\rho_0 \beta \cdot \int_0^d z \cdot s(z) dz = 0\,, \tag{2}$$

where $\rho = \rho_0[1 - \alpha \cdot (T - T_0) + \beta \cdot (S - S_0)]$, $S = S_0 + s(z)$ is the initial density distribution with the requirement $\int_0^d sdz = 0$. Since the variables B_T, B_S, s(z), d, ΔS^L must be set, finally, we have three equations for determination of three unknown time dependent functions: d, ΔT^U, ΔS^U.

The process of BHL formation may be considered as complete, when the conditions of the balance of heat and salt are achieved. When $d = d_e$:

$$f(R_\rho)(\alpha \cdot \Delta T^U)^{4/3} = B_T \quad (3)$$

$$B_S = \gamma \cdot B_T, \gamma \cong 0.15 \quad (4)$$

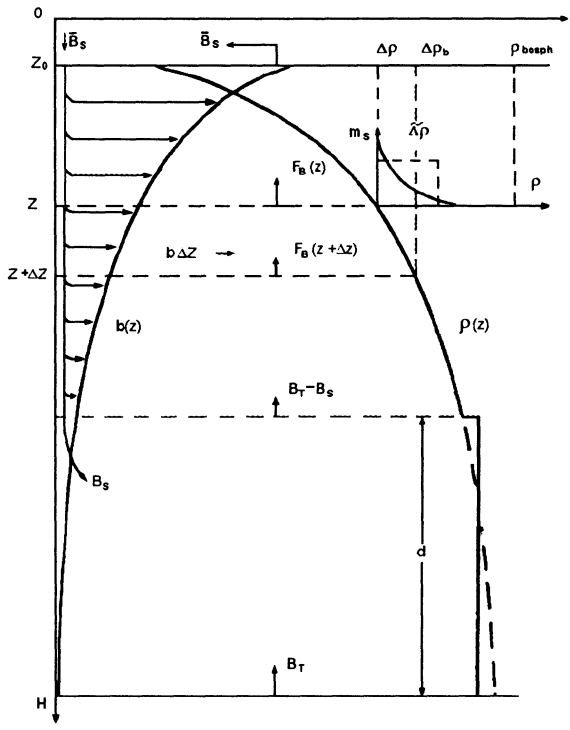


Figure 3. The scheme of the salt balance in the Black Sea (see definitions in the text).

Here, f is the known function of R_ρ [3,8], and (4) corresponds to the results of the laboratory modeling [8] concerning the constancy of the ratio of fluxes ($\gamma \cong 0.15$) in a broad range of R_ρ ($R_\rho \geq 2$) when the exchange is controlled by double diffusion.

Inevitably, the process of BHL formation from the time when the saline Marmara Sea water began to intrude the Black Sea is rather sophisticated and can not be described in detail using the above approach. Herein we shall consider only the basic knowledge available about the contemporary state of the sea. In particular, we consider the bottom geothermal heat flux to be a constant value. For salt flux from the Bosphorus, we assume the more realistic model that takes into account its dependence on stratification. Accordingly, it is possible to introduce buoyancy flux B_S due to salt flux from the Bosphorus source into the BHL of variable depth (d) in the form:

$$B_S = b_S(d)(1-K_r), \qquad b_S(d) = \int_{H-d}^{H} b dz \tag{5}$$

where $b(z)$ is the specific rate of buoyancy production. The factor $b_S(d)$ depends upon the stratification in the 'undisturbed' (prior to BHL formation) fluid, and K_r depends upon stratification in the transition layer above the top BHL interface.

Within the one dimensional approach used in these studies, let us consider the following model of 'stirring' of salt from the Bosphorus effluent in the Black Sea.

Let $\overline{M_S}$ be the salt mass coming into the basin per unit time, which is continuously mixed with the ambient fluid. At some moment, part of this salt $\overline{M}_S - M_S(z)$ reaches a depth level z. The salt is distributed in a volume that is inhomogeneous in terms of density. The total range of density variations in the volume can be defined as $\Delta\rho_b = \rho_{bosp} - \rho(z)$, where ρ_{bosp} is the density of the incoming water (Fig.3) that reaches the upper boundary of the main pycnocline. The function m_S in Figure 3 is a function of salt distribution in the density range $\Delta\rho_b$ normalised by $\overline{M}_S - M_S(z)$.

Under the action of buoyancy forces, the mass of salt in the volume with the range of density variations $\Delta\rho$, will pass into the layer Δz :

$$(\overline{M}_S - M_S(z)) \cdot m_S^0 \cdot \Delta\rho, \tag{6}$$

and the rest of the salt penetrates deeper. Here, $m_S^0 = m_S(0)$. Multiplying (6) by $g\beta / \overline{S}_{BS}$, where $\overline{S}_{BS}$ is the area of the Black Sea, we obtain:

$$(\overline{B}_S - \int_{z_0}^{z} b dz)k\frac{\Delta\rho}{\rho} = \Delta z, \quad \overline{B}_S = g\beta \cdot \overline{M}_S, \; k = \rho \cdot m_S^0 \tag{7}$$

If the process of Bosphorus salt 'stirring' is self-similar then m_S^0 is a constant value. With $\Delta z \to 0$, we obtain:

$$\frac{g}{k} N^2 b + \int_{z_0}^{z} b dz - \overline{B}_S = 0. \tag{8}$$

Differentiating (8) by z, finally, we obtain equation for b :

$$b_z + [\frac{k}{g} N^2 - \frac{(N)_z^2}{N^2}] \cdot b = 0 \tag{9}$$

The function $N(z)$ for the Black Sea may be approximated by the function $N(z) = N_0(\frac{z_0}{z})$. Then, the solution (9) has the form: $b = b_0 N^2 \exp(Nk\frac{N_0 z_0}{g})$,

and the constant b_0 is found from the condition $\int_z^H b dz = \overline{B}_S$. After integrating, we get

$$b_S(d) = \overline{B}_S\{\exp(\frac{kr}{H-d}) - \exp(\frac{kr}{H})\}\{\exp(\frac{kr}{z_0}) - \exp(\frac{kr}{H})\}^{-1} \; r = \frac{N_0^2 z_0}{g} \quad (10)$$

This value determines buoyancy flux due to salinity input from the Bosphorus into the near bottom layer of thickness d when convection is absent. The existence of convective motions within the layer increases the vertical density gradient at the top interface when compared to background values. As a result, less salt penetrates into the convective layer than into an 'undisturbed' layer of the same thickness. Part of the total amount of salt that reaches BHL top interface is withheld there by buoyancy forces, and diffuses upwards. Respectively, a value of K_r determines a 'reflection coefficient'. In accordance with (7), we define: $B_S = b_S(d) - b_S(d) \cdot k(\frac{\Delta\rho^U}{\rho})$ and, consequently, K_r can be expressed in the form:

$$K_r = k \cdot \alpha \cdot \Delta T^U (R_\rho - 1) \quad (11)$$

In the last expression, $\cdot\cdot\alpha \cdot \Delta T^U (R_\rho - 1) = (\Delta\rho^U / \rho)$ is the density 'step' at the top of the benthic layer. Substitution of (10) and (11) into (5) gives the form for $B_S(z)$. Equation (5) is also valid for the equilibrium state, i.e. when $d = d_e$. For such conditions and in accordance with (4), we get:

$$b_S(d_e) \cdot [1 - k \cdot \alpha \cdot \Delta T_e^U (R_\rho - 1)] = \gamma \cdot B_T \quad (12)$$

Now, excluding R_ρ from the system of equations (3), (12), it is possible to depict the function $d_e = d_e(\alpha \cdot \Delta T_e^U)$. The unknown equilibrium values of d_e and $\alpha \cdot \Delta T_e^U$ are found at the intersection point of the curve $d_e = d_e(\alpha \cdot \Delta T_e^U)$ and the curve $d = d(\alpha \cdot \Delta T_e)$ which is obtained from the system of equations (1), (2). As a result, the problem of formation of equilibrium BHL can be completely solved.

For the determination of the d_e value, we shall use the equation (12) and an estimate for K_r. For this, the value of $\alpha \cdot \Delta T^U$ may be estimated using known parameters and R_ρ, for example, from the expression for the heat flux from [6]. An estimate for $R_\rho = [\beta \cdot (\Delta S^L + \Delta S^U)] / \alpha \cdot \Delta T^L$, we can get from the condition of potential energy constancy (2). In the cases of linear and exponential distribution of $\rho(z)$, respectively, we get:

$$2.7 < R_\rho < 3, \qquad 2.21 < R_\rho < 2.43.$$

Both estimates are close to the observed value of R_ρ at the top of the BHL.

It is possible to find an expression for d_e from (10) and (12):

$$d_e = H \cdot \{1 - \frac{k \cdot r}{H} \ln^{-1}[\exp(\frac{k \cdot r}{H}) + (\frac{\exp(\frac{k \cdot r}{z_0}) - \exp(\frac{k \cdot r}{H})}{1 - k \cdot 10^{-6}}) \cdot \frac{\gamma \cdot B_T}{B_S}]\} \quad (13)$$

Since we consider a stationary, one dimensional model for the Black Sea, we need to choose typical or averaged parameters for calculations: z_0 = 50 m, H = 2000 m, $N_0 = 1.75 \cdot 10^{-2} s^{-1}$, g = 9.8 m·s^{-2}, γ = 0.15. Expressions for fluxes have the form:

$$B_T = (g \cdot \alpha \cdot H_Q) / C_P, \qquad \overline{B}_S = (g \cdot \beta \cdot 350000) / \overline{S}_{BS}$$

The numeric factor in the expression for $\overline{B}_S$ reflects the salt flux from the Bosphorus, equal to 350 tons of salt per second [9]. Taking $3.8 \cdot 10^{11}$ m^2 for the typical Black Sea area, $H_Q = 3 \cdot 10^{-2} w / m^2$, $\alpha = 1.3 \cdot 10^{-4} (^oK)^{-1}$, we finally get:

$$B_T = 1.4 \cdot 10^{-12} m^2 s^{-3}, \quad \overline{B}_S = 7.8 \cdot 10^{-9} m^2 s^{-3}.$$

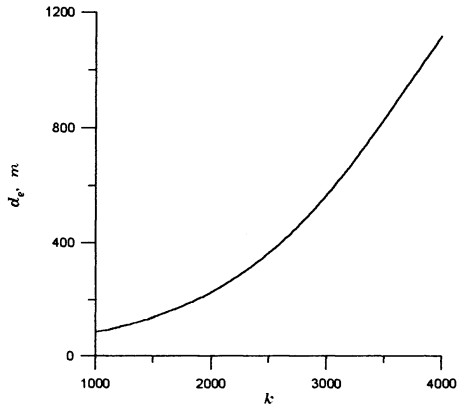


Figure 4. The relationship between equilibrium BHL thickness and parameter *k*..

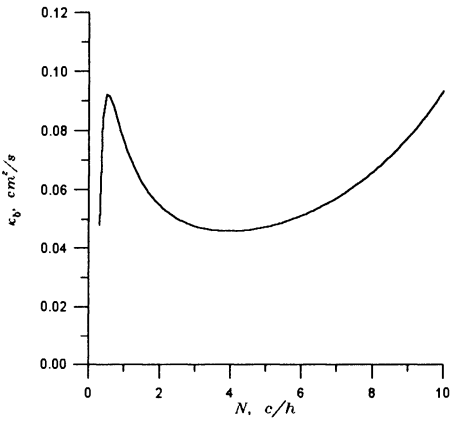


Figure 5. Diffusive coefficient of salt dependence on stratification.

Since we lack detailed information on the character of Bosphorus water penetration into the deep layers of the Black Sea, some uncertainties still exist in the determination of d_e, which are parameterised by k. Consequently, the parameter k parameterises the process of down-slope flow of the Bosphorus water and its mixing with the ambient fluid. Taking into account that the apparent age of the deep water is, at least, hundreds of years, it is possible to conclude that the effects of the processes resulting in mixing and dispersal are well parameterised (i.e. their time scales are *a priory* much less than the age of the water) by such a procedure. Figure 4 shows the

relationship between the equilibrium BHL thickness and k. The latter estimate is useful for calculations of the diffusion coefficient in the main halocline of the Black Sea.

4. Summary and Conclusions

In the following paragraph we would like to outline some important conclusions and consequences of the present study.

(1) The analysis of field data as well as the presented modelling approach can be considered as preliminary diagnosis that does not contradict with the basic hypothesis of the existence of stationary BHL. The results of the model support the general claim that the observed BHL exists due to the geothermal heat flux, and due to the dependence of mixing properties on stratification. Indeed, if we were to assume a specific constant value for the vertical salt flux, we would get an equilibrium BHL thickness of only 0.5 m.

(2) One of the conclusions is the impossibility of existence of a system of stationary convective layers above the BHL interface. This is because the incoming salt flux is distributed in the vertical. The conditions of salt balance at the interface can only be achieved for the lowest layer.

(3) It is necessary to emphasise that an upward transport of heat and salt due to the double diffusion mechanism is possible when $(B_S/B_T) \leq 1$. Hence, we can calculate the corresponding scale (changing $\gamma \cdot B_T / \overline{B}_S$ for $B_T / \overline{B}_S$ in 13): to be $d_1 \cong 1150$ m. In the vertical, the corresponding depth level, $z_1 \cong 850$ m, coincides with the boundary between intermediate and deep water masses.

(4) What is the vertical distribution of salt diffusion coefficient for the Black Sea? The Bosphorus is the only source of salt for the Black Sea. The balance for salt requires that the total amount of salt penetrating from the Bosphorus is transported backwards. Shear instabilities, breaking of internal waves, bottom friction, double diffusion, come into play in the vertical fluxes of salt and heat. The results of the model allow to make an estimate of the vertical diffusion coefficient for the Black Sea (which occur due to a summary action of vertical mixing mechanisms) as a function of depth or Brunt Vaisala frequency.

Let the buoyancy flux be basically determined by the salt flux. For simplicity, we neglect the influence of another factors. The buoyancy flux into the layer Δz consists of $b(z)\Delta z$, and of an inputs from horizontal boundaries $F_B(z+\Delta z)$ and $-F_B(z)$. The balance equation for buoyancy has the form:

$$b(z) \cdot \Delta z = F_B(z) - F_B(z+\Delta z).$$

Dividing both parts of this equation by Δz and putting the limit $\Delta z \to 0$, we get:

$$b(z) = -(dF_B / dz)$$

Assuming the above approximation for Brunt-Viasala frequency $N = N_0(z_0 / z)$ and taking $b(z)$ from solution of (9), we get:

$$F_B = \overline{B}_S[\exp(\frac{k \cdot r}{z_0}\frac{N}{N_0}) - \exp(\frac{k \cdot r}{H})] / [\exp(\frac{k \cdot r}{z_0}) - \exp(\frac{k \cdot r}{H})] \quad (14)$$

$$\kappa_B = \frac{F_B(N)}{N^2}, \quad (15)$$

where κ_B is the salt vertical diffusion coefficient. The vertical buoyancy flux $F_B(N)$ is zero at the bottom ($z = H$) and equals $\overline{B}_S$ at z = z_0. Dependence of κ_B upon N is presented in figure 5.

(5) In what extent does the BHL thickness depend upon the amount of salt penetrating from the Bosphorus? To reveal sensitivity of the Black Sea to possible climatic changes of salt flux from the Bosphorus, a function $d_e(\overline{M}_S)$ has been calculated for reasonable range of $\overline{M}_S$ variations. If the amount of the incoming salt would be reduced (increased), accordingly, this would make the BHL thicker (thinner).

(6) The above conclusions were derived under the condition for stationary BHL and we consider that there are grounds for such a claim. However, as stated in [5,7], there are grounds to consider that the bottom mixed layer is in the 'low stability' regime [2]. If so, how can this alter the conclusions of this studies?

For the 'low stability' regime, $B_S / B_T = 0.15 \cdot R\rho$ at the upper mixed layer interface [2]. Since $R_\rho \cong 2.6$, numerical values for k will be changed. However, this can not alter speculative conclusions of the present studies. Actually, in 'low stability' regime, same as for the stationary conditions, the BHL in the Black Sea can exist only if some part of the total amount of the incoming salt penetrates into the bottom layer. Only in such a case the condition for salt balance can be satisfied for this layer.

References

1. Duchkov, A.D., Kazantsev, S.A (1979) Heat flux in the deep Black Sea. In: *Geophysical fields of the Atlantic ocean*, M: Nauka, pp. 121-130. (in Russian)
2. Fernando, H.J.S. (1989) Oceanographic implications of laboratory experiments on diffusive interfaces, *J. Phys. Oceanogr.* **19**, 1707-1715.
3. Kelley, D.E (1990) Fluxes through diffusive staircases: a new formulation, *J. Geophys. Res.* **95**, 3365-
4. Murray, J.M., Top, Z. and E. Ozsoy (1991) Hydrographic properties and ventilation of the Black sea, *Deep-Sea Res.* **38**, suppl.**2**, 663 - 689.
5. Ozsoy, E., Top, Z., White, G. and J. Murray (1991). Double Diffusive intrusions, mixing and deep sea convection processes in the Black Sea, in: E. Izdar and J. M. Murray (eds.), *Black Sea Oceanography*, NATO/ASI Series, Dordrecht, Kluwer Academic Publishers, 17-42
6. Ozsoy, E., Unluata, U. and Z. Top (1993). The evolution of Mediterranean water in the Black Sea: interior mixing and material transport by double diffusive intrusions, *Prog. Oceanogr.*, **31**, 275-320.
7. Ozsoy, E. and Besiktepe, S. (1994). Sources of double diffusive convection and impacts on mixing in the Black Sea, in: A.Brandt and H.J.S.Fernando (eds.), *Double-Diffusive Convection*, American Geophysical Union.
8. Turner , J.W. (1973) *Buoyancy effects in fluids*, Cambridge University Press, New York.
9. Unluata, U., Oguz, T., Latif, M.A. and E. Ozsoy (1989) On physical oceanography of the Turkish Straits. In: L.J.Pratt (ed.) *The Physical Oceanography of Sea Straits*, Kluwer Academic Publishes, Dordrecht.

PHYSICAL PROCESSES OF SURFACE-DEEP LAYERS EXCHANGE IN THE BLACK SEA

ENCHO DEMIROV[1], MOHAMMED A. LATIF[2] AND VASILE DIACONU[3]
[1]*Institute of Oceanology,*
Varna 9000, P.O. Box 152, Bulgaria
[2]*Institute of Marine Sciences,*
Middle East Technical University,
P. O. Box 28 Erdemli 33731, İçel, Turkey
[3]*Romanian Marine Research Institute*
300, Mamaia Blvd.,
Constantza 3-8700 Romania

Abstract. The relatively strong vertical stratification in the Black Sea significantly restricts the exchange between the surface and deep layers. The surface layer, where the anthropogenic flow enters, is separated from the deep layer by a sharp halocline (at depths 120-150m). Questions of changes in the Black Sea environment related to anthropogenic influences require investigation of physical processes which control the intensity of vertical mixing and advection in regions where they may be significant, as well as development of parameteriztion schemes in circulation models. Data from three CoMSBlack expeditions suggest that relatively intense upwelling, downwelling and the related processes of vertical exchange can be observed in some areas over the north-west continental shelf slope of the basin. The existence of these events is connected to nongeostrophic dynamics of waters in the Danube canyon and in the cape Kaliakra area. The buoyancy flux stipulated by vertical exchange processes in these regions is considered as a possible reason for the permanent existence of anticyclonic gyres near cape Kaliakra and Crimea.

1. Introduction

The Black Sea is a semi-enclosed sea, connected with the Marmara and Azov seas respectively by the narrow Bosphorus and Kerch Straits. The

E. Özsoy and A. Mikaelyan (eds.), Sensitivity to Change: Black Sea, Baltic Sea and North Sea, 285–294.
© 1997 *Kluwer Academic Publishers.*

strong salinity stratification, formed due to weak exchanges with the adjacent basins and the large volume of fresh water input, significantly restricts vertical mixing processes. According to [5] the maximum depth of winter convection in the Black Sea is about 50 m. In comparison with other basins, where this depth is of the order of several hundered meters, the Black Sea is a poorly ventilated basin. Some authors(see [13] and [1]) suggest that under the conditions of weak vertical turbulent mixing, the processes of upwelling, downwelling and isopycnical mixing become significant factors which determine the vertical exchange below the seasonal thermocline.

The present article is an attempt to clarify some aspects of the dynamics of these vertical exchange processes as related to the mesoscale variability of the cyclonic Black Sea Main Rim Current (MRC). The results presented are mainly for the north-west shelf. However, they are considered applicable for other parts of the sea where similar dynamic conditions may exist.

Previous studies of the vertical exchange are considered in Section 2. An analysis of CTD and ADCP measurements obtained during CoMSBlack and NATO-TU Black Sea expeditions is presented in Section 3.

2. Background

The relatively stable stratification and quasigeostrophic (i.e. quasi-non-divergent) dynamic balance in the deep regions of the Black Sea restrict the processes of vertical advection and mixing here. Under these conditions the upwelling and downwelling (forced by Ekman pumping processes in cyclonic MRC) and isopycnical mixing are considered by different authors (see [4],[1], [13]) as the most significant dynamic processes determining the vertical exchange in the sea.

The cyclonic MRC is a jet-like current, and has maximum intensity over the continental slope. Upwelling and downwelling are observed in the central part and periphery of the deep water area of the sea respectively (see [1], [13] and [2]). [13] showed that winter cooling has maximum intensity in the central part of the basin because of the relatively low depth of mixed layer(ML), which is limited here by the upwelling of the saltier deep waters, and the relatively strong vertical salinity gradient at the bottom of ML. The surface cooled and dense waters during this season sink into CIL following the isopycnical surfaces.

Downwelling is observed along the periphery of the deep water area (see [4])in almost the entire basin. In this connection the region of MRC periphery over the North-West continental shelf slope is of particular significance, because the chemical properties of waters sinking in this area are strongly influenced by the anthropogenic input from rivers (see [1]). Following [1] we will refer to this region as Convergence Zone (CZ). In Figure 3 CZ coincides

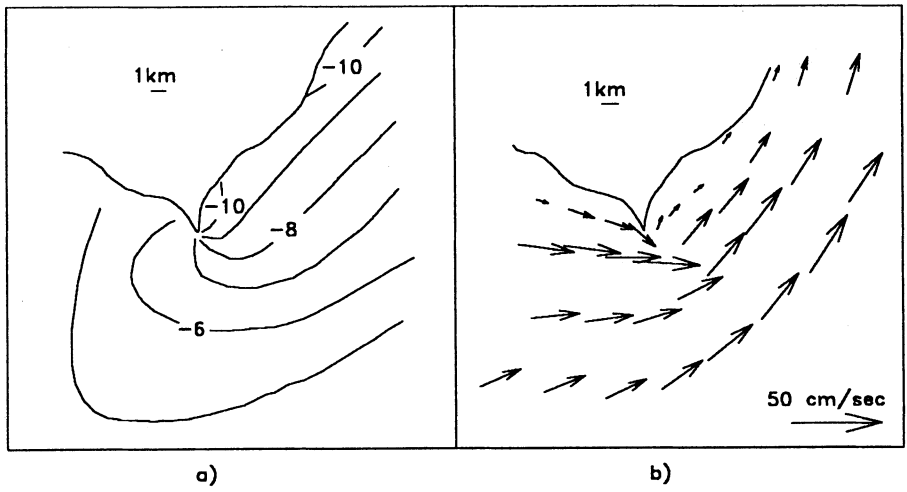


Figure 1. Model solution for distribution of a) sea level (cm) and b) vertically mean current velocity near cape Kaliakra under conditions of south(10 m/sec) wind

with the full isolines (downwelling) area over the North-West continental shelf slope.

An important feature of CZ are anticyclonic gyres, which exist in some parts of CZ almost continuosly (see [6]). In the north-west part of the Black Sea anticyclonic gyres are usually observed in CZ near cape Kaliakra and to the south-west of Crimea. Presently the physical reasons for their permanent character are not well known. [10] hypothesized that their stability is due to the vertical buoyancy flux determined by deepening of surface waters in CZ.

[7] used a nonlinear barotropic model on nonregular coordinate system for studying the processes of anticyclonic gyres formation in the region near Cape Kaliakra. The relatively fine grid step near the cape (500 m) allowed to reproduce precisely the vorticity balance in this region. Numerical experiments showed that anticyclonic vorticty here is generated when the model is forced by south and south-west winds. Considerable lowering of sea level is observed in the model solution for this case in a small region, of about 2-3 km extent, around Cape Kaliakra, (Figure 1). This result is in good agreement with field observations which show that under south and south-west winds intensive upwelling occurs in a small region (of scale of several

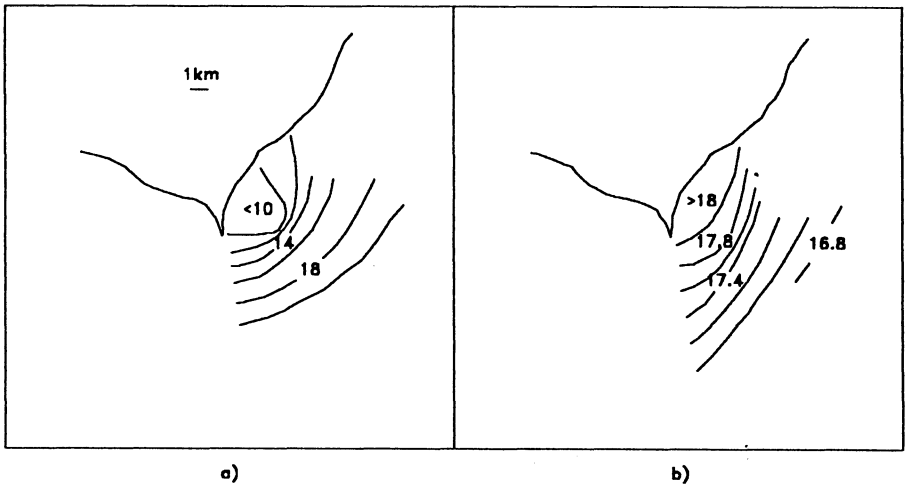


Figure 2. Surface a)temperature and b) salinity distributions observed during upwelling near Cape Kaliakra (in July 1987)

kilometers) near Cape Kaliakra (see Figure 2).

According to [7], the dynamic balance in the upwelling region differs significantly from the geostrophical balance, and is characterised by local intensification of horizontal circulation and relatively high divergence of current velocity. Evaluation of vorticity equation terms, presented in Table. 1, shows that vorticity production near Cape Kaliakra is mainly due to the processes of vorticity stretching and turbulent diffusion. Vorticity production in this region has values several orders higher than in the middle shelf and open sea areas.

We should mention that the barotropic model applied by [7] is not able to simulate the complicated baroclinic processes of gyre dynamics in CZ. However, evaluation of the vorticity balance using this model allows us to hypothesize that the nonlinear processes of vorticity production in the small upwelling region near the cape could play an important role in Kaliakra anticyclonic gyre dynamics.

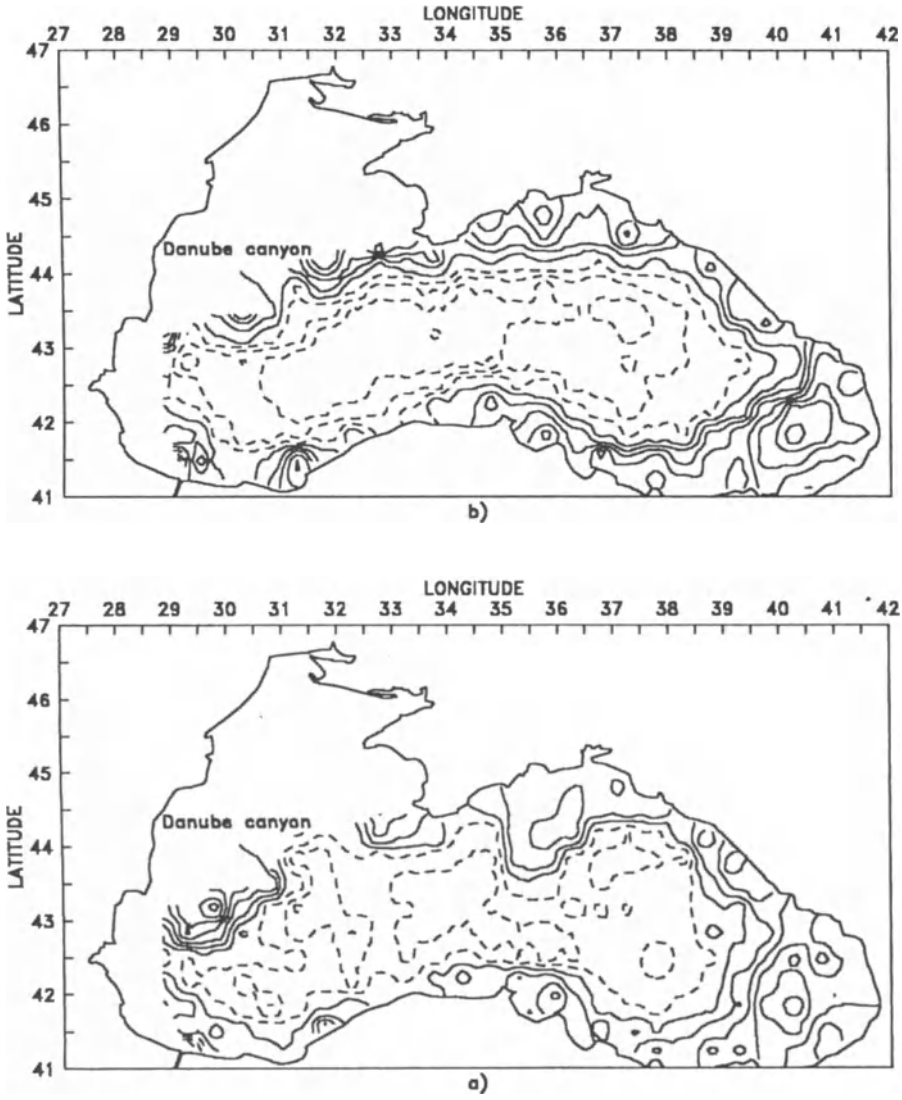


Figure 3. Topography of $\sigma_t = 16$ isopycnical surface as measured during a)HydroBlack 91 and b) ComSBlack 92a expeditions. Contour interval is equal to 10 m. Full lines correspond to negative values and broken lines - to positive

TABLE 1. Model estimation of barotropic vorticity balance equation terms (sec^{-2}), determining the main mechanisms of vorticity production at four positions in Western part of the Black Sea

	Vorticity stretching	Bottom friction	Wind forcing	Turbulent diffusion
Cape Kalikra	$-1,42.10^{-9}$	$-5,87.10^{-10}$	$1,16.10^{-13}$	$-1,84.10^{-9}$
Cape Emine	$-2,02.10^{-9}$	$2,39.10^{-10}$	$-9.65.10^{-10}$	$7,23.10^{-10}$
middle shelf area	$-2,45.10^{-11}$	$1,89.10^{-10}$	$-2,51.10^{-10}$	$-1,18.10^{-10}$
deep water area	$2,06.10^{-13}$	$3,18.10^{-15}$	$5,55.10^{-17}$	$4,08.10^{-14}$

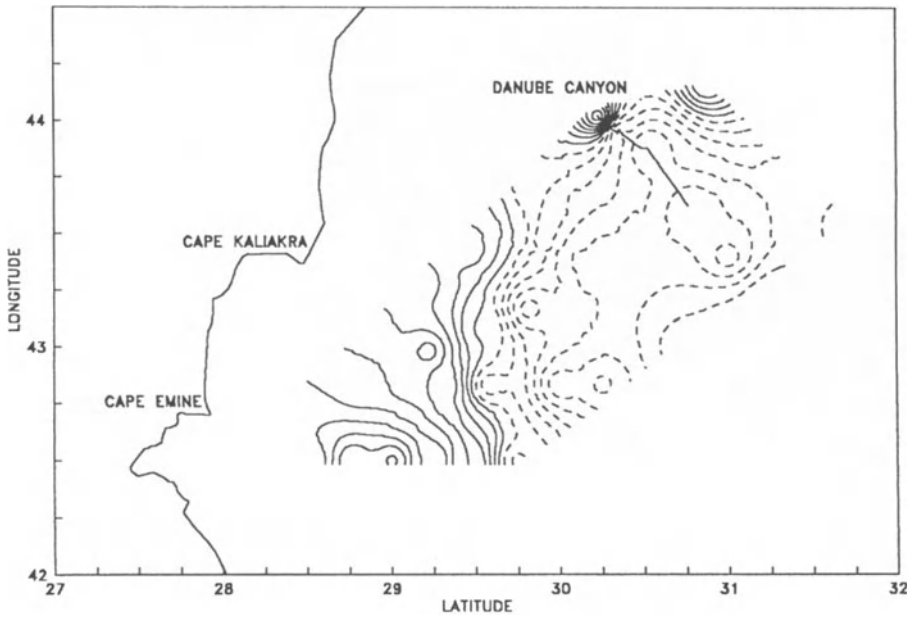


Figure 4. Topography of $\sigma_t = 16$ isopycnical surface as measured during CoMSBlack 94a expedition. Contour interval is equal to 5 m. Full lines correspond to negative values and broken lines - to positive

3. On Vertical Exchange Processes in the Convergence Zone

The experimental data presented in this section were obtained during three cruises conducted as part of the CoMSBlack and NATO TU Black Sea inter-

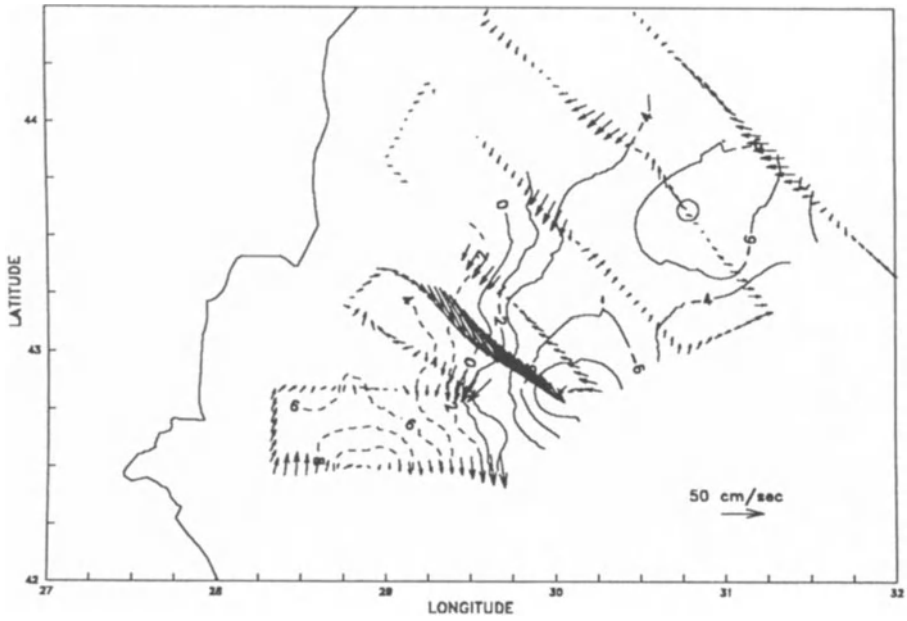


Figure 5. Optimally interpolated surface velocity ADCP measurements and 5 db dynamic topography (referenced to 500 db) distributions during CoMSBlack 94a. Contour interval is 2 cm.

national projects. The HydroBlack 91, CoMSBlack 92a and CoMSBlack 94a expeditions were conducted in September 1991, July 1992 and April 1994 respectively. Detailed description of these expeditions as well as some preliminary results of data analysis are presented in [3]; [11]; [12]; [2]. Some ecological aspects of the vertical exchange processes and particularly the processes which take place in CZ as observed during CoMSBlack 92a are discussed in [2].

The topography of the isopycnal surface $\sigma_t = 16$ for the HydroBlack91 and CoMSBlack92a cruises are shown in Figure 3. The positive values of the surface elevations in the central part correspond to the upwelling area whose formation and variability is connected to the MRC dynamics. The CZ in the north-west part of the sea lies in downwelling area over the continental shelf slope.

In both the CoMSBlack 92a and HydroBlack 91 cruises, two anticylonic gyres were observed in the CZ, to the east of cape Kaliakra and to the

south-west of Crimea respectively. Downwelling areas in the centres of both anticyclones correspond to the minimum values of depths of the isopycnal surface $\sigma_t = 16$. In both cruises, upwelling was observed in the area between the anticyclons (see Figure 3), which is in the vicinity of Danube canyon.

As mentioned above, the Kaliakra and Crimea anticyclones are relatively stable gyres (see [6]). This gives rise to the question: Is the upwelling above the Danube canyon also a persistent feature? In this connection we should mention that the long term data of [4] show that minima in surface temperature distribution are often observed during spring in this (upwelling) region. The relatively low temperatures are explained [4] as being due to the divergence of the flow here. According to [4], the temperature minimum near the Danube canyon is not well pronounced in other seasons, possibly due to the fact that the upwelling has a greater influence on the surface temperatures during spring, when the mixed layer is relatively shallower, as it starts to develop.

One can expect that the upwelling is related to the dynamic processes which occur in the canyon. On the other hand, the size of the upwelling area is much larger than the width of the canyon, i.e. a relatively large area outside canyon is involved in the upwelling process. During HydroBlack'91 the upwelling area size was comparable to the size of anticyclonic gyres.

The cruise plan of CoMSBlack 94a expedition included a hydrographic section over the canyon in order to obtain data which may help in understanding the upwelling in this area.

It is known that persistent vertical motions are observed in the regions over many canyons of the world ocean (see [8]). According to [9] a dynamicaly significant reason for upwelling or downwelling in canyons can be the specific dynamics here. These are characterized by a relatively small scale (determined by the canyon width) of motion and a dynamic balance which is away from geostrophity. Persistent vertical motion is observed especially in the regions of relatively constant direction of pressure gradient (see [9]). The diagnostic computations of the Black Sea circulation by different authors (see [3]; [6]; [11]; [12]; [15]; [16]) showed that the pressure over the shelf is usually higher than in deep water area, i.e. there exists a relatively constant direction of pressure gradient from the deep water area to the coast. One can expect that in this case downwelling should take place over the Danube canyon.

The topography of the isopycnal surface $\sigma_t = 16$ during the CoMSBlack 94a expedition, Figure 4, supports this conclusion. A sharp area of downwelling is observed over the canyon. Since the downwelling area has a relatively small size it is observed at only one station over the Danube canyon section. The downwelling is supported indepentently by ADCP measurements. Optimaly interpolated data of ADCP measurements of currents

in the surface layer are presented on Figure 5. The optimal interpolation method suggested by [14] was applied for smoothing of the ADCP data over each shelf section. The distribution of the current velocity shows the convergence of the surface flow in a relatively wide area around the canyon and hence supports the presence of downwelling here.

The surface current velocities, Figure 5, are approximately parallel to the isolines of dynamic topography in almost the whole region. A significant crossisosterical (ageostrophical) flow is observed mainly in the region over the Danube canyon.

The downwelling region over the canyon has a relatively small size (comparable with the size of the canyon), however, the surface flow divergence and upwelling occur over a much larger region(see Figures 4 and 5).

We should mention that in the earlier cruises (HydroBlack 91, CoMS-Black 92a) no hydrographical stations were made in the vicinity of the canyon and only the upwellig area was observed near the Danube Canyon, because the douwnwelling area has a size much less the distance between the stations (see Figure 5 and [3]).

4. Conclusions

On the basis of the observations and model results discussed above regarding the processes of vertical exchange in CZ over the north-west part of the Black Sea, it can be concluded that relatively intense and permanent regions of upwelling and downwelling exist near Cape Kaliakra and Danube canyon, as a result of dynamic processes occuring in a relatively small area (with space scale of about several kilometers). The high slope of isopycnical surfaces here, which result from the upwelling and downwelling, provides conditions for intensive alongisopycnal mixing between the surface coastal waters (near cape Kaliakra and Danube canyon) and the central downwelling area of anticyclonic gyres. The vertical buoyancy flux, which is due to alongisopycnal flux and topographically induced processes of upwelling and downwelling, can be considered as a possible mechanism for providing potential energy to anticyclonic gyres and as a factor which maintains their persistency.

5. Acknowledgments

This work was done as a part of international projects NATO TU-Black Sea and CoMSBlack. The study was supported in part by the Bulgarian Science Foundation. We would like to thank B. Kagan, G. Korotaev and E. Stanev for helpful discussions.

References

1. Adrianova O.P., I.M. Ovchinnikov 1991. Pecularities in transformation of fresh waters in the western part of the Black Sea.*Meterologya i Hydrologya* (Meteorology nad Hydrology), **7**, 57–64
2. D. Aubrey, S. Moncheva, E. Demirov, V. Diaconu. (1995) On the global change in the bio-chemical regime of Black Sea North-Western Shelf as related to Specific Anthropogenic and Natural Conditions . In print *Journal of Marine Systems* (Proc. XVI - th Liege International Colloquium on Ocean Hydrodynamics)
3. Aubrey D. G., T. Oguz, E. Demirov, V. Ivanov, T. McSherry, V. Diaconu, E. Nikolaenko. (1992). HydroBlack'91. International Workshop, UNESCO, Intergovernmental Oceanographic Comission. Workshop Report No. 91, 56pp.
4. Blatov A.S., N.P. Bulgakov, V.A. Ivanov, A.N. Kosarev, V.S. Tujilkin. (1984) Variability of Black Sea hydrophysical fields. St. Petersburg, (in Russian)
5. Boguslavskij S.G., G.S. Chernucho. (1979) Temperature field and heat contents of the activ layer. In: Complex investigations of the Black Sea, Sevastopol, MHI, 9-16. (in Russian)
6. Bulgakov S.N., Demyshev S.G., Korotaev G.K. (1992). Modelling of the Black Sea circulation and water stratification (review). In V.N. Eremeev, D.Aubrey and N.P. Bulgakov (eds), Problems of the Black Sea, MHI, Sevastopol, 34-53.
7. Demirov E.K. (1991) Numerical modeling of the Black Sea eigen oscillations and wind driven circulation, PhD thesis, Russian Hydrometorological Institute, St. Petersburg (in Russian)
8. Gardner W.D. 1989 Baltimore Canyon as a modern conduit of sediment to deep sea, *Deep-Sea Res.*, **36**, 323-358.
9. Klinck J.M. (1988) The influence of a narrow transverse canyon on initially geostrophic flow, *J. Geoph. Res.*, **93**, 509-515
10. Latun V.S. (1989) Anticyclonic eddies in the Black in summer 1984, Journal of Marine Hydrophysics (MHI), **3**, 27-35. (in Russian)
11. Oguz T., Ş. Beşiktepe, Ö. Baştürk, İ. Salihoğlu, D. Aubrey, A. Balcı, E. Demirov, V. Diaconu, L. Dorogan, M. Duman, L. Ivanov, S. Konovalov, A. Stoyanov, S. Tuğrul, V. Vladimirov, A. Y i lmaz. (1993) CoMSBlack 92-Report of the Physical and Chemical Intercalibration Workshop, 15-29 January, 1993, Middle East Technical University, Erdemli, Turkey
12. Oguz T., D. Aubrey, A. Koleshnikov, E. Demirov, L. Koveshnikov, H.I. Sur, V. Diaconu, Ş. Beşiktepe, M. Duman, R. Limeburner, V. Eremeev (1994) Mesoscale circulation and termohaline structure of the Black Sea observed during HydroBlack 91, *Deep-Sea Res.*, **41**(4), 603-628.
13. Ovchinikov I.M., Yu.I. Popov (1984). On the problem of the Cold Intermediate Layer formation in the Black Sea, Doklady Akademiy Nauk SSSR, **279**(4), 986-990. (in Russian)
14. Robinson A.R., M.A. Spall, L.J. Walstad, W.G. Leslie (1989) Data assimilation and dynamical interpolation in Gulfcast experiments, *Dyn. Atm. Oceans*, **13**, 301-316.
15. Stanev E.V. 1990. On the mechnisms of the Black Sea circulation, *Earth-Science Reviews*, **28**, p.285-319
16. Staneva J. (1995) Cold water mass formation in the Black Sea. Model Sensitivity to space and time variability, in E. Özsoy and A. Mikaelyan (eds.) Abstr. NATO ARW Sensitivity of North Sea, Baltic Sea and Black Sea to anthropogenic and climatic changes, Varna, Bulgaria 14-18 November, 1995, 48.

CONVECTION IN THE BALTIC SEA

- a numerical process study -

JAN O. BACKHAUS AND HENNING WEHDE
Institut für Meerskunde, Universität Hamburg
Troplowitzstr. 7, D-22529 Hamburg

Abstract. A non-hydrostatic convection model was applied to investigate convective water mass formation in the Baltic in winter. The model domain is a vertical ocean slice with cyclic lateral boundary conditions. The slice, which is resolved by an isotropic grid-size of 5 m, covers a horizontal and vertical extent of 1,500 m and 100 m, respectively. The non-linear model includes rotational accelerations but, due to its 2.5-dimensionality (all gradients normal to model plane vanish), it cannot simulate geostrophic adjustment. A model experiment was conducted over half a year from autumn to spring by prescribing a schematic atmospheric forcing (cooling and warming). The simulation was initialised by an observed T,S-profile from late summer. Although the experiment should be viewed as a pilot process study it confirms importance of convection in water mass formation, ventilation and heat budget of the Baltic. A cold intermediate layer (CIL) situated beneath the summer thermocline and above the perennial halocline of the Baltic is first eroded and later re-established by convection. The CIL is isolated from the atmosphere by a thermocline in both summer and winter. Establishment and convective erosion of both thermoclines were simulated. Convection originating at the sea surface induces internal mixing beneath the actual convective penetration depth by transmitting pressure fluctuations across isopycnals.

1. Introduction

The investigation of convection appears to be a key topic in oceanography since the late seventies (MEDOC Group 1970, Killworth 1976, 1979, 1983; Rudels 1990, Quadfasel and Rudels 1991, Brugge et al. 1991, Smith and Morrison 1992, Jones and Marshall 1993, Visbeck 1993, Schott et al. 1994,

E. Özsoy and A. Mikaelyan (eds.), Sensitivity to Change: Black Sea, Baltic Sea and North Sea, 295–309.
© 1997 *Kluwer Academic Publishers.*

Akitomo et al. 1995, Backhaus 1995, Backhaus et al. 1996). The climate discussion, which involves the global conveyor belt (Broecker 1991), has drawn attention to the role of convective water mass formation in high latitudes (GSP Group 1990). Little attention however, has as yet been devoted to investigate the role of this process in mid-latitude temperate seas. The intention of this investigation is to provide an initial indication of the role of convection on water mass formation in the Baltic. Parallels will be drawn to the Black Sea because both seas are governed by an excess in freshwater supply.

In the Black Sea both convection in the open ocean (water column) and on the continental slope appear to contribute to water mass formation (Özsoy et al. 1993, Murray et al. 1991, Sur et al. 1994). Slope convection involves intrusions of dense bottom arrested gravity plumes into intermediate layers of the Black Sea. The generation of a dense water body however, i.e. the initial phase of slope convection, requires convection in the shelf water column. It appears, by comparing typical T,S-profiles from Baltic and Black Sea, that a cold intermediate layer (CIL) exists in both seas. The CIL is situated beneath the summer thermocline and above the halocline. In the Black Sea the CIL is maintained by both slope- and open ocean convection (Murray et al., 1991, Özsoy 1993). In the Baltic, due to the absence of shallow shelves, apart from the Bay of Bothnia, convection in the open water column will primarily contribute to a maintenance of the CIL.

The result of a temporally confined occurrence of convection in the Baltic as inferred from a numerical process study is discussed in this contribution. The discussion is confined to thermodynamics because an inclusion of salinities and sea ice, which are both predicted by the model, would go beyond the scope of this contribution. Beforehand a brief outline of the Baltic hydrography and of the convection model will be given. General descriptions of the Baltic hydrography can be found in Dietrich und Schott (1974) and in Tomczak and Godfrey (1994). An account of the sensitivity of the hydrographies of both Baltic and adjacent North Sea with respect to climate change is described by Backhaus (1993, 1996). To set the scene for this investigation only some important facts of the Baltic hydrography need to be given here.

The Baltic receives a net annual freshwater input of 480 km/y from the catchment of large river systems in north-eastern Europe. At first order evaporation equals precipitation (Dietrich und Schott, 1974). In wide parts of the Baltic, in particular in its eastern portions, salinities are well below 10 psu. The freshwater surplus maintains a large scale zonal salinity gradient and a perennial halocline. The haline stratification induces a difference in mean sea level in the order of one meter between eastern Baltic Proper and North Atlantic Ocean (Backhaus 1993, 1996). The sea level slope, due

to dynamic interactions with the North Sea, also depends on the circulation within the North Sea which appears to be particularly sensitive to atmospheric forcing (Backhaus 1989, 1990, 1993). A complex and very shallow topography at the western entrance to the Baltic (Kattegat and Belt Sea) inhibits a direct import of waters of Atlantic and North Sea origin (see also: Skogen, this volume). Occasional intrusions of Atlantic water modified in the North Sea (frequency: approx. 5 to 15 years) are the only means for a deep water renewal (Matthäus and Franck 1988), the most recent of which occurred in January 1993. The poor exchange situation in the Baltic - in particular for the waters in the deep basins of the Baltic Proper - is reflected in estimates of a basin wide flushing time which is in the order of decades (Dietrich und Schott, 1974). Tomczak and Godfrey (1994) draw a parallel between the Baltic and the Black Sea by stating that both seas are 'mediterranean dilution basins susceptible to anoxic conditions due to poor ventilation and renewal of the deep water'.

The existence of a perennial halocline and of low salinities in the Baltic, in particular in the Baltic Proper, constitutes the most significant difference in marine climates of the Baltic and the adjacent North Sea (Backhaus, 1996). Whereas the water column in the North Sea is homogenised in winter due to cooling, convection and wind- and tide-induced mixing the Baltic remains stratified throughout a year. This has wide-spread implications for both its heat budget and the regional climate. Only the water column above the Baltic halocline may potentially store and release heat during the annual cycle (neglecting the effect of an occasional import of heat with salt intrusions) because the stable halocline inhibits a deeper reaching heat transfer. In the course of a winter the water column which is in direct contact with the atmosphere, and which potentially can release heat to the atmosphere, is reduced from an initial depth of about 60 m, i.e. average halocline depth, to about 20 m, i.e. thickness of a well mixed surface layer in winter. This is a result of the non-linear behaviour of the density of sea water with low salinities at low temperatures. With the onset of cooling in autumn the water column is first destabilised allowing for convection. However, after the temperature of the density maximum has been passed a 'winter thermocline' is established which largely inhibits a further release of heat to the atmosphere and prevents convection in the underlying water column. Therefore, in terms of thermodynamics, the Baltic in winter is seen from the atmosphere as a sea that is only as shallow as the depth of the thermocline. Only wind-induced entrainment would allow to release some of the heat stored beneath the winter thermocline after its establishment. The exchange of heat with the atmosphere will be reduced even more with the onset of ice formation and ice-covered regions will finally attain an albedo and surface temperatures similar to the surrounding snow-covered

land. This causes much colder air temperatures in the Baltic region during a winter in contrast to the North Sea.

The subtle thermodynamics of the brackish Baltic waters imply a second convection episode which should occur in spring because then increasing sea-surface temperatures have again to pass the temperature of the density maximum before a stable summer stratification can be established. Positive buoyancy provided by freshwater runoff may allow for an establishment of a thermocline even before the temperature of maximum density was reached (Eilola, 1996). In conclusion, convection in the Baltic may penetrate down to the depth of the halocline twice during a winter season. Duration and success of convective ventilation will depend on both stratification (and freshwater runoff) and actual atmospheric conditions which largely control heat and momentum fluxes.

2. The non-hydrostatic Convection Model

The non-hydrostatic, 2.5-dimensional ocean model is based on the non-linear, primitive Boussinesq equations for an incompressible fluid. It predicts perturbations from a hydrostatic background pressure distribution in a vertical plane. Coriolis terms are incorporated in the equations of motion for all three space co-ordinates. All gradients in the plane-normal are assumed to vanish. The model therefore cannot simulate a geostrophic adjustment between velocity and pressure field. Rotational adjustment however, was found to be of minor importance for active convection phases in view of its small scales in both space and time. Prognostic equations for salinity and potential temperature together with non-linear equations (UNESCO) of state and temperature of freezing point in dependence to salinity are applied for the prediction of the density field. The model includes the thermobaric effect i.e. the compressibility of sea water which is most pronounced at low temperatures. For applications in high latitudes the convection model was coupled to a prognostic thermo-hydrodynamic ice-model (Backhaus 1995, Backhaus et al. 1996) by adopting approaches proposed by Maykut (1986) and Semtner (1976, 1987).

Sub-grid scale turbulence is parameterised by a diagnostic closure scheme (Kochergin, 1987). It assumes that the rate of turbulent exchange is described by an instantaneous (im-)balance between shear production derived from the local velocity field and stability expressed by the buoyancy frequency (N). A turbulent Prandtl number of unity is assumed following observations under drifting Wedell Sea pack ice (McPhee and Martinson, 1993).

Horizontal and vertical motions are expected to be of same order of magnitude in convective dynamics. The model is therefore defined on an

isotropic, equidistant grid to avoid any distortions of convective dynamics and of the parameterisation of sub-grid scale turbulence by the choice of a non-uniform grid. Accordingly, equal eddy viscosity and diffusivity coefficients are applied for the horizontal as well as for the vertical co-ordinates. The scheme of Kochergin (loc.cit.) was originally developed for predominantly horizontal motions which a priori does not hold for convective dynamics. Therefore, an additional term for shear production due to horizontal gradients of the vertical velocity component was added to Kochergin's (loc.cit.) shear production term which originally only considered vertical gradients of the horizontal velocity components. Good experiences from model applications for the Greenland Sea seem to support this approach (Backhaus 1995). The diagnostic closure scheme applied to dynamics in our high-resolution convection model yields values in the range of 0.005 to 0.05 m^2/s for the turbulent eddy viscosity which appear to be close to estimates derived from observations by McPhee and Martinson (1993).

The grid size of the model was determined experimentally from a number of tests and by comparing simulated scales of convection with observations from the Greenland Sea (Quadfasel, pers. com., 1995). A final choice of 5 meters for the grid size turned out to be an acceptable compromise between computational demands and process oriented resolution. Smith and Morrison (1993) used a similar (but not isotropic) grid size in their convection study. With this resolution the convection model works well below the internal Rossby radius of deformation. The space domain is discretised by means of a staggered Arakawa C-grid (Arakawa and Lamb 1977). The advection of momentum and heat and salt is simulated by means of a conservative explicit (numerically diffusive) vector- upstream scheme. As a result of the explicit character of the advection scheme the time step of the model is largely governed by the energetics of convective dynamics. Typically the model is run with time steps in the order of one minute.

The artificial diffusivity of the vector-upstream scheme, as judged from previous experiences with the model, appears to be of minor significance. The diagnostic (elliptic) Poisson equation for perturbation pressure, which is needed in a non- hydrostatic model to obtain actual pressure fields (Backhaus 1995), is solved at each time step by means of an iteration utilising a successive over-relaxation (SOR) scheme (Varga 1962). At the sea surface a rigid-lid condition for the pressure is applied to filter out surface gravity waves.

The application of a cyclic boundary condition avoids prescription of lateral boundary conditions in the model. However, care has to be taken to avoid that the boundary condition gains influence on the model solution. This is avoided by choosing the lateral scale of the model 'slice' in a way that the model domain always at least covers 3-5 convection cells. In this

application to Baltic convection, considering a water column of 100 meters, a horizontal dimension of 1.5 Km was chosen for the model slice. Typical convective aspect ratios (vertical versus horizontal scale) are in the order of 1.5 to 2.5. This ensures a validity of cyclic lateral boundary conditions. For the fluxes of heat, salt and momentum at the sea surface standard bulk formulae are used (Gill 1982).

3. Experimental Set-up

The Baltic CIL appears in a typical T,S-profile (figure 1a) measured in the central Baltic Proper (source: BOSEX 1977, ICES data base). For the Baltic model experiment the model slice should be visualised as being placed in the region (cf. figure 1b) where the T,S-profile was obtained. This profile is prescribed for the entire model domain as an initial condition implying homogeneity in the horizontal. The applied cyclic boundary conditions account for a closed system; it excludes lateral advection and allows to investigate convective modification of the water column in isolation.

The model is forced by prescribing an ambient air temperature and a constant wind of 10 m/s. The wind direction was turned by 45 degrees to the right relative to the normal axis of the model slice. This was done because experiments with a fully three-dimensional convection model (Kämpf, 1996) have shown that the convection is sensitive to the prescribed wind direction. With the given tilt of the wind direction both models predicted very similar water mass properties for the same forcing and initial stratification.

The air temperature in the experiment is decreased/increased linearly in order to simulate a cooling phase in autumn and winter and a subsequent warming phase in spring. In this time of the year the two potential 'convection windows' are expected to occur. On purpose, with the intention to obtain a first guess of convective water mass formation in the Baltic Proper, the applied forcing simulates cooling and warming phases in an evidently schematic way. It accounted for heat fluxes which varied in magnitude between 20 and 500 W/m^2 in dependence on difference between predicted SST and prescribed air temperature. Bearing this in mind the applied forcing just reflects the basic seasonal trend of heat and momentum fluxes and excludes transient fluctuations which confines this process study to the most simple case.

4. Results

By applying the schematic forcing the model was run for a total simulation time of 4000 hours, i.e. about 5.6 months. The cooling phase lasted for about 2100 hours. Both cooling and warming phase in the experiment were

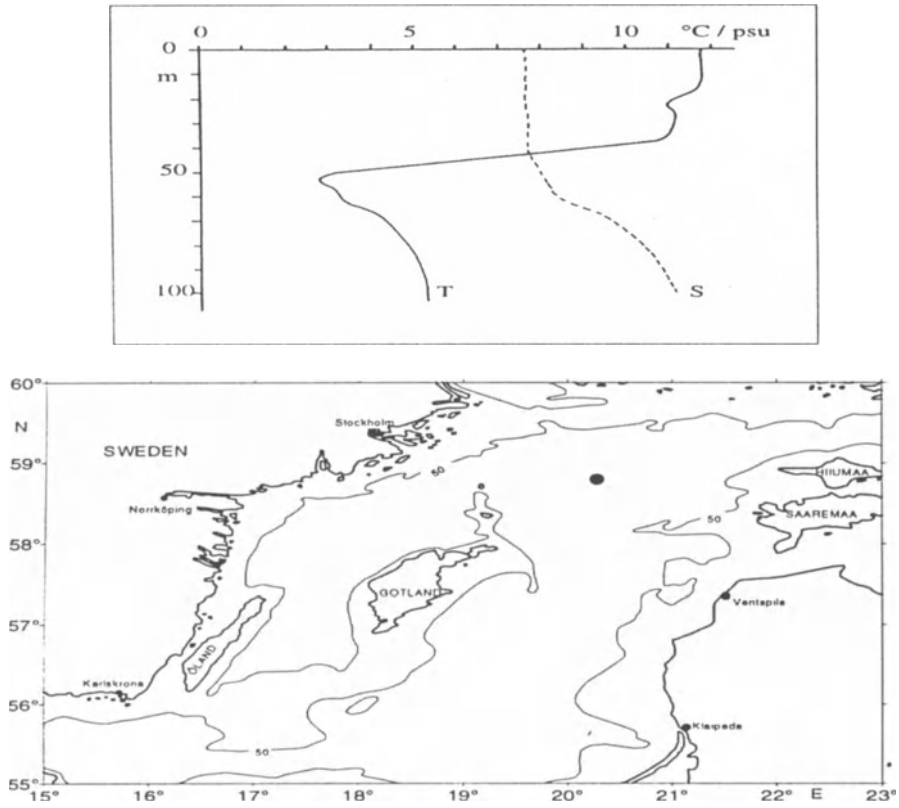


Figure 1. a: T,S-profile from BOSEX 1977 (Top) b: Location of T,S-profile in Baltic Proper (bottom)

initialised by a laterally homogeneous T,S-profile and assuming an ocean at rest. The warming phase was initialised from the final result of the cooling phase by applying a horizontal mean over the entire model domain on all predicted properties. An effective data compression was obtained by computing horizontal averages of predicted fields over the model domain. Standard deviations obtained from this procedure will be used as an integral measure to quantify fluctuations of convective dynamics.

The evolution of temperature profiles during the course of the experiment for both cooling and warming phase is described by profile-ensembles (figure 2) which cover time intervals of 100 hours, respectively with a 10-hourly sub- sampling. For the sake of clarity individual groups of profiles are separated by data gaps of 100 hours in the display. The cooling phase (figure 2a) is characterised by a transition from a summer to a winter thermocline. A reversed sequence is obtained for the warming phase (figure 2b) which ends with the establishment of a summer thermocline. The initially

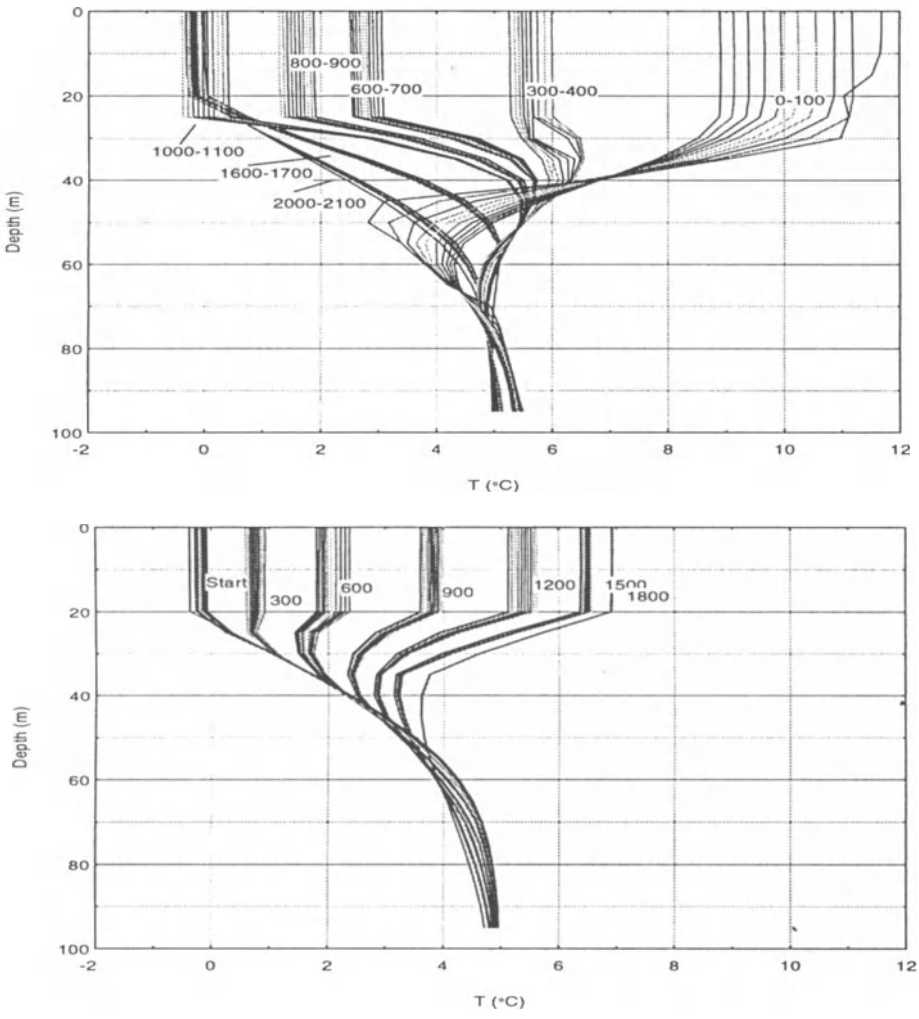


Figure 2. Predicted evolution of temperature (° C) for entire model experiment, i.e. cooling and warming phase. Profile-ensembles are given for time intervals of 100 hours with 10-hourly sub-sampling. Ensembles are separated by data gaps of 100 hours for the sake of clarity of display. a: Cooling phase (top); b: Warming phase (bottom)

pronounced CIL (figure 1a) beneath the summer thermocline is rapidly destroyed during the cooling phase (figure 2a). However, the CIL re-appears at the end of the warming phase (figure 2b) but with a less pronounced signature as compared to the initial profile (cf. figure 1).

4.1. COOLING PHASE

The particularly dramatic evolution of temperature profiles during the cooling phase (figure 2a) deserves a more detailed inspection. Temperature profiles during the cooling phase are given by means of a time-sequence of 10-hourly ensembles of predicted mean temperature profiles (figure 3). Convective erosion of the summer thermocline occurs after a simulation time of about 400 hours (cf. figure 3a). Apparently convective dynamics also erode the signature of the CIL which is situated well below the actual penetration depth of the convection (at this stage about 35 meters). The CIL is warmed by about 2.5 ° C during the first 400 hours of the experiment and it looses its initially pronounced signature (figure 3a). The first 'convective window' occurs after the erosion of the thermocline (figure 3a) as can be seen by fluctuations in temperature profiles (figure 4a) reaching down to depths around 40 m. Soon after the water column re-stratifies (figure 3b) and a winter thermocline is established. The applied (relatively strong) wind forcing causes a pronounced homogeneity of the surface layer. During re-stratification penetration depths of convection decrease from initially around 40 to 25 meters.
A comparison with the initial temperature profile (cf. figures 1 and 3) reveals a drastic change of the thermal stratification within the first 990 hours of the experiment. Evidently temperatures even beneath the halocline, at depths below about 60 meters, have increased by about half a degree. The temperature inversion of the CIL has disappeared (cf. figures 3a,b).

In the final cooling phase (figures 3c,d) a rapid establishment and a strengthening of the winter thermocline is obtained. While surface temperatures approach the freezing point (at about -0.5° C) temperature gradients between sea surface and underlying waters are initially very sharp as can be seen from the first series of profiles in figure 3c. However, thereafter gradients begin to decrease in conjunction with a shallowing of the thermocline from initially 25 to about 20 m (figure 3c). The final hours of the simulated cooling phase (figure 3d) are characterised by a gradual decrease of temperature gradients beneath the thermocline. Surface waters remain close to the freezing point but show a slight tendency to warm. A continuous and ongoing cooling can be observed at depths between 30 and 70 meters. Temperatures at depths around 50 meters appear to approach values of the initial minimum in the temperature inversion of the CIL (cf. figure 1).

The entire cooling phase covered 2100 simulation hours. Apparently, with the onset of the winter thermocline, a warm intermediate layer (WIL) establishes beneath the thermocline (cf. figure 3c,d). Temperatures around the original depth of the CIL, and within the halocline (below 60 m), tend to decrease with increasing stability of near surface waters. Towards the end

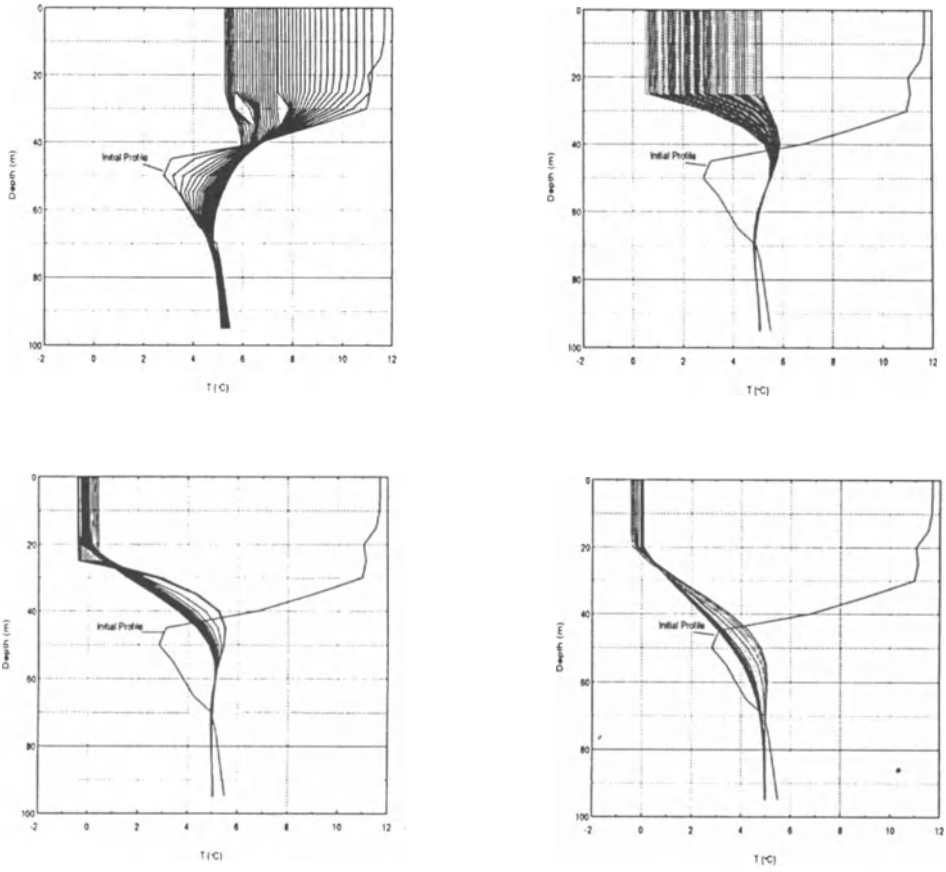


Figure 3. Predicted ensembles of temperature profiles (° C) for cooling p hase as depicted by 10-hourly sub-sampling. a: simulation time: 2 to 392 hours (upper left) b: simulation time: 402 to 992 hours (upper right) c: simulation time: 1002 to 1292 hours (lower left) d: simulation time: 1302 to 1992 hours (lower right)

of the cooling phase the WIL is increasingly eroded. However, temperature contrasts between sea surface and waters above the halocline are still in the order of 4 to 5 ° C. In the North Sea, where convection prevails throughout a winter due to salinities well above 30 psu, the corresponding amount of heat would principally be available to be released to the atmosphere. However, according to our predictions for the Baltic this heat reservoir appears to be trapped beneath the winter thermocline.

Predicted profiles of convective temperature fluctuations (figure 4), i.e. standard deviations obtained from horizontal averaging over the width of the model slice, should be viewed at in conjunction with mean temperature profiles (figure 3) depicted for the same time intervals. Convective erosion of the summer thermocline causes considerable temperature fluctuations

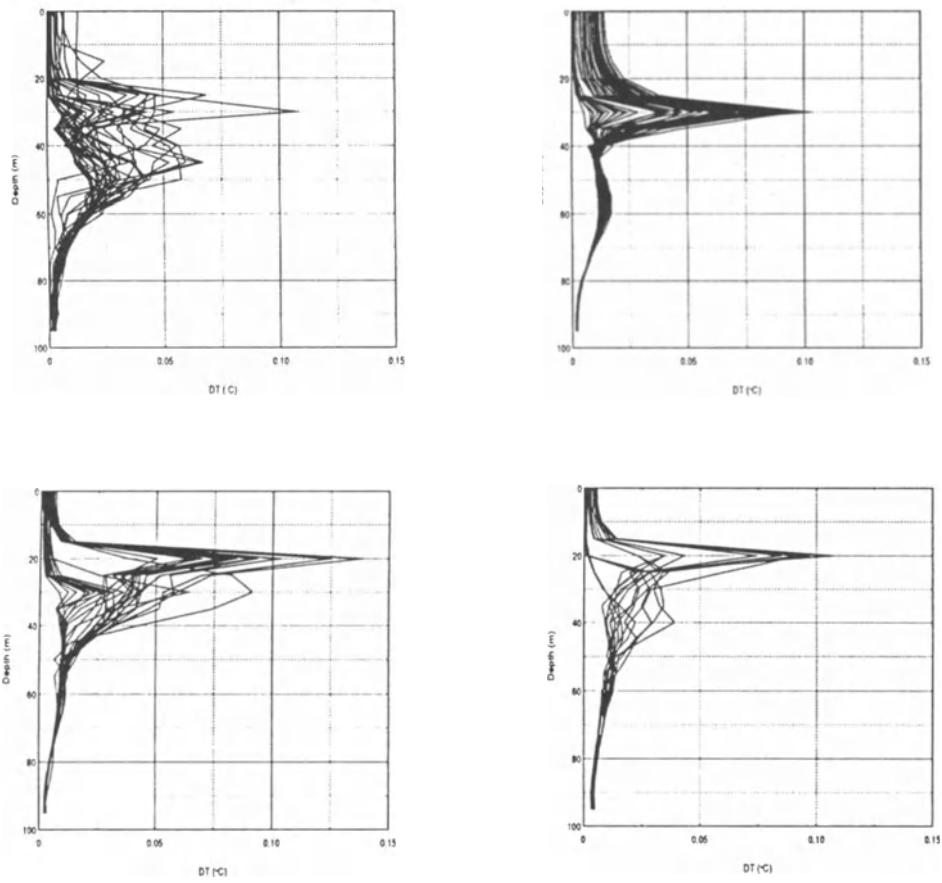


Figure 4. Predicted temperature fluctuations (° C) for cooling phase, i.e . standard deviations from horizontal averaging, depicted by profile-ensembles with 1 0-hourly sub-sampling. a: simulation time: 2 to 392 hours (upper left) b: simulation time: 402 to 992 hours (upper right) c: simulation time: 1002 to 1292 hours (lower left) d: simulation time: 1302 to 1992 hours (lower right)

(figure 4a) which are most pronounced in the depth range between 20 and 70 meters. A double-peak structure emerges which reflects highest activities at the base of the thermocline and within the CIL. This is the signature of the first convective window which apparently reaches down to the halocline. With the establishment of the winter thermocline, i.e. with the closure of the convective window, extremes of fluctuations appear to be confined around depths of 30 meters, that is at the base of the new thermocline (figure 4b). With the beginning erosion of the short-lived WIL fluctuations cover a larger depth range and a double-peak structure (figure 4c) emerges which prevails until the end of the cooling phase. It is characterised by a pronounced and sharp peak at the base of the now shallower winter thermocline and by a broader, weaker peak around depths between 30 and 50 meters (figure 4d).

4.2. WARMING PHASE

The warming phase (figure 2b) shows a less dramatic development than the cooling phase as judged from the modality of temperature profiles. With the onset of warming a slight deepening of the winter thermocline is obtained (cf. profile ensemble for 300 hours in figure 2b). Apparently the second convective window that was expected in spring does not occur. As explained in the introduction one would expect it to open up while increasing surface temperatures approach the temperature of the density maximum. Instead, the simulation predicts an unexpectedly early establishment of the summer thermocline (cf. ensemble for 600 hours in figure 2b) which occurs while surface temperatures are still below the temperature of the density maximum. The early onset of the thermocline is explained by a fresh water input from the melting ice cover. The additional buoyancy provided by the freshwater allowed for an early establishment of the summer thermocline and apparently prevented deep reaching convection in spring.

The further development of the predicted thermal stratification shows the establishment of a new CIL beneath the increasing gradient of the summer thermocline (ensembles for 600 to 1800 hours in figure 2b).

5. Discussion

The model experiment revealed that the CIL is first eroded in autumn and winter by convective dynamics and then re-established in spring. Obviously convection originating from the sea surface never penetrates deep enough to reach the depth of the halocline. However, internal dynamics appear to contribute in a significant way to water mass formation beneath the actual convective penetration depth. The internal mixing is induced by non-hydrostatic pressure fluctuations which are caused by convection originating from the sea surface and which act across isopycnals. They were also obtained in model applications for the Greenland Sea (Backhaus 1995) where pressure disturbances from surface convection triggered internal instabilities at depths well below 1000 meters.

Apparently the water column beneath the Baltic winter thermocline, after SSTs have reached the freezing point, continuously looses heat towards the thermocline (cf. ensembles of temperature profiles for hours 800 to 2100 in figure 2a). This thermal leakage goes along with a weakening of temperature gradients beneath the thermocline and accounts for a slight increase of SSTs in late winter (cf. figures 3c,d). The resulting cooling of the water column above the halocline pre- conditions the new CIL which re-appears towards the end of the warming phase (cf. figure 2b). The ongoing internal

mixing is also seen in the temperature fluctuations below the thermocline (cf. figures 4c,d). Note that dynamics in the well mixed surface layer are always turbulent due to the applied constant wind forcing (10 m/s) in our experiment. Turbulence in the winter thermocline accounts for the leakage of heat towards the atmosphere. This should change significantly with a transient forcing. In that event even lower temperatures would be expected for waters above the halocline.

In general the results of our model experiment seem to reflect the expected temperature evolution in the Baltic. Despite the schematic forcing the convection model provided detailed information about the complex internal temperature evolution in the Baltic Proper. In particular the trapping of a considerable heat reservoir beneath the winter thermocline was successfully reproduced. However, the model failed to simulate the postulated second convection window but it provided an explanation for the early onset of a new thermocline which agrees with findings described by Eilola (1996). According to this simulation a direct convective ventilation of the entire water column above the halocline appears to be by far more difficult than expected. This might have been caused by the applied schematic forcing. With a transient forcing peaks in oceanic heat loss should cause a more energetic and hence more penetrative convection.

Active convection causes internal mixing well beneath its actual penetration depth. It would have been impossible to simulate this phenomenon with a conventional mixed-layer model because it cannot predict non-hydrostatic pressure fluctuations. With a realistic transient forcing insight into temporal variability of penetration depth and convective water mass formation during a winter could be provided by the model. An application of the model to both Baltic and Black Sea would allow for an inter-comparison of convective water mass formation in both seas.

6. Acknowledgements

The authors are grateful to their colleagues Bert Rudels and Corinna Schrum for many fruitful discussions and encouragement. Thanks in particular is due to Emin Özsoy for his constructive impetus and careful editing of the joint volume but also to all colleagues from Bulgaria who hosted an extremely informative and interesting workshop at Varna in late 1995. This work was partly funded by the EU under grant ESOP 1 MAS II-CT 93-0057

References

1. Akitomo K., T. Awaji, N. Imasato (1995): Open-ocean deep convection in the Wedell Sea: two-dimensional numerical experiments with a non- hydrostatic model. Deep Sea Res. 1, Vol. 42, No. 1, pp 53-73.

2. Arakawa A. and V.R. Lamb (1977) Computational design of the basic dynamical processes of the UCLA general circulation model. Meth. comp. Physics., Vol.16, 173-263.
3. Backhaus, J.O., 1984: Estimates of the Variability of low frequency currents and flushing times for the North Sea. ICES, C.M. 1984/C:24
4. Backhaus, J.O.,1989: The North Sea and the Climate, Dana, Vol.8, 69-82.
5. Backhaus, J.O.,1990: On the Atmospherically induced Variability of the Circulation of the NW-European Shelf Sea and related Phenomena, in: Modelling Marine Systems Vol. I, A.M.Davies (ed), pp 93-134
6. Backhaus, J.O.,1993: Das Wetter im Meere, in: Klimaänderung und Küste - Einblick ins Treibhaus - ; Schellnhuber, Sterr (Hrsg.), Springer Verlag 1993
7. Backhaus, J.O., H. Fohrmann, I.H. Harms, J.H. Jungclaus, A. Rubino, 1995: Convective watermass and ice formation in Arctic shelf seas - a numerical process study -. WMO-Report (to appear), Proceedings of conference on Arctic Climate System Study (ACSYS), held in Gothenburg, 1994.
8. Backhaus, J.O., 1995: Prozeßstudien zur ozeanischen Konvektion. Habilitationsabhandlung im Fachbereich Geowissenschaften der Universität Hamburg.
9. Backhaus, J.O.,1996: Climate-Sensitivity of European Marginal Seas as derived from the Interpretation of Modelling Studies. Journal of Marine Systems Vol. 7, 361-382.
10. Backhaus, J.O., I.H. Harms, J. Kämpf, A. Rubino, 1996: Formation of dense bottom water in Arctic shelf seas. ICES Journal of Marine Science (to appear).
11. Broecker, W.S., 1991: The great Ocean Conveyor, Oceanography, 4, 79-89.
12. Brugge, R., H.L. Jones & J.C. Marshall, 1991: Non-hydrostatic Ocean Modeling for Studies of Open-Ocean Deep Convection. In: CHU, P.C. & J.C. Gascard (Hrsg.): Deep Convection and Deep Water Formation in the Oceans. Elsevier, New York, 325-340.
13. Dietrich, G. F. Schott, 1974: Wasserhaushalt und Strömungen der Ostsee. in: Meereskunde der Ostsee, Editoren: Maagaard, Rheinheimer. Hochschultexte, Springer-Verlag, Berlin, Heidelberg, New York
14. Eilola, K. (1996): The development of a spring thermocline at temperatures below the temperature of maximum density with application to the Baltic Sea Journal Geophys. Res. (to appear)
15. Gill A.E. (1982) Atmosphere Ocean Dynamics. Academic Press, San Diego, Cal.
16. GSP Group (1990): Greenland Sea project - a venture towards improving our understanding of the oceans' role in climate, EOS, 71 (24), 750-755.
17. Hibler, W.D., 1979: A dynamic thermodynamic sea ice model. J. Phys. Ocean. 9, 815-846.
18. Jones H. and J. Marshal (1993) Convection with rotation in a neutral ocean; a study of open ocean deep convection. J. Phys. Ocean.23,109-123
19. Kämpf, J. (1996) Thermohaline Konvektion in Polynien arktischer Schelfmeere. Institut für Meereskunde der Uni. Hamburg, April 1996
20. Killworth, P.D., 1976: The mixing and spreading phases of MEDOC. I. Progr. in Oceanogr. 7, Pergamon Press, 59-90.
21. Killworth, P.D., 1979: On chimney formations in the oceans. J. Phys. Ocean., 9, 531-554.
22. Killworth, P.D., 1983: Deep convection in the world ocean. Rev. Geophys. Space Physics 21, 1-26.
23. Kochergin V.P. (1987) Three-dimensional prognostic models. in: Three- dimensional coastal ocean models (ed. N. Heaps); AGU: coastal and estuarine science 4, 201-208.
24. Maykut G.A. (1986) The surface heat and mass balance. in: Geophysics of sea ice (Untersteiner ed.). Plenum Press, New York.
25. Matthäus, W., H. Franck, 1988: The seasonal Nature of major Baltic Inflows. Kieler Meeresforschung, Suppl. Vol. 6, 64-72
26. McPhee M. and D.G. Martinson (1994) Turbulent mixing under drifting pack ice in the Weddell Sea. Science, 236, 218-221
27. MEDOC Group (1970): Observations of formation of deep water in the Mediter-

ranean sea, 1969. Nature, 227, 1037-1040.
28. Murray J., Z. Top, E. Özsoy (1991) Hydrographic properties and ventilation of the Black Sea. Deep-Sea Res., 38, Suppl. 2, S663-S689.
29. Özsoy E., Ü.Ünlüata, Z. Top (1993). The evolution of Mediterranean water in the Black Sea: interior mixing and material transport by double diffusion. Prog. Oceanog. Vol. 31, 275-320.
30. Özsoy E., Z Top, G.White and J.Murray (1991) Double diffusive intrusions,mixing and deep sea convection processes in the Black Sea .In:The Black Sea Oceanography, E.Izdar and J.M.Murray(editors),NATO/ASI Series,Dordrecht,Kluwer Academic Publishers,17-42
31. Rudels B. and D. Quadfasel (1991) Convection and deep water formation in the Arctic Ocean - Greenland Sea System. J. Marine Systems, 2, 435-450.
32. Rudels B. (1990) Haline convection in the Greenland Sea. Deep-Sea Research, vol. 37, 1491-1511.
33. Schott, F., M. Visbeck & J. Fischer,. 1993: Observations of vertical currents and convection in the central Greenland Sea during the winter of 1988-1989. J. Geophys. Res. 98, 14402-14421.
34. Semtner A.J. (1976) A model for the thermodynamic growth of sea ice in numerical investigations of climate. J. Phys. Ocean., 6, 379-389.
35. Semtner A.J. (1987) A numerical study of sea ice and ocean circulation in the Arctic. J. Phys. Ocean., 17,
36. Skogen, M. (1996) this volume
37. Smith D.C. and J.H. Morrison (1993) A numerical study of haline convection beneath leads. JGR, vol 98, 10069-10083.
38. Sur, H.I., E. Özsoy, . nlata (1994) Boundary current instabilities, upwelling shelf mixing and eutrophication processes in the Black Sea. Prog. Oceanog. Vol. 33, 249-302.
39. Tomczak, M., J.S. Godfrey, 1994: Regional Oceanography, an introduction. Pergamon Press, 297ff.
40. Varga R.S. (1962) Matrix iterative ananlysis. Englewood Cliffs, NJ, Prentice Hall.
41. Visbeck, M., 1993: Konvektion im offenen Ozean. Interpretation von Beobachtungen aus der Grnlandsee und dem westlichen Mittelmeer. Ber. Inst. Meeresk. Christian-Albrechts-Universität Kiel 237, 187 pp.

AN ICE/OCEAN MODEL FOR NORTH AND BALTIC SEA

CORINNA SCHRUM
Institut für Meerskunde, Universität Hamburg
Troplowitzstr. 7, D-22529 Hamburg

Abstract. A coupled ice/ocean model for the region of North Sea and Baltic Sea was developed to carry out realistic hindcast simulations on climatological time scales. By comparing model results and observations, it could be shown that the model is able to reproduce the annual cycle of surface temperature in both marginal seas, North Sea and Baltic Sea. Comparisons of model results and climatological mean distributions showed that it was possible to calculate vertical stratification of temperature and salinity in a realistic manner and that the permanent halocline in the Baltic is preserved during the calculation period of one year. Beyond, it was also possible to calculate the realistic development of sea ice in the Baltic Sea. Thus, the model represents an important tool for climate research in the North Sea and the Baltic Sea.

1. Introduction

During the last decade, scientific research has focussed on the discussion of climate variability and climate change. Most of the studies were carried out on the global scale with grid resolutions in the order of 500 km and more. Processes on the regional scale are below the resolution of global climate models, which was earlier discussed by v. Storch (1994). In principle, there are two strategies to conclude from results of global climate research to the regional scale. The first one is statistical downscaling, carried out for example by Heyen *et al.* (1995). They investigated correlations between the sea level in the Baltic Sea and North Atlantic air pressure gradients. The second strategy, which will be applied here, is the dynamical downscaling, i.e. the application of regional models, which use the results of global climate models as boundary conditions.

E. Özsoy and A. Mikaelyan (eds.), Sensitivity to Change: Black Sea, Baltic Sea and North Sea, 311–325.
© 1997 *Kluwer Academic Publishers.*

There are some requirements on such a regional model for Baltic Sea and North Sea. Firstly, it is necessary to include both marginal seas in one model, to be able to resolve the sea level gradient between North Sea and the Baltic, because the exchange of salty North Sea water and brackish Baltic Sea water depends strongly on the sea level gradient between both. Consequently the model needs to be a prognostic baroclinic model, because water exchange and sea level gradient between North and Baltic Sea are influenced by large scale density gradients between North Sea and the Baltic and by the inclination of the permanent halocline in the Baltic, as briefly discussed by Backhaus (1996).

In the climatological mean, nearly one third of the Baltic Sea area is covered by ice for more than one month during the winter, and parts of the Baltic are usually ice covered up to several month during the year. Since sea ice is important for momentum and heat exchange between ocean and atmosphere, a model, that is suitable for investigations of climate sensitivity and climate change, needs to be coupled dynamically and thermodynamically to an ice-model.

Thirdly the model needs to be stratification resolving. Not only near the surface, to resolve the processes of thermocline development, but also up to nearly $100m$ depth, to resolve the permanent halocline in the Baltic.

The last requirement is a technical one: The integration of the model over climate time scales, say up to decades, must be performable with realistic effort in computation time and storage. This makes the usage of long timesteps, and therefore implicit schemes, necessary.

A great number of regional scale models exists for Baltic Sea and North Sea. Examples are the North Sea model of Pohlmann (1996a and b) and the Baltic Sea model of Lehmann (1992). However, coupled ice-ocean models which include both marginal seas are rare. Up to now, there is only one such model available, namely the operational model of the BSH [1] (Huber *et al.*, 1994). However, this model was designed for operational forecasts. It uses explicit numerical methods and has long computation times (in the order of realtime modelling). Therefore, the development of a North and Baltic Sea model, suitable for climate investigations is one effort that is necessary for the regional climate impact research. Such a model was developed and is presented in the following. It will be shown, that the model is able to calculate the thermohaline circulation, the seasonal cycle of temperature and salinity and the sea ice development.

[1] Bundesamt für Seeschiffahrt und Hydrographie in Hamburg, Germany

2. Model Description

The model is the combination of two sub-models, a hydrodynamic- and an ice-model. These two sub-models are thermodynamically and dynamically coupled. Heat and momentum fluxes between ice and water are considered and the atmosphere/ocean heat and momentum fluxes are reduced as a function of ice compactness.

The hydrodynamic part of the model has its origin in the HAMSOM (HAMburg Shelf Ocean Model), a nonlinear semi-implicit 3-d baroclinic model, based on the equation of motion in Boussinesq-approximation, the continuity equation, the hydrostatic approach, the equation of state and the nonlinear advection equations for temperature and salinity. Brief model descriptions were given by Backhaus (1983 and 1985), Stronach *et al.* (1991), Pohlmann (1991 and 1996a) and Schrum (1994).

The dynamic ice model is based on the viscous plastic ice model of Hibler (1979) and the Baltic Sea ice model of Leppäranta (1981). It was coupled to a simple two-dimensional ocean model by Zhang and Leppäranta (1992) and is now used by the Swedish Meteorological and Hydrological Institut (SMHI) in an operational mode (Omstedt *et al.*, 1994, 1995).

The area of the North Sea, Baltic Sea and the transition region between both marginal seas is covered by the model. The grid is a spherical grid with horizontal resolutions of $\Delta\varphi = 6'$ and $\Delta\lambda = 10'$. In the vertical, the model consists of 20 layers with layer thickness from 5m (surface to 40 m depth), 8m (48 to 88 m) and a coarser resolution for the deeper layers (lower boundaries 100, 125, 150, 200, 400 and 600 m).

Because of the semi-implicit numerical schemes, the model is able to run with long time steps. Two different time steps are used: the hydrodynamic model and the thermodynamics are calculated with a time step of 40 minutes, whereas the dynamic ice model uses a time step of four hours.

The model was running on an Apple MacIntosh Power PC 8100/80. For the simulation of one year, it takes seven days of computation time and memory of 53 MB are needed.

2.1. BOUNDARY CONDITIONS

The model receives time dependent lateral boundary values for surface elevation, salinity and temperature from models for the area of the Northwest Europaen Shelf and the North Sea (Backhaus and Hainbucher, 1987; Pohlmann, 1991), which were integrated for the same period as the present model. At the estuaries, lateral boundary conditions are given. Additional surface elevation and salinity decrease, depending on river runoff data in m^3/s (Baltic Sea: Bergström and Carlsson (1994); North Sea: pers. comm.

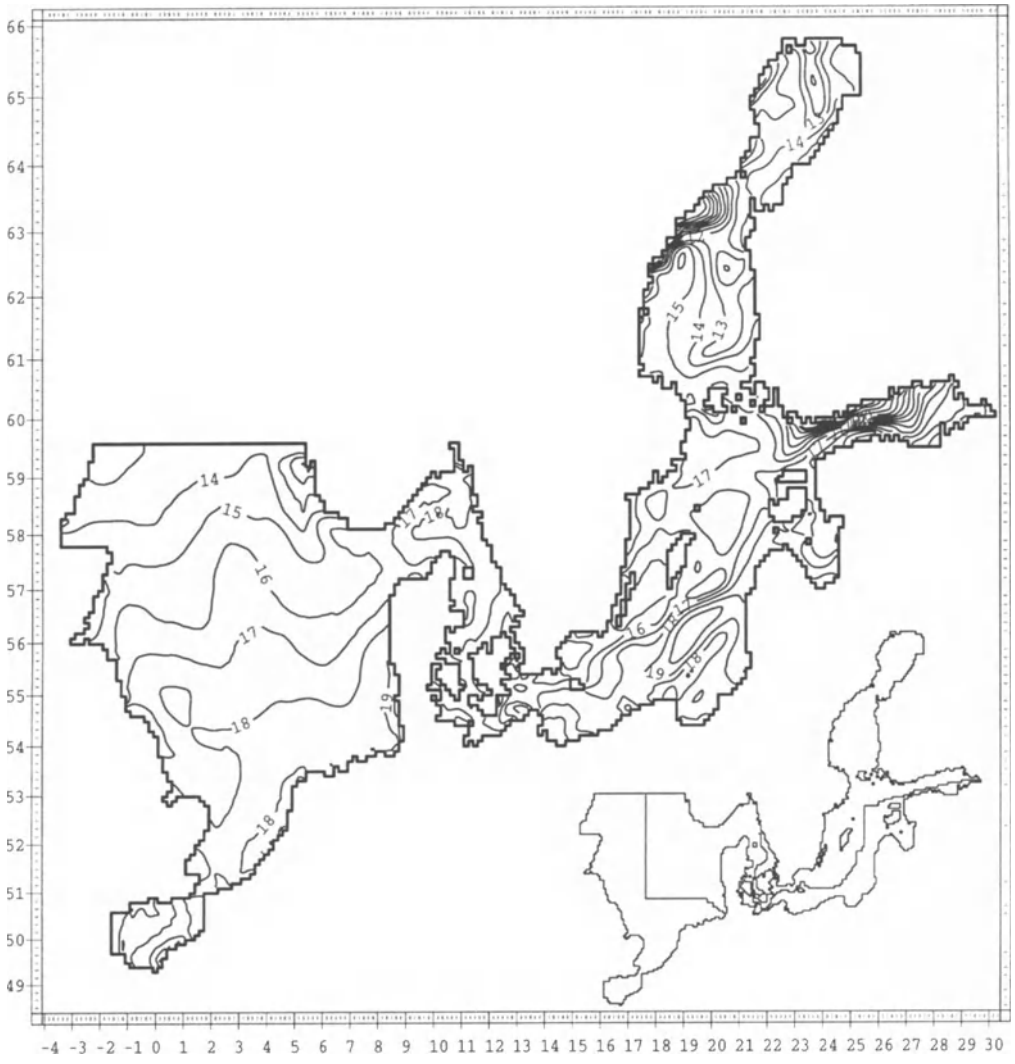


Figure 1. Calculated sea surface temperatures (in ° C) for the 25^{th} of August 1983, mean for the upper two layers. The course of the two vertical sections in North Sea and Baltic Sea, discussed in section 3.4, are marked in the lower left corner.

J. Paetsch and P. Damm, Institut f. Meereskunde in Hamburg, Germany), are assumed.

Heat and momentum fluxes at the sea surface and the ice interfaces are estimated with common bulk formulae as earlier described by Schrum (1994) and Harms (1994). To calculate the fluxes, meteorological observation data (for the North Sea: datasets compiled by the Deutschen Wetter-

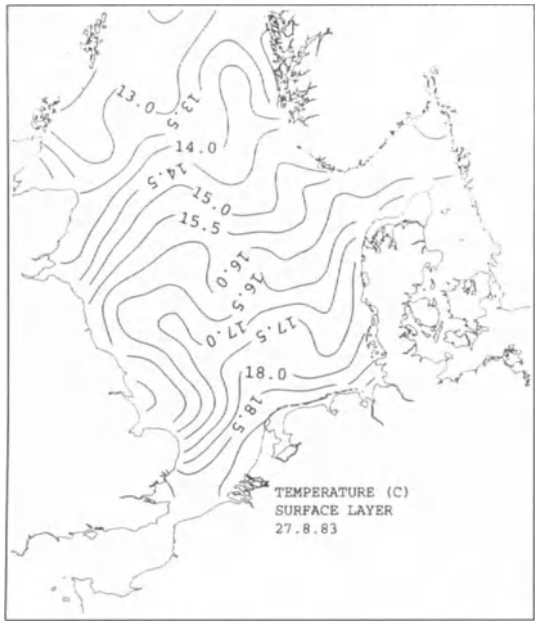


Figure 2. Observed sea surface temperature for the week of 24^{th} to 30^{th} of August 1983 (in $^{\circ}$ C) for the North Sea, The data were provided by the Bundesamt für Seeschiffahrt und Hydrographie in Hamburg, Germany.

dienst, Seewetteramt Hamburg; for the Baltic Sea: the Baltic Sea ice climate dataset, compiled by Haapala *et al.* (1996)) were used. A simple bi-modal decay law after Paulson and Simpson (1977) is assumed to estimate the vertical distribution of the incoming global radiation.

3. Results

A prognostic hindcast, starting with climatological monthly means of temperature and salinity for May, for the period from May 1983 to the end of April 1984 was carried out. This period was selected because it is well investigated and found to represent conditions close to the mean: Omstedt and Nyberg resume that during the winter 1983/1984 ice conditions were normal (Omstedt and Nyberg, 1996) and the period was selected in the Baltic Sea Ice Climate Modelling Program (Haapala *et al.*, 1993) as representative for a normal ice winter. The heat storage during the summers of the years 1983 to 1992 in the North Sea was evaluated by Pohlmann (1996b). His results show, that during the summer 1983 the North Sea heat content was close to the mean heat content of this period. Bergström and Carlsson

(1994) found that the river runoff to the Baltic Sea during the hindcast period was close to climatological mean runoff for the period 1950 to 1990. Therefore it can be assumed, that the hindcast period is representative for a mean state in Baltic Sea and North Sea, especially in the questions of heat content, ice conditions and river runoff.

3.1. SEA SURFACE TEMPERATURES

By comparing the computed mean temperatures in the upper 10 m for the North Sea and the Baltic Sea to observed weekly sea surface temperatures in the North Sea (compiled and published by the BSH) and to observations for the Baltic Sea (compiled and published by the SMHI), it could be shown, that the model succeeded to reproduce the sea surface temperature in the North Sea and the Baltic Sea. An example of the comparisons, the surface temperature for the 25^{th} of August 1983 is shown in the Figures 1, 2 and 3 and discussed in the following.

The calculated range of the surface temperature was, from less than $8°C$ in the Bothnian Sea up to $19°C$ in the Baltic Proper and the southern North Sea, similar to the observed range. Regional scale structures, as the colder area off the eastern Norwegian coast, the upwelling off the western Swedish coast and in the northern part of the Gulf of Finland could be successfully reproduced with the model.

The good agreement between observations and model results for the end of August was confirmed by comparisons of numerous other periods (observation charts for each hindcast week have been compared to model results), not shown here.

3.2. ICE CONDITIONS

The calculated ice distributions in the Baltic have been compared to observed distributions during the hindcast period for every two weeks. One example, the ice conditions for the 16^{th} of February 1984 (Figure 4 computed and Figure 5 observed) will be discussed in the following.

At the 16^{th} of February 1984, the Bothnian Bay was fully ice covered with a small belt of new ice in the southwestern part of the Bothnian Bay. Ice thickness was typically between $15 - 50cm$ in the southern part of the bay and up to $75cm$ in the northern part. Ridging was observed in the northern part.

The Bothnian Sea was ice-free in its eastern central part and a new ice belt along the Swedish coast was observed. The belt of new ice along the western Bothnian Bay and western Bothnian Sea was interrupted by a local thong of very close (compactness between 0.9-1.) and close (compactness between 0.7-0.8) ice in the entrance of Bothnian Bay. The transi-

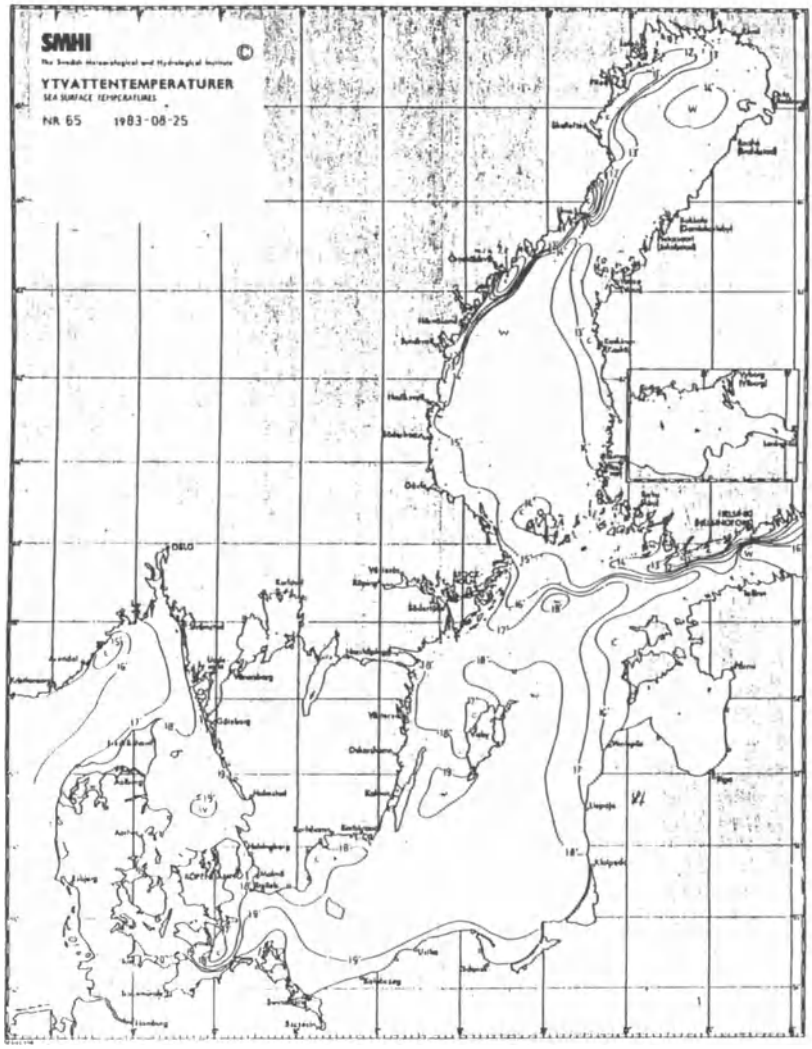


Figure 3. Observed sea surface temperatures (25^{th} of August 1983, in ^{o} C). The chart was published by the Swedish Meteorological Hydrological Institut in Norrköping, Sweden.

tion area between Bothnian Sea and Baltic Proper, the Åland Sea and the Archipelago Sea, was closed by ice. The Åland Sea was covered by new ice and the Archipelago Sea by older fast ice.

Calculated ice distributions in the Bothnian Bay and Sea are similar to the observed. In the northern part of the Gulf of Riga and in the northern and eastern parts of the Gulf of Finland, fast ice and very close ice was observed and calculated. Ice concentrations were slightly overestimated by

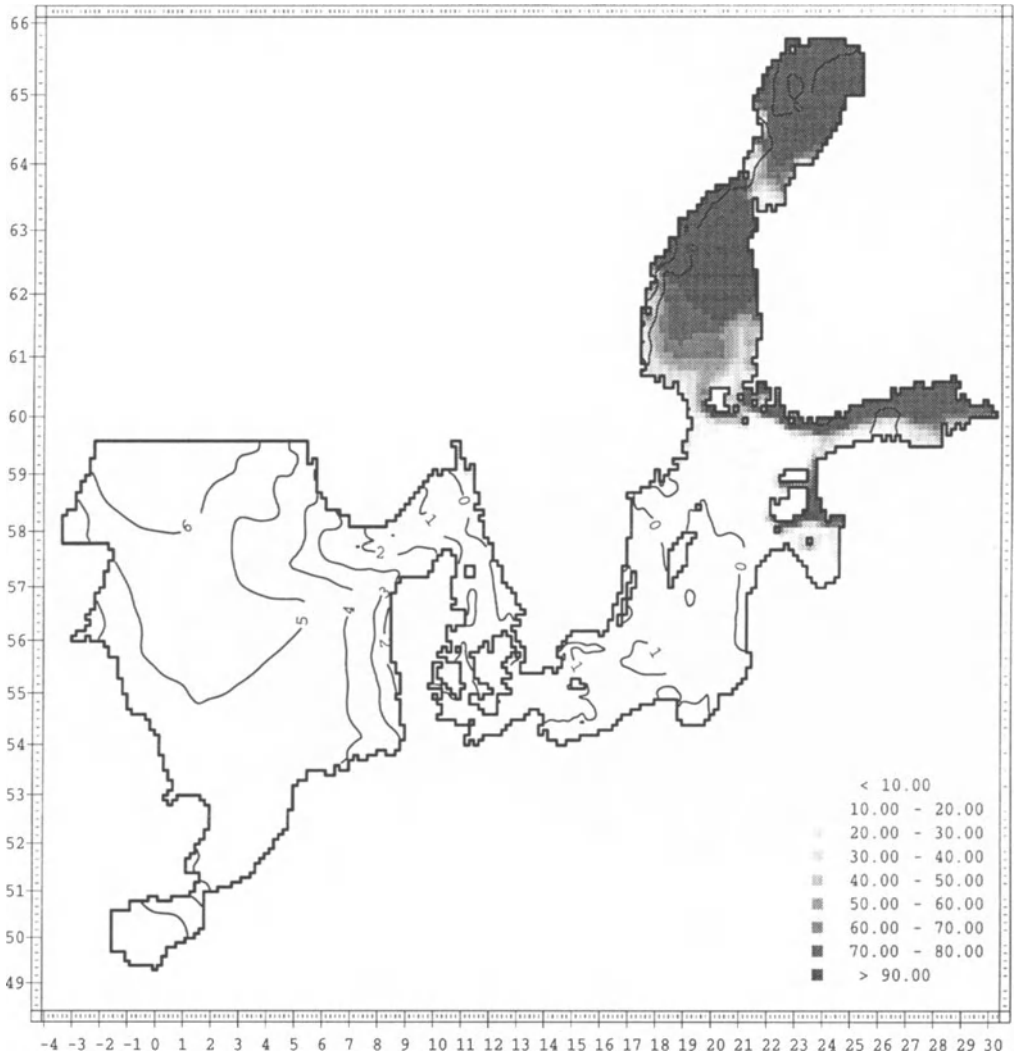


Figure 4. Calculated sea surface temperatures (in ° C, mean for the upper two layers) and ice concentrations in percent for the 16^{th} of February 1984.

the model, but well reproduced in structure.

Computed ice thicknesses were close to observed ice thicknesses and ridging was predicted with the model in the north of Bothnian Bay and in the eastern part of Gulf of Finland, as observed. However, there are discrepancies between model results and observations. In general the calculated surface temperatures are less than observed. The range of differences between model results and observations is in the order of $1 - 2°C$. This is

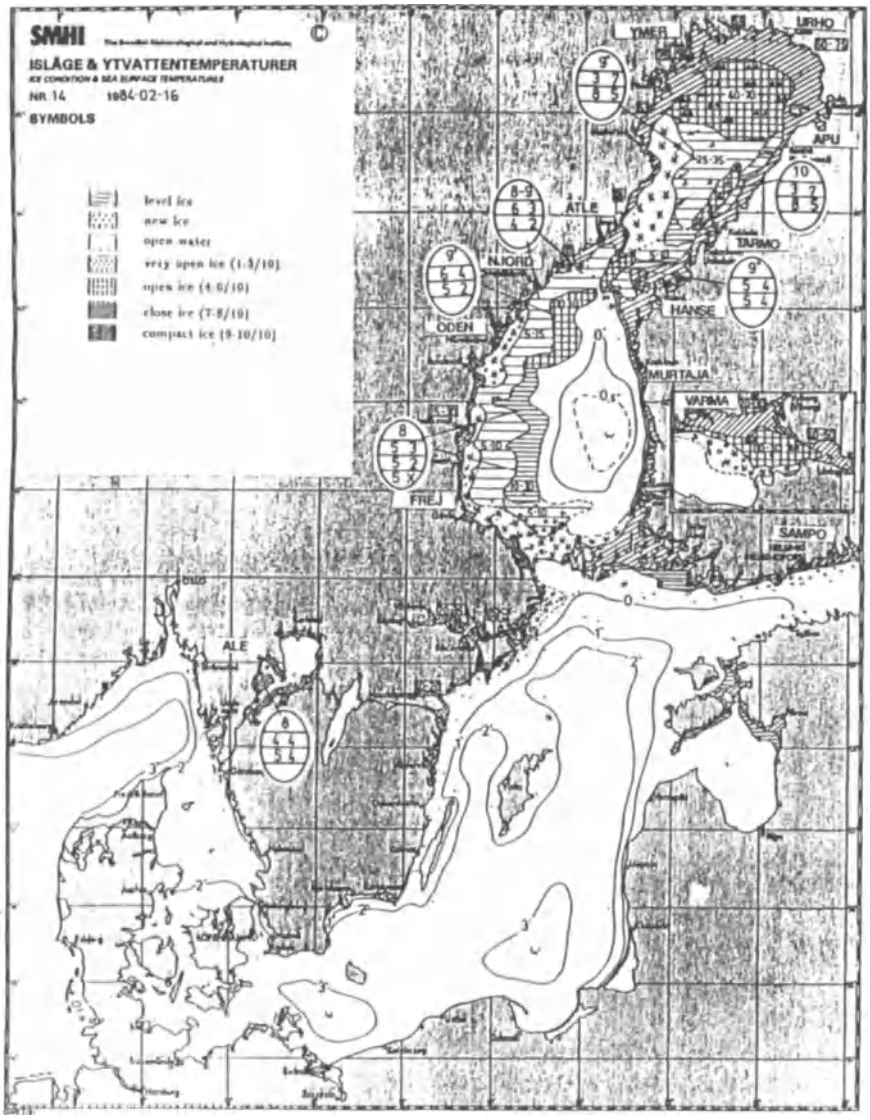


Figure 5. Sea surface temperature (in $^{\circ}$ C) and ice map (16^{th} of February 1984) for the Baltic Sea. The chart was published by the Swedish Meteorological Hydrological Institut in Norrköping, Sweden.

responsible for the slight overestimation of ice compactness, by the model. However, the discrepancies are small and processes of ice growing, advection and melting could be reproduced with the model. These results were confirmed by comparisons of other ice periods.



Figure 6. Upper: Calculated monthley mean temperature (in ^{o} C, July 1983) along the section through the North Sea (course cf. Figure 1). Lower: Gridded climatological means of the temperature (in ^{o} C) in the North Sea for July (course cf. Figure 1). The data were provided by Damm (1989). The climatological temperatures are given on a coarser grid, the resolution is: $\Delta\phi = 12'$, $\Delta\lambda = 20'$. In the vertical direction grid layer depths are 10, 20, 30, 40, 60, 80, 100, 150 and 200 m.

3.3. STRATIFICATION

It was shown, that the annual cycle of surface temperature and the development of sea ice could be successfully simulated with the model. Another open question is the simulation of thermocline and halocline, i.e. the questions: 'Is the model able to describe the processes of thermocline development and is the model able to preserve the permanent halocline in the Baltic?'

In the following, computed temperatures and climatological mean temperature (for the Baltic Sea after Lenz (1971), for the North Sea after Damm (1989)) along two sections, the first from the Skagerrak to the Gulf of Finland and the second from the northern North Sea to the German Bight (courses are given in Figure 1) are compared for different seasons. Two examples will be shown in the following, namely the North Sea section for July 1983 (compared to climatological mean temperature for July, Figure 6) and the Baltic Sea section for October (compared to climatological mean temperature for October, Figure 7).

During July the climatological mean depth of the thermocline in the

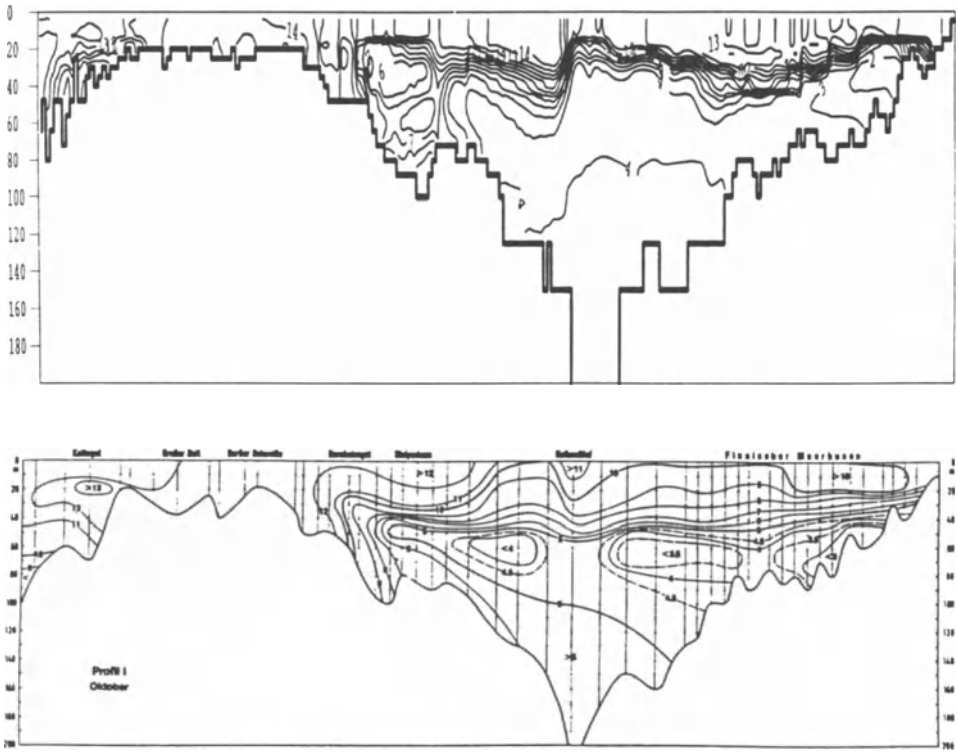


Figure 7. Calculated (left) and climatological monthley mean (right, published by Lenz, 1971) temperature (in ° C) for October along the section through the Baltic Sea (course cf. Figure 1).

North Sea is between 20 and 30 m. This was modelled as well. Considering the coarser vertical resolution of the climatological mean field, the differences between modelled and climatological temperatures are in the range of the mean differences between single observations and climatological means, given by Tomczak and Goedecke (1964). For the deeper areas they gave mean differences of 1.2° C for the bottom water temperature. In shallow areas they found mean differences in the order of 2.4° C. In the Baltic Sea, the depth of the thermocline during the summer is smaller than in the North Sea (Lenz, 1971). This difference was reproduced by the model and the stratification in the Baltic Sea was also simulated realistically during the summer period.

During October thermocline deepening is usually observed in the North Sea and the Baltic Sea, while the surface temperatures decrease. The thick-

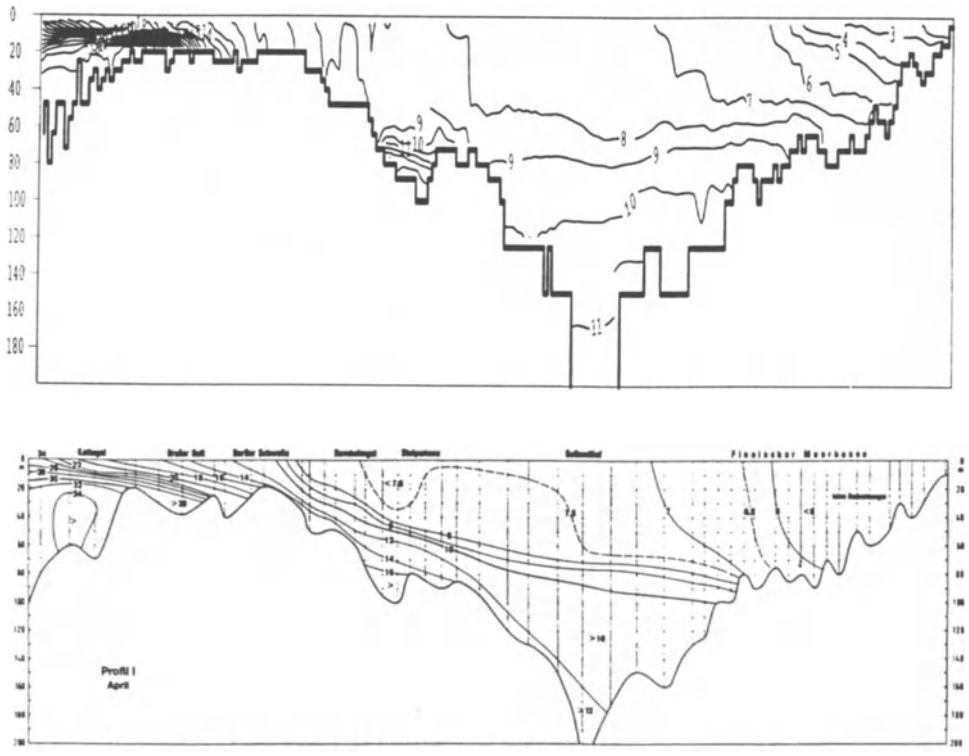


Figure 8. Calculated and climatological monthley means (climatological chart for April, published by Bock, 1971) of the salinity (in PSU) for April along the section through the Baltic Sea (course cf. Figure 1).

ness of the turbulent surface layer increases, it is in general more than 20 m. This deepening was modelled as well. Computed and mean thicknesses of well mixed surface layers are comparable. In the area of the Gotland deep the calculated thermocline depth is shallower, upwelling occured. This is a feature which is evident in climatological mean distributions. Beneath the thermocline, a cold intermediate layer with temperatures between $3 - 3.5°$ C is usually observed from May to November (Lenz, 1971). A similar layer can be found in the model results, too. In climatological mean sections, the thickness of this dense intermediate layer decreases from nearly 50 m in the late spring to less than 20 m in the end of autum. This was modelled as well, and the calculated thickness was in the same range.

The deep water in the Gotland deep is warmer and saltier, with salinities of more than 11 PSU. The characteristics of this water mass are preserved

by the model during the hindcast period. This decrease is not observed in the climatological means. This can be seen by comparisons of calculated monthley means of salinity for April 1984 to climatological means for April (Figure 9). The calculated salinity in the Bornholm basin is less than the climatological mean salinity. The salinity in the deep Bornholm basin decreased in the order of two PSU during the simulation of the hindcast period. However, the modelled decrease is in the order of the observed decrease from the beginning of May 1983 to the end of April 1984, measurements were shown by Matthäus and Carlberg (1990).

4. Summary and Conclusions

A fully prognostic model (in temperature and salinity) was developed and it was shown that the model is able to describe the regionally different answer of the marginal seas on time dependent atmospheric weather conditions. Processes of thermocline development and sea ice development were realistically simulated and preservation of the permanent halocline and the water mass characteristics below the halocline was possible with the model.

The next step towards achieving predictions of the impact of climate change and towards investigating climate variability on the regional scale is now to show which items in climate variability are described by such a model. Intensive analysis of hindcasts for decades and comparisons to observations and climatological means for the same period will be necessary. It will take years to carry out these analyses. Nevertheless, a first step was done with the development of this model, which is an important tool for climate research on a regional scale in the North Sea and Baltic Sea.

5. Acknowledgements

I would like to thank Prof. A. Omstedt (SMHI) and Dr. M. Leppäranta for their kindness of making available the dynamic part of the ice model .

For the valuable forcing database of river runoff and atmospheric data I would like to thank my colleagues P. Damm and J. Paetsch from the IfM, J. Haapala (Department of Geophysics, University of Helsinki, Finland), and once more A. Omstedt. The database for river runoff to the Baltic Sea was kindly placed at disposal by the SMHI for this study. My special thanks are also due to the Deutscher Wetterdienst, Seewetteramt Hamburg and the Meteorologisches Institut der Universität Hamburg for the valuable meteorological database for the North Sea. Thanks also to Dr. T. Pohlmann (IfM), who delivered boundary conditions for temperature and salinity, and to the colleagues from the BSH, Dr. E. Kleine and S. Dick for the topographic data and the climatological temperature and salinity database for

the Baltic Sea. For the North Sea, my colleagues D. Hainbucher (IfM) and P. Damm kindly made available these data to me.

Beyond, I thank Prof. J. Backhaus, Prof. A. Omstedt and Dr. I. Harms for valuable discussions and helpful comments and Dr. H. Langenberg for reviewing the paper.

The study was financed by the German Ministery of Science and Technology (BMBF) under the grant number 01 LK 9326/0.

References

1. Backhaus, J. O. (1983): A semi-implicit scheme for the shallow water equations for application to shelf sea modelling. *Continental Shelf Research*,**2**, 243-254.
2. Backhaus, J. O. (1985): A three-dimensional model for the simulation of shelf sea dynamics. *Dt. Hydrogr. Z.*,**38(4)**, 165-187.
3. Backhaus, J. O. and Hainbucher, D. (1987): A finite difference general circulation model for shelf seas and its application to low frequency variability on the North European Shelf. Three-dimensional models of marine and estuarine dynamics, J. C. J. Nihoul and B. M. Jamart (Ed.), *Elsevier Oceanography Series*, **45**, 221-244.
4. Backhaus, J. O. (1996): Climate Sensitivity of European Coastal Seas. *J. of Mar. Syst.*, **7**, 361-382.
5. Becker, G. A. (1981): Beiträge zur Hydrographie und Wärmebilanz der Nordsee. *Dt. hydrogr. Z.*, **34 (5)**, 167-262.
6. Bergström, St. and Carlsson, B. (1994): River Runoff to the Baltic Sea: 1950-1990. *Ambio*, **23, No. 4-5**, 280-287.
7. Bock, K. H. (1971): Monatskarten des Salzgehaltes der Ostsee. *Dt. Hydrogr. Z., Erg.-H., Reihe B*, **12**, 126 p.
8. Damm, P. (1989): Klimatologischer Atlas des Salzgehaltes, der Temperatur und der Dichte in der Nordsee, 1968-1985, *Technical report of the Institute of Oceanography of the University of Hamburg*, **6-89**.
9. Haapala, J. , J. Dubra, S. V. Klyachkin, T. Kouts, M. Leppäranta, G. Matisone, A. Omstedt, L. Pakstys, K. Strübing, N. Schmelzer, C. Schrum, M. Sztobryn, E. Zaharchenko (1996): A data bank for Baltic Sea ice climate studies., *Report Series in Geophysics, University of Helsinki, Department of Geophysics (in press).*
10. Haapala, J., Leppäranta, M. and Omstedt, A. (1993): Forcing data for the Baltic Sea ice climate modelling. Proc. from the first workshop on the Baltic Sea Ice Climate, Tvärnime, Finland $24^{th} - 26^{th}$ August, 1993. *Report Series in Geophysics University of Helsinki, Department of Geophysics*, **27**, 95-107.
11. Harms, I. (1994): Numerische Modellstudie zur winterlichen Wassermassenformation in der Barentssee. *Berichte aus dem Zentrum für Meeres- und Klimaforschung der Universität Hamburg, Germany, Reihe B*, **7**, 97 p.
12. Heyen, H., Zorita, E. and v. Storch, H. (1995): Statistical downscaling of monthley mean North Atlantic air-pressure to sea-level anomalies in the Baltic Sea. Submitted to *Tellus.*
13. Hibler, W. D. (1979): A dynamic thermodynamic sea ice model. *J. Phys. Oceanogr.*, **9(4)**.
14. Huber, K., Kleine, E., Lass,H.-U. and Matthäus, W. (1994): The Major Baltic Inflow in January 1993 - Measurements and Modelling Results. *Dt. hydrogr. Z.*, **46(2)**, 103-114.
15. Leppärranta, M. (1981): An ice drift model for the Baltic Sea. *Tellus*, **33**, 583-596.

16. Lehmann, A. (1992): Ein dreidimensionales baroklines wirbelauflösendes Modell der Ostsee. *Berichte aus dem Institut für Meereskunde der Christian-Albrechts-Universität Kiel*, **231**, 104 p.
17. Lenz, W. (1971): Monatskarten der Temperatur der Ostsee dargestellt für verschiedene Tiefenhorizonte. *Dt. Hydrogr. Z., Erg.-H., Reihe B*, **11**, 148 p.
18. Luthardt, H. (1987): Analyse der wassernahen Druck- und Windfelder über der Nordsee aus Routinebeobachtungen. *Hamburger Geophysikalische Einzelschriften.* , **83**.
19. Matthäus, W. and Carberg, S. (1990): Meteorological, ice and water exchange conditions, *Baltic Sea Environment Proceedings*, **No. 35 B**, Baltic Sea Environment Protection Commission, Helsinki Commission 1990, 39-43.
20. Maykut, G. A. (1986): The surface heat and mass balance. *The Geophysics of Sea Ice.* Plenum Press, New York.
21. Omstedt, A., Nyberg, L. and Leppäranta, M. (1994): A coupled ice-ocean model supporting winter navigation in the Baltic Sea. Part 1. Ice dynamics and water levels. *SMHI Reports*, **RO 17**, 17 p.
22. Omstedt, A. and Nyberg, L. (1995): A coupled ice-ocean model supporting winter navigation in the Baltic Sea. Part 2: Thermodynamics and meteorological coupling. *SMHI Reports*, **RO 21**, 30 p.
23. Omstedt, A. and Nyberg, L. (1996): Response of Baltic Sea ice to seasonal, interannual forcing and climate change. *Tellus, in press.*
24. Paulson, A. und Simpson, J., J. (1977): Irradiance measurements in the upper ocean. *Journal of Physical Oceanography*, **7**, 952-956.
25. Pohlmann, T. (1991): Untersuchung hydro- und thermodynamischer Prozesse in der Nordsee mit einem dreidimensionalen numerischen Modell. *Berichte aus dem Zentrum für Meeres- und Klimaforschung der Universität Hamburg, Germany*, **23**, 116 p.
26. Pohlmann, T. (1996a): Predicting the thermocline in a circulation model of the North Sea. Part I: Model description, calibration and verification. *Cont. Shelf Res.*, **16(2)**, 131-146.
27. Pohlmann, T. (1996b): Simulating the heat storage in the North Sea with a three-dimensional circulation model. *Cont. Shelf Res.*, **16(2)**, 195-213.
28. Schrum, C. (1994): Numerische Simulation thermodynamischer Prozesse in der Deutschen Bucht. *Berichte aus dem Zentrum für Meeres- und Klimaforschung der Universität Hamburg, Germany. Reihe B*, **15**, 175 p.
29. v. Storch, H. (1994): Inconsistencies at the interface of climate impact studies and global climate research. Report No. 122, Max-Planck-Institut für Meteorologie Hamburg, Germany.
30. Stronach, J. A., Backhaus, J. O. and Murty, T. S. (1993): An update on the numerical simulation of oceanographic processes in the waters between Vancouver Island and the Mainland: the GF8 model. *Oceanogr. Mar. Biol. Annu. Rev.*, **31**, UCL Press, 1-87.
31. Tomczak, G. and Goedecke, E. (1964): Die thermische Schichtung der Nordsee auf Grund des mittleren Jahresganges der Temperatur in $1/2^{\circ}$ und 1° Feldern. *Dt. Hydrogr. Z., Erg.-H.*, **8**, 148 p.
32. Zhang, Zh.-H. and Leppärranta, M. (1988): Modelling the influence of sea ice on water in the Gulf of Bothnia. Internal Report 4, Finnish Institute of Marine Research, 40 p.

QUANTIFICATION OF TRANSPORTS TO SKAGERRAK

A modeling approach

MORTEN D. SKOGEN, GRO ERIKSRØD AND EINAR SVENDSEN
Institute of Marine Research
Pb.1870, N-5024 Bergen, Norway

Abstract. A coupled 3-dimensional physical, chemical and biological model system, NORWECOM (the NORWegian ECOlogical Model system), is used to identify and quantify the variability of the different water masses being transported in and out of Skagerrak. The model system consist of a fine grid for the Skagerrak/Kattegat area, embedded in a coarse grid for an extended North Sea.

The model has been run for several years, and the interannual variability in the transports has been identified and quantified. By running the model with real atmospheric forcing, it has become a tool for explaining some of the ecological characteristics in the same period.

1. Introduction

The Skagerrak ($36000km^2$) and the Kattegat ($22000km^2$) are a transition zone between the much larger Baltic Sea and the North Sea. Especially the Skagerrak is heavily influenced by the water exchange with the North Sea, and due to its relatively deep basin reaching down to about 700 meters, it acts as a "dustbin" for suspended matter (including contaminants) from major parts of the North Sea [4]. The inflow of different water masses from the North Sea is highly variable on time scales of a few days [10, 11], making realistic estimates of transports (based only on measurements) very difficult. The strong vertical stratification and frontal dynamics are also quite variable, and therefore 3-dimensional modeling (including baroclinic forcing) is needed if realistic averaged transports of matter shall be achieved.

The hydrodynamics are quite complicated due to the major water exchanges with the North Sea, large supplies of freshwater (both from the Baltic and some major rivers) and strong topographic steering. Figure 1 demonstrates the general circulation of the relevant water masses. Due to general strong vertical density stratification, sharp fronts and large supplies of both natural and anthropogenic nutrients, the area is highly productive and acts as an important feeding area for several fish species.

The main weakness of 3-D modeling activities is the lack of comparison with adequate real data. The present model has [32, 35] been compared with the extensive SKAGEX-90 dataset [22], focusing the attention around the simulation of the processes and variabilities in Skagerrak and northern Kattegat in May-June 1990.

E. Özsoy and A. Mikaelyan (eds.), Sensitivity to Change: Black Sea, Baltic Sea and North Sea, 327–339.
© 1997 *Kluwer Academic Publishers.*

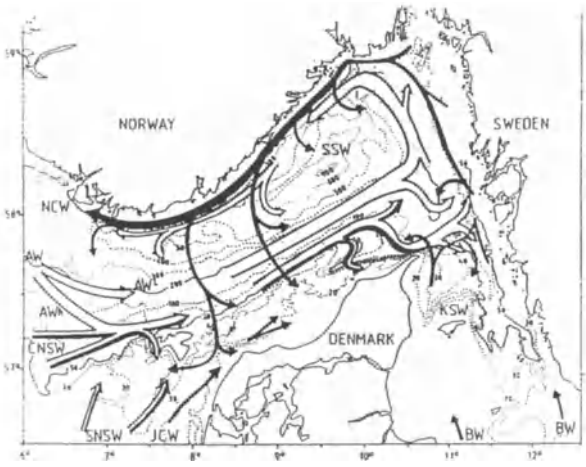


Figure 1. Schematics of the general circulation of the relevant water masses in the Skagerrak and adjacent areas. Open and filled arrows indicate roughly subsurface and surface water respectively (from Danielssen et al.,1995)

In this work the focus has been on different transports to Skagerrak, and some of the main conclusions from [32] have been further investigated. The model system has been run for several years. The wind driven pulsation of the Jutland Coastal Water (JCW) has been studied, and it's interannual variability has been quantified and compared with field data. Using average values for nitrogen in this water, an estimate of that transport from the German Bight to the Skagerrak is given. The seasonal cycle of the total volume transport from the North Sea to Skagerrak is estimated from the modeled circulation, and finally the primary production has been investigated for two of the modeled years.

2. The model design

The NORWegian ECOlogical Model system (NORWECOM) is a coupled physical, chemical, biological model system applied to study primary production and dispersion of particles (fish larvae pollution). The model is fully described in [30]. See also [2, 31].

In the present study a nested version of the model is used, with a coarse 20 × 20 km grid on an extended North Sea, and a fine 4 × 4 km mesh in the Skagerrak/Kattegat area (see Figure 2). The coarse model was run initially, providing the necessary boundary and initial values for the fine grid model.

The forcing variables are six-hourly hindcast atmospheric pressure fields provided by the Norwegian Meteorological Institute (DNMI) [13, 24], 6-hourly wind stress (translated from the pressure fields by assuming neutral air-sea stability), four tidal constituents (coarse model only) and freshwater runoff. In the lack of data on the surface heat fluxes, a "relaxation towards climatology" method is used [9]. During calm wind conditions, the surface temperature field will adjust to the climatological values after about 10 days [21]. The net evaporation precipitation flux is set to zero.

The biological model is coupled to the physical model through the subsurface light, the hydrography and the horizontal and the vertical movement of the water masses. The incident irradiation is modeled using a formulation based on Skartveit & Olseth [26, 27]. Data for global daily radiation from 1990 is taken from a station at Taastrup (Denmark)

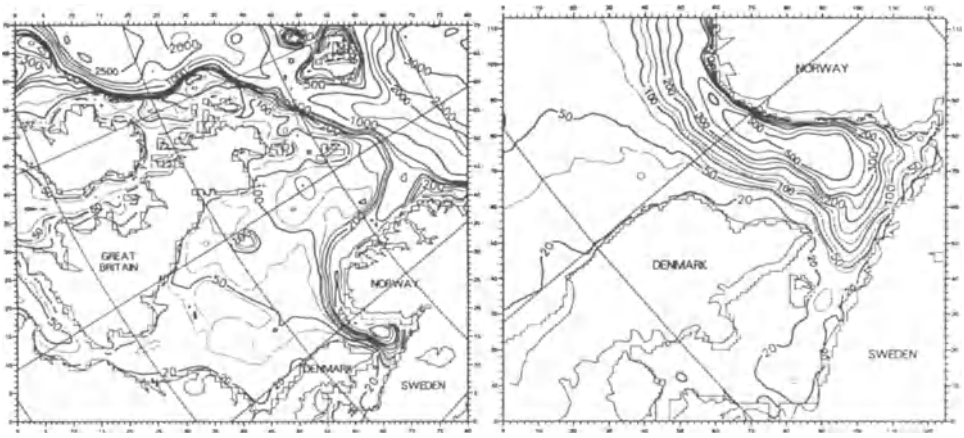


Figure 2. Bottom topography, North Sea 20 × 20 km. left, and Skagerrak 4 × 4 km. right

[3]. Nutrients are added to the system from the rivers and from the atmosphere (only nitrate).

In the coarse model initial values for velocities, water elevation, temperature and salinity are taken from monthly climatologies [20]. Interpolation between monthly fields are also used at all open boundaries, except at the inflow from the Baltic where the volume fluxes have been calculated (using an algorithm of Stigebrandt [33]) from the modeled water elevation in Kattegat and the climatological monthly mean freshwater runoff to the Baltic. In the model, the water entering Kattegat from the Baltic has throughout the year a salinity near 8 psu.

The nutrient fields are derived and extrapolated/ interpolated [23] from data (obtained from ICES) together with some small initial amounts of diatoms and flagellates ($2.75 mgNm^{-3}$). Very few (continuous) time series of nutrients are available from the inflow of Atlantic water. At the open boundaries (outside the North Sea) nutrient values from station M ($66\,^oN, 2\,^oE$) from 1992 (F. Rey, pers. comm., 1993) have been used and assumed valid everywhere in the inflow area. Nutrient data (monthly means) measured in the Baltic (ICES) are used for the water flowing into Kattegat.

Monthly data for freshwater runoff (or annual averaged data), including nutrient data, from main rivers are taken from [8]. In addition extra freshwater is added along the Norwegian and Swedish coast to fulfil requirements to estimated total freshwater runoff from these coastlines [12].

The fine grid model is initiated from the coarse grid model with interpolated data. New boundary values are read and interpolated hourly from the coarse run on the boundary facing the North Sea, and imported through a FRS-zone [19] to the model domain. The open boundary towards the Baltic, as well as freshwater runoff, are treated as in the coarse model.

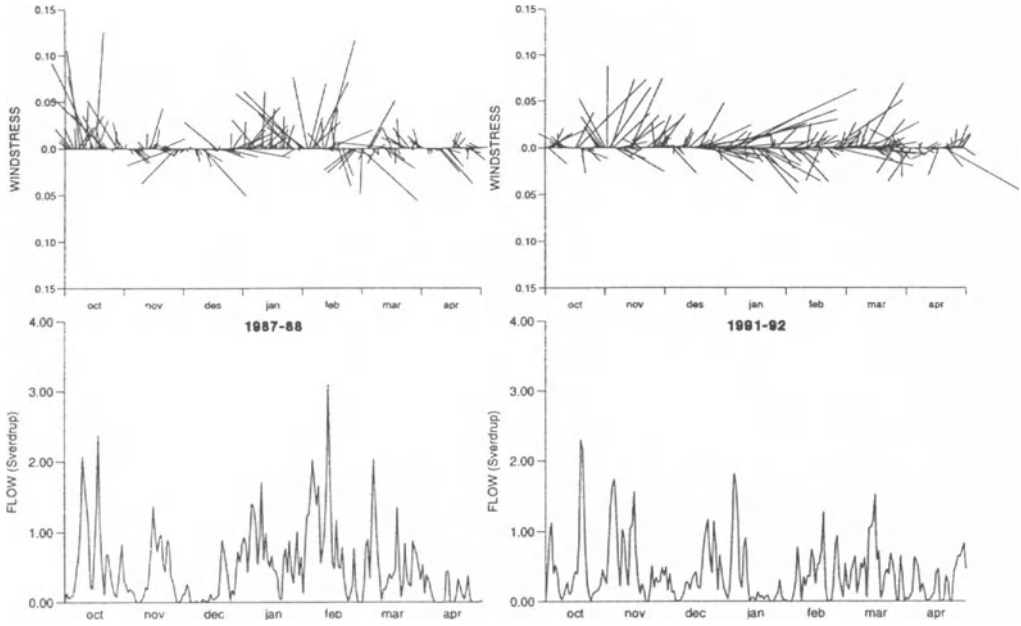


Figure 3. Wind stress (upper) and transports (lower) on the Danish coast through the Tyborøn section, 1987/88 (left) and 1991/92 (right)

3. Transports to Skagerrak

To investigate the interannual variabilities in the transports to Skagerrak, the physical part of the model has been run several years with real atmospheric forcing and river flows. In these model runs the coarse North Sea model has been initiated and started on June 1, while the fine grid Skagerrak-Kattegat model was initiated from the coarse model and was run for an 8 months period starting on September 1, and ending on May 4. This has been done for all years from 1987/88 to 1993/94.

3.1. JUTLAND COASTAL WATER

The especially nutrient rich Jutland Coastal Water (JCW) originates from the German Bight and is influenced by fresh-water from the continental rivers being gradually mixed with relatively nutrient poor Southern North Sea Water (SNSW) on its way northward [11]. At the entrance to Skagerrak the JCW must "compete" with other water masses possible present in the area, and the result is often that there is no inflow of this water. When there is an inflow it is most often located close to the shore.

In [32] a strong correlation between wind direction and the pulsation of the JCW was found during SKAGEX. In the new simulations the relationship between the windstress and the transport through a section going from Tyborøn ($56.7\,^oN$,$8.1\,^oW$) on the Danish coast and 90 kilometers west, has been studied. In Figure 3 results from two years (1987/88 and 1991/92) of simulations are presented. The pulsative transport through this section seems to be strongly wind driven. In periods with winds towards south, the transport is

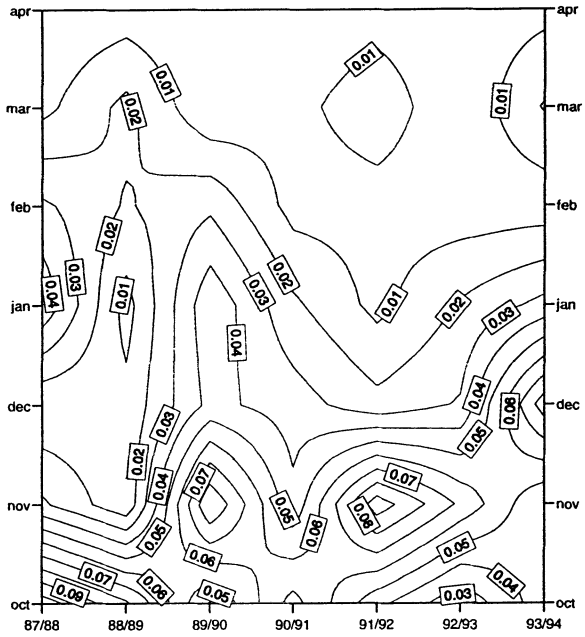


Figure 4. Monthly mean transport in Sverdrup of GBW through the Tyborøn section

blocked, while the strength of the transport northwards shows the same pattern as the north component of the wind stress.

This indicates that under periods with winds from the south, pulses of nutrient rich water are transported into Skagerrak, causing great geographical variability in the nutrient conditions. These changes often take place in a time scale of a few days.

The high nutrient values in the JCW, are mainly linked to low saline water. A new variable, German Bight Water (GBW), was included in the model. On the southern boundary of the fine-scale model, all water was labeled according to modeled salinity under the assumption that this will characterize the amount of water originating from the German Bight.

$$GBW = \begin{cases} 100 & S \leq 31 \\ \frac{100}{3.5}(34.5 - S) & 31 < S \leq 34.5 \\ 0 & S > 34.5 \end{cases}$$

From this southern boundary GBW was transported and diluted as a passive tracer by the modeled circulation (there are no further backcoupling between modeled salinity and GBW).

Focusing on the way the GBW is implemented, 1 litre of fresh water can mix with approximately 9 litres of 34.5 psu water, giving 10 litres of 31 psu GBW water. In this way a run off of $1000 m^3 s^{-1}$ should equal .01 Sv of GBW.

In Figure 4 the modeled monthly mean transports of GBW into Skagerrak (section Tyborøn) are shown. The transport shows a clear seasonal cycle with the highest transports

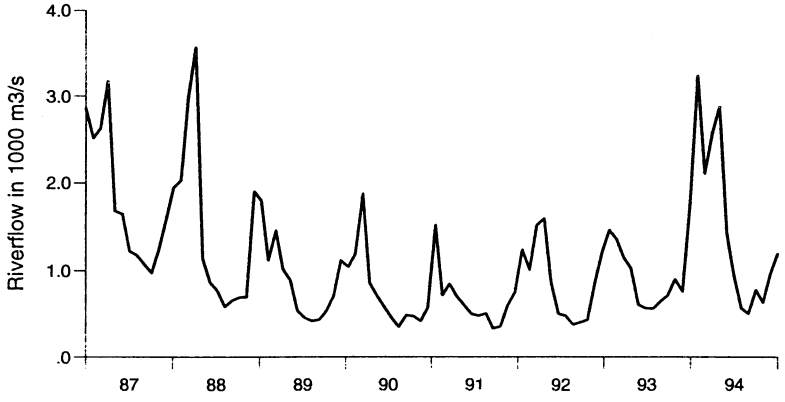


Figure 5. Monthly mean freshwater flow from German rivers Elbe, Ems and Weser

in the fall and nearly no inflow in March and April. At least two factors will influence this variability. The first one is the wind direction, which triggers the JCW, and thereby also the transport of GBW into Skagerrak, and the second one is the amount of freshwater in the system which will increase the concentration of GBW.

A comparison with the total transport in Figure 3 shows some agreement in the first half of the period. Compared to 1991/92, 1987/88 has a general high transport in January and February, and this is also the case for GBW in Figure 4. The opposite situation takes place in December, when the 1991/92 transport is significantly higher.

In Figure 5, the monthly mean freshwater run off for Elbe, Ems and Weser are given. Two years have a large runoff, 1987/88 and 1993/94. The first year has a high flow in the whole model period, while the second has a flood starting in January. For the other years, the annual cycles are much weaker. These variations in the river flow are not clearly seen in the flow of GBW through the Tyborøn section. This indicates that the transportation of water from the German rivers to the Skagerrak is wind driven. The German Bight and west coast of Denmark seems to be a storage area for the river water, which during southerly wind events, are let to flow north and into the Skagerrak.

The dependency of the river run off is also seen in Figure 6, where the comulative transport of GBW for 1987/88 (high run off) and 1991/92 (low run off) are given. The value for 1987/88 is more than 20 % higher than in 1991/92 [1]. This indicates that in the long run the modeled amount of GBW transported northward along the Danish coast is correlated with the German river flow. Such a comparison can be done for all years with a similar result, except for 1989/90 (moderate run off) when the comulative transport is slightly higher than that in 1987/88. From Figure 4 this year gives high transports of GBW from October until February. Investigating the wind field shows strong winds from south west in both January and February, and the comulative *total* transport through this section during the spring has its maximum value this year. In the spring of 1990 the highest salinity values ever were found in the North Sea [14, 17], and other simulations

[1] An extra fresh water flow of 1000 $m^3 s^{-1}$ in seven months, gives approximately $0.2 \times 10^{12} m^3$ of GBW

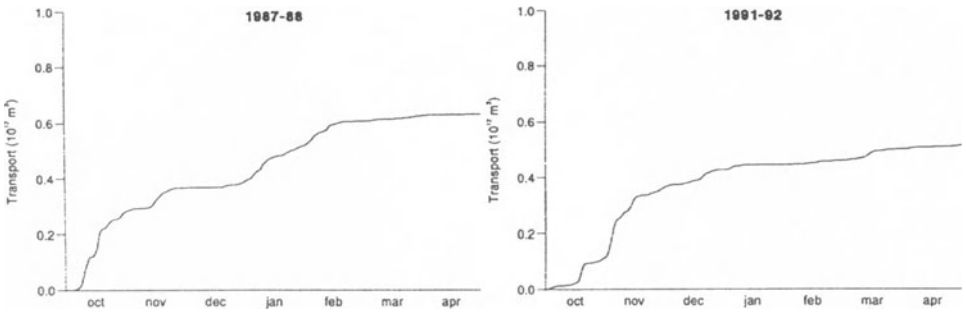


Figure 6. Comulative transport of German Bight water through the Tyborøn section

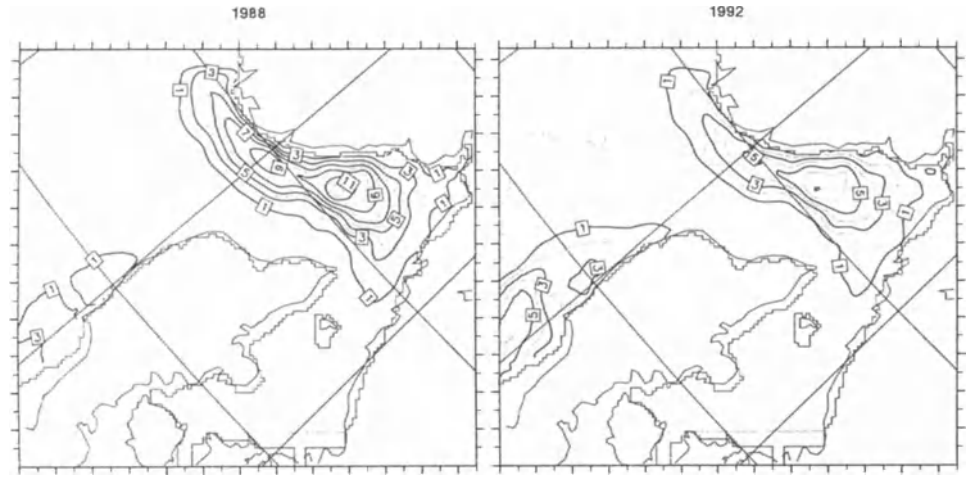


Figure 7. Averaged distribution of GBW (m^3/m^2) April 15-30 in 1988 (left) and 1992 (right)

(Svendsen, pers comm.) shows very high Atlantic inflow to the North Sea this year. The reason for the the high transport in 1990 might therefore be found outside the area.

3.2. NITRATE FROM THE GERMAN BIGHT

Assuming a concentration of total nitrogen (organic and inorganic) of $40\mu M$ (Aure, pers comm.), this transport from the German Bight to the Skagerrak can be estimated. With a total transport of $0.5 \times 10^{12} m^3$ in the seven months period this equals 280 kilo Tons (kT) of nitrogen. Knowing that the main part of this takes place during fall and winter, this agrees quite well with other estimates of the *annual* transport of 250 kT [31] and 400 kT [28].

By following the signal of the different pulses of GBW through various sections inside Skagerrak, the estimated time for the surface water to pass through and leave the area is

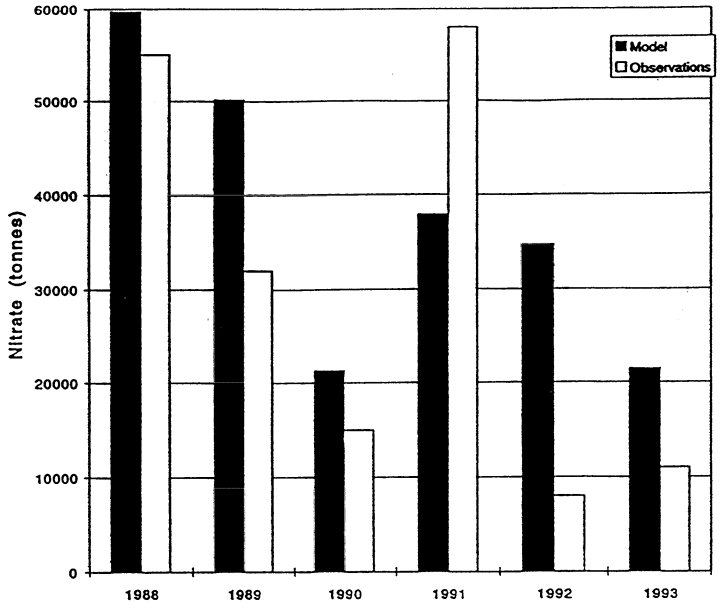


Figure 8. A comparison of modeled and measured nitrate from the German Bight

2-3 weeks. This means that only nitrate entering Skagerrak from the beginning of February will be available for primary production. From Figure 6 this amount is about $0.1 \times 10^{12} m^3$ of GBW. By distributing this nitrogen equally in the whole of Skagerrak and assuming an intercellular $C : N$ relationship of six, this gives a new production of approximately $10 gCm^{-2}$.

In Figure 7 the modeled averaged distribution of GBW in the second half of April 1988 and 1992 are given. The unit are m^3/m^2, which equals the integrated depth of 100 % GBW in each water column. As expected the values are higher in 1988, but it is interesting to notice the high values along the Danish coast in 1992 caused by the high inflow of GBW in March 1992 (see Figure 4). The Institute of Marine Research has surveyed nitrate concentrations in Skagerrak in the second half of April all years since 1988. From these data it is possible to give an estimate of the amount of nitrate originating from the German Bight [6]. By assuming a nitrate concentration of the modeled field fixed to $40 \mu M$, a comparison of modeled and estimated amounts of GBW are given in Figure 8.

The interannual variability in modeled and measured nitrate gives a reasonable agreement in both relative and absolute values. Note that the GBW is not very well defined from available parameters in nature (Aure, pers.comm), and that the measurements are based on instantaneous values. The modeled estimates are a two weeks average, and it is assumed that the nitrate concentration in German Bight water are constant. The timing of the spring bloom also represents an uncertainty.

It is interesting to note the maximum values of GBW in the spring of 1988. Within the last decade an increasing number of harmful flagellate blooms have been reported in coastal areas in the southern part of the North Sea. This trend culminated in the spring of 1988 with the *Chrysochromulina polylepis* bloom [1, 18, 29]. Eutrophication has been

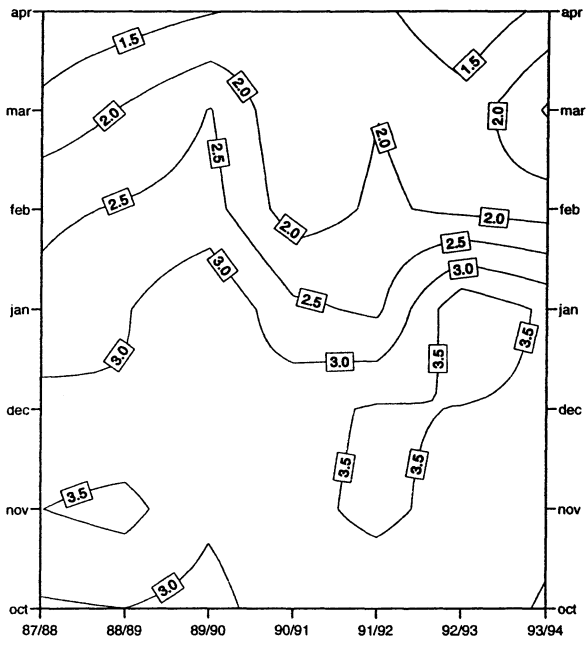


Figure 9. Monthly mean transport in Sverdrup to Skagerrak through the Hanstholm - Kristiansand section

focused as causal mechanism of these blooms, although to what extent this might have contributed remains unclear.

3.3. MEAN VOLUME TRANSPORT

The total volume transport to Skagerrak has also been studied. In Figure 9 the modeled monthly mean volume transport into Skagerrak through a section going from Hanstholm (Denmark) to Kristiansand (Norway) is given

The transport shows a clear seasonal pattern going from more than 3 Sverdrup in November and December to less than 1.5 Sverdrup in April. Recirculation is known to take place in the area, but this is small compared to the total transport. The interannual variability seems moderate, but it is worth noticing that once again the spring of 1990 has the highest transport values. In [32] the model system proved to give realistic transport estimates in accordance with ADCP measurements during SKAGEX. In this period (May/June 1990) an average transport of 1.2 Sv was found, a number that also agrees quite well with what is believed to be the mean transport from the North Sea to Skagerrak (0.5-1 Sv) [25, 34].

In this respect, the new model estimates during winter seems much too high. Nevertheless, Svansson [34] refers to geostrophic measurements based on surface currents in calm weather, and Rodhe [25] has calculated the mean transient barotrophic outflow from 9 velocity observations at 8 cross section stations to be 0.5 Sv.

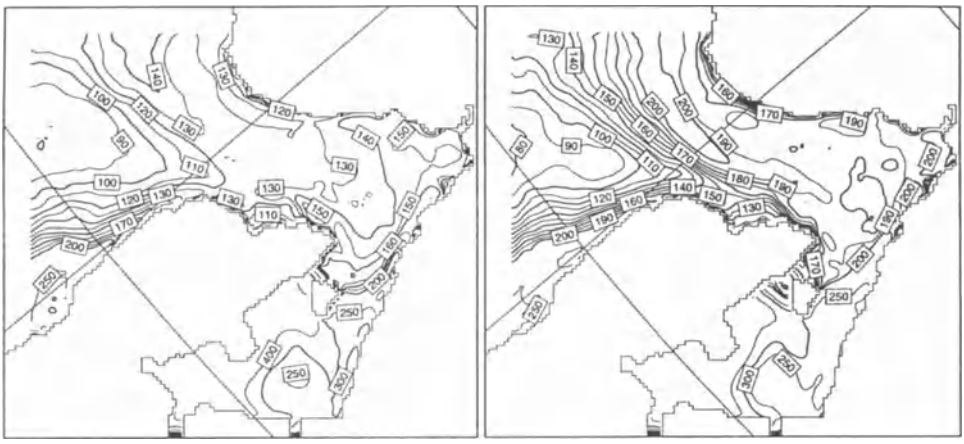


Figure 10. Total production (gCm^{-2}) (February 1 - November 1) for 1988 (left) and 1993 (right)

Furnes & Sælen [15] report on the transport by the same method at the eastern side of the Norwegian Trench at the sill of the Skagerrak in a 1.5 months period in the spring of 1976. They report on the net mean northward flow of 1 Sv, but the transport varies in an interval from -0.5 to +3.0 Sv. Some calculations by Rodhe [25] from a part of his section in the same period, shows that there seems to be no significant difference in amplitude or phase between the two sections. These estimates give another indication that the proposed 0.5-1 Sv mean transport might be an underestimate.

Aure and Sætre [7] estimates the outflow in January - March 1979 to be 0.5 Sv in the *upper* layer, while Gammelsrød and Hackett [16] calculates the transport to 0.4 Sv (May-75) and 1.1 Sv (Nov-77) by assuming geostrophy and using an inverse method.

Rodhe also calculates the standard deviation of the transport pr. unit width, m^2/s, which most places are higher than the absolute value of the same transport. This indicates large uncertainties in his estimate. Since in addition Svansson doesn't take into account the important wind effects we postulate that the winter transport from the North Sea to Skagerrak is higher than the previous believed 0.5-1 Sv, and that the transport has a clear seasonal cycle.

3.4. PRIMARY PRODUCTION

Finally NORWECOM (included the biological module) has been run for two selected years (1988 and 1993) to investigate the primary production. To get a full annual cycle of the production the fine grid model was initiated on February 1, and ran until November 1, while the coarse model was given an extra 2 months of spin up. The total production for the two years are given in Figure 10.

There are great differences between the two years, with a mean production in central Skagerrak of approximately $180gCm^{-2}$ in 1993 and $130gCm^{-2}$ in 1988. The 40 % increased production is seen both for diatoms and flagellates. From the figure it seems like this difference is caused by a high production in the Atlantic inflow, while the production in

the JCW is almost unchanged these two years. In Figure 8 both model and data showed the highest values for GBW in Skagerrak in 1988, while 1993 gave very low values. This also agreed with the comulative total transport and the transport of GBW through the Tyborøn section in the spring months, that gave much higher values in 1988.

To explain the big differences in the modeled production, the Atlantic inflow therefore has to be further investigated. Focusing on the total inflow of water with salinity higher than 35 psu. through the Kristiansand - Hanstholm section, the integrated transport from March 1 to November 1 is a factor two higher in 1993 than in 1988. Limiting the same transport to the upper 50 meters, there is a factor three in difference. Adding that the comulative transport of the total water masses through this section shows very small differences between the two years, we conclude that the inflow in 1993 was dominated by nutrient rich Atlantic water, while the inflow in 1988 had a larger fraction of water with Central and Southern North Sea origin.

Finally, the model has been used to estimate the inflow of nitrate to the Skagerrak in the two years. The total inflow in 1988 (March 1 to November 1) were approximately 4800 kT (2100 kT in upper 50 meters), and almost 30 % higher (also if limited to upper 50 meters) in 1993. As a comparison, the modeled transport of nitrate through the Tyborøn section is found to be 370 kT in 1988 and 250 kT in 1993.

4. Conclusion

The NORWECOM model system has in earlier works [35, 32] proven to give realistic transport estimates and to reproduce short term variabilities during SKAGEX. Based on these experiences, the same model should also be able to give new insight in the identification and quantification of longterm variabilities in the transports to the Skagerrak.

The present study indicates that the Jutland Coastal Water is wind driven, and that during southerly wind events this water is transported into the Skagerrak. Labeling this water with respect to salinity, the model shows a clear seasonal cycle in the transport of water with origin in the German Bight, a transport that is also correlated with the river run off. The interannual variability in this transport gives a reasonable agreement with measurements from late April.

The total transport from the North Sea to Skagerrak shows a clear seasonal cycle varying from more than 3 Sverdrup in winter to 1 Sverdrup in summer. The winter values are somewhat higher than what is believed to be the mean transport to Skagerrak, but other transport estimates are either from calm weather periods, or measurements of barotrophic flow only. This study estimates the total volume transport, and also includes short term variabilities in the estimates. The wind generated short term variations are believed to be of the same magnitude as the transport, and no previous estimates of the magnitude of the seasonal variations exists [5].

The model also gives indications of large year to year variations of the primary production in Skagerrak. Variability in the inflow of Atlantic water, rather than freshwater discharge, seems to be the main reason for this.

The present model represents a tool for getting new insight in the complex dynamics between physics and biology in nature. However, limitations have to be taken into consideration when interpreting the results. There are no zooplankton eating the algae, and no "particle" bottom settlement and resuspension routines are incorporated in the model. Neither are there at present routines for regeneration of silicate. A very clear limitation

is also the lack of realistic light attenuation due to riverine inputs of gelbstoff, suspended particulate matter and resuspended sediments.

Clearly the horizontal resolution is a limiting factor with respect to correct simulation of, for example, near-shore and mesoscale processes. The model does not incorporate *real* surface heat fluxes, surface irradiance and surface freshwater fluxes. A clear limitation in the investigation of interannual variability is also the use of monthly climatological fields around the open boundaries. Except for variations in the river run-off, the model is therefore reporting on the variability in the wind-driven circulation.

Large supplies of freshwater has a great impact on the Skagerrak circulation. The Baltic outflow contributes considerably to this discharge, and a prescribed climatological fresh water run off to the Baltic is therefore an oversimplification. A more or less constant salinity of the Baltic outflow might also contribute to bias of model results. For this reason the transport from Kattegat to Skagerrak has not been discussed in this paper. Inclusion of data for the water level and the salinity in the Baltic is necessary for a reliable discussion of the interannual variability of this transport.

References

1. D.L. Aksnes, J. Aure, G.K. Furnes, H.R. Skjoldal, and R. Sætre. Analysis of the Chrysochromulina Polyepis Bloom in the Skagerrak, May 1988, Environmental Conditions and Possible Causes. Technical Report 1, Bergen Scientific Centre, 1989.
2. D.L. Aksnes, K.B. Ulvestad, B. Baliño, J. Berntsen, J. Egge, and E. Svendsen. Ecological modelling in coastal waters : Towards predictive physical-chemical-biological simulation models. *Ophelia*, 41:5–36, 1995.
3. Anon. Solar radiation and radiation balance data, 1990, 1991. The world radiation data centre.
4. Anon. North sea quality status report, 1993. North Sea Task Force.
5. Anon. North Sea Subregion 8, Asessment report. State Pollution Control Authority, Oslo, Norway, 1993. ISBN 82-7655-157-2.
6. Jan Aure, Didrik Danielssen, and Einar Svendsen. The impact of Southern North Sea water on the nutrient conditions in the Skagerrak in late spring 1988-1994, 1995. Symposium on Changes in the North Sea Ecosystem and their causes : Århus 1975 revisited. Poster CNS No. 52.
7. Jan Aure and Roald Sætre. Wind effects on the Skagerrak outflow. In R. Sætre and M. Mork, editors, *The Norwegian Coastal Current, vol.1*, pages 263–293, 1981.
8. Beatriz M. Baliño. Nutrient inputs to the North Sea, Skagerrak and Kattegat. River concentrations and loads from 1980- to 1990. Technical report, HOV-senteret, Høyteknologisenteret, Bergen, Norway, 1993.
9. Michael D. Cox and Kirk Bryan. A numerical model of the ventilated thermocline. *J. of Physical Oceanography*, 14:674–687, 1984.
10. D. S. Danielssen, L. Edler, S. Fonselius, L. Hernroth, M. Ostrowski, E. Svendsen, and L. Talpsepp. Oceanographic variability in Skagerrak/Northern Kattegat, May-June 1990, 1995. Submitted to the ICES Journal of Marine Science.
11. D.S. Danielssen, L. Davidsson, L. Edler, E. Fogelqvist, S. Fonselius, L. Føyn, L. Hernroth, B. Håkanson, I. Olsson, and E. Svendsen. SKAGEX: Some preliminary results, 1991. ICES C.M.1991/C:2.
12. Bjørn Egenberg. The relationship between hydrographical variability in coastal water and meteorological and hydrological parameters. Master's thesis, Geophysical Institute, University of Bergen, Norway, 1993. In Norwegian.
13. L.I. Eide, M. Reistad, and J. Guddal. Database av beregnede vind og bølgeparametre for Nordsjøen, Norskehavet og Barentshavet, 1985. DNMI report.
14. D.J. Ellett and R. Turrell. Increased salinity levels in the NE Atlantic, 1992. ICES C.M.1992/C:20.
15. G. Furnes and O.H. Sælen. Current and hydrography in the Norwegian Coastal Current off Utsira during JONSDAP 76. Technical Report Norwegian Coastal Preoject, Rep. 2/77, Univ. of Bergen, Norway, 1977.
16. Tor Gammelsrød and Bruce Hackett. The circulation of the Skagerrak determined by inverse methods. In R. Sætre and M. Mork, editors, *The Norwegian Coastal Current, vol.1*, pages 311–330, 1981.
17. M. Heath, E. Henderson, G. Slesser, and E. Woodward. High salinity in the North Sea. *Nature*,

352:116, 1991.
18. S.E. Maestrini and E. Graneli. Environmental Conditions and Ecophysiological mechanisms which led to the 1988 Chrysochromulina polylepis bloom and hypothesis. *Oceanologica Acta*, 14(4), 1991.
19. E.A. Martinsen and H. Engedahl. Implementation and testing of a lateral boundary scheme as an open boundary condition in a barotropic ocean model. *Coastal Engineering*, 11:603–627, 1987.
20. Eivind A. Martinsen, Harald Engedahl, Geir Ottersen, Bjørn Ådlandsvik, Harald Loeng, and Beatriz Balino. MetOcean MOdeling Project, Climatological and hydrographical data for hindcast of ocean currents. Technical Report 100, The Norwegian Meteorological Institute, 1992.
21. Lie-Yauw Oey and Ping Chen. A model simulation of circulation in the North-East Atlantic shelves and seas. Contribution No. 6 of the Stevens Institute of Technology Ocean Modeling group, January 1991.
22. Marek Ostrowski. The SKAGEX Atlas. A User's Guide. Technical Report TemaNord 1994:635, Nordic Council of Ministers, 1994.
23. Geir Ottersen. MODgrid, a Model Oriented Data grider. Technical Report 6/1991, Havforskningsinstituttet, 1991.
24. M. Reistad and K.A. Iden. Updating, correction and evaluation of a hindcast data base of air pressure, winds and waves for the north sea, norwegian sea and the barents sea. Technical Report 9, Det Norske Meteorologiske Institutt, 1995.
25. Johan Rodhe. The large-scale circulation in the Skagerrak; interpratation of some observations. *Tellus*, 39A:245–253, 1987.
26. Arvid Skartveit and Jan Asle Olseth. Modelling slope irradiance at high lattitudes. *Solar Energy*, 36(4):333–344, 1986.
27. Arvid Skartveit and Jan Asle Olseth. A model for the diffuse fraction of hourly global radiation. *Solar Energy*, 37:271–274, 1987.
28. Hein Rune Skjoldal. Eutrophication and Algal growth in the North Sea. In Norberto F.R. Della Croce, editor, *Symposium Mediterranean Seas 2000*, pages 445–478. Universita di Genova, 1993.
29. H.R. Skjoldal and I. Dundas. The chrysochromulina polylepis bloom in the Skagerrak and the Kattegat in May - June 1988 : Environmental conditions, possible causes and effects. Technical Report ICES cooperative research report 175, International Council for the exploration of the Sea, Copenhagen, Denmark, 1991.
30. Morten D. Skogen. A user's guide to NORWECOM, the NORWegian ECOlogical Model system. Technical Report 6, Institute of Marine Research, Division of Marine Environment, Pb.1870, N-5024 Bergen, 1993.
31. Morten D. Skogen, Einar Svendsen, Jarle Berntsen, Dag Aksnes, and Kåre B. Ulvestad. Modelling the primary production in the North Sea using a coupled 3 dimensional Physical Chemical Biological Ocean model. *Estuarine, Coastal and Shelf Science*, 41:545–565, 1995.
32. Morten D. Skogen, Einar Svendsen, and Marek Ostrowski. Quantifying volume and nutrient transports and primary production with the NORWegian ECOlogical Model system (NORWECOM), 1995. Submitted.
33. Anders Stigebrandt. Barotropic and baroclinic response of a semi-enclosed basin to barotropic forcing of the sea. In H.J. Freeland, D.M. Farmer, and C.D. Levings, editors, *Proceeding of the NATO Conference on Fjord Oceanography*. Plenum Press, New York, 1980.
34. Artur Svansson. Physical and chemical oceanography of the Skagerrak and the Kattegat. Technical Report 1, Fishery Board of Sweden, Inst. of Marine Res., 1975.
35. E. Svendsen, J. Berntsen, M.D. Skogen, B. Ådlandsvik, and E. Martinsen. Model simulation of the Skagerrak circulation and hydrography during SKAGEX, 1996. In press, J.of Mar.Syst.

EDDY DYNAMICS CONTROLLED BY BASIN SCALE, COASTLINE AND TOPOGRAPHY

N. H. RACHEV and E. V. STANEV
Department of Meteorology and Geophysics,
University of Sofia,
5 James Bourchier street, 1126, Sofia, Bulgaria

Abstract

The paper addresses the physical mechanisms of eddy variability in the Black Sea and is based on analyses of simulation data. The model, used as a research tool, is the Bryan-Semtner-Cox model with 11 km horizontal resolution, forced by annual mean data. The study focuses on the basin oscillations, meanders, eddy formation and dissipation. Sub-basin scale eddies are spontaneously formed and propagate to the west. The dissipation is extremely strong in the western basin, where eddies slow down and their scales decrease. Simplistic models, corresponding to the Black Sea conditions, demonstrate the impact of different physical processes, basin shape, and forcing for the formation of the circulation. The bottom topography control has an utmost importance for enhancing baroclinic oscillations with interannual time periods. Model simulated phenomenology, time and length scales are compared against observations.

1. Introduction

The coastal and semi-enclosed seas present challenging test areas to study oceanographic phenomena, which are dominated by coastline (orientation, shape) and topography (shelf, continental slope). The relative impact of these factors increases moving from the open ocean to the coast. It was previously shown by Rachev and Stanev (1996, hereafter RS) that the well known turbulent cascade in some seas (e. g. the Black Sea) is affected by their small scales, and the eddy variability is dominated by the basin-scale baroclinic oscillations. This interesting dynamics could become dominant if the basin scales are of the order of the Rossby radius of deformation. This is perhaps the case in other semi-enclosed seas as the North Sea, the Baltic Sea, and the Mediterranean Sea. The last has a very complicated coastline and large diversity of basin scales, topographic and strait control.

E. Özsoy and A. Mikaelyan (eds.), Sensitivity to Change: Black Sea, Baltic Sea and North Sea, 341–364.
© 1997 *Kluwer Academic Publishers.*

The relative impact of the regional factors on the eddy processes still presents an open question. We see a gap between the theoretical studies, dealing with basin-scale oscillations (most of them focusing on the barotropic oscillations), and the increasing number of observational findings in the Black Sea (Oguz *et al.*, 1993, 1994; Sur *et al.*, 1994) waiting for profound theoretical explanations. The numerical modeling presents an effective tool to address issues such as: (1) How do the scales of the ocean affect the eddy processes if they become comparable with the Rossby radius of deformation. (2) How relevant are the dynamics simulated in simplistic models to those observed in real basins. (3) How does the regional topography control the dynamics and the transition between different quasistable states in the circulation.

We analyze in the present study some simulated characteristics of the baroclinic oscillations in the Black Sea. Basin-type oscillations with periods of about 0.5 year have been previously found by RS, whereas longer period ones (period of about 2 years, found in the present study) are a result of the adjustment of the eddy dominated circulation to the wind forcing. These different oscillations correspond to two different circulation regimes. The first one (known from the work of RS) is dominated by eddies. The second one is dominated by basin wide cyclonic gyre. There is a periodic trend of the gyre-type circulation to break into smaller eddies, when the currents become unstable, followed by a readjustment of the model to the forcing (see also Stanev and Staneva, 1996).

The paper includes description of the model and formulation of the model experiments (section 2), analysis on the simulation results in basins with idealized and realistic coasts and topographies (section 3), followed by conclusions.

2. Description of the model, parameters and experiments

The model is based on the well known primitive equation numerical model of Bryan (1969) in the version documented by Cox (1984). Its application to studying the Black Sea eddy variability is discussed in RS. Therefore the model description is kept rather short here, referring to the above publications. The density is used as a thermodynamic variable. As in the standard Cox (1984) code, the lateral boundaries are insulating and nonslip, and the bottom is taken to be insulating and free slip. The model assumes the following boundary conditions at z=0:

$$\rho_0 A_v V_{hz} = \tau, \tag{1}$$

$$K_w \rho_z = \eta(\rho^* - \rho)\, \Delta z, \tag{2}$$

where V is the velocity vector, V_h-its horizontal component, ρ is the density, τ is the wind stress vector, ρ^* is the climatological density, η is an inverse time scale, the subscript $(_z)$ denotes differentiation in the vertical, and Δz is the thickness of the first model layer. The numerical algorithms are documented by Bryan (1969) and Cox (1984).

The model resolution is $1/10^0$ in the latitude and $1/6^0$ in the longitude, giving almost square grid elements with grid size of about 11 km. The mixing and diffusion in the horizontal are parameterized with biharmonic operators, with coefficients of turbulent diffusion for momentum and density A_h=0.1 10^{19} cm^4 s^{-1} and K_h=0.4 10^{19} cm^4 s^{-1}, respectively (see also Cox, 1985; Holland, 1989; Böning and Budich, 1992; RS), which are just sufficient to prevent noise. The vertical mixing coefficient A_v =1.5 cm^2 s^{-1} and the vertical diffusion coefficient K_v=0.1 cm^2 s^{-1} are chosen small enough not to create unrealistically strong mixing in the deep layers.

We carry out two types of experiments, which show to what extent the basin shape, coast, topography and driving forces dominate the circulation. The common feature between all experiments is that the zonal extension of the basins is the same, specified as 1150 km, which is equal to the zonal extension of the Black Sea. The experiments discussed in the paper are listed in Table 1, where IC and RC refer to Idealized and Real Coast, respectively. In the IC-type of experiments, the basin is rectangular, with latitudinal extension in the first experiment (IC1) equal to the latitudinal extension of the Black Sea, that is 630 km. This basin is resolved by 88x58 points with the horizontal resolution, specified above. In the second idealized experiment (IC2), the basin is twice wider (1270 km).

Table 1. Model experiments

Experiment	Coastline	Vertical resolution	Max. depth (m)	Area (10^5 m^2)	Volume (10^5 m^3)	Wind forcing	$(We+Wi)/(De+Di)$
IC1	idealized	coarse	1540	7.158	7.764	Eq. (3)	2.6
IC2	"	"	1540	14.316	15.528	Eq. (5)	2.4
RCFA1(WR91)	real	"	1540	3.921	4.266	R91	2.6
RCFA	"	fine	1640	3.921	4.444	R91	2.8
RCRA	"	"	2250	3.921	5.249	R91	3.7

Notations and abbreviations: **IC** - **I**dealized **C**oastal line, **RC** - **R**ealistic **C**oastal line, **FA** - **F**lat **A**byssal, **RA** - **R**ealistic **A**byssal, **R91** - Annual mean wind stress from **R**achev *et al.* (1991), W_e, W_i, D_e, D_i - see Equations (7).

We retain some important Black Sea topographic features in the idealized basins, such as the wide shelf and the continental slope. We specify the shelf as a slightly slopped plane along the western coast only. The narrow continental slope in the real basin is specified as a narrow model continental slope along the northern, southern and eastern coasts. The continental slope is wider in the western part of the Black Sea, thus the width of the model continental slope there is 250 km. The model representation of the bottom slope in the IC1 and IC2 experiments is given in Figure 1a.

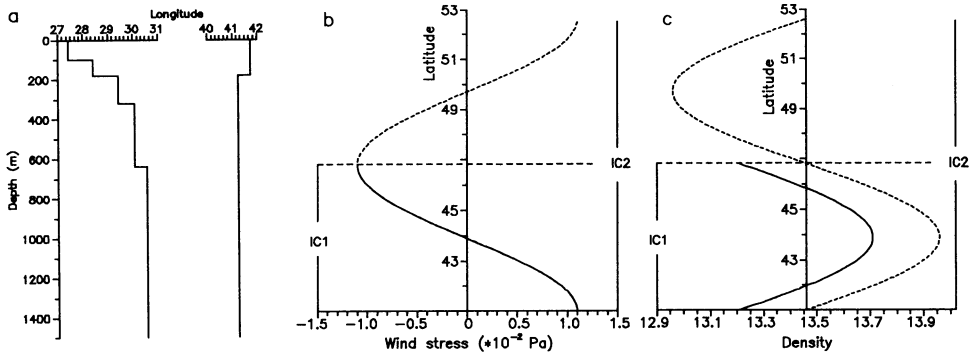


Figure 1. Zonal shape of topography and meridional shape of forcing functions in the experiments with idealized coastal line. (a) Topography pattern in the IC1 and in the IC2 experiments (left - about the western coast, right - in the remaining coastal area). The extension of the shelf from the coast can be seen in Figure 3b. (b) Wind stress pattern in the IC1 and in the IC2 experiments. The wind stress amplitude is 0.022 Pa. (c) Sea surface density in the IC1 (solid line) and in the IC2 (dash line) experiments

We specify idealistic (but consistent with the observations) model forcing. The wind stress over the Black Sea is cyclonic, with a mean curl of 6.8 10^{-8} Pa m^{-1} (Rachev *et al.*, 1991; Staneva and Stanev, in the present volume). We substitute in the model this real forcing by zonal wind stress,

$$\tau(y) = \tau_0 \cos(\pi y/L_y), \tag{3}$$

where τ_0 =0.011 Pa, and L_y is the meridional extension of the basin (Figure 1b). The maximum of *curl* (τ) is 5.4x10^{-8} Pa m^{-1}.

It is more difficult to specify a simplified buoyancy forcing, since the heat and fresh water fluxes for the Black Sea are not well known (Staneva and Stanev, 1996). Therefore, we use relaxation boundary condition (2) in the equation for the water density. It is known from the observations, that the density increases in the interior Black Sea due to upwelling. To take this into account, we specify the meridional distribution of sea surface density as:

$$\sigma_t(y) = \sigma_{t0} + \sigma_{t1}(\sin \pi y/L_y - 0.5), \tag{4}$$

where σ_{t0} =13.46 is the horizontally averaged sea surface climatological density, and σ_{t1} =0.5. This simplified forcing is shown in Figure 1c. We keep the relaxation constant equal to 1/10 days in all experiments, which is adequate to the Black Sea conditions, as shown by the sensitivity experiments, carried out by RS. This ensures that the simulated mass field is dominated by the internal dynamics.

The model forcing in the IC2 experiment is formulated in a similar simplistic way. Our motivation now is to "give the eddies more freedom to propagate", keeping

in the same time forcing patterns similar to the ones in the IC1 experiment. Thus, the wind forcing is prescribed as:

$$\tau(y) = \tau_0 cos\,(2\,\pi\, y/L_y), \tag{5}$$

and the sea surface density as:

$$\sigma_t(y) = \sigma_{t0} + \sigma_{t1}\, sin\,(2\,\pi\, y/L_y). \tag{6}$$

These forcing functions are shown in Figure 1b and Figure 1c.

Our model forcing is similar to the one of Holland and Lin (1975a, 1975b). They used zonal wind stress, which varied with the latitude in a simple sinusoidal way, but their single and double gyre wind patterns were reversed to 180^0, compared to our wind stress (see equations 3 and 5, and also Figure 1b). It is noteworthy that their wind stress has a magnitude, which is nine times stronger (τ_0 = 0.1 Pa). Further in the text we will refer again to this work, illustrating the similarities and the differences between the model responses. Now, we will introduce the second type of experiments, the ones with Realistic Coastal line (the first two initials in the model nomenclature is RC, see Table 1). The first of these models has very coarse vertical resolution of 6 levels and its dynamics is analyzed in RS, where its specification was WR91. In this model, we enable intense eddy processes by limiting the depth in the abyssal area to 1540 m. We do this simplification purposely, since using the realistic abyssal plane results in less intense circulation, than what is usually observed in this sea. The alternative is to increase the strength of the forcing. This is practically the case in the real sea, where the seasonal variability and the variability due to the synoptic processes in the atmosphere provides enough energy to develop intense eddy dynamics, as shown by the comparison of the recent satellite altimetry data (Kantha and Drexler, 1996) and the model simulations, forced by twice daily atmospheric analysis data (Stanev and Staneva, in the present volume). We will show in the present paper that the driving versus the damping ratio is strongly dependent on the damping in the deep layers. The different physical balances, resulting from the different model representation of the basin shape and topography are illustrated in Table 1, where we show the ratio between the work done by wind versus the dissipation. These different dynamics result in different types of simulated variability. Therefore we will consider another two experiments, in which the principal difference is the description of the bottom in the deep ocean. The first model basin with realistic coast has **F**lat **A**byssal (RC**FA**), limited to 1640 m. The second one has **R**ealistic **A**byssal (RC**RA**). The thickness of each of the first four levels is 5 m, of the following 7 levels 10 m, and it constantly increases in the deep layers as follows: 30, 40, 50, 60, 80, 100, 130, 170, 240, 310, 340, 360 and 250 m. As shown by RS, very coarse vertical resolution of 6 layers only (RCFA1, see Table 1) do not give principal deviations from the simulations carried out with higher resolution (RCFA). Therefore, the difference between the simulations in the RCRA and the RCFA, RCFA1 experiments is mainly due to the description of the shelf area and the bottom relief in the deep sea.

We force the RCRA and the RCFA experiments with the annual mean wind stress of Rachev *et al.* (1991). The density at the sea surface is relaxed to the annual mean sea surface density. To save place, we do not show the forcing functions, but recommend to the interested reader the work of RS. The relaxation parameter has the same value as in the experiments with idealized coasts. All experiments are initialized with the density stratification, which corresponds to the Black Sea conditions. The volumes and the areas of the model basins are shown in Table 1. The different intensity of the circulation in the RCRA and RCFA experiments could be due to the differences between the volumes and depths of the basins, when the same forcing functions are prescribed at the sea surface.

If we take for the depth of the main pycnocline the value of 400 m, we obtain for the Rossby radius of deformation $L_r=NH/f$ the value of 30 km. Here N is the Väisälä frequency, H is the depth of the pycnocline, f is the Coriolis parameter. This number could vary about 4%, depending on the regional stratification. The value of L_r for the ocean is about 50 km.

We give below the magnitudes of some other physically important numbers. For the mean Black Sea latitude of 43^0 (f=9.92 10^{-5} s^{-1}, and β = 1.66 10^{-11} m^{-1} s^{-1}), the barotropic radius of deformation $L_e=(gH)^{1/2}/f$ is 1200 km, which is comparable to the length of the large axis of this sea. Taking for the mean ocean velocity the value of 10 cm s^{-1} and β=2 10^{-11} m^{-1} s^{-1}, we estimate for the scale $L_\beta=(2U/\beta)^{1/2}$ (which corresponds to the parameter of nonlinearity $\delta = 2\ U/(\beta\ L) = 1$) the value of 100 km. This parameter determines the length scale $\pi\ L_\beta$, at which transition between eddies and waves occurs. An interesting peculiarity in the model simulated circulation in the Black Sea is that the mean velocities simulated in the model are smaller than in the ocean, giving for L_β the value of 82 km (πL_β=260 km) in the RCFA experiment, and about 75 km (πL_β=230 km) in the RCRA experiment. Two important consequences are noteworthy, before starting the description of the model results: (1) the wave-eddy transition in the RCFA experiment occurs at larger scales, which explains the pronounced wave-like patterns of the circulation, previously reported in the work of RS; (2) this transition occurs in the RCRA model at smaller scales, which will less tolerate the increase in the scales of the meanders and eddies. This type of different model behavior is one of the main issues of the paper.

3. Analyses of the model results

3.1. MODELS WITH IDEALIZED COASTLINE

It was shown by RS that eddies are formed in the eastern Black Sea and propagate to the west, increasing their scales, until they reach the basin scales. Similar trend exists in the IC1 and IC2 experiments. The eddies become less constrained by the basin scales in the IC2 experiment. However, this seems not to be the case in the IC1 experiment, as seen from the snapshot of the sea surface currents in Figure 2. The cyclones are elongated in the north-south direction, and are more intense along the

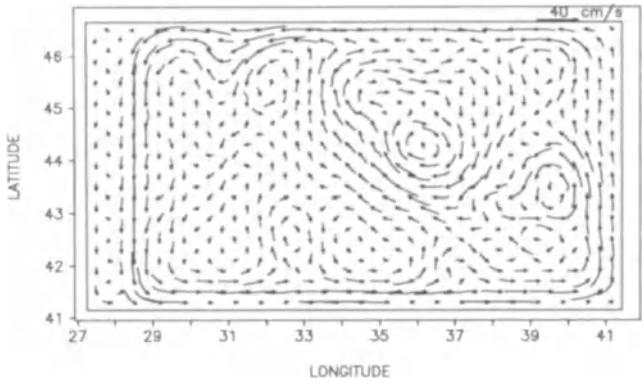


Figure 2. Instantaneous sea surface currents in the IC1 experiment. The scaling arrow in the upper right corner corresponds to 40 cm s^{-1}

southern coast. The anticyclones reach the meridional basin scales and tend to occupy the northern part of the basin. This tendency of differentiation was found earlier in the model with realistic coasts (RS). In the present simulations it is a result of the conservation of potential vorticity, whereas in the work of RS the realistic coastline and the bottom topography dominated the propagation of eddies. The tendency of separation of cyclones and anticyclones has a pronounced impact on the time mean circulation in the model (Figure 3), showing a pronounced north-south asymmetry. We refer here to the work of Holland and Lin (1975a), who studied the circulation in a square basin (1000x1000 km, and two layers in the vertical) forced with similar winds as in Figure 1b. From their model simulations, we could expect that the model would produce one gyre circulation. While this is roughly the case in the surface layer (Figure 3a), the vertically integrated circulation is far from this pattern, mainly due to the reversed currents in the northern part of the model sea (Figure 3b). Though our model basin and the one of Holland are forced in a similar ways, there are large differences, related to the aspect ratio of the basins, different topography and stratification, different impact of the planetary vorticity when the circulation is reversed. All this in combination, results in very different model responses in strongly nonlinear models.

The main gyre at the sea surface encompasses the whole basin, with strongest currents, trapped over the continental slope. They follow the northern, western and southern boundaries, but show more unexpected behavior close to the eastern coast, where a large meander forms. This meander gives rise to the mid basin jet. North and south of the jet, the circulation is dominated by quasipermanent sub-basin scale eddies. The comparison of the circulation pattern with the model forcing (Figure 1b, c), along with the analysis on the magnitudes of the different terms in the momentum equations, shows that the model is far from the Sverdrup balance.

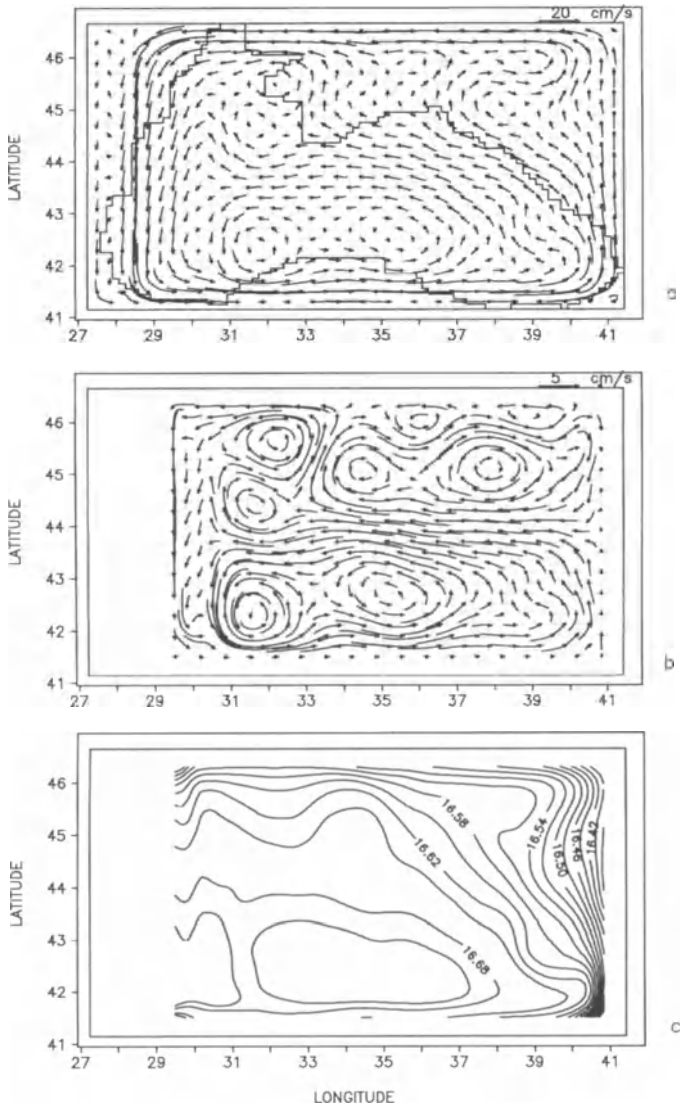


Figure 3. Time mean fields in the IC1 experiment. (a) Sea surface currents. The coastal line of the Black Sea is also plotted. (b) currents at 260 m. (c) density at 260 m, contour interval is 0.02.

The broken line in Figure 3a is the one of the Black Sea coast, used in the RC-models. The comparison of the time mean currents with the ones of RS (see also Figure 6 further in the text) reveals several noteworthy features: (1) There is an amazing correlation between the main gyre simulated in the models with quite

different coasts. (2) The formation of anticyclonic sub-basin scale eddy in the northern part of the basin in the IC-and RC-types of models correlates with the observations in this area. (3) The mid-ocean jet in the IC1 experiment is parallel to the real Black Sea coast. (4) The gyre increases its instability when reaching the eastern coast and turns to the north. These are perhaps the main peculiarities in the Black Sea circulation, which the simplistic model IC1 demonstrates rather well.

A compact anticyclonic gyre is simulated in the deep layers. There are two quasipermanent cyclonic eddies between this gyre and the northern coast (Figure 3b). Unlike the circulation in the northern part of the basin, which shows a reversal with depth, the one in the southern part do not change qualitatively at different levels. The magnitude of the currents decreases 2-3 times between the sea surface and the halocline. Surface currents reach maximum values of 48 cm s^{-1} along the western boundary. The corresponding value at 260 m is 14 cm s^{-1} and is reached along the south-western corner of the model basin.

The density patterns give a good illustration about the vertical motions (Figure 3c). The downwelling in the eastern basin (negative density anomaly) is a model analogue of the downwelling in the area of the Batumi quasipermanent eddy. In this area the model simulates a quasipermanent meander (Figure 3a), after the jet detaches from the coast. The large value of the Eddy Kinetic Energy (EKE), the low value of the Mean Kinetic Energy (MKE), and the large *rms* of the density in the easternmost part of the sea indicate instabilities in the circulation. Similar meandering/instabilities in the real Black Sea could give a trend for the formation of anticyclonic circulation in the area of the Batumi eddy (RS; Stanev and Staneva, in the present volume).

Detailed analyses of the model simulated snapshots show that the coastal jets are dominated by meanders with wavelength of 320 km. Standing waves with about the same length are well pronounced along the southern coast in the time averaged patterns (Figure 3a). The mean phase speed of the westerly propagating oscillations is 8-9 km day^{-1} and the major periodicity occurs at 63 day. The mean kinetic energy is 40 cm^2s^{-2}.

The larger meridional extension of the basin in the IC2 experiment gives the eddies more freedom to freely evolve, as seen from the snapshot of the sea surface currents (Figure 4). The model simulates wide spectrum of eddies, with scales ranging from 70 to 240 km. The mean phase speed is 7.9 km day^{-1} and the mean kinetic energy is 33 cm^2 s^{-2}, which is lower than in the IC1 experiment. The "macro-cyclones", with scales larger than 450 km, have several centers. The formation of these "macro-eddies" can be regarded as a trend of the circulation to self integrate. This is followed by a disintegration of the "macro-eddies" into smaller scale ones. It is noteworthy that no basin-scale eddies are simulated in the IC2 experiment, as this was the case in the IC1 one. This is an indication that the constraint imposed by the basin scales on the eddy formation and dissipation decreases in the IC2 experiment, compared to the constraint in the IC1 experiment, or in the experiments with realistic Black Sea coast (RS).

The time averaged circulation in the IC2 experiment (Figure 5) shows two easterly propagating jets, confined in a narrow coastal band along the southern and

northern boundary. The compensating westward current occupies a wide zone in the central part of the sea. Currents at the sea surface reach maxima of about 30 cm s^{-1} They decrease to about 10 cm s^{-1} in the pycnocline, thus the vertical shear is smaller in the IC2 than in the IC1 experiment, indicating stronger barotropization.

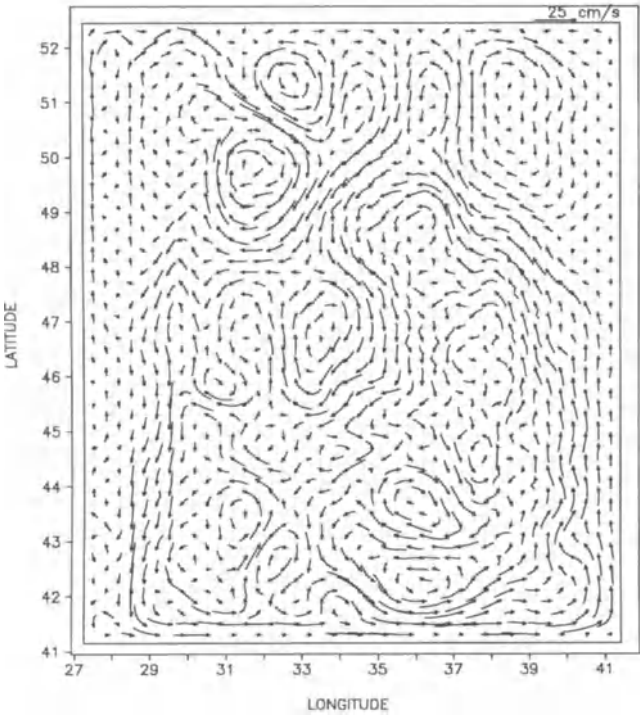


Figure 4. Snapshot of the sea surface currents in the IC2 experiment.

There are areas with very different stability of the circulation, which is proved by the analysis of the EKE and the MKE. The model simulates the largest EKE in the central part of the basin. However, the EKE/MKE ratio is also large along the northern coast. The strong meander just after the detachment zone, having a wavelength of 320 km (Figure 5) supports this conclusion. The inverse transport (to the south) in the detachment zone is a significant element of the jet instability. Number of quasipermanent eddies form between the eastern jet and the northern coast, which are better seen in the deep layer. The north-south asymmetry in the circulation, illustrated by the different stability in the currents, results also in a weaker intensity of the northern gyre. We remind that the largest variability is simulated in the central region.

On the contrary, the largest stability of the circulation is observed along the western and the southern coasts.

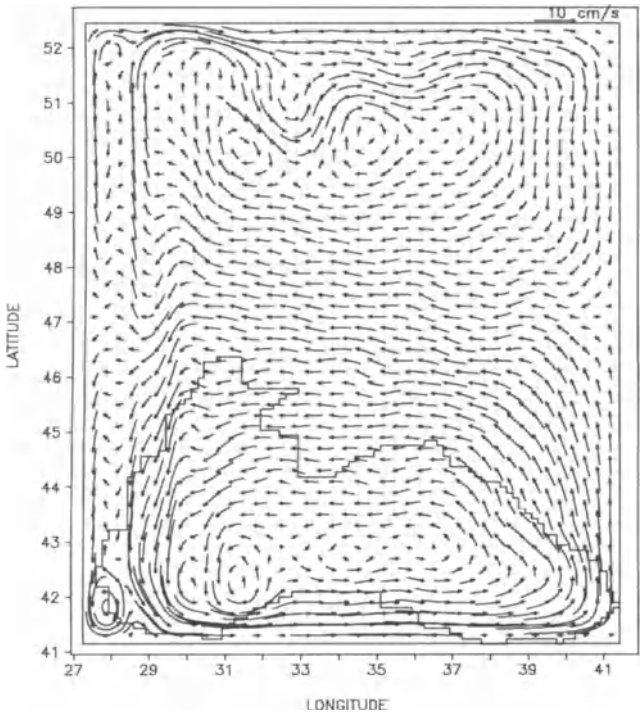


Figure 5. Time mean sea surface currents in the IC2 experiment. The coastal line of the Black Sea is plotted at the downpart of the figure.

There is a small difference between the circulation in the two experiments with idealistic coasts, illustrated in the IC2 experiment by the smaller amplitude of the meander in the eastern part of the southern gyre. This indicates that not only changing the direction of the current, when it approaches the eastern coast, tends to form the quasipermanent anticyclonic eddy. The small width of the easternmost basin (which is the case in the Black Sea) additionally amplifies the meandering. At the end of this section, we will stress on the amazing agreement between the circulation in the southern part of the model area and the one in the model with a realistic coast. We illustrate this by projecting the Black Sea coast on the plot in Figure 5 and comparing the circulation in the contoured area with the one simulated in the model with realistic coast (RCFA1 experiment, Figure 6).

3. 2 BASINS WITH REALISTIC COASTLINE

The time averaged circulation in the RCFA1 experiment (WR91 experiment of RS, Figure 6) and in the RCFA experiment (Figure 7a), correlates with the patterns, known from dynamic and diagnostic calculations (Bogatko *et al.*, 1979; Blatov *et al.*, 1984)

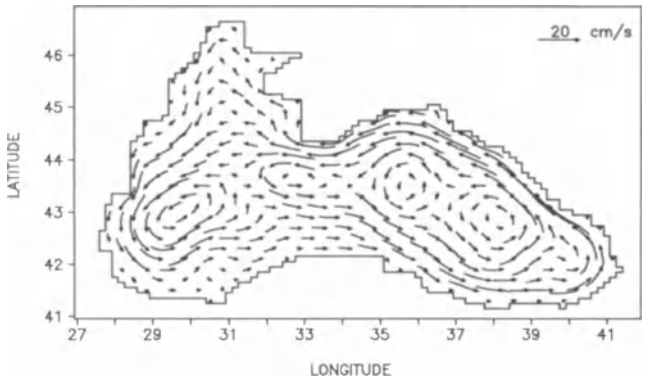


Figure 6. Time mean sea surface currents from RS, experiment

and with earlier model estimates (Bulgakov and Korotaev; 1987, Stanev, 1988). The anticyclonic eddy in front of the Sakarya Canyon (Oguz *et al.*, 1993; Sur *et al.*, 1994) is simulated both in the RCFA and RCRA experiments, with some differences, which are due to the different topography. It seems that this is one of the most stable sub-basin scale quasipermanent features of the circulation. Differently from the time mean patterns, the stream function snapshots (Figure 9) are dominated by eddies and give quite a different view of the circulation. This is mostly due to the fact that the stream function gives an integrated view on the circulation, which might not coincide with the circulation patterns in the surface layer. The last is predominantly cyclonic, both in our model estimates, as well as in the estimates based on observational data. Sub-basin scale eddies form in the easternmost Black Sea (once every six months) and constantly grow with time. After about twelve months, they enter the western Black Sea and dissipate. Some regularities in the eddy evolution, which are different for cyclonic and anticyclonic eddies, are simulated. The anticyclones have almost equal scales zonally and meridionally at the initial phase of their evolution. Five months after they appear (at this time the eddy center reaches about 37^0 E), eddies start to elongate in the meridional direction and become sandwiched between the two cyclonic eddies. The one to the west is still intense but its westward velocity starts to decrease in the narrow section. The cyclonic eddy, to the east of the anticyclone, intensifies, moves rather fast to the west, and "flattens" the anticyclone. The change of the aspect ratio between the meridional and zonal scales of the model eddies indicates

a similarity with the propagation of basin oscillations. Similar changes of the aspect ratio are observed when the moving nodes approach the fixed ones (Longuet-Higgins, 1965; Özsoy *et al.*, 1992). The elongated anticyclone follows further west, but its meridional extension starts to decrease when it enters the narrow section between the Sinop and Crimea. Next, its pathway turns to the south-west (towards the Bosphorus Strait). In such a way the anticyclonic circulation in this area (the Sakarya eddy) is constantly maintained. The cyclones continue their propagation to the west and merge with the quasi-permanent near coastal cyclonic eddy, thus contributing to maintaining the cyclonic circulation in the western Black Sea.

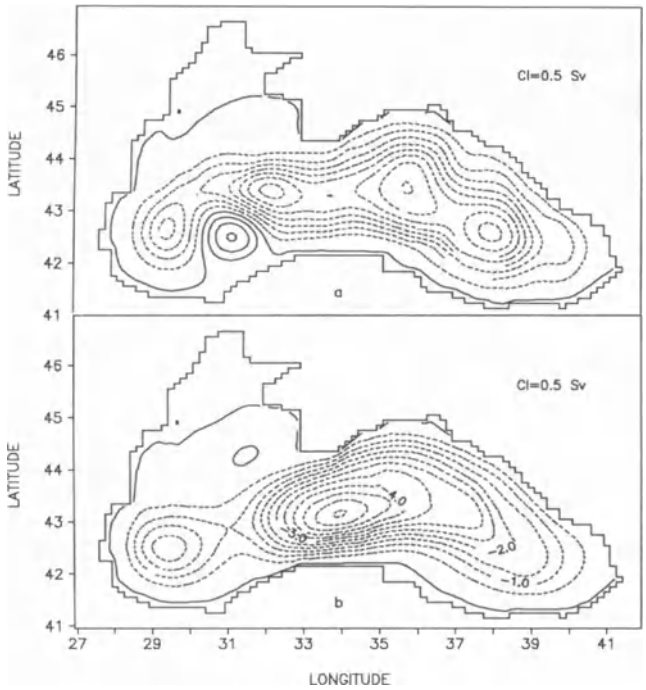


Figure 7. Time mean total transport stream function in: (a) RCFA experiment and (b) RCRA experiment. The contour interval is 0.5 Sverdrup. Solid lines correspond to positive values, dash lines correspond to negative values.

The comparison of the model and survey data by RS revealed number of similarities in the dynamics of the anticyclonic eddies in the central Black Sea (Altman *et al.*, 1984; Latun, 1990). The vertically integrated transport, estimated for the observed by Golubev and Tuzhylkin (1990) eddies, ranges from 1.2 to 3.3 Sverdrup. The corresponding numbers estimated from the model are between 3 to 5

Sverdrup, when the eddy is in the area of the narrow section. Sea surface velocities reach maxima of about 45 cm s^{-1} (60 cm s^{-1} in RCFA experiment), which is in a good agreement with the observations compiled by Blatov *et al.* (1984). The maxima decrease with increasing depth to about 25-30 cm s^{-1} at 70 m, and to 5-10 cm s^{-1} at 1100 m.

The instabilities (meanders) are created in the area of Batumi quasi-permanent eddy and propagate against the southern part of the gyre (to the west). The excitation of the Sinop anticyclonic eddy could be regarded as stimulated by the growing instability moving to the west. From the comparison between the magnitudes of the mean and eddy transports, we see that the sub-basin scale modes start to dominate the solution. Though the correctness of the comparisons of transport patterns of suspended matter and plankton derived from satellite observations and the model simulated patterns is questionable, we refer to the results of Sur *et al.* (1994). They show that the horizontal scales (100-250 km) and the speed of propagation of the eddies/meanders west of the Caucasian coast (couple of centimeters per second) almost coincide in the model simulations and in the observations.

There are two different regimes dominating the circulation: a wave-like regime in the eastern and central Black Sea and turbulent-like regime in the western basin. More detailed understanding on the time-space variability could be obtained by analyzing the Hovmoeller diagram (meridional velocity at 43° N, plotted as a function of time and longitude, Figure 9). The time averaged velocity along the section line is also given in Figure 9. The diagram indicates Rossby wave propagation. The phase speed in the eastern sub-basin (the slope of the contours) in the RCFA experiment is about 2.4 km day^{-1} (2.8 cm s^{-1}). For comparison, we refer to the results of Latun (1990), who estimated for the speed of the eddy propagation 1.5 cm s^{-1}. This speed has almost constant magnitude in the eastern basin, but eddies slow down in the narrow section (between 32° E and 34° E) and to the west of it. This is illustrated in the Hovmoeller diagram by the changing slope of the contours (Figure 9) and is in agreement with the decrease of the eddy size in the western sub-basin (Figure 8). The orientation of the isolines becomes almost parallel to the ordinate in a close proximity to the coast, which indicates a very slow propagation. The decrease in the eddy size and speed suggests intense dissipation of eddy energy, therefore, we name the western sub-basin a dissipation basin. The position of the velocity maxima in the Hovmoeller diagrams indicates that the group velocity is towards the East. This correlates with the well-known mechanism of Rossby wave reflection from the western coast, and shows that the western coastal zone is an important source of instabilities in the RCFA experiment.

The time averaged circulation in the RCRA experiment (Figure 7b), is qualitatively similar to the one simulated in RCFA experiment (Figure 7a). It correlates well with the estimates from independent sources, as well as with the circulation simulated by RS. The maximum transport is 5.6 Sverdrup against 4.7 Sverdrup in the RCFA experiment. We see an intensification of the cyclonic circulation in the western basin and a westward shift of the center of the main cyclonic gyre. It is now located at 34° E (35.5° E in the RCFA experiment). Less realistic,

compared to the observations, is the absence of anticyclonic eddies between the main gyre and the coast in the RCRA experiment, and in particularly the Batumi and Sakaria eddies. The last one is well pronounced in the time mean circulation, simulated in the RCFA experiment (Figure 7a).

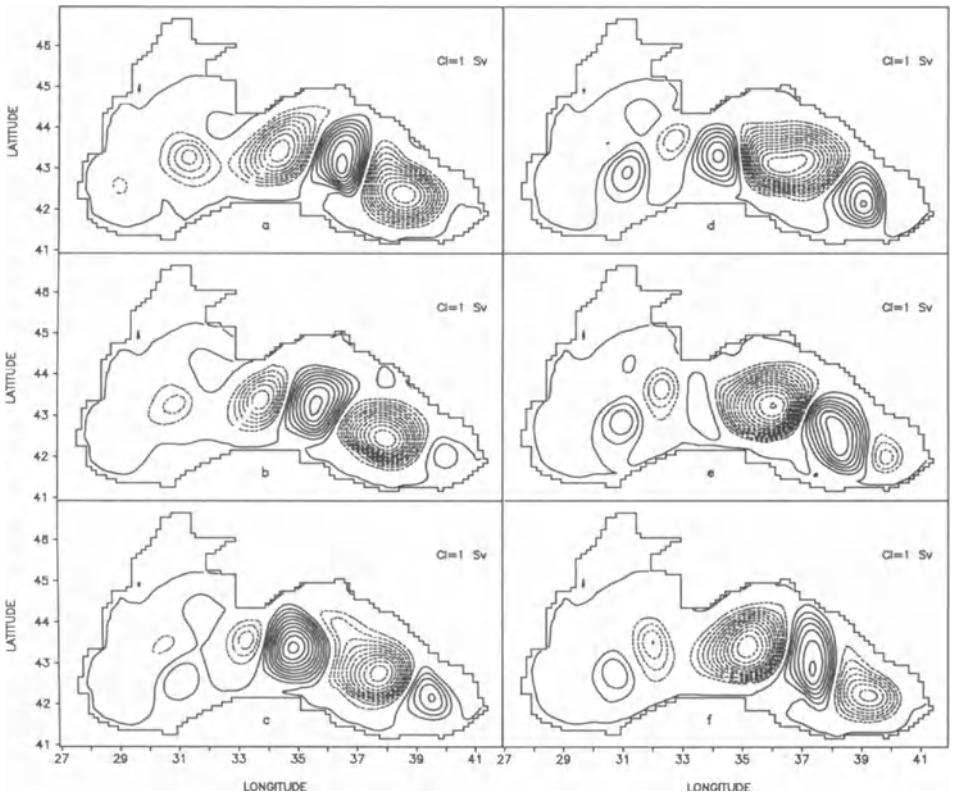


Figure 8. Snapshots of the vertically integrated mass transport stream function in the RCFA experiment. The time interval between the snapshots (in alphabetical order) is 30 day; the contour interval is 1 Sverdrup. Solid lines correspond to positive values, dash lines correspond to negative values.

The time mean density patterns in the RC-type experiments (not shown here) have larger horizontal gradients in the RCRA experiment. This correlates with the larger dooming of the pycnocline and with the resulting increase in the potential energy. The major difference between the two experiments is demonstrated by the analysis of the time evolution of circulation (Figure 10). Unlike to the circulation in the RCFA experiment, which is dominated by eddies, the one in RCRA experiment is much more

"organized" with prevailing cyclonic rotation. One important difference between Figure 8 and Figure 10 has to be mentioned. The time interval between the subsequent snapshots in Figure 8 is 1 month, and 6 plots are enough to fully represent one eddy cycle. Differently, the time discretization in Figure 10 is 97 days, and more individual patterns are needed to sufficiently resolve the time evolution.

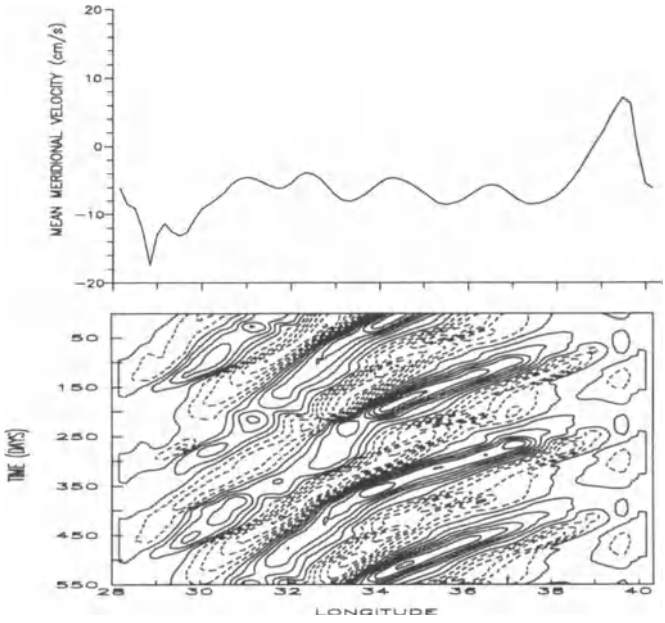


Figure 9. Time evolution of zonal section at 43° *N* (*x-t* plot) of the meridional velocity at sea surface in the RCFA experiment, the contour interval is 5 cm s^{-1}. Solid lines correspond to positive values, dash lines correspond to negative values. The slope of the contours gives a measure of the zonal phase speed of the eddies. Time averaged velocity (upper panel) is subtracted from the actual velocity data.

We remind that, while the variability in the RCFA experiment has a regular "wavelike" behavior, the one in the RCRA experiment is more irregular (quasi-repeating), and one cycle takes about 20.7 months. This type of circulation is characterized by a large scale gyre from day 1700 to day 1900, which is rather similar to the time mean circulation. The maximum value reached by the total transport, at day 1847 is about 11.3 Sverdrup, compared to 5.6 Sverdrup in the annual mean transport (see Figure 10c and Figure 7b). This type of circulation starts to change at day 1847 (Figure 10c), when three anticyclonic meanders/eddies are formed: (1) northwest of Trabzon, (2) west of the Crimea Peninsula, and (3) east of the Sakaria Canyon. The Trabzon eddy grows, while the anticyclonic areas in the western basin split the gyre into two parts at day 1944 (Figure 10d). This process develops further, and the Trabzon eddy, moving to the north and west, splits completely the eastern

gyre (Figure 10g, day 2236). The circulation in the westernmost part of the sea shows anticyclonic sign at that time. Unlike the simulations in the RCFA experiment, where the cyclones and anticyclones have comparable intensity, the anticyclones in the RCRA experiment are weaker and disappear in the area of the narrow section (between day 1653 and day 1750, Figure 10a and Figure 10b).

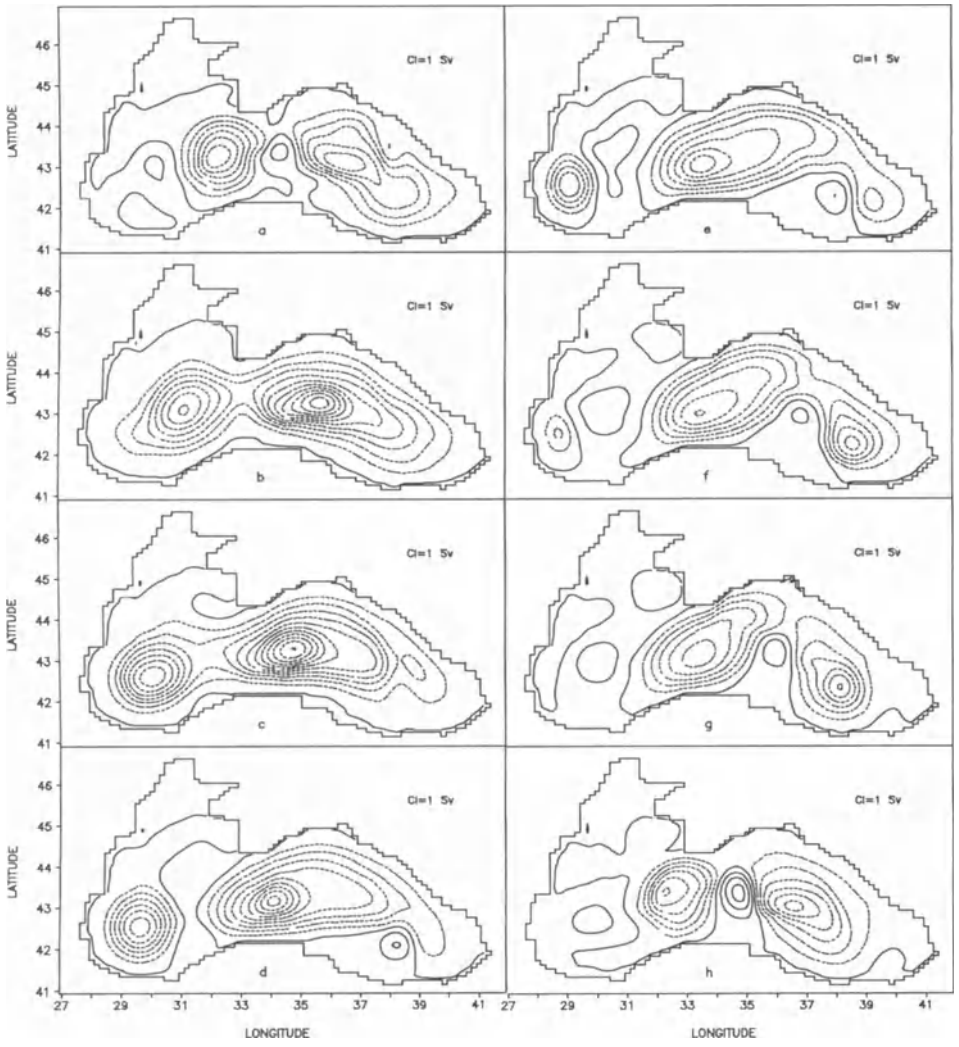


Figure 10. Snapshots of the vertically integrated mass transport stream function in the RCRA experiment. The time interval between snapshots (in alphabetical order) is 97 days; the contour interval is 1 Sverdrup. The solid lines correspond to positive values, dash lines correspond to negative values. (a) day 1653; (b) day 1750; (c) day 1847; (d) day 1944; (e) day 2042; (f) day 2139; (g) day 2236; (h) day 2333.

The above comparison of the results in the two experiments with realistic coastline shows that the RCRA experiment tends to periodically form a gyre-type circulation, dominating the pattern for about 30% of the time of one quasiperiodic cycle of variability. During the rest of the time, the model gives disintegrated circulation (dominated by sub-basin scale eddies), similar to the one in the RCFA experiment. However, the cyclonic circulation is better pronounced in the RCRA experiment, thus masking the appearances of basin oscillations with anticyclonic rotation. The above analysis on the time evolution of the circulation is well illustrated in the Hovmoeller diagram of the meridional flow (Figure 11), along the same zonal line as in Figure 9. The slope of the contours demonstrates again a westward propagation. We purposely subtracted the time mean velocity at each point to enable the plot to better illustrate the propagation of the anomalies. We have to keep this in mind when comparing Figure 11 with the consecutive patterns in Figure 10, where the anticyclone (seen in the vertically integrated mass transport stream function) disappears to the west of the narrow section.

The mean phase speed of the waves is 0.91 km day^{-1} (1.05 cm s^{-1}). However, the oscillations are characterized by non-uniform westward propagation in some particular areas. The stagnation of the eddies along the western coast was explained in the RCFA experiment as due to their dissipation in these areas. More interesting is the second stagnation zone in the narrow section (between 32 -33^0 E), but this is only for the negative velocity anomalies (dash lines in Figure 11). The changing speed of the westward propagation gives an indication that specific anomalies in the currents dominate the circulation in some areas (e. g. 31 - 33^0 E). These anomalies can change sign for relatively short time. This presents an indication that a transition between different circulation states is possible in the model.

The transition between the two regimes of the circulation (gyre-type and eddy-type) is accompanied by a transition in the vertical circulation (Figure 12). The zonally averaged meridional mass transport was previously analyzed by Stanev (1988, 1990) in a model with full thermodynamics and under different forcing. It was found that the vertical circulation is much weaker (0.1 Sverdrup), compared to the horizontal circulation (about 3 Sverdrup). This corresponds to the concept that the Black Sea is a poorly ventilated basin. The present results support our earlier ones, giving for the ratio between the horizontal and vertical transport a value of about 60.

The model simulates an intense vertical circulation (particularly in the central basin) just before the eddy-type circulation starts to transform into a gyre-type one (Figure 12b). This is accompanied by an intensification in the horizontal (predominantly cyclonic) circulation (Figure 10h). At the end of the time interval dominated by gyre-type circulation (maximum values in the horizontal transport are reached at that time (Figure 10c), the vertical overturning is the weakest (Figure 12a). It is noteworthy that the intensification of the upwelling in the basin interior (42.5-43^0 N) is accompanied by an intense sinking in the continental slope area. This could enhance the vertical mixing in the Black Sea (see Staneva and Stanev, in the present volume).

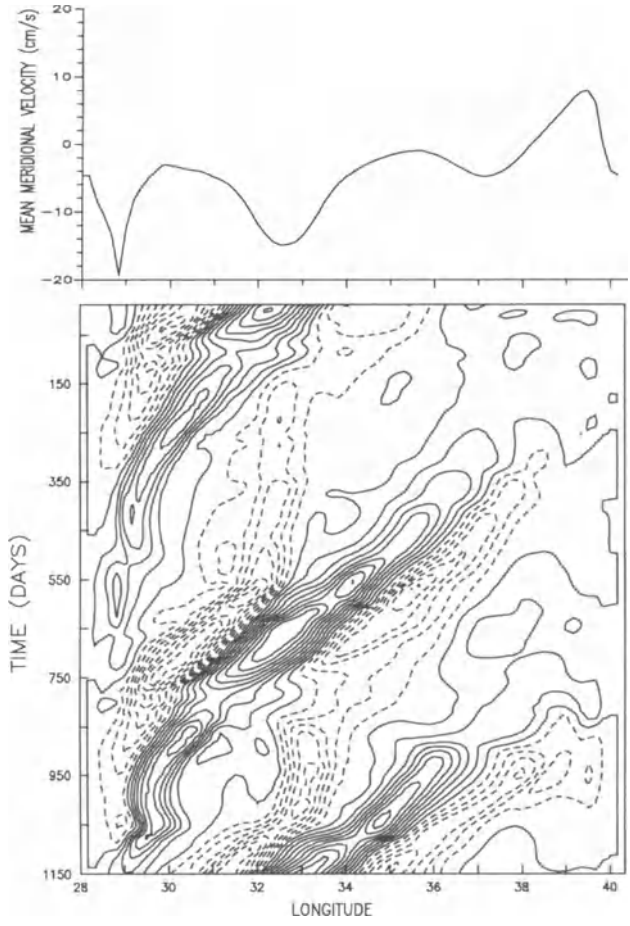


Figure 11. Time evolution of zonal section at 43° N (*x-t* plot) of the meridional flow at sea surface in the RCRA experiment. The contour interval is 5 cm s^{-1}. Solid lines correspond to positive values, dash lines correspond to negative values. Time averaged velocity (upper panel) is subtracted from the actual velocity data. The plot begins at day 1750.

As it is well known, the ratio between available potential energy and kinetic energy is larger in large scale motions, than in eddies. This ratio could be used to identify transitions in our model. The analysis of the model energetics and of larger number of vertical snapshots supports the correlation between the available potential energy and the type of circulation. The model simulates a decrease in the potential energy when the circulation is dominated by eddies, and *vice versa*, under gyre type circulation. This correlates with changing the horizontal density contrasts. They are larger in the case of gyre-type circulation and smaller in the case of eddy-type

circulation. The transition between the two types of circulation is also accompanied by changes in the current shear in the vertical. Instantaneous velocities below the pycnocline are stronger in the case of gyre-type circulation, compared with the velocities during the eddy-type circulation, but this situation reverses at levels above the pycnocline.

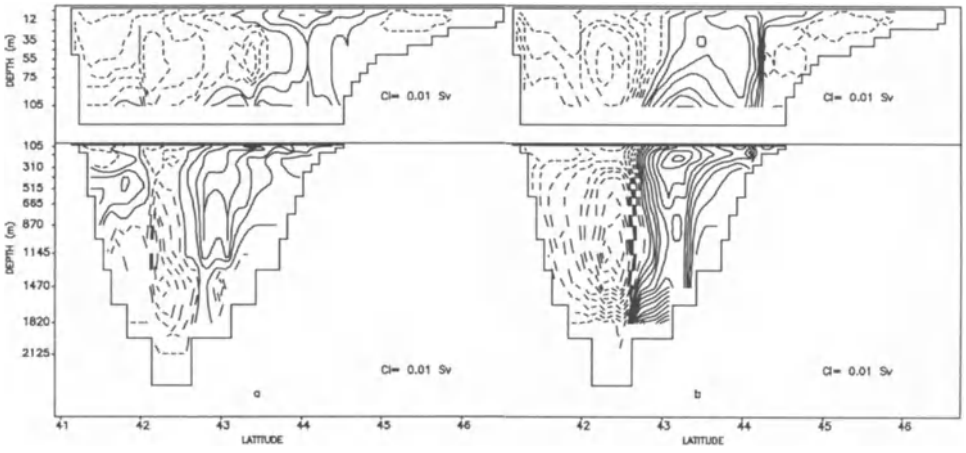


Figure 12. Zonally averaged meridional mass transport in the RCRA experiment: (a) day 1847; (b) day 2333

The phenomenological analyses above lead to the speculation that transitions between the two model states are due to the instabilities, developing in the gyre after the slope of the pycnocline reaches some critical value. Then the circulation enters into the eddy regime, tending again to adjust to the forcing, and to amplify. This could be proved by the analysis of the model energetics.

Short description on the energetic terms and analysis of the energetics of the present model is done by RS, therefore we will remind below only the meaning of different terms, referring for more details to the above publication and to Holland (1975). For the time rate of change of the kinetic energy of the external and internal modes, we have:

$$E_t = N_e + B_e + W_e + D_e \qquad \text{and} \qquad E_t = N_i + B_i + W_i + D_i \qquad (7)$$

where the terms on the right hand side of equations (7) represent the work done on the external/internal mode by the nonlinear terms (N_e, N_i), the pressure forces (B_e, B_i), the wind stress (W_e, W_i) and the dissipation forces (D_e, D_i). In a mechanically closed basin $N_i = - N_e$, the net transfer between the external and internal modes due to topography is $T= B-B_i$, where $B=B_e+B_i$ is the work done by buoyancy forces. We will analyze below the energetic terms (Figure 13a) using the scheme of Treguier (1992).

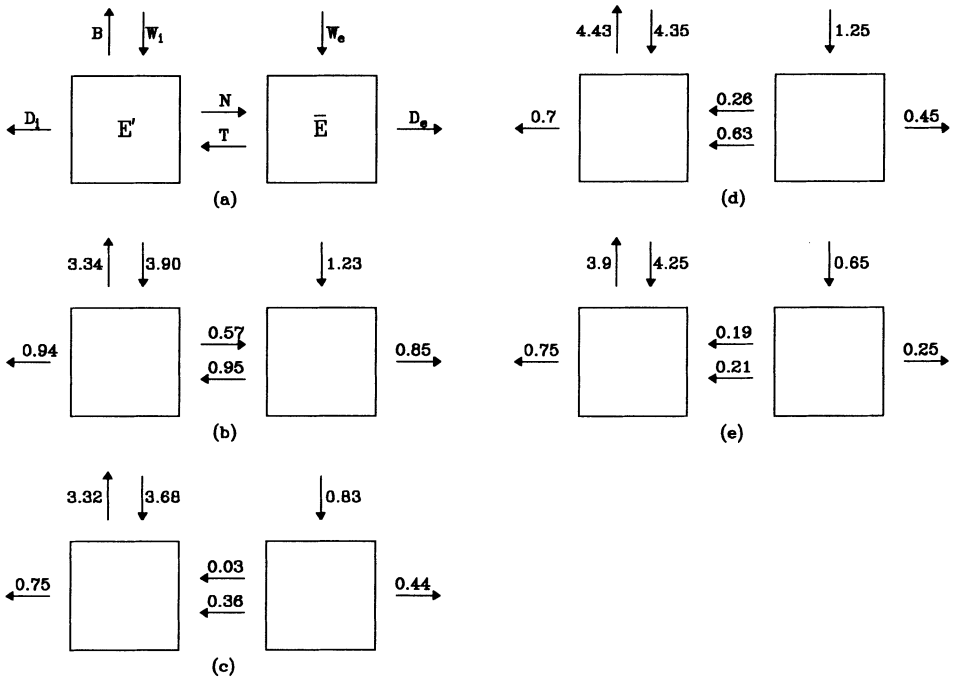


Figure 13. Energy box diagrams showing the magnitude and direction of work done by the energetic terms in equations (7). The numbers ($cm^2 s^{-3}$) are multiplied by 10^{-6}. (a) notations (see also equations 7); (b) RCFA experiment (time mean); (c) RCRA experiment (time mean); (d) RCRA experiment - day 1847 (e) RCRA experiment - day 2333.

The model simulates different energetic regimes, depending on the vertical resolution. These differences are due to the impact of the vertical discretization on the resolution of bottom topography, which is a specific feature of the model. The model approximation of the abyssal plane under different resolution has, in particular, a very pronounced effect on the model energetics. The coarse vertical resolution in the main experiment of RS (RCFA1 experiment in the present study) tends to create a large transfer of energy from internal to external mode. This was analyzed in detail by RS, with a focus on the opposing actions of the nonlinear transfer and the topographic control. In the RCFA experiment, which has finer vertical resolution than the RCFA1 experiment, and essentially the same abyssal topography, the relative importance of the internal mode increases. This is accompanied by a relative change in the rate of works done by horizontal/vertical motion. The increased vertical resolution makes the model more dependent on the vertical motions, particularly on the vertical friction. The energy balance changes if we resolve the topography in the abyssal plane (RCRA experiment). The circulation is less intense in RCRA than in the RCFA experiment,

the nonlinear transfer decreases strongly, and even changes sign (Figure 13b, RCFA, and Figure 13c, RCRA experiments). The terms W_e, D_e, and T decrease about two times and the terms W_i, D_i, and B_i increase approximately two times. It is important to note that the main balance in all experiments is between the work done by wind and pressure forces on both external and internal modes. The changes of W_e and W_i are coherent in the RCRA experiment, whereas the maxima of W_e coincide with minima of W_i, and *vice versa* in the RCFA experiment. Here we remind that the structure of the energy exchange is qualitatively similar to the one, found earlier by Stanev (1988, 1990).

It is impossible to make a definite conclusion which scheme of the energy transfer corresponds better to the real Black Sea conditions. We admit that there are no appropriate observations to check this. However, both possible circulation mechanisms are related to specific energy balances, and their analysis could help in understanding the possible circulation mechanisms in the Black Sea, and how they are maintained.

We will illustrate the transition between both types of circulation by the comparison of model energetics, corresponding to the gyre-type circulation (Figure 13d) and eddy-type circulation (Figure 13e). The work done by wind on the external mode W_e decreases two times when the circulation is dominated by eddies (Figure 13e), compared to W_e in the case of gyre type circulation (Figure 13d). This term measures the correlation between the wind stress and the sea surface currents (Holland, 1975). One plausible explanation on the circulation mechanisms follows from here. The wind stress provides the major driving in the model (as seen by the comparison between the signs of the rate of energy change due to the wind and to the buoyancy) and tends to form a doom-shaped pycnocline. After some critical limit, the nonlinearity increases, and the circulation breaks into several sub-basin scale eddies, thus decreasing the correlation between the wind stress and the surface currents. Note that the work done by wind on the internal mode remains approximately the same under the two regimes of circulation (W_i has smaller value in the beginning of the eddy-type circulation). The formation of the sub-basin scale type circulation seems to be the mechanism, which enables the model to pass into a state with a lower energy. A smaller energy transfer between the external and internal modes is simulated, correspondingly. In the same time, the JEBAR term shows that the correlation between the currents and the topography decreases. Thus, the eddy-type circulation, dominated by sub-basin scale eddies, is less constrained by the topography than the gyre one. The period of one energy cycle, (e. g. one cycle in Figure 11) is practically the time needed by the model to readjust to the wind forcing.

Conclusions

The simulations with the IC-models show some very interesting differences from the results of earlier simulations, which will be commented below. Though our model basin and the one of Holland and Lin (1975a, b) are forced in a similar way, the model

dynamics, which is strongly nonlinear, result in a different, asymmetric, response of the present model. The anticyclones reach basin scales and tend to occupy the northern part of the basin. Similar tendency of differentiation was found earlier by RS in the model with realistic coasts. This differentiation has a pronounced impact on the time mean circulation (Figure 3), showing north-south asymmetry. The basin scale constraint on the eddy processes decreases in the IC2 experiment, compared to the one in the IC1 experiment, or in the experiments with a real basin coast of RS. This result speaks for the major role, which the coast has in the formation of the circulation when the Rossby radius of deformation is comparable to the basin scales. In such dynamical systems the basin-scale oscillations start to dominate the model solution, and induce a strong baroclinic response. The model simulated snapshots of currents show rather chaotic behavior in the IC-type of experiments, which is dominated by synoptic/sub-basin scale eddies. However, there is an amazing correlation between the time-mean circulation and the one simulated in the models with realistic coast, provided that the forcing incorporates the main features, typical for the Black Sea forcing: the cyclonic wind stress and the increased sea surface density in the Black Sea interior. Such simplistic models give some confidence to speculate about the major driving forces and about the utmost importance of the basin scales and specific aspect ratios for the formation of the circulation in the real basin.

Two important results are noteworthy when drawing conclusions from the RC-experiments: (1) the wave-eddy transition occurs at larger scales in the in the RCFA experiment, which is demonstrated by the pronounced wave-like behavior of the mesoscale eddies; (2) this transition occurs in the RCRA experiment at smaller scales, which limits the increase of the meanders and eddies. The formation of circulation dominated by sub-basin scale eddies enables the model to pass into a state with lower energy. In this new physical state, smaller energy transfer between the external and internal modes is simulated. This type of circulation is less constrained by the topography than the gyre one. The major period of the basin oscillations (Figure 11) corresponds to the energy cycle, which is 20.7 months. This is practically the time needed by the model to develop instabilities and to readjust to the constant in time wind forcing. The seasonality in this forcing could change the appearance of the model variability, as it was recently shown by Stanev and Staneva (1996). In any case, the periodic intensification of the basin oscillations, which is illustrated by the intensification of sub-basin scale eddies, seems to be a major physical mechanism, providing the adjustment between the model circulation and the external forcing.

References

1. Altman, E. N., V. I. Kalatskyi, G. K. Korotaev and Latun V. S. (1984). The Black Sea multi-institutional expedition, 1984. Organization and main results. *Marine hydrographycal Journal* **5**, 58-64 (in Russian).
2. Blatov, A. S., Bulgakov, N. P., Ivanov, V. A., Kosarev, A. N., and Tuzhylkin, V. S. (1984). *Variability of the hydrophysical fields in the Black Sea*, Gidrometeoizdat, Leningrad (in Russian).
3. Bogatko, O. N., Boguslavskiy, S. G., Beliakov, M., and Ivanov, R. (1979). Surface currents in the Black Sea. *In: Complex studies of the Black sea*, Marine Hydrophysical Inst., Sevastopol, pp. 26-33 (in Russian).

4. Böning, C. W. and Budich, R. G. (1992). Eddy dynamics in a primitive equation model. Sensitivity to horizontal resolution and friction, *J. Phys. Oceanogr.* **22**, 361-381
5. Bryan, K., (1969). A numerical method for the study of the circulation of the World Ocean, *J. of Computational Physics* **4**, 347-378.
6. Bulgakov S. N. and Korotaev, G. K. (1987). Diagnostic calculations of the Black Sea climatic circulation on full nonlinear model, *Morsk. Gidrofiz. Zh.*, 2987(1), 7-13 (in Russian).
7. Cox, M. D. (1984). A primitive equation, 3-dimensional model of the ocean, GFDL *Ocean Group Technical Report* No 1, 143 pp.
8. Cox, M. D. (1985). An eddy-resolving model of the ventilated thermocline, *J. Phys. Oceanogr.* **15**, 1312-1324.
9. Golubev, Y. N. and Tuzhylkin, V. S. (1990). Kinematics and water structure of anticyclonic vortex formation in central part of the Black Sea, *Okeanologyia* **30** (4), 575-581 (in Russian).
10. Holland, W. R. (1975). Energetics of baroclinic oceans, in *Proceedings of symposium of Numerical models of ocean circulation*, National Acad. of Sci., Washington, D. C., 168-177.
11. Holland, W. R. (1989). Experiences with various parameterizations of sub-grid scale dissipation and diffusion in numerical models of ocean circulation. in P. Muller and D. Henderson (eds.), *Parameterization of small-scale processes,* Proceedings, 'Aha Huliko'a, Hawaiian Winter Workshop, pp. 1-9.
12. Holland, W. R. and Lin, L. B. (1975a). On the generation of mesoscale eddies and their contribution to the oceanic general circulation. I. Preliminary numerical experiment, *J. Phys. Oceanogr.* **5**, N 4, 642-657.
13. Holland, W. R. and Lin, L. B. (1975b). On the generation of mesoscale eddies and their contribution to the oceanic general circulation. II. A parameter study, *J. Phys. Oceanogr.* **5**, N 4, 658-669.
14. Kantha, L. H. and Drexler, L. (1996). Altimetry in marginal, semi-enclosed and coastal seas. Part I. Multimedia document, *http:/www.cast.msstate.edu/Altimetry.*
15. Latun, V. S. (1990). Anticyclonic eddies in the Black Sea in summer of 1984, *Sov. J. of Phys. Oceanogr.* **1** (4), 279-286.
16. Longuet-Higgins, M. S. (1965) Planetary waves on a rotating sphere. II, *Proc. Roy. Soc. A*, **284**, 40-54.
17. Oguz, T., Latun, V.S., Latif, M. A., Vladimirov, V. V., Sur, H. I., Markov, A. A., Özsoy, E., Kotovshchikov, B. B., Eremeev, V. V., and Ünlüata, Ü. (1993). Circulation in the Surface and Intermediate Layers of the Black Sea, *Deep Sea Res.* **40**, 1597-1612.
18. Oguz, T., Aubrey, D. G., Latun, V. S., Demirov, E., Koveshnikov, L., Sur, H. I., Diaconu, V., Besiktepe, S., Duman, M., Limeburner, R., and Eremeev, V. (1994). Mesoscale circulation and thermohaline structure of the Black Sea observed during HydroBlack '91, *Deep Sea Res.*,**41**, 603-628.
19. Özsoy, E., Lozano, C. J., and Robinson, A. R. (1992). A consistent baroclinic quasigeostrophic ocean model in multiply connected ocean domains, *Mathematics and Computers in Simulations* **34**, 51-79.
20. Rachev, N. H., Roussenov, V. M., and Stanev, E. V. (1991). The Black Sea climatological wind stress, *Bul. J. Meteorol. and Hydrol.* **2**, 72-79.
21. Rachev, N. H. and Stanev, E. V. (1996). Eddy processes in semi-enclosed seas. A case study for the Black Sea, *J. Phys. Oceanogr.*, (submitted manuscript).
22. Stanev, E. V. (1988). Numerical study on the Black Sea circulation. Mitteilungen des Instituts für Meereskunde der Universität Hamburg, **28**, 232 pp.
23. Stanev, E. V. (1990). On the mechanisms of the Black Sea circulation, *Earth-Science Rev.*, **28**, 285-319.
24. Stanev, E. V. and Staneva, J. V. (1996). The impact of baroclinic eddies and basin oscillations on the transitions between different quasistable states of the Black sea circulation, *J. Mar. Sys.*, in Ch. Mooers (ed.), special issue on the *Circulation of the semi-enclosed seas*, (accepted manuscript).
25. Staneva J. V. and Stanev, E. V. (1996). Oceanic Response to Atmospheric Forcing Derived from Different Climatic Data Sets. Intercomparison Study for the Black Sea *Oceanologica Acta* (accepted manuscript).
26. Sur, H. I., Özsoy, E., and Ünlüata, Ü. (1994). Boundary current instabilities, upwelling, shelf mixing and eutrophication processes in the Black Sea, *Progress in Oceanography* **33**, 249302.
27. Treguier, M. (1992). Kinetic energy analysis of an eddy resolving, primitive equation model of the North Atlantic, *J. Geoph. Res.* **97** (C1), 687-701.

SEASONAL VARIABILITY OF THE BLACK SEA CLIMATIC CIRCULATION

DIMITUR I. TRUKHCHEV[1] AND RASHIT A. IBRAYEV[2]
[1]*Institute of Oceanology, Bulgarian Academy of Sciences, P.O. Box 152, Varna 9000, Bulgaria*
[2]*Institute of Numerical Mathematics, Russian Academy of Sciences, Leninski pr. 32A, Moscow 117 334, Russia*

Abstract. A 3-D PE GCM is used for diagnostic study of seasonal variability of the Black Sea. A diagnostic study is made, using the hydrodynamic adjustment method, and based on climatological monthly data sets of temperature and salinity. The monthly climatological circulation shows strong variability. The intensity of the Rim Current is seasonal, with a maximum in winter - early spring. The circulation pattern, the Rim Current, and the Cold Intermediate Layer (CIL) are quite realistic and comparable with measurements. Strong influence on current is caused by winter mixing, producing different water masses in the shelf and deep sea regions. There are indications of positive feedback between Rim Current Intensification and upwelling/downwelling rates.

1. Introduction

Experimental studies of sea currents in the Black Sea are rather limited and non-systematic - to date, they only provide the most general ideas on the large-scale circulation [16]. Long term measurements of currents were carried out mostly in the shelf zone, and showed considerable synoptic variability. The rarely available measurements of currents in deep- water areas are of a local character and are not sufficient for the reproduction of the general pattern of the dynamics. The only method for the reconstruction of the Black Sea steady-state circulation today is presented by numerical modelling. The present study includes results from semi-diagnostic (adjust-

E. Özsoy and A. Mikaelyan (eds.), Sensitivity to Change: Black Sea, Baltic Sea and North Sea, 365–374.
© 1997 *Kluwer Academic Publishers.*

ment) calculations, made on the basis of temperature T and salinity S observational data. The aim is to reconstruct the 3-Dimensional climatic circulation of the basin, and to achieve a better understanding of its seasonal variability, the cold intermediate layer (CIL) evolution, and the interaction mechanisms between the shelf and interior flows.

2. Input Data and the Model

The climatic hydrological data is a good basis for detailed model examination of the Rim Current - the Main Black Sea Current [17, 18] and of its barotropic-baroclinic instability [1]. In the present calculations is used an array of 64 300 hydrological stations for a period of the last 50 years. The monthly averages of the salinity and temperature data set [4] are represented for every month on a model grid with a spatial resolution of 12 x 15 arc min on 26 levels from the sea surface to the bottom $H = H(x, y)$. The monthly wind stress fields have been taken from Hellerman and Rosenstein [5]. In order to determine the velocities, use is made of the hydrodynamical adjustment method [14, 15] by means of a PE model of the general circulation developed in the Institute of Numerical Mathematics of the Russian Academy of Sciences [3, 6]. It is well known that the quality of any data assimilation method is determinated first of all by the quality of the hydrodynamic model itself. That is why, we implement for this study a model, which is tested successfuly in the model calibration experiment in the former USSR [14].

The initial system includes equations (of motion, continuity, sea level, heat and salt diffusion, and sea water state) and boundary conditions, which are traditional for a model of ocean hydro-thermodynamics. The finite-difference approximation of the model equations is based on the balance of properties within the "boxes" on Arakawa B-grid. One important feature of the solution is the choice of the sea level ζ as a model integral function [15]. This is a key function to the analysis of the dynamic character: its behavior is determined mainly by the density distribution in the upper baroclinic layer (300-500 m) and by the currents corresponding to this density distribution. The difference analogue of the equation for ζ is derived by the transformations of the basis of discrete analogues of continuity equation and equations of motion. Boundary conditions for the equation for the sea surface height are the projection of the continuity equation on the domain boundary with respect to boundary conditions for velocities.

3. The Adjustment Method

Briefly, the hydrodynamic adjustment procedure for every month of the 12 months of runs consists of the following. At the first *(diagnostic)* stage, the

T and S functions are "frozen" and the equations of motion are integrated until a steady-state solution is obtained. At the second *(adaptation)* stage, the two equations for the salt and heat evolution are added to the input system of equations. The duration of this stage process (3 days) is determined by the completion of the initial stage of adjustment for the T, S and **U** functions. The boundary conditions of the system are as follows: *on the ocean surface* are given the tangential wind stress fields, the "rigid-slip" condition and zero values for the heat and salt fluxes; *on the bottom* are given the heat and salt isolation conditions, a zero value for the normal velocity component and the quadratic bottom friction; *on the side boundaries* are given the zero normal flow component and the free slip conditions, as well as the heat and salt isolation conditions. In the adjustment study, we do not specify transport conditions on the coastal boundary, i.e. we do not account directly for the influence of river run-off and for the water exchange with the Mediterranean and the Azov Sea - the basin is "closed". The seawater state equation is a 3-rd order polynomial with respect to T and S with coefficients taken from the UNESCO formula [19].

The CIL appears to be one of the Black Sea hydrological peculiarities [1, 8, 9, 12]. The presence of this layer in the adapted fields is a sensitive indicator of the correct parameterization of eddy and turbulent vertical mixing in the model. If the coefficients of vertical mixing processes are constant, the CIL structure would be considerably distorted, even after a short adaptation term of 3 days. Therefore, the vertical coefficients depend on the Richardson number Ri, according the Pacanowsky and Philander's method, used for modelling of tropical ocean [13]:

$$\nu = \nu_o(1 + \alpha Ri)^{-n} + \nu^b, \tag{1}$$

$$\nu_T = \nu_o(1 + \alpha Ri)^{-1} + \nu_T^b, \tag{2}$$

where $Ri = g\frac{\partial \rho}{\partial z}[(\frac{\partial u}{\partial z})^2 + (\frac{\partial v}{\partial z})^2]^{-1}$; ν^b, ν_T^b, ν_o, α, n are parameters. These parameteres were varied within the next limits: $0.1\ cm^2/s \leq \nu^b \leq 1\ cm^2/s$; $0.01\ cm^2/s \leq \nu_T^b \leq 2\ cm^2/s$; $10\ cm^2/s \leq \nu_o \leq 50\ cm^2/s$; $0.5 \leq \alpha \leq 5$; $n = 1, 2, 3$. The good coincidence of the seasonal basin-wide averaged vertical distribution of the temperature values in the initial and adapted fields for summer and winter provides support for the use of the coefficients in (1) – (2) we have chosen: $\nu_o = 30\ cm^2/s$, $\alpha = 1$, $\nu^b = 1\ cm^2/s$, $\nu_T^b = 0.2\ cm^2/s$, $n = 2$.

4. Dynamics of the Upper Layer Circulation

The results confirm the general cyclonic character of the Black Sea circulation. All year around, the minimum sea surface level is located in the

centres of the eastern and wetern parts of the basin (Figure 1). Both gyres are most intensive in winter. But the Rim Current does not appear to be a stable cyclonic current flowing regularly along the shelf edge. As a rule, both the large-scale and the sub-basin scale (according to the general Knipovich scheme) movements are clearly expressed, and on this background - the developing mesoscale features of the circulation (eddies and local jets). The influence of the mesoscale processes on the dynamic character increases along with the weakening of the factors maintaining the main cyclone. Most of the eddies and meanders spread into the whole water layer from the seasurface to the bottom. The different factors forming and supporting the cyclonic movements in the western and eastern subbasins work out of phase and with different intensities. Therefore the Rim Current occupies the whole basin only when the reasons causing the cyclone gyres in both parts of the sea coincide in time. This happens during the winter convection period in February - March and in summer (Figure 1, Figure 2).

We shell mention a possible relationship between the variability of the thermohaline fields and the Rim Current intensity. In January - April the convective mixing process results in a nearly homogeneous water massive, formed on the whole north-west shelf. The sea surface amplitude in this zone in this period is not more than 4 cm. The river run-off is almost completely entrained in the mixing area on the shelf and does not penetrate into the central areas of the sea where from January to April the salinity on the surface reaches a maximum annual value of 18.4 ppt. The cold and fresh waters are distributed mainly along the Rim Current periphery and are transported by the latter in southern direction along the coast to the central and eastern regions. As a result, a stronger density gradient appears between the central and the shelf areas, and consequently - a stronger amplitude in the sea surface level and higher intensity of the cyclonic motion are being observed. At this time, the maximum surface level gradients are observed in the zone above the continental slope, the speed in the Rim Current reaches its maximum ($\approx 40\ cm/s$ on the average), and the current itself is quite narrow (Figure 1, Figure 2). The maximum speed ($\approx 70\ cm/s$) is observed in March to the south of the Crimean Peninsula. The cyclonic circulation intensification causes an upwelling intensification in the center of the basin and a downwelling intensification over the continental slope. This, in its turn, increases additionally the sea surface amplitude. This positive feed-back connection between the sea surface gradients on the slope and the circulation exists until the beginning of the water warming in summer.

Currents in the eastern part with an intensity, comparable to the currents in the western part, can be observed only south from the Kerch Strait. Here are created conditions similar to those of the north-west shelf. The Rim Current along the coast of the North Caucasus and of the south-east

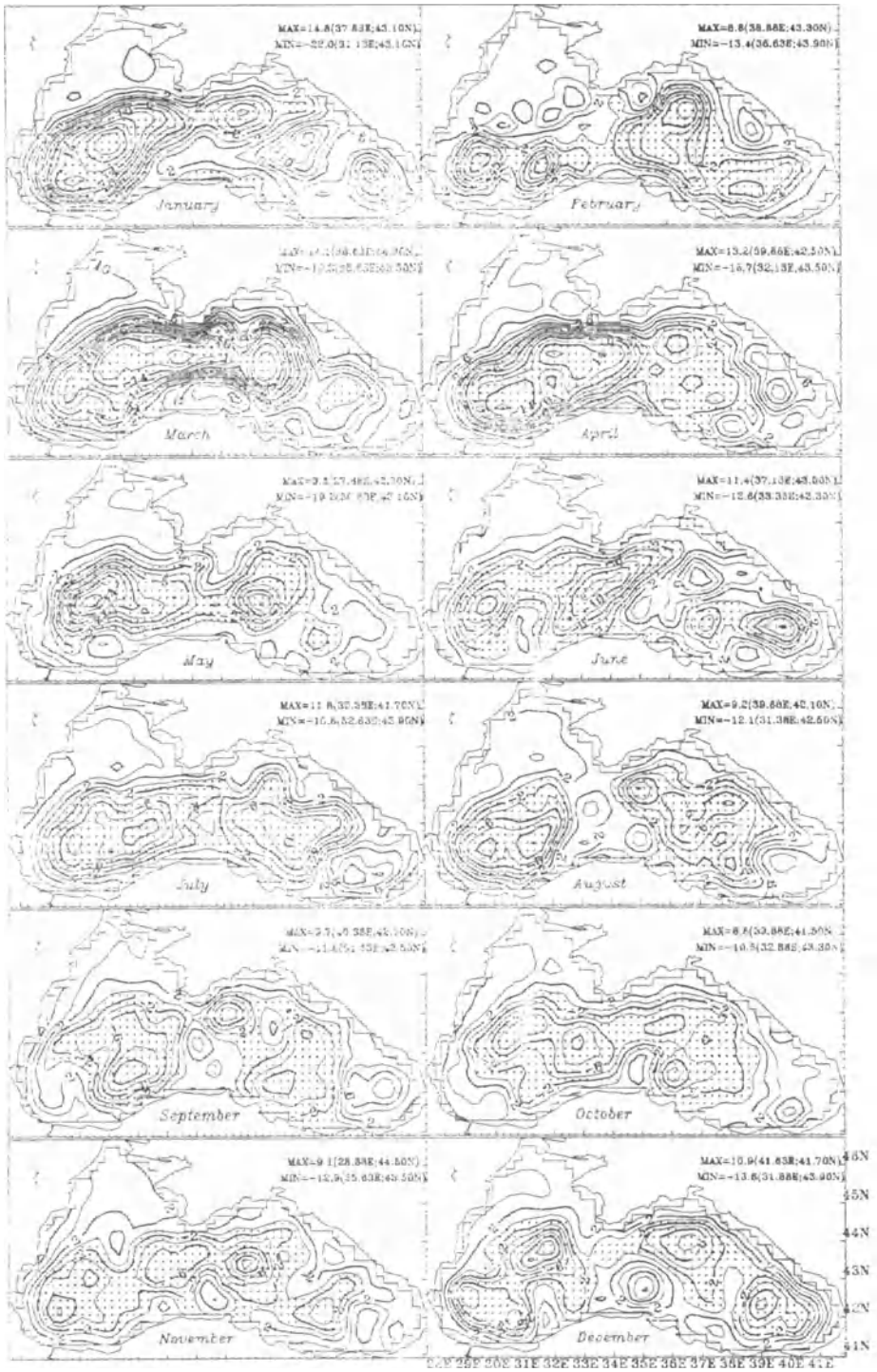


Figure 1. The Black Sea climatic sea-level (cm) topography.

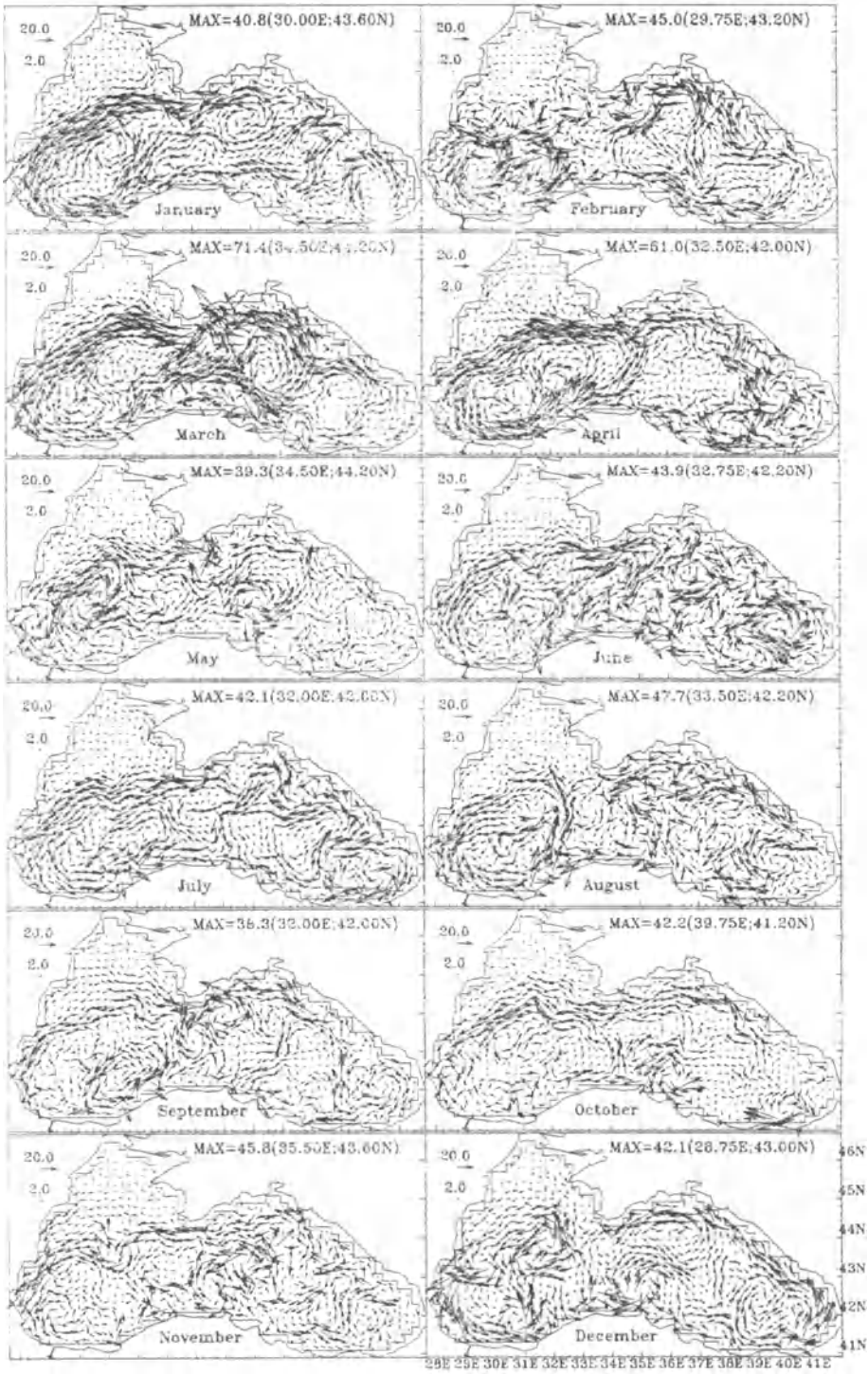


Figure 2. Climatic fields of sea currents (cm/s) at 5 m depth.

area of the Anatolian is less intensive and does not follow the coastal line. In the Sochi area there exists an anticyclonic eddy almost throughout the whole year.

In May starts an intensive sea heating and the thermocline formation, at this time begins also the winter fresh waters influx. The co-influence of both factors causes the formation of relatively light waters and of a pycnocline. As a result of this, the amount of fresh waters, which participated in the mixing process on the shelf zone, is now distributed in the upper 20-30 m of the sea including the central regions. Simultaneously, along the edge of the north-west shelf at a depth of 50-150 m penetrates water with a higher salt contents from the open sea. The sea level amplitude on the north-west shelf reaches 6-8 cm (Figure 1). As a consequence, the density gradients are weakened and so are the "shelf - interior" sea level differences: from May till October - November those differences along the shelf edge are much smaller and the zone of the maximum sea level gradient is not very clearly outlined.

5. Deep Layer Circulation

There is an obvious deep-sea current variability at a depth of 1000-2000 m and of the stream function correlated with it (Figure 3). As for the general charact of the circulation, there is, obviously an approximate equality of the relative strength and occupied area of the cyclonic and anticyclonic eddies. In the western part of the basin, the deep-sea circulation has more cyclonic character throughout the year; in the eastern part the anticyclonic eddy is better developed. A relatively stable anticyclonic eddy is observed in the central region of the sea from November to June. From month to month this eddy shifts from the Crimean peninsula to the Anatolian coast.

6. Evolution of the Cold Intermediate Layer

In winter, the cold, fresh waters from the shallow North-West regions reach the Rim Current periphery and are transfered by it along the shore to the south and east, towards the Bosphorus. Along this route, this water sinks down the slope because of downwelling. A certain part of north-west cold waters is entrained by the current, which forms the internal cyclonic gyre and is transferred to the central part of the cyclonic gyre. Simultaneously, a convective mixing process takes place above the dome of the cyclonic gyre. From the sea surface to a depth of 50 m, the north-western shelf waters and the cold centers are separated by relatively warm water. At a depth of 75 m both masses of cold waters join together forming a tongue.

The basic mechanism of upper layer homogenization in the eastern sub-basin is the more intensive cooling of the water above the dome of the

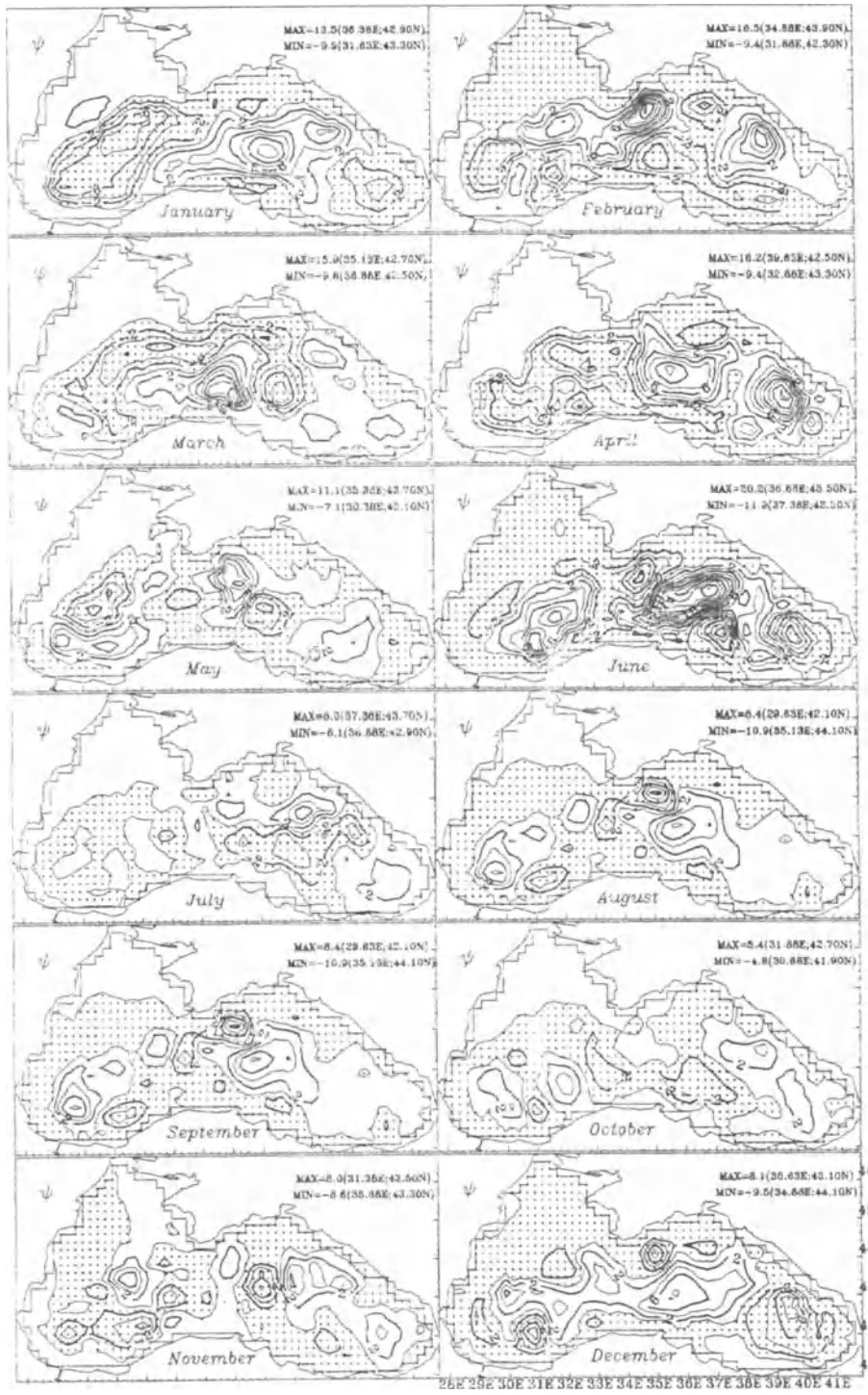


Figure 3. The stream finction of the Black Sea.

cyclonic gyre, the spreading of the cold water from the cyclonic gyre dome, the entrainment by the anticyclonic gyre and the corresponding deepening of the cold waters. Beginning with March, near the coast, at the central part of the basin and over the anticyclonic eddy, there exist sources with temperature inversions, formed during the earlier season. In April the water begins warming up; the time for the gradual increasing of the temperature with depth proves to be insufficient and the new season's inversions are formed.

7. Conclusion

A common problem for all studies on ocean circulation diagnosis is the reliability of the results obtained. In this respect, some independent climatic parameters would be necessary for comparing and estimating the closeness of the circulation obtained to the one, observed in Nature. The reconstructed currents' picture generally agrees with the currents' map of Neumann [7] and of Bogatko et al. [2]. We had at our disposal the data from direct velocity measurements of buoy stations given in [16], and took into account all measurements with time-length more than 12 hours in the winter and in the summer months at a depth of 0-50 metres. Both maps - of the velocity vectors measured and of the model reconstructed currents averaged by seasons and by the same layer, as a whole, are not contradictory to each other.

The present study contains the results from a reconstruction of the mean long-term circulation of the Black Sea waters, made on the basis of temperature and salinity data. When considering the results we obtained, we tried not only to analyze the variability of the circulation of the upper and deep sea layers, but to follow some "cause-effect" relationships between the basic dynamic factors too. Our analysis does not claim to be a conclusive one, nor have our suppositions been completely proved. More reliable statements could be made on the basis of a further analysis of the results obtained and on the results from the numerical reproduction of the seasonal evolution of the Black Sea dynamics.

8. Acknowledgements

This investigation was carried out with the financial support of the National Science Funds of Bulgaria (*Grant NZ-412*) and Russia (*Grant 94-05-9 09*).

References

1. Blatov, A.S., Bulgakov, N.P., Ivanov, V.A, Kossarev, A.N and Tuzhilkin, V.S. (1984) *Variability of hydrophisical fields of the Black Sea, (in Russian)*, Gidrometeoizdat,

Leningrad (S. Petersburg).
2. Bogatko, O., Bogusavsky, S., Belyakov, Yu. and Ivanov, R. (1979) Surface currents in the Black Sea, in *Complex studies of the Black Sea, (in Russian)*, Marine Hydrophysic Institute, Sevastopol, Ukraine, pp. 25–33.
3. Demin, Yu. and Ibraev, R. (1989) A numerical method of calculation of currents and sea surface topography in multiply connected domains of the ocean, *Soviet J. of Numerical Analysis and Mathematical Modelling*, **No 4**, pp. 179–252.
4. Eremeev, V., Ivanov, V., Trukhchev, D. and Tuzhilkin V. (1994) Climatic circulation of the Black Sea waters derived from the adaptation calculations with mesoscale resolution, in *Diagnosis of the state of marine enviroment of the Azov-Black Sea basin*, MHI UAS, Sevastopol, pp. 121–135.
5. Hellerman, S. and Rosenstein, M. (1983) Normal monthly wind stress over the World ocean with error estimates, *J. Phys. Oceanogr.*, **No 13**, pp. 1093–1104.
6. Ibraev, R. (1993) Reconstruction of climatic characteristics of the Gulf Stream current, *Izv. Russian Acad. Sci. Atmos. Oceanic. Phys., (in Russian)*, **6**, pp. 803-814.
7. Neumann, G. (1942) Die absolute Topographie des physikalischen Meeresniveaus und die Oberflachenstromungen des Schwarzen Meeres, *Ann. Hydrograph. Marit. Meteorol.*, **No 70**, pp. 265–282.
8. Oguz, T., Aubrey, D., Latun, V., Demirov, E., Koveshnikov, L., Sur, H.I., Diaconu, V., Besiktepe, S., Duman, M., Limeburner R. and Eremeev, V. (1994) Mesoscale circulation and thermohaline structure of the Black Sea observed during Hydro-Black'91, *Deep-Sea Res. I*, **14**, pp. 603–628.
9. Oguz, T., La Violette, P. and Unluata, U. (1992) The upper layer circulation of the Black Sea: Its variability as inferred from hydrographic and satellite observations, *J. Geophys. Res.*, **97 (C8)**, pp. 12569–12584.
10. Oguz, T., Malanotte-Rizzoli, P. and Aubrey, D. (1995) Wind and thermohaline circulation of the Black Sea driven by yearly mean climatological forcing, *J. Geophysi. Res.* **100 (C4)**, pp. 6845–6863.
11. Oslu, O. (1992) Strategy decisions for the protection of coastal waters against pollution, in *Problems of the Black Sea*, MHI UAS, Sevastopol, pp. 29–42.
12. Ovchinnikov, I. and Popov, Yu. (1984) On the formation of a cold intermediate layer in the Black Sea, *Dokl.AN USSR, (in Russian)*, **279(4)**, pp. 986–989.
13. Pacanowski, R. and Philander, S. (1981) Parameterization of vertical mixing in numerical models of tropical oceans, *J. of Phys. Oceanogr.*, **11**, pp. 1443-1451.
14. Sarkisyan A. (1995) Analysis of model calibration results: Atlantic Ocean climatic circulation, *J. of Marine Systems*, **6**, pp. 47–66.
15. Sarkisyan, A. and Demin, Yu. (1983) A semidiagnostic method of sea currents calculation, in *Large-scale oceanogrphic experiments in the WCRP, WCRP Publications Series, Tokyo*, **2, 1**, pp. 201–214.
16. Simonov, A., Altman, N. (eds.) (1991) *Reference book "The USSR Seas" Project, Hydrometeorology and marine chemistry of USSR seas. Volume IV. The Black Sea. Issue 1. Hydrometeorological conditions, (in Russian)*, Gidrometeoizdat, St. Petersburg.
17. Trukhchev, D. (1992) Numerical modelling of the Black Sea climate based on hydrological data from observation - results and problems, in *Problems of the Black Sea, MHI UAS, Sevastopol*, pp. 83–90.
18. Trukhchev, D. and Demin, Yu. (1992) *The Black Sea general circulation and climatic temperature and salinity fields*, Woods Hole Oceanog. Inst. Rept., WHOI-92-34, CRC-92-02.
19. UNESCO (1976) Seventh report of the joint panel on oceanographic tables and standarts, *UNESCO Techn. Papers. Mar. Sci.*, **24, App. 1**, pp. 39–54.

COLD INTERMEDIATE WATER FORMATION IN THE BLACK SEA. ANALYSIS ON NUMERICAL MODEL SIMULATIONS

J. V. STANEVA and E. V. STANEV
Department of Meteorology and Geophysics
University of Sofia
5, J. Bourchier street, 1126 Sofia, Bulgaria

Abstract

We use numerical ocean circulation model as a tool to produce data, which are analyzed with a focus on the water mass formation. Some hypotheses about the mechanisms of cold water formation, based on observations, are validated using model simulations. The results indicate that the cold water is formed mostly on the shelf and on the continental slope and then is transported by the main cyclonic gyre into the basin interior and into the deeper layers (up to 100-120 m). Anticyclonic eddies between the Black Sea front and the coast enhance the penetration of cold water into the halocline. This mechanism is very efficient west of Crimea Peninsula. The areas of maximum cooling and the ones of formation of extremely low temperatures do not coincide. This suggests that the regionalization of cold water formation needs to be further elucidated in its intimate relation with the ocean-atmosphere heat exchange.

1. Introduction

Ocean convection initiates when the surface forcing is sufficiently strong, and is facilitated in the areas of weak vertical stratification. The Gulf of Lions, where the deep Mediterranean Sea water forms, is a typical example of efficient preconditioning. As shown by numerous studies in this area, the upwelling, associated with cyclonic circulation, supplies surface layers with more saline water, thus reducing the stability of the stratification. It could be expected that the displacement of the pycnocline in the Black Sea, associated with the gyre and synoptic circulation, will also dominate the water mass formation. This is the main issue, which we address in the present study.

The autumn-winter cooling is very effective in the northwestern Black Sea. The atmospheric conditions in the cold part of the year are characterized by bursts of cold winds, causing large differences between atmospheric temperature and Sea Surface

E. Özsoy and A. Mikaelyan (eds.), Sensitivity to Change: Black Sea, Baltic Sea and North Sea, 375–393.
© 1997 *Kluwer Academic Publishers.*

Temperature (SST). This results in a strong cooling, triggering the winter convection. However, it is blocked by the stable stratification, and does not penetrate below the halocline. The reduced mixing in the seasonal thermocline tends to decrease heat flux from above, and the cold water remains sandwiched between surface and deep layers as in a thermostat (Friedrich and Stanev, 1988; Stanev, 1988, 1990). The observations show that the Black Sea Cold Intermediate Layer (CIL) is usually observed between depths 40-120 m (the 8°C isotherms mark its upper and lower boundaries).

The first ideas about the CIL (Knipovich, 1932; Zubov, 1938) suggested that it was a result of basin-wide local convection. Later, it was found that in most of the sea the temperature in its core was lower than the minimum temperature in the mixed layer (Kolesnikov, 1953; Filippov, 1965). This fact gives an evidence that Cold Intermediate Water (CIW) is advectively penetrating throughout the sea. This idea was explored by Georgiev (1972), based on analysis of survey data, and by Stanev (1988, 1990), based on model simulations, where it was proved that the cold water originated from the shelf area. The analysis of model simulations in the above studies elucidated new details of the CIW formation, proving that the low salinity at the sea surface, originating from rivers, tends to decrease the cooling capabilities and the penetration of cold waters into the deeper layers.

A different view point on the mechanisms of the CIW formation (Ovchinnikov and Popov, 1987) suggests that substantial amount of CIW are formed in the centers of the cyclonic eddies. Newly generated cold surface waters spiral along the dome-shaped isopycnal surfaces. This idea focuses on the existence of different (dynamically and regionally) mechanisms and sources of CIW. Recently, Ivanov *et al.* (1996, see also their paper in the present volume) found that CIW form on the Northwestern shelf, but most of them are stored in the regions, where the circulation is anticyclonic.

We will not discuss here the interpretation of the observational data, but will only remind that finding clear illustrations of convection is a difficult task. The survey data are insufficient to distinguish which areas favor the CIW production. Even more difficult is to specify the local characteristics of the convection. Much intuition was perhaps involved in the speculations about the origin and the fate of the CIW. We have to admit that the existing hypothesis are based on analyses of experimental data, taken usually in limited regions and for relatively short time. No comprehensive process studies exist, thought its has been studied, along with other thermohaline features, in the model simulations by Stanev (1988, 1990). However, the horizontal resolution was insufficient to estimate the impact of eddies on the CIW formation.

The present paper could be regarded as a complementary study to the experimental works, aiming to verify some of the existing hypothesis. We will confine our task to giving illustrations of the preconditioning of winter convection and on the phenomenology of CIW, as simulated by the model. In contrast to the previous studies (Friedrich and Stanev, 1988; Stanev, 1988; Stanev 1990) we focus on the effect of eddies on the CIW formation.

2. Model description

This study employs Pakanowski *et al.* (1991) version of Bryan-Semtner-Cox model. Convection is parameterized by convective adjustment. Solid boundaries are non-slip and insulating for temperature and salinity. The bottom is free sleep and insulating. The horizontal resolution is 1/12 in latitude and 1/9 in longitude, giving almost square grid elements. The model has 24 vertical levels, with model depths at 2.5, 7.5, 12.5, 17.5, 25, 35, 45, 55, 65, 75, 85, 105, 140, 185, 240, 310, 400, 515, 665, 870, 1145, 1470, 1820, 2125m. Bottom topography (Figure 1) is discretized from UNESCO bathymetric map with the model resolution. The wide and rather shallow shelf in the northwestern Black Sea is resolved correctly, since the first four model levels are sufficiently thin (5 m).

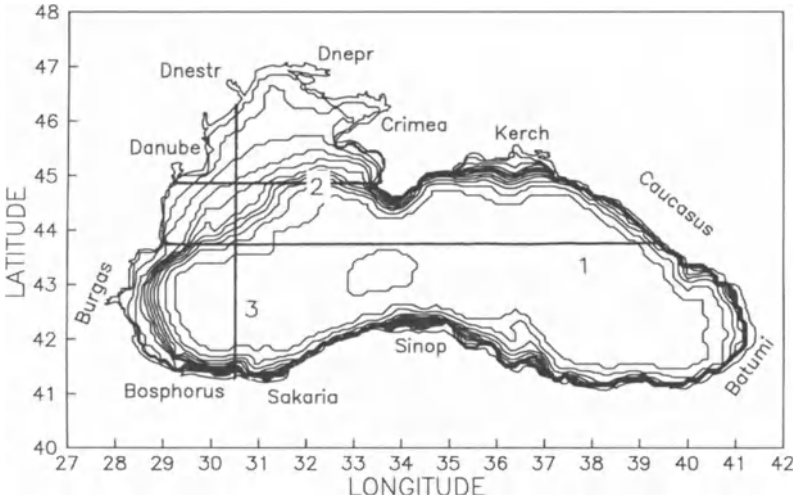


Figure 1. Model topography. Isolines are plotted at 12 model levels: 7.5 17.5, 35, 55, 75, 105, 185, 310, 515, 870, 1470, 2125 m. The three strait lines (1, 2, and 3) specify the vertical cross-sections, which are analyzed further in the text.

Subgrid scale processes in the horizontal are parameterized with biharmonic operators. The coefficients of mixing and diffusion are 0.1×10^{19} cm^4 s^{-1} . The vertical mixing coefficient is 1.5 cm^2 s^{-1}, the vertical diffusion coefficient is stability dependent (Gargett, 1984; Lewis and Landing, 1991; Stanev and Staneva, 1996a, b).

The model is forced by wind stress and net heat flux, which are parameterized using bulk formulae (Staneva *et al.*, 1995). The meteorological data needed for the parameterization are winds, atmospheric temperature, vapor pressure at 1000 mb, and cloudiness. The value of SST in the parameterizations for wind stress and for heat flux is set to be equal to the current model SST.

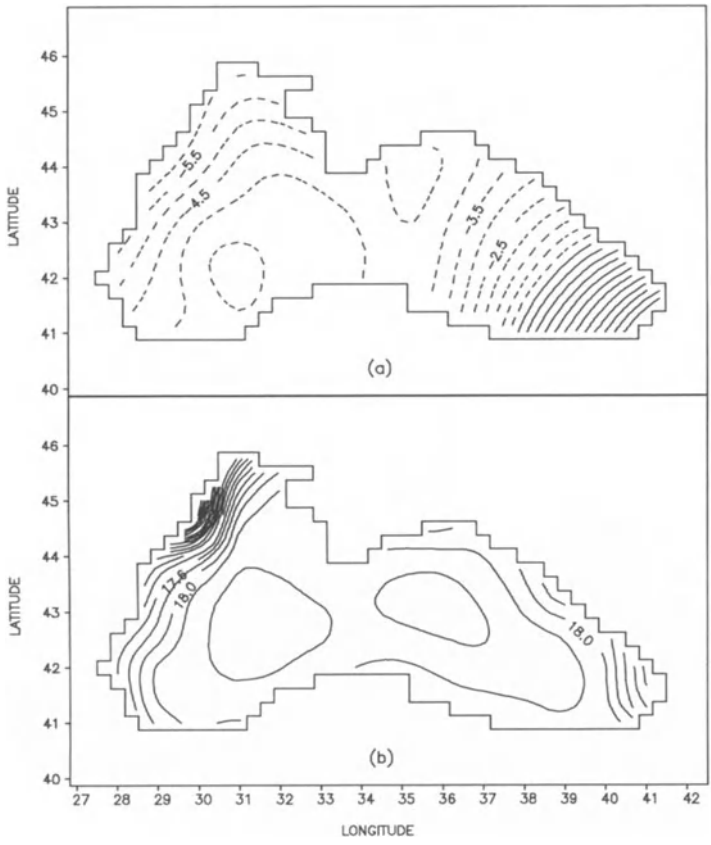


Figure 2. Model thermohaline forcing at 28 February 1986. (a) air temperature (Contour Interval, CI=0.5 °C); (b) climatological salinity (CI=0.2 psu). Negative temperatures are plotted with dash lines. The horizontal resolution is 0.25°, corresponding to the resolution of the original forcing data (Stanev and Staneva, 1996b).

The atmospheric forcing data is based on twice daily atmospheric analysis data and climatic data. For more details about the forcing data set we refer to the paper by Stanev and Staneva (1996b). As an illustration of the cooling potential, we show in Figure 2a the atmospheric temperature for 28 February 1986.

The sea surface salinity is relaxed to time variable data, interpolated linearly at every model time step from monthly mean climatological data. The salinity forcing for the same moment as in Figure 2a is shown in Figure 2b. The salt balance in the model is closed at the Strait of Bosphorus, where the salt flux is calculated from diagnosed at sea surface salt flux, using simple model for the water exchange in the strait. This approach, its relevance to the Black Sea conditions and the details related to its implementation are described by Stanev and Staneva (1996b).

We integrate a coarse resolution version of the model (Stanev and Staneva, 1996b) for 20 years with seasonally variable atmospheric forcing until quasiperiodic

solution is reached. Then the fine resolution model is initialized with the data, simulated in the coarse resolution model and is integrated further for 6 years (beginning from 1 January 1980). The forcing has seasonal, as well as high frequency variability and corresponds to the real time atmosphere. Most of the results in this paper are shown for 1986. More detailed analyses on the model performance, focused on basin mode oscillations, baroclinic instabilities and eddy formation, can be found in the paper by Stanev and Staneva (1996a).

3. Model circulation and preconditioning for convection.

The model circulation provides the local peculiarities, preconditioning winter convection, therefore we give a short analysis on this physical background. The currents (Figure 3) show one gyre system. The total transport is about 5.5 Sv, ranging from 4 Sv in summer to 7 Sv in winter. A typical feature in the simulations is the existence of anticyclonic eddies between the main gyre and the coast. They are very well pronounced along the southern coast and persist during the whole year. This result is in a good qualitative agreement with the patterns, based on observations (Oguz *et al.*, 1992). The vertical circulation, associated with these eddies, could enhance water mass formation, which we will prove in the paper.

Eddies form in the eastern Black Sea and propagate westwards, dissipating along the western coast. This behavior is a combined effect of the basin oscillations, Rossby and topographic waves. The synoptic/subbasin scale eddies have diameters between 50 and 200 km. More careful analyses on their evolution (see further in the text) indicates that there are periodic transitions of circulation from a state of intense eddy activity (as in Figure 3) to states with smaller meanders and eddies (Figure 4c). This process has interannual time scales and is related to oscillations in the baroclinic field (Stanev and Staneva, 1996a; Rachev and Stanev, in the present volume).

The minimum SST is about 2 °C in the western coastal area. The dashed lines, originating from this area, follow the coast, reaching Sakarya Canyon. The SST is much higher in the eastern Black Sea (about 11 °C at sea surface). Unlike the smooth atmospheric forcing (Figure 2a), the simulated temperature in the mixed layer (Figure 3b) is dominated by strong fronts, meanders and filaments. This gives an example how close the mixed layer temperature (further in the text we will refer to mixed layer temperature as to SST) "follows" the air temperature. The large differences between the two patterns suggest that the correlation between SST and air temperature could have an important impact on the ocean-atmospheric exchange. This impact, and particularly the contribution of eddies, is underestimated in the coarse resolution models.

The Black Sea meanders, and eddies are of primary importance for the water exchange between coastal and open sea waters, and could have crucial biogeochemichal consequences. Their correct simulation is very important in the coupled physical/biological models because significant amount of nutrients are delivered in the coastal areas by rivers and transported by the meandering currents to

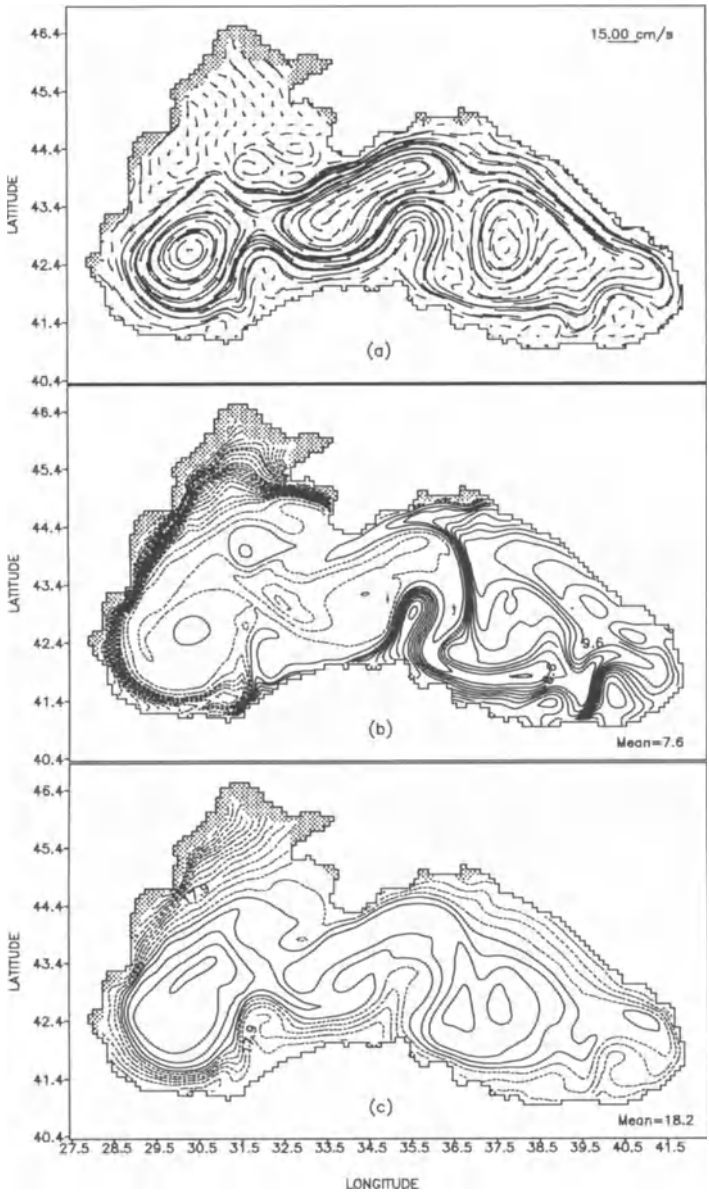


Figure 3. Simulated horizontal patterns at 17.5 m for 28 February 1986. (a) velocity, the arrow in the upper right corner gives the magnitude of the current; (b) temperature, CI=0.2 °C; (c) salinity, CI=0.1 psu. Mean values are given in the lower right corner of each plot. Values, lower than the mean, are plotted with dash lines.

the south and in the basin interior. We refer here to the patterns of plankton and suspended matter, observed using satellite data (Sur *et al.*, 1993) as an indirect prove that the model simulations give consistent mesoscale features. From the viewpoint of the present study, more important for the formation and fate of the CIW is the role of mixing induced by eddies. The close correlation between the simulated temperature and the Advanced Very High Resolution Radiometer data for the same time of the year (Figure 21 from the paper by Sur *et al.*, 1993) proves that simulated cooling is realistic.

The salinity pattern at 17.5 m (Figure 3c) shows that the model dynamics dominates salinity in the mixed layer (no filaments or meander-like features are observed in the climatoliogical data, Figure 2). It is noteworthy that the model generates anticyclonic circulation in the area, where the well known Batumi eddy is usually observed. The horizontal gradients of salinity in the shelf area decrease rapidly with increasing depth, and the isolines tend to follow the continental slope. At deeper layers salinity is very homogenous, which is in agreement with the observations (the maximum contrast at 450 m for the whole basin reaches about 0.2 psu).

It follows from the above discussion that the preconditioning for convection depends not only on the local atmospheric conditions (strong cooling of the northwestern shelf), but it has also dynamical dependency (basin circulation, pronounced eddies and meandering). To better understand the fate of the CIW, we show several snapshots of the depth of the isopycnal surface σ_t =14.8 (Figure 4) and the temperature patterns (Figure 5) for the same surface. To facilitate reading the figures, we plot the negative anomalies with dash lines (mean values are also shown). The depth of the isopycnal surface ranges from 30-40 m in the interior Black Sea to about 100 m at the periphery. Strong meanders are simulated in winter along the southern coast (Figure 4a), and more than five anticyclonic eddies are observed between the gyre and the coast in spring (Figure 4b). The pattern is smoother in summer (Figure 4c) and much smoother in fall (not shown here). This seasonal evolution is dominated by strong interannual signal (Stanev and Staneva, 1986b; Rachev and Stanev, in the present volume).

Though the vertical mixing in the Black Sea is small, due to strong stratification, the diapycnal fluxes are not negligible, particularly in the surface layers. The temperature exhibits large variations throughout the year (Figure 5). There are some important common features in the warm part of the year: (1) the temperature increases in the basin interior, where the distance between the pycnocline and the sea surface is small, (2) the water at the periphery has the T-S characteristics of the CIW. The fact that the temperature field shows large contrast on the isopycnal surfaces, speaks that it has an important (independent from salinity) role for the thermodynamics of surface layer. This becomes more clear if we compare the patterns in the warm and cold part of the year. The opposite sign of temperature anomalies shows that the buoyancy flux due to heating from the atmosphere changes direction, thus the instability increases in winter.

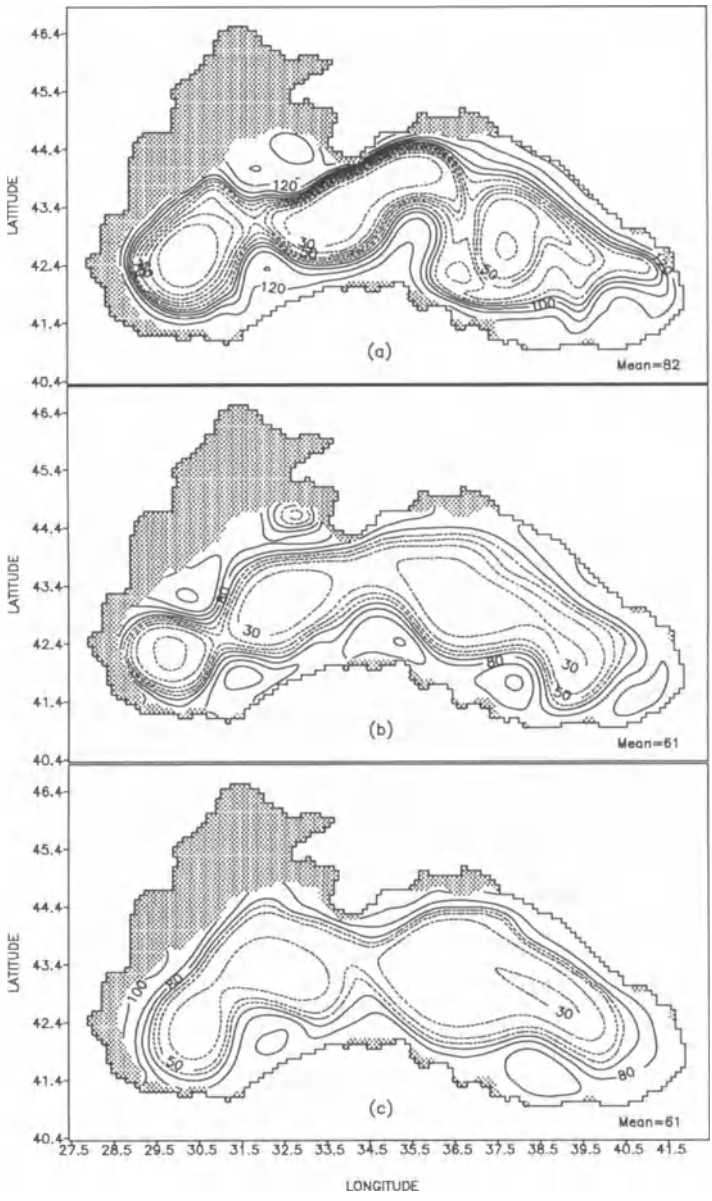


Figure 4. Depth of the isopycnal surface σ_t=14.8, CI=10 m. Mean values are given in the lower right corner of each plot. Values, lower than the mean, are plotted with dash lines. (a) 28 February 1986; (b) 28 May; (c) 28 August.

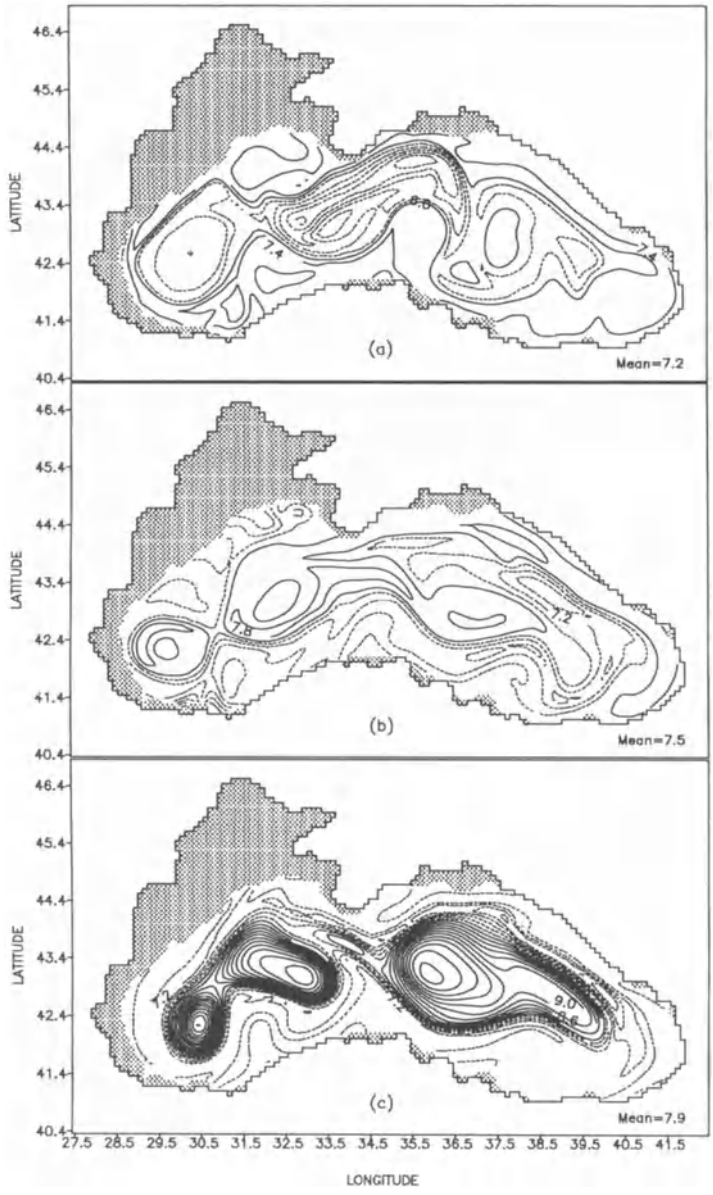


Figure 5. Temperature on the isopycnal surface σ_t=14.8, CI=0.2 °C. Mean values are given in the lower right corner of each plot. Values, lower than the mean, are plotted with dash lines. (a) 28 February 1986; (b) 28 May; (c) 28 August.

To the west of the Crimea Peninsula temperature patterns in spring indicate cold water intrusions from the shelf. These waters reach the deepestmost part of the isopycnal surface at the southern boundary of the anticyclonic area (approximately in the frontal zone, compare Figure 4b and Figure 5b). Not everywhere is the coldest water simulated at the deepestmost part of the isopycnal surfaces. In spring (Figure 5b), it is associated with the southern branch of the gyre. This pattern can be traced along the jet current in the eastern Black Sea, and reaches the area south of Crimea Peninsula. In summer and fall (Figure 5c), the model simulates much narrower (than in spring) band of cold water, associated with the areas with largest slope of the pycnocline. It originates from the eastern Black Sea and makes almost a complete loop, reaching the area north of Sakaria Canyon in fall. It is obvious that the isopycnic cross-sections in Figure 5 "see" the core of the CIL just at the area of the strongest slope of the pycnocline. This presents a nice illustration how important is the horizontal advection for the fate of the CIW.

4. Formation and fate of the CIW

The vertical cross-sections (Figure 6-Figure 8) are plotted along the section lines, shown in Figure 1: "1" is east-west section along 43.6 °N, that is crossing the central part of the sea, "2" is north of" 1", and crosses the Crimea Peninsula at 44.6 °N, "3 is meridional section, plotted across the shelf. The vertical patterns of meridional velocity make easier to identify the location of the eddies and to illustrate the role of baroclinicity for velocity change with increasing depth. The shape of the isolines illustrates the areas of the CIW formation and the blocking of convection in the halocline. We analyze the model results for 28 February 1986, when the atmospheric temperature was extremely cold (Figure 2a).

There is a good correlation between the temperature and salinity plots (Figure 6a, b) and the one of meridional velocity (Figure 6c) below 100-150 meters, particularly in the western and central Black Sea. The centers of eddies coincide with the doomed isolines. The upwelling, associated with the cyclonic gyre in the central Black Sea, results in a shallower position of the halocline than in the coastal area (the corresponding locations are marked by numbers 2 and 3 on the plot). The layer down to about 50-70 m is rather homogeneous, and the processes depend on the local interaction with the atmosphere. One general rule is noteworthy: the waters in the areas of anticyclones are warmer than in the areas of the cyclones. A simple explanation of this result can be given, having in mind that the depth of convection depends on position of the pycnocline. Relatively smaller volume of water releases heat to the atmosphere in the area of cyclonic circulation, thus the thermal capacity is smaller, and the cooling is stronger. On the opposite, SST is higher in the anticyclones, due to the larger thermal capacity. In brief, cooling in the areas of cyclones (measured by temperature) is stronger, but this does not mean that the heat, released to the atmosphere is largest there. This issue was overlooked in some interpretations of the observations, mainly due to insufficient amount of winter data.

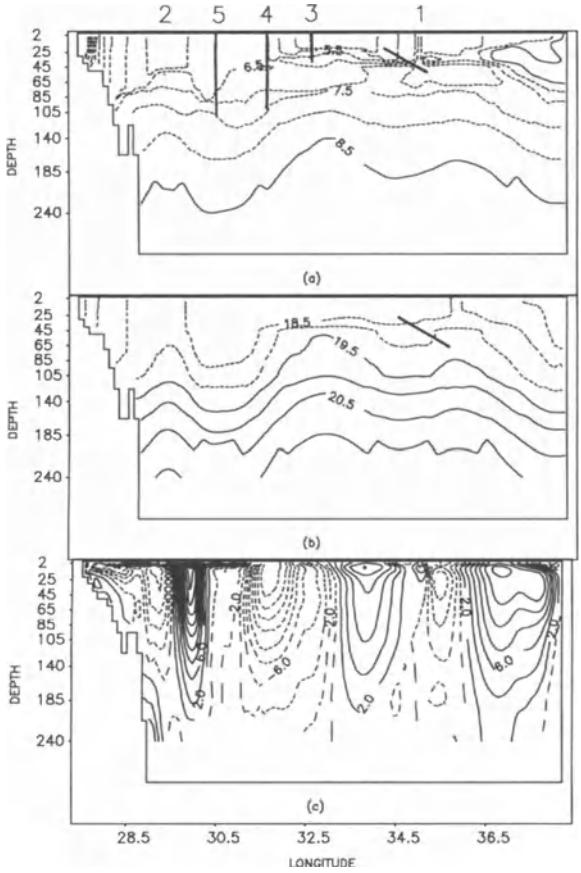


Figure 6. Vertical cross-sections (28 February 1986) along 43.6 °N, the zonal line 1, shown in Figure 1. (a) temperature, values lower than 8 °C are plotted with dash lines, CI=0.5 °C; (b) salinity, values lower than 19 psu are plotted with dash lines, CI=0.5 psu; (c) meridional component of velocity, negative values are plotted with dash lines, CI=2 cm s^{-1}. The difference of the bottom line in (c) from the ones in (a) and (b) is due to the specific location of model grid points for temperature/salinity and velocity.

We argue that the regionalization of winter cooling has to take into account the heat exchange with the atmosphere, or the heat content during the cooling events.

The cyclones are filled with very cold water (Figure 3b and Figure 5a), which is further advected and mixed in the horizontal by eddies. This can be regarded as a support of the hypothesis of Ovchinnikov, but we stress here that we have to distinguish between formation of cold water and its further transport or modification by mixing or slant-wise propagation.

The role of the downwelling in the area of the anticyclones for the CIW formation is illustrated by the zonal cross-section across the southern Crimea Peninsula (Figure 7). We remind that the circulation west of the Peninsula is dominated by anticyclonic

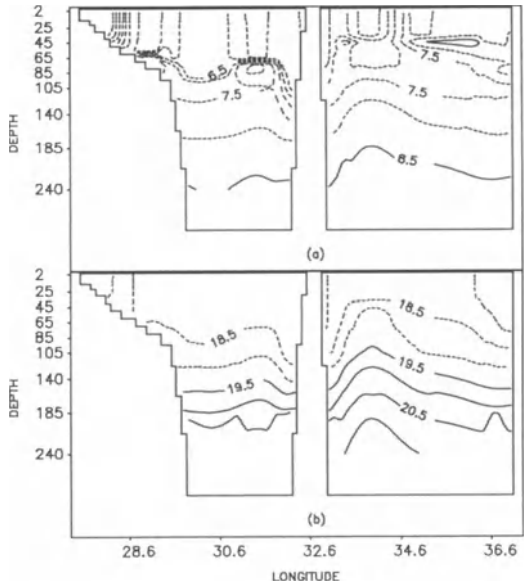


Figure 7. Vertical cross-sections (28 February 1986) along 44.6 ° N, the zonal line 2, in Figure 1. (a) temperature; (b) salinity. The notations are as in Figure 6.

eddy (see also Figure 3a, 4a and 5a). This contributes to increasing depth of the mixed layer to 120-140 m, which is an extremely deep penetration of CIW for this basin.

The cold subsurface anomaly along the southern coast on the meridional cross-section of temperature (Figure 8) illustrates the role of advection for the propagation of CIW basinwide. The local downwelling north of Sakaria Canyon results in the vertical elongation of cold water core. This water is transported from the northern area, following the coast. The cooling of the northwestern shelf, seen on the same figure, deserves more explanation. Cold waters are "trapped" on the shelf and separated from the open sea waters by the Black Sea frontal zone (see the vertical isotherms, which are close one to another over the slope). Convective coiling reaches the bottom layer, and the isotherms follow the slope, down to about 65-75 meters. Currents and mixing carry this cold water further south in the basin interior. This simulation correlates with the speculations of Georgiev (1967, 1972), proving that part of the CIW is formed on the shelf. Here we stress on two important details, which are often overseen, when addressing the CIW formation. First, the slope of the isotherms on the shelf is smaller than over the continental slope. This proves that the lower salinity in the shelf area inhibits convective cooling. Second, the isotherms tend to follow the continental slope. Similar trend can be found in the western part of the zonal cross-section (Figure

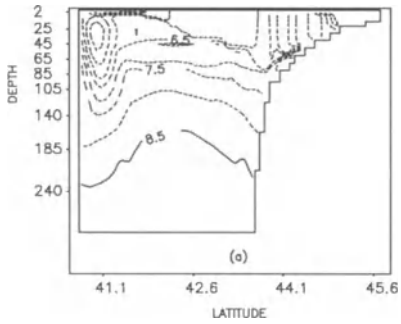


Figure 8. Vertical cross-section of temperature (28 February 1986) along 30.5 °E, the meridional line 3 in Figure 1. The notations are as in Figure 6.

7a). Obviously, the continental break favors deeper penetration of cold water, whereas the northwestern shelf limits geometrically (small depth) and thermodynamically (low salinity) the depth of convection (see also Stanev, 1990). The anticyclonic circulation on the continental slope tends to increase this depth. On the opposite, convection reaches smaller depths in the interior basin (Figure 8) and in its eastern part (Figure 7a) due to cyclonic circulation and less cooling from the atmosphere. The transport of warmer water from the eastern basin (see the advection pattern in Figure 3b) also tends to locally decrease the depth of the convection (Figure 7a).

The formation of CIW and their evolution is controlled by diapycnal processes, thus presenting some of the simulations in σ_t-λ coordinates (λ is the longitude) can give more insight into the mixing of CIW and their penetration into the halocline. Vertical cross-sections along 43.6 °N (the zonal line 1 in Figure 1) for temperature and the depth of isopycnal surfaces are plotted in Figure 9-Figure 11 for the three moments, corresponding to Figure 5. We will discuss the above figures parallel with the z-λ plots in Figure 6. Several comments to the new type of plots are needed. The depth of the isopycnic surfaces in σ_t-λ coordinates (Figure 9b, 10b, 11b) shows an inverse shape to the one of the isohaline surfaces in z-λ coordinates (the isohaline surfaces approximately coincide with the isopycnic surfaces, particularly in the deep layers). Stronger stratification in the surface layer corresponds to larger σ_t-"thickness", and *vice versa* in the deep layers. This gives better resolution of the strongly stratified upper layer. In winter, some of the isopycnals outcrop, therefore the plots have evolving upper boundary. Most of the density volume (between σ_t=14 and σ_t=14.5) is empty in Figure 9 due to formation of heavy waters. The largest outcropping occurs in the area marked by 2 in Figure 6 and Figure 9. The isohalines S=18.5 psu cross the sea surface, and water with temperatures lower than 7.5 °C reaches the isopycnal surface σ_t=15 (about 100 m). We remind that "horizontal" tongues of temperature in the σ_t-λ coordinates indicate isopycnic mixing/penetration, whereas "vertical" gradients in the

same coordinates indicate diapycnal penetration. The last is well pronounced in winter and summer at the sea surface, indicating direct cooling or heating.

The largest gradients of temperature in the area of extreme cooling are identified by the thick line in area 3 (Figure 9a). This is the area of the dome-shaped pycnocline, marked by the same number in Figure 6a. The relatively small length of the vertical thick line indicates that large transformation of temperature, or diapycnal flux in the surface layers ($5°/1\sigma_t$ unit) are observed both in z and σ_t coordinates. The corresponding numbers for the areas marked by lines 4 and 5 (located on the slant of the pycnocline and in its trough) are $2°/1\sigma_t$ and $1.3°/1\sigma_t$. It is noteworthy that the extremely cold water, formed in the area of the central cyclone (Figure 3 and Figure 5a), shows a tongue propagating towards the area occupied by downwelling (line 1 in Figure 6a and Figure 9a). This cold water tends to penetrate into the "old" CIL. This type of transport is associated with the very strong temperature gradients in Figure 3a, extending from the area south of Crimea into the basin interior, and supports the mechanism, proposed by Ovchinnikov and Popov (1987). Even better illustration on this mechanism, is the cold tongue in Figure 5a propagating southwards.

The three plots in σ_t-λ coordinates demonstrate that the thickness of the CIL varies in wide rang. The weaker stratification in spring (than in summer) explains why the thickness, measured in σ_t coordinates, is larger. The space -dependency is well pro-

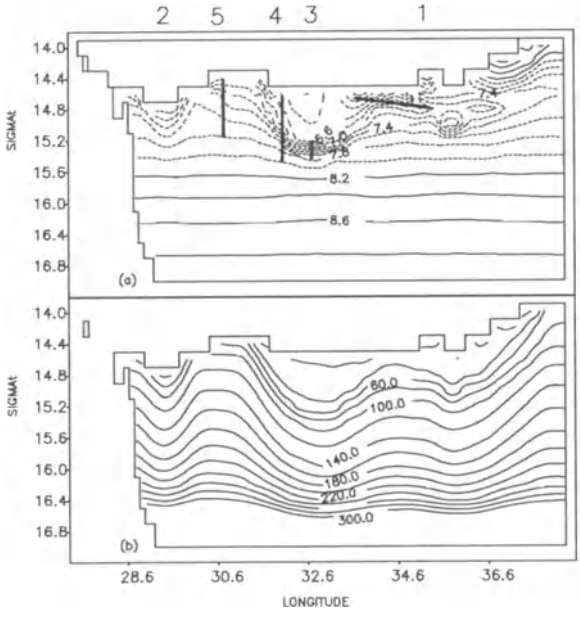


Figure 9. Vertical σ_t-λ, cross-sections (28 February 1986) along 43.6 °N, the zonal line 1 in Figure 1. (a) temperature, the isolines are plotted as in Figure 6; (b) depth of isopycnal surfaces, CI=20 m.

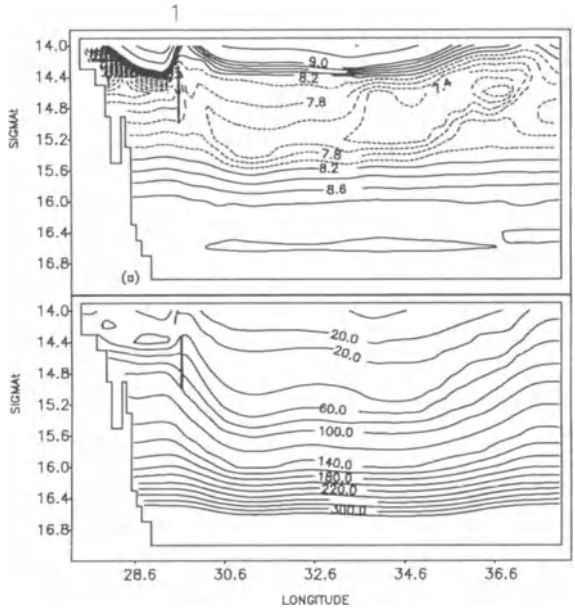


Figure 10. As in Figure 8, but for 28 May, 1986.

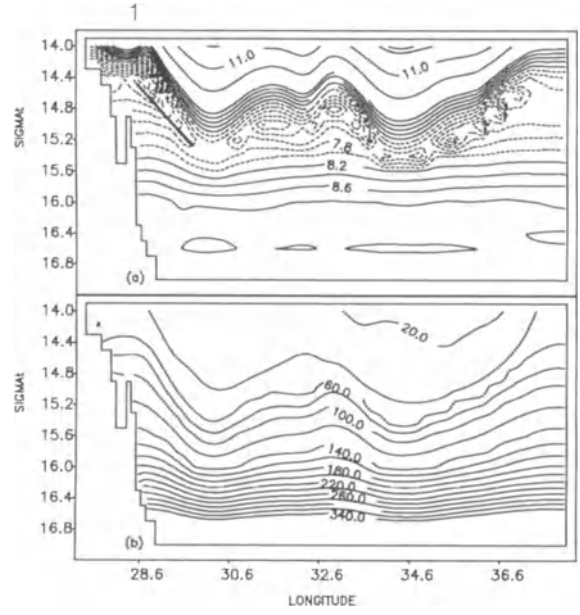


Figure 11. As in Figure 8, but for 28 August, 1986.

nounced in the summer cross-section (Figure 11), showing that the thickness of the pycnocline increases in the eastern Black Sea and in the areas of downwelling. It decreases in the areas dominated by cyclonic circulation. A source of cold water is seen in the westernmost part of this figure, indicating that cold waters penetrate into the basin interior from their reservoir, which is in the shelf/continental slope area. The propagation pattern is identified by the tongue in Figure 11a (see the thick line in the core). This water penetrates into the halocline (almost without deepening, at about 80 m) and constantly increases temperature. As seen from the spring cross-section (Figure 10a), the penetration of the CIW in the same area is along the isopycnals (horizontal in σ_t-λ coordinates). West of this area of intrusion, the model simulates an intense and localized downwelling (thick lines in area 1, Figure 10a, b), and the cold coastal waters reach σ_t =15. The two areas with cold waters (the one originating from` the shelf) and the CIL of the basin interior are separated by the Black Sea front.

5. Discussion and conclusions

The cooling capabilities and the cooling efficiency are of utmost importance for the CIW formation, but it is practically impossible to estimate them from the limited amount of survey data. Model estimates could give complementary understanding on this fundamental issue. Before making the final conclusions we will show the simulated heat flux between the Black Sea and the atmosphere for 28 February 1986, the mean heat flux for February 1986, and the annual mean heat flux for 1986 (Figure 12). The instantaneous patterns, or the ones averaged for shorter time, are characterized by very strong gradients (the three plots have the same contour interval of 20 W m^{-2}). The maximum cooling reaches locally more that 500-600 W m^{-2}. The eastern area exhibits less cooling at 28 February 1986, which can be explained by the higher atmospheric temperatures in the same region (Figure 2a). More unexpected is that the shelf region is less cooled than the eastern area (about 20 W m^{-2}). This can be explained having in mind that the heat flux depends on the local difference between SST and air temperature. Due to the limited heat capacity on the shelf, the SST approaches the atmospheric temperature, which results in a decrease of the heat flux.

The pattern in Figure 12a is dominated by the model dynamics. The strongest cooling is in the area south of the Kerch Strait and north of the Turkish coast. The advection of warmer waters from the eastern basin enhances the cooling capabilities of the first area, whereas the anticyclonic circulation enhances the deep penetration of cold surface water in the second area and its thermal capacity (compare with the observation data of Sur *et al.*, 1994 for the same time of the year, their Figure 12). Comparison between the snapshot for 28 February 1986 and the monthly mean heat flux indicates that short periodic variability dominates the heat exchange. Thus, limited number of instantaneous patterns is not sufficiently representative for the cooling conditions (cooling in the area of the southern coast is not seen, and the north-western shelf is cooled relatively more efficiently in the monthly mean patterns). More important is that there is a good agreement between the patterns of maximum depth of winter convection, estimated from observations (Figure 2.29 of Gertman,

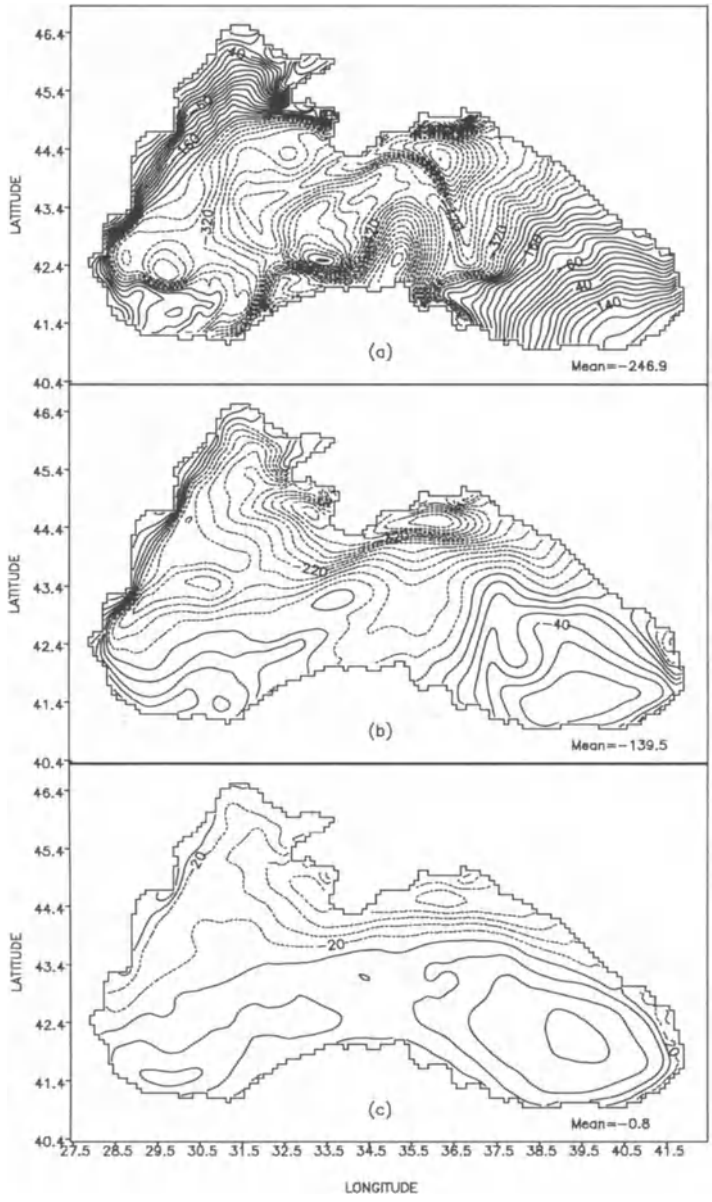


Figure 12. Heat flux at sea surface, CI=20 W m^{-2}. Mean values are given in the lower right corner of each plot. Values, lower than the mean, are plotted with dash lines. (a) 28 February 1986; (b) mean for February 1986; (c) annual mean for 1986.

1991), and the maximum of simulated cooling, west of Crimea. Obviously, this is dynamically important area, where the downwelling, associated with anticyclonic eddies and the slope convection, contribute substantially for the CIW formation. Not less important is the second cooling area, south of Kerch Strait, where the cooling capacity is a function of local forcing and advection from the eastern Black Sea. The narrow band of reduced cooling along the western coast also deserves attention. This feature correlates with the simulated salinity in the surface layer (Figure 3c), and can be explained by the large river discharge in this area, diluting waters at sea surface and increasing stability of the stratification. This results in smaller depth of convection, thus cooling capabilities decrease. SST approaches the atmospheric temperature, and further cooling stops.

Coming back to the hypotheses about the formation of CIW, we argue that areas of extreme cooling (measured by SST) and of most efficient cooling (measured by the heat exchange) do not coincide. This could motivate further studies, aiming to quantify the details related to the CIW formation. We believe that the contribution from the areas of most intense cooling, as specified in Figure 12b (part of the shelf, the area of anticyclonic circulation west of Crimea, and the local area south of Kerch Strait), will be demonstrated by further process studies and observations. The extremely good correlation between the simulated annual mean heat flux (Figure 12c) and the estimates from observations (Figure 1.12 of Gertman, 1991) is very promising. Below we summarize briefly the more important results of the paper.

A typical feature in the model simulations is the existence of anticyclonic eddies between the main gyre and the coast, enhancing the downwelling and giving a net contribution to the pumping of cold water into the CIL. Three types of penetration of CIW in the halocline were considered, which are *related to mesoscale processes*. The first one is illustrated by the slant-wise motions along the doomed isohalines, which supports the speculations of Ovchinnikov and Popov (1987). The second type is dominated by the downwelling in the areas of the anticyclones. This is perhaps a very efficient mechanism, supplying the halocline with cold water. It is important to note that this efficiency is mostly due to the specific circulation in the Black Sea: anticyclonic eddies are located between the main gyre and the coast, which approximately coincides with the zone of most intense cooling. Cold waters are usually "trapped" along the shelf edge/continental slope in the upper layers, and follow the isobaths 65-75m. The continental break favors the slope convection, and we classify this as the third type of CIW penetration.

Acknowledgments. We thank L. Ivanov for the useful comments. This work was supported by the contract with the CEC No ERBCIPDCT940501.

References

1. Filippov D. M. (1965). The cold intermediate layer in the Black Sea. *Oceanology*, **5**, 47-52.

2. Friedrich, H., J, and Stanev E. V., 1988: Parameterization of the vertical diffusion in a numerical model of the Black Sea. in J. C. J. Nihoul and B. M. Jamart (eds.), *Small-scale turbulence and mixing in the ocean.* Elsevier, pp.151-167.

3. Gargett, A., E., 1984. Vertical eddy diffusivity in the ocean interior., *J. Mar. Res.*, **42**, 359-393.

4. Georgiev, Yu. S. (1967). On dynamic of cold intermediate layer in the Black Sea. in *Okeanograficheskiye issledovaniy Chernogo Morya (Oceanographic Investigations of the Black Sea).* Naukova Dumka, Kiev, pp. 105-113, (In Russian).

5. Georgiev, Yu. S. (1972). About the advective nature of the cold intermediate layer in the Black Sea. *Biologiya moria*, **24**, 81-89, (In Russian).

6. Gertman, 1991. Struktura vod moria. (Composition of sea water). in A. I. Simonov and E. N. Altman (eds.) *Hydrometeorology and hydrochemistry of the USSR Seas.* Vol. **4**: The Black Sea. pp. 166-174, (in Russian).

7. Ivanov, L I., Besiktepe S., Nikolaenko E., Özsoy E., Diaconu V., and Demirov E. (1996). Volumetric fine structure of the Black Sea cold intermediate layer. *Deep Sea. Res.* (Submitted manuscript).

8. Knipovich, N. M. (1932). The hydrological investigations in the Black Sea, Trudi Azovo-Chernomorskoy Nauchnopromyslovoy Ekspeditsii, 1932, **10**, 274 p., (In Russian).

9. Kolesnikov (1953), Seasonal course of temperature, stability and vertical turbulent heat exchange in the open part of the Black Sea, *Trudi Mor. Gudrol. Inst. USSR AS*, **3**, 3-13, (In Russian).

10. Lewis, B. L. and Landing W. N. (1991). Manganese and iron in the Black Sea., *Deep Sea Res.*, **38**, S773-S805.

11. Oguz, I, La Violette P. E., and Ü. Ünluata (1992). The upper layer circulation of the Black Sea: its variability as inferred from hydrographic and satellite observations, *J. Geophys. Res.* **97**, 12569-12584.

12. Ovchinnikov, I. M. and I. Popov Yu. (1987). Evolution of the Cold Intermediate Layer in the Black Sea. *Oceanology*, **27**, 555-560.

13. Stanev, E. V., 1988 Numerical study on the Black Sea circulation. *Mitteilungen des Instituts für Meereskunde der Universität Hamburg*, **28**, 232 p.

14. Stanev, E. V., 1990. On the mechanisms of the Black sea circulation. *Earth-Science Rev.*, **28**, 285-319.

15. Stanev, E. V. and Staneva J. V., (1996a). The impact of the baroclinic eddies and basin oscillations on the transitions between different quasi-stable states of the Black Sea circulation. *J. Mar. Sys.*, in Ch. Mooers (ed.), special issue on the *Circulation of the semi-enclosed seas* (accepted manuscript).

16. Stanev, E. V. and Staneva J. V. (1996b). Numerical model of the Black Sea water mass formation. Tracer study on the surface and intermediate water. *Deep Sea Res.*, in D. Aubrey (ed.), special issue on the *Black Sea: Oceanographic variability*, (accepted manuscript).

17. Staneva J. V., Stanev E. V., and Rachev N. H. (1995). Heat balance estimates using atmospheric analyses data: A case study for the Black Sea. *J. Geophys. Res.*, **100**, 18581-18596.

18. Sur, H. I., Özsoy E., and Ünluata Ü. (1993). Boundary current instabilities, upwelling, shelf mixing and euthrophication processes in the Black Sea. *Progr. Oceanogr.*, **33**, 249-302.

19. Zubov, N. N. (1938). Marine waters and ice. Hydrometeoizdat, Moscow, 451p., (In Russian).

CIRCULATION IN SEMI-ENCLOSED SEAS INDUCED BY BUOYANCY FLUX THROUGH A STRAIT

G. K. KOROTAEV
Marine Hydrophysical Institute
Sevastopol, Crimea, Ukraine 335000

Abstract. A numerical study of the stratification and circulation in a circular basin under the influence of the lateral buoyancy fluxes is carried out. It is shown that the stratification and the horizontal circulation are supported by the upwelling in the open part of the basin, downwelling near the coast and diffusion. Numerical simulations confirm previous results predicting the three-layer structure of the circulation (cyclonic current- anticyclonic undercurrent- cyclonic current) under the influence of the lateral buoyancy flux for a set of parameters that are typical of the Black Sea.

1. Introduction

The famous papers by Robinson and Stommel [1], and Stommel and Arons [2] have given rudimentary explanations of the world ocean stratification and the mid-ocean and the deep-ocean thermohaline circulations. The ocean thermocline is supported by deep water upwelling in the major part of the ocean, and deep water is formed in the near-polar regions due to the winter convection penetrating to large depths.

It is interesting to note that the deep water in semi-enclosed seas is also formed in very restricted areas. The formation of the deep water in the Mediterranean occurs in localised regions and it is sporadic in time. The Black Sea deep water has been formed due to the mixing of the Black Sea upper layer water and salty Mediterranean water of the Marmara Sea supplied by the flow through the Bosphorus Strait. The depth on which the salty water penetrates and spreads in the Black Sea is the fundamental problem of the Black Sea hydrology [3,4,5,6].

The stratification of the Black Sea is mainly haline and defined by the salinity of the Mediterranean water entering from the Marmara Sea. The haline circulation in the Black Sea should be more intensive than the thermal circulation in the world ocean since the Black Sea and Marmara Sea salinities are 18 and 36 respectively, equivalent to a difference of about 120°C in temperature if the linear state equation for the density is used. Therefore, if the thermal circulation at the world ocean is estimated as 0.1 cm/s [7] and it is produced by the equator-pole temperature difference of about 30°C,

E. Özsoy and A. Mikaelyan (eds.), Sensitivity to Change: Black Sea, Baltic Sea and North Sea, 395–401.
© 1997 *Kluwer Academic Publishers.*

then, remembering the size ratio, we can expect the haline circulation to be of the order of 10 cm/s in the Black Sea.

A simple non-linear model is proposed in this paper for the investigation of the stratification and the circulation of the semi-enclosed sea under the influence of the lateral buoyancy fluxes. The model is based on the following: Any field distribution on an offshore section of the Black Sea shows similar dynamical structures and features. Then, to a first approximation, it is helpful to consider the fields averaged along the coast (similar to zonal averaging applied to atmospheric models) and to model the Black Sea as a circular basin. Then the azimuthally averaged fields yield the first approximation to more complex three-dimensional dynamics, which we use to investigate the stratification and the circulation induced by the lateral buoyancy flux in the circular basin.

2. The Model

We consider a circular basin with the radius R and the depth H. All fields depend only on radial and vertical coordinates. In this case, the equations that describe the field distribution along the radial section have the following form

$$-fv = A_z \frac{\partial^2 u}{\partial z^2} + A_l \frac{1}{r}\frac{\partial}{\partial r} r \frac{\partial u}{\partial r} \tag{1}$$

$$fu = -\frac{\partial p}{\partial r} + A_z \frac{\partial^2 v}{\partial z^2} \tag{2}$$

$$-g\gamma s = -\frac{\partial p}{\partial z} \tag{3}$$

$$\frac{1}{r}\frac{\partial rv}{\partial r} + \frac{\partial w}{\partial z} = 0 \tag{4}$$

$$\frac{\partial s}{\partial t} + v\frac{\partial s}{\partial r} + w\frac{\partial s}{\partial z} = \kappa_z \frac{\partial^2 s}{\partial z^2} + \kappa_l \frac{1}{r}\frac{\partial}{\partial r} r \frac{\partial s}{\partial r} \tag{5}$$

where r is the radial co-ordinate, z is the vertical one, t is time, u, v, w are azimuthal, radial and vertical velocity components, s is the salinity, p is the pressure anomaly normalised with the mean density. Equation (1) is the azimuthal momentum projection which is written in the linear approximation. Equation (2) represents the radial momentum balance where the lateral viscosity is omitted in addition to the non-linear terms as it is only important in the coastal boundary sublayer that is too thin to be resolved in our finite-difference scheme. The Coriolis parameter f is taken as constant, and A_z, A_l are coefficients of vertical and horizontal viscosity. The linear state equation is used in the hydrostatic equation (3) where γ is the salinity coefficient and g is the gravity acceleration. (4) and (5) are continuity and salt diffusion

equations, κ_z, κ_l are vertical and horizontal diffusion coefficients, respectively. The vertical axis is directed downward where $z = 0$ is the basin surface and $z = H$ corresponds to the bottom.

The following boundary conditions are prescribed at the surface and the bottom

$$\frac{\partial u}{\partial z} = \frac{\partial v}{\partial z} = 0, \; w = w_0(r), \; \kappa_z \frac{\partial s}{\partial z} - w_0(r)s = 0 \quad \text{at } z = 0 \tag{6}$$

$$u = v = w = 0, \frac{\partial s}{\partial z} = 0 \quad \text{at } z = H \tag{7}$$

where $w_0(r)$ is the precipitation-evaporation and fresh water input that models the river inflow from a point source at $r = R$. The boundary conditions at the center of the basin and on the side wall have the following form

$$u = v = 0, \frac{\partial s}{\partial r} = 0 \quad \text{at } r = 0 \tag{8}$$

$$\frac{\partial u}{\partial r} = 0, \; v = 0, \; \kappa_l \frac{\partial s}{\partial r} - v_b(z)(s - s_b(z)) = 0 \quad \text{at } r = R \tag{9}$$

where $v_b(z)$ is the strait inflow and outflow and

$$s_b(z) = \begin{cases} s, if v_b(z) > 0 \\ s_m, if v_b < 0 \end{cases} \tag{10}$$

where s_m is the Marmara Sea salinity.

The exchange through the Bosphorus Strait is parameterised by the following way: The total volume transport through the strait Q is assumed to be equal to the river inflow in any moment of time. The volume transport of the upper flow Q_+ and the lower flow Q_- are parameterised by the following formulae

$$\frac{Q_+}{Q} = \frac{11}{16} + \frac{21}{8}\frac{s_m - s}{s_m}, \qquad \frac{Q_-}{Q} = \frac{5}{16} - \frac{21}{8}\frac{s_m - s}{s_m} \tag{11}$$

where s is the upper layer salinity near the strait. Coefficients in these formulae are chosen in such a way that the present volume transports through the Bosphorus Strait and the salinity of the upper layer of the Black Sea satisfy (11). Linear approximation is used in (11) since only a stationary solution of the problem it is considered.

The system of equations (1)-(5) with boundary conditions (6)-(9) are solved numerically. Spatial derivatives are approximated on the shifted grids by central differences. The explicit Euler approximation is used for the time derivative.

3. Numerical experiments

Numerical experiments are carried out for a circular basin with a radius of 200 km and a depth of 2 km, i.e. a volume of about of 250 km^3. The depth, perimeter and volume of the basin roughly correspond to the deep basin of the Black Sea. The values of the Coriolis parameter is $f = 10^{-4} s^{-1}$, gravity acceleration is g=10 m/s, and $\gamma = 8 \times 10^{-4}$. The river inflow, uniformly distributed on the to have an average value of $Q = 46.3 \times 10^{-4} m^2/s$ per unit length of the perimeter, amounts to a total fresh water transport of about 200 km^3/yr. The salinity of the Marmara Sea water that flows into the Black Sea is equal to 36. The uniform grid contains 20x20 points. The horizontal resolution is 10 km and the vertical one is 100 m. The fresh water input is specified at the surface, and the salty water inflow is distributed between depths of 100-200 m along the perimeter. Mixed salty water leaves the basin within the upper 100 m of the perimeter. The volume transport through the strait is describes by formulae (11) where the salinity of the upper near-coastal box is substituted as the salinity for water leaving the basin. The basin is at rest, and filled by the fresh water at the beginning of calculations.

Two experiments are carried out using the same coefficients with and without convective adjustment. The reason to compare two runs is that the coast in the model is approximated by a vertical wall. The salty water input through the strait creates unstable stratification which is removed by means of convective adjustment. In the real sea the shelf slope does not allow unstable stratification to develop and salt water should be transformed at a slower rate than in the case of the convective mixture. Thus the experiment without the convective adjustment helps to estimate the significance of the salty water transformation near the strait.

The turbulent coefficients of horizontal viscosity and diffusion are taken as 57.9 m^2/s and 5.79 m^2/s, coefficients of vertical viscosity and diffusion are 11.6 $x10^{-4}$ m^2/s and $3.47x10^{-5}$ m^2/s, respectively for both runs. This set of coefficients will be cited as the basic ones in the following discussion. Numerical calculations show that, the only difference between the two experiments is the settling time to reach a stationary state. The stationary state is achieved after 15000 years of integration without the convective adjustment, instead of 2200 years when the convective adjustment is taken into consideration. The final stationary states are practically the same in both cases. The explanation is in the structure of the vertical cell that is developed at the end of integration (Fig.1). Strong downwelling near the coast promotes salt water mixing near the strait and the mixed water spreads to the bottom forming the neutral stratification even without the convective adjustment. Additional numerical experiments are carried out for different values of coefficients to study the sensitivity of modelled fields..

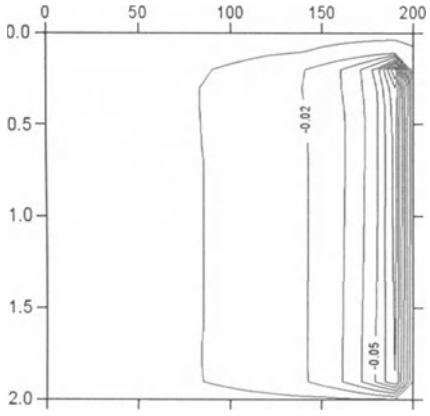


Figure.1. The stream function isolines for the basic experiment in 10^6 m^3/s. Vertical axis is the depth in kilometres Horizontal axis is the distance along the radius in kilometres.

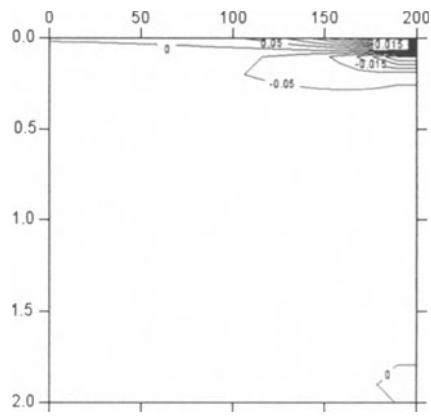


Figure.2. The azimuthal velocity isolines for the basic experiment in m/s. Axes are the same as for Fig.1.

The deep water salinity is close to that observed in the Black Sea for the basic set of coefficients. It varies from 23.009 near the coast to 22.995 in the center of the basin. The deep water salinity is very sensitive to the vertical diffusion coefficient. Decreasing the vertical diffusion coefficient by a factor of three increases the deep water salinity to a value of 25.7.

The halocline is supported by upwelling in the central part of the basin. The vertical velocity maximum is $3\text{-}4 \times 10^{-6}$ m/s and the volume transport of the vertical cell is 15 times larger than the transport of the lower Bosphorus flow. The intensity of the vertical cell depends significantly on coefficients of horizontal diffusion and vertical viscosity. Ten times decrease of the vertical viscosity produces almost three times decrease of the intensity of the vertical cell. Five times increase of the horizontal diffusion yields almost two times higher intensity of the vertical cell.

The salinity of the near-coastal upper box is determined by the outer salt balance. It is near 18 and depends slightly on the model properties using formulae (11) for parameterisation of the exchange through the strait. The salinity of the upper layer in the center of the basin is found to be always greater than the value for the open part of the Black Sea in all experiments, changing from 21.688 to 22.253 for the set of parameters used. Freshening of the surface layer in the center of the basin depends mainly on lateral diffusion. Smaller lateral diffusion coefficient gives rise to an increase of the salinity at the center of the basin.

The azimuthal velocity distribution has three-layer structure for all experiments similar to the prediction of the linear analytical model [8] and the laboratory experiments [9]. Cyclonic circulation is developed in the upper layer, an anticyclonic one occurs at intermediate depth and a weak cyclonic circulation is located near the bottom. The typical azimuthal velocity section is shown on Fig.2 for the basic experiment. The surface cyclonic flow has the maximum velocity of about 0.5 m/s and

concentrates within upper 100m. The surface velocity increases with increasing vertical viscosity and decreasing horizontal diffusion. The anticyclonic undercurrent of intermediate depth has a maximum velocity about of 0.3 m/s and occupies the layer between 100m and 1800m. The maximum of undercurrent velocity is 0.75 m/s when the coefficient of the horizontal diffusion decreases to $116m^2/s$. The deep cyclonic flow is very weak. It is observed below 1800m and its velocity does not exceed 0.01 m/s.

4. Discussion

The numerical study of the lateral buoyancy flux-driven circulation in a rotating basin, carried out within the framework of a simplified model, qualitatively confirms our previous conclusions in [8,9]. The stratification and the circulation are supported by a vertical cell with downwelling near the coast and upwelling in the open part of the basin. The volume transport of the cell exceeds significantly the water exchange through the Bosphorus Strait, corresponding to the ideas of Vodyanitsky [10] on the intensity of the vertical motion in the Black Sea. The intensity of the vertical cell is not sensitive to the way in which Marmara Sea water is transformed, since the numerical results are the same when the convective mixing is taken into account or absent. At the same time the salinity of transformed Marmara Sea waters is sensitive to coefficients of vertical and horizontal diffusion. The Marmara Sea water is transformed mainly under the influence of the advection of the water from the open basin, and vertical diffusion. This is why a decrease of the vertical diffusion coefficient results in an increase in the deep layer salinity.

The surface salinity at the center of the basin is unrealistic and depends on the value of the horizontal diffusion coefficient. Adding Ekman transport in the upper layer should induce near coastal downwelling and promote additional mixing of the Marmara Sea and fresh waters, resulting in a decrease in deep-water salinity as well as the surface salinity in the center of the basin.

The azimuthal circulation in the model depends quantitatively on the coefficients of viscosity and diffusion, which influence the circulation through at least two different mechanisms: The first one is through the sharpening of horizontal gradients of salinity, determined by horizontal diffusion and by the intensity of the vertical cell. The second mechanism is related to the bottom Ekman layer flux. If bottom friction is absent, the vertically integrated volume transport will be equal to zero. The current-undercurrent structure is necessary in this case. The bottom friction prescribes the azimuthal velocity redistribution inside the water column.

5. References

1. Robinson,A.R.,Stommel,H.:1959,'The Oceanic Thermocline and the Associated Thermohaline Circulation', Tellus,11, 295--308.
2. Stommel,H.,Arons,A.B.:1960,'On the Abyssal Circulation of the World Ocean. 2. An Idealised Model of the Circulation Pattern and Amplitude in Oceanic Basins', *Deep-Sea Res.*, **6**, 217--233.

3. Stanev, E. V., 1988 Numerical study on the Black Sea circulation. Mitteilungen des Instituts fuer Meereskunde der Universitaet Hamburg, 28, 232 pp.
4. Stanev, E. V., 1990. On the mechanisms of the Black sea circulation. *Earth-Science Rev.*, **28**, 285-319.
5. Latif,M.A., Ozsoy,E.,Oguz,T.,Unluata,U.:1991,'Observations of the Mediterranean Inflow into the Black Sea', *Deep-Sea Res.*, **38**, Suppl. 2, S711-S723.
6. Simeonov,J., E. V. Stanev, J. O. Backhaus, J. H.Jungclaus, and V. M. Roussenov, (1996). Heat and salt intrusions in the pycnocline from sinking plumes. Test case for the entrainment in the Black Sea. (the present volume).
7. Bryan,K.:1975,'Three-Dimentional Numerical Models of the Ocean Circulation' in R.O.Reid, A.R.Robinson, K.Bryan (ed.), *Numerical Models of Ocean Circulation,* U.S. Nat. Acad. Sci., pp.94-106.
8. Bulgakov,S.N.,Korotaev,G.K.:1987,'Analytical model intensive circulation in the semiclosed basins', *Marine Hydrophys. Journ.*, **3**, 18--24 (in Russian).
9. Bulgakov,S.N.,Korotaev,G.K,. Whitehead,J.:1993,'Salt flux as a mechanism of large-scale circulation in the Black Sea', in Proceedings of American Geoph.Union Meeting, San-Francisco, p.358.
10. Filippov,D.M.: *'Circulation and Waters of the Black Sea'*, Nauka, Moscow, 1968, 136pp.(in Russian).

MODELLING OF STRAIT DYNAMICS: THE BALTIC EXPERIMENTS

ERDEM SAYIN
Marine Sciences and Technology Institute
35340 İnciraltı-İzmir, Turkey

Abstract. The stratified free surface Princeton Model is used to analyse dynamics in the Danish Straits, which connect the Baltic with the North Sea. Two basic experiments were done. The first one is the density–driven and the second one is the forced Baltic experiments . Buoyancy–driven circulation produces bi–directional flow in the Danish Straits with the fresh layer moving north above the southward flowing deeper layer. This circulation alone can not supply the transport required for a renewal of the deep Baltic bottom water. The thermohaline circulation loses its two–layer character with barotropic forcing. Unidirectional flow permits larger transport of volume and salt than bidirectional flow in the straits. The straits are geostrophically controlled. On the other hand the combination of Belt and Sound flows supply more transport through the Belt and the Sound for the inflow and the outflow case respectively. The model results are suited for comparison with laboratory and field studies. Particularly the dense rotating water in the Arkona basins can be explained with the processes over a sill. The inflowing water forms a dome–like feature in the basin after passing the sill.

1. Introduction

The Danish Straits are narrow and shallow channels which connect the Baltic Sea and the Kattegat. They are Great Belt, Little Belt and Sound. Little Belt will not be taken into account in this study. Some parameters for the Straits and Basins are given in Table 1 and in Table 2 respectively. Buoyancy–driven circulation produces bi-directional flow in the Danish Straits (Wyrtki 1954 and Mälkki and Tamsalu 1985). The less dense Baltic water flows to the North Sea in the upper layer, above the denser water

E. Özsoy and A. Mikaelyan (eds.), Sensitivity to Change: Black Sea, Baltic Sea and North Sea, 403–416.
© 1997 *Kluwer Academic Publishers.*

TABLE 1. Some parameters related to the Strait geometries (from Sayın and Krauß, 1996)

	minimum sill depth	narrowest sill width	mean depth	narrowest cross–sect.
G. Belt	Darss S. 18 m	8.0 km	13.0 m	255 000 m^2
Sound	Drodgen 8 m	6.0 km	15.0 m	80 000 m^2

TABLE 2. Some parameters related to the Arkona and Kattegat Basins (from Sayın and Krauß, 1996)

	mean depth	salinity range
Arkona	40 m	8.0 – 16.0
Kattegat	23 m	15.0 – 35.0

flowing into the Baltic. Bi-directional flow is often observed in the summer months or during calm wind situations. During most of the year bi-directional flow occurs in the Fehmarnbelt. This is observed in 50 % of all cases in summer and 29 % in winter (Wyrtki, 1954). In the Great Belt the corresponding numbers are 95 % in summer and 65 % in winter (Farmer and Møller, 1990).

Magaard and Krauß (1966) computed energy and amplitude spectra from the sea level records along the Baltic coast and explained the energy concentration in the range of about 120 h with a standing wave forced by wind. Because of meteorological forcing, during most of the time barotropic processes dominate in the Baltic Sea. However, Kielmann et al. (1973) used mode decomposition and found that the major baroclinic mode contains 10 times the energy of the barotropic one near the inertial frequency. They also found the strongest baroclinicity in the period range from approximately $10h - 40h$. For periods longer than about 50 hours the energy becomes nearly independent on depth, which means that the Baltic responds mainly barotropically at low frequencies.

The paper is organised as follows: In section 2, we introduce the model, which is used. In section 3 we give the properties for the thermohaline

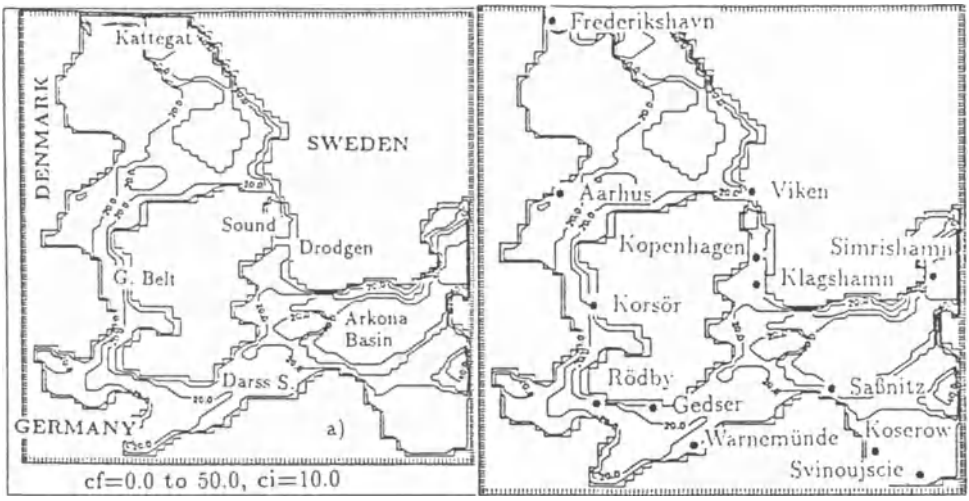


Figure 1. a) Model topography and b) Location of the stations.

circulation in model basin. We compare inflow and outflow from different viewpoints in section 4 and we discuss the circulation with and without wind forcing especially for the inflow case in section 5. In section 6 we try to find out, which theoreticall transport relation fits to the model transport relation better. In section 7 we make a comparison between model and observed surface elevations. The paper is brought to an end by conclusions.

2. Model Description

The model used here – the time dependent 3–dimensional stratified Princeton model – has 12 layers in the vertical with reduced thickness at the surface and the bottom. This is necessary to resolve the internal dynamics of the stratified fluid. Fennel et al. (1991) calculated Rossby radii for different seasons in various part of the Baltic Sea. In the Belt Sea they found maximum values during summer (about 4 km) and minumum values during autumn and winter (about 1.4 km). The horizontal resolution of 2.5 km of the model may be critical for the latter period. The model area extends from the Kattegat, over the Danish straits to the Arkona basin. The model-topography are shown in figure 1. Salinity and temperature values are from Bock (1971) and Lenz (1971) respectively.

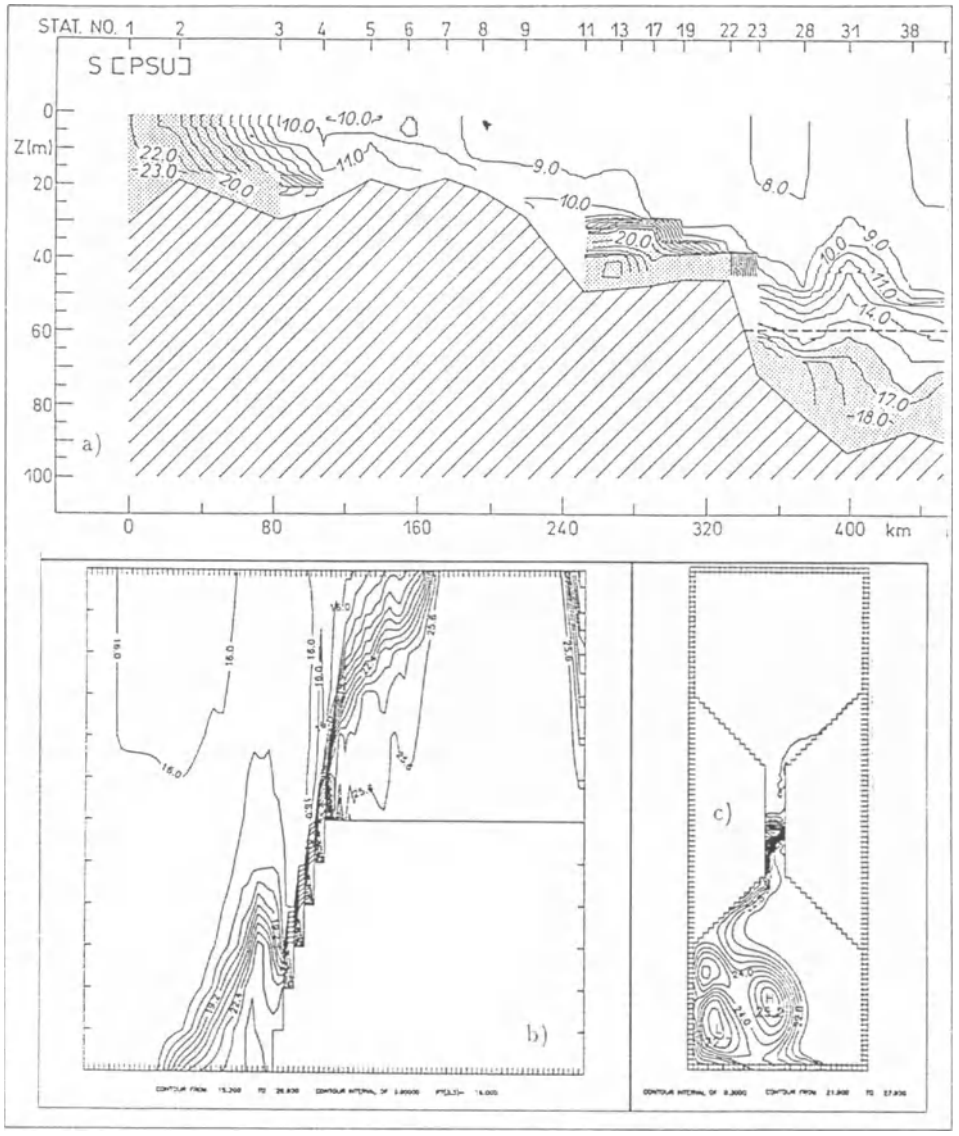


Figure 2. a) Observed salinity values. Vertical section from the south of the Belt Sea, Arkona to Borholm Basin (Alkor February cruise 1993) b) Salinity values, vertical section for density driven case c) Horizontal density field for spin-down experiment (layer 7).

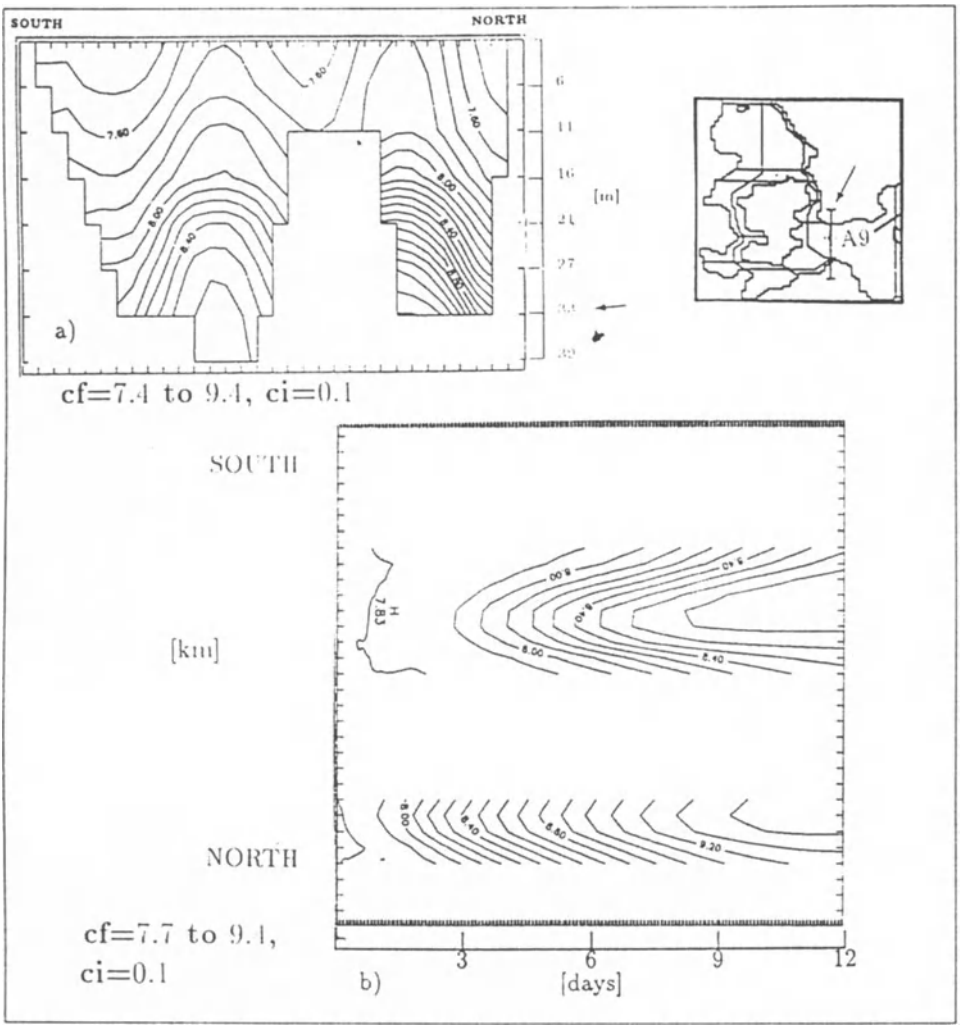


Figure 3. Salinity values, Arkona vertical section A9 for the case of small density gradients between the two ends of the Danish Straits a) after 12 days b) space-time contour plot for the salinity of layer 7, as indicated in plot a.

3. Thermohaline Circulation

Before the description of the Baltic Experiments, a comparison is made between the results obtained for the density driven circulations (from two–basin experiments, Sayın, 1996a, hereafter Part I) and observations. An eddy formation begins at the bottom as rotation of the dense fluid in the adjacent model basin. This dense fluid is described as *dome-shaped* by Gill

(1977) and as *convective chimney* by Killworth (1992). The experiment performed in Part I shows close agreement between the model and the pattern of observed salinity fields, which make a dome in Borholm Basin (Alkor February cruise 1993, Fig.2). Density gradient and topographic effect are important in the establishment of this saline dome. However, this dome is not a stagnant one. A spin-down experiment was done, where after 4 days the barotropic forcing was switched-off. The resulting density field is shown in figure 2c. Two small eddies are generated near the main eddy. One of them is anticyclonic. All eddies have propagated away from the sill.

Model results indicate that the currents near the coast at the north (in the Kattegat) have more baroclinic character; whereas the currents flowing to the NE direction in the Arkona Basin are more or less barotropic. The dense water entering the Arkona Basin domes up and forms a cyclonic gyre there. Stigebrandt (1987a) calculated the flow of dense water into the Baltic that leaks from the deepest part of the Arkona basin. He considered that this leakage is contolled by the vertical stratification in the Arkona Basin and the rotation (rotational baroclinic control).

The saltier water which comes from the Kattegat flows preferentially through the northern part of the Arkona Basin. The dense bottom current entering the basin lifts the lighter fluid upwards (Fig.3) as a result of vertical advection induced in the basin by the intruding dense current. This result is in agreement with Stigebrandt (1987b) and with the two-basin experiment described in Part I.

The currents are stronger in the southern part of the Arkona Basin than the currents in the northern part. They decrease from the surface to the bottom in the south. On the other hand the currents are intensified at the bottom in the north of Arkona Basin. The near–inertial and superinertial oscillations effect the surface and bottom velocity fields and the system reaches a quasi–steady state in the Arkona Basin after 4–5 inertial periods. The topographic waves have a wavelength of approximately 30 km, in agreement with observations by Aitsam and Elken (1982).

The dense flow into the Arkona Basin as a result of the thermohaline circulation is not sufficient for the renewal of deep water in the Baltic. For the mean density distribution of November the volume transport through the Belt into the Arkona Basin is about 13000 $m^3\ s^{-1}$ and same volume is transported through the Sound into the Kattegat.

The common characteristics of thermohaline circulation in the Belt are:

(a) The surface displacements are always higher at the right hand side of the straits in the flow direction.

(b) The water in the lower layer becomes gradually saltier in time in the direction to the Arkona Basin. Salt intrusion speed is approximately $2.5 km/day$.

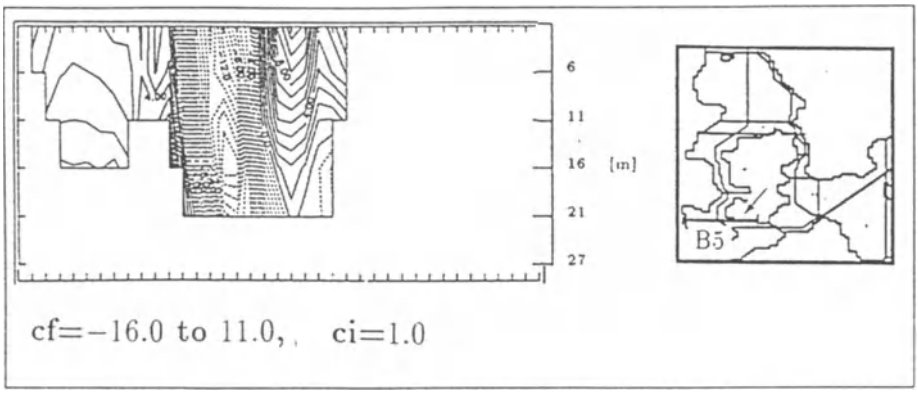


Figure 4. Velocity values (v–component), Belt section B5 after 12 days.

(c) The lower layer maximum velocity in the direction to the Baltic are greater (about 20 $cm\ s^{-1}$) than the upper layer velocity in the direction to the Kattegat (about 10 $cm\ s^{-1}$).

A *bore* formation can be seen in the Belt (Fig.4). It may be a result of the time-dependent circulation, also nonlinearities may be important. Stern (1980) examined the bore intrusion and commented that after arresting the bore a large eddy is expected to form. Pratt (1984) stated that a bore-like reflected wave is a sufficient (but not necessary) evidence that the flow is hydraulically controlled. Helfrich and Melville (1990) found analytic bore solutions. They explained that bores are generated by unsteady transcritical forcing and they are complementary pairs of solitary waves. Nof (1986) explained the bore formation with the help of shock waves, associated with a sudden change in depth accompanied by local energy loss.

In the Sound the current flows more or less only in the direction to the Kattegat, but the surface layer maximum velocity (about 20 $cm\ s^{-1}$) is greater than the velocity in the lower layer (about 5 $cm\ s^{-1}$). Less dense water flows along the east coast in the Sound to the Kattegat and the surface elevation is higher at the right hand side of the channel.

4. Barotropic Forcing

The barotropic and baroclinic respons of a semi-enclosed basin to barotropic forcing are discussed by Stigebrandt (1980). He emphasized that the velocity at topographical features must be considered in order to study the baroclinic response to barotropic forcing which causes larger transport through the channel. Some examples for this situation were computed by using two-basin experiments (Part I) and realistic topography in the present study.

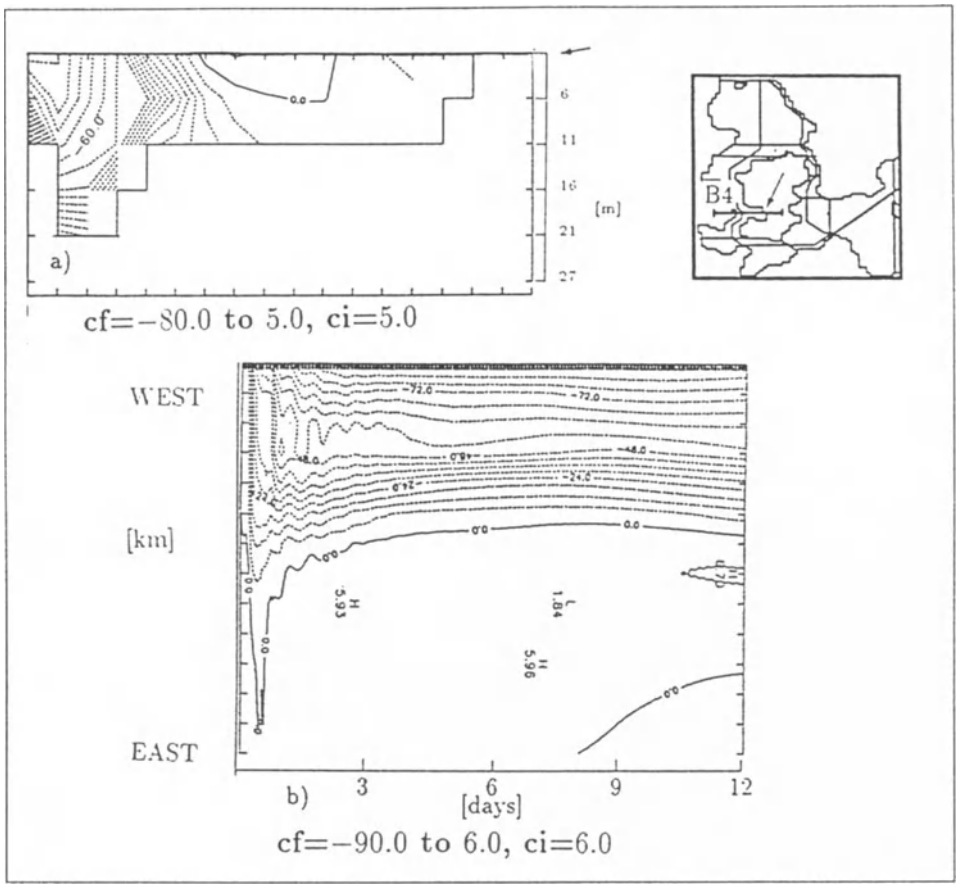


Figure 5. Section B4 at the end of Day 12 (INFLOW) a) v-component of velocity b) Space-time contour plot for the surface layer velocity.

Barotropic forcing displaces the density front over great distances and intensifies the horizontal density gradient. Volume and salt transport depend strongly on the sea level difference between the Kattegat and the Arkona Basin. The sea level difference can be established also by wind surge and barotropic circulation. The sea level at a certain position is influenced by seiches (Wübber and Krauß, 1979).

The upper layer density front extends along the Swedish coast to the north during outflow and through the Belt along the southern Arkona Basin, where it forms a small tongue towards NE during inflow. In the Sound the separation of the density front from the left coast is observed during inflow. It can be concluded from the comparison of the barotropic velocities with the total velocities that both inflow and outflow velocities

are mostly barotropic.

The direction of the currents is different from the thermohaline case. In general, from the surface to the bottom the velocities are to the south in the case of inflow and to the north in the outflow case. Only in the Belt the barotropic forcing used is not strong enough to overcome the thermohaline component in the bottom layer completely in the outflow case.

The maximum velocity values for the inflow are approximately three times as large as the values for the outflow case, although the strength of the barotropic forcing is the same for both cases. The question arises, why the velocities for the inflow case are greater than those for the outflow. The answer can be, that during outflow continuous stratification is maintained (topographic breaktrough, Killworth, 1989). A finite amount of mass can be transported (oscillatory) along the topography. On the other hand during inflow the dense fluid over the topography has a fundamental effect on the transmission of wave energy. In this case topography does not intersect all density–layers.

After the quasi–steady state is reached in the Belt, the maximum velocities are 90 cm/s for inflow and 30 cm/s for outflow in the upper layer and 24 cm/s for inflow (Fig 5) and 12 cm/s for outflow in the lower layer. In the Sound maximum velocities are 36 cm/s and 27 cm/s for inflow in the upper and lower layers, respectively and 20 cm/s and 16 cm/s for outflow. Maximum velocities during outflow occur in the upper layer and during inflow the maximum appears close to the bottom in shape of a bore. As mentioned before, in case of inflow barotropic and baroclinic components are in balance with the external forcing in the upper layer. Consequently maximum velocities must occur in the lower layer due to the addition of the thermohaline component and barotropic external forcing there. This can also be explained by the hydraulic theory, suggesting strong lower layer flow if the Froude number $F > 1$. In the present study it is found that the Froude number is always greater than 1 for the inflow case.

Values of the volume transport in the Belt are greater than the values in the Sound. The transport values depend strongly on the difference in surface elevation prescribed between the ends of the straits. A constant difference in surface elevations causes almost constant volume and salt transports in both straits. The propagation of salt for the outflow case is very slow and the phase speed of the front is approximately 2.8 km/day. Given the sea surface elevation difference of 20 cm between the Kattegat and the Arkona basin, the volume transport in the Sound amounts to $4. \times 10^{10}$ cm^3/s in the inflow case. In the Belt the volume transport is 11.9×10^{10} cm^3/s. Thus, 25% of the volume transport occur in the Sound and 75% in the Belt.

For the inflow case the same relation holds for the salt transport, 22% in the Sound and 78% in the Belt. The outflow case gives a different relation.

The reason is the density stratification is concentrated in the straits region. This density field drives internal dynamics and affects the transport relations in the outflow case. In the stratified case an outflow in the upper layer and also in the lower layer occurs very rarely in the Belt (Wyrtki, 1954). If the model density stratification is weak in the straits, the calculated volume and the salt transport relation agree with the observed relations in the Belt and the Sound.

5. Wind Effects

An additional experiment was performed to determine the effect of wind forcing. The constant wind stress is taken in x-direction ($\tau = 2 dynes/cm^2$) and the same sea level difference between the northern and eastern boundary is used as in the previous experiments. The differences to the inflow case with barotropic forcing only are the following:h

- Short wave oscillations and small-scale structures disappear in both straits for the wind-driven case. Velocities decrease gradually from the surface to the Ekman depth.
- Vertical density homogenization occur in the straits. Also the horizontal density differences are smaller across the straits.
- In the Arkona basin homogenization occurs in the salinity field in the lower layer and also in the upper layer. Consequently, a strong vertical salinity gradient is established at mid-depth. The more saline water reaches the Arkona basin in a shorter time for the case with constant westerly wind than for the case without wind forcing.
- An important result is the salt transport in the Belt. At the beginning of the adjustment process the salt front has an intrusion speed of 26.8 km/day and at the end of day 12 with 16.0 km/day. In the wind driven case during the first adjustment phase salt is intruded faster with an speed of 28.5 km/day and at day 12 with 15.9 km/day. The calculated intrusion speeds for both cases at the beginning of the adjustment do agree with the values observed for mid-November 1976 by Lass and Schwabe (1988). They found the speed of the salinity front to be 30 cm/s (25.9 km/day).
  The salt intrusion is weak in the outflow case compared to the two inflow cases. The stratification occur in the lower layer for the outflow case which can cause that less transport through the Belt. Salt intrusion during outflow is very slow and the intrusion speed is approximately 2.8 km/day.
- Volume and salt transport are increased in the wind-driven case. The total volume transport is $15.9 \times 10^4\ m^3\ s^{-1}$ without wind and $20.0 \times 10^4\ m^3\ s^{-1}$ for the wind–driven case in both straits . The relative

transport in the Sound and the Belt change with wind forcing. The volume and salt transports increase in the Sound and decrease in the Belt.

6. Transport Relations

We can conclude that the transport can be described by the geostrophic relation during outflow in the Belt and during inflow in the Sound. The small difference between the values of the geostrophic relation and the model results is due to the baroclinic and topographic effects. This means that we must add a correction term to the geostrophic relations due to the density currents. For the inflow situations in the Belt and for the outflow situations in the Sound, however, transport values deviate from geostrophy in considerable amount. The reason is the combination of the Belt and the Sound currents near the opening of Belt Strait in the direction to the Arkona Basin for the inflow and near the opening of the Sound in the direction to the Kattegat for the outflow case. More information about the transport relation is in paper Sayın and Krauß, 1996.

7. Sea Surface Elevations

TABLE 3. Results of the linear regression analysis for 9 stations for the months January, July, September and November 1989. Here r–correlation coefficient. *– no data available (Locations of the stations are shown in figure 1).

	JAN	JUL	SEP	NOV
Aarhus	r=0.77	r=0.60	*	r=0.69
Kopenhagen	*	r=0.63	*	r=0.64
Korsör	*	r=0.61	r=0.54	r=0.85
Viken	r=0.69	r=0.67	r=0.52	r=0.68
Warnemünde	r=0.75	r=0.70	r=0.73	r=0.86
Saßnitz	r=0.89	r=0.87	r=0.94	r=0.91
Gedser	r=0.70	*	*	r=0.80
Rödby	r=0.66	*	r=0.85	r=0.80
Klagshamn	r=0.77	r=0.70	r=0.90	r= 0.75

If surface elevations of the model are compared with observed values at 9 stations during November, one recognizes good agreement especially for the stations in the east of the area. Although the surface elevations are prescribed at both the eastern and northern boundaries, the same high correlation could not be obtained for the stations in the north. The agreement

for the stations in the central region and in the north in November and also for the months January, July and September is not always satisfactory. A high correlation is between the model values and the observed surface elevations of Saßnitz (correlation coefficient, $r = 0.94$). Table 3 gives the results of the linear regression analysis for 9 stations for the months January, July, September and November. From the estimated intercepts and slopes of the fitted line a constant bias between model and observed surface elevations cannot be determined. In general, the correlation is higher for the stations in the eastern part of the area than in the other regions. Some explanations can be given for the discrepancies between the model and the observed values:

(a) The closed model region favours seiches oscillations different from the real basin oscillations.

(b) The currents at the north have more baroclinic character, whereas the currents flowing into the Arkona Basin are more or less barotropic. The nonlinear interraction between barotropic and baroclinic current affects the values of surface elevations in the northern part of the basin more than in the eastern part.

There is a good agreement between data and model results at frequency bands lower than the inertial frequency. The short period oscillations could not be modelled very well, they show phase differences compared to the model results.

8. Conclusions

The results of the Baltic experiments can be summarized as follows:

- Model transport values were compared with some transport relations. For the outflow case in the Belt and for the inflow case in the Sound the transport may be determined by using the geostrophic relation. The transport values for the inflow case in the Belt and for the outflow case in the Sound deviate from geostrophy. This deviation can be explained by the combination of the Belt and Sound flows.
- The inflowing dense water forms a dome–like feature in the Arkona Basin. The possibility of hydraulic control can be said with the occurance of dome, namely advective process takes place between the dome and the sill. The rotating dense water can only penetrate further by external forcing or after the rim of the dome reaches the next sill.
- Altough the first mode shelf wave speed faster than the first mode baroclinic Kelvin waves at high and mid latitudes, we can not conclude that the barotropic adjustment proceeds baroclinic one for the Danish straits. The complex basin geometries and topographies, non–linear

barotropic–baroclinic interractions can effect the adjustment processes in the straits.

- The well known relation that 75 % of the total transport in the Danish Straits occurs through the Belt is established for the inflow in the strongly stratified case and for inflow and outflow in the weak stratified case with a slightly less percentage. For outflow situations in the strongly stratified case this relation is changed due to topographic breakthrough (stratified outflow case).
- At the northern coast of the basin solitary waves were detected in the two–basin experiments (Part I) for the density–driven case. These waves can probably explain the bottom process of the coastal current along the Swedish coast in the Kattegat.

References

1. Aitsam, A. and J. Elken, (1982) Synoptic scale variability of hydrophysical fields in the Baltic proper on the basis of CTD measurements, *Hydrodynamics of semi–enclosed seas*, J.C.C. Nihoul, Editor, Elsevier, Amsterdam, pp. 433–468.
2. Bock, K.H., (1971) Monatskarten des Salzgehaltes der Ostsee, *Ergänzungsheft zur Deutschen Hydrographischen Zeitschrift*, **Reihe B, Nr.12**.
3. Farmer, D.M. and J.S. Møller, (1990) Measurements and modeling in the Great Belt: A unique opportunity for model varification, *In: The Physical Oceanography of Sea Straits*, edited by L.J. Pratt, 125–152, Kluwer, Boston.
4. Fennel, W., T. Seifert and B. Kaiser, (1991) Rossby radii and phase speeds in the Baltic Sea, *Continental Shelf Res.*, **11**, 23–36.
5. Gill, A.E., (1977) The hydraulics of rotating–channel flow, *J. Fluid Mech.*, **80**, 641–671.
6. Helfrich, K.R. and W.K. Melville, (1990) Review of dispersive and resonant effects in internal wave propagation, *In: The Physical Oceanography of Sea Straits*, edited by L.J. Pratt, 391–420, Kluwer, Boston.
7. Kielmann, J., W. Krauß and K.H. Keunecke, (1973) Currents and stratification in the Belt Sea and the Arkona Basin during 1962–1968, *Kieler Meeresf.*, **XXIX**, 90–111.
8. Killworth, P.D., (1989) Transmission of a two–layer coastal Kelvin wave over a ridge, *J. Phys. Oceanogr.*, **19**, 1131–1148.
9. Killworth, P.D., (1992) The time–dependent collapse of a rotating fluid cylinder, *J. Phys. Oceanogr.*, **22**, 390–397.
10. Lass, H.U. and R. Schwabe, (1990) An analysis of the salt water inflow into the Baltic in 1975 to 1976, *Dt. Hydrogr. Z.*, **43**, 97–125.
11. Lenz, W., (1971) Monatskarten der Temperatur der Ostsee, *Ergänzungsheft zur Deutschen Hydrographischen Zeitschrift*, **Reihe B, Nr.11**.
12. Magaard, L. and W. Krauß, (1966) Spektren der Wasserstandsschwankungen der Ostsee im Jahre 1958, *Kieler Meeresf.*, **XXII**, 155–162.
13. Mällki, P. and R. Tamsalu, (1985) Physical features of the Baltic Sea, *Finn. Mar. Res.*, **No. 252**, 110 pp.
14. Nof, D., (1986) Geostrophic shock waves, *J. Phys. Oceanogr.*, **16**, 886–901.
15. Pratt, L.J., (1984) A time–dependent aspect of hydraulic control in straits, *J. Phys. Oceanogr.*, **14**, 1414–1418.
16. Sayın, E., (1996) Modelling of strait dynamics: The two–basin experiments (prepared).
17. Sayın, E. and W. Krauß, (1996) A numerical study of the water exchange through

the Danish Straits, *Tellus*, **48A**, 324–341.
18. Stern, M.E., (1980) Geostrophic fronts, bores, breaking and blocking waves, *J. Fluid Mech.*, **99**, 687–703.
19. Stigebrandt, A., (1980) Barotropic and baroclinic response of a semi–enclosed basin to barotropic forcing from the sea, *In: Fjord Oceanography*, edited by H.J. Freeland, D.M. Farmer and C.D. Levings, 141–163, Plenum, 715 pp.
20. Stigebrandt, A., (1987a) Computations of the flow of dense water into the Baltic Sea from hydrographical measurements in the Arkona Basin, *Tellus*, **39A**, 170–177
21. Stigebrandt, A., (1987b) A model for the vertical circulation of the Baltic deep water. *J. Phys. Oceanogr.*, **17**, 1772–1785.
22. Wübber, C. and W. Krauß, (1979) The two-dimensional seiches of the Baltic Sea, *Oceanologica Acta*, **2**, 435–446.
23. Wyrtki, K., (1954) Die Dynamik der Wasserbewegungen im Fehmarnbelt II, *Kieler Meeresf.*, **X**, 162–181.

HEAT AND SALT INTRUSIONS IN THE PYCNOCLINE FROM SINKING PLUMES. TEST CASE FOR THE ENTRAINMENT IN THE BLACK SEA

J. A. SIMEONOV[1], E. V. STANEV[1], J. O. BACKHAUS[2],
J. H. JUNGCLAUS[2], and V. M. ROUSSENOV[1]
[1]*Department of Meteorology and Geophysics, University of Sofia*
James Bourchier street 5, 1126 Sofia, Bulgaria
[2]*Institute of Oceanography, University of Hamburg*
Troplowitzstrasse 7, 22529 Hamburg, Germany

Abstract

The paper describes the slope convection, heat and salt intrusions, which provide key mechanisms for internal mixing and water mass formation in the Black Sea. The high salinity plume of Mediterranean origin entrains Black Sea surface and intermediate waters and carries this mixture into the intermediate and deep layers. This is potentially the most important mechanism for mixing in the interior and deep layers, which was recently confirmed by the analyses of penetration rates of Chernobyl tracers. We apply a numerical reduced gravity model with a horizontal resolution of 600m to the Bosphorus inflow area, which covers 72 km in the East-West and 54 km in the North-South directions, respectively. The ambient stratification is constant in time. Pronounced intrusions of cold waters, entrained from the cold intermediate layer, are simulated at different depths in the area of the continental slope. The model simulated mixing ratio and different characteristics of the sinking plume are compared with observations. The sensitivity of the depths of the intrusions in dependence to the magnitude of the heat inflow is studied.

1. Introduction

The Black Sea is a typical inland ocean basin, where the large river discharge, and the limited water exchange with the Mediterranean Sea result in the formation of extremely stable vertical stratification. The exchange flow is controlled by the hydraulic processes in the Strait of Bosphorus (Oguz *et al.*, 1990, Ozsoy *et al.*, 1996), as well as by the density differences between the Black Sea and Mediterranean Sea waters. There is an important link between the external forcing of the Black Sea (e. g. the river discharge and Mediterranean Sea buoyancy flux) and the Black Sea response. This response is dependent on the Mediterranean effluent, which distributes the

E. Özsoy and A. Mikaelyan (eds.), Sensitivity to Change: Black Sea, Baltic Sea and North Sea, 417–438.
© 1997 *Kluwer Academic Publishers.*

negative buoyancy signal originating from the strait between the sill depth and deep layers. This intimate mechanism makes the issues, related with the sinking and spreading characteristics of the Mediterranean Sea water, key issues in the Black Sea oceanography.

The response of the Black Sea to the Mediterranean inflow has been evolved within the last 10 thousands years. During this time, the sea changed from a fresh water lake to its present state. This change resulted from the pronounced sea level rise of the world ocean. After the link with the Mediterranean Sea was established, the Mediterranean Sea Water (MSW) began to sink to large depths, forming gradually saltier deep water body below less saline surface waters. Some speculations exist (Özsoy *et al.*, 1993) that the present day deep water has been formed long time ago, and the deep layers remain nowadays unaffected by the sinking plume.

The recent interest in the Black Sea oceanography resulted in an important progress in the data base (both in quantity and quality), including the MSW data (Yuce, 1990, Latif *et al.*, 1991, Oguz and Rozman, 1991), but there still remains much to be done for understanding physical processes in the close proximity of the Bosphorus Strait. Some interpretations for entrainment and penetration of the MSW were discussed by Friedrich and Stanev (1988) from the view point of coarse resolution three-dimensional numerical model. However, the scales of the plume (it spreads a couple of tens of kilometres from the strait) dictates a separate process-oriented model study addressing the small-scale processes, which take place during the different stages of the plume evolution along the shelf, and on the continental slope. One important characteristic of this evolution is the transition (trough the slope convection) from hydraulic dominated processes in the strait to the open sea dynamics on the continental slope area.

There is another important motivation to address the penetration of the MSW into the Black Sea by means of a numerical model. Observations in this region require fine profiling and extremely dense coverage. Large number of surveys is needed to obtain reliable estimates. The detection of the plume is difficult, as the modified MSW approaches the properties of the Black Sea Water (BSW) on the continental slope (Oguz and Rozman, 1991). Numerical simulations provide a powerful tool to trace MSW in the areas, where existing observations are rather sparse. Finally, analysing the results from different scenarios can help our understanding entrainment of BSW by the sinking MSW.

There is a growing interest in studying slope convection as a key mechanism for the ocean water mass formation. Although streamtube models (Smith, 1975) are still applied in studying the fundamental processes of the outflows from marginal seas (Price and Baringer, 1994), reduced gravity plume models (Jungclaus and Backhaus, 1994) or the fully 3D primitive equation models (Gawarkiewicz and Chapman, 1995 and Chapman and Gawarkiewicz, 1995) give more complete view on the dynamics of the sinking plumes.

The aims of this paper are: (1) to apply a rather simple numerical model, which realistically simulates gravity plume, in the Bosphorus outflow region, (2) to study the phenomenology of the plume, as simulated by the model and to validate the results

against observations; (3) to analyse the model estimates for the entrainment and intrusions.

2. The Mediterranean plume as an important element of the Black Sea circulation

A number of attempts to trace the MSW in the Black Sea have been made, provoking discussions on the pathways of the plume, on the possible blocking of the dense MSW by the sill near the exit of the channel and on the question where to search for the MSW. A review of the scientific activities, related to the fate of the MSW in the Black Sea is given by Tolmazin (1985). In the past, insufficient observations on the bottom topography resulted in some false speculations about the pathways of the MSW.

If the bottom in the inflow area had a uniform north-south slope, we could expect that the plume would propagate to the north and then to the north-east, deflected by the Coriolis force and the eastward currents of the basin circulation. Some observations failed in tracing the plume to the east of the Bosphorus exit, which led to the hypothesis that its penetration in the Black Sea is often blocked by the sill (Ulyott and Ilgaz, 1946, quoted from Tolmazin, 1985). For the first time, using the data from the 15 year long IMBYUM (Institute of the Southern Seas of the former Soviet Union) program, Tolmazin (1985) has shown that the northern sill does not prevent the MSW from exiting the strait and the plume persistently takes a Northwest track within the shelf. However, the lack of bottom topography data in the vicinity of the strait led him to some misinterpretation of the reasons for the westward deflection.

Recent progress in understanding the pathways of the Mediterranean effluent was manly due to the Turkish oceanographers (Yuce, 1990, Latif *et al.*, 1991, Oguz and Rozman, 1991), who showed for the first time a new bathymetric map and explained the westward deflection of the plume as being due to the guidance by a narrow underwater channel. Now it is widely accepted that the MSW entrains cold surface or near surface water and forms the Black Sea deep water. The entrainment mechanism could help to answer such fundamental question, as why the residence time at intermediate depth is shorter than the one estimated from the renewal via the Bosphorus inflow only. However, there is still a large uncertainty about the degree of entrainment and the depth of injections (Murray *et al.*, 1991).

The restricted diffusive mixing in the Black Sea interior results from the extremely strong stratification, identified by salinity values of 18 psu in the sea surface layer and 22.3 psu in the deep layers. The consequences of stability control on the water mass formation in the intermediate layers was demonstrated by Stanev (1988) and Friedrich and Stanev (1988). Later, the stability analysis (Murray *et al.*, 1991) showed that vertical diffusion by itself could hardly explain the mixing in the intermediate layers. The importance of the entrainment was proved in a very convincing way by Buesseler *et al.* (1991) from the penetration of Chernobyl tracers. The above results are discussed in detail by Özsoy *et al.* (1993), who conclude that the entrainment of the BSW by sinking MSW and the lateral intrusions of the plume dominate the

penetration of the MSW in the deeper levels and provide an important mechanism for internal mixing.

3. The numerical model

3.1. GOVERNING EQUATIONS

The basic model configuration is depicted in Fig. 1. The model consist of a turbulent lower layer of height H (the plume) underlying an upper layer at rest. The lateral extent of the plume is determined by the movable boundary technique, described by Jungclaus and Backhaus (1994). Wherever the plume is absent, the interface depth $-\zeta$ and the sea-bottom depth $-D$ coincide.

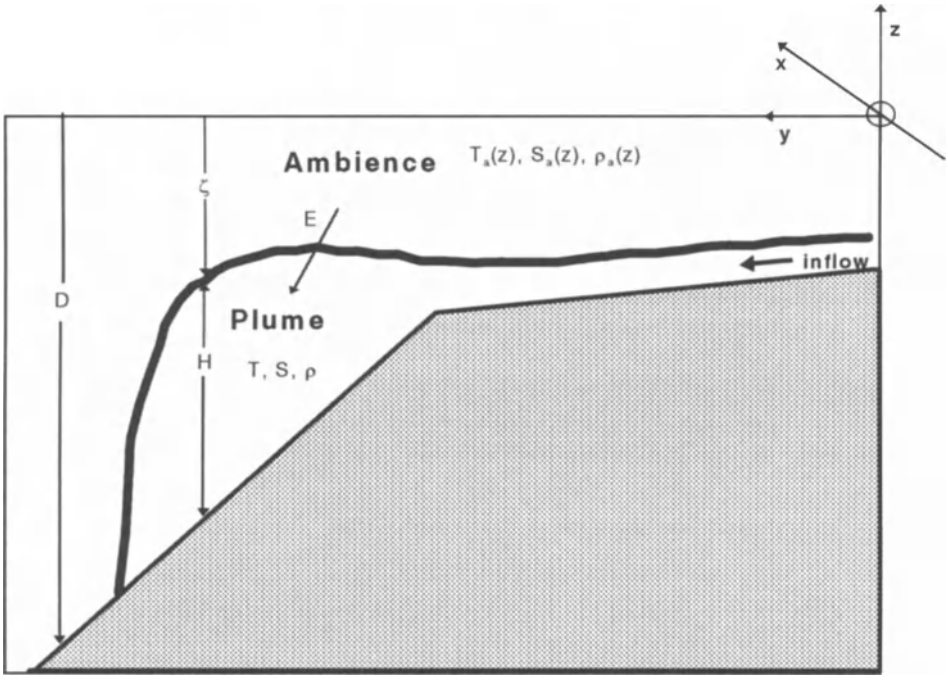


Figure 1. Schematic view on the reduced gravity model used in this study. See for the notations in text.

We define first the integrated transports:

$$\vec{V} = (U,V), \quad U = \int_{-D}^{-\zeta} u dz, \quad V = \int_{-D}^{-\zeta} v dz \tag{1}$$

and averaged velocities:

$$\bar{u} = \frac{U}{H}, \quad \bar{v} = \frac{V}{H}, \quad H = D - \zeta . \tag{2}$$

The model equations in vertically-integrated form read:

$$\frac{\partial U}{\partial t} + \nabla.[\vec{V}\frac{U}{H} - A_h H \nabla \frac{U}{H}] - fV = -g' H \frac{\partial \zeta}{\partial x} - \frac{gH^2}{2\rho_o}\frac{\partial \rho}{\partial x} - \frac{\tau_{bx}}{\rho_o}, \tag{3}$$

$$\frac{\partial V}{\partial t} + \nabla.[\vec{V}\frac{V}{H} - A_h H \nabla \frac{V}{H}] + fU = -g' H \frac{\partial \zeta}{\partial y} - \frac{gH^2}{2\rho_o}\frac{\partial \rho}{\partial y} - \frac{\tau_{by}}{\rho_o}, \tag{4}$$

where A_h is the coefficient of horizontal turbulent exchange,

$$g' = \frac{\rho - \rho_a}{\rho_o} g \tag{5}$$

is the "reduced gravity", subscripts "a" denote ambient quantities, and ρ_o is the reference density. The continuity equation reads:

$$\frac{\partial \zeta}{\partial t} + \frac{\partial U}{\partial x} + \frac{\partial V}{\partial y} = w_e, \tag{6}$$

where w_e is the entrainment velocity. Bottom stress in the model obeys a quadratic drag law:

$$\frac{\vec{\tau}_b}{\rho_o} = r|\vec{v}|\vec{v}, \tag{7}$$

where r is the dimensionless friction coefficient. Integrated conservation equations for heat and salt read:

$$\frac{\partial T}{\partial t} + \bar{u}\frac{\partial T}{\partial x} + \bar{v}\frac{\partial T}{\partial y} + w_e \frac{T - T_a}{H} = \frac{A_h^T}{H}\nabla(H\nabla T), \tag{8}$$

$$\frac{\partial S}{\partial t} + \bar{u}\frac{\partial S}{\partial x} + \bar{v}\frac{\partial S}{\partial y} + w_e \frac{S - S_a}{H} = \frac{A_h^T}{H}\nabla(H\nabla S), \tag{9}$$

where A_h^T is the coefficient of horizontal turbulent diffusion. The density

$$\rho = f(T,S) \tag{10}$$

is calculated using linear equation of state.

3. 2. MODEL AREA AND MODEL PARAMETERS

The model domain (Fig. 2) is resolved by 90 grid points in the north-south and by 120 grid points in the east-west direction, with a horizontal resolution of 600 m. The model topography is digitised from the bathymetric maps of Latif *et al.* (1991). It shows that the strait of Bosphorus has an underwater extension in the shelf area, reaching 10 km from the exit of the strait. The channel has the same orientation as the strait in the first 8 km. Then it turns to the north and continues for about 2 km. Later it turns to the north-west. The width of the underwater channel is about 1000 m in the narrowest transect, but it is resolved by at least 3 points in the model (see Fig 2b). At about 10 km from the Bosphorus Strait the channel reaches depth of about 70 m. Further down, in the north western direction, the 70 m isobaths at the two sides of the channel open sharply, thus marking the end of the channel.

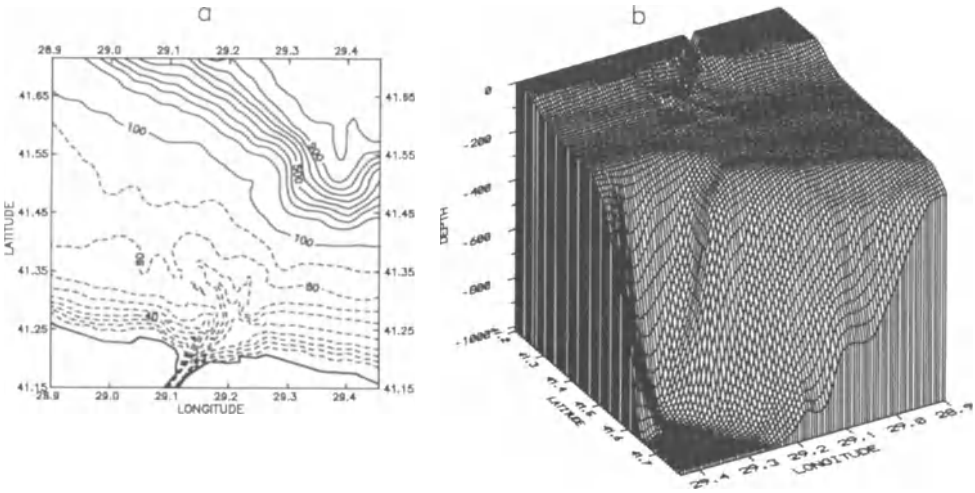


Figure 2. Model topography
(a) isobaths, the contour interval is 10 m in the shelf region (dashed lines) and 100 m on the continental slop (full lines).
(b) isometric plot of the model area, looked from Northeast.

Some important topographic characteristics in Fig. 2, which may affect the spreading of the MSW are noteworthy.

•To the right of the second trough there is a small underwater hill, reaching a depth of 55 m, which blocks effectively the propagation of the plume to the Northeast, and deflects the current to the Northwest.
•There is a distance of about 10-12 km between the underwater channel and the continental slope. This is a very wide and flat shelf area (Fig. 2b).
•The continental slope has orientation from North-west to South-east (Fig. 2a) and an abrupt change of the depth between 100 and 1000 m occurs in about 10 km only. A good illustration on the steepness of the slope, compared to the canyon forms and shelf, is given by the isometric Fig 2b.
•The North-eastern corner (the angle from which we look the isometric depths) of the model area is a deep and flat area.
The mixing of ambient water into the turbulent flow is parameterized in equations (8) and (9) by means of entrainment velocity w_e. We use the parameterization given by Jungclaus and Backhaus (1994)

$$w_e = \frac{{c_L}^2}{S_m}\sqrt{\overline{u}^2 + \overline{v}^2 + \frac{g'H}{S_m}}, \tag{11}$$

where, c_L is a proportionality constant and Sm is the turbulent Schmidt number, defined by the formula given by Mellor and Durbin (1975)

$$S_m = \frac{R_i}{0.725(R_i + 0.186 - \sqrt{{R_i}^2 - 0.316R_i + 0.0346})}, \tag{12}$$

where

$$R_i = \frac{g'H}{\overline{u}^2 + \overline{v}^2} \tag{13}$$

is the Richardson number.
A time step of 30 s provides a stable model behaviour. A number of tuning experiments and comparisons with the existing observations led us to set the bottom friction coefficient at $r=3\text{x}10^{-2}$ and $c_L=0.086$.
The ambient stratification is kept constant during the integration. It corresponds to the annual mean profiles of temperature and salinity and is resolved with a vertical discretization of 10 m. These values are taken as initial data for the entire model domain. In Fig. 3 we show the temperature and salinity at the bottom. This is a rather unusual way of presenting the stratification, but it is useful to obtain later an idea of the evolution of temperature and salinity due to the plume, which displaces the ambient bottom water. Two topographic features are well pronounced in Fig. 3: the underwater channel and the shelf break. The flat shelf is filled with Cold Intermediate Water (CIW), with temperatures lower than 8°C.

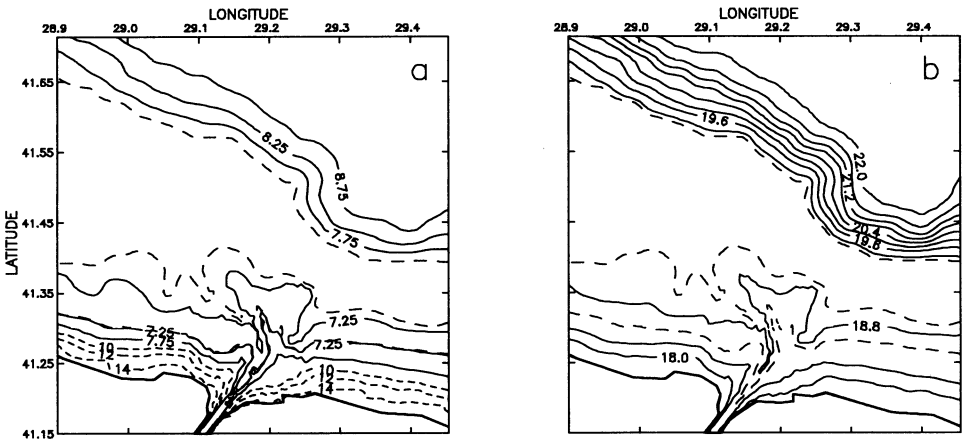


Figure 3. Bottom temperature in °C (a) and salinity in psu (b), corresponding to the ambient stratification. Contours are: (a) 7.25 to 14.75 by 0.50 °C, (b) 18.0 to 22.0 by 0.4 psu. Longer dash curves are the 60-, 80-, and 100-m isobaths.

3.3. BOUNDARY CONDITIONS

As seen from Fig. 2, the model area has an almost solid boundary in the south, with a small opening, where the model forcing is specified in the exit of the Strait of Bosphorus. The other three boundaries are open, and the following boundary conditions are prescribed there:

$$\left.\frac{\partial S}{\partial n}\right|_L = 0, \quad \left.\frac{\partial T}{\partial n}\right|_L = 0, \quad \left.\frac{\partial \bar{u}}{\partial n}\right|_L = 0, \quad \left.\frac{\partial \bar{v}}{\partial n}\right|_L = 0, \quad \left.\frac{\partial \zeta}{\partial n}\right|_L = 0, \tag{14}$$

where L corresponds to Eastern, Northern and Western boundaries. The zero normal gradients imply that the plume freely propagates through the open boundary.
The model area is extended towards the basin interior with a buffer zone (10 points), where the horizontal grid size is increased linearly up to a maximum value of 30 km. This buffer zone is not shown in Fig. 2 and is also excluded in the presentation of model results since the model does not simulate any unrealistic features there.
At solid boundary M (M corresponds to the Southern boundary):

$$U|_M = 0, \quad V|_M = 0. \tag{15}$$

The model forcing is specified in the exit of the Bosphorus Strait, where the thickness of the plume is tuned to initiate a water transport that is comparable to observations

(10^4 m^3 s^{-1}, Unluata *et al.*, 1990). This corresponds to 310 km^3 $year^{-1}$. The insufficient resolution in the exit area and on the first several kilometres in the strait results in small inaccuracies in the simulated variables. The interface depth in the area of the sill is about 48 m, whereas the corresponding depth, observed by Latif *et al.* (1991) is 45m. The inaccuracies are partially due to the lack of a piece of the Strait with its specific physics.

The salinity in the inflow points is set to 37 psu, which corresponds to observational data. This large value, compared to the ambient salinity, provides the negative buoyancy flux and maintains the slope convection in the model.

The heat and salt fluxes from the plume to the ambience are defined as the product of the entrainment velocity and the respective temperature and salinity differences between the plume and its environment. These fluxes are calculated in the model at each time step and at each grid point. Their evolution in time shows that the model reaches a balance between the input and output of heat and salt after about 20 days of integration. Practically, the ambience acts as a motionless sponge, where the intrusions from the plume enter. This one way exchange is an important model simplification. The question how the ambience is changed by the sinking MSW is an important issue of the Black Sea oceanography. In this paper, however, we confine ourselves to the analyses of the evolution of the MSW intrusion.

3.4. EXPERIMENTS

As known from the experimental data for the MSW in the Black Sea, the buoyancy flux is mainly due to the salinity anomaly

$$BS = g\beta Q_b \ (S_b - S_a) \tag{16}$$

where Q_b is the water transport by the Bosphorus undercurrent with temperature T_b and salinity S_b, β is the coefficient of haline contraction. The contribution of the buoyancy due to temperature is

$$BT = g\alpha Q_b (T_b - T_a) \tag{17}$$

where α is the heat expansion constant. Dividing equations (16) and (17), and taking the values of 0.13×10^{-3} and 0.78×10^{-3} as α and β, respectively, we see that the buoyancy flux due to temperature is approximately one order of magnitude smaller than the one due to salinity. In order to illustrate the impact of the buoyancy due to temperature, we carry out two experiments. In the first one, we keep the temperature in the inflow 14°C, which corresponds to the estimates from observations (Yuce, 1990, Murray *et al.*, 1991, Oguz and Rozman, 1991, Özsoy *et al.*, 1993). In the second experiment, we assume that the temperature at the inflow points is equal to the ambient temperature. In this way the initial buoyancy due to the temperature is zero, and the plume is driven only by the buoyancy due to salinity. We refer this experiment as to Zero Heat Flux (ZHF) experiment.

4. Horizontal patterns

The simulated plume shows similar patterns in both experiments. It has the form of a very thin wedge with well defined boundaries along the underwater canyon and on the continental shelf. The thickness in these areas ranges from 1 m at the edge of the plume to 17 m in the channel (Fig. 4 and Fig. 5). These values might seem slightly different from the estimates based on observations (10 m in the channel, Latif *et al.*, 1991), but we must keep in mind here that in the reduced gravity model, the temperature and salinity are homogeneous in the vertical and are bounded by a material interface whereas in the observed data there is a continuous transition between the dense bottom layer and the ambience. Therefore, the calculation of the interface depth is subject to interpretation. We note here that Fig. 5 is plotted from time averaged simulation data for a five day period at the end of the integration. This concerns also all plots of time averaged plume characteristics in the remainder of the paper.

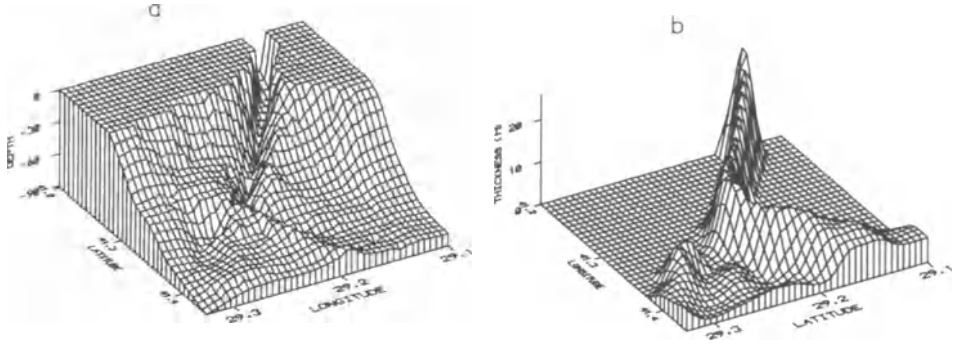


Figure 4. Isometric plots of the underwater channel bathymetry (a), and the thickness of the plume (b) in the main experiment.

There is a very good agreement between Fig. 6 and the observed salinity at the bottom (compare with Fig. 4 of Latif *et al.*, 1991). The Mediterranean outflow is guided by the orientation of the channel, and we observe north-eastward propagation along the first several kilometres, followed by a turn to the Northwest. The plume turns again to the right on the flat shelf, which is an indication that the Coriolis force starts to dominate the solution in this region (compare with Fig. 11 of Yuce, 1990 and Fig. 4 of Latif *et al.*, 1991). The simulations in the main experiment and in the ZHF experiment give very close estimates for the thickness of the plume (Fig. 5a, b) and for the bottom salinity (Fig. 6a, b). The last clearly shows that the buoyancy due to heat flux has secondary effect.

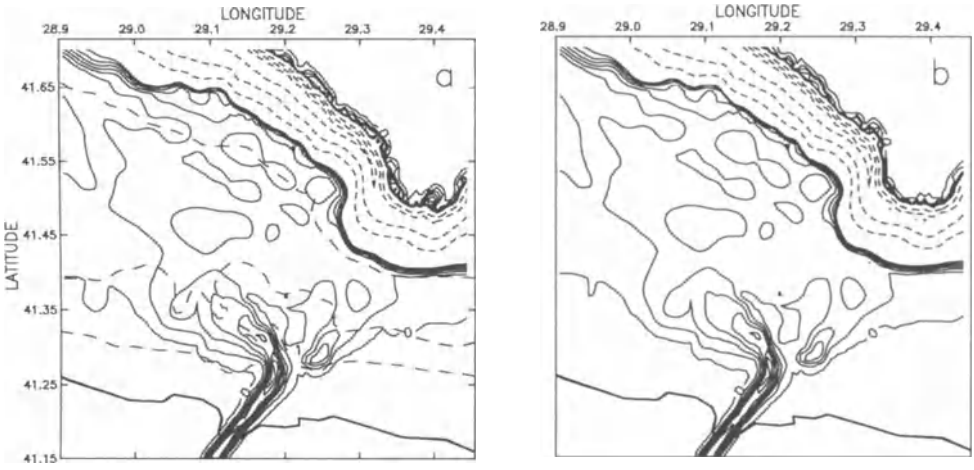


Figure 5. Five day averaged (from day 25 to day 30 of the integration period) thickness of the plume (in m) in the main experiment (a) and in the ZHF experiment (b). Solid contours are 0 to 18 by 3 m, dashed contours are 100 to 300 by 100 m. Longer dash curves are the 60-, 80-, and 100-m isobaths.

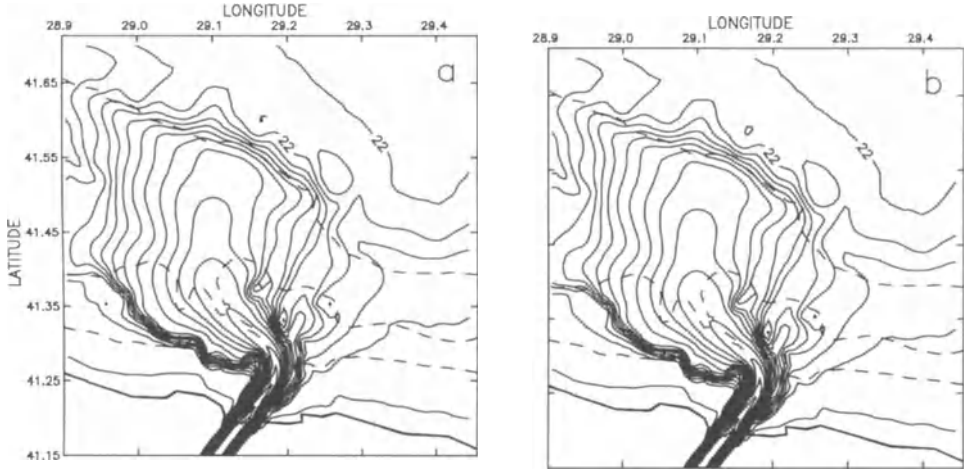


Figure 6. Time averaged bottom salinity (psu) in the main experiment (a) and in the ZHF experiment (b). Contours are 18 to 36 by 1 psu. Dashed curves are the 60-, 80-, and 100-m isobaths.

The form of the simulated plume is very similar to the one shown in Fig. 4 of Latif *et al.* (1991). The plume can be traced down to the continental slope, where it becomes rather diluted and the salinity drops to about 22 psu (close to the ambient salinity). This happens approximately 35 km north-north-west from the strait. As in the

experimental data, the effluent becomes thinner at the edge of the continental slope (about 3 m in the simulation, versus 2 m in the data, reported by Latif *et al.*, 1991).

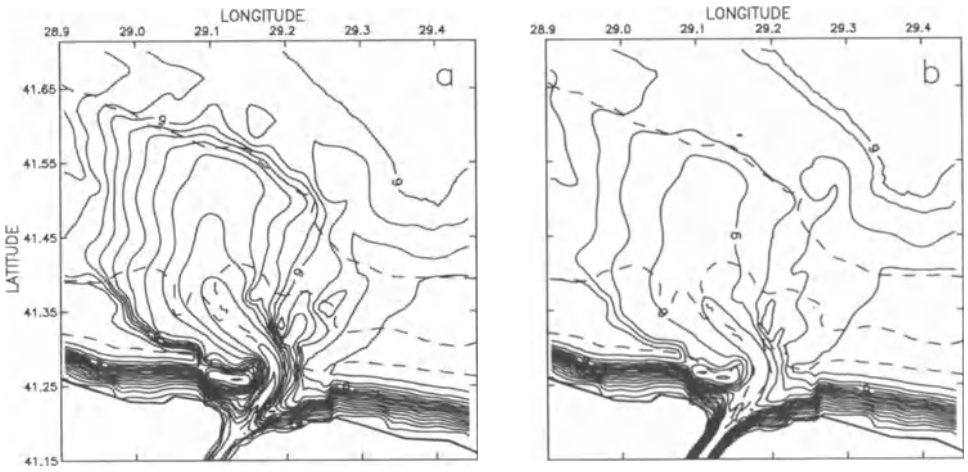


Figure 7. Time averaged bottom temperature of the plume in the main experiment (a) and in the ZHF experiment (b). Contours are 7.5 to 14.0 by 0.5 °C. Dashed curves are the 60-, 80-, and 100-m isobaths.

The model plume does not reach the open boundaries of the model area. This supports the observations of Oguz and Rozman (1991), showing that the plume can not be found to the west of 28°50'E. According to the same observations, the plume is almost undetectable on the continental slope, which is due to the small differences between the plume and the ambient water mass properties. As shown by Özsoy *et al.* (1993), lateral intrusions and internal mixing dominate the penetration of the MSW in the deeper levels. These processes are not simulated in our model (the plume is arrested to the bottom), but the model entrainment further dilutes the plume. Thus, its thickness increases, reaching about 300 m on the slope. This is an indication that the MSW is totally mixed on the continental slope with the ambient water, and the plume loses its individuality. This part of the simulation is not adequate to the real process, due to the model simplifications. However, it presents the model substitute of the deep intrusions in the real basin and has as a main result the termination of the plume at some particular depth (the depth where the plume reaches its neutral density level roughly corresponds to the depth of the intrusions in the real basin). The analysis of the model data shows that the penetration of the plume in the basin interior terminates before the MSW reaches the abyssal plane. Different heat fluxes at the inflow location in the main experiment and in the ZHF experiment do not change the pattern of the bottom temperature, but the gradients decrease strongly in ZHF experiment. More important is that the patterns in the area of the plume are completely dominated by its dynamics,

and are very different from the bottom temperatures dominated by the ambient stratification and topography only (compare Fig. 6 and Fig. 7 with Fig 3b and Fig 3a).

5. Mixing and intrusions

Bogdanova (1961) postulated that the MSW mixed significantly with surface water and did not sink to the bottom but to intermediate depths. Later this idea was confirmed many times and became basic assumption in developing different scenarios to estimate entrainment of the MSW. The plume propagates on the shelf through the CIL (see the bottom temperatures in Fig. 3a), thus it becomes colder after mixing with ambience water. Further down, it reaches the continental slope, with temperatures lower than those of the surrounding water (compare Fig. 7a with Fig 3a). The intrusions on the continental slope carry this cold signal in the basin interior. One of the main issue of this paper is to adequately simulate these processes. A major uncertainty in understanding the ventilation in the Black Sea results from the unknown entrainment of the CIW by the sinking Mediterranean plume. Most of the models for the deep water formation postulate different entrainment of the CIW by the Mediterranean plume: Ostlund (1974) gives for the ratio of the entrained water versus the Bosphorus inflow the value 4:1; Boudreau and Le Blond (1989) use in their box model for the evolution of the salinity during the Holocene an entrainment ratio of 1:4; Murray *et al.* (1991) estimate this ratio as 3,3:1 from the balance of a simple box model. A more direct estimate on the entrainment was given by Buesseler *et al.* (1991) by using Chernobyl isotopes. They showed that ventilation in the upper layer occurs by the lateral injection of 1:10 mixture of inflowing MSW and CIL water. Entrainment and lateral mixing of oxic waters into the anoxic depths explains why the stratification in the chemocline is less sharp than expected. As speculated by Buesseler *et al.* (1991) and Özsoy *et al.* (1993), the chemocline is a region of rapid ventilation, which may occur on quite short time scales, mostly due to lateral injections.
If we assume that Q_b km^3 s^{-1} Mediterranean water with salinity S_b entrains Q_e km^{3}s^{-1} CIL water with salinity S_e and forms a mixture with salinity S_p:

$$S_p = \frac{\sum_p S(i,j)H(i,j)}{\sum_p H(i,j)},$$

where $\sum_p$ is a sum over the plume points, then

$$Q_b S_b + Q_e S_e = (Q_b + Q_e) S_p, \tag{18}$$

and the entrainment ratio is

$$E = \frac{Q_b}{Q_e} = \frac{(S_b - S_p)}{(S_p - S_e)} \tag{19}$$

If we take for the Mediterranean salinity S_b=37.0 psu, for the salinity in the CIL S_e=18.5 psu (see Fig. 3b) and for the salinity of the mixture S_p=21.0 psu (we assume that this is the salinity value, below which we can not detect the plume, see Fig. 6) then E is about 6.4. If we assume that S_e=19.5 psu, which includes not only the mixing with the CIL waters, but also the mixing with deep waters, then E=10.7.

The model constants and forcing were varied in sensitivity experiments to achieve a reasonable tuning. It seems that the best agreement with the observation data (thickness of the plume, bottom temperature and salinity, pathway of the plume) is simulated when the entrainment of CIW by the MSW is about 6.4. This value is between the value of 3-6 (known from the study of Özsoy, *et al.*, 1993) and the one estimated as 10 by Buesseler *et al.* (1991). As we showed above, this ratio could become larger when the entrainment into the outflow along the continental slope is added (see also Özsoy *et al.*, 1993). The evolution of the entrainment of the CIW with time (Fig. 8) shows that 20 days are sufficient for the plume to reach quasi-stationary state.

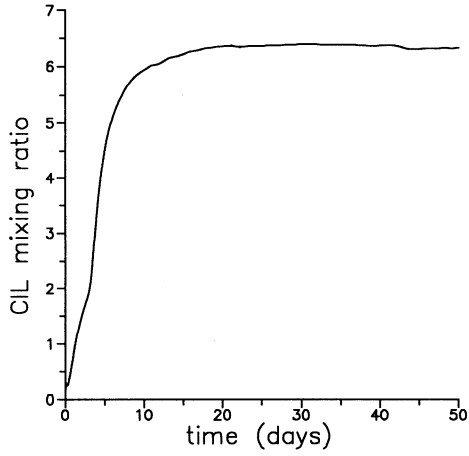


Figure 8. The establishment of the quasistationary state in the main experiment.

The model simulated entrainment velocity (see equations 6-9 and 11-13) shows clearly that there are two well pronounced mixing regions. The first one is just at the shelf break and the second one is close to the downslope edge of the continental slope (Fig. 9). No substantial differences could be found between the results of the two

experiments. We remind again the assumption that the plume is arrested to the bottom, thus the model physics in the second entrainment area does not correspond to the real

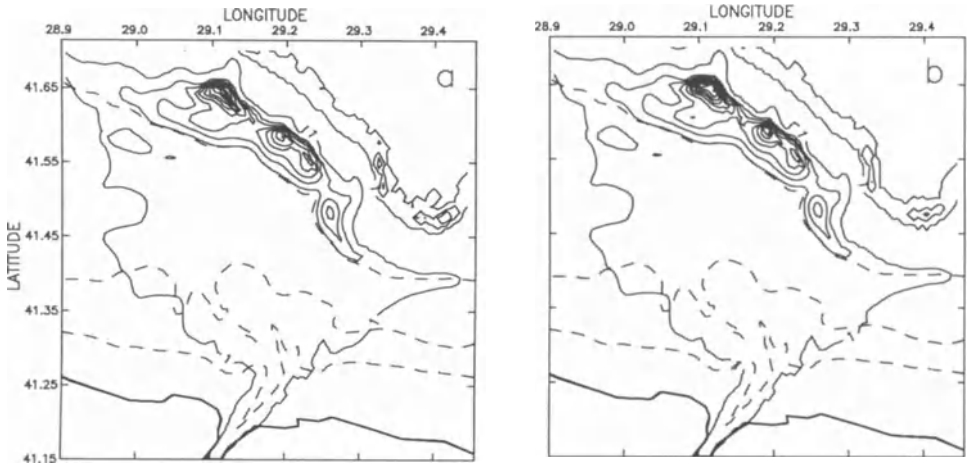


Figure 9. Time averaged entrainment in one model cell (in $m^3 s^{-1}$), calculated from equation (11). Contours are: 1 to 451 by 50 in the main experiment (a), 1 to 501 by 50 in the ZHF experiment (b). Dashed curves are the 60-, 80-, and 100-m isobaths.

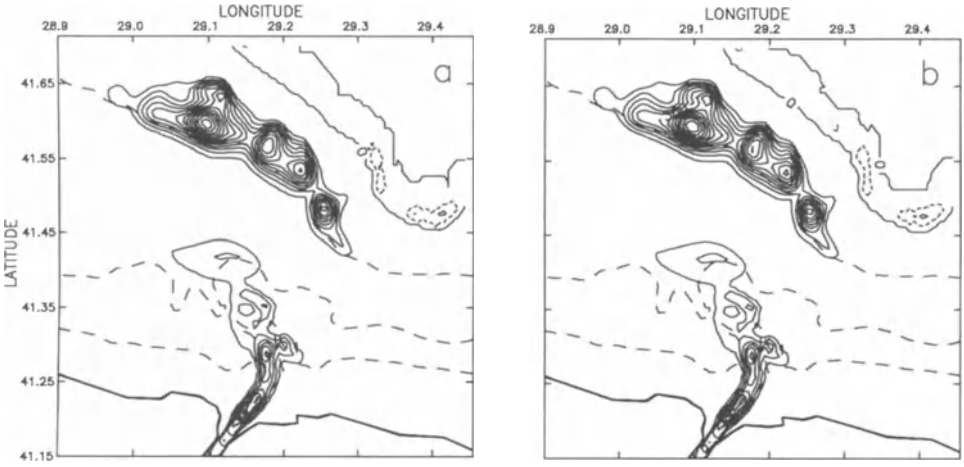


Figure 10. Time averaged salt intrusion in one model cell in units kg s^{-1}, the last term in the left hand side of equation 9. Contours are: -80 to -20 by 60 and 0 to 780 by 60 in the main experiment (a), -100 to -40 by 60 and 0 to 780 by 60 in the ZHF experiment (b). Dash line corresponds to negative values, full line corresponds to positive values. Longer dash curves are the 60-, 80-, and 100-m isobaths.

processes in the deep part of the continental slope. By simulating strong entrainment, the model fulfils the requirement that the plume finds its neutral buoyancy level. This occurs in the second entrainment area. Since this simulation is rather a model artifact, we will not discuss in detail the results in this part of the model domain.
The entrainment velocities do not give enough information about the intrusions of salt and heat at different locations. These variables depend on the difference between the plume temperature and salinity and the ambience water mass properties (equations 8, 9). There is a substantial difference between the salt and heat intrusion patterns, and the ones of the entrainment velocity (Fig. 10 and Fig. 11). Three areas of intrusions are

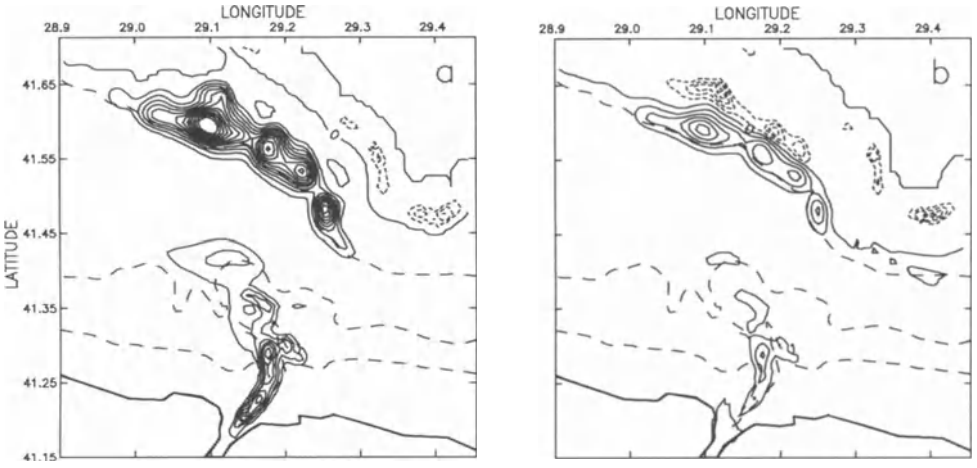


Figure 11. Time averaged heat intrusion in one model cell (in $10^7 J\ s^{-1}$), the last term in the left hand side of the equation 8. Contours are: -20 to -4 by 8 and 0 to 96 by 8 in the main experiment (a), -40 to 40 by 8 in the ZHF experiment (b). Dash line corresponds to negative values, full line corresponds to positive values. Longer dash curves are the 60-, 80-, and 100-m isobaths.

noteworthy. The first one is dominated by strong contrasts between the plume and the ambient in the area of the underwater channel. The intrusions are rather small on the flat shelf, but they increase again in the second area, which is at the shelf break. The third area (at the end of the continental slope) coincides with the area, where entrainment velocities reach secondary maxima. The heat/salt intrusions are not as large as in the other two intrusion zones due to the small temperature/salinity contrasts at the interface. This proves that the plume completely loses its identity in this area.
The differences between the heat flux in the main experiment and the one in the ZHF experiment have small impact on the salinity flux (Fig. 10a, b). However, the heat exchange between the plume and the ambience in the two experiments is very different (Fig. 11a, b). In the experiment with realistic temperature in the inflow location (positive heat flux), cooling of the plume on the shelf and on the

shelf/continental slope edge is much stronger (Fig. 11a). Though heat flux in the inflow location is zero in ZHF experiment, higher temperatures at the level of the inflow than in the underlying CIL result in simulating similar patterns as in the main experiment, but with much weaker gradients.

The area averaged plume characteristics, shown in Fig. 12, give a more general view on the fate of the MSW in the Black Sea. The averaging is done only for the points at the interface. The first depth range, with a maximum at about 100 m, corresponds to the entrainment zone at the edge of the continental shelf. In this depth range, the model simulates positive salt flux, that is salt penetrates from the plume to the ambience. In the same depth range the plume exports heat to the ambience, since it is

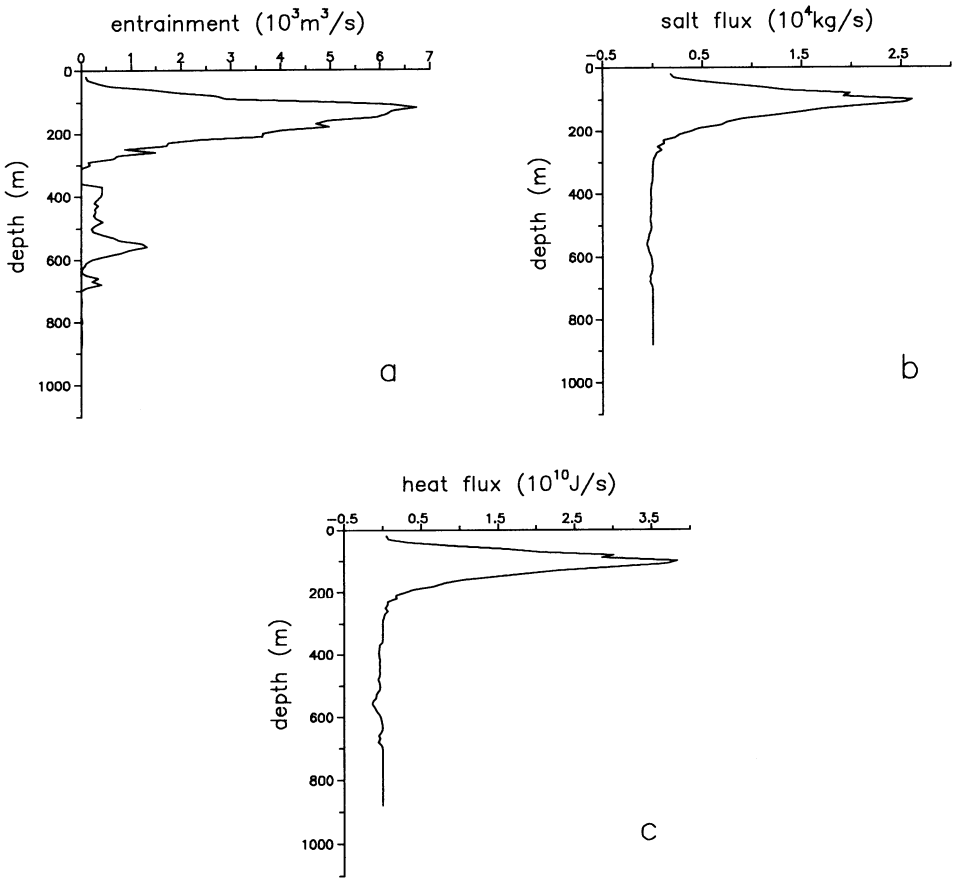


Figure 12. Time averaged vertical profiles of the mean for the plume interface entrainment (a), salt flux (b), and heat flux (c) in the main experiment.

warmer than the CIL. The maxima of heat and salt flux are about 20 m shallower than the one of the entrainment velocity, which results from the specific correlation between entrainment velocity and temperature/salinity differences at the interface.
The second depth range, where entrainment has a maximum, lies at about 550 m. We just showed that the plume reaches its neutral density level at this depth and tends to completely mix with the surrounding water. The model simulates randomly changing maxima of the intrusions and different depths of penetration. However, intrusions never reach the deepest most level, which supports the hypothesis of Özsoy *et al.* (1993) that in the present époque the deep layers remain untouched by the surface water. Radiocarbon data show rather short residence times at depths less than 500 m (Ostlund, 1974 and Ostlund and Dyrssen, 1986), which is consistent with the intrusion mechanism simulated in the model.

6. *T-S* analysis

The vertical profiles of the difference between the ambience and plume temperature/salinity, averaged for the plume interface (Fig. 13), show in a generalised way the transformation of the MSW. There is no principal difference between the profiles simulated in the two experiments. Salinity of the plume tends to the one of the ambience, and most of the dilution occurs in the upper 100m (Fig. 13 a). The temperature difference at the interface shows a different behaviour in the upper levels. It increases sharply with depth down to the upper boundary of the CIL. The difference between the shape of the curves in Fig. 13a and Fig 13 b is due to the different shape of the vertical profiles of the temperature and salinity of the environment. While ambient salinity constantly increases with depth, its temperature first decreases, and below the core of the CIL, starts to increase. The plume constantly warms with increasing depth and reaches the ambience temperature at 200m.
The density difference at the interface (Fig. 13c) shows that the plume dynamics is dominated by salinity anomalies (the shapes of Fig. 13c and Fig. 13a are the same). More detailed understanding about the individual contribution of temperature and salinity anomalies in the formation of buoyancy anomaly at the interface is given in Fig. 13 d, where the terms $\alpha(T-T_a)$ and $\beta(S-S_a)$ are compared. There is an area in the extension of the Bosphorus Strait, where the effect of buoyancy due to temperature opposes the one due to salinity (the intruding MSW is warmer and saltier than the ambience water). However, below 50 m the plume entrains sufficiently CIW. Below the core of the CIL it becomes cooler than the ambience water, thus the sign of the slope changes. The dash curve has a slope corresponding to $\alpha(T-T_a)/\beta(S-S_a)=1$. The difference between the slopes of the dash and the full lines measures the relative importance of the two thermodynamic characteristics in the formation of the buoyancy of the plume. It is noteworthy that this ratio is constant between core of the CIL and the continental slope (60-110m). Below, the relative importance of the temperature slightly increases.

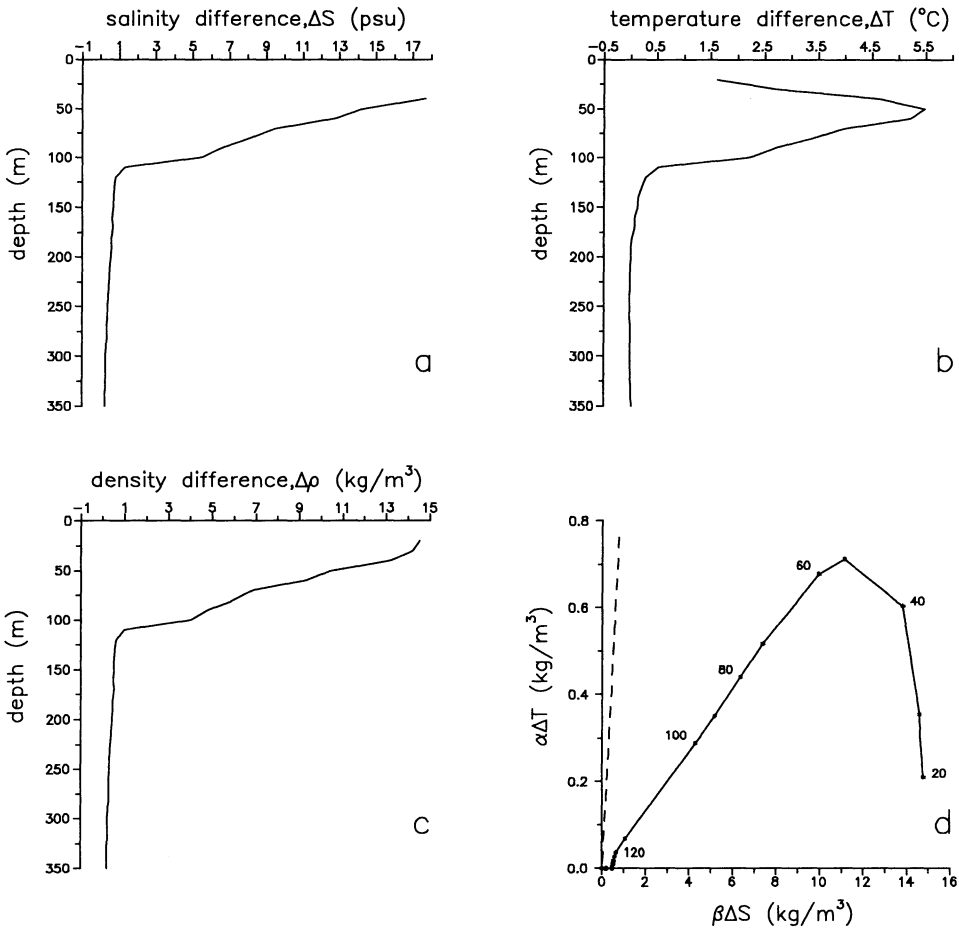


Figure 13. Time averaged vertical profiles of the mean for the plume interface difference between the ambience and plume salinity (a), temperature (b), density (c), and the contribution of temperature versus the one due to salinity in the density anomaly (d). Dash line has a slope $\alpha(T-T_a)/\beta(S-S_a)=1$, numbers denote the depth in meters.

Further insight in the details of the mixing processes could be achieved from the analysis of the simulated *T-S* diagrams (Fig. 14), which compare well with Fig. 7 of Özsoy *et al.* (1993), showing the ambient *T-S* diagram and the mixing path of the MSW. The *T-S* points are below the ambient curve, which indicates that cold anomalies are injected from the plume into the surrounding BSW. We note that no full correspondence with the mixing curves of Özsoy *et al.* (1993) exists, since they show *T-S* plots for all depths, and ours are only for the bottom water. More detailed examination of the mixing paths indicates that MSW first decrease temperature and salinity, and after reaching values of 7.1°C and 18.8 psu *T-S* points move again to the

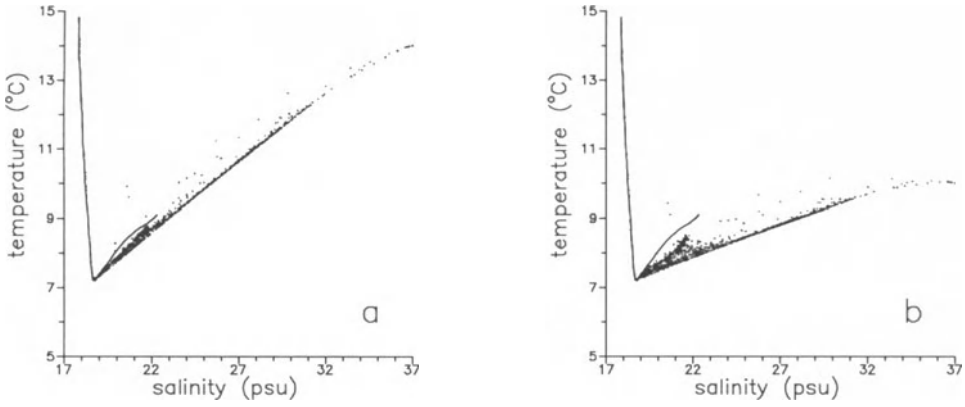


Figure 14. Time averaged *T-S* diagrams in the main experiment (a), and in the ZHF experiment (b). The scattered points give *T-S* characteristics of the mixed MSW at sea bottom. Full line corresponds to the ambient.

upper-right corner of the diagram and tend to touch the ambience curve. The ZHF experiment gives geometrically similar mixing paths, but the difference in the temperatures at the inflow location of about 4°C result in much wider mixing sector.

7. Conclusions

The evolution of the intermediate and deep water is a fundamental issue in the physical oceanography of the Black Sea. It is related to the physical mechanisms of circulation, water mass formation, and internal mixing. However, it has far reaching implications for the understanding of climatic change in this basin, as well as the sensitivity of its water masses to external climatic and antropogenic impacts. The changing depth of penetration of the MSW could give a spectacular illustration of the evolution of the Black Sea physical system from a state, typical for a fresh water lake, into its present stagnant state. As we showed, this penetration depends both on the morphometric characteristics, and on the entrainment of the BSW by sinking MSW. However, there is no common understanding how entrainment operates, and this open question necessitates further theoretical and model studies. The present paper presents a small contribution to elucidating this issue.

For the first time the phenomenology of the sinking plume, originating from the Strait of Bosphorus, is illustrated by model simulations. They show encouraging agreement with the observations. In particular, the coincidence of nepheloid layers with the cold intrusions indicates that common physical mechanism exists, which produces these anomalies (Özsoy *et al.*, 1993). Our model simulated intrusions correlate rather well with the observations just below the base of the CIL. Model simulated intrusions does not penetrate deeper than 500-600m. This depth range was previously estimated from

the observation data as the ultimate depth of penetration of the modified water (Özsoy *et al.*, 1993).

Model studies could go beyond the simplistic comparative tasks, elucidating the regional physical balances. The numerical model can be regarded as a tool for the examination of subtle characteristics of the plume. The best agreement with the observations (thickness of the plume, bottom temperature and salinity, pathway of the plume) is simulated when the entrainment of CIW by the MSW is about 1:6.4. This entrainment rate correlates with other independent estimates, proving again that the model is sufficiently tuned. This resulted in a number of encouraging agreements of the simulated plume phenomenology with the results from observations. These agreements are the best on the shelf and on the shelf edge, where most of the transformation of the MSW occurs. The simulated plume has the form of a very thin wedge with well defined boundaries along the underwater canyon and on the continental shelf. It is guided by the orientation of the channel, and propagates to the North, Northwest. The plume turns then to the right on the flat shelf, deflected by the Coriolis force. The form of the plume on the shelf correlates well with the one found by Latif *et al.* (1991) from survey data. It can be traced down to the continental slope, where its salinity approaches the ambient salinity. After this phase of the evolution, the MSW is totally mixed or intruded in the ambience on the continental shelf, which agrees with the more general results of Price and Baringer (1994).

We admit that there are number of simplifications in the present study, some related to the model, as "arresting the plume at the bottom" and considering it as fully mixed in the vertical, others related to the formulation of model driving. We have chosen the simplest driving configuration here. Further model development has to be related to improving the resolution, which is still insufficient in the strait exit area, and combining strait and shelf physics in one model.

Acknowledgements

We thank E. Özsoy for the comment about the temperature of the inflowing water during the NATO ARW and the anonymous reviewer for the useful suggestions, related to some interpretations of the results. The study was supported by the International Atomic Energy Agency, Contract No 7814/R1/RB.

References

1. Bogdanova, A. K. (1961) The distribution of Mediterranean waters in the Black Sea, *Okeanologiya* **1**, 983-991 (in Russian).
2. Bourdreau, B. P. and Leblond, P. H. (1989) A simple evolutionary model for water and salt in the Black Sea, *Paleoceanography* **4**, 157-166.
3. Buesseler, K. O., Livingston, H. D., and Casso, S. (1991) Mixing between oxic and anoxic waters of the Black Sea as traced by Chernobyl cesium isotopes, *Deep Sea Research* **38**, S725-S745.
4. Chapman, D. C. and Gawarkiewicz, G. (1995) Offshore transport of dense shelf water in the presence of a submarine canyon, *J. Geophys. Res.* **100**, 13373-13386.

5. Friedrich, H. J and Stanev, E. V. (1988) Parameterization of the vertical diffusion in a numerical model of the Black Sea, *Small-scale turbulence and mixing in the ocean.* J. C. J. Nihoul and B. M. Jamart (editors), Elsevier, 151-167.
6. Gawarkiewicz, G. and Chapman, D. C. (1995) A numerical study of dense water formation and transport on a shallow, sloping continental shelf, *J. Geophys. Res.* **100**, 4489-4507.
7. Jungclaus, J. H. and Backhaus, J. O. (1994) Application of a transient reduced-gravity plume model to the Denmark Strait overflow, *J. Geophys. Res.* **99, C6,** 12375-12396
8. Latif, M. A., Özsoy, E., Oguz, T., and Unluata, U. (1991) Observation of the Mediterranean inflow into the Black Sea, *Deep Sea Research* **38**, Suppl. 2, S711-S723.
9. Mellor, G. L. and Durbin, P. A. (1975) The structure and dynamics of the ocean surface mixed layer, *J. Phys. Oceanogr.* **5**, 718-728.
10. Murray, J., Top, Z., and Özsoy, E. (1991) Hydrographic properties and ventilation of the Black Sea, *Deep-Sea Research* **38**, Suppl. 2, S663-S689.
11. Oguz, T. and Rozman, L. (1991) Characteristics of the Mediterranean underflow in the south-western Black Sea continental shelf/slope region, *Oceanologica Acta* **14**, 433-444.
12. Oguz, T., Özsoy, E., Latif, M. A., Sur, H. I., and Unluata, U. (1990) Modeling of hydrographically controlled exchange flow in the Bosphorus Strait, *J. Phys. Oceanogr.* **20**, 945-965.
13. Ostlund, H.G. (1974) Expedition Odysseus 65: Radiocarbon age of Black Sea water, *The Black Sea Geology, Chemistry and Biology*, E. T. Degens and D. Ross (editors), The American Association of Petroleum Geologist, Memoir 20, pp. 127-132.
14. Ostlund, H. G. and Dyrssen, D. (1986) Renewal rates of Black Sea deep water, *The chemical and physical oceanography of the Black Sea.* University of Goteborg, Report on the Chemisrtry of the Sea XXXIII Presented in the Meeting on the Chemical and Physical Oceanography of the Black Sea, Goteborg, Sweden, June, 1986.
15. Özsoy, E., Unluata, U., and Top, Z. (1993) The evolution of Mediterranean water in the Black Sea: interior mixing and material transport by double diffusive intrusions, *Progress in Oceanogr.* **31**, 275-320.
16. Özsoy, E., Latif, M. A., Sur, H. I., and Goryachkin, Y. (1996) A review of the exchange flow regimes and mixing in the Bosphorus Strait, *Bulletin de l' Institut oceanfgraphique* , Monaco, n^0 special 17.
17. Price, J. F., Baringer, M. O'Neil (1994) Outflows and deep water production by marginal seas, *Prog. Oceanogr.* **33**, 161-200.
18. Smith, P. C. (1975) A streametube model for bottom boundary currents in the ocean, *Deep Sea Res.* **22,** 853-873.
19. Stanev, E. V. (1988) Numerical study on the Black Sea circulation, *Mitteilungen des Instituts fuer Meereskunde der Universitaet Hamburg* **28**, 232 pp.
20. Stanev, E. V. (1990) On the mechanisms of the Black sea circulation, *Earth-Science Rev.* **28**, 285-319.
21. Tolmazin, D. (1985) Changing coastal oceanography of the Black Sea. Part II: Mediterranean effluent, *Progress in Oceanogr.* **15**, 277-316.
22. Unluata, U., Oguz, T., Latif, M. A., and Özsoy, E. (1990) On the Physical Oceanography of the Turkish Straits, *The Physical Oceanography of Sea Straits*, L. J. Pratt (editor), *NATO/ASI Series, Kluwer, Dordreht*, pp. 25-60.
23. Yuce, H. (1990) Investigation of the Mediterranean Water in the Strait of Istanbul (Bosphorus) and the Black Sea, *Oceanologica Acta* **13**, 177-186.

COASTAL EUTROPHICATION OF THE SOUTHERN BIGHT OF THE NORTH SEA : ASSESMENT AND MODELLING

CHRISTIANE LANCELOT, VERONIQUE ROUSSEAU, GILLES BILLEN AND DENIS VAN EECKHOUT
Groupe de Microbiologie des Milieux Aquatiques, GMMA
Université Libre de Bruxelles, CP 221
Boulevard du Triomphe
B-1050, Bruxelles

Abstract

Massive blooms of the colony-forming Haptophyte *Phaeocystis* sp. are a recurrent phenomenon in the eutrophicated continental coastal waters of the North Sea. This coastal zone is receiving the discharge of seven major west-european rivers the watershed of which is characterized by high population densities and intense industrial and agricultural activities. The basic mechanisms of *Phaeocystis* blooms development in response to riverine nutrient enrichment are being investigated since 1988 in the scope of national and EC research projects on *Phaeocystis* bloom dynamics. The ultimate objective is to set up a computer tool that could provide guidance for making selection among the control actions available for counteracting coastal eutrophication in this area. For this purpose, an integrated research methodology has been implemented, combining field observations of *Phaeocystis* blooms development and associated physico-chemical and biological variables at reference coastal stations, physiological studies of *Phaeocystis* nutrient metabolism and the development of the mechanistic biogeochemical MIRO model. Results of this long-term study are presented here. Observational and mathematical evidence is given that the present-day extent of *Phaeocystis* colony development observed in the whole area, mainly results from changes in riverine nitrate and silicate delivery, driven by changes in both anthropogenic activities and rainfall conditions on the watershed. Furthermore, realistic nutrient reduction scenarios as scheduled for North-Western Europe for the next 25 years, making use of the current MIRO model, gives additional illustration of the complex interaction between the continent and coastal sea systems and of the appropriateness of the mechanistic model as a decision support for selecting the most appropriate measure to counteract coastal eutrophication.

E. Özsoy and A. Mikaelyan (eds.), Sensitivity to Change: Black Sea, Baltic Sea and North Sea, 439–453.
© 1997 *Kluwer Academic Publishers.*

1. Introduction

The coastal zone, at the interface between land, ocean and atmosphere, plays a major role as recipient of large amounts of nutrients from human activities, including industrial effluents, agricultural runoff, and municipal sewage. Manifest effects of man-induced coastal eutrophication usually appear as qualitative changes of the structure and functioning of the pelagic and benthic food-web with resulting undesirable effects (e. g. invasions of undesirable or toxic phytoplankton species, extinctions of key species on higher trophic levels, reduced yields of harvestable fish or invertebrate populations...). This alteration of the ecosystem structure and functioning is primarily driven by changes in nutrient ratios available to coastal phytoplankton with respect to silicon availability - severely deficient compared to nitrogen and phosphorus -, resulting from the interplay of several factors as anthropogenic activities (land use modification, waste water purification treatments, hydraulic managments, farming practices,...), biogeochemical transformations occuring in the river systems and meteorological conditions [1].

Such harmfull events are occurring in the eutrophicated continental coastal waters of the North Sea. This area receives the discharge of 7 major west-european rivers draining regions characterized by high population densities and intensive industrial and agricultural activities (Fig.1). Transient foam accumulations observed, indeed, every spring at sea surface and on the beaches are resulting from food chain disruption due to the proliferation of one single non-siliceous species, the gelatinous colony-forming *Phaeocystis*, largely unpalatable for mesozooplankton and apparently hardly biodegradable [2]. Even if no toxicity is attributable to *Phaeocystis* to date, its dramatic invasion is being seriously considered regarding the nuisances it causes to the coastal ecosystem and to recreative and aquaculture activities. Most of these - including their impact on the higher trophic levels of the planktonic and benthic food chain, the exportation of organic matter to the oxygen depleted bottom waters of the Danish coastal area, the accumulation of foam on the beaches and the production of volatile sulphur compounds into the atmosphere - are the consequence of the peculiar physiology and life cycle of *Phaeocystis*, especially in its capacity to form large unpalatable gelatinous colonies causing food chain disruption [3] and to synthetize dimethyl-sulphide precursors [4].

Reduction of harmful *Phaeocystis* blooms in the continental coastal waters of the North Sea through the formulation of national and international regulations on sewage treatment facilities and farming practices aiming at the reduction of riverine nutrient delivery to the coastal sea is nowadays a main concern of public authorities. However the basic scientific knowledge required to properly assess the extent of nutrient reduction as well as its priority target (ammonium, nitrate, phosphorus) was up to now lacking. Yet, the choice between phosphorus or nitrogen reduction for controlling coastal eutrophication has considerable economical consequence.

In the scope of national and EC research projects, an integrated land-coastal sea system approach that combines field observations, process-level studies and numerical experimentation has been implemented since 1988. The purpose is to improve

knowledge on eutrophication mechanisms in the coastal North Sea and give guidance for making selections among the possible measures to counteract eutrophication in this coastal sea. The feasibility and the appropriateness of this integrated research methodology to identify and solve coastal eutrophication problems is illustrated in this paper which synthetizes (i) knowledge on the present-day eutrophication level of the continental coastal waters of the North Sea and its natural and man-induced controlling mechanisms; (ii) shortly describes the mechanistic biogeochemical model MIRO; (iii) appraises the model performance in its ability to predict present-day *Phaeocystis* blooms; and (iv) explore the response of the current *Phaeocystis*-dominated coastal North Sea ecosystem to environmental policies scheduled for the next decade by North-Western European countries with respect to EC guidelines.

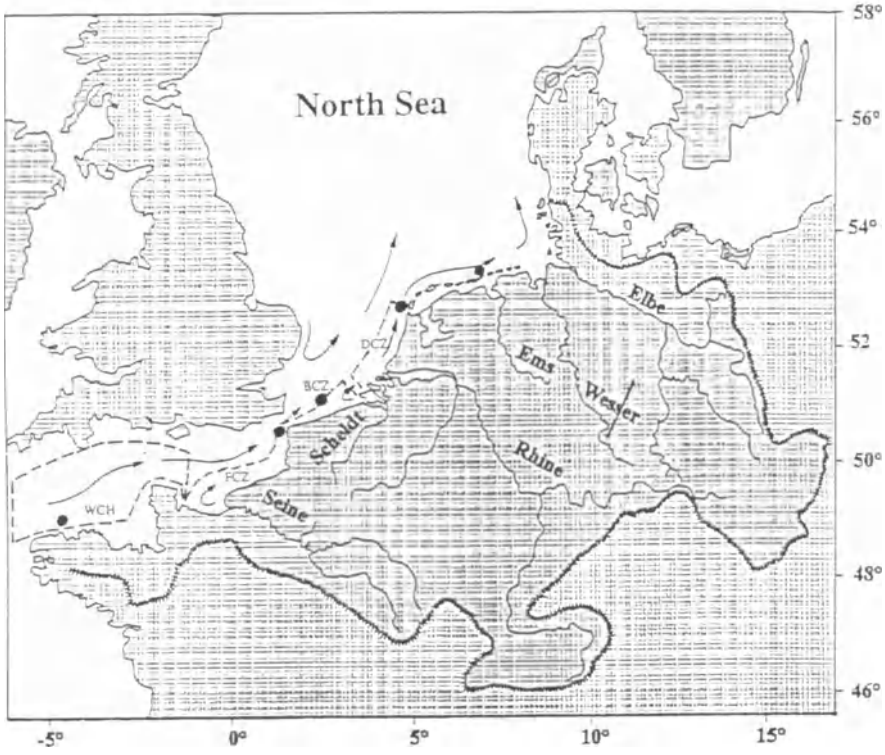


Figure 1. Map showing the watershed of the main rivers discharging in the continental coastal waters of the North Sea; the location of the monitoring stations (●); and the sub-areas (dotted contours) considered for the application of the MIRO model (WCH Western Channel; FCZ : French coastal zone; BCZ : Belgian coastal zone; DCZ : Dutch coastal zone)

2. The eutrophication phenomenon of the continental coastal waters of the North Sea : assesment and mechanisms

The present-day features of coastal North Sea eutrophication were appraised from the comprehensive analysis of high resolution time-series data on nutrients, phytoplankton and heterotrophic organisms yearly collected during the period 1988-1993 at selected reference stations within the area extending from the Western Channel to the Dutch coastal waters (Fig.1) [5], in relation to nutrients riverine loads and meteorological conditions. When combined with physiological studies on *Phaeocystis* nutrient metabolism [3, 6] and on the biodegradability of *Phaeocystis*-derived material [7], this comprehensive analysis allows to identify the basic mechanisms behind eutrophication of coastal North sea, in particular those ecological events that lead in spring to transient accumulations of foams on beaches bordering the North Sea.

2.1. THE NUTRIENT ENVIRONMENT OF COASTAL NORTH SEA PHYTOPLANKTON

The general nutrient enrichment of the coastal area from continental sources is reflected by N, P, Si winter concentrations (Table 1) which display a one-order-of-magnitude increase from the Western Channel to the Dutch coastal waters. Riverine nutrients discharging in the North Sea are indeed cumulating along a SW-NE axis as a result of the mean residual circulation of the water masses. Qualitative changes induced by freshwater sources of nutrients as exhibited by the N:P, N:Si and P:Si molar ratios of the winter inorganic nutrient pool (Table 1) clearly evidence in the whole area a nitrate excess over silicate and phosphate with respect to coastal diatom silicon requirements (average N:Si molar ratio of 1.2) [8] and phytoplankton phosphorus needs (Redfield's N:P molar ratio of 16).

TABLE 1. Nutrient discharge and winter concentration in the coastal North Sea

Coastal area	WCH	FCZ	BCZ	DCZ
River inputs :				
nitrogen : 10^3 T y^{-1} (% nitrates)		125 (80)	58 (44)	500 (70)
phosphorus :10^3 T y^{-1}(% phosphate)		12 (77)	7.3 (45)	29 (70)
silicates : 10^3 T y^{-1}		67	27	191
molar N:P - N:Si - P:Si		24 - 3 - 0.13	29 - 3.4 - 0.11	31 - 4.2 - 0.14
Average winter concentrations				
nitrate : µM	8	25	35	80
phosphate : µM	0.6	1.5	1.2	2
silicate : µM	6	9	12	40
molar N:P - N:Si - P:Si	17 - 1.4 - 0.11	17 - 2.7 - 0.17	30 - 3 - 0.11	28 - 2.7 - 0.1
Maximum spring chl a : mg m^{-3}	4	10	45	75

2.2. STRUCTURE AND FUNCTIONING OF THE COASTAL NORTH SEA PLANKTONIC FOOD-WEB

2.2.1. *The phytoplankton community*

Nutrient enrichment of coastal waters stimulates in spring the development of phytoplankton of which the biomass exhibits a one-order-of-magnitude increase from the Western Channel to the Dutch coastal waters (Table 1). The severely unbalanced nutrient enrichment with respect to diatoms requirements, however, stimulates, after the early spring development of a silicate-controlled diatom bloom (Fig.2a), the explosive development of the colony-forming *Phaeocystis*, sustained by new sources of nitrate of anthropogenic orgin (Fig.2b). The link between *Phaeocystis* colony blooms and the anthropogenic nitrate enrichment of the continental coastal waters of the North Sea is clearly evidenced by the positive relationship between the maximum *Phaeocystis* cells density reached in spring and the nitrate standing stock available at diatom decline (Fig.3).

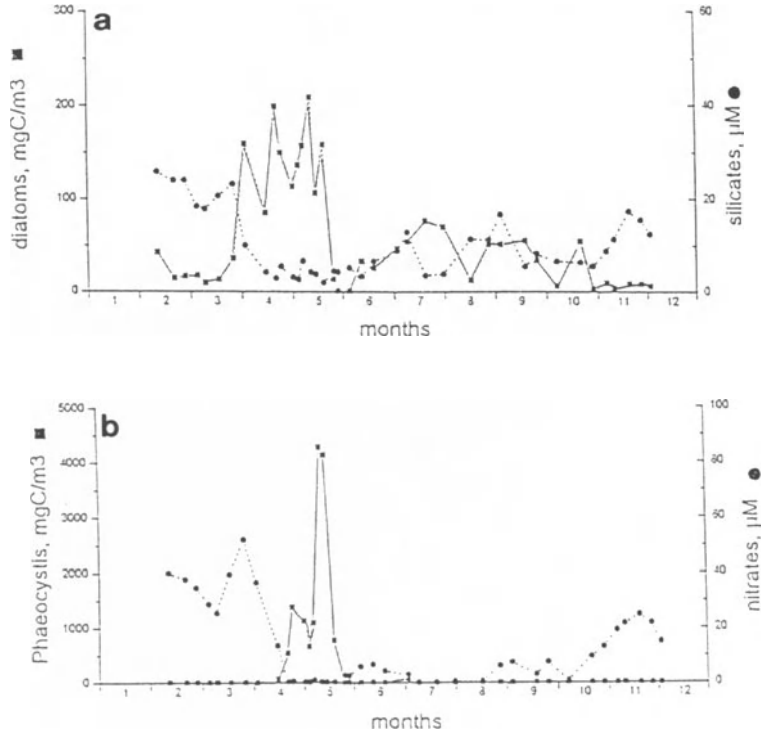


Figure 2 Typical spring phytoplankton succession and nutrients cycle in the Belgian coastal waters Monitoring data 1993 of Rousseau et *al.*[9]

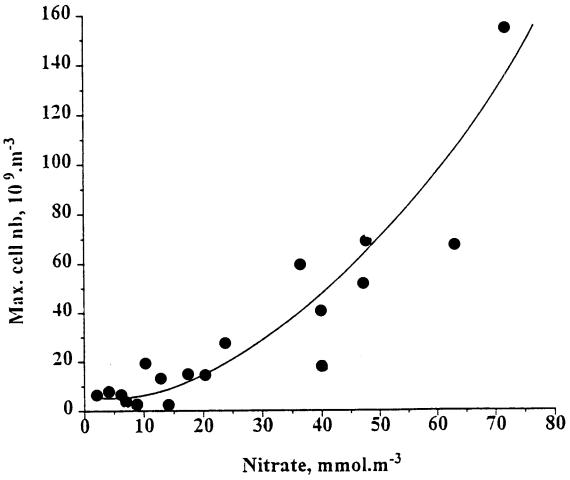


Figure 3 Relationship between *Phaeocystis* colony bloom magnitude and nitrate concentration at *Phaeocystis* onset. 1988-1995 data of Rousseau *et al.* [9]

Superimposing changes in anthropogenic activities - in particular those supplying nitrates to the freshwater and marine systems -, as driving forcing of *Phaeocystis* colonies development in the coastal North Sea, variations of late winter meteorological conditions on the watershed, in particular rainfall, were shown to induce contrasting changes in the spring diatom-*Phaeocystis* dominance as well [9]. Accordingly, the relative importance of diatom *versus Phaeocystis* colony blooms is positively related to late winter rainfall conditions (Fig.4) with persistant intense precipitations in winter driving the development of a diatom-dominated spring bloom while less intense rainfall promoting *Phaeocystis* colonies. To which extent this alternation in phytoplankton species dominance is affecting the trophic efficiency and the geochemical significance of the coastal North Sea is not known yet.

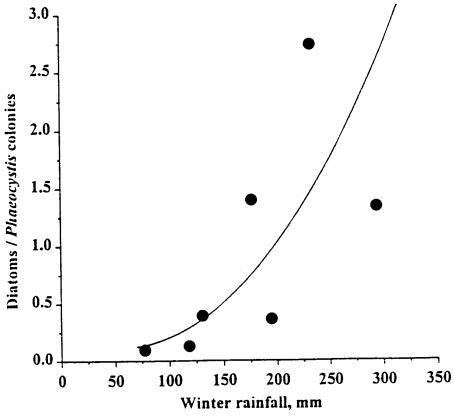


Figure 4 Relationship between late winter rainfall on the Scheldt watershed and the relative importance of the diatom :*Phaeocystis* carbon biomass. After Rousseau *et al.* [9]

2.2.2. *Planktonic food-web structure*

Phaeocystis is one of the few marine phytoplankters exhibiting phase alternation between free-living cells of 3-9 μm in diameter and 1 mm gelatinous colonies typically composed of thousands of cells embedded in a gel-like matrix made of polysaccharides [e.g. 3, 10, 11]. These *Phaeocystis* life forms are characterized by different ecological and geochemical fate [12]. The successfull development of *Phaeocystis* colonies is explained by an apparent higher ability of the colonial form tu use nitrate as nitrogen source [12, 13], and by their high resistance to grazing by indigeneous mesozooplankton [14]. The dominance of mesozooplankton-unpalatable *Phaeocystis* colonies has been deviating the classical linear food chain towards a complex microbial network. The latter is primarily stimulated by the release of *Phaeocystis* free-living cells and dissolved organic matter after disruption of non-grazed colonies. The outstanding aggregation of foam deposited on beaches during periods of onshore winds then results from transient accumulation of *Phaeocystis*-derived organic matter resistant to immediate microbial degradation. Interestingly enough, a positive relationship exists between the magnitude of *Phaeocystis* blooms and mesozooplankton [15]. This positive feedback might be explained by the existence of an active microbial food-web in which protozoa play a key role as grazers of *Phaeocystis* free-living [16, 17] and as food ressources for indigeneous mesozooplankton [18]. This stresses the high flexibility of this coastal ecosystem and its adaptability to environmental changes.

3. Modelling the eutrophication of the continental coastal waters of the North Sea

An integrated network of mechanistic biogeochemical models, consisting of the offline coupling of a biogeochemical model of *Phaeocystis* blooms development in the coastal North Sea - the MIRO model [5] - with a river system model calculating riverine nutrient delivery to the coastal zone, as a function of hydrology, land use and waste water purification policies - the RIVERSTRAHLER model [9] - is being developed for predicting the response of the *Phaeocystis*-dominated coastal ecosystem to changes in riverine nutrient loads resulting from changes occuring in the watershed. Basically these mechanistic models are describing and predicting the cycling of carbon, nitrogen, phosphorus and silicon through aggregated key components of the freshwater and coastal ecosystems over seasons and years in response to the physical and nutrient forcing. Such mathematical models, therefore, are based on physiological and geochemical principles. The numerical code synthetizes knowledge on the kinetics and the factors controlling the main auto- and heterotrophic processes involved in the functioning of the river and marine coastal ecosystem. The code is continuously in development relying on progress in experimental aquatic ecology. Current development of the MIRO model, in particular its ability to reproduce the present-day eutrophication in the continental coastal waters of the North Sea, in particular the magnitude and extent of *Phaeocystis* blooms, and explore the coastal ecosystem

response to nutrient reduction scenarios scheduled for the next 25 years is shortly presented below.

3.1. THE MIRO MODEL : MODELLING PRESENT-DAY *PHAEOCYSTIS* BLOOMS DEVELOPMENT IN THE COASTAL NORTH SEA.

3.1.1. *Description of the ecological model*

The MIRO ecological model describes the cycling of carbon, nitrogen, phosphorus and silicon through aggregated chemical and biological compartments of the planktonic and benthic components of the coastal area (Fig.5). Thirty-two state variables and twenty-six processes linking them were identified as important from the knowledge of the structure and functioning of *Phaeocystis*-dominated ecosystems. The model results of the assemblage of 4 modules describing the dynamics of phytoplankon, zooplankton, organic matter degradation and nutrient regeneration in the water column and the sediment. Mathematical formulation of kinetics, parameters and forcing functions are described in [5].

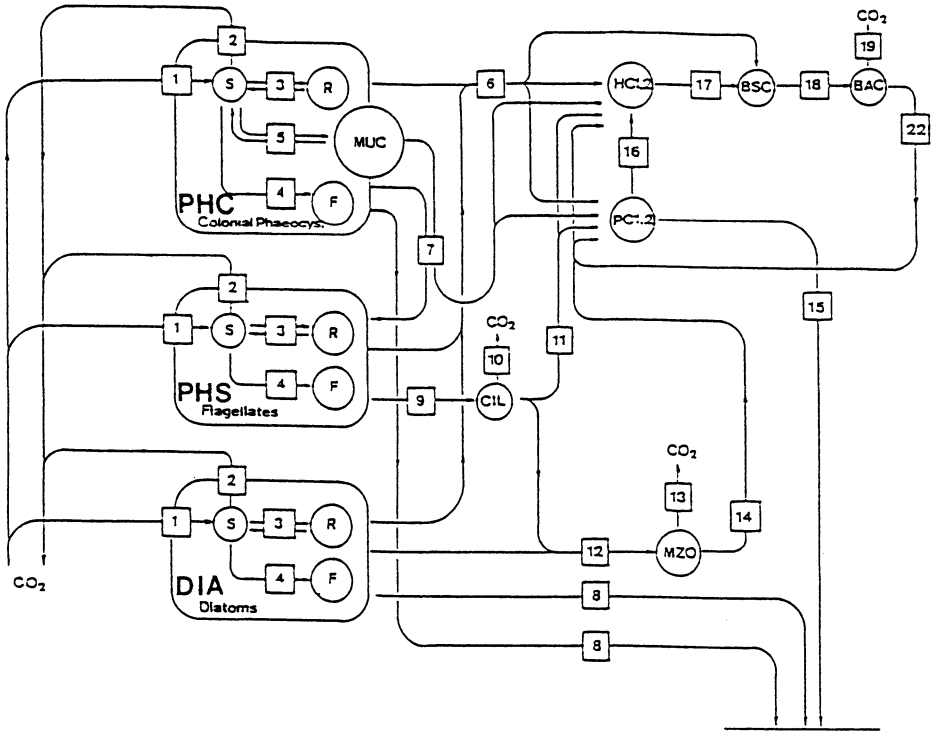


Figure 5 Structure of the MIRO model : carbon cycling. Legend for state variables (circles) and processes linking them (numbers) in text.

The phytoplankton module considers 3 phytoplankton groups: diatoms (DIA), free-living nanoflagellates (PHS) and *Phaeocystis* colonies (PHC). Due to their trophic fate, *Phaeocystis* free-living cells and colonies are considered as separate state variables, even though they constitute two different stages of the life cycle of the same phytoplankter (e.g. Rousseau *et al.*, 1994). The kinetics of phytoplankton activities is described according to the AQUAPHY model of Lancelot *et al* [20]. It considers 3 intracellular pools - monomers (S); reserve material (R); functional and structural metabolites (F) - and distinguishes the processes of photosynthesis (1) directly dependent on light availability, from the process of growth (4) controlled by the availability of intracellular monomers and ambiant nutrients. One single nutrient is limiting phytoplankton growth, according to the Liebig law of minimum. With respect to *Phaeocystis* colonies, an additional pool of extrapolymers (MUC) has been added to consider the mucilaginous matrix in which the cells are embedded and which serves as reserve of energetic material (5). Beside respiration (3), loss processes include excretion, cellular lysis (6), under control of nutrient stress; sedimentation (diatoms and *Phaeocystis* colonies) (8); zooplankton grazing (12).

The zooplankton module of the MIRO model considers two groups of zooplankton : the microzooplankton (CIL) feeding on free-living flagellates (9) and the mesozooplankton (MZO) grazing (12) on diatoms and microzooplankton according to a preference for the latters (F. Hansen, pers. com.). *Phaeocystis* colonies escape grazing. Colonies are however submitted to a nutrient stress-dependent process of colonial disruption (7) which releases in the water column free-living cells and dissolved organic polymers. A simplified description of zooplankton dynamics has been chosen, considering grazing as an hyperbolic Michaelis-Menten function of food items with however a threshold value below which no grazing is possible. Zooplankton growth and excretion (14) are calculated from grazing rates based on growth efficiency, zooplankton stoechiometry and the calculated nutrient composition of food. First-order mortality is considered.

Organic matter degradation by planktonic bacteria is described according to the HSB model of Billen[21], considering two classes of biodegradability for both dissolved (HC1 and HC2) and particulate (PC1 and PC2) organic matter. Ectoenzymatic hydrolysis of these polymers (17) produces monomers (BS) that can be taken up by bacteria (18). These processes are described by standard Michaelis-Menten kinetics. According to their origin, carbon and nitrogen contribute in variable proportions to the pools of organic matter. This proportion, compared to the bacterial C:N ratio determines whether net ammonification or ammonium uptake accompanies bacterial activity. All organic phosphorus is assumed to be released directly as ortho-phosphate during hydrolysis of polymeric organic matter and phosphorus is taken up by bacteria in its inorganic form only.

Benthic organic matter degradation and nutrient (N, P, Si) recycling is calculated making use of the algorythms developed by Lancelot and Billen [22] and Billen *et al.*, [23]. These algorythms, by solving steady-state diagenetic equations expressing the mass balance of organic carbon, oxygen, inorganic forms of nitrogen and phosphorus in the sedimentary column, calculate the fluxes of nitrate, ammonium and phosphate

accross the sediment-water interface resulting from a given sedimentation flux of particulate organic matter. Furthermore, a first-order kinetics describes benthic silicon redissolution and release of silicic acid to the water column.

3.1.2. *The multi-box MIRO model*

For a first application of the MIRO model to the continental coastal waters of the North Sea, a multi-box model has been considered on the basis of the hydrological regime. Such a low resolution of the hydrodynamics is reasonable in this tidally-well-mixed area. Three successive boxes , assumed to be homogeneous, have been chosen from the Baie de Seine to the Wadden Sea area of the Dutch coastal zone, on the basis of the hydrological regime (Fig.1). The offshore limit of the boxes is taken along a residual streamline so that inshore-offshore exchanges can be neglected. Each successive box is treated as an open system, receiving waters from the upwards adjacent box and exporting water to the downwards box. The seasonal variation of the state variables are calculated by solving the different equations expressing mass conservation in the system according to the Euler procedure.

The boundary conditions are provided by the results of the calculations performed for the conditions existing in the western Channel area, considered as a quasi oceanic closed system. Forcing functions are observed seasonal irradiance and seawater temperature and monthly riverine nutrient discharges of 1985 (source : North Sea Task Force, 1992).

The prediction capability of the MIRO model can be appraised from Fig.6 and 7 which compares respectively predicted chlorophyll a and *Phaeocystis* cellular density and nutrients concentration in the 3 sub-areas of the continental coastal waters of the North Sea with observations at the respective reference stations of the observational network, from 1988 to 1993. In spite of a reasonable general agreement between predictions and observations, in particular in the timing and magnitude of *Phaeocystis* blooms, the model does not predict properly the fast decline of *Phaeocystis* blooms, especially in the northern part of the simulated area where non-observed elevated biomass is predicted along the summer season. This discrepancy between predictions and measured data could originate either from the oversimplification of the hydrological regime, neglecting for instances the influence of the Wadden Sea in the Dutch coastal area or from a low description of mechanisms prevailing for *Phaeocystis* blooms termination and degradation. Further research in this field is in progress.

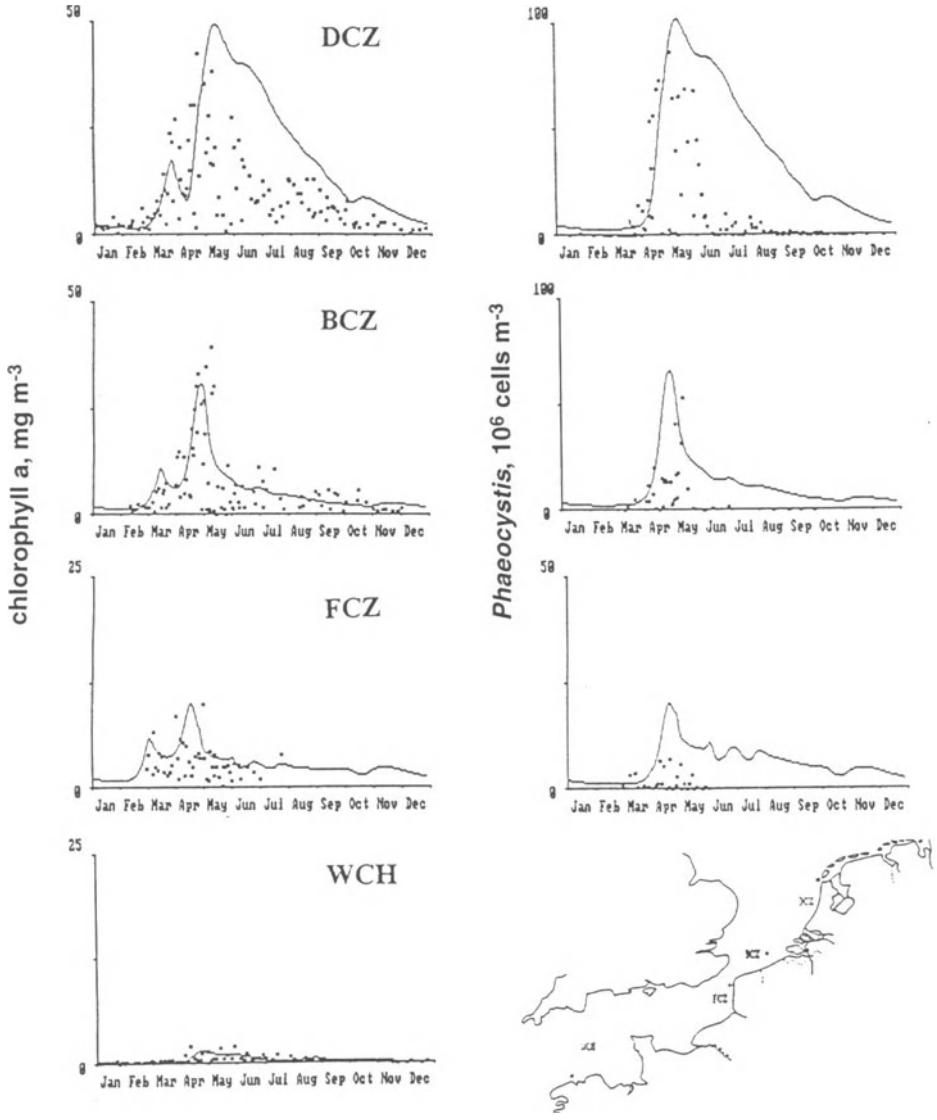


Figure 6 Observed (dots) and predicted (line) phytoplankton development in the coastal North Sea. Total chlorophyll a (a) and *Phaeocystis* cells (b)

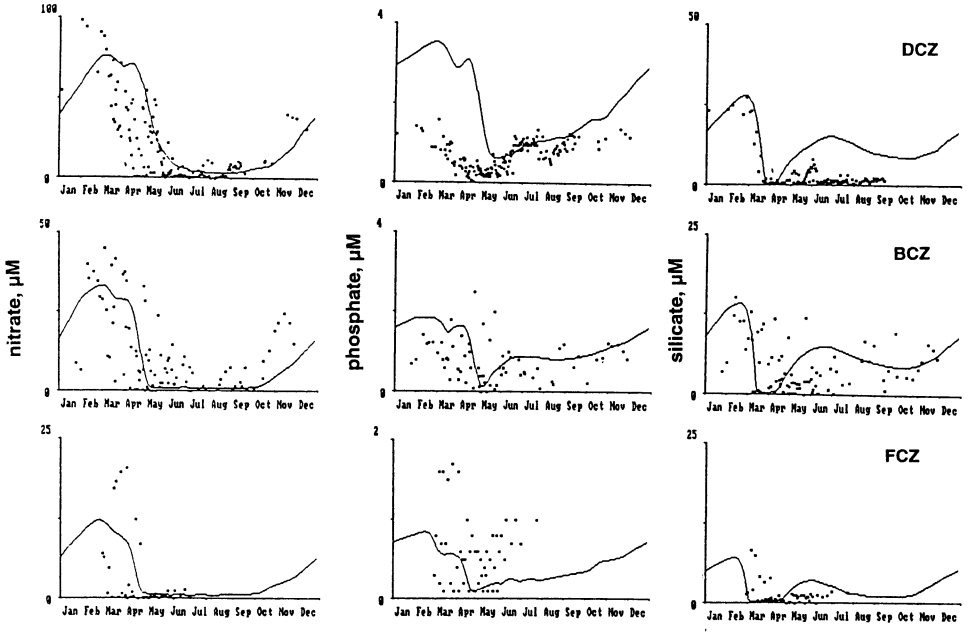


Figure 7 Observed (dots) and predicted (line) nutrients concentration in the coastal North Sea.

3.2. MODELLING *PHAEOCYSTIS* BLOOMS IN RESPONSE TO NUTRIENT REDUCTION SCENARIOS

The appropriateness of the integrated modelling approach for coastal management purpose is shown by exploring the response of the MIRO model to reduction scenarios of riverine nutrient delivery of the coastal zone consequent to the application of the EC guideline of May 1991 on urban waste water treatment for sensitive areas, *i.e.* 90 % phosphate removal and/or 75 % denitrification.

Nutrient reduction scenarios were established by modifying nutrient riverine inputs of 1985, according to the results generated by application of the RIVERSTRAHLER model to watersheds similar to those of the rivers Seine, Scheldt and Rhine and for various scenarios of urban waste water treatment. These calculations were based on published level of urban waste water treatment reached in the different watersheds. Due to the marked seasonality of both river flow discharge and nutrient transformation within the river system, a summer (April-September) and a winter (October-March) nutrient reduction factors were considered.

The extent of *Phaeocystis* colony blooms reduction expected from the application of the EC guideline of May 1991 can be appraised on Fig.8 which compares predicted *Phaeocystis* blooms after nutrient abatement scenarios with present-day predictions. Slight differences in the response of the coastal ecosystem are to be observed between subareas. Severe reductions of *Phaeocystis* blooms colonies are predicted after 90 % P removal. By contrast, very little bloom reduction is achieved in the scenario involving the denitrification treatment of waste waters. This is explained by the importance of diffuse sources of nitrogen. Interestingly enough, the simultaneous application of phosphorus removal and denitrification treatment of urban waste waters is not required for obtaining the largest reduction of *Phaeocystis* blooms in the coastal North Sea.

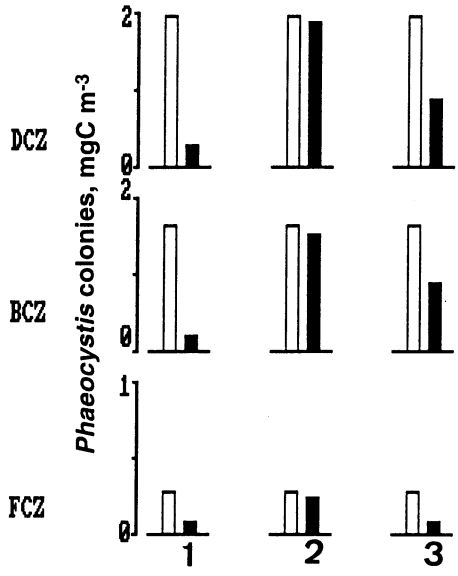


Figure 8 Predicted present-day magnitude of *Phaeocystis* blooms (white block) and after nutrient reduction scenarios (black block) : 1 = 90% P removal; 2 = 75% denitrification; 3 = 90% P removal and 75% denitrification

These exploratory nutrient reduction scenarios highlight the complex interactions between the continental and coastal marine systems and provide guidance to better select the available control actions on the watershed in order to reduce the development of *Phaeocystis* colony blooms. Further numerical work has to be done in this direction and should be supported by infrastructure development i.e. the setting up of permanent monitoring stations of *Phaeocystis* colony bloom development in the key sites of the coastal North Sea for assessing long-term changes of the ecosystem functioning resulting of waste water purification policies and climate change and verify model predictions.

Acknowledgements

This work has been financially supported by the EC research projects entitled "Modelling *Phaeocystis* blooms, their causes and consequences" (contract STEP-CT90-0062) and "Biogeochemistry of *Phaeocystis* colonies and their derived aggregates" (contract EV5V-CT94-0511) and the Belgian Impulse Programme "Marine Sciences" (contract MS/11/070). G. Billen is research director of the FNRS. We are grateful to participants of the joint EC research project, especially, S. Becquevort, G. Cadée, W. van Boekel, W. Gieskes, H. Grossel, F. Hansen, S. Mathot, Y. Rahmel, R. Riegman, M. Veldhuis, T. Weisse, whose scientific contributions provided material for most ideas developed in this synthesis.

References

1. Billen,G., Lancelot, C. and Meybeck, M. (1991) N, P and Si Retention along the Aquatic Continuum from Land to Ocean, in R.F.C. Mantoura, J.M. Martin and R. Wollast (eds), *Ocean Margin Processes in Global Change*, John Wiley & Sons, Ltd, pp. 19-44.
2. Lancelot, C. (1995) The mucilage phenomenon in the continental coastal waters of the North Sea. *The Science of the Total Environment. Special issue Marine Mucilages* **165**, 83-102
3. Lancelot, C. and Rousseau, V. (1994) Ecology of *Phaeocystis*-dominated ecosystems : the key role of colony forms, in J.C. Green and B.S.C. Leadbeater (eds), *The Haptophyceae Algae*, The Systematics Association, special volume **51**. Publisher Oxford University Press, pp. 229-245.
4. Liss, P.S., Malin, G., Turner, S.M. and Holligan, P.M. (1994) Dimethyl sulphide and *Phaeocystis* : a review, in C. Lancelot and P. Wassmann (eds), *Ecology of Phaeocystis-dominated ecosystems, J. Mar. Syst.* **5**, 41-54.
5. Lancelot, C., Billen, G. and Rousseau, V. (1994). Modelling *Phaeocystis* blooms, their causes and consequences. EC final synthesis report (contract STEP CT90-0062).
6. Baumann, M., Lancelot, C., Brandini, F., Sakshaug, E., and John, D (1994). The taxonomic identity of the cosmopolitan prymnesiophyte *Phaeocystis*, in C. Lancelot and P. Wassmann (eds), *Ecology of Phaeocystis-dominated ecosystems, J. Mar. Syst.* **5**, 5-22.
7. Thingstad, F. and Billen, G. (1994). Microbial degradation of *Phaeocystis* material in the water column, in C. Lancelot and P. Wassmann (eds), *Ecology of Phaeocystis-dominated ecosystems, J. Mar. Syst.* **5**, 55-66.
8. Brzezinski, M.A. (1985) The Si:C:N ratio of marine diatoms : interspecific variability and the effect of some environmental variables, *J. Phycol.* **21**, 347-357.
9. Rousseau, V., Dandois, JM. and Lancelot C. (1996) Impact of rainfall on the diatom-*Phaeocystis* succession in the eutrophicated continental coastal waters of the North Sea. Revised version submitted to *Aquatic Microbial Ecology*.
10 Rousseau, V., Vaulot, D., Casotti, R., Carcou, V., Lenz, J., Gunkel, J. and Baumann, M. (1994) *Phaeocystis* (Prymnesiophysae) life cycle : evidences and hypotheses, in C. Lancelot and P. Wassmann (eds), *Ecology of Phaeocystis-dominated ecosystems, J. Mar. Syst.* **5**, 23-40
11. van Boekel, W.H.M. (1992). *Phaeocystis* colony mucus components and the importance of calcium ions for colony stability, *Mar. Ecol. Progr. Ser.* **87**, 301-305.
12. Lancelot, C., Keller, M., Rousseau, V., Smith, W.O.Jr. and Mathot, S. (1997) Physiology and Ecology of the Haptophyte *Phaeocystis* sp. In D.M. Anderson, A.D. Cembella and G. Hallegraef (eds), *The Physiological Ecology of Harmful Algal Blooms*, NATO-ASI Series, in press.
13. Smith, W.O.Jr. (1993) Nitrogen uptake and new production in the Greenland Sea : The Spring *Phaeocystis* bloom, J. Geophys. Res. **98**, 4681-4688.

14. Hansen, F.C. and van Boekel, W.H.M. (1991) Grazing pressure of the calanoid copepod *Temora Longicornis* on a *Phaeocystis*-dominated spring bloom in a Dutch tidal inlet, *Mar. Ecol. Progr. Ser.* **78**, 123-129.

15. Franz, G., Gonzales, G.C., Cadée, G.and Hansen, F.H. (1992) Long term change of *Temore longicornis* (Copepoda, Calanoida) abundance in a Dutch tidal inlet (Marsdiep) in relation to eutrophication, *Neth. J. Sea Res.* **30**, 23-32.

16. Weisse, T. and Scheffel-Moser, U. (1990) Growth and grazing loss rates in single-celled *Phaeocystis sp* (Prymnesiophyceae), *Mar. Biol.* **106**, 153-158.

17. Weisse, T., Tande, K., Verity, P., Hansen, F. and Gieskes, W. (1994) The trophic significance of *Phaeocystis* blooms. In C. Lancelot and P. Wassmann (eds), *Ecology of Phaeocystis-dominated ecosystems. J. Mar. Syst.*, **5**, 67-80.

18. Hansen, F.C., Reckermann, M., Klein Breteler, W.C.M. and Riegman, R. (1993) *Phaeocystis* blooming enhanced by copepod predation on protozoa : evidence from incubation experiments, *Mar. Ecol. Progr. Ser.* **102**, 51-57.

19. Garnier, J., Billen, G. and Coste, M. (1995) Seasonal succession of diatoms and Chlorophyceae in the drainage network of the Seine River : Observations and modeling, *Limnol. Oceanogr.* **40(4)**, 750-765.

20. Lancelot, C., Veth, C. and Mathot, S. (1991) Modelling ice-edge phytoplankton bloom in the Scotia Weddell Sea sector of the Southern Ocean during Spring 1988, *J. Mar. Syst.* **2**, 333-346.

21. Billen, G. (1991) Protein degradation in Aquatic Environments, in R. Chrost (ed), *Microbial Enzymes in Aquatic Environments,* Springer Verlag, Berlin, pp. 123-143.

22. Lancelot, C. and Billen, G. (1985) Carbon-Nitrogen relationship in nutrient metabolism of coastal marine ecosystem, in HW. Jannash and P.J. Leb Williams (eds), *Adv. Aquatic Microbiol.*, Academic Press London **3**, pp. 263-321.

23. Billen, G., Dessery, S., Lancelot, C. and Meybeck, M. (1989) Seasonal and interannual variations of nitrogen diagenesis in the sediments of a recently impounded basin, *Biogeochemistry* **8**, 73-100.

MODELLING THE FUNCTIONING OF THE NORTH-WESTERN BLACK SEA ECOSYSTEM FROM 1960 TO PRESENT

DENIS VAN EECKHOUT and CHRISTIANE LANCELOT
Groupe de Microbiologie des Milieux Aquatiques, GMMA
Université Libre de Bruxelles, CP 221
Boulevard du Triomphe
B-1050 Bruxelles, Belgium

Abstract

The north-western Black Sea, a shallow semi-enclosed area, is highly sensitive to eutrophication receiving the discharge from the Danube, Dniestr and Dniepr rivers. Since the 1960's, riverine nitrogen and phosphorus loads dramatically increased respectively by a factor 3 and 10, as a consequence of urban and industrial development and intensive use of fertilisers in agriculture. Over the same period, silicon carried out by rivers significantly decreased as a result of hydraulic management programmes. Changes that occurred in the nutrient environment of the north-western Black Sea have had as consequences dramatic modifications in the structure and functioning of the coastal ecosystem. We present here an explanatory model describing the carbon, nitrogen, phosphorous and silicon circulation through the coastal ecosystem over seasons and years, in response to physical and nutrient forcing. The performance of the model, in particular its ability to reproduce the ecological events which took place since 1960, is assessed by exploring the response of the model to scenarios of nutrient concentrations reproducing different conditions that were encountered since 1960.

1. Introduction

1.1. CHANGES IN THE NUTRIENT ENVIRONMENT

Since the 1960's, nitrogen and phosphorous inputs into the north-western Black Sea by the Dniestr, Dniepr and Danube rivers dramatically increased respectively by a factor 3 and 10, as a consequence of the important urban and industrial development and the intensive use of fertilisers in agriculture [1, 2]. Over the same period, silicon carried out by rivers significantly decreased as a result of hydraulic management programmes [1, 2]. As a consequence, the nutrient environment of coastal phytoplankton was dramatically modified in both quantity and quality. Inorganic forms as expressed by the N:P:Si ratios show an excess of phosphorus over nitrogen with respect to phytoplankton requirements and over silicon with respect to diatoms requirements (Table 1.). Oxidized:reduced

E. Özsoy and A. Mikaelyan (eds.), Sensitivity to Change: Black Sea, Baltic Sea and North Sea, 455–468.
© 1997 *Kluwer Academic Publishers.*

nitrogen and inorganic:organic ratios were also modified with an increased importance of reduced and organic forms (Table 1.).

TABLE 1. Long-term mean values of nutrients and organic matter at Constanta [3, 4].

Years	PO_4	Si	NO_3+NO_2	NH_4	DBO_5
	µM	µM	µM	µM	mg O_2/l
1960-1970	0.3	36.8	1.6	-	1.96
1971-1975	5.7	61.2	-	-	2.32
1976-1980	6.4	30.6	15.4	12.8	2.75
1981-1985	4.3	12.9	7.3	5.3	2.58
1986-1990	7.0	11.2	8.4	5.6	2.34

Years	N/P	N/Si	P/Si
	molar	molar	molar
1960-1970	4.9	0.09	0.01
1971-1975	-	-	0.09
1976-1980	4.4	0.9	0.21
1981-1985	2.9	0.9	0.33
1986-1990	2.0	1.2	0.62
coastal diatoms [5]	16	1.2 (0.9-1.7)	0.07 (0.06-0.1)

1.2. ECOSYSTEM FUNCTIONING AND EVENTS

1.2.1. The response of the phytoplankton community

This impressive man-induced nutrient enrichment caused deep modifications in the structure and functioning of the coastal ecosystem. As an immediate response to nutrient enrichment, both the frequency and the amplitude of algal blooms were increased in the 1970's [6, 7]. Before this period, large phytoplankton developments were exceptional and diatoms were dominating the phytoplankton community. Phytoplankton developments were occurring in the early spring (Fig. 1.). After 1970, numerous phytoplankton blooms were developing during the summer period and the phytoplankton community was dominated by multiple blooms of non-siliceous phytoplankton (Fig. 1.). As reported by Bodeanu [4] 46 algal blooms occurred in the Romanian coastal waters from 1981 to 1990. Among the bloom-forming species the most frequently reported one is the mixotrophic dinoflagellate *Prorocentrum cordatum* causing blooms every summer since 1973. The explosive development of large opportunistic phytoplankters (*P. cordatum* and other peridinians) that are unpalatable to meso-zooplankton species [8] represents an important modification in the structure and functioning of the food-web of the north-western Black Sea ecosystem.

1.2.2 The response of the higher trophic levels

Larger developments of secondary (copepods) and higher trophic levels (fishes) organisms have been occurring after 1970 in response to the increased development of phytoplankters [10]. The higher fish availability led to an increase of fish catches and as a matter of consequence of the fishing pressure [1].

1.2.3. The explosive development of gelatinous organisms

In the mid 1980's, the giant omnivorous dinoflagellate *Noctiluca scintillans* started to exhibit explosive developments (Fig. 2.) [11, 12]. *N. scintillans* is a non-specific consumer feeding on living and detritical particles such as diatoms, nanoflagellates,

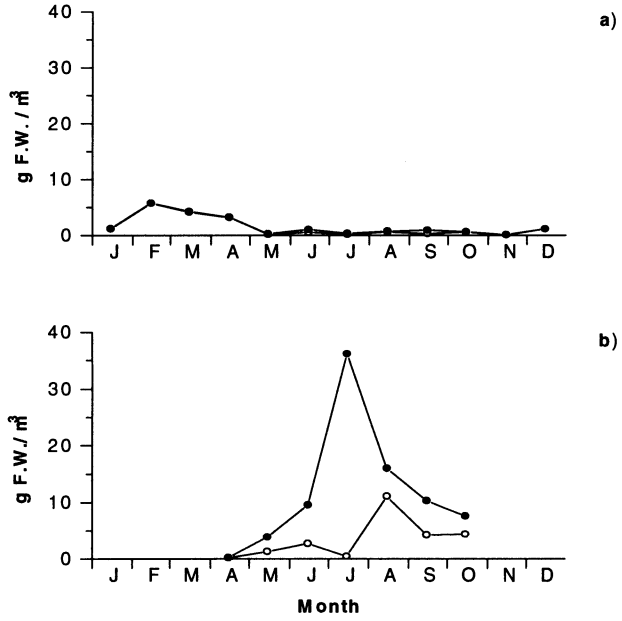


Figure 1. Total phytoplankton biomass (●) and diatoms biomass (O) in the Romanian coastal waters. (a) mean value for the period from 1960 to 1970; (b) values for 1989. After Bodeanu and Roban [9].

opportunistic phytoplankters, micro-zooplankton, bacteria and particulate organic matter. Deprived of known predators *N. scintillans* constitutes a trophic dead-end in concurrence with the upper part of the linear food chain leading to copepods and fishes.

The copepods populations have been further threatened by the massive development of the jellyfish *Aurelia aurita* in the 1980's [13] and by the development of the exotic ctenophore *Mnemiopsis ledyi* in the mid-1980's [14] (Fig. 2.). The explosive development of gelatinous carnivorous organisms such as *A. aurita* and *M. ledyi* brought an important competition with fishes for copepods. Lacking predators in the Black Sea these gelatinous organisms constitute trophic dead-ends. The organic matter derived from their mortality further enhances the development of bacterial populations.

The increased predation pressure on copepods by *A. aurita* and *M. ledyi* combined with the over-fishing and the fact that *M. ledyi* is eating fish eggs and larvae as well may account for the almost total collapse of fish catches in the late 80's [15, Shiganova, this volume]. The relative importance of these factors remains unclear. Both carnivorous are growing very fast at high food resources. Accordingly tremendous biomass of 3.5 g C/m^2 was reached by *A. aurita* in 1988 and by *M. ledyi* in 1989 (Fig. 3). Inter-annual variation (Fig. 3.) suggests that both gelatinous are in competition for food resource.

1.3. MODELLING A CHANGING ECOSYSTEM

Explanatory models discussing carbon and other biogenic elements cycling through the coastal ecosystem over seasons and years, in response to physical and nutrient forcing constitute useful research tools for analysing ecosystem resistance to destabilisation. Moreover such mechanistic models are of great value for determining the measures to be

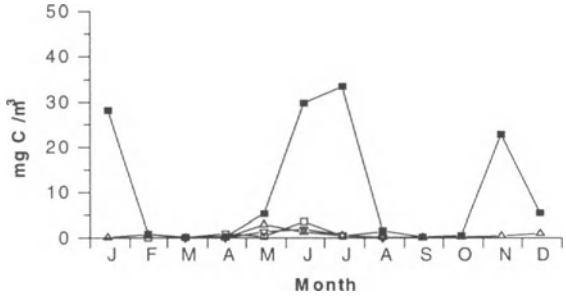


Figure 2. Intra- and inter-annual variations *N. scintillans* in the Romanian coastal waters. Open symbols: years before 1980. Solid squares: mean values for the period from 1980 to 1986. After Porumb [11].

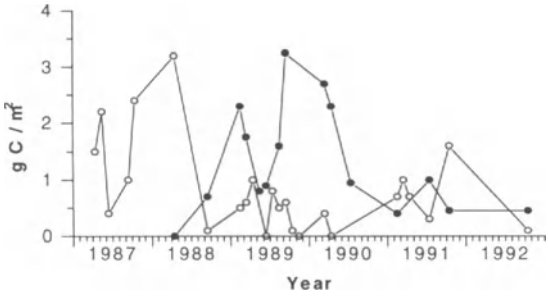


Figure 3. Changes in the biomass of *M. ledyi* (●) and *A. aurita* (○) during the period 1978-1992. Redrawn from Vinogradov [14].

taken for recovering sustainable water quality and biodiversity in the north-western Black Sea. To achieve this goal, these models should be part of an integrated framework of coupled biogeochemical models of river and marine systems.

These models have to be based on the best available understanding of key biological processes in particular those governing food-chain changes and bifurcations. In the specific case of the north-western Black Sea where dramatic ecosystem changes have been recorded since 1960 in response to changes in the nutrient environment, the coastal zone evolved from a highly diversified ecosystem with a "muscular-type food-web" toward a low-diversity ecosystem with a gelatinous-dominated food-web. This bifurcation in the food-web structure contrasts with most eutrophicated coastal ecosystems which exhibit a high ability to develop complex alternate pathways in response to phytoplankton community changes.

We present here a 0-D biogeochemical model describing the functioning of the north-western Black Sea shelf ecosystem and its evolution over the three past decades. This model focused on the water column describes the evolution of key biological functional groups and is based on the biological processes of importance, in particular those governing:

- the response of the phytoplankton community to nutrient change,
- the feeding activities of the dominant micro- and meso-zooplankton populations with particular emphasis on the feeding behaviour of opportunistic gelatinous species,

- the mechanisms of organic matter degradation and its coupling with nutrient regeneration,
- the nutrient regeneration by local sediments.

Special attention had to be given to the newly introduced species *M. ledyi*. On the one hand the cause of *M. ledyi* explosive development could be its introduction in a suitable environment in the early 1980's. On the other hand *M. ledyi* could have been introduced earlier but was unable to develop in the absence of suitable conditions. Such suitable conditions being brought later on by eutrophication.

Developing a mechanistic model describing the ecological changes recorded in the north-western Black Sea since 1960 is particularly exemplar considering the extreme ecological changes encountered for this marine system. When operational such a model gives the basis for developing a generic model of coastal eutrophication.

2. Description of the ecological model

2.1. CHOICE OF THE STATE VARIABLES AND LINKING PROCESSES

The state variables describing the biological functioning of the ecosystem were chosen according to the sequence of events described above. Figure 4. gives a diagrammatic representation of the whole conceptual biogeochemical model. Solid lines show an idealised description of the non perturbed north-western Black Sea marine ecosystem in the 1960's. Dotted and dashed lines represent the extended model structure needed for an adequate representation of recent ecological changes in this ecosystem.

Primary producers are described as three different functional groups according to their different physiological properties and trophic fates: diatoms (DIA), nanophytoflagellates (NAN) and autotrophic opportunistic species (OPP) (Fig. 4.). NH_4, NO_3, and PO_4 are taken up by all three groups while silicic acid is assimilated by the only DIA. Primary producers are either grazed by the upper trophic levels, or converted to dissolved organic matter (DOM) by exudation and to DOM and particulate organic matter (POM) by cell lysis. A part of DIA and OPP is removed from the water column by sedimentation. Due to their small size NAN are not submitted to sedimentation.

The secondary trophic level is composed of bacteria (BAC), micro-zooplankton (MUZ), copepods (COP) and *N. scintillans* (NOC), the latter feeding on all living micro-organisms and detrital particles (Fig. 4.). COP are grazing on DIA initiating the so-called linear food-chain. MUZ is feeding on BAC and NAN but constitutes a prey of high food-value for COP. MUZ occupies a key trophic position linking the microbial and the linear food-chains.

Among carnivorous organisms only *A. aurita* (AUR) and *M. ledyi* (MNE) are considered explicitly. Gelatinous are feeding on COP and thus compete with fishes for food resources. Fishing pressure is described as a first-order forcing function.

All gelatinous organisms are deprived of predators and no trophic link exists between them. Furthermore all zooplankters are producing DOM and POM either by autolysis, excretion or egestion. POM is submitted to sedimentation.

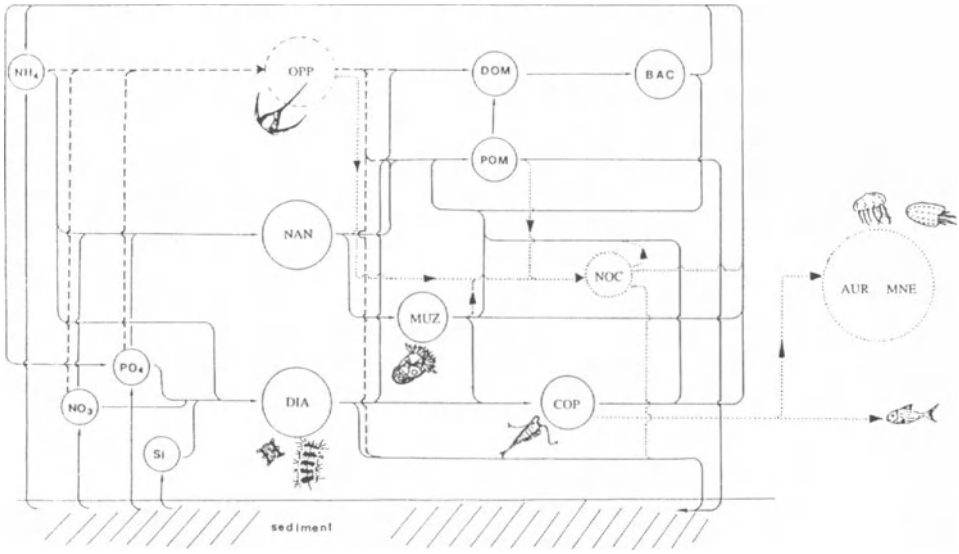


Figure 4. Structure of the north-western Black Sea ecosystem. Solid lines show an idealised description of the food web representative of the 1960's. Dashed lines correspond to the incorporation of autotrophic opportunistic species. The gelatinous food-chain is represented by dotted lines.

On the basis of this complex food-web composed of three branches -the linear, the microbial and the gelatinous pathways- the cycling of carbon, nitrogen, phosphorus and silicon through aggregated chemical and biological compartments of the planktonic and benthic components of the coastal area can be established.

For instance the cycling of carbon is illustrated by figure 5. Thirty-four state variables and thirty-three processes linking them were identified as needed to describe the structure and functioning of the north-western Black Sea ecosystem.

2.2. MATHEMATICAL REPRESENTATION

The model results from the assemblage of five different modules describing respectively the dynamics of phytoplankton, micro- and meso-zooplankton, gelatinous organisms, microbial degradation in the water column and early diagenetic processes in the sediments. The phytoplankton compartments (DIA, NAN and OPP) are described by the AQUAPHY module [16]. Feeding mechanisms of copepods and micro-zooplankton are described by Monod-type kinetics with saturation of the specific ingestion rate at high food concentrations [17]. The specific ingestion rate of MUZ and COP on a given prey (i) is described by:

$$graz_i = graz_i^{\max} \frac{P_i}{P_i + K_i^{app}} G \qquad \text{with} \qquad K_i^{app} = K_i \left(1 + \sum_{j(\neq 1)}^{n} \frac{P_j}{K_j} \right)$$

where K_i^{app}= apparent half-saturation constant of grazing on prey i , K_j = half-saturation constant of grazing on prey j, $graz_1^{\max}$ = maximum specific ingestion rate, P_i = concentration of prey i, G = grazer concentration.

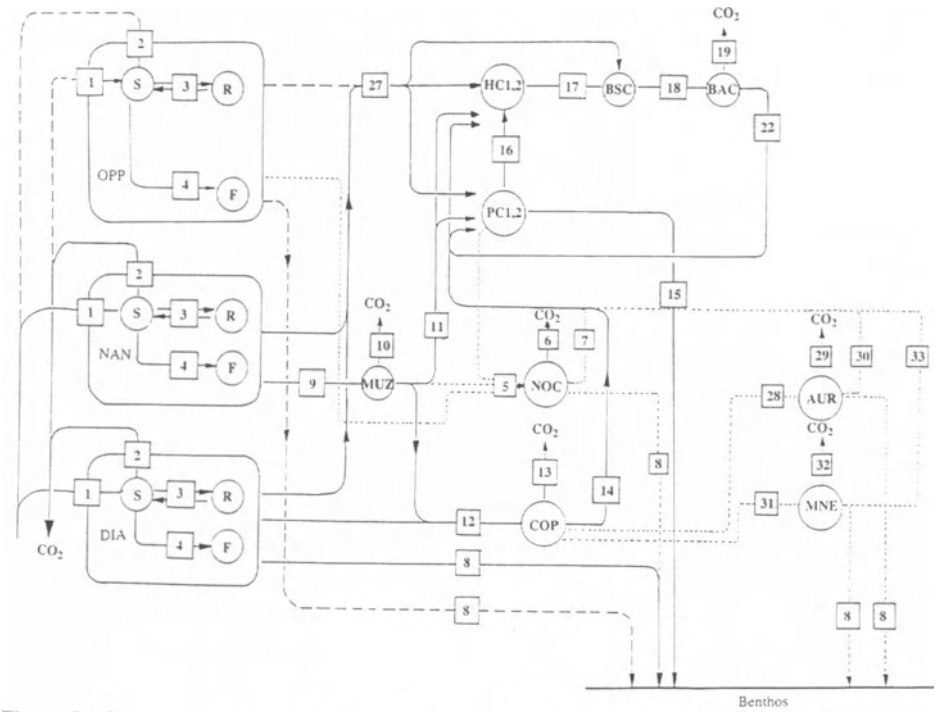


Figure 5.: Carbon cycling trough aggregated biological and chemical compartments of the north-western Black Sea ecosystem model. State variables (circles) not mentionned in the text: R, reserve metabolites; F, functional metabolites; S, monomeric precursor metabolites; SBC, Monomeric organic carbon. Processes (numbers): photosynthesis (1); phytoplankton respiration (2); synthesis and catabolism of intracellular reserves (3); growth (4); grazing by NOC (5), MUZ (9), COP (12), AUR (28) and MNE (31); respiration by NOC (6), MUZ (10), COP (13), BAC (19), AUR (29) and MNE (32); excretion and mortality of NOC (7), COP (14), MUZ (11), AUR (30) and MNE (33); sedimentation (8); POM sedimentation (15); POM ectoenzymatic hydrolysis (16); DOM ectoenzymatic hydrolysis (17); bacterial uptake of monomeric organic matter (18); bacterial mortality (22) and cell lysis (27).

Conversely experimental evidences show that the specific food ingestion rate of gelatinous organisms -NOC, AUR and MNE- does not display saturation for high food concentrations. Above a minimum food concentration (lower feeding threshold) the specific ingestion rate of these organisms increases linearly with respect to food concentration [18]. The specific ingestion rate of grazing NOC, AUR and MNE can be expressed by:

$$graz_i = \alpha \left(\sum_i P_i - \beta \right) G \frac{P_i}{\sum_i P_i}$$

where α = ingestion coefficient and β = feeding threshold.

The microbial degradation of DOM and POM pools is described according to the HSB model of Billen and Servais [19]. Two classes of organic matter biodegradability are considered for both polymeric DOM ($HC_{1,2}$, $HN_{1,2}$, $HP_{1,2}$) and POM ($PC_{1,2}$, $PN_{1,2}$, $PP_{1,2}$). These polymers have to be hydrolysed through bacterial exoenzymes prior to be

taken up by bacteria. This model also take into account either the net ammonification or the ammonium uptake that can be carried out by bacterial activity. All organic phosphorous is assumed to be released directly as ortho-phosphate after hydrolysis of polymeric organic matter and phosphorous is assumed to be taken up by bacteria under its inorganic form only.

The benthic module describing nitrate, ammonium and phosphate fluxes across the sediment-water interface as well as the denitrification rate as functions of the downward flux of POM is based on a diagenetic model established by Billen et al.[20]. The cycling of silica involves the uptake by diatoms and the storage in a benthic pool which is slowly released to the water column by dissolution.

2.3. PARAMETRISATION

The parmetrisation procedure constitutes a key step for a successful implementation of a mechanistic model. Usually parameters are determined experimentally, based on processes-oriented studies [see e.g. Lancelot et al., this volume]. The scarcity of process studies that have been carried out in the Black Sea do not allow yet the use of an existing self-consistent set of parameters. Such process-oriented studies are currently under way in the scope of the EROS-21 project. Due to the large number of parameters needed and the need of self-consistency we have used a set of parameters obtained for the Southern Bight of the North Sea. The use of a parameter set obtained for another coastal zone allows to test the model by exploring it response to changes in the nutrient environment. Parameters used for the AQUAPHY module, the HSB module and the benthic module can be found in [21]. The feeding parameters used for the micro-/meso-zooplankton and the gelatinous organisms modules are detailed in Table 2. and Table 3.

TABLE 2. Micro- and meso-zooplankton module: parameters.

Parameters (units)	Micro-zooplankton	Copepods
Maximum grazing rate (h^{-1})	0.09	0.12
Lower feeding threshold ($mgC.m^{-3}$)	1	2.5
Half-saturation constant on bacteria ($mgC.m^{-3}$)	15	-
Half-saturation constant on nano-flagellates ($mgC.m^{-3}$)	10	-
Half-saturation constant on microzooplankton ($mgC.m^{-3}$)	-	25
Half-saturation constant on diatoms ($mgC.m^{-3}$)	-	50
Growth yield	0.1-0.3*	0.25
Egested fraction of ingestion	0.1	0.25
Mortality constant (h^{-1})	0.003	0.001**

* 0.3 on nanoflagellates and 0.1 on bacteria; **a mortality by fish predation (0.001 h^{-1})is added

TABLE 3. Gelatinous module: parameters.

Parameters	*N. scintillans*	*A. aurita*	*M. ledyi*
Lower feeding threshold ($mgC.m^{-3}$)	10*	5**	10
Ingestion coefficient ($h^{-1}.mgC^{-1}.m^3$)	0.00005*	0.0004**	0.0006
Growth yield	0.25	0.25	0.35
Egested fraction of ingestion	0.25	0.25	0.25
Mortality constant (h^{-1})	0.007	0.0003	0.0003

* calculated from [22] ;** calculated from [23].

3. Application

The model has been run as an 20 meters-depth open-box with a residence time of 50 days until a steady state is reached (less than 5 years). Boundary conditions are obtained by a 1-year run of the model as a closed box. The performance of the model, in particular its ability to reproduce the ecological events which took place since 1960, is assessed by exploring the response of the model to the changes of nutrient concentrations that were encountered since 1960.

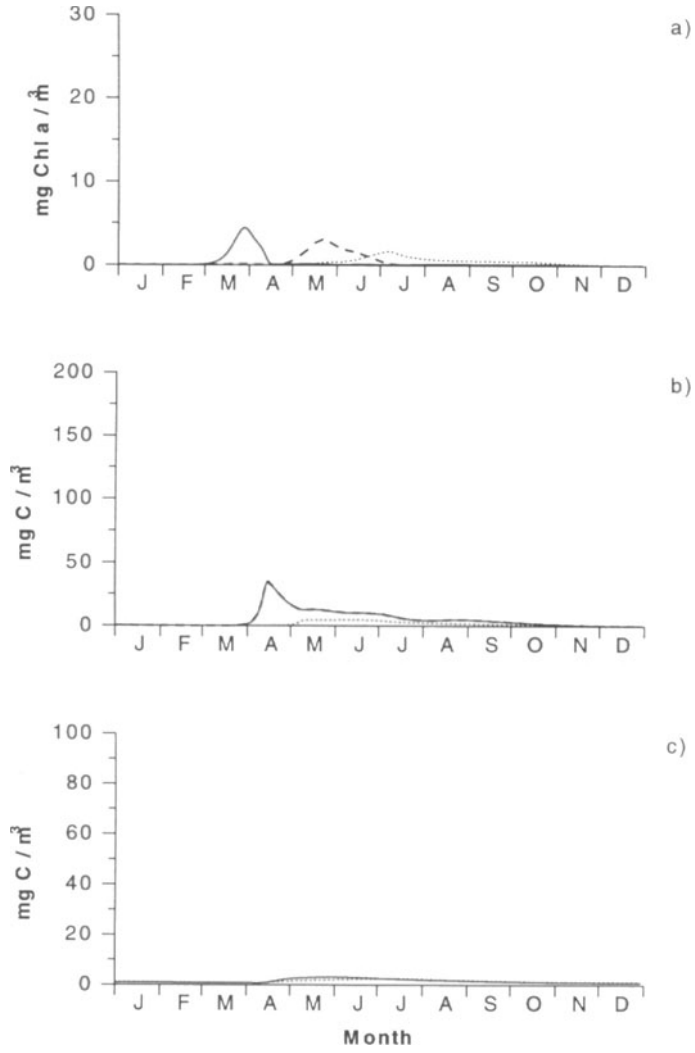


Figure 6. Model prediction for the nutrient coastal environment of the 1960's (N/Si/P = 8.3/122/1).
(a) Phytoplankton development: diatoms (solid line), nanoflagellates (dashed line), large opportunists (dotted line). (b) Zooplankton development: copepods (solid line), micro-zooplankton (dashed line), *N. scintillans* (dotted line). (c) *M. ledyi* (solid line) and *A. aurita* (dotted line)

Figure 6. shows the model predictions when forced by the nutrient concentrations of the 1960's (Table 1.). The model predicts an early spring bloom of diatoms in agreement with observations. The diatom bloom is followed by the development of nanoflagellates sustained by regenerated nutrients. A small development of opportunists phytoplankters is predicted in summer. The zooplankton is composed of copepods and to a lesser extent of micro-zooplankton. *N. scintillans, A. aurita* and *M. ledyi* are not growing in this nutrient environment.

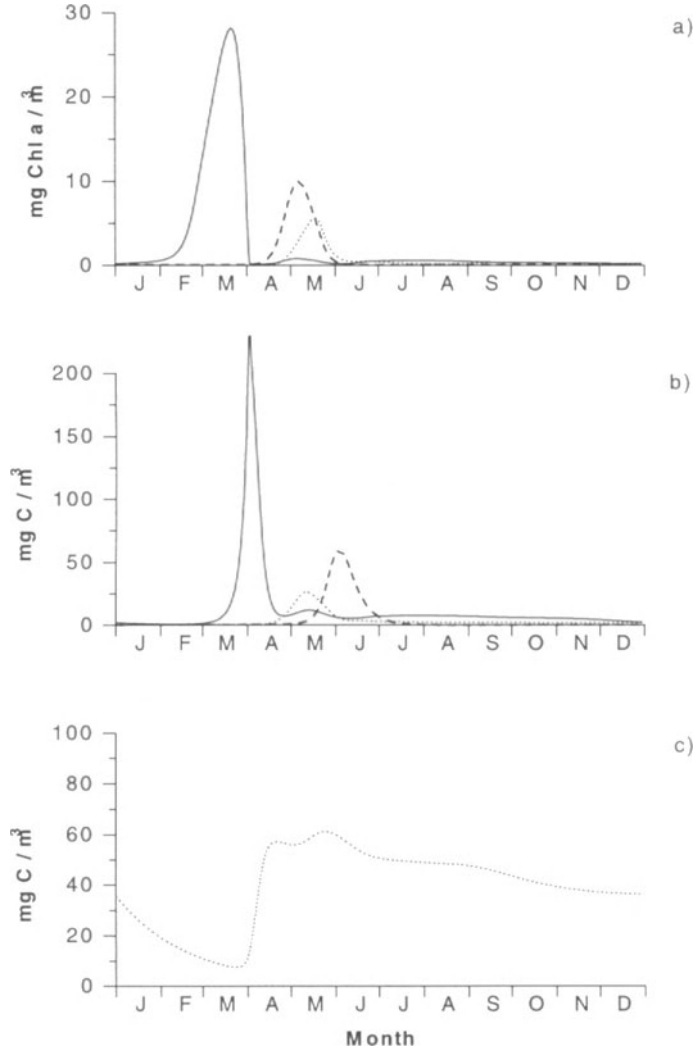


Figure 7. Model prediction. Scenario: 1976-1980 (N/Si/P = 4.4/4.8/1). *M. ledyi* has been removed from the model. (a) Phytoplankton development: diatoms (solid line), nanoflagellates (dashed line), large opportunists (dotted line). (b) Zooplankton development: copepods (solid line), micro-zooplankton (dashed line), *N. scintillans* (dotted line). (c) *A. aurita* (dotted line)

Figure 7. shows the predictions obtained by imposing as initial conditions the nutrient concentrations reported for the period 1976-1980 (Table 1.). For this scenario and in agreement with the real ecological situation, *M. ledyi* has been removed from the model. Compared to the reference ecological situation of 1960 (Fig. 6.), the model predicts - under these particular conditions of nutrient load- a general enrichment for every trophic level. Of particular interest is the explosive development of the early spring diatom population stimulating an important development of copepods.

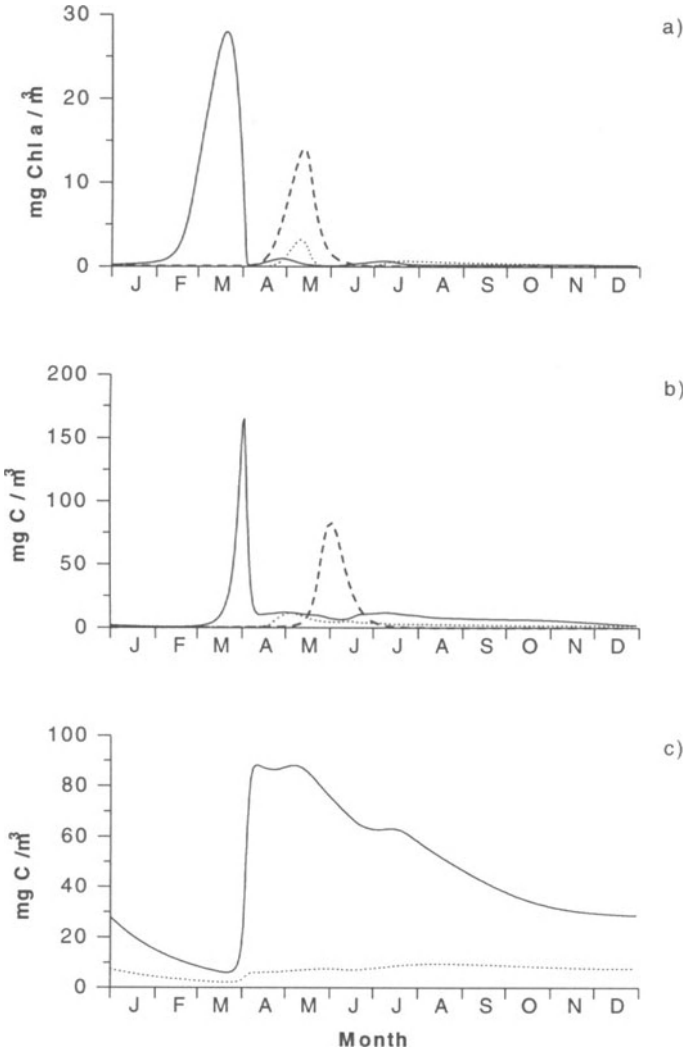


Figure 8. Model prediction the model for the nutrient coastal environment of 1976-1980 (N/Si/P = 4.4/4.8/1) after the introduction of *M. ledyi*. (a) Phytoplankton development: diatoms (solid line), nanoflagellates (dashed line), large opportunists (dotted line). (b) Zooplankton development: copepods (solid line), micro-zooplankton (dashed line), *N. scintillans* (dotted line). (c) *M. ledyi* (solid line) and *A. aurita* (dotted line)

Interestingly these nutrient conditions allow the significant late spring development of gelatinous organisms(Fig. 7.). Indeed the general increase of ecosystem productivity allows the development of the omnivorous *N. scintillans* (up to 60 mg C/m^3) which control the development of opportunist phytoplankters. The peak of *N. scintillans* remains smaller than the peak of copepods because of the dependence of the specific ingestion rate of *N. scintillans* on the total food concentration. In this simulation where *M. ledyi* has been removed from the model significant development of *A. aurita* is predicted. Once the population of *A. aurita* reaches significant biomass, this organism controls the development of copepods.

Introducing *M. ledyi* in the model under the same nutrient conditions shows that this ctenophore outcompetes *A. aurita* which remains at very low concentrations (Fig. 8.). Once copepods are controlled by *M. ledyi,* copepods population remains at a level corresponding to the feeding threshold of *M. ledyi* (Fig. 8.). This result tends to show that *M. ledyi* could have been developing earlier than the mid-80's if it had been introduced earlier.

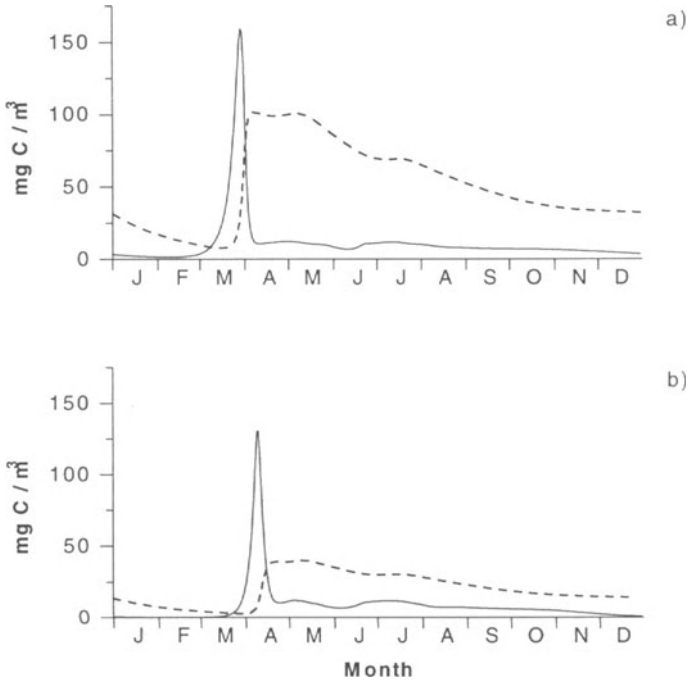


Figure 9. Influence of the fishing pressure on the development of *M. ledyi.* Model prediction for the nutrient coastal environment of 1976-1980 (N/Si/P = 4.4/4.8/1). (a) Increase of the fishing pressure with respect to the predictions presented in figure 8: two-fold decrease of copepods mortality by fish predation. (b) Decrease of the fishing pressure with respect to the predictions presented in figure 8: two-fold increase of copepods mortality by fish predation. Copepods (solid line), *M. ledyi* (dashed line).

It has been recently hypothesised that over-fishing rather than man-induced increase of the nutrient load was responsible of the successful development of *M. ledyi* in the north-western Black Sea [Shiganova, this volume]. Over-fishing by decreasing fish biomass

increases food resource for carnivorous gelatinous. The influence of fisheries on the successful development of *M. ledyi* was tested by running the model with nutrient conditions of the period 1976-1980, under increasing (Fig. 9.a.) and decreasing (Fig. 9.b.) fishing pressure. Predictions show a high sensitivity of the ecosystem functioning to fishing pressure. An explosive *M. ledyi* development is predicted for high fishing pressure while the abundance of the ctenophore is reduced when fishing pressure decreases because of the higher competitivity of fishes at low food concentrations.

4. Conclusion

The explanatory ecosystem model - BIOGEN - developed in this paper synthesises the knowledge available on the Black Sea ecosystem structure and functioning. The model is able to reproduce the historical sequence of ecological modifications that were reported for the north-western Black Sea from 1960 to present. As such it constitutes also a tool for the identification of experimental needs. By the mean of sensitivity analysis, it allows the identification of the key factors determining the ecosystem response and therefore which processes should deserve more attention from the experimentalists.

The model also allows the testing of different hypothesis regarding the structure of the ecosystem and the forcing functions acting on it -e.g. the impact of the fishing pressure or the diet composition of *M. ledyi*, the effects of nutrient load reduction. The ability to test such hypothesis is of interest either for policy-makers or for experimentalists.

The use of parameters determined by process-oriented studies conducted in the north-western Black Sea should extend the scope of application of the model. In a latter stage this model will be coupled with an hydrodynamical model in order to be able to relate the changes occurring in the shelf ecosystem to modifications in the nutrient discharge by the Danube, Dniestr and Dniepr river. Considering the large number of state variables described by this model a preliminary aggregation of state variables might be necessary before coupling biology and physics.

The ability of the model to reproduce the different ecological events that were observed in the north-western Black Sea over the past three decades (including changes in the relative importance of major trophic pathways within the foodweb) shows that a generic modelling approach can be used for the description of changing ecosystems. This approach can be used whether or not different food-web structures are present across time.

5. Acknowledgements

This work has been conducted with the financial support of the European Union research project entitled EROS-2000 (contract EV-CT94-0501). The authors would like to thank Thomas Weisse and Sylvie Becquevort for useful discussions on the feeding behaviour of zooplankton and Pierre Duponcheel for the figures.

References

1. Mee, L.D. (1992) The Black Sea in crisis: a need for concerted international action, *AMBIO* **21** (4), 278-286.
2. Tolmazin, D. (1985) Changing coastal oceanography of the Black Sea. 1: North-western Shelf, *Prog. Oceanog.* **15**: 217-276.
3. Popa, A., Cociasu, A., Popa, L., Voinescu, I., and Dorogan L. (1985) Long-term statistical characteristics of several physico-chemical parameters of the near shore waters in the Constantza zone, *Cercetari marine* **18,** 7-51.
4. Bodeanu, N. (1992) Algal bloom and development of the main phytoplanktonic species at the Romanian Black Sea littoral in conditions of intensification of the eutrophication process, in R.A. Vollenweider, R. Marchetti and R. Viviani (eds.), *Marine coastal eutrophication,* Elsevier, pp. 981-906.
5. Brzezinski, M.A. (1985) The Si:C:N ratio of marine diatoms : interspecific variability and the effect of some environmental variables, *J. Phycol.* **21,** 347-357.
6. Bodeanu, N. (1984) Le phytoplancton du littoral roumain de la Mer Noire sous l'influence de l'eutrophisation, VIIe s Journées Etudes Pollutions, Lucerne, CIESM, 745-752.
7. Bologa, A.S., Bodeanu, N., Petran, A., Tiganus, V., and Zaitsev Yu. (1995) Major modifications of the Black Sea benthic and planktonic biota in the last three decades, *Bulletin de l'Institut océanographique, Monaco,* n° spécial **15,** 85-110.
8. Gomoiu, M.-T (1992) Marine eutrophication syndrome in the north-western part of the Black Sea, in R.A. Vollenweider, R. Marchetti and R. Viviani (eds.), *Marine coastal eutrophication,* Elsevier, pp. 683-692.
9. Bodeanu, N. and Roban, A. (1989) Les développement massifs du phytoplancton des eaux du littoral roumain de la Mer Noire, *Cercetari marine* **22,** 127-146.
10. Porumb, F. (1989) The influence of eutrophication on zooplankton communities in the Black Sea waters, *Cercetari marine* **22,** 233-246.
11. Porumb, F. (1989) On the development of *Noctiluca scintillans* (Macartney) kofoid and swezy under the eutrophication of Romanian Black Sea waters. *Cercetari marine* **22,** 247-262.
12. Porumb, F. (1992) On the development of *Noctiluca scintillans* under eutrophication of Romanian coastal Black Sea waters, in R.A. Vollenweider, R. Marchetti and R. Viviani (eds.), *Marine coastal eutrophication,* Elsevier, pp. 907-920.
13. Gomoiu, M.-T and Kuprianov S.S. (1981) Données préliminaires concernant la répartition de la méduse *Aurelia aurita* L. dans la Mer Noire, *Rapp. Comm. int. Mer Médit.* **27** (7), 151-152.
14. Vinogradov, M.E. (1992) Long-term variability of the pelagic community structure in the open Black Sea, in: *Problems of the Black Sea,* International Conference, Sevastopol, Ukraine. November 10-15, 1992. MHI-UAS Publication; pp.19-23.
15. Zaitsev, Y.P. (1993) Impacts of eutrophication on the Black Sea fauna. Fisheries and environment studies in the Black Sea system. Report FAO n° **64,** 63-86.
16. Lancelot, C., Veth, C., and Mathot, S. (1991) Modelling ice-edge phytoplankton bloom in the Scotia Weddell Sea sector of the Southern Ocean during spring 1988, *J. Mar. Syst.*, **2,** 333-346.
17. Fenchel, T. (1980) Suspension feeding in ciliated protozoa: functional response and particle size selection, *Microb. Ecol.*, **6,** 1-11.
18. Hoffmeyer, M.S. (1990) Algunas observatciones sobre la alimentation de *Mnemiopsis mccradyi* Mayer, 1900 (Ctenophora, Lobata), *Sér. Zool., Porto Alegre* **70**, 55-65.
19. Billen, G. and Servais, P. (1989) Modélisation des processus de dégradation bactérienne de la matière organique en milieu aquatique, in M. Bianchi, D. Marty, J.-C. Bertrand, P. Caumette, Gauthier M. (eds.) *Micro-organismews dans les milieux océaniques,* Masson, pp. 219-245.
20. Billen, G., Dessery, S., Lancelot, C., and Meybeck, M. (1989) Seasonal and inter-annual variations of nitrogen diagenesis in the sediments of a recently impounded basin, *Biogeochemistry* **8,** 73-100.
21. Lancelot, C., Billen G., and Rousseau V. (1994). Modelling *Phaeocystis* blooms, their causes and consequences, EC synthesis report (contract STEP CT90-0062).
22. Weisse , T. (1994) The trophic significance of *Phaeocystis* blooms, *J. Mar. Sys.* **5,** 67-79.
23. Olesen, N.J. (1995). Clearance potential of jellyfish *Aurelia aurita,* and predation impact on zooplankton in a shallow cove, *Mar. Ecol. Prog. Ser.* **124,** 63-72.

TOWARDS COUPLING THREE DIMENSIONAL EDDY RESOLVING GENERAL CIRCULATION AND BIOCHEMICAL MODELS IN THE BLACK SEA

TEMEL OĞUZ[1], PAOLA MALANOTTE-RIZZOLI[2], HUGH DUCKLOW[3]

[1] *Institute of Marine Sciences, Middle East Technical University, Erdemli, TURKEY*
[2] *Department of Earth, Planetary and Atmospheric Sciences, Massachusetts Institute of Technology, Cambridge, USA*
[3] *Virginia Institute of Marine Sciences, The College of William and Mary, Gloucester Point, VA, USA*

Abstract. An overview of our ongoing efforts on modeling the Black Sea general circulation and lower trophic level pelagic food web is presented. Using an eddy resolving ocean circulation model endowed with active thermodynamics and turbulence closure parameterization, a synthesis of the yearly mean and monthly varying circulations driven by the climatological wind stress, air-sea thermohaline fluxes and lateral buoyancy fluxes is given first. The main features of the vertically resolved, three dimensional biochemical model involving interactions between the inorganic nitrogen (nitrate, ammonium), phytoplankton, herbivorous zooplankton and bacterial biomasses, detritus and dissolved organic nitrogen are then described. A simplified version (depth and time) of the coupled physical-biochemical model without having the horizontal variabilities is applied to the central Black Sea conditions. Given a knowledge of physical forcing, solar radiation and subsurface nutrient source, the coupled model simulates main observed seasonal and vertical characteristic features such as formation of the Cold Intermediate Water mass, yearly evolution of the upper layer stratification, the annual cycle of phytoplankton production with the fall and spring blooms, the subsurface maximum layer in summer, as well as realistic patterns of bacterial biomass and particulate and dissolved organic materials.

E. Özsoy and A. Mikaelyan (eds.), Sensitivity to Change: Black Sea, Baltic Sea and North Sea, 469–485.
© 1997 *Kluwer Academic Publishers.*

1. Introduction

The biogeochemical state of the Black Sea has undergone catastrophic changes within the last two-three decades. Among other reasons, the primary causes were the intense eutrophication as a result of increased antropogenic nutrient supply, and other man made activities (Mee, 1992; Bologa et al., 1995). Complementary to field observations, interdisciplinary modeling approach appears to be the proper tool to investigate the roles of major biochemical processes leading to the present state of the sea, to nowcast/forecast the system's response to various measures, and is therefore of vital importance to the success of any environmental management plan. Some objectives of the basinwide coupled physical-biochemical models are (i) to determine pathways of nutrient transport and how they correlate with productivity on the regional scale, (ii) to examine the influence of changes in the nutrient influx rates on the productivity and biomass distribitions in the northwestern shelf and nearby parts of the deep basin, (iii) to describe exchange of nutrients and biogenic materials between the shelf and the interior by a variety of physical processes responsible cross-shelf exchanges (iv) to describe large scale patchiness of chlorophyll concentrations in relation with large scale general circulation modulated by mesoscale motions.

The fundamental dynamics which need to be incorporated in such interdisciplinary models involve biogenic element cycling, pelagic and benthic ecosystems carbon and energy flows, as well as their coupling to the physical circulation, horizontal/vertical transport mechanisms. Even a very modest idealization of this highly nonlinear, complex system is, however, an extremely challenging task. The models should necessarily be four dimensional to incorporate mesoscale-to-gyral scale spatial variabilities, buoyancy input from major rivers, from the Bosphorus Strait and at the sea surface, topographic control of the rim current and its dynamics and instability, the coastal-deep sea interactions as well as day-to-year temporal variability. They should include different nutrients (nitrogen, phosphate, silicate, their new and recycled inorganic forms as well as dissolved and particulate organic forms) and biological groups (various size clasess of phytoplankton and zooplankton, and bacteria) in order to be able to incorporate strong regional and temporal variations of dominant planktonic species and of the nutrient limitation.

Implementation of this type of a comprehensive and interdisciplinary model should naturally follow a series of systematic exploratory studies carried out independently for both the physical and biochemical models. In the present paper, we describe our ongoing efforts leading to development of a coupled physical-biochemical model for the Black Sea. The coupled model is comprised of three interactive modules, dealing separately with

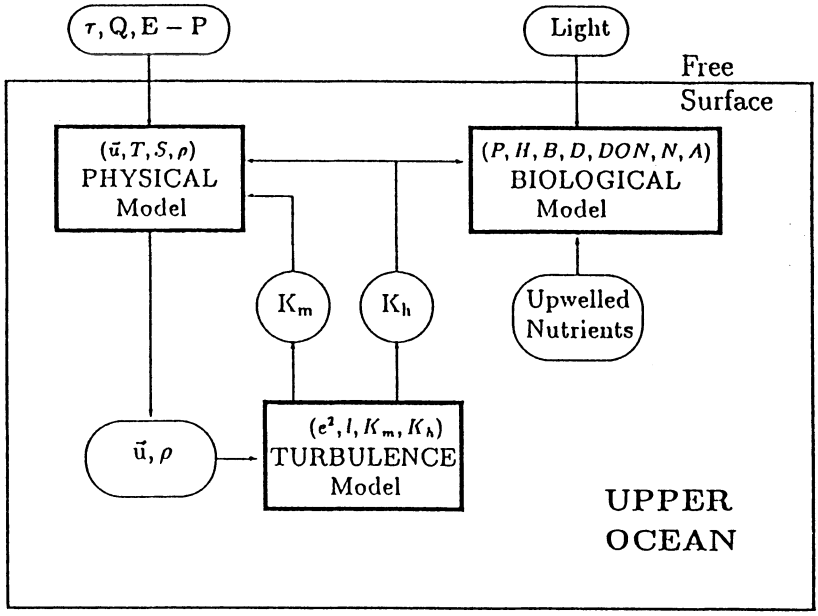


Figure 1. Schematic representation of the interactions between the physical, turbulence and biochemical modules of the interdisciplinary model.

the physical, turbulence and biological components of the system (Fig. 1). The physical module computes vertical structures of the horizontal velocity components and of density of the flow in response to wind stress, surface and lateral buoyancy forcings. The flow characteristics are then used in the turbulence module to compute the vertical eddy viscosity and diffusivity using Mellor-Yamada level 2.5 turbulence closure parameterization. The vertical turbulent diffusivity forms the main coupling of the mixed layer dynamics with the biological system. In this approach, internal structure of the physical-biological system is evolved solely in response to external forcings applied as the boundary conditions at the free surface and bottom of the ocean. This makes its main difference from the mixed layer-based biological models. In the latter type modeling approach, on the other hand, both the mixed layer structure and the interfacial mixing have to be specified a priori throughout the year.

The paper is organized as follows: In Sections 2 and 3, Numerical modeling approaches for simulation of the Black Sea general circulation and for describing the basic biochemical processes associated with the nutrient

cycling and the bacteria-plankton dynamics are presented in Sections 2 and 3, respectively. Neglecting contribution of the lateral variability in the sea for the time being, a one-dimensional application of the coupled model to the central Black Sea conditions is provided in Section 4.

2. General Characteristics of the Circulation Model

The Princeton Ocean Model of Mellor (1991) is implemented to the Black Sea configuration. It is an eddy-resolving, primitive equation model endowed with active thermodynamics, and Mellor and Yamada level 2.5 turbulence closure parameterization. The model accommodates a bottom-following σ coordinate in the vertical and a boundary fitted orthogonal curvilinear coordinate system in the horizontal. The model resolves steep topographical changes around the periphery of the basin using $O(10km)$ grid spacing and 18 vertical levels which are compressed towards the free surface to resolve the thin, $O(150m)$, upper layer of the Black Sea stratification.

Using standard climatological data sets (wind stress of Hellerman and Rosenstein [1983] and surface fluxes of Altman et al. [1987], and initializing the model with a horizontally uniform one dimensional stratification obtained by basinwide averaging of the yearly mean climatological data the individual roles of climatological forcings by the wind stress, surface thermal and salt fluxes and the lateral fresh water discharge in generating major features of the yearly mean circulation and its seasonal evolution are studied in Oguz, Malanotte-Rizzoli and Aubrey (1995) and Oguz, Malanotte-Rizzoli (1996b). The main findings from these studies are summarized below.

The model domain with orthogonal curvilinear coordinates has the average grid spacings of 8.5 km and 11.5 km in the meridional and zonal directions, respectively. The grid spacing attains a resolution of about 5 km along the Turkish coast where the topography undergoes its most pronounced variations. It increases maximally to about 15 km within the rest of the basin. Considering that the first baroclinic radius of deformation is about 20-30 km in the Black Sea, mesoscale processes are resolved reasonably well with the model grid. 18 vertical sigma levels are used to represent the vertical stratification. They are compressed towards the free surface in order to better resolve the thin upper layer stratification with about 3-to-6 kg/m^3 density changes. For example, for a water column of 2000 m depth, the upper 200 m layer has nine vertical levels.

The model experiments indicate that, under all forcing mechanisms, the overall basin circulation is characterized by a very strong seasonal cycle controlled primarily by the seasonal evolution of the surface thermohaline fluxes. The wind driven circulation possesses some sub-basin and gyral scale

structures which persists throughout the year. They are also seen in the circulation pattern driven by the annual mean wind stress. The rim current undergoes continuous evolution within the year. The cyclonic cell, covering the entire basin interior shown in the yearly mean circulation (see Fig. 10a,b in Oguz, Malanotte-Rizzoli and Aubrey, 1995) therefore exhibit a strong seasonal evolution. As a result, sub-basin scale cyclonic gyres of the interior cell interact, split and coalesce throughout the climatological year. The sub-basin scale circulation is also modulated by strong mesoscale activity leading to the formation of cyclonic/anticyclonic eddies along the peripheral current system. The intense mesoscale activity is evidently linked to the meanders and instabilities of the rim current, and reminescent of the surface patterns observed in satellite imagery. The overall wind-driven circulation seems therefore to be more strongly affected by the seasonal cycle with the exception of only a few localized structures that persists throughout the year. The monthly mean February and August circulation patterns representing, respectively, the winter and summer conditions of the wind driven motion are shown in Fig. 2a,b.

Contrary to the wind stress forcing, the horizontally varying surface flux distributions tend to generate a much simpler circulation pattern. In winter the circulation is characterized by a pair of zonally elongated basinwide cells. The northern cell is induced by the response to stronger cooling in the northern half of the basin, whereas the southern cell is developed by the dominant effect of precipitation. In summer both warming and excess of evaporation generate a basinwide anticyclonic cell. When the freshwater discharge is introduced in the northwestern shelf, the wintertime anticyclonic cell of the southern basin breakes into two separate gyres in the western and eastern basins, separated by a cyclonic gyre in between. Thus, also the circulation induced by the surface cooling alone and the surface and buoyancy forcings together exhibit a strong seasonal cycle. An important result of the purely thermally driven circulations is that the observed seasonal reversal of the coastal-deep water temperature gradients can be generated solely by the seasonal cycle of the surface thermal fluxes.

The fresh water discharge from the Danube is able to generate basinwide circulation comparable to circulation caused by the wind stress or surface fluxes. Although the freshwater input is only 10,000 m^3/sec, the buoyancy source introduces a strong baroclinic pressure gradients which eventually drive a strong depth integrated along-isobath flow under the action of jebar effect. This process ultimately give rise to a well-developed, strongly meandering Rim Current and accompanied temperature and salinity variations around the basin. Locally, the Danube inflow drives a strong anticyclonic circulation over the northwestern shelf. This cell is closed by a southwestward current flowing along the shelf break topography. The anti-

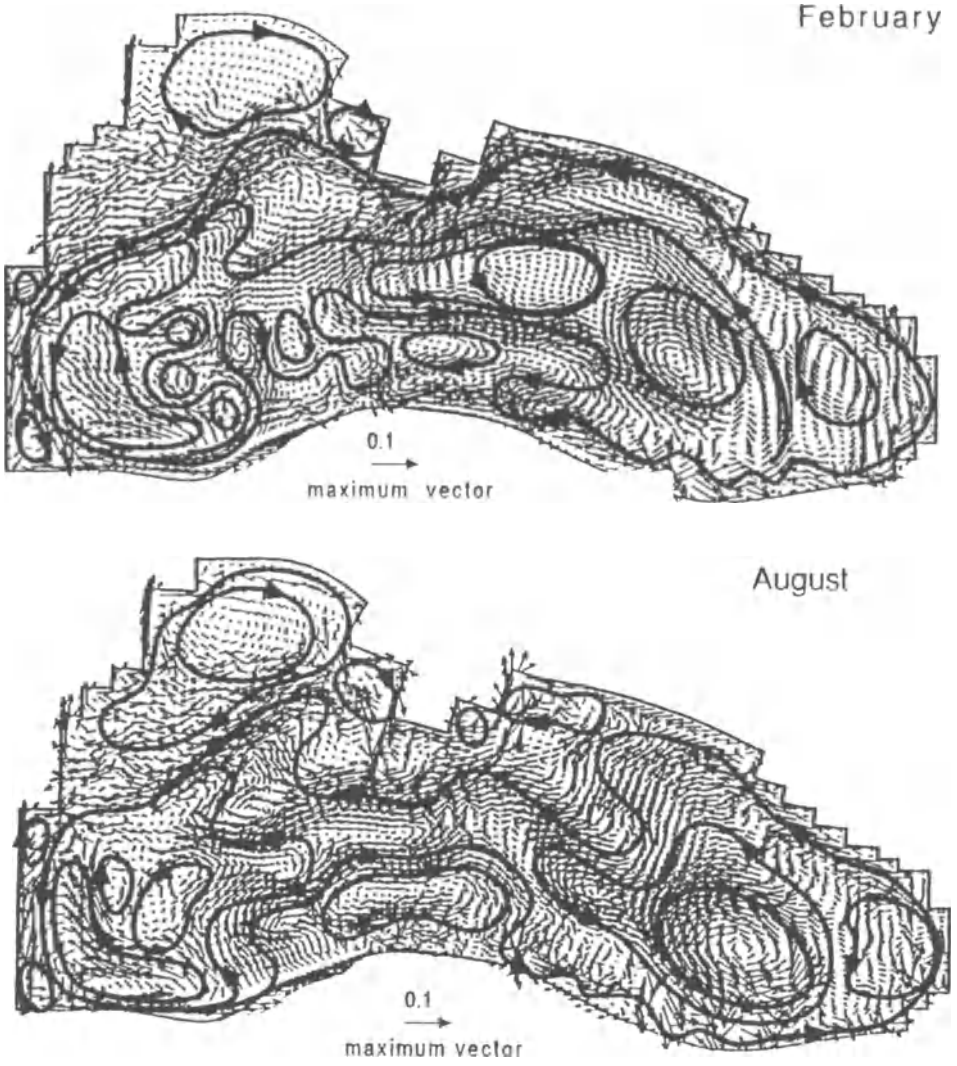


Figure 2. 5 m monthly mean wind driven circulation pattern for (a) February, (b)August. Maximum currents are scaled by 10 cm/sec for clarity of presentations. A schematic pattern of circulation is also included on the figures (after Oguz and Malanotte-Rizzoli, 1996b).

cyclonic tendency of the shelf circulation is often supported by the satellite imagery.

The wind stress and surface/lateral buoyancy forcings are all found

to be equally important in the yearly mean circulation. In the seasonal patterns the surface thermohaline fluxes, however, seem to be the dominant mechanism under the climatological data used for this study. They reduce considerably the richness in interior structures produced in the purely wind driven circulations. Topography remains a crucial factor in controlling the pattern of the rim current system, as explored previously in the yearly mean circulation studies of Oguz, Malanotte-Rizzoli and Aubrey (1995).

The regional variability of the surface forcings also affects crucially the spatial variability of the seasonal circulation. Again, as the surface wind stress pattern does not exhibit dramatic winter-to-summer changes, the horizontal variability of the surface thermohaline fluxes is the determining factor. Particularly important is the persistence of excess precipitation in the easternmost part of the basin throughout the year. This drives one of the permanent circulation features, called the Batumi eddy. Finally, the mesoscale activity associated with the peripheral current system is mostly intense along the Turkish and Caucasian coast. They are obviously linked to the dynamical instabilities of the rim current that produce strong meandering and eddy formation especially along the southern coastline.

The model circulation can be classified as a two-layer system with vertical homogeneity in each layer. In the upper layer of about 150 m, the individual forcing mechanisms contribute to the generation of the most of the known features of circulation in the sea. The Rim Current and the interior cell are the main blocks of the basin scale circulation system. The anticyclonic gyres on the northwestern shelf and the southeastern corner, as well as the cyclonic gyres of the interior cell constitute the main sub-basin scale features. A series of anticyclonic eddies confined between the coast and the meandering Rim Current zone are products of the mesoscale variability. Other mesoscale features, such as offshore filaments, dipole structures and detached eddies are originated from the evolution of propogating meanders.

The circulation in the lower layer, below 300 m depth, is separated from the upper layer by a transition zone. It is interesting to note that the lower layer circulation is always similar under all forcings. It consists of an elongated mildly meandering cyclonic cell over the flat interior of the basin. The shoreward side of the cell is covered by an anticyclonic recirculation zone which is wider and encircles the entire basin, as compared with the one in the upper layer. The transition zone reflects essentially the motion induced by the horizontal variability of the pycnocline and varies depending on the intensity and horizontal structure of the surface fluxes. The circulation below $\sim$300 m is basically barotropic, driven by the surface elevation whose patterns are similar for all the forcings. Hence the baroclinic component of the circulation generated in response to the deformation of the pycnocline is only limited to a transitional layer immediately below the

pycnocline.

An important byproduct of this modeling study is the necessity of re-analysis of the heat flux climatology. The existing data seem to impose a too strong local cooling and/or warming which leads to inconsistency between the computed water mass characteristics and the available observations. This does not critically alter the overall upper layer circulation characteristics, but prevents reasonably realistic horizontal distributions of temperature at the near-surface levels. Another important finding of the present work is to quantify the secondary role of the NWS region in the CIW formation process. Even though the most intensified cooling and subsequent formation of coldest waters take place in the NWS, the fresh water supply from the Danube prevents the shelf waters from being dense enough to spread into the deep interior layers of the basin by crossing over the topographic slope. Thus, during moderate-to-high discharge winters, as in the present simulations, the NWS does not contribute significantly to the overall newly formed CIL.

3. The Biochemical Model

The biochemical model describing the nutrient cycling and bacteria-plankton dynamics in the Black Sea consists of interactions and transformations between phytoplankton P, herbivorous zooplankton H, bacteria B, labile pelagic detritus D, labile dissolved organic nitrogen DON, nitrate N and ammonium A. Their temporal variations are expressed by an equation of the general form

$$\frac{D\tilde{C}}{Dt} = \frac{1}{H^2}\frac{\partial}{\partial\sigma}\left[(K_b + \nu_b)\frac{\partial\tilde{C}}{\partial\sigma}\right] + \Re_c + HmnF_C \tag{1}$$

The material derivative on the left hand side of eq. (1) is expressed as

$$\frac{D\tilde{C}}{Dt} = \frac{\partial\tilde{C}}{\partial t} + \frac{\partial}{\partial\xi}\left(\frac{u\tilde{C}}{m}\right) + \frac{\partial}{\partial\eta}\left(\frac{v\tilde{C}}{n}\right) + \frac{1}{H}\frac{\partial}{\partial\sigma}\left(\omega\tilde{C}\right) \tag{2}$$

K_b and ν_b are the vertical eddy and molecular diffusion coefficients, respectively. They are assumed to be same with those of the heat and salt equations. F_C represents the biological interaction terms which are expressed for each of the biological variables as (e.g. Fasham et al., 1990)

$$F_P = (1-\kappa)\,\Phi_p P - G_p(P)\,H - m_p P \tag{3}$$

$$F_H = \gamma_p G_p(P)\,H + \gamma_b G_b(B)\,H - m_h H - \mu_h H \tag{4}$$

TABLE 1. Biological model parameters and definitions

Parameter	Definition	Value	Units
ν_b	Background (molecular) value of kinematic viscosity and diffusivity	$1x10^{-6}$	m^2s^{-1}
σ_m	Maximum phytoplankton growth rate	1.5	day^{-1}
a	Photosynthesis efficiency parameter	0.01	nondimensional
k_w	Light extinction coefficient for PAR	0.08	m^{-1}
k_c	Phytoplankton self-shading coefficient	0.07	m^2 $(mmol\text{-}N)^{-1}$
R_n	Nitrate half saturation constant	0.5	mmol-N m^{-3}
R_a	Ammonium half saturation constant	0.2	mmol-N m^{-3}
ψ	Ammonium inhibition parameter	3.0	$(mmol\text{-}N)^{-1}$
m_p	Phytoplankton death rate	0.04	day^{-1}
κ	Phytoplankton exudation fraction	0.05	nondimensional
r_g	Herbivore maximum grazing rate	0.6	day^{-1}
m_h	Herbivore death rate	0.04	day^{-1}
μ_h	Herbivore excretion rate	0.12	day^{-1}
γ_p	Herbivore assimilation efficiency	0.75	nondimensional
R_g	Herbivore grazing half saturation constant	0.5	mmol-N m^{-3}
σ_b	Maximum bacterial growth rate	0.35	day^{-1}
γ_b	Bacterial assimilation efficiency	0.7	nondimensional
r_b	Bacterial maximum grazing rate	0.25	day^{-1}
R_b	Bacterial grazing half saturation constant	0.5	mmol-N m^{-3}
μ_b	Bacteria excretion rate	0.05	day^{-1}
ϵ	Detrital remineralization rate	0.1	day^{-1}
w_s	Detrital sinking rate	2.0	m day^{-1}
Ω_n	Ammonium nitrification rate	0.5	m day^{-1}
Ω_d	nitrate denitrification rate	0.5	m day^{-1}
λ	partition of detritus between DON and Ammonium	0.5	nondimensional

$$F_D = (1-\gamma_p)\,G_p(P)\,H + (1-\gamma_b)\,G_b(B)\,H + m_p P + m_h H - \epsilon D + \frac{w_s}{H}\frac{\partial D}{\partial \sigma} \tag{5}$$

$$F_{DON} = -\Phi_b B + \kappa \Phi_p P + \lambda \epsilon D \tag{6}$$

$$F_B = \Phi_b B - G_b(B)\,H - \mu_b B \tag{7}$$

$$F_A = -\sigma_m \alpha(I)\,\beta_a(A)\,P + \mu_h H + (1-\lambda)\,\epsilon D + \mu_b B - \Omega_n A \tag{8}$$

$$F_N = -\sigma_m \alpha(I)\,\beta_n(N)\,P + \Omega_n A - \Omega_d N \tag{9}$$

where the definition of parameters are given in Table 1.

In the phytoplankton equation, the primary production is expressed as a function of light, nitrate and ammonium uptakes by

$$\Phi_p = \sigma_m \alpha(I)[\beta_a(A) + \beta_n(N)] \tag{10}$$

The maximum specific production rate under optimum light and nutrient conditions does not have the temperature dependence. Daily variations of the photosynthetically available radiation are neglected. The losses are due to the herbivore grazing and natural mortality. The effects of respiration and phytoplankton excretion are included in the latter loss term. 5% of the total primary production is assumed to be exudated as DON.

The nutrient limitation functions for the ammonium $\beta_a(A)$ and for the nitrate $\beta_n(N)$ are expressed by the standard Michaelis-Menten formulations

$$\beta_a(A) = \frac{A}{R_a + A} \qquad \beta_n(N) = \frac{N}{R_n + N} \exp(-\psi A) \tag{11}$$

where R_n and R_a are the half-saturation constants for nitrate and ammonium, respectively. The exponential term represents the inhibiting effect of ammonium concentration on nitrate uptake, with ψ signifying the inhibition parameter. The light limitation is parameterized by

$$\alpha(I) = tanh[aI(z,P,t)] \tag{12}$$

$$I(z,P,t) = I_s \exp[-(k_w + k_c P)z] \tag{13}$$

where a denotes photosynthesis efficiency parameter, I_s is the surface intensity of the PAR, k_w is the light attenuation coefficient due to sea water, and k_c is the phytoplankton self-shading coefficient. The grazing rates of herbivores on phytoplankton is represented by

$$G_p(P) = r_g \frac{P}{R_g + P} \tag{14}$$

where r_g is the maximum grazing rate, and R_g denotes the half-saturation constant. A similar expression is also used to express the bacterial grazing of herbivores.

The zooplankton are fed by assimilating 70%'s of the phytoplankton and bacterial grazing. The losses are excretion and mortality. The excretion occurs in the form of ammonium. The mortality term represents dead zooplankton biomass as well as losses by higher predators which are not considered explicitely in the model. The main source of the detrital pool is the fecal pellets constituting 30%'s of the zooplankton grazing of phytoplankton and bacteria. All the phytoplankton losses and the dead zooplankton biomass constitute additional detrital sources. Detritus sink downward with

a fall speed w_s. It is assumed that only 50% of the particulate matter is converted into DON form, the rest is converted instantly into ammonium form, and does not take place in the bacterial production process.

In addition to the detrital breakdown, the other DON production mechanism is the phytoplankton exudation. The bacteria take up the DON, excrete ammonium and are grazed by zooplankton. No bacterial mortality is modeled separately; its effect is embedded in the excretion term. The bacterial uptake of the dissolved organic nitrogen is expressed by

$$\Phi_b = \sigma_b \frac{DON}{R_b + DON} \tag{15}$$

with σ_b and R_b signifying the maximum bacterial growth rate and the half saturation constant, respectively. Thus, the nitrogen requirement of the bacterial growth process is met simply by the DON, and the ammonium contribution (see Fasham et al., 1990) is not incorporated in this process.

The zooplankton and bacterial excretion as well as a part of detrital breakdown signify the three mechanisms in the ammonium equation responsible for the nitrogen cycling and the regenerated production. The ammonium consumption of the phytoplankton during the photosynthesis and nitrification process consitute the sink terms. The nitrification process is parameterized as a direct conversion of ammonium to nitrate without the intermediate level of nitrite transformation. The nitrification rate is taken vertically uniform above the depth of the 15.6 kg/m^3 sigma-t level, decreasing linearly to zero towards the depth of the 16.2 kg/m^3 sigma-t level (Ward and Kilpatrick, 1991). At deeper levels (i.e. within the anoxic layer), no nitrification takes place. But, nitrate is denitrified to N_2 at these depths.

No-flux conditions are specified for all variables both at the surface and the bottom.

4. One Dimensional Simulation with the Coupled Physical - Biochemical Model

As a step towards the three dimensional ecosystem modeling, we present here a one-dimensional version of the coupled model with no horizontal dependence. A similar model with five compartments of the biological module (without DON and bacteria) was described in Oguz et al. (1996c). This simplified approach provides a basic understanding of the first order biological processes relevant for the central Black Sea, away from the shelf and the Rim Current frontal zone.

The model is initialized with the stably stratified upper ocean temperature, salinity, nitrate and ammonium profiles representative of the autumn

conditions for the interior part of the sea. A total of 51 vertical levels is used for the water column of 200 m depth representing the upper layer of the Black Sea. The grid spacing is compressed slightly towards the surface to increase the resolution near the uppermost levels. A typical grid spacing is about 5 m, except near the boundaries. The vertical diffusion terms and some of the biological terms in each of the equations (1)-(9) are solved implicitely using a time step of 5 minutes. The physical and turbulence modules, without the biological module, is first integrated for five years until an equilibrium state is achieved with repeating yearly cycles of the physical variables. The physical model is forced by the monthly varying wind and surface heat flux climatologies given by Efimov and Timofeev (1990). The monthly surface salinity values, obtained from the climatological atlas of Altman et al. (1987), are stipulated as the boundary condition in the salinity equation. Using the fifth year's cycle of the physical-turbulence models, the biological model is then forwarded in time for four years to obtain yearly cycles in all the biological variables.

Using the parameter values given in Table 1, a simulation run describing basic features of the nitrogen cycling and bacteria-plankton dynamics in the central Black Sea are shown in Figs. 3 and 4. The temporal and vertical distributions of nitrate (Fig. 3) exhibit an almost complete depletion within the shallow surface mixed layer during the period from May to November. The lack of vertical mixing across the sharp thermocline leads to consumption of the entire nitrate stocks within the mixed layer during the summer. This layer is separated from the waters having relatively richer nitrate concentrations by a seasonal nutricline confined between the depths of 20-to-30 m. It is only after November, once the seasonal thermocline is eroded, the surface layer begins to accumulate nitrate by entrainment from nitrogen-rich subsurface waters. The entire convectively generated mixed layer of about 50 m thus attains a vertically uniform nitrate concentrations during the winter period. The winter mixed layer is separated from the subsurface nitrate maximum zone by a strong permanent nutricline centered approximately at 60 m. In the rest of the year, when the mixed layer is much shallower, the layer bounded by the permanent and seasonal nutriclines signifies the biochemically active zone of nitrification process. Consequently, this layer exhibits more uniform variations between the depleted surface waters and subsurface nitrate maximum. At depths below the maximum, nitrate concentrations does not change much as compared with the initial profile. It tends to zero at a depth of about 120 m corresponding here to the level of oxic/anoxic interface.

The phytoplankton distribution (Fig. 4a) reveals a major peak during March with concentrations of 1.8 mmolN/m^3 within the upper 30 m layer, decreasing gradually towards the base of the euphotic zone at 50m. The

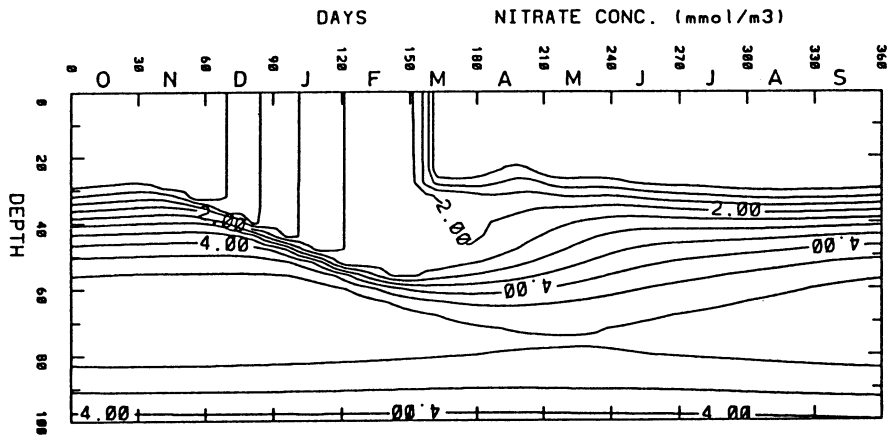


Figure 3. Depth and time variations of the nitrate concentrations computed by the one-dimensional coupled model. Day zero corresponds to the begining of October.

early spring bloom of approximately two weeks duration is followed by a shorter secondary bloom event during the third week of April. Contrary to the March bloom, the latter is related with the regenerated production due to the excess of ammonium (Fig. 4b) produced in the water column following the March bloom due to the remineralization process. In summer, a relatively weaker subsurface phytoplankton production exists below the seasonal nutricline where, in addition to nitrate, there is enough solar radiation to trigger the primary production. The summertime subsurface production is eventually combined with the surface production during November, once the atmospheric cooling starts to generate sufficiently strong vertical mixing. This is however a weaker bloom as compared with those reported by the observations. Because the model considers the vertical mixing due only to the atmospheric cooling, and does not incorporate strong short term wind induced mixing events which are very common during late autumn and early winter seasons.

All the three phytoplankton bloom events are followed by the specific periods of high zooplankton production with a time lag of about two-to- three weeks (Fig. 4c). The peak herbivore concentration is about 1.0 mmol N/m^3 occuring within the last week of March. In April, its concentration is about 0.5 mmolN/m^3 and approximately 0.20 mmolN/m^3 in November. The winter season is completely inactive in terms of plankton production. Both

phytoplankton and herbivore concentrations are almost zero in the period between the autumn and early spring blooms. While the herbivore concentrations decrease gradually inside the surface mixed layer during the summer, there exists subsurface concentrations of the order of 0.40 mmolN/m^3 within the late spring and entire summer period. The zooplankton community in the model is concentrated within the euphotic zone within the upper 50 m layer since they are grazed primarily by phytoplanktons.

The detritus distribution (not shown) exhibits its most dense concentrations of about 0.6 mmol N/m^3 right after the March bloom. Concentrations gradually reduce towards summer as they partially sink to deeper levels and, at the same time, are continually converted to dissolved organic nitrogen and ammonium forms. The DON reveals maximum concentrations during late spring and summer seasons. The peak values of about 1.0 mmolN/m^3 occurs near the surface during May, decreasing to about 0.25 mmolN/m^3 during the summer. June corresponds to the period with most drastic DON variations due to its consumption in the bacterial production process. The bacteria concentration reaches a value of 0.6 mmolN/m^3 in this month. The bacteria population is of the order of 0.1 mmolN/m^3 within the rest of the year.

4.1. MODEL-DATA COMPARISON

The nitrogen deficiency of surface waters during the summer season is supported by the nitrate measurements (Codispoti et al., 1991; Basturk et al. 1994). To our knowledge, there are not much nutrient measurements performed within the interior part of the sea during the late autumn and winter periods. The systematic measurements carried out outside the northern exit of the Bosphorus Strait (see Fig. 4 in Polat and Tugrul, 1995), on the other hand, reveal an almost one order of magnitude changes in the nitrate concentrations within the year. The mixed layer averaged concentrations of less than 0.1-0.2 mmolN/m^3 in the August-October period increase to about 2.5 mmolN/m^3 during winter, and then decrease sharply towards the summer values in spring, following the bloom event. The model results are consistent with these variations.

When the computed phytoplankton distributions is compared with the observed Chlorophyll-a distributions (see Fig. 2b in Oguz et al. 1996c), it is shown that the model is able to reproduce the two major peaks during early spring and late autumn, as well as the subsurface maximum layer during the summer period. The layer averaged peak concentration of about 1.5 mgChl-a/m^3 agrees fairly well with the data. The typical post-bloom and early summer values computed by the model is about 0.1-0.2 mgChl-a/m^3 whereas the data suggest slightly higher values of 0.3-0.4 mgChl-a/m^3 at the

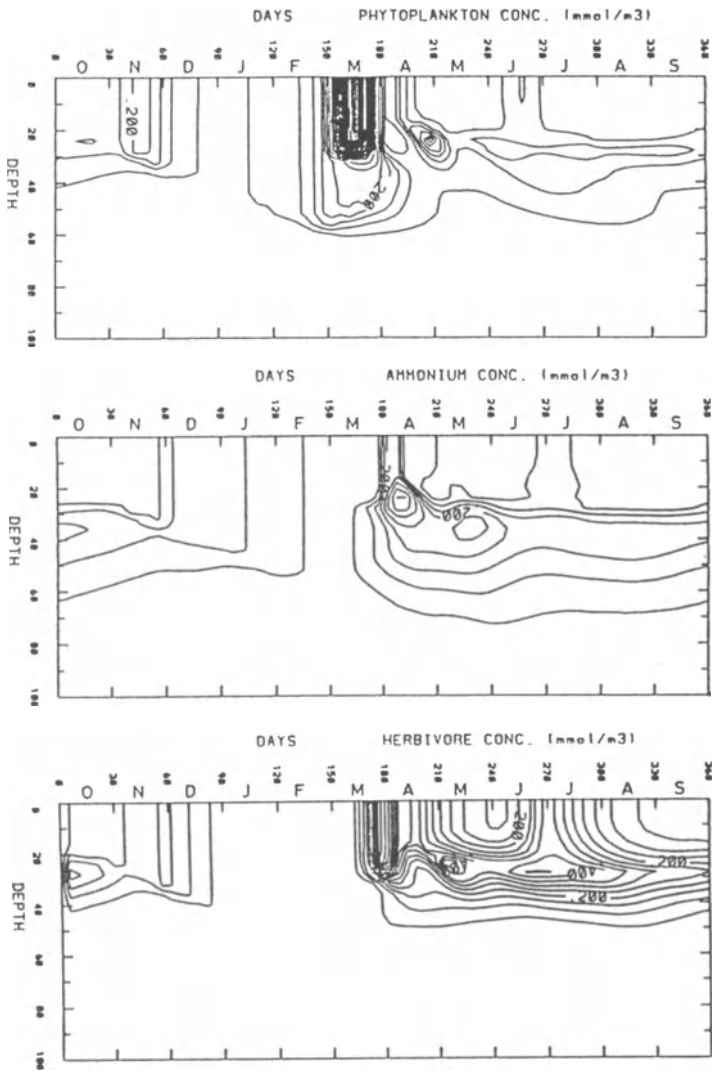


Figure 4. Depth and time variations of (a) phytoplankton, (b) ammonium, (c) zooplankton concentrations. Day zero corresponds to the begining of October.

same period. The model, on the other hand, underestimates intensity of the autumn bloom. The computed values of 0.2-0.3 mgChl-a/m^3 are lower than the observations which suggests a range of variations between 0.4 and 1.0 mgChl-a/m^3, depending on the location and the year. As we have already

emphasized above, incorporation of strong wind-induced mixing events on weekly time scales may provide a better model-data agreement.

The euphotic layer integrated peak herbivore concentration in the model amounts to ~25 mmolN/m^2 (≃2.5gC/m^2) at the begining of April, decreasing to the values of about 1.0 gC/m^2 later in the summer season, and to about 0.5 gC/m^2 during the autumn period. These values are consistent with the estimates of the mesozooplankton biomass as reported by Vinogradov (1992). The detritus exhibits similar distribution within the year. The total PON content (the sum of phytoplankton, zooplankton and detritus) within the euphotic layer are about 3.5 mmolN/m^3 during March-April period, decreasing to the values of about 2.0 mmolN/m^3 during summer months. These values are comparable with the PON values measured in the Bosphorus exit region (Polat and Tugrul, 1995).

It is difficult to compare the DON concentrations with the available observations, because of the wide range of discrepencies reported in the measured DOC values. According to data shown in Polat and Tugrul (1995), DON concentrations within the euphotic layer varies between 15 and 20 mmolN/m^3 within the year with slightly higher values in the summer months and lower ones during the winter months. If the labile fraction of DON is assumed to be around 5% of the total, then the measured labile DON concentrations should be about 0.75-1.0 mmolN/m^3. Our computed DON values are in good agreement with this estimate. The bacterial biomass has the summer peak value of 0.4 mgC/m^3 during June. The average concentration within the euphotic layer is about 0.2 mgC/m^3 in spring season, and around 0.10 mgC/m^3 within the late summer and autumn season. These are the typical range of variations in the photoautotrophic bacterial biomass concentrations as suggested by the observations (Sorokin, 1983).

5. Acknowledgements

This work was supported in part by TU-Black Sea Project sponsored by the NATO Science for Stability Program, in part by the National Science Foundation, Grant No: INT.9310226 and the Office of Naval Research, Grant No: N00014-95-1-0226. Under these grants, Temel Oguz was visiting scientist at MIT-USA during June 1993-July 1994 and June-July-August 1995.

References

1. Altman, E.N., I.F. Gertman, Z.A. Golubeva (1987) *Climatological fields of salinity and temperature in the Black Sea.* State Oceanographical Institute, Sevastopol Branch, 109pp (in Russian).
2. Basturk, O., C. Saydam, I. Salihoglu, L.V. Eremeeva, S.K. Konovalov, A. Stoyanov, A. Dimitrov, A. Cociasu, L. Dorogan, M. Altabet (1994) Vertical variations in the

principle chemical properties of the Black Sea in the autumn of 1991. *J. Marine Chemistry*, **45**, 149-165.

3. Bologa, A.S., N. Bodeanu, A. Petran, V. Tiganus, Yu. P. Zaitsev (1995) *Major modifications of the Black Sea benthic and planktonic biota in the last three decades.* In: Mediterranean tributary Seas, CIESM Science Series No 1, Ed. Frederic Briand, Monaco, Musee Oceanographique, pp.85-110.
4. Codispoti,L.A., G.E. Friederich, J.W. Murray, C.M. Sakamoto (1991) Chemical variability in the Black Sea: implications of continuous vertical profiles that penetrated the oxic/anoxic interface. *Deep Sea Res.*, **38**, Suppl.2, S691-S710.
5. Efimov, V.V., and N.A. Timofeev (1990) *Investigation of the Black Sea and Azov Sea heat balance.* Technical Report, Ukranian Academy of Sciences, Sevastopol, 237pp.
6. Fasham, M.J.R., H.W. Ducklow, S.M. McKelvie (1990) A nitrogen-based model of plankton dynamics in the oceanic mixed layer. *J. Mar. Res.*, **48**, 591-639.
7. Hellermann, S. and M. Rosenstein (1983) Normal monthly wind stress over the world ocean with error estimates. *J. Phys. Oceanogr.*, **13**, 1093-1104.
8. Mee, L.D. (1992) The Black Sea in crisis: The need for concerted international action.*Ambio*, **21**, 278-286.
9. Mellor, G.L. (1991) *User's guide for a three dimensional, primitive equation, numerical ocean model.* Prog. in Atmos. and Ocean. Sci., Princeton University, 35pp.
10. Oguz, T., V.S. Latun, M.A. Latif, V.V. Vladimirov, H. I. Sur, A.A. Markov, E. Ozsoy, B.B. Kotovshchikov, V.V. Eremeev, U. Unluata (1993) Circulation in the surface and intermediate layers of the Black Sea. *Deep Sea Res. I*, **40**, 1597-1612.
11. Oguz, T., D.G. Aubrey, V.S. Latun, E. Demirov, L. Koveshnikov, V. Diacanu, H.I. Sur, S. Besiktepe, M. Duman, R. Limeburner, V. Eremeev (1994) Mesoscale circulation and thermohaline structure of the Black Sea observed during HydroBlack'91. *Deep Sea Research I*, **41**, 603-628.
12. Oguz, T., P. Malanotte-Rizzoli, D. Aubrey (1995) Wind and thermohaline circulation of the Black Sea driven by yearly mean climatological forcing. *J. Geophys. Res.*, **100**, 6845-6863.
13. Oguz, T., D. Aubrey, S. Besiktepe, L. Ivanov, V. Diacanu, U. Unluata (1996a) ADCP observations of the western Black Sea Rim Current. *to appear in Deep Sea Res.*
14. Oguz, T. and P. Malanotte-Rizzoli (1996b) Seasonal variability of wind and thermohaline driven circulation in the Black Sea. *J. Geophys. Res.*, **101**(C7), 16585-16599.
15. Oguz, T., H. Ducklow, P. Malanotte-Rizzoli, S. Tugrul, N. P. Nezlin, U. Unluata (1996c) Simulation of annual plankton productivity cycle in the Black Sea by a one-dimensional physical-biological model. *J. Geophys. Res.*, **101**(C7), 16551-16569.
16. Oguz, T., L.I. Ivanov, S. Besiktepe, E. Demirov, V. Diacanu, A.V. Grigorev, M. Duman, D.G. Aubrey (1996d) Kinematical description of basinwide circulation and thermohaline characteristics of the Black Sea during July 1992. *Submitted to J. Marine Systems.*
17. Polat, S.C. and S. Tugrul (1995) Nutrient and organic carbon exchanges between the Black and Marmara Seas through the Bosphorus Strait. *Cont. Shelf Res.*, **15**, 1115-1132.
18. Vinogradov, M.E. (1992) *Long-term variability of the pelagic community structure in the open part of the Black Sea.* In: Problems of the Black Sea. Proc. International Conference, Sevastopol, Ukraine. November 10-15, 1992. MHI-UAS Publication, pp.19-33.
19. Ward, B.B. and K.A. Kilpatrick (1991) *Nitrogen transformations in the oxic layer of permanent anoxic basins: The Black Sea and Cariaco Trench.* In: Black Sea Oceanography, NATO ASI Series C-Vol.351, E.Izdar and J.W. Murray, editors, Kluwer Academic Publishers, Dordrecht, pp.111-124.

COUPLED HYDRODYNAMIC ECOSYSTEM MODEL OF THE BLACK SEA AT BASIN SCALE

Model description and first results

M. GRÉGOIRE[1], J.-M. BECKERS[2], J.C.J. NIHOUL, E. STANEV[3]
G.H.E.R. - Université de Liège
Sart-Tilman B5, B-4000 Liège (Belgium)
[1] *Research Assistant and* [2] *Research Associate,*
National Fund for Scientific Research, Belgium
[3] *Permanent address: University of Sofia, Dept. of Meteorology and Geophysics, 5 J. Bourchier Str., 1126 Sofia, Bulgaria*

Abstract. A hydrodynamical model of the general circulation in the Black Sea has been build up, using the GHER primitive equation model. In a first experiment, a model with 15 km horizontal resolution and 20 vertical levels is used to compute the typical seasonal cycle by forcing the model with climatological monthly mean fields of temperature, salinity and wind stress at the air sea interface. Furthermore, the corresponding river discharges of the Danube, Dnestr, Dnepr and Rioni are taken into account. The simulation results are presented in view of their later use in a 3D ecosystem model. An ecosystem model at basin scale is then defined by a nitrogen cycle, which is described by 5 state variables, i.e. NO_3^-, NH_4^+, Phytoplankton, Zooplankton and Dissolved organic matter. This model has been chosen as a first test for coupling the 3D hydrodynamical model and the ecosystem model. The ecosystem model is imbedded on-line into the 3D hydrodynamical model with a superimposed cycle for the light intensity. In this paper, the main findings of the hydrodynamic model are summarized stressing those aspects of the current and hydrological fields that affect the ecosystem. The ecosystem model is briefly described emphasizing the modifications made to adapt the equations to the Black Sea's environmental conditions.

E. Özsoy and A. Mikaelyan (eds.), Sensitivity to Change: Black Sea, Baltic Sea and North Sea, 487–499.
© 1997 *Kluwer Academic Publishers.*

1. Introduction

The three-dimensional PE turbulent closure ecohydrodynamic mathematical model developed at the **GeoHydrodynamics** and **E**nvironment **R**esearch Laboratory (GHER) of the University of Liège has been described in various earlier publications (e.g. Nihoul and Djenidi 1987, 1991, Nihoul et al 1989, Nihoul and Beckers 1989, Adam 1991, Beckers 1991, Nihoul et al 1994). In its general formulation, it consists in two sectorial submodels :

1. the hydrodynamic model, the state variables of which are the three components of the velocity vector, the pressure, temperature, buoyancy (or salinity), the turbulent kinetic energy and the turbulent dissipation rate (or the mixing length) ;
2. the plankton ecosystem model, the state variables of which are defined, according to the recommendations of the GLOBEC Numerical Modelling Group, as those which are necessary and sufficient to assess the effects of the physical processes on primary and secondary productions (the so-called "minimum critical set") (GLOBEC 1995).

In this preliminary application to the Black Sea, the simple version of the GHER plankton model, applied previously with success to the Northern Bering Sea, has been used, - in a version adapted to the Black Sea -, and the state variables are NO_3^-, NH_4^+, the phytoplankton and zooplankton biomasses and dissolved organic matter.

The ecosystem model is embedded on-line into the 3D hydrodynamic model with a superimposed light intensity cycle.

In this paper, the main findings of the hydrodynamic model are summarized stressing those aspects of the current and hydrological fields that affect the ecosystem. The ecosystem model is briefly described emphasizing the modifications made in the original formulation to adapt the equations to the Black Sea's environmental conditions. Exemplary results are given in illustration.

2. Hydrodynamic results

It is widely accepted in the Black Sea oceanography that the sea surface elevation has a maximum in the coastal zone and decreases with increasing distance from the coast (Filippov, 1968, Gamsakhurdia and Sarkysian, 1976, Stanev et al., 1988, Oguz et al., 1994). This general pattern explains the cyclonic currents at the sea surface encompassing the whole basin, as a result of the adjustment between the velocity and mass fields. The mean position of the surface currents coincides approximately with the position of the continental slope, but important deviations are observed due to eddy variability, direct impact of extreme atmospheric forcing or interannual

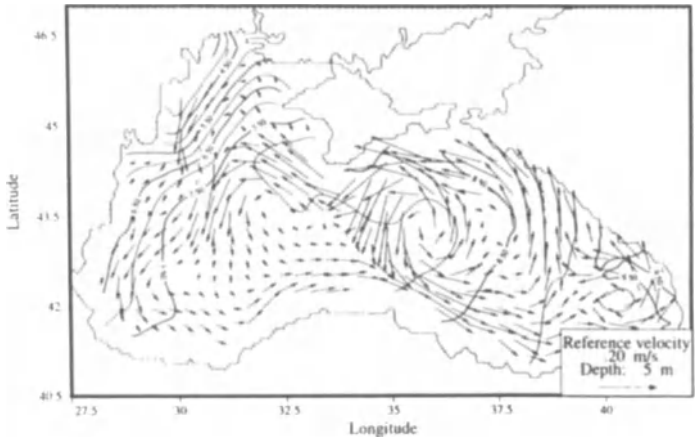


Figure 1. Model simulated results with currents superimposed, 20 February. Temperature at 5m ($^{\circ}C$).

variability. This cyclonic type of circulation dominates the vector plots, Fig. 1, 2, and 3, but shows pronounced seasonal dependency, which is important for the transport of plankton and other biological components. One begins by analyzing the seasonal variability, simulated by the model, using Figures 1-3, which show the daily averaged sea surface temperature (SST). Each figure corresponds to one specific state of the sea during its seasonal evolution. Fig. 1 (20 February) corresponds to winter, that is to the state when the cooling, and the resulting formation of the cold waters is strongest; Figure 2 (1 June) corresponds to the end of spring, when the sea is very strongly affected by the river discharge; Figure 3 (10 September) corresponds to the time immediately after the strongest summer heating and just before the thermohaline fields start to change, due to the cooling in fall.

Currents reach maximal values along the Caucasian Coast in fall. Qualitative time-changes of the circulation (reversals) are very pronounced between the main gyre and the coast, and in particular in the western basin. The circulation in the central and eastern parts of the sea remains relatively stable during the year, and the patterns do not show reversals of the circulation. The variability in these areas is illustrated rather by the large meander, off the Caucasus Coast, Figures 1 and 2, which disappears in fall; and by the meander off the eastern Turkish coast, which shifts to the east in winter, to the west in summer, and to the north in fall. The circulation on the shelf exhibits the largest changes over the year. The current follows the coast in winter, starting from the southern coasts of the Crimea Peninsula, and reaching the Bulgarian coast to the south west.

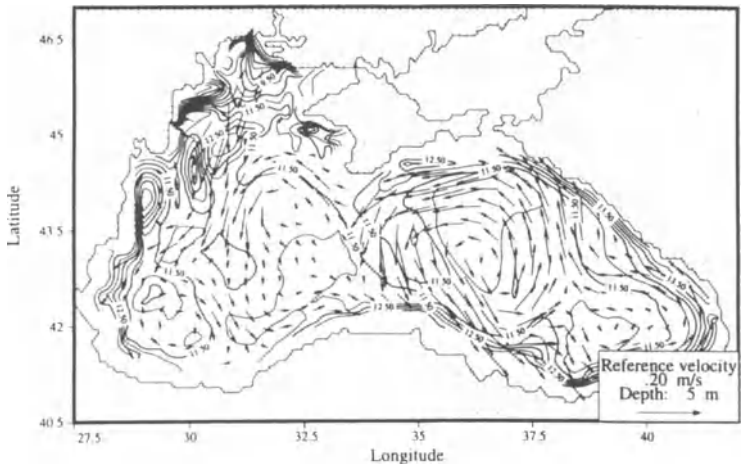


Figure 2. Model simulated results with currents superimposed, 1 June. Temperature at 5 m ($^{\circ}C$).

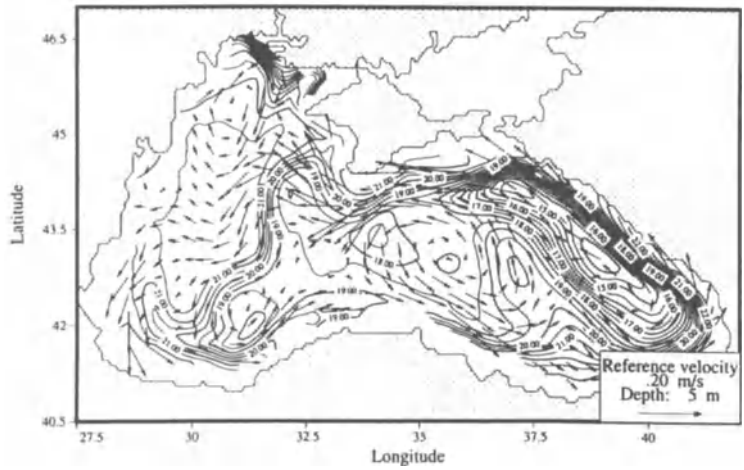


Figure 3. Model simulated results with currents superimposed, 10 September. Temperature at 5 m ($^{\circ}C$).

An anticyclonic eddy is formed on the shelf, off the Danube delta, in late spring, Figure 2. This area widens to the east in summer.

The large loop of the western branch of the main gyre, formed in late spring could have an important impact on the ecological processes in this area. After the current reaches the northern Bulgarian coast, it abruptly turns towards the Danube inflow area. After reaching the coast there it turns again to the south. Such meandering type of behavior is typical for non-linear currents, which could be regarded as extensions of the river plumes into the open sea (Chao and Boicourt, 1986). The analysis of the

dynamics of river plumes (see Figure 2 by Oey and Mellor, 1993) proves that the inertia tends to balance the Coriolis acceleration, which results in the formation of intrusion of the open sea water towards the plume.

The simulated SST, Figures 1, 2, and 3 show pronounced seasonal variability. The winter minimum of about 3.5 $^{\circ}C$ is reached on the most part of the north-western shelf. Water, cooler than $^{\circ}C$ can be found between the isobath 100 m and the coast, which correlates well with the pattern derived from the satellite data (Sur et al., 1995). Temperature maximum in February of about 9.5 $^{\circ}C$ is simulated in the easternmost Black Sea.

When one analyzes the SST in the warm part of the year, one has to take into account the fact that the sea surface is much warmer than the intermediate layer. The core of the CIL is about 50 m below the sea surface, and it is 10-15 $^{\circ}C$ colder than the surface waters. Thus it is potentially a very good "tracer", which could dye surface waters with low temperatures, and show the existing upwelling, Figure 2. However, these strong gradients are not crucial dynamically, since the circulation in the Black Sea is dominated by salinity.

3. The ecosystem model

The model used in this preliminary investigation of the Black Sea's ecohydrodynamics is very simple and must be regarded rather as a tool for testing the coupling of hydrodynamic and ecosystem submodels, while acquiring some preparatory assessment of the effect of physical processes on the ecodynamics (A more sophisticated model is now in process and new results will be reported later). The model has five state variables : NO_3^-, NH_4^+, phytoplankton, zooplankton and dissolved organic matter. Bacterioplankton has been eliminated assuming quasi-equilibrium prey-predator relationships within the microbial loop (Walsh et al 1989, Nihoul et al 1994), and no independent state variable is introduced to account for the particulate organic matter; particles are included in the sedimenting fractions of both the phytoplankton (dead cells) and the zooplankton (dead animals, faecal pellets) biomasses (with appropriate sedimentation velocities determined by inspection of the data base). The nitrification process (ammonium oxidation into nitrate) is assumed to be too slow to enter the spectral window of the simulation. If the model is kept integrated for several years to reach a statistical equilibrium state, the ammonium concentration could keep increasing as the nitrate keeps decreasing (Oguz et al., 1996). Thus, the simulation can not be performed during several years to see if a steady state solution can be reached. Matter exchanges between compartments are described in the form of a nitrogen cycle and the state variables are measured in nitrogen content units. The interaction

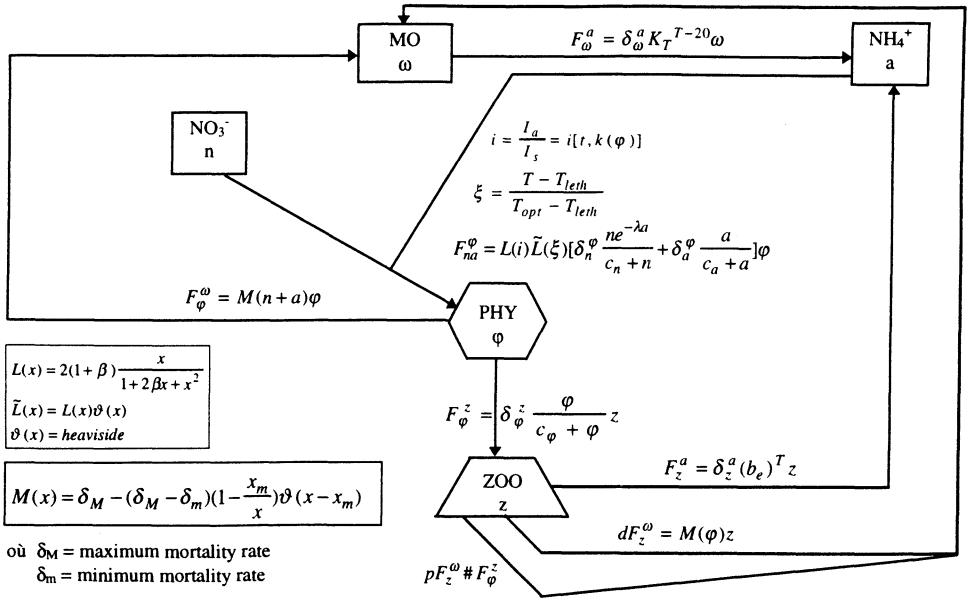


Figure 4. Schematic representation of the ecosystem model. The interaction rates Q^y are written on the arrows. The parameters dependent on the temperature are circled

rates used in the Black Sea calibrated model are written on the box-arrow representation of the model shown in figure 4. In the winter, important sea surface temperature gradients are observed. For instance, a winter minimum of 3.5 $°C$ is reached on most of the north western shelf while in the eastern part, the temperature is about 9 $°C$ (Stanev and Beckers 1995). One may thus expect strong temperature limitation effects on the phytoplankton's distribution. It is well known that all biological processes have a temperature dependence. Generally, process rates double for each 10 $°C$ increase in temperature. However, in this preliminary study, only the phytoplankton's growth, the remineralization rate and the zooplankton's excretion rate depend on the temperature following the model of Nival and Andersen (1988). This model introduces a lethal temperature and this concept will undoubtedly have to be reexamined in further studies as it excludes the possibility that particular resisting species may develop below the lethal threshold.

The calibration and sensitivity study of the model is not straightforward

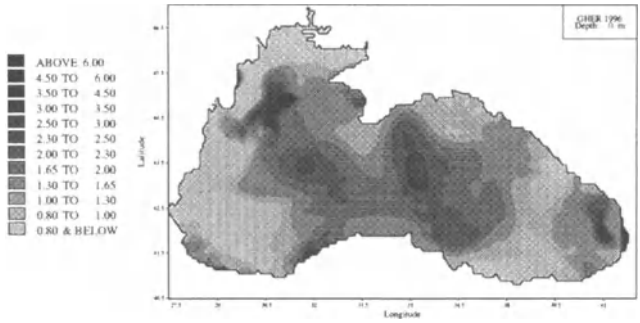


Figure 5. Surface phytoplankton field at the end of February (in $\mu at - gN/l$) ; the bloom begins at the central parts of the eastern and western main cyclonic gyres. High phytoplankton concentrations are also observed at the Danube's mouth.

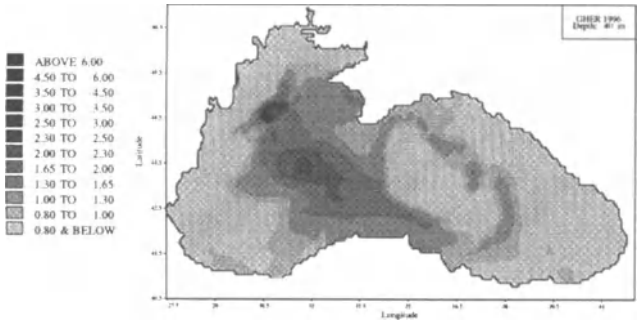


Figure 6. Horizontal distribution of phytoplankton at 40 m at the end of February (in $\mu at - gN/l$). In the region of the eastern main cyclonic gyre, the shallow mixed layer (the upper border of the pycnocline is located at 20 to 30 m owing to the upwelling) creates unfavorable light conditions for phytoplankton development at 40 m ; a white patch can be observed in this area in the phytoplankton distribution.

in the 3D model due to the large number of simulation experiments needed. Thus, a box version of the model has been used to determine the most sensitive parameters of the ecosystem model. Once these parameters are known, the calibration of the 3D model can be realised by adjusting them.

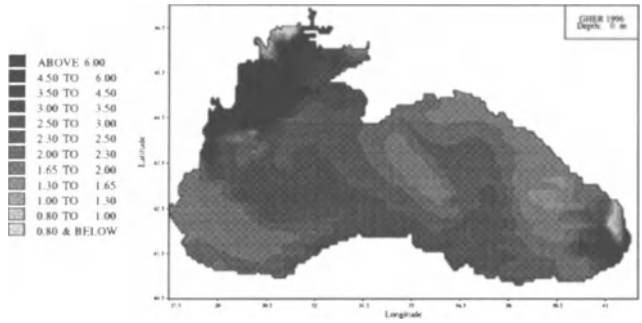


Figure 7. Surface phytoplankton field at the end of March (in $\mu at - gN/l$). In the north-western region, the increasing temperatures allow phytoplankton growth, and the bloom occurs in the region of the Danube's plume. In the region of the eastern gyre, the increasing grazing pressure leads to the decrease of phytoplankton concentrations.

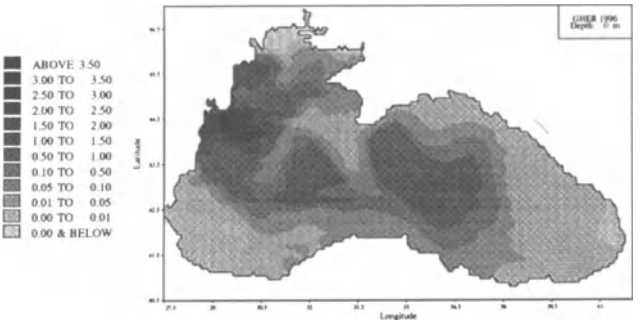


Figure 8. Surface zooplankton field at the end of March (in $\mu at - gN/l$). Zooplankton development is important in the phytoplankton bloom regions.

4. Discussion

The simulation is performed by solving the ecosystem model conjointly with the physical model. The results suggest that the initiation of the bloom is essentially influenced by the water column stability and by the temperature. In the winter, on most of the north western shelf, the water column is not stratified, the mixed layer extends to the bottom (further than the euphotic layer) leading to the light limitation of winter phytoplankton,

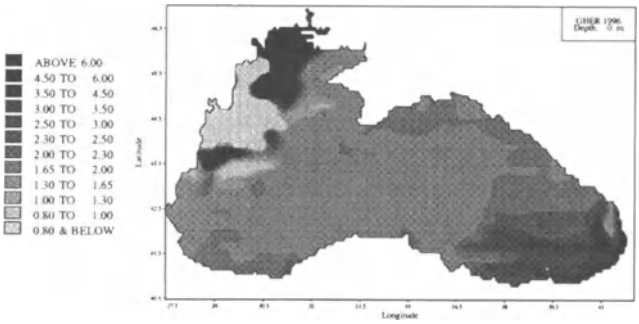


Figure 9. Surface phytoplankton field at the end of May (in $\mu at - gN/l$). The phytoplankton population decreases as nutrient are progressively exhausted and the grazing pressure increases. In the region of the Danube's plume consumed nutrients are constantly replaced by the discharge river waters.

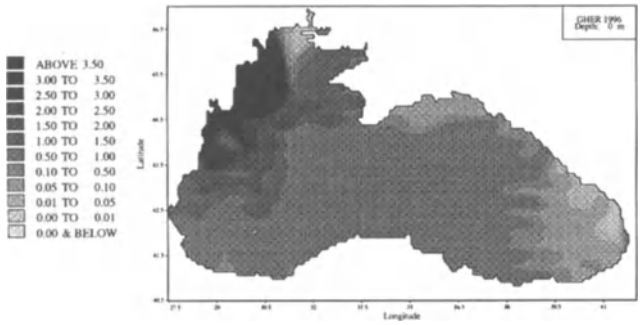


Figure 10. Surface zooplankton field at the end of May (in $\mu at - gN/l$). This picture shows the important zooplankton development in the region of the Danube's plume.

while in the central parts of the eastern and western main cyclonic gyres, the mixed layer doesn't extend further than 20 to 40 m and becomes shallower than the critical depth . Besides, as has been explained before, the existence, in the winter, of important gradients in the sea surface temperature distribution, makes us to introduce a temperature limitation function of phytoplankton's growth. This limiting effect of temperature introduces a delay in the beginning of the bloom in the cold water region.

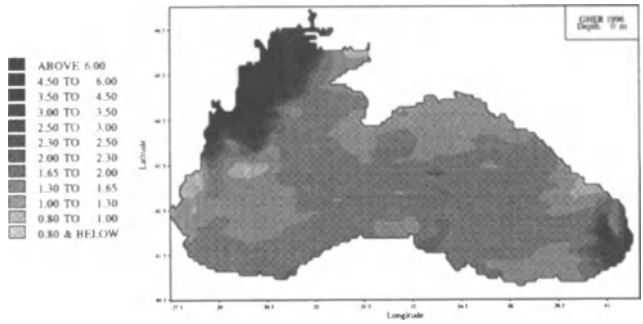


Figure 11. Surface phytoplankton field : mean values in Spring (in $\mu at - gN/l$). The competition between phytoplankton growth and grazing is very likely responsible for the spatial structure of the phytoplankton concentration in the region of the Danube's plume.

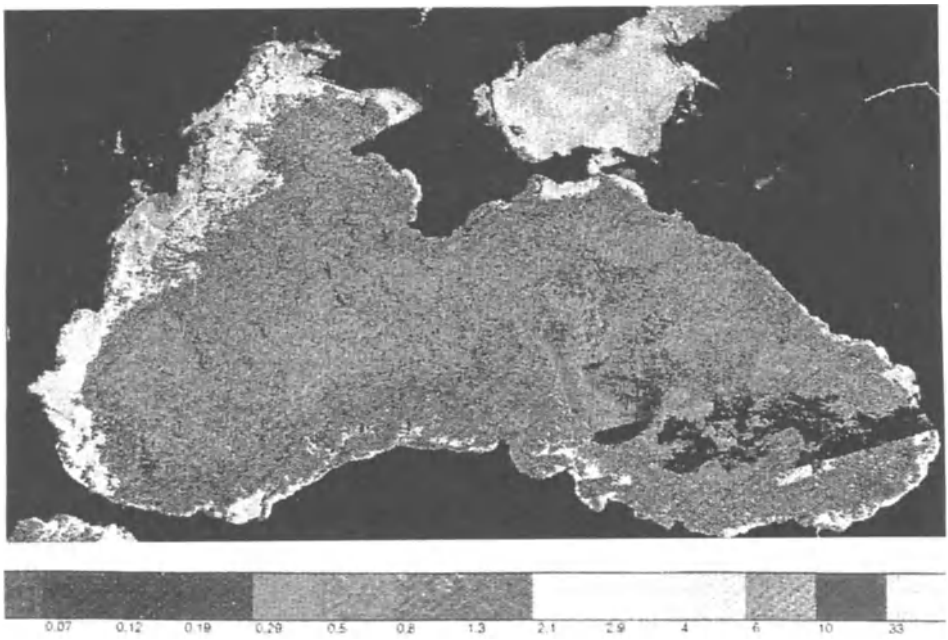


Figure 12. CZCS estimate of the sea surface chlorophyll filed : mean values in spring 80 ($\mu at - gN/l$).

The hydrodynamical results show permanent upwelling of deep waters to the surface layer in the central parts of the eastern and western main cyclonic gyres. These upwellings bring to the surface cold nutrient rich

water and allow phytoplankton growth.
The results show that the bloom begins in the region of the western and eastern main cyclonic gyres (figure 5). This winter bloom is also observed by A. Mikaelyan (1995) and identified as made of the diatom Nitzschia delicatula. On most of the north western shelf , the very low temperatures (temperatures reach 3.5 $°C$ and are below the lethal temperature used in this model ($T_{lethal} = 4\ °C$)), and the extreme convective cooling resulting in the formation of a cold intermediate layer don't allow phytoplankton's development In the eastern main cyclonic gyre, the mixed layer doesn't extend further than 20 to 30 meters and is completely included in the euphotic layer; the shallow pycnocline creates favorable light conditions for phytoplankton development in the upper 20 to 30 meters, while below, a white patch of phytoplankton's depletion can be observed (figure 6).

At the end of March, the bloom occurs in the region of the Danube's plume (figures 7 and 8).

After April, the phytoplankton population decreases as nutrient are progressively exhausted and the grazing pressure increases. The latter is particularly important in the region of the Danube's plume where consumed nutrients are constantly replaced by the discharged river waters (figures 9 and 10). The competition between phytoplankton growth (feeding on river plume nutrients) and grazing - and not the local hydrodynamics - is very likely responsible for the spatial structures of the mean spring phytoplankton concentration shown in figure 11.

The simplicity of the model and the lack of sufficient data available at the time of this preliminary simulation did not allow a thorough validation of the model. It is illuminating however to compare the model's results with CZCS images of surface chlorophyll - figure 12 shows for instance the surface chlorophyll field for the spring 1980. Since 1980, the extending and amplifying eutrophication process has led to an important increase in the nutrient content. Then, a qualitative comparison rather than a quantitative one is made and shows a good agreement. However, two main differences should be noted : - in the CZCS picture, the spring bloom occurs along the whole western coast ; - in the central parts of the two main cyclonic gyres, simulated phytoplankton concentrations are higher.

5. Conclusions

In this paper, one showed how a hydrodynamical model was implemented and extended to include an ecosystem model. The representation of the general circulation in the Black Sea by the hydrodynamical model is probably accurate enough for the simulation of a phytoplankton bloom at basin scale. In particular, the cyclonic circulation and interior upwellings

induced by the wind fields are taken into account as well as cold intermediate water formation and frontal systems on the north western shelf.

Among the problems which remain in the model version used here, is the fact that the calibration and initialization of the ecosystem model is still not optimal. In particular, the temperature limitation function of phytoplankton's growth is for the lack of something better, calibrated with data relative to specific species of phytoplankton, whereas the model handles the phytoplankton as an aggregate of different species, with different temperature limitations. The temperature limitation function must thus be interpreted as some kind of envelope of the different species specific limitation curves and should be subjected to a critical sensitivity analysis.

In this simple version of the model, silicate is not taken into account, no distinction is made between diatoms and other phytoplankton populations. The possibility of the development of opportunistic species is not tackled by the model. The representation of particulate organic matter and the short-circuiting of the microbial loop are very likely oversimplifications.

On the shelf, the informations provided by the model are primarily related to the physical constraints imposed on the system; a fine resolution interdisciplinary model will be implemented to simulate eutrophication processes. But this regional high resolution model depends on the information flowing in by the large scale circulation. In this case again the basin scale hydrodynamical and ecosystem model will be very useful.

6. Acknowledgments

This research was financed by the European Union Project EROS-2000 (contracts EVSV-CT94-0501). The authors are endebted to IBM International Foundation for supercomputer assistance in the scope of the SALMON Project.

References

1. Adam P., (1991). Sensitivity analysis of a 3D mathematical model of the Northern Bering Sea. Dissertation, GHER, Lige University, 89 pp.
2. Andersen V. and Nival P., (1988). Modle d'ecosystme plagique des eaux ctires de la Mer Ligure. Oceanologica Acta, NSP, 211-217
3. Aubrey D.G., Oguz T., Demirev E., Ivanov V., McSherry T., Diaconu V. and Nikolaenko E., (1991). Hydroblock '91 CTD Intercalibration Workshop, 1-10 December 1991, Woods Hole, USA, Intergovernmental Oceanographic Commission, Workshop Report N91, 56 pp. and 5 annexes.
4. Beckers J.M., (1991). Application of a 3D model to the Western Mediterranean. Journal of Marine Systems, 1, 315-332.

5. Chao S.-Y. and Boicourt W.C., (1986). Onset of estuarine plume. J. Phys. Oceanogr., 16, 2137-2149.
6. Filippov D.M., (1968). Circulation and water composition of the Black Sea. Nauka, Moscow, 136 pp.
7. Gamsakhurdiya G.R. and Sarkisyan A.S., (1976). Diagnostic calculations of the current velocities in the Black Sea. Oceanology, Engl. Transl., 15, 164-167.
8. Globec 1995. Report of Working Group 1, "Critical variables and dominant scales", Globec Numerical Modelling Group Meeting, Nantes, July 17-20, 1995.
9. Mikaelyan A.S., (1995). Winter bloom of the diatom Nitzschia delicatula in the open waters of the Black Sea. Marine Ecology Progress Series, 129, 241-251.
10. Nihoul J.C.J. and Djenidi S., (1987). Perspective in three-dimensional modelling of the marine system. In : J.C.J. Nihoul and B.M. Jamart (editors), Three-dimensional Models of Marine and Estuarine Dynamics, Elsevier Oceanogr. Ser., 45, 1-34.
11. Nihoul J.C.J. and Beckers J.M., (1989). Preliminary results of a three-dimensional model of the Western Mediterranean's general circulation. In : Research in the North Western Mediterranean, H. Barth (editor), Commission of the European Communities, Brussels, 7-26.
12. Nihoul J.C.J., Deleersnijder E. and Djenidi S., (1989). Modelling the general circulation of shelf seas by 3D k-ϵ models. Earth Sci. Rev., 26, 163-189.
13. Nihoul J.C.J. and Djenidi S., (1991). Hierarchy and scales in marine ecohydrodynamics. Earth Sci. Rev., 31, 255- 277.
14. Nihoul J.C.J., Adam P. and Brasseur P., (1994). Mathematical visualisation of the Northern Bering Sea's summer ecohydrodynamics. In : Data Assimilation, P. Brasseur and J.C.J. Nihoul (eds), NATO ASI Series, vol. I. 19, Springer Verlag, 107-134
15. Oey L.Y. and Mellor G.L., (1993). Subtidal variability of estuarine outflow, plume and coastal current : a model study. J. Phys. Oceanogr., 23, 164-171.
16. Oguz T.D., Aubrey S., Besiktepe S., Ivanov L., Diaconu V. and Unluata U., (1994). On the ADCP observations of the western Black Sea rim current. Deep Sea Res., II (submitted manuscript).
17. Oguz T., Ducklow H., Malanotte-Rizzoli P., Tugrul S., Nezlin N., Unluata U., (1996). Simulation of annual plankton productivity cycle in the Black Sea by a one-dimensional physical-biological model. Journal of Geophysical Research, revised.
18. Saydam C., Tugrul S., Basturk O., Oguz T., (1993). Identification of the oxic/anoxic interface by isopycnal surfaces in the Black Sea. Deep Sea Research, 40, 1405-1412.
19. Sorokin J.I., (1983). The Black Sea estuaries and enclosed seas ecosystems of the world. (ed. Elsevier), 26, 253-292.
20. Stanev E.V. et al., (1988). Numerical study on the Black Sea circulation. Mitteilungen des Instituts fr Meereskunde der Universitt Hamburg, 28, 1-232.
21. Stanev E.V., (1991). On the mechanisms of the Black Sea circulation. Earth Science Rev., 28, 285-319.
22. Stanev E.V. and Beckers J.M., (1995). Barotropic and baroclinic oscillations in strongly stratified ocean basins. Numerical study. Continental Shelf Research, submitted.
23. Sur H.I., Ozsoy E., Ilyin Y.P. and Unluata U., (1995). Coastal/deep ocean interactions in the Black Sea and their ecological/environmental impact. Journal of Marine Systems (accepted).
24. Walsh J.J. Mc Roy C.P., Coachman L.K., Wirich C.D., Shuert P.G., Grebmeier J.M., Springer A.M., Tripp R.D., Hansell D., Djenidi S., Deleersnijder E., Henriksen K. Lund B.A., Andersen P., Muller-Karger F.E., and Dea K., (1989). Carbon and nitrogen cycling within the Bering/Chukchi Sea : source regions for organics matter affecting AOU demands of the Arctic Ocean. Progress Oceanogr., 277-359

ATMOSPHERIC TRANSPORT OF DESERT DUST TOWARD EUROPEAN SEAS: MODEL PARAMETERISATION AND A SIMULATED CASE

SRDAN DOBRICIC
Dept. of Applied Physics, University of Athens, Greece[1]
Present Address: TP-690, Space Applications Institute, JRC, I-21020 Ispra (Va), Italy

Abstract. Long range transport of dust from the desert and its deposition into remote areas may significantly contribute to the local atmospheric deposition. Although the North, Baltic and Black Seas are not close to Sahara, the dust originating from Sahara is deposited in these regions, especially by precipitation, and therefore has influence on the local chemical properties of the water. A full Eulerian prognostic model for the atmospheric dust transport is described in this study. The model simulates the processes of the dust suspension from the ground, vertical turbulent mixing, horizontal and vertical advection, horizontal diffusion and dry and wet deposition. A case study of a very intense dust storm in early July 1991 is simulated to quantify the dust deposition into the sea, as it is very difficult to estimate it from the ground station measurements. The results showed that the wet deposition into North, Baltic and Black Seas was of the same order of magnitude as into the Mediterranean Sea near the Sahara desert. These short but intense episodes of a large deposition of minerals during several hours may have significant influence on the local marine ecology in those seas.

1. Introduction

The deposition of mineral aerosols from the atmosphere may represent a significant source of nutrients over the open ocean water (Donaghey et al. 1991). Even in closed seas like North, Baltic and Black Sea, during very intensive episodes of Saharan dust transport, wet deposition of the Saharan dust during relatively short events can contribute in large part to the total annual deposition of atmospheric aerosols.

The number of Saharan dust transport events to southern Europe increased rapidly from early 1980's indicating climatic changes in the general circulation of the atmosphere (Dessens and Van Dinh 1990), and during the last 100 years the rate of the suspension of the dust in northern Africa increased by factor of 10 (Hjelmroos and

E. Özsoy and A. Mikaelyan (eds.), Sensitivity to Change: Black Sea, Baltic Sea and North Sea, 501–507.
© 1997 *Kluwer Academic Publishers.*

Franzen 1989). This increased occurrence of the dust storm events may result in more frequent long range transport of the desert dust and its more important influence on the environment in seas that appear rather remote from Sahara.

2. Model description

The meteorological model used to provide the meteorological fields determining the atmospheric transport of dust is the ETA/NMC model (Janjic 1994).

The dust model in the atmospheric model follows the transport equation for the concentration of a passive substance, assuming that there is no influence of the atmospheric dust on other meteorological fields:

$$\frac{\partial C}{\partial t} + \vec{v} \cdot \nabla C + w \frac{\partial C}{\partial z} = \nabla K_L \nabla C + \frac{\partial}{\partial z} K_H \frac{\partial C}{\partial z} + F$$

where u, v and w are wind components, K_L is the lateral diffusion coefficient, K_H the turbulent exchange coefficient and F represents the source and the sink of the dust in the atmosphere.

The potential source area for the dust suspension is the semidesert land cover as suggested by Westphal (1988).

The main difference in the simulation of atmospheric dust, compared to the simulation of other atmospheric passive substances, is in the parameterisation of the dust suspension from the surface and the turbulent mixing in the lowest model layer. The model is designed so that it produces the dust over the desert through parameterisation of the dust uptake. The author's parameterisation of the dust uptake splits the scheme into separate treatment of two different physical processes:

- the kinematic mobilisation of the dust particles at the ground
- the vertical turbulent mixing of those mobilised particles with the dust in the lowest model layer.

By splitting the parameterisation into two physically distinguished phases the calculation of the mobilisation at the ground becomes independent of vertical stability, and in the second phase, the vertical mixing is calculated by the Mellor-Yamada 2.0 scheme (Mellor and Yamada 1982), assuming that the vertical mixing is the same as that for other meteorological variables.

Above the surface layer the vertical turbulent mixing is calculated by the Mellor-Yamada 2.5 scheme, with a van Leer type scheme (Lin et al. 1994) for the advection.

The model calculates fall, turbulent and wet deposition and these fields are used to specify the source of the material into the sea. The fall deposition is calculated by a single fall velocity, assuming that all particles are of the same size. This assumption may have influence on the dust quantification close to the source area as it excludes the influence of the larger particles on the concentration. The turbulent deposition is

calculated by the Mellor-Yamada 2.0 scheme, and the wet deposition is calculated by the constant scavenging ratio.

Testing of the model was showed its ability to realistically simulate the atmospheric dust fields with results quantitatively comparable with the available satellite measurements.

3. The Simulation

The yellow coloured snow was observed at the Arctic Circle in northern Sweden and Finland on 10 march 1991 (Franzen and Mattson 1994). At the first instance it was believed that the colour originated from the Central European pollution, but after snow samples analysis, the main part of the aerosols were shown to be the dust from Sahara (Franzen and Mattson 1994).

In their paper Franzen and Mattson (1994) give detailed evidence of long range dust transport originating from Western Sahara between 6 and 8 March, which was observed over many places in Northern Africa, Southern, Western and Central Europe between 8 and 9 March, finally reaching the Arctic Circle on 10 March.

The simulation of the atmospheric dust model was started on 5 March 1991 and ended on 11 march 1991. The model is initialised with zero dust concentration and therefore it is needed to start the simulation several days before the main dust storm occurs to produce the background concentration over the desert.

The meteorological situation was characterised by a depression with strong winds passing over Northern Africa during 7 and 8 March and producing long range transport of the dust towards Northern Europe (Fig. 1).

Figure 2 shows the simulated atmospheric dust concentration integrated in the vertical for the period 7-10 March 1991. The dust entered the atmosphere in a strong dust storm in southern Algeria (Fig. 2a), the area that is one of the main sources of the Saharan dust in the atmosphere (Westphal et al. 1988). On 8 March (Fig. 2b) the Saharan dust cloud reached Scandinavia at high altitudes. Part of the cloud spread over eastern Europe and Turkey. In following days (Fig. 2c and 2d), the dust cloud covered a large area of Central and Eastern Europe and spread far north over the Arctic Circle.

Figure 3 shows the wet dust deposition accumulated for 24 hours on 9 and 10 March. On 9 March a large deposition occurred over the North Sea, in an area between Norway and Netherlands, while on 10 March the deposition was over the northern part of the Baltic Sea. The deposition over Scandinavia on 10 March had a peak exactly at the place where it was measured (Franzen and Mattson 1994). On 10 March the model simulated wet deposition over the western coast of the Black Sea.

This picture shows that the deposition of the Saharan dust to the North and Baltic Seas was of the same order of magnitude as the deposition over the Mediterranean. This process of deposition by precipitation occurs during several hours and it is a sudden large flux of external nutrients into the sea.

The dry deposition had a more simple structure and is mainly located close to the source area.

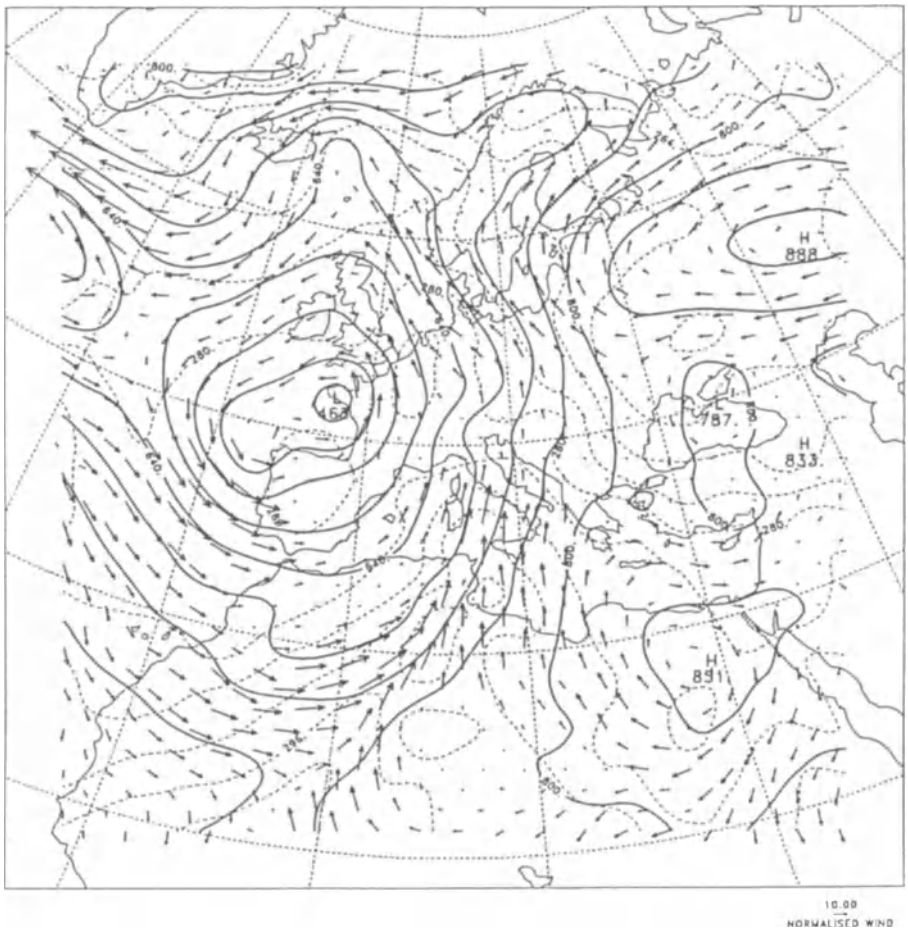


Fig. 1: Weather situation on 8 March 1991. at 00UTC. The figure shows the ECMWF analysis of the 925Mb isosurface. Full lines show geopotential heights and dashed lines show temperature. Wind direction and intensity are represented by arrows. The area of convergence and strong winds over Western Sahara is visible on the figure.

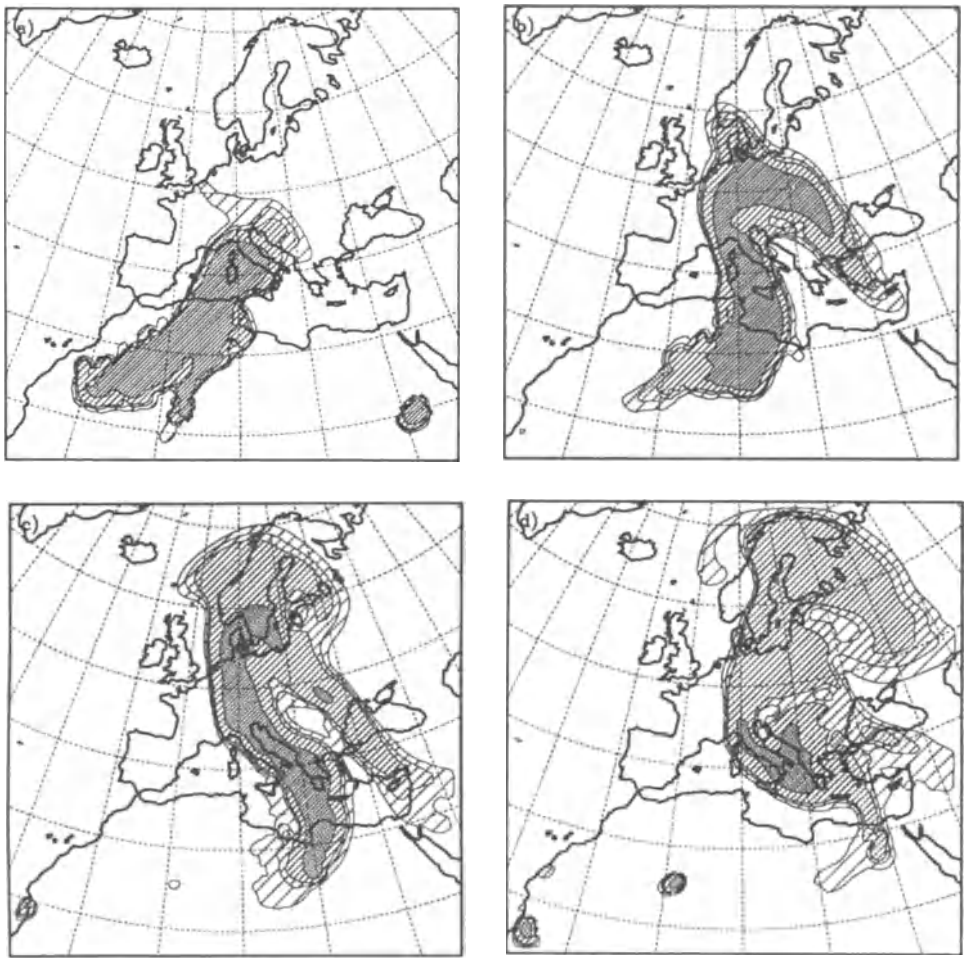


Fig. 2: Simulated dust load 8 March 1991 at 00UTC (a), 9 March 1991 at 00UTC (b), 10 March 1991 at 00UTC (c) and 11 March 1991 at 00UTC (c). The isolines represent dust load of 0.1, 0.5, 1.0 and 2.0 gm^{-2}

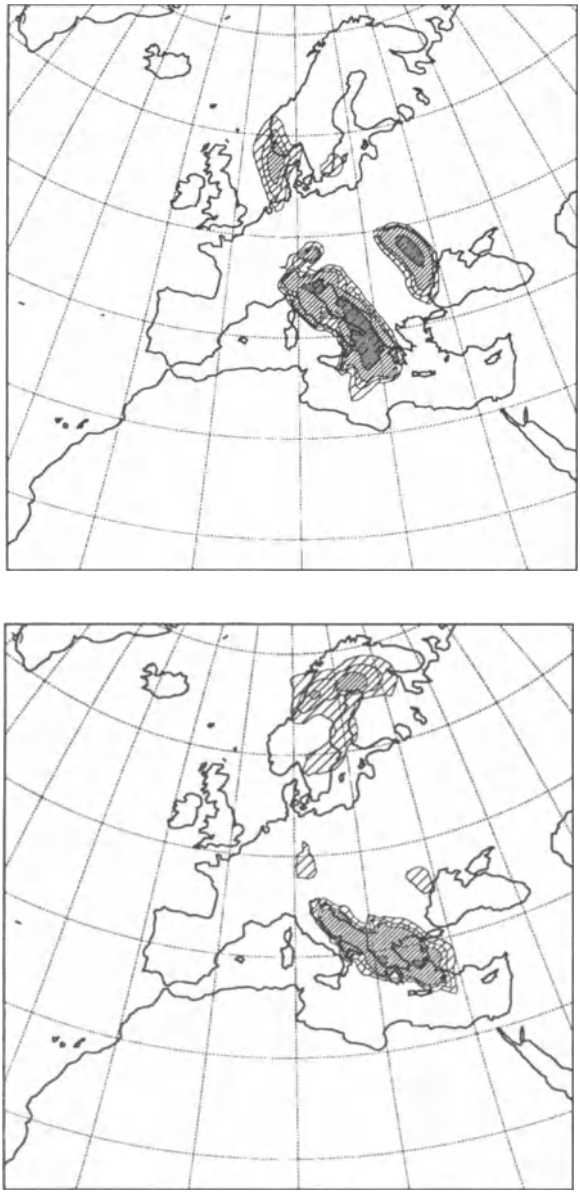


Fig. 3: Simulated wet dust deposition accumulated for 24h for 10 March 1991 at 06UTC (a) and 11 March 1991 at 06UTC (b). The isolines represent deposition of 0.1, 0.2, 0.3 and 1.0 gm^{-2}

4. Conclusions

An atmospheric dust model is used to simulate a very intense dust transport event in early March 1991, described by Franzen and Mattson (1994). The simulation was in qualitative agreement with measurements and reports about this event over Europe.

The simulation showed that there was large quantities of wet dust deposition over the North, Baltic and Black Seas. The amount of the deposited dust into these seas was locally as high as that occurred into the Mediterranean Sea, which is closer to the Saharan desert. This result suggests that the impact of Saharan dust deposited into remote areas can not be neglected, when the total atmospheric flux is calculated in order to understand the role of external nutrients on the local marine ecology.

An atmospheric dust transport model that can resolve all the phases of the atmospheric dust input, transport and deposition, and give the quantitative picture of the process is an important tool for better understanding of the phenomena in the future.

5. Acknowledgements: I am grateful to Prof. Emin Özsoy who introduced to me the problem of the atmospheric nutrient inputs into the sea and encouraged me in my work.

6. References

1. Donaghey, P.L., Liss, P.S., Duce R.A., Kester, D.R., Hanson, A.K., Viliareai, T., Tindaie, N. and Gifford, D.J., (1991) The role of episodic atmospheric nutrient inputs in the chemical and biological dynamics of oceanic ecosystems. Oceanography. 4: 62-70
2. Dessens, J. and Van Dinh, P. (1990) Frequent Saharan dust outbreaks north of the Pyrenees: A sign of climatic change?. Weather, 45: 327-333.
3. Franzen, G.L. and Mattson, O.J., (1994) Yellow snow over the Alps and Subarctic from dust storm in Africa, March 1991. Ambio. 23: 233-235.
4. Hjelmroos, M. and Franzen, L.G. (1989) Desertification and soil damage in Central Tunisia during the Halocene. Proceedings of the European Workshop "Airborne particles and their negative effects on the cultural heritage, the environment and Man". Ravello 12-13 December 1989.
5. Janjic, Z.I., (1994) The step-mountain eta coordinate model: Further developments of the convection, viscous sublayer, and turbulence closure schemes. Mon. Wea. Rev. 122: 927-945.
6. Lin, S., Chao, W.C., Sud Y.C., Walker J.K. (1994) A class of the van Leer type transport schemes and its application to the moisture transport in a general circulation model. Mon. Wea. Rev. 122: 1575-1593
7. Mellor, G.L., and Yamada T., (1982) Development of a turbulence closure model for geophysical fluid problems. Rev. Geophys. Space Phys. 20: 851-875.
8. Saydam, C., (1994) April 1994 dust storm events, Unpublished manuscript
9. Westphal, D. L., O. B. Toon and Carlson T.N., (1988) A case study of mobilization and transport of saharan dust. J. Atmos. Sci. 45: 2145-2175.

SUBJECT INDEX

-A-

abundance, 89,127
  of M. Leidyi, 121-122
  of recruitment, 169
  of zooplankton, 142
advection, 285
algal production, 49
ammonia, 52-62
ammonium, 479
anchovy, 70-71,75,125-126,149-159,163
  biomass, 165-170
  catch of, 126
  decline in the stock of, 164
  fishery, 153-154
  spawning, 70,149,156-157
anoxia, 151
anoxic
  boundary, 197
  water, 184,190,192,197,265
anticyclone, 347
anticyclonic
  area, 384-385,392
  circulation, 387,390,391,399
  region, 183,184
antropogenic
  activities, 449,440,444
  effects, 79
  eutrophication, 91,111
  factors, 164
  flow, 285
artificial reefs, 25,28

-B-

Bacillariophyta, 79-91
  biomass ratio (Bacill.:Dinophytha), 79,80
bacteria, 472
  coliform, 28
baroclinic
  oscillations, 341,342
  pressure gradients, 473
  radius of deformation, 472
barotropic-baroclinic instability, 366
basin
  oscillations, 341,363,353,358,379
  shape, 341,343,345
benthic, 80,470
biodiversity, 26,79,85,458
biogenic matter, 211,219,470
bio-indicator, 103-104
biomass, 89,90,97,119-120
  bacterial, 469,470
  living, 211,218
biomass:abundence (B:N) ratio, 82
  planktonic, 40
Black Sea Water (BSW), 419,428,436
bloom, 79,80,163,172,469,494,495

algal, 456
frequency of, 79-91
intensity of, 79
phytoplankton, 151
blooming
areas, 25
density, 85
of phytoplankton, 135
period, 72
blue fish, 163
bonito, 163
bottom homogenius layer (BHL), 275-283
bottom topography, 341,347
boundary conditions, 342,367,424-425
Brunt-Vaisala frequancy, 282
buoyancy, 298
flux, 278,280,285,287,293,381,395,425
flux, lateral, 395,396,400

-C-

C/Chl ratio, 223-237
C/N ratio, 223-237,447
Carbon cycling, 455
Cesium profiles, 246

chemocline, 265,429
interannual variability, 265
chernobyl, 239
isotopes, 429
tracers, 417
penetration of, 419

chlorophyll, 213,216,220
patchiness, 470
chlorophyll-a, 106,131,136,223
circulation, 342-361,365,367,371,373,376,385, 387,392,395,396,400,403,469-475
buoyancy driven, 403
climatological, 365,366
formation of, 341
haline, 395,396
horizontal, 395
ocean, 469
physical, 470
scheme, 255
steady-state, 365
thermal, 395
thermohaline, 395,403,404,407-409
time changes of, 489
upper layer, 49
vertical, 379
climate change, 1,311,312
indicators of, 2
model, 311
variability, 311
climatic
data, 261
field, 40
variability, 65,75
coccolitophores, 46
coefficient of
diffusion, 377
horizontal, 396-400
vertical, 396-400
light attenuation, 33,37,41-44
mixing, 377
of exploitation, 165
Cold Intermediate Layer (CIL), 50,62,188,240, 253-263,295-306,365,367,376,384, 388,392,417,429-436,491,497
formation, 498
evolution, 366
temperature, 256,267
thickness, 186,192,260
volume of, 256-257,261,263
Cold Intermediate Water (CIW), 253-263,376, 381,384,423,434,437,469
characteristics, 261
formation, 376,384-387,390,392
interannual variability in, 257
penetration of, 375,376,386,387,390,392

temperature/salinity analysis of, 253
temperature of, 257
volume of, 258,262
cold water formation, 375
color
index, 33
purity, 45-46

scale, 45
continental slope, 417,418,427-429,432-434
convection, 34,255,276,280,295,296,303,304, 376,377,381,384,387,392
ocean, 375
slope, 417,418
winter, 376,379,390
convective
cooling, 497

layer, 275-277

convergence zone (see also anticyclonic region), 253-256,263,,286,287,293
copepod, 26,72,153,456
correlation coefficient, 23
Coastal Zone Color Scanner (CZCS), xiv,131
data, 136-138
cooling, 375,376,385,382,489
134Cs, 239
134Cs/137Cs ratio, 240
137Cs, 239

137Cs/90Sr ratio, 240
currents, 365,366,368,371
cyclone, 346
main, 368
cyclonic
area, 384-385
circulation, 253,259,375,384,387,390,399,489
eddies, 376
gyre, 200,473
main, 375,379
region, 183-185
rings, 40

-D-

deep water structure, 275
de-eutrophication, 104
degradation, 223
distribution, 366
surface, 188,239
stratification, 412
variability of, 14
detrivores, 26
diatom, 89,105,456,498

bloom, 90
dinoflagellates, 105
Dinophyta, 79-91
dissolved organic nitrogen (DON), 194
dissolved oxygen (DO), 186-188,192,197,198,200,203
downwelling, 365,368,371,386,388,390,392, 395,398,400
dust

model, 502
suspension, 501,502
transport, 507
uptake, 502

-E-

eddy, 261,262,341-363,367,368,371,379,381, 384,385,412,469-473
anticyclonic, 371,373,490
cyclonic, 376
dissipation, 341
formation, 341
kinetic energy (EKE)
variability, 341,342
Ekman

layer flux, 400
transport, 400
EKE/MKE ratio
El-Nino Southern Oscillation (ENSO), 20
euphotic layer, 37,198,203,209,494,497
euphotic zone, 211,218,219,223,480
depth of, 40
eutrophication, xvi,25,46,75,79,95,105,124,212, 218,439-442,455,470,497,498
coastal, 439,440
determination of, 114
primary and secondary
eutrophic waters, 132-135

exotic comb jelly (see also Mnemiopsis Leidyi), 25

-F-

filtration, 106
finite-difference approximation, 366
fish, 80,125,163,456
  fauna, 150
  seasonal migration of, 151
  species, 179
  stock, 163
fishery, 65
  of anchovy, 153-154
fishing, 125,149,163
  fleet, 154-155
  over-fishing, 157
food
  availability, 117,151
  chain, 440,445
  web, xvii,440,443,445,456,458,460,469
forcing, 300,341,342-346,362,378-379,392,469, 471-474
  atmospheric, 327,328
  baroclinic, 327
  barotropic, 403,409-412
  meteorological, 404
  physical nutrient, 457

-G-

gelatinous
  animals, 66
  colonies, 440
grazing, 105,112,497
Green Revolution, 26
Gulf of Gdansk, 1
gyre, 347,348,368
  anticyclonic, 349,373,475
  cyclonic, 342,368,371-373,384,475
  main, 392
    cyclonic, 495,496,497

-H-

halocline, 186,265,285,295-307,311
  diffusion coefficient of, 282
  interannual variability, 265
heat flux, 272,277,367,377,390,425,428,432
  geothermal, 275
  Zero Heat Flux (ZHF), 425,426,428,433
herbivores, 26,481
herring, 139-147
  biomass, 141
  feeding, 142
  stock, 145
horse mackerel, 163
  biomass, 177-179
    spawning, 177-178
    total, 177
hydrochemical properties, 197,198
hydrogen sulfide, 188
hypertrophic waters, 132-135
hypoxia, 27,50,80

-I-

ichthyoplankton, 68
  monitoring of, 65
interannual variability, xv
interdecadal variability, xv
isohaline surfaces, 387
isopycnal interface, 265
isopycnal surface, 376,381,382,387
  topography of, 290-292

-J-

jelly fish, 66,457
jet
  coastal, 349
  local, 368
  mid-ocean, 349

-M-

man-made
  changes, 25
  disturbances, 152
meanders, 381

mean kinetic energy (MKE)
Mediterranian Sea Water (MSW), 419-437
  penetration of, 420,428,436
megaplankters, 170
mesotrophic waters, 134
mixing, 200,239,282,376,381,386
  convective, 368,371
  internal, 420
  process, 371
Mnemiopsis Leidyi,
33,46,65,97,101,105,110,117-
127,149,152,179,457
  abundance, 121-122
  biomass, 170,179
  blooming, 71
  life cycle, 118
  long term fluctuations of, 119
  period of adaptation of, 124
  seasonal dynamics of, 123-124
  size groups, 118
model, 295,296,298-300
  3-D model, 428,569,492
    ecosystem, 487-498
  3-D PE GCM, 365
  atmospheric dust model, 502,503,507
  BIOGEN, 467
  Bryan-Semtner-Cox model, 341,342
    description of, 377-379
  climate, 311
  ETA/NMC model, 502
  GHER plankton model, 488
  GHER primitive equation model
  hydrodynamic, 487,488
  ice/ocean model,311-313
  MIRO Model, 439,445,446-448,450
  non-linear model description, 396-398
  NORWECOM, 327,328-329
  numerical ocean circulation, 375
  numerical reduced gravity model, 417,418
  one-dimensional model of formation, 275
  Princeton Model, 403,405,472
  turbulence, 471
mortality, 164
  coefficient, 164,169
  rate, 165-171,171
movable boundary, 420

-N-

N:P ratio, 49,56,60,62,183,192,442
N,P,Si concentrations, 442
N:P:Si ratio, 455
N:Si ratio, 56,60,442
natural factors, 164
net, 96,106
new species, 74

nitracline, 183,190,192,209
nitrate, 197,203,208-209,439-440,443,476-481
nitrogen, 29,46,89,455,479,480
  cycling, 455,487
  dissolved organic (DON), 476-479,482,484
  in fish tissue, 159-160
  inorganic (IN), 49
  organic, 479
  stock, 49
  total inorganic (TIN), 52-62
  transport, 333-334
Northern Atlantic atmospheric circulation, 4
North Sea, 311, 327, 439
nutrient, xvi,40,197,476,478,
  enrichment, 151,159,439,442,443,456
  fluxes, 50
  profile, 197,198
  ratio, xvi,79,80,89,440
  reduction, 450,451
  stock, 51,58-62
nutricline, 188

-O-

ocean-atmosphere
  heat exchange, 375
  system, 14
opportunistic phytoplankters, 456,457
organic matter, 29,218
  particulate, 29
oxic/anoxic interface, 239
oxic water, 188,265

oxycline,
183,186,188,190,192,194,198,200,203,265
shoaling, 265
oxygen, 197,200
deficiency, 30
profile, 197,198

-P-

Pacific Southern Oscillation index, 20

particulate organic matter (POM),
211,213,215,217,218,220,223-237,457,484,491
distribution, 223-237
patchiness, 132-134
pelagic species, 65
phosphate, 49,188-190,194,197,203,206-207
concentration in RIM Current, 109
interannual variations, 52
phosphorus, 29,46,89,440,455
cycling, 455
in fish tissue, 159
inorganic (IP), 49,52-62
phosphocline, 183,188,192,194
photosynthesis, 217,219
phytoplankton, 34,46,79,456,469-470,479,495
bloom, 151
biomass, 25,26,106,218,220,488,491
changes in, 109
interannual variability of, 81
total, 108
community changes, 80
winter blooming of, 135
plankton, 37,381,472,481
fauna, 95
structure, 89
plant pigment, 131,135
surface concentration, 132
seasonal fluctuations of, 132-137
plume, 417
pollution, 79,163
POM/SM ratio, 211,218
potential vorticity, 260-261,263
primary production, 29,37,211-220,328,334,336-337,488
level of, 106

production, 223,481
productivity, 131,135,212,218,220,470
biological, 40
fish, 28
level of, 114,211,218
primary, 223
P:Si ratio, 442
pycnocline, 186,188,197,198,200,203,206,208,209,240,265-273,384,475,476,497
seasonal, 214

-R-

radiance index, 45
spectral, 41
radiation shift, 44-45
radionuclide, 239
red-tide species, 85
reflection coefficient, 280
Regions of Freshwater Influence (ROFI), xiv
residence time, 419
Richardson number, 367,423
Rim Current, 49,112,254,260-263,470,473
area, 106
intensity, 368
main (MRC), 286,291
meandering, 256,266
biomass, 105,112
river dicharge, 13,105,487,489
anomalies, 13
seasonal cycle of, 15
river input, 211,212
interannual fluctuations of, 15
interdecadal fluctuations of, 23
plume, 490,491
predictability of low frequency, 23
river influence, 211,212,218,220
Rossby
index (RI), 13
trend, 20
radii, 405

radius of deformation, 342

wave, 354,379

-S-

salt
flux, 367,433
transport, 412
salinity, 253,258,261,275,276,296,297,
365-367,373,399,405,423,425-430,434,491
at Heligoland Roads, 74
change, 270-272
flux, 432
in Baltic Sea, 139-145
montly averaged, 13
pattern, 381
sea surface, 378
upper layer, 397,399
variability of, 14,267

vertical profiles of, 268,270
satellite, 211,212,215,474
sea ice, 1,2,4,311

sea level, 1,2,371,404
difference, 410
increase in, 1
variability, 5-6
temperature anomalies, 1,13
seasonal variability, 365,489
sea suface temperature (SST), 489,491,
distribution, 495
gradient, 492
Secchi Disk, 27
variability of visibility, 33-47

sedimentation, 29
settling technique, 106
sigma-t interface, 265,267,268
sigma-t surface
temperature in, 267
silicate, 52-62,470,498
silicon (Si), 91,455
annual cycle of, 90
content, 90
cycling, 455
depletion hypothesis, 89
Si:N ratio, 89,90,91
Si:P ratio, 56,60,89,90,91
solar activity, 80,172
cycle, 47
solar radiation, 469481
spawning, 141,145
biomass, 165, 168-174

of anchovy, 156-157
sprat, 163
biomass, 170
90Sr, 239
storm surges
frequancy of, 1,3-4
duration, 2-3
statistical analysis of data, 6
stratification, 142-
145,282,286,381,395,396,398,400,423,429,469,4
72
stability of, 375
unstable, 298
suboxic zone, 188-190,192,194,197,203,
206-208,214
thickness, 203
suspended matter (SM), 211-219,381
vertical distribution of, 214

-T-

taxonomic
composition, 89
structure, 84,90
of phytoplankton, 105
temperature, 253,258,275,276,366,367,373,405,
425,426,434,437
air, 112-114,265,273,300,379,390
at Heligoland Roads, 74
atmospheric, 375,377,378,390
change, 270,272
gradients of, 388,473
mixed layer, 379
montly averaged, 13
sea surface (SST), 375,377,379,390
surface, 311
variability of, 14,267

vertical profiles of, 268,270
thermal capacity, 384
thermocline, 34,113,186,295-307
thermohaline flux, 469,472
topographic wave, 379

toxic
phytoplankton bloom, 91
T,S
diagrams, 258-264
profiles, 295,296,300,301

-U-

upwelling, 172,285-293,384,395

-V-

ventilation,
197,200,203,239,265,295,297,298,307,429
vertical
advection, 501
circulation, 379
mixing, 142,197,198,285,286,381
stratification, 285,327,375,408,417
of salinity, 311,320-323
of temperature, 311,320-323
coefficient, 343
turbulent, 367,501,502
profiles,
of temperature, 434
of salinity, 434
stability, 502
velocity, 265,271-273
viscosity,396-400,471
volume transport, 335-336,397-400,412
vorticity, 288,347

-W-

Warm Intermediate Layer (WIL), 303-305
water
cold water formation,
colour, 41-46
deep water formation, 395
mass formation, 295
water transparency, 25,47,106
of Black Sea, 27
interannual variability of, 34
longterm variability of, 35
substances, 25

wave-eddy transition, 346,363
wet dust deposition, 503,507
whiting, 163,174-176
wind stress, 342,344-346,362,472-475
climatological, 469
field, 366
winter
bloom, 137
convection, 395
period, 368
mixing, 255,365

-Y-

yellow substance (gelbstoff), 44

-Z-

zooplankton, 25,71,74,75,476,478,479,481-484
abundance, 142
biomass, 95-104,112,127,488,491
composition, 95
monitoring, of 65
species, 66-70
zooplanktivores, 170